Energy, Mines and Resources • *Yukon Geological Survey*

YUKON EXPLORATION & GEOLOGY 2006

- Mining & Exploration Overview
- Yukon Geological Survey
- Geological Fieldwork
- Property Descriptions

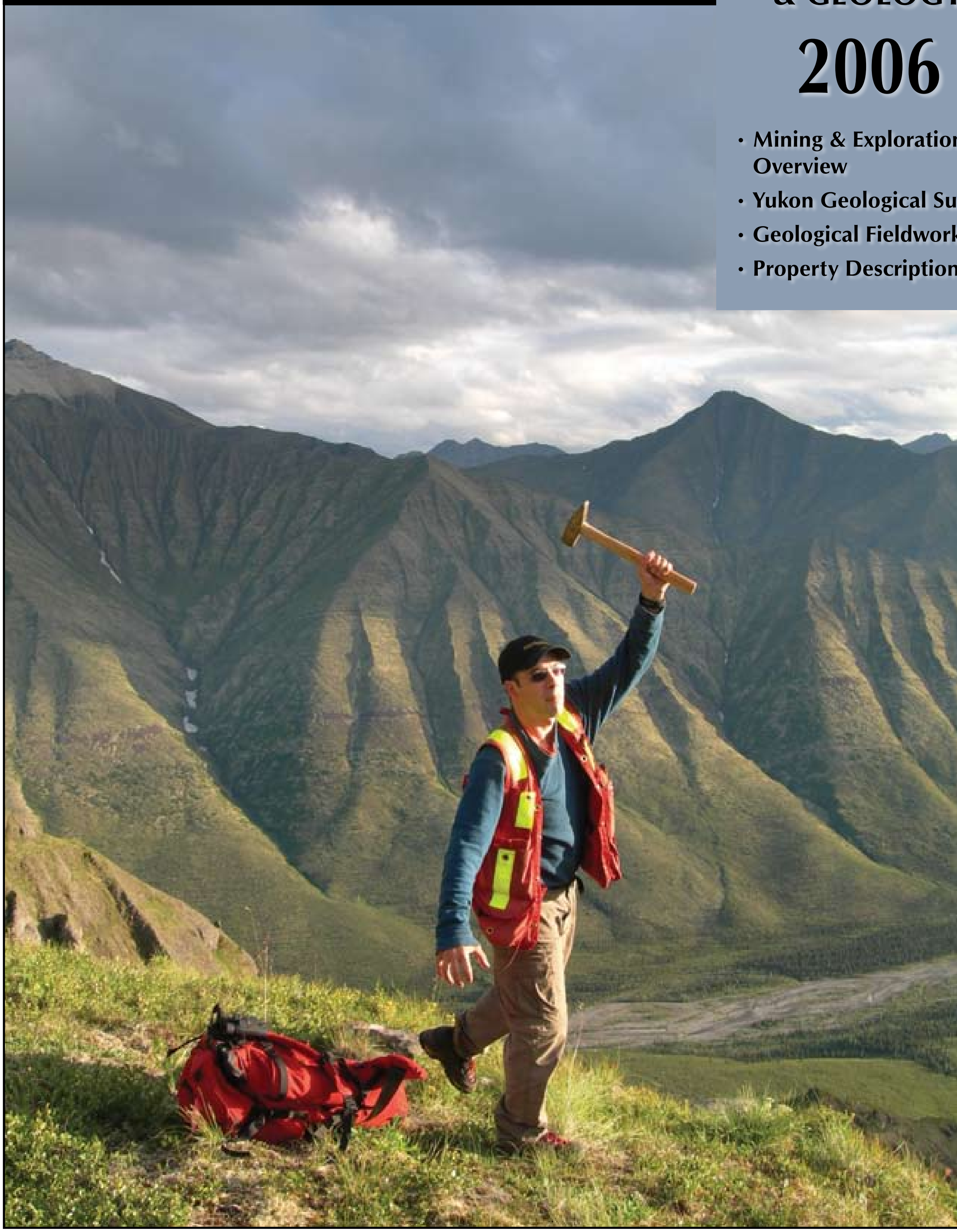

Yukon Geological Survey

Yukon
Energy, Mines and Resources

YUKON
EXPLORATION & GEOLOGY
2006

Edited by
D.S. Emond, L.L. Lewis and L.H. Weston

Yukon Geological Survey
Energy, Mines and Resources
Government of Yukon

Published under the authority of the Minister of Energy, Mines and Resources, Government of Yukon

http://www.emr.gov.yk.ca

Printed in Whitehorse, Yukon, 2007.

Publié avec l'autorisation du ministre de l'Énergie, des Mines et des Ressources
du gouvernement du Yukon

http://www.emr.gov.yk.ca

Imprimé à Whitehorse (Yukon) en 2007.

ISSN 1208-2937 (print version), 1718-8326 (on-line version)

This, and other Yukon Geological Survey publications, may be obtained from:

Geoscience and Information Sales
c/o Whitehorse Mining Recorder
102-300 Main Street
Box 2703 (K102)
Whitehorse, Yukon, Canada Y1A 2C6
phone (867) 667-5200, fax (867) 667-5150

Visit the Yukon Geological Survey web site at www.geology.gov.yk.ca

In referring to this publication, please use the following citation:

Yukon Exploration and Geology 2006. D.S. Emond, L.L. Lewis and L.H. Weston (eds.), 2007.
Yukon Geological Survey, 268 p.

Production by K-L Services, Whitehorse, Yukon.

PHOTOGRAPHS

Front cover: Geoff Bradshaw (Yukon Geological Survey) strikes a 'hero pose' at the Crest Iron property, Yukon. Photo by Lara Lewis, YGS.

PREFACE

Yukon Exploration and Geology (YEG) continues to be the main publication of the Yukon Geological Survey (Energy, Mines and Resources, Yukon government). This is the 29th volume of the series.

YEG 2006 contains up-to-date information on mining and mineral exploration activity, studies by industry, and results of recent geological field studies. Information in this volume comes from prospectors, exploration and government geologists, mining companies and students who are willing to contribute to public geoscience for the benefit of the scientific community, general public, and mineral and petroleum industries of the Yukon. Their assistance and patience is sincerely appreciated.

This year our editing team consisted of Lara Lewis, Leyla Weston and myself. It is an honour to work with such a dedicated, efficient team. We have, however, greatly missed our co-editor from past years, Geoff Bradshaw, who was tragically killed in an accident this summer. He was a huge asset to our team in the past, but his spirit is still hugely inspiring for us (see Dedication).

We thank the Translation Bureau, Public Works and Government Services Canada for translating the French abstracts. Appreciation is also extended to Maurice Colpron of the Yukon Geological Survey (YGS) for his able assistance in the review of French translations of abstracts. We also thank all the geologists who contributed by critically reviewing YEG manuscripts: M. Allan, J. Bond, M. Burke, R. Friedman, S. Israel, C. Kearns, P. Lipovsky, G. Lowey, D. Murphy, L. Ootes, L. Pigage and B. Ward.

Wynne Krangle and Peter Long of K-L Services continue to provide excellent service in putting this production together, including editing suggestions, design of diagrams, volume layout, and working under the pressure of a tight deadline. Sherry Tyrner of the Queen's Printer once again ensured that the printing process went smoothly.

The 2006 volume has four parts. The first — Mineral Industry — includes overviews of hardrock and placer mining, development and exploration in the Territory as well as a summary of the Yukon Mining Incentives Program. The second part — Government — outlines the activities and organization of the Yukon Geological Survey, and includes announcements of the seventh Mining Land Use Reclamation Awards, the Robert E. Leckie Awards. The third part — Geological Fieldwork — contains reports describing regional mapping, and more detailed geoscience studies. The last part — Property Descriptions — is meant for submissions from the mineral industry on mineral occurrences and deposits.

We welcome any input or suggestions that you may have to improve future YEG publications. Please contact me at (867) 667-3203 or by e-mail at diane.emond@gov.yk.ca.

Diane Emond

PRÉFACE

Yukon Exploration and Geology (YEG) continue d'être la publication principale de la Commission géologique du Yukon (Énergie, Mines et Ressources, gouvernement du Yukon). Ce volume est le 29e de la série.

YEG 2006 contient une mise à jour sur l'exploitation et l'exploration minières, les études réalisées par l'industrie et les résultats des travaux géologiques exécutés récemment sur le terrain. L'information est fournie par des prospecteurs, des géologues d'explorations et du gouvernement, des sociétés minières et des étudiants qui souhaitent en faire bénéficier la communauté scientifique, le grand public, ainsi que les industries minières et pétrolières du Yukon. Nous apprécions leur aide et leur dévouement.

Cette année les co-rédacteurs du YEG sont Lara Lewis, Leyla Weston et moi-même. C'est un honeur de travailler avec une équipe aussi dédiée et éfficace. Nous manquons toutefois grandement la contribution de notre co-rédacteur des années précédentes, Geoff Bradshaw, qui fût tué tragiquement dans un accident au cours de l'été. Il était un grand atout au sein de notre équipe dans le passé, et son esprit continu de nous inspirer énormément (voir "Dédication").

Nous remerçions le Bureau de la traduction, Travaux publics et Services gouvernementaux du Canada, pour la traduction française des résumés. Nous remerçions également Maurice Colpron de la Commission géologique du Yukon pour son aide avec la révision des traductions françaises. Il faut aussi souligner la contribution de plusieurs géologues à la lecture critique des manuscrits, au cours de cette année; il s'agit notamment de M. Allan, J. Bond, M. Burke, R. Friedman, S. Israel, C. Kearns, P. Lipovsky, G. Lowey, D. Murphy, L. Ootes, L. Pigage and B. Ward.

Wynne Krangle et Peter Long de K-L Services ont une fois de plus fourni un excellent service de production, incluant des suggestions de révision, la conception de diagrammes, la mise en page et le respect d'échéances serrées. Sherry Tyrner de l'Imprimeur de la Reine a, pour sa part, veillé au bon déroulement de l'impression.

Le volume de 2006 comprend quatre parties. La première — Industrie minérale — renferme des survols sur l'exploitation, le développement et l'exploration minières des roches dures et des placers dans le territoire, de même qu'un résumé sur le Programme d'encouragement des activités minières du Yukon. La deuxième partie — Gouvernement — décrit dans les grandes lignes les activités et l'organisation de la Commission géologique du Yukon, et présente la sixième édition des prix Robert E. Leckie, récompensant les meilleurs travaux de remise en état des sites miniers. La troisième partie – Travaux géologiques sur le terrain — contient des rapports décrivant la cartographie régionale et des études géoscientifiques plus détaillées. La dernière partie — Descriptions des propriétés — vise les présentations des sociétés minières concernant des indices et des gîtes minéraux.

Pour tout commentaires ou suggestions afin d'améliorer les futures publications du YEG, vous être priés de communiquer avec moi par téléphone au (867) 667-3203 ou par courriel à l'adresse suivante : diane.emond@gov.yk.ca.

Diane Emond

TABLE OF CONTENTS

MINERAL INDUSTRY

Yukon Mining, Development and Exploration Overview 2006
M. Burke, S. Traynor and L.L. Lewis 2
Appendix 1: 2006 exploration projects 41
Appendix 2: 2006 drilling statistics 46

Yukon Placer Mining Overview 2006
W. LeBarge 49

Yukon Mining Incentives Program Overview 2006
S. Traynor 53

GOVERNMENT

Yukon Geological Survey
G. Abbott and staff 57

La Commission géologique du Yukon
G. Abbott et M. Colpron 73

Robert E. Leckie Award for Outstanding Reclamation Practices
J. St. Amand 77

GEOLOGICAL FIELDWORK

Investigating a Triassic overlap assemblage in Yukon: On-going field studies and preliminary detrital-zircon age data
L.P. Beranek and J.K. Mortensen 83

Evaluation of the origins of gold hosted by the conglomerates of the Indian River formation, Yukon, using a combined sedimentological and mineralogical approach
D.P.G. Bond and R.J. Chapman 93

Late Wisconsinan McConnell glaciation of the Big Salmon Range, Yukon
J.D. Bond 105

The Dawson City landslide (Dawson map area, NTS 116B/3), central Yukon
M.A. Brideau, D. Stead, V. Stevens, C. Roots, P. Lipovsky and P. VonGaza 123

Developing a new method to identify previously unrecognized geochemical and morphological complexity in placer gold deposits in western Yukon
E.C. Crawford, R.K. Chapman, W.P. LeBarge and J.K. Mortensen 139

Micropetrology and mineral geochemistry of the Tombstone and Deadman plutons, Tombstone Plutonic Suite, central Yukon
A.M. Flanders, M.J. Harris, L. Kearns and C.J.R. Hart 149

continued

Field investigations of the Upper Devonian to Lower Carboniferous Tuttle Formation, eastern Richardson Mountains, Yukon
T.A. Fraser and T.L. Allen 157

Are mafic dykes in the Nor and Hart River areas of the Yukon correlative to the Bonnet Plume River Intrusions? Constraints from geochemistry
J. Hunt and D. Thorkelson 175

A reconnaissance inventory of permafrost-related landslides in the Pelly River watershed, central Yukon
P.S. Lipovsky and C. Huscroft 181

Structure of schist in the vicinity of the Klondike goldfield, Yukon
D. MacKenzie, D. Craw, J.K. Mortensen and T. Liverton 197

Laser ablation ICP-MS U-Pb zircon ages for Cretaceous plutonic rocks in the Logtung and Thirtymile Range areas of southern Yukon
J.K. Mortensen, A. Brand and T. Liverton 213

The three 'Windy McKinley' terranes of Stevenson Ridge (115JK), western Yukon
D.C. Murphy 223

Morphological and compositional analysis of placer gold in the South Nahanni River drainage, Northwest Territories
K.L. Rasmussen, J.K. Mortensen and H. Falck 237

PROPERTY DESCRIPTIONS

New data on the geology and mineralization of the Skukum Creek gold-silver deposit, southern Yukon (NTS 105D/3)
S.G. Soloviev 253

YUKON EXPLORATION AND GEOLOGY 2006

GEOLOGICAL FIELDWORK

1	**Beranek & Mortensen**	Triassic overlap assemblage
2	**Bond & Chapman**	Gold in conglomerates, Indian River formation
3	**Bond**	McConnell glaciation, Big Salmon Range
4	**Brideau *et al.***	Dawson City landslide
5	**Crawford *et al.***	Characterizing placer gold
6	**Flanders *et al.***	Tombstone and Deadman plutons
7	**Fraser & Allen**	Tuttle Formation
8	**Hunt & Thorkelson**	Mafic Dykes, Nor and Hart River
9	**Lipovsky & Huscroft**	Landslides, Pelly River watershed
10	**Mackenzie *et al.***	Structure of Schist, Klondike
11	**Mortensen *et al.***	Geochronology, Logtung and Thirtymile
12	**Murphy**	Windy McKinley, Stevenson Ridge
13	**Rasmussen *et al.***	Placer gold, South Nahanni River

PROPERTY DESCRIPTION

14	**Soloviev**	Skukum Creek Gold-silver Deposit

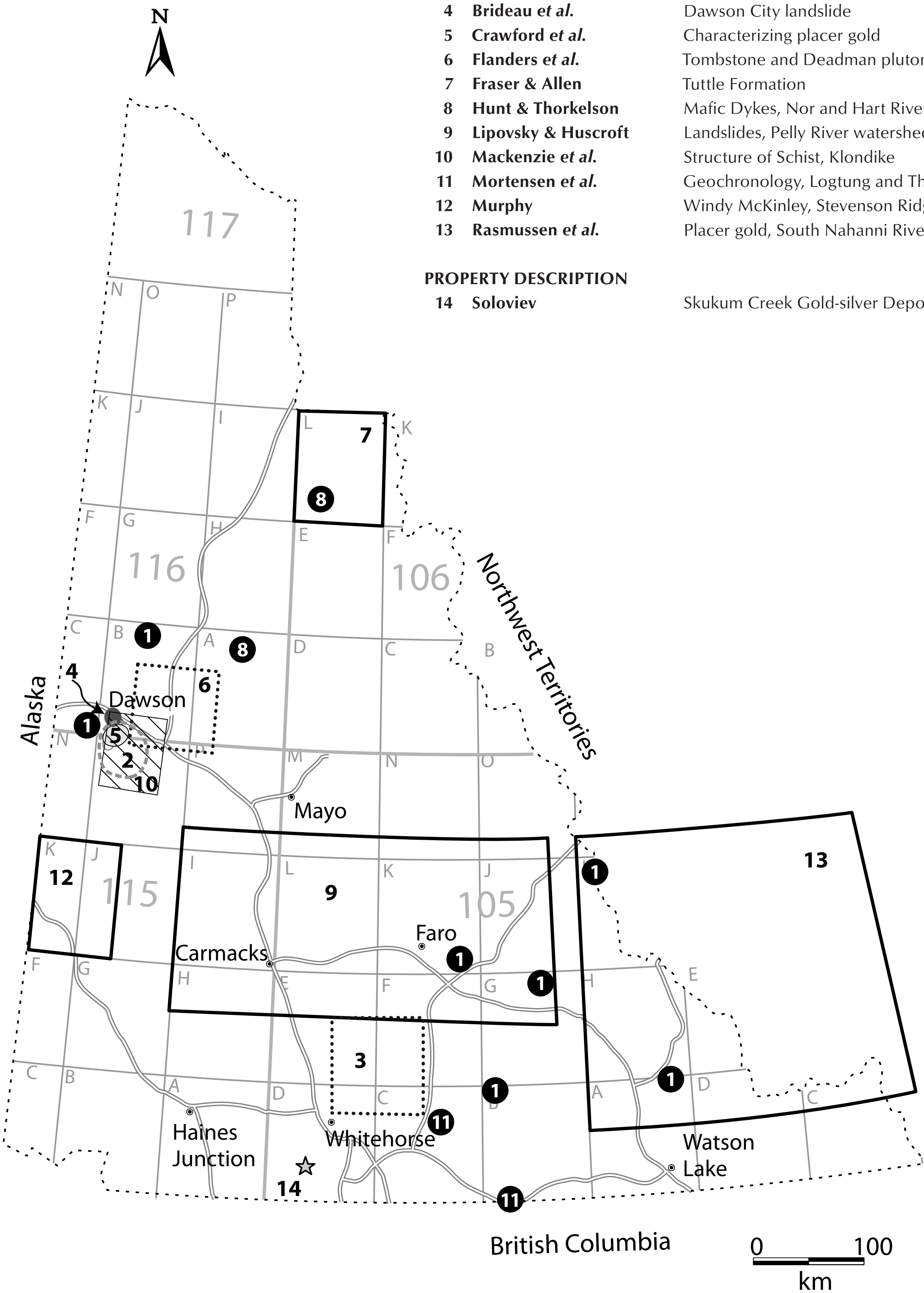

Geoffrey Bradshaw

On July 22, 2006, the Yukon geological community suffered a great loss with the death of Geoff Bradshaw. Geoff joined the Yukon Geological Survey in the fall of 2003 after a number of years working in the private sector on both Yukon and international projects.
He will be well remembered for his enthusiasm, work ethic and his unique ability to bring people together.

ANECDOTE FROM JULY 22, 2006, *by Jeff Bond*

It was a sunny Saturday afternoon. My family and I were fully immersed in the Dawson City Music Festival. For our afternoon entertainment, we chose to take in a workshop entitled, "I've Been Everywhere", featuring a host of musicians, most of whom I hadn't heard of before. We found a pew near the front, and took our seats as the musicians and technical staff prepared for the show. Around 2 p.m., the workshop host, John Samson of the Weakerthans, introduced himself, as well as the other musicians on stage. He opened the workshop with a song that I did not know the title of, but instantly recognized. My friend and co-worker, Geoff Bradshaw, had included the song on a CD compilation that he had given my wife, Leyla. The song had found its way into our car stereo and we had listened to it numerous times over the last several months. Even my five-year-old daughter, Sofia, recognized the tune and looked up at me when she first heard the recognizable sound coming from John's guitar. With big eyes and a smile, she said "Bradshaw". The four of us sat there and enjoyed the song and the feeling of coincidence that came with it.

The following day, we learned Geoff had died in the Wernecke Mountains while on traverse with co-worker and friend, Lara Lewis. An ordinary helicopter pickup had left us reeling in sorrow and disbelief. How could our friend leave us so soon? Since that day, it has been a difficult time for many. Geoff left behind many loved ones including his partner, Zoë, his parents, Jennifer and Gary, his brother, Mike, sister in-law, Jana, and niece, Edelle, many close friends, and of course, his co-workers at the Yukon Geological Survey.

A couple of weeks after Geoff passed away, my wife reminded me where we had been at the time Geoff died. We had been sitting in St. Mary's church listening to John Samson's familiar song. She said the song is entitled "Left and Leaving". The meaning of this song seems open to interpretation, but the more I listen to it, the more I feel that it symbolizes the grief felt by those left behind. Some days seem ordinary enough, but when you least expect it, a moment becomes engraved in your memory. The important part of that day for me is that I can take comfort in knowing that the moment Geoff was leaving us, we were thinking of him ... with smiles on our faces.

We love you Geoff and miss you dearly. Thank you for the good times.

Jean François Pagé

In loving memory of our friend,
Jean François Pagé, a beautiful person
whose spirit will live on.

À la douce mémoire de notre ami
Jean-François Pagé, un homme remarquable
qui restera dans nos cœurs.

Jean François Pagé came north in the late 1990s and found a home in Whitehorse. With a ready smile, a love of adventure and a wide range of interests, J.F. made friends wherever he went, from Nunavut to the Yukon. In 2004, after completing a course at the Chamber of Mines, J.F. began working in mineral exploration with Aurora Geosciences. Starting as a field-hand and working his way up, he staked, cut line, soil sampled, ran geophysics and packed core at a score of projects across the Yukon and northern B.C. He loved the work — the travel, camps, hard days and adventure — and became an experienced field worker, valued wherever he worked. Whether building a sauna, whipping up a great meal from a bland food list or sparking a lively discussion on music or film, J.F. found a way to liven up every camp. He was a real coureur des bois — and he left his mark on the north. He died on the first day of his third season doing what he loved.

Jean François Pagé est arrivé dans le Nord à la fin des années 90 et a établi son domicile à Whitehorse. Toujours souriant, passionné d'aventure et s'intéressant à divers sujets, il s'est fait des amis à tous les endroits qu'il a visités, depuis le Nunavut jusqu'au Yukon. En 2004, il a commencé à travailler dans le domaine de l'exploration minière à Aurora Geosciences après avoir terminé un cours à la Chambre des mines. Il a entrepris sa carrière en tant qu'assistant sur le terrain et a gravi les échelons en posant des jalons, dégageant les tracés de prospection, prenant des échantillons de sol, menant des tests géophysiques et emballant des carottes dans le cadre de divers projets au Yukon et dans le Nord de la Colombie Britannique. Il adorait son travail – les déplacements, les camps, les journées difficiles et l'aventure – et il est devenu un homme de terrain expérimenté dont la présence était appréciée partout où il travaillait. Lorsqu'il construisait un sauna, préparait un excellent repas avec des aliments fades ou entamait une discussion animée concernant la musique ou le cinéma, il trouvait le moyen de rendre la vie de camp plus intéressante. Véritable coureur des bois, il a laissé son empreinte dans le Nord. Il est décédé le premier jour de sa troisième saison en faisant un travail qu'il aimait.

by Mike Power

With a ready smile, a love of adventure and a wide range of interests, J.F. made friends wherever he went, from Nunavut to the Yukon.

Son sourire facile, sa passion pour l'aventure et ses divers intérêts ont permis à Jean-François de se faire des amis partout où il a voyagé, depuis le Nunavut jusqu'au Yukon.

MINERAL INDUSTRY

Yukon Mining, Development and Exploration Overview 2006

Mike Burke, Steve Traynor and Lara L. Lewis
Yukon Geological Survey

Yukon map 2
Abstract 3
Résumé 3
Introduction 4
Mine development 5
Precious metals – gold 7
Precious metals – silver 18
Base metals – zinc 21
Base metals – copper 25
Base metals – nickel ± platinum group elements (PGE) 29
Base metals – tungsten ± molybdenum 30
Base metals – molybdenum 32
Base metals – tin 32
Uranium 33
Gemstones 37
Coal 38
References 40
Appendix 1: 2006 exploration projects 41
Appendix 2: 2006 drilling statistics 46

Yukon Placer Mining and Exploration Overview 2006

William LeBarge
Yukon Geological Survey

Placer mining 49
Placer exploration 51
Aperçu 52

Yukon Mining Incentives Program 2006

Steve Traynor
Yukon Geological Survey

.... 53
Résumé 53

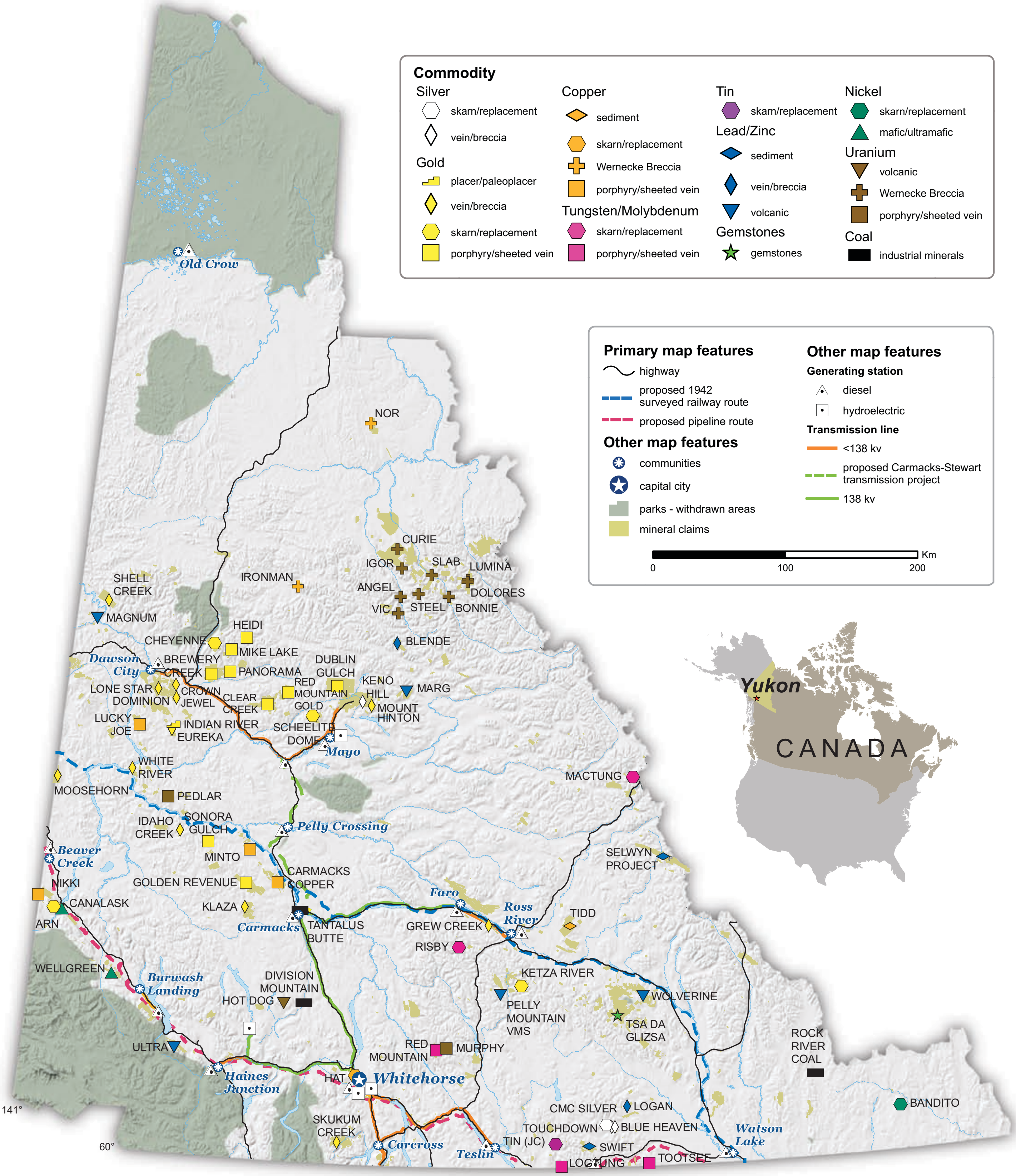

Figure 1. Location map of advanced (>$100 000 expenditures) exploration projects in Yukon, 2006.

Yukon Mining, Development and Exploration Overview 2006

Mike Burke*[1]*, Steve Traynor and Lara L. Lewis
Yukon Geological Survey

Burke, M., Traynor, S. and Lewis, L.L., 2007. Yukon Mining, Development and Exploration Overview 2006. *In:* Yukon Exploration and Geology 2006, D.S. Emond, L.L. Lewis and L.H. Weston (eds.), Yukon Geological Survey, p. 2-47.

ABSTRACT

Mineral exploration in Yukon has reached record levels with over $80 million spent on the search for base and precious metals, coal, gemstones and uranium in 2006. Exploration for gold attracted the largest share of the exploration dollars, capturing 35%, followed by zinc at 22%, uranium 15%, copper 12%, silver 7%, tungsten and molybdenum 6%, and the remainder being spent on coal and gemstones.

Mine development expenditures have also increased dramatically with an estimated $50 million being spent on the Minto mine, which is scheduled to be in production in the second quarter of 2007. The total development costs at Minto, including a 50% mill expansion in the first year of mining, are estimated to be $107 million.

Exploration activity at all levels in Yukon, from grassroots stages to advanced exploration, has experienced a dramatic increase. A total of 70 of the approximately 150 exploration projects in Yukon had expenditures of greater than $100 000, with 21 of these projects spending more than $1 million. The largest program was the Selwyn project, where drilling continued into December, with expenditures of over $12 million, confirming and expanding the huge zinc resources at Howards Pass (Selwyn Project).

RÉSUMÉ

L'exploration minière au Yukon a atteint des niveaux records avec plus de 80 millions $ consacrés en 2006 à la recherche de métaux communs et précieux, de charbon, de pierres précieuses et d'uranium. La prospection axée sur l'or a attiré la plus grande part des budgets, soit 35 %, suivie par le zinc (22 %), l'uranium (15 %), le cuivre (12 %), l'argent (7 %), le tungstène et le molybdène (6 %), le charbon et les pierres précieuses se partageant le reste.

Les dépenses consacrées aux développements miniers ont également augmenté de façon spectaculaire. Près de 50 millions $ ont ainsi été dépensés pour la mine de cuivre et d'or de Minto qui devrait entrer dans sa phase de production au second trimestre de 2007. Le total des dépenses pour la mine de Minto, y compris le coût de l'expansion de 50 % du malaxeur au cours de la première année, est estimé à 107 millions $.

Au Yukon, les activités d'exploration à tous les niveaux, de la phase initiale aux étapes avancées, s'intensifient de manière remarquable. Au total, 70 des 150 projets d'exploration mis en œuvre au Yukon s'accompagnent de dépenses supérieures à 100 000 $, et 21 de ces projets affichent des coûts dépassant le million de dollars. Le programme le plus important est le projet Selwyn, pour lequel les forages ont continué jusqu'en décembre et les dépenses dépassent maintenant 12 millions $. Le projet confirme la présence d'énormes réserves de zinc et de plomb à Howards Pass (le projet Selwyn).

[1]*mike.burke@gov.yk.ca*

INTRODUCTION

Mineral exploration expenditures in Yukon experienced a significant increase for the fifth consecutive year, rising to an estimated $80 million, a huge increase over the low of $7.4 million spent on exploration in 2001 (Figs. 1 and 2). In addition to the increase in mineral exploration, an estimated $50 million was spent on mine development, all at Sherwood Copper Corporation's Minto (copper-gold-silver) mine. Construction at the mine was on schedule at year-end, and production is slated for the second quarter of 2007. Yukon Zinc Corporation completed a bankable feasibility study on the Wolverine (zinc-silver-lead-copper-gold) deposit in May, 2006 and proceeded with an optimization study during the year. A quartz mining license was issued for the Wolverine project; upon completion of the optimization of the feasibility study and the securing of project financing, the company expects to make a production decision in 2007. Cash Minerals Ltd. completed a feasibility study on their Division Mountain (coal) project. While the feasibility study concluded that current conditions did not support the development of a mine to serve the export market, it did prove technically and economically feasible to develop an open-pit mine, and the product sold to a potential 50-megawatt mine-mouth power station.

A significant amount of claim staking took place in 2006, with a total of 14 034 claims staked during the season (Fig. 3), which increased the number of claims in good standing to 57 968 by the end of the year (Fig. 4).

The Yukon government continued to support the mineral industry in several areas including: 1) the Yukon Mining Incentives Program, which offered approximately $880 000 to 53 successful applicants (Traynor, this volume); and 2) the Yukon Mineral Exploration Tax Credit, which offers a refundable corporate and personal income-tax credit of 25% of eligible mineral exploration expenditures incurred by qualified individuals and corporations conducting off-minesite exploration in the Yukon between April 1, 2004 and March 31, 2007. Control over the Territory's natural resources was transferred from Canada to the Yukon government in 2003. Decisions regarding oil and gas, mining, lands, forests and water are now made by the Yukon government. Internally, the government has initiated an Integrated Resource Management Strategy. This strategy streamlines the review process by addressing policies and legislation gaps, and it establishes better collaboration between government departments. An example of this strategy is the Project Management Process that assists mining companies in their efforts to secure permits for development proposals. Project coordinators are assigned to individual projects to assist with the reviews and timely resolution of issues. The project coordinators report to a team of deputy ministers that is responsible for regulatory approvals. This committee is chaired by the Department of Energy, Mines and Resources. Currently, six Yukon projects have been assigned project coordinators: Yukon Zinc Corporation's Wolverine (zinc-silver-lead-copper-gold), Cash Minerals Ltd.'s Division Mountain coal, Western Copper Corporation's Carmacks Copper (copper-gold), Tintina Mines Ltd.'s Red Mountain (molybdenum)

Figure 2. *Exploration expenditures in Yukon, 1971 to 2006.*

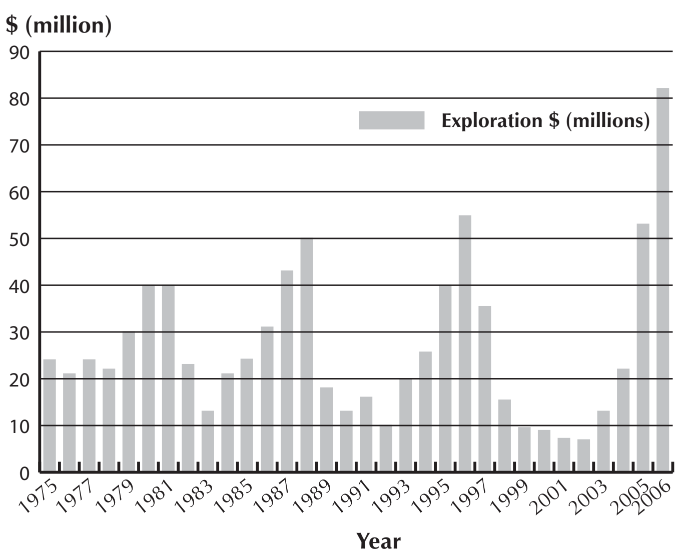

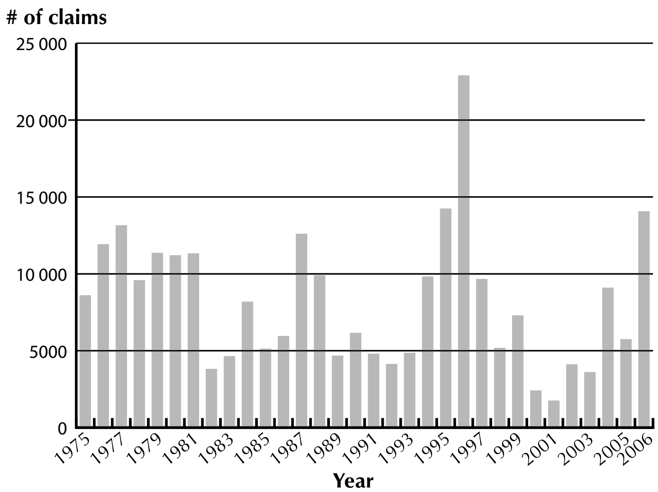

Figure 3. *Mineral claims staked, 1975–2006.*

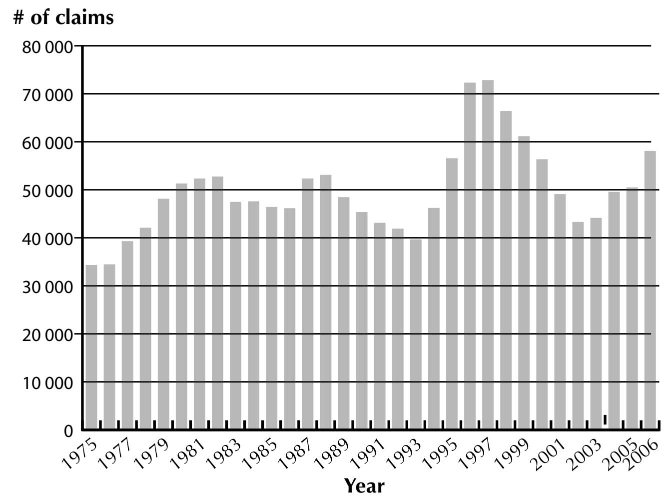

Figure 4. *Mineral claims in good standing, 1975–2006.*

deposit, YGC Resource's Ketza River (gold) and Tagish Lake Gold Corp's Skukum Creek (gold-silver) project.

The Government of Yukon also maintained current levels of funding for geoscience projects, under the auspices of the Yukon Geological Survey. In addition, 11 of 13 Yukon First Nations have ratified their land claim agreements.

All of the Yukon mineral occurrences and properties mentioned in this report are documented in detail in the Yukon MINFILE (Deklerk and Traynor, 2005), which can also be accessed online (*www.geology.gov.yk.ca*).

Exploration results for many of the projects were still pending when this report went to press. The reader is encouraged to visit company websites for the most recent results.

MINE DEVELOPMENT

Figure 5. *Pre-stripping of the Minto copper-gold-silver deposit, July, 2006.*

Sherwood Copper Corporation (*www.sherwoodcopper.com*) began development of the open-pit **Minto** (copper-gold-silver) mine in 2006 (Fig. 5). Production from the deposit is scheduled to begin in the second quarter of 2007. The deposit is a magmatic-hydrothermal copper-gold deposit hosted in foliated zones within granodiorite of the Jurassic Klotassin Batholith. The deposit bears similarities to porphyry and iron oxide-copper-gold deposits, but the origin of the deposit is still subject to debate (Fig. 6).

The deposit has Measured and Indicated reserves of 9.06 Mt grading

Figure 6. *High-grade chalcopyrite-bornite mineralization from the Minto deposit.*

1.78% Cu, 0.62 g/t Au and 7.3 g/t Ag at a 0.5% Cu cut-off grade, and contains a high-grade core of 4.03 Mt grading 2.82% Cu, 1.02 g/t Au and 11.6 g/t Ag at a 1.5% Cu cut-off. The feasibility study indicates the head grades will average 3.3% Cu and 0.94 g/t Au in the first year, and 2.4% Cu and 0.88 g/t Au in the first six years of operation. Production will average 41 million pounds (19 million kg) copper, 17,295 ounces (490 300 g) gold and 250,000 ounces (7 087 000 g) silver in the first six years of operation, at a cash cost of US$0.57 net of byproduct credits. Financing for completion of the construction of the mine was provided by a debt package with Macquarie Bank Ltd., totaling C$85 million. The project has a very attractive Net Present Value of C$173.4 million at a 7.5% discount rate pre-tax and an internal rate of return of 53.2%. The company continues to optimize the feasibility study and expects that several modifications, such as tying in to the proposed expansion of the Yukon power grid, will lead to further improvements to the project.

The Minto project has had great success in exploration on the mine property. Several areas have had historical (1970s) drill intersections with significant copper grades that had not previously received any follow-up. Geophysics in these areas has helped to refine and expand the exploration targets on the property. Sherwood concentrated their drilling efforts mainly on one of these targets just south (130 m) of the planned open pit called Area 2. The company drilled 79 holes in the target area intersecting mineralization that appears to be an extension of the main Minto deposit. The drilling intersected a similar thickness of mineralized rock to the Minto deposit, including high-grade bornite-rich mineralization that was assayed at 5.1% Cu, 2.6 g/t Au over 8.1 m within a 13.4-m interval grading 3.4% Cu, 1.7 g/t Au in hole 06SWC-146. Sherwood has engaged SRK Consulting to conduct an independent pre-feasibility study on the Area 2 mineralization. Many more compelling exploration targets exist on the property and the potential to extend the mine life is excellent.

PRECIOUS METALS – GOLD

Epigenetic gold mineralization is recognized in several different settings within Yukon. These consist of intrusion-related gold, associated with mid-Cretaceous plutonism; orogenic gold, related to Jurassic and Eocene events; epithermal gold, related to late Cretaceous to Eocene sub-aerial volcanism; and gold skarns, related to Cretaceous oxidized and reduced intrusions. Exploration for intrusion-related gold occurred mainly within the western portion of the Tintina Gold Belt between Dawson and Mayo, where accessibility is greatest, and also in the Dawson Range in central Yukon, north of Carmacks, an area well known for its placer-gold and copper-porphyry potential.

SKARN/REPLACEMENT

YGC Resources Ltd. (*www.ygcr.ca*) conducted the largest exploration program for gold on the **Ketza River** gold property (Yukon MINFILE 105F 019), where diamond drilling occurs year-round (Fig. 7). Mineralization at Ketza consists of massive, pyrrhotite-pyrite manto deposits hosted in Lower Cambrian limestone (Fig. 8), as well as quartz-pyrrhotite-pyrite veins hosted in Lower Cambrian argillite, which stratigraphically underlie the limestone unit. Oxidized mantos mined at the Ketza River deposit between 1988 and 2000 produced approximately 3.1 million grams of gold. YGC Resources Ltd. is concentrating on increasing the sulphide mineral resources on the property. A 43-101-compliant[1] resource for the property was completed in November, 2005 (see Table 1).

Table 1. *Sulphide resources at the Ketza River property (43-101-compliant).*

Classification	Tonnes (t)	Gold (g/t)	Contained ounces	Cut-off grade
Measured	1 410 000	3.54	160,500	1.0 g/t
Indicated	7 130 000	2.60	596,200	1.0 g/t
Inferred	14 580 000	2.25	1,054,000	1.0 g/t

Figure 7. *Winter drilling at the Ketza River gold property of YGC Resources.*

[1]*Note that where this standard is mentioned, it refers to Canadian Securities Administrators (2001).*

Figure 8. *Massive pyrrhotite-pyrite mineralization in drill core from the Calcite zone, a new discovery at Ketza River.*

In 2006, YGC Resources completed 34 663 m in 271 diamond drill holes on the property, expanding the existing resources and testing previously undrilled areas. New discoveries were made. The results of this year's drilling will be used to update the existing resource and complete the pre-feasibility study that was initiated in 2006. The company is planning on making a production decision in 2007.

Dynamite Resources Ltd. (*www.dynamiteresources.com*) completed a program on the **Mike Lake** property (Yukon MINFILE 116A 012) that included 2250 m of diamond drilling in 17 holes (Fig. 9). The bulk of the drilling was directed at the North Vein zone, a skarn horizon developed within calcareous sedimentary rocks adjacent to a Cretaceous Tombstone Suite intrusion. Intersections up to 17.23 m of 3.48 g/t Au were encountered in the drilling. Drilling also tested additional geochemical and geophysical targets on the property.

Figure 9. *Helicopter-supported drilling at the Mike Lake project of Dynamite Resources***.**

Logan Resources Ltd. (*www.loganresources.ca*) conducted a program of VLF/EM surveying and prospecting confirming previous results from known showings on the **Cheyanne** (Yukon MINFILE 116B 001, 094, 096) property, in addition to re-sampling the Golden Wall showing (discovered in 2005). The Golden Wall showing consists of pyrrhotite-pyrite skarn hosted in calcareous sedimentary rocks adjacent to a Cretaceous Tombstone Suite intrusion. Grab samples from the Golden Wall assayed up to 5.04 g/t Au.

Logan Resources Ltd. conducted a drilling program late in the season on the **Heidi** (Yukon MINFILE 116A 037) property. Skarn mineralization in calcareous sedimentary rocks was targeted and two drill holes (427 m) were

Figure 10. Late-season drilling on the Heidi gold property of Logan Resources.

completed before winter conditions suspended the program (Fig. 10). Drill results were not available by year-end.

ATAC Resources (*www.atacresources.com*) optioned their **Arn** (Yukon MINFILE 115F 048) property to a private company. The Arn property covers a number of gold skarn occurrences that have returned values up to 11.92 g/t Au and 0.18% Cu over 12.67 m in previous drilling. The company completed a program of line-cutting and geophysics (IP and magnetic surveys) in 2006.

PORPHYRY/SHEETED VEIN

Intrusion-related gold targets related to the mid-Cretaceous Tombstone Suite that forms a part of the Tintina Gold Belt were explored mainly in the Dawson-Mayo area.

The **Dublin Gulch** (Yukon MINFILE 106D 025) property of StrataGold Corporation (*www.stratagold.com*) hosts Indicated resources in the Eagle Zone of 66.54 Mt grading 0.916 g/t Au and an additional 14.39 Mt grading 0.803 g/t Au in the Inferred category, calculated prior to the 2006 drilling program. Mineralization in the Eagle Zone consists of gold in sheeted quartz veins, shears and fractures within a Cretaceous Tombstone Suite granodiorite intrusion (Fig. 11).

Figure 11. Craig Hart examining sheeted quartz veins at the Dublin Gulch gold deposit.

Drilling targeted the Eagle Zone at depth and the Steiner Zone that is located to the north of the Eagle Zone. Drilling at the Eagle Zone had previously tested to a maximum depth of 250 m, while drilling in 2006 intersected mineralization grading up to 0.910 g/t Au over a true width of 26.75 m approximately 180 m below the maximum depth of previous drilling. A mineralized zone, located 130 m north of the Eagle Zone, that had no previous intersected mineralization assayed up to 1.037 g/t Au over a true thickness of 28.18 m. Drilling on the Steiner Zone, located 700 m northwest of the Eagle Zone, intersected sheeted quartz-sulphide veins in granodiorite with up to 22.14 m averaging 1.106 g/t Au and 35.73 m averaging 0.835 g/t Au. StrataGold also conducted a small exploration program on its Clear Creek (Yukon MINFILE 115P 023) property that hosts numerous intrusive-related gold targets.

Alexco Resource Corp. (*www.alexcoresource.com*) conducted a 9-hole, 1184-m drill program at the **Brewery Creek** (Yukon MINFILE 116B 160) property. The program, managed by NovaGold Resources (19% equity shareholder of Alexco Resources), focused on similarities that the NovaGold exploration team has identified with their Donlin Creek deposit in Alaska. Similar to Donlin Creek, Brewery Creek is related to a series of high-level porphyritic dykes and sills that intrude fine-grained sedimentary rocks, including carbonaceous shale, siltstone and sandstone. Disseminated arsenopyrite and stibnite, and illite and clay alteration is characteristic of both deposits (Fig. 12). Drilling at the Bohemian zone intersected several high-grade intervals including DDH BC06-126, which intersected 9.01 g/t Au over 13.74 m, including 14.47 g/t Au over 7.9 m. The Classic Zone, a potentially large low-grade oxide resource, was also successfully tested in the drill program and had intersections such as 0.99 g/t Au over 19.88 m.

The **Klondike** property (Yukon MINFILE 116A 027) of Alexco Resources is located approximately 30 km east of the Brewery Creek project. Alexco completed a small

Figure 12. *Siliceous quartz monzonite from the Bohemian zone at Brewery Creek. The core in this interval assayed 4.16 g/t Au.*

Figure 13. *Rock sampling on the Harlan property of Alexco Resources.*

program of geological mapping and sampling on the property in 2006. The property hosts gold mineralization associated with Cretaceous Tombstone Suite altered intrusive dykes and sills, hosted by siltstone, calcareous siltstone, and chert of the Ordivician to Lower Devonian Road River Group.

Alexco Resources also conducted a small program of geological mapping, sampling (Fig. 13) and geophysical surveys on the **Harlan** property (Yukon MINFILE 105O 051), located 150 km north of Ross River. Intense alteration and silicification at Harlan is associated with quartz veining in calcareous chert-pebble conglomerate, greywacke, siltstone, and shale of the Devonian to Mississippian Earn Group, as well as with altered Cretaceous Tombstone Suite quartz monzonite dykes and sills. The property remains untested by drilling.

Atac Resources optioned their **Panorama** (Yukon MINFILE 116A 031) property to a private company. Panorama is located approximately 15 km northeast of Brewery Creek and encompasses a small Tombstone Suite granodiorite pluton. The company conducted a program of airborne and ground geophysical surveys (VTEM and IP) on the property this year.

Regent Ventures Ltd. (*www.regentventuresltd.com*) carried out diamond drilling on their **Red Mountain** Project (Yukon MINFILE 115P 006). Two areas of gold

Figure 14. *Versatile Time-Domain ElectroMagnetic (VTEM) surveying of the Red Mountain gold project of Regent Ventures.*

mineralization were tested, the 50/50 fault zone and the Saddle Zone. The 50/50 zone is a marked by a prominent surface linear with a coincident gold-silver-zinc-copper soil geochemical anomaly. Drilling intersected up to 1.8 m of 0.25 g/t Au, 43.2 g/t Ag and 1.44% Zn. Drilling in the Saddle Zone delineated a swarm of Tombstone Suite intrusive dykes with up to 6.1 m of 0.86 g/t Au. The company also flew the property with an airborne geophysical survey utilizing the VTEM (Versatile Time-Domain ElectroMagnetics) system (Fig. 14).

International Gold Resources Ltd. (*www.intlgold.com*) flew the **Mahtin** (Yukon MINFILE 115P 007) property with a VTEM survey. The Mahtin property has extensive gold-arsenic-antimony-bismuth geochemical anomalies on the claims that cover the mid-Cretaceous Sprague Creek intrusion and adjacent calcareous siltstone. The property remains untested by drilling.

Curlew Lake Resources (*www.curlew-lake.com*) conducted a program of geochemistry and geophysics (magnetic surveys) on their **Typhoon** (Yukon MINFILE 115P 060) property in the Clear Creek area. The company had planned a drilling program in the fall, but was unable to secure a drill to complete the proposed program. Geophysics and geochemistry suggest the property is underlain by an intrusion.

Copper Ridge Exploration (*www.copper-ridge.com*) performed an exploration program on their extensive **Scheelite Dome** (Yukon MINFILE 115P 004) property. The work program consisted of additional soil sampling, induced polarization (IP), magnetic and VLF-EM (very low-frequency-electromagnetic) geophysical surveying on 21 km of grid, plus 1430 m of mechanical trenching. The work focused on a previously untested gold-arsenic-bismuth-antimony soil anomaly, the Toby zone. A new zone of gold-bearing quartz-arsenopyrite veins were discovered in the trenching program. Assays of up to 14.9 g/t Au in grab samples, and up to 4.2 g/t Au over a 2.0-m continuous chip sample, were obtained from the trenches. The Scheelite Dome property covers numerous intrusive-related gold targets within a 10-km coincident gold-arsenic-bismuth-antimony soil geochemical anomaly. The Toby zone is located at the southwestern extent of the extensive anomaly.

The Dawson Range in west-central Yukon is underlain by Early Mississippian and older metamorphic rocks of the Yukon-Tanana Terrane intruded by several plutonic suites that range in age from Early Jurassic to Early Tertiary. The area is host to numerous styles of magmatic-hydrothermal mineralization related to the various intrusive events. Porphyry gold ± copper, molybdenum and associated styles of epigenetic mineralization are found throughout the Dawson Range including the enigmatic Minto copper-gold-silver deposit of Sherwood Copper Corporation that is currently under development.

Northern Freegold Resources (*www.northernfreegold.com*) successfully assembled a large land package (166 km^2) in the Dawson Range. The package encompasses numerous mineral occurrences and the entire package is referred to as the **Freegold Mountain** project. The property hosts various styles of mineralization including porphyry, skarn and veins. The acquisition of the land package will allow the company to evaluate the entire mineralization system. The main focus of Northern Freegold's effort this year was to acquire and compile the large amount of historical data that exists on the property, prospecting and sampling, geological mapping, differential GPS mapping, airborne geophysical surveys (VTEM) and diamond and Rotary Air Blast (RAB) drilling. The property hosts a 43-101-compliant Inferred resource, in five zones, of 14 455 800 tonnes at 1.51 g/t Au. The diamond drilling concentrated on the Golden Revenue (Yukon MINFILE 115I 042) property (Fig. 15) optioned from Atac Resources (*www.atacresources.com*). Mineralization at the Golden Revenue zone is associated with quartz-feldspar porphyry dykes, and typically consists of pyrite with minor chalcopyrite and/or arsenopyrite occurring on hairline fractures, or is disseminated in the dykes, in narrow quartz veinlets and breccia zones in the dykes, and adjacent metasedimentary and metavolcanic rocks. Only partial results from the laboratory had been received by year-end. The first 5

Figure 15. *Diamond drilling on the Golden Revenue deposit. Mechanic Creek, an active placer mining creek, is visible (top right) below the deposit.*

Figure 16. *Visible gold in drill core from the Golden Revenue deposit.*

of 26 drill holes returned values up to 19.81 m of 1.74 g/t Au and 27.01 m of 1.02 g/t Au. Visible gold was also noted in the drilling (Fig. 16).

Firestone Ventures Inc. (*www.firestoneventures.com*) conducted an exploration program consisting of geological mapping, prospecting, geochemistry and geophysics, followed by diamond drilling of 1821 m in 12 holes on the **Sonora Gulch** (Yukon MINFILE 115J 008) property in the Dawson Range. The exploration program defined five new gold ± copper and molybdenum targets within the larger K-467 zone that were subsequently tested by the drilling campaign. Strongly clay-altered, silicified and sulphidized (pyrite plus additional unidentified sulphide minerals; Fig. 17) intrusive rocks, shear-hosted mineralized quartz veins, and quartz stockwork were some of the styles of mineralization intersected in the various zones. The drilling encountered significant gold-silver intersections in four of the five zones. The Amadeus zone had the most significant result, with hole SG-06-06 intersecting 153 m of 6.21 g/t Au and 3.0 g/t Ag, including 5.0 m of 12.19 g/t Au and 4.8 g/t Ag. This new discovery has greatly enhanced the potential of the property.

Figure 17. *Silicified and sulphidized quartz-feldspar porphyry from the Sonora Gulch property.*

VEIN/BRECCIA

The road-accessible **Skukum Creek** gold-silver (Yukon MINFILE 105D 022) deposit of Tagish Lake Gold Corp. (*www.tagishgold.com*) is located 80 km southwest of Whitehorse (Fig. 18). Tagish Lake also owns two other deposits in the area, Mt. Skukum and Goddell Gully (Yukon MINFILE 105D 158 and 025), but is focused on bringing the Skukum Creek deposit into production. The Skukum Creek deposit is a polymetallic vein deposit containing structurally controlled mineralization within northeast-trending faults and shear zones (Soloviev, this volume). The company extended the underground workings at Skukum Creek by 300 m, and conducted a 6500-m underground drilling program designed to upgrade and expand the resources at the deposit as part of the ongoing feasibility study. Drilling returned numerous high-grade gold-silver intersections that will upgrade and expand the known resource of 800 000 tonnes of 6.78 g/t Au and 248 g/t Ag (Measured and Indicated), plus 90 000 tonnes of 6.53 g/t Au and 225 g/t Ag (Inferred) in the Rainbow, Kuhn and Ridge zones. The drilling also resulted in a new discovery called the Berg zone. In addition to the exploration, the company continued with environmental and metallurgical studies for the ongoing feasibility study. Metallurgical testwork resulted in a significant increase in overall silver recoveries to 77% and gold to 85.5%. Improvements to silver and gold recoveries have allowed the company to lower the cut-off grade for the deposit to 4 g/t Au equivalent from the pre-feasibility study that used a 5 g/t Au equivalent cut-off. This will result in an increase in the contained gold and silver in the resource. The company plans on completing the feasibility study and making a production decision in 2007.

Figure 18. *The Skukum Creek gold-silver deposit.*

Klondike Star Mineral Corporation (*www.klondikestar.com*) continued to work on their extensive mineral exploration properties, totaling approximately 370 km^2, south of Dawson City in the historical Klondike placer mining district. Klondike Star's claims cover numerous mineral occurrences in the district. The company added to their landholdings in the district by optioning the DOM claims from KSL (Yukon) Exploration and the King Solomon Dome (Yukon MINFILE 115O 068) property from J.A.E. Resources. The company conducted geological mapping, geochemistry, geophysics (IP) and trenching on a number of properties, and diamond drilling on the **Lone Star**

Figure 19. *Diamond drilling on the Lone Star property in the Klondike.*

(Fig. 19) and **Buckland** properties (Yukon MINFILE 115O 072, 077). Gold at the properties occurs with disseminated pyrite, and locally is associated with narrow discordant quartz veins. The mineralized zones are associated with quartz-carbonate-pyrite alteration and are hosted by felsic metavolcanic schist. The mineralized horizon at Lone Star trends northwest and dips gently to the northeast. Drilling at the Buckland zone returned values up to 98.7 g/t Au over 0.90 m. Drilling on the Lone Star continued to expand the zone, intersecting wide intervals of low-grade mineralization that include short intervals of higher grade mineralization, such as 32 m grading 0.40 g/t Au, including 1.0 m of 6.61 g/t Au in hole 06LS-04.

Strategic Metals Ltd. (*www.strategicmetalsltd.com*) conducted a program of excavator trenching and reverse circulation drilling on their **Eureka** (Yukon MINFILE 115O 057) property. Previous work has identified gold-bearing vein and breccia zones in this area that are in an area characterized by very rich placer creeks. Results were not available at year-end.

International Gold Resources Inc. *(www.intlgold.com)* performed geochemical sampling on their **Crown Jewel** and **Bonanza** claims (Yukon MINFILE 115O 139, 080) in the Klondike placer mining district. Previous work has identified gold-quartz veins, while the current work was directed at obtaining high-quality geochemical samples through the use of soil augers.

Yukon Gold Corporation (*www.yukongoldcorp.com*) conducted a program of geological mapping, geochemical sampling and road building on the **Mt. Hinton** gold-silver (Yukon MINFILE 105M 072) property near Keno Hill. Quartz-sulphide veins are numerous on Mt. Hinton and have returned some spectacular results, with individual specimens assaying up to 693 g/t Au and 8959 g/t Ag. A program of reverse-circulation drilling on the property was cancelled due to the mechanical failure of the drill.

Figure 20. *High-grade gold-silver bearing quartz-pyrite-galena vein from the Hartless Joe property.*

Mountain Rio Resources, a private exploration company, explored the **Moosehorn** (Yukon MINFILE 115N 024) property with geological mapping, sampling and diamond drilling. The company completed approximately 2250 m of diamond drilling in 24 holes, testing the extent of the gold-bearing veins. High-grade auriferous quartz veins on the Moosehorn property have been subjected to small-scale historical open-cut mining. Auriferous quartz veins in granodiorite occur mainly along northwest-trending joints, with shallow easterly dips (20° to 40°). The veins host two types of gold mineralization: (1) micron gold within sulphide minerals; and (2) visible blebs of free gold up to 1-2 mm in width.

New Shoshoni Ventures Ltd. (*www.newshoshoni.com*) optioned the **Hartless Joe** (Fig. 20; Yukon MINFILE 105 203) and **Byng** (Yukon MINFILE 105 184) properties from ATAC Resources. The properties,

Figure 21. *The gentle slope in the foreground, located on the Horn property, contains gold-in-soil anomalies of up to 1060 ppb.*

located approximately 40 km northeast of Whitehorse, host high-grade epithermal gold-silver veins in Middle Triassic Joe Mountain volcanic rocks. The company performed an airborne VTEM geophysical survey and follow-up prospecting on the claims. Prospecting confirmed earlier high-grade results and float samples assayed up to 29.97 g/t Au and 9487 g/t Ag.

In the Upper Hyland River area in eastern Yukon, Ryanwood Exploration conducted soil geochemistry and magnetic surveys over the **Horn** (NTS 105H/15) claims (Fig. 21). The claims are the northernmost in a 50-km belt of gold properties. Work by Hart and Lewis (2006) suggests that auriferous quartz veins in the belt have characteristics similar to orogenic gold veins, and thus potentially relate to regional metamorphism and large structural features. Soil sampling outlined an area over 1 km^2 with gold-in-soil anomalies up to 1060 ppb.

Northern Freegold Resources' large **Freegold Mountain** property encompasses numerous mineralized occurrences including the Goldstar (Yukon MINFILE 115I 053), Rage and Seymour (Yukon MINFILE 115I 121) zones. The company sampled mineralized veins and dykes that range from trace values to 3.7 g/t Au and 13.7% Cu (2006 grab samples). Central to these zones is the Stoddart (Yukon MINFILE 115I 121) porphyry, which has similar characteristics to the Nucleus zone, yet remains untested by drilling. The company also conducted geological mapping, sampling and core re-logging on the Tinta Hill (Yukon MINFILE 115I 058) property, where a polymetallic vein occupies a shear zone cutting a Jurassic quartz diorite (Fig. 22).

Figure 22. *Historical drill core, properly preserved and undisturbed from the Tinta Hill property of Northern Freegold Resources.*

Bannockburn Resources Limited optioned the Klaza (Yukon MINFILE 115I 067) property from ATAC Resources and completed a program of line-cutting and ground-based geophysics (IP). At Klaza, polymetallic gold-silver veins cut the Cretaceous Dawson Range Batholith. Previous drilling has intersected mineralization assayed at up to 6.27 g/t Au and 15.1 g/t Ag over 8.9 m.

Klondike Silver Corp. (*www.klondikesilver.com*) optioned the ***Idaho Creek*** (Yukon MINFILE 115J 099) property from ATAC Resources and completed a program of ground geophysics (IP) and reverse circulation drilling. The property covers an area of poor exposure that has a large multi-element soil geochemical anomaly. Previous work has identified different styles of mineralization including manganiferous quartz veins, consisting of limonite boxwork with minor pyrite, arsenopyrite, galena and sphalerite. The veins occur in altered shear zones cutting mid-Cretaceous granitic rocks. Specimens of vein material assayed up to 15 g/t Au and 1389 g/t Ag.

PRECIOUS METALS – SILVER

Exploration for silver has increased significantly in Yukon and is led by the renewal of exploration in the Keno Hill mining district. Keno Hill is known as being the second largest silver producer in Canada. Between 1941 and 1989, the district produced more than 217 million ounces of Ag (5.37 million tons) that included average grades of 1389 g/t (40.52 oz/ton) Ag, 5.62% Pb and 3.14% Zn. In southern Yukon, numerous occurrences of silver veins in the Rancheria district have produced grades similar to those in the Keno Hill district. Veins in the Rancheria district, however, only have a small production history. Some of the veins in the Rancheria district were high-graded and ore was shipped to southern smelters. Current exploration in both districts is focused on increasing known resources to support production. Exploration for silver has also increased in the Ketza River area and the Dawson Range, which are previously known silver districts.

VEIN/BRECCIA

Alexco Resources Corp. (*www.alexcoresource.com*) conducted a comprehensive exploration program in the Keno Hill mining district (Yukon MINFILE 105M 001) in central Yukon. The district consists of 14 980 hectares of mining leases, quartz claims and crown grants. The lands controlled by Alexco have numerous occurrences of mineral deposits and prospects, including 35 mines with a history of production. The 2006 program culminated with over 11 000 m of diamond drilling in 42 holes. Drilling was conducted in the areas of the historical Silver King, Bellekeno, Husky, Husky Southwest, Lucky Queen, Shamrock and Ruby mines. A new discovery was made in the Silver King East area that is approximately 600 m from the Silver King mine. This discovery at the western end (Fig. 23) of the Keno Hill mining district is characterized by a silver-dominated and gold-bearing disseminated and vein-related mineralized system that is depleted in base metals. The mineralization is hosted in argillically altered greenstone and has high-grade vein mineralization within wide, lower grade stockwork zones. Partial results were returned by year-end and included hole K06-13 which intersected 15.2 m grading 978.6 g/t Ag, 1.37 g/t Au, 0.31% Pb, 0.66% Zn, including a 3.1-m interval that returned 4478.1 g/t Ag, 3.47 g/t Au, 1.12% Pb and 1.83% Zn. The discovery in the Silver King East area is characteristic of a high-level epithermal system and has significant implications for future exploration and potential production for the western end of the Keno Hill mining district. In the eastern end of the district, more typical galena-dominated, vein-fault mineralization was intersected in drilling. Partial

Figure 23. *View of the new exploration camp (centre) and the headframes of the Husky mine at the western end of the Keno Hill silver camp.*

results from the Bellekeno mine (Fig. 24) included assay values from intersections such as in hole K06-11 which contained 2.0 m grading 4628.5 g/t Ag, 63.39% Pb and 7.54% Zn. The Bellekeno mine has a historical (non 43-101 compliant) Measured and Indicated resource of 229 813 tonnes grading 1251 g/t Ag, 0.34 g/t Au, 12.4% Pb, 7.1% Zn, plus an Inferred resource of 34 427 tonnes grading 789 g/t Ag, 0.34 g/t Au, 6.0% Pb, 4.0% Zn. The resource is being upgraded to 43-101 standards. The exploration in 2006 targeted the along-strike and down-dip mineralization from the historically reported resource. Alexco's exploration target at Bellekeno is to develop a 20-million-ounce silver resource.

Approximately 30 km northeast of the Keno Hill mining district, CMC Metals Ltd., (*www.cmcmetals.ca*) acquired an option on the **Clarke-Cameron** properties (Yukon MINFILE 106D 11 and 12). The properties host a non-43-101-compliant resource of 327 373 tonnes grading 254.79 g/t Ag, 4.6% Zn and 5.6% Pb in vein and manto styles of deposits. The company performed an airborne geophysical survey in an effort to trace the dominant mineralized structure between the two adjacent properties.

In the Rancheria District in southern Yukon, CMC Metals explored the **CMC** silver property (formerly Silver Hart property; Yukon MINFILE 105B 21) and conducted geological and geochemical surveys, as well as diamond drilling. In addition to the exploration work, environmental studies were initiated, resulting in the

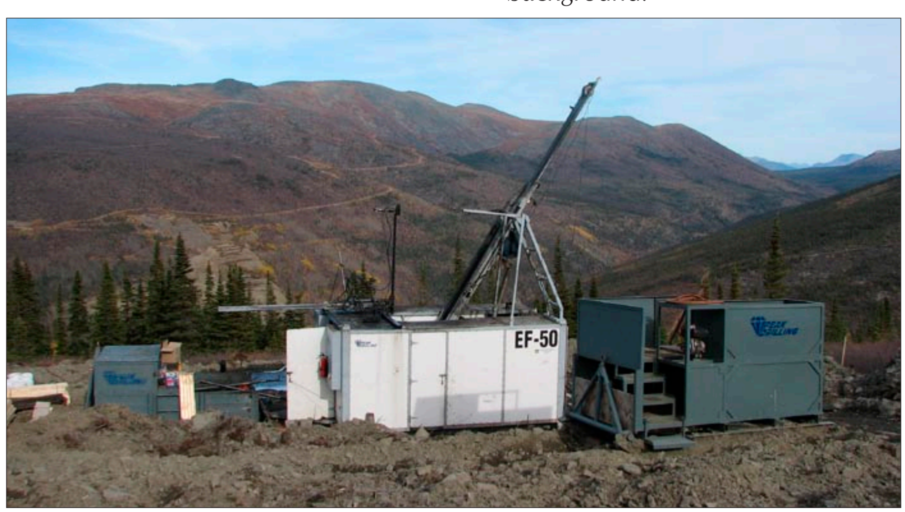

Figure 24. *Diamond drilling at the Bellekeno mine; Keno Hill is in the background.*

Figure 25. *Kel Sax with Aurora Geosciences of Whitehorse examines drill core on the CMC silver property.*

completion of metallurgical testwork, and road upgrading and construction. Mineralization occurs as veins and replacement bodies in Cambrian or older biotite-quartz schist, limy hornfels and calcareous horizons near the margin of the mid-Cretaceous Cassiar Batholith. Trenching resulted in the discovery of a new vein, the 'D' vein, that averaged a width of 1.31 m over a 20.1-m length of the trench. Chip samples have mineral assay values up to 1896 g/t Ag and 73.0% Pb over 1.0 m. Infill drilling on the 'S zone', a high-grade vein hosted in granodiorite, has mineral assay values up to 4619 g/t Ag, 29.3% Zn and 0.36% Pb over 0.15 m (Fig. 25). Additional results from other zones drilled were not yet available at year-end.

CMC Metals acquired an option on the **Logjam** property (Yukon MINFILE 105B 038), located approximately 60 km to the southwest of their CMC Silver property. The company performed an initial property evaluation of historical work that had identified eight quartz veins cutting a steeply dipping diorite dyke that is approximately 610 m wide. The dyke is mineralized with galena, sphalerite, arsenopyrite and pyrite over widths of up to 0.9 m.

Valencia Ventures Inc. (*www.valenciaventures.com*) acquired an option on several properties in the Rancheria district from Strategic Metal Ltd. and conducted varying levels of exploration on all the claims. The properties include the **Blue Heaven, Touchdown, Qb, End Zone** and **Pigskin** (Yukon MINFILE 105B 20, 22, 98, 101 and 107). All of the properties host a variety of styles of silver-lead-zinc mineralization, which are mainly vein type, but some occur as carbonate replacements. On the Blue Heaven property, trenching in the Hall zone exposed clay-altered granitic rocks that contain zones of manganese staining, silicification and galena mineralization. Assay values from trench samples are up to 10.45 m grading 446.5 g/t Ag and 1.12% Pb. Drilling at the H zone on the Blue Heaven property intersected variably mineralized quartz-vein and quartz-breccia zones that have assay values up to 16.5 g/t Ag, 8.52% Zn and 0.046% Pb over 1.81 m. At the Blue zone, a single drillhole intersected semi-massive galena and sphalerite mineralization that have two intervals grading 348 g/t Ag, 3.37% Pb and 0.92% Zn, and 1400 g/t Ag, 0.14% Pb and 14.9% Zn over 1.0 m and 0.49 m, respectively. On the Touchdown property, excavator trenching and four diamond drillholes were completed on a structural zone hosting manganiferous and silica alteration within granitic and metasedimentary rocks. Modest silver and zinc mineralization was intersected.

Klondike Silver Corp. (*www.klondikesilver.com*) optioned the **Connaught** property (Yukon MINFILE 115N 040) from ATAC Resources and completed an airborne geophysical survey (VTEM). Historical work on the property in the Dawson Range of central Yukon identified mineralization consisting of lenses of galena and arsenopyrite, and minor sphalerite, tetrahedrite and boulangerite in northeast-striking quartz veins. The mineralized quartz veins cut Late Devonian- to mid-Mississippian Nasina Assemblage schists of the Yukon-Tanana Terrane. The schists are cut by sills of Early Mississippian granitic augen gneiss and by Late Cretaceous monzonitic to granodioritic intrusive rocks.

Klondike Silver also optioned the **Stump** property (Yukon MINFILE 105F 056) that is located just east of the Ketza River gold property. The property has historical underground workings that intersect a fine-grained galena vein that has mineral assays up to 528.8 g/t Ag over 3 m in a raise. The company collected samples for metallurgical testing.

YGC Resources (*www.ygcr.ca*) optioned claims that cover the **Ketzakey** property (Yukon MINFILE 105F 057) immediately east of their Ketza River gold property. The company completed some late-season diamond drilling on the property. The property hosts vein-type mineralization that consists of galena, pyrite and minor tetrahedrite, as well as sphalerite in a carbonate gangue. Samples from historical underground workings have mineral assays of up to 692.6 g/t Ag and 12.4% Pb over a 1.7 m width. Results of the drilling were not available at year-end.

BASE METALS – ZINC

SEDIMENTARY

Selwyn Basin is a continental-margin basin characterized by the deposition of thick sequences of black carbonaceous shales in euxinic conditions, and by the development of second-order basins through periodic extensional tectonism, subsidence and faulting. Over 800 mineral occurrences have been discovered within the limit of Selwyn Basin; 19 of these have been identified as sedimentary-exhalative (SEDEX) deposits. An additional 89 occurrences have been described as SEDEX-type mineralization. Of the three main SEDEX districts (e.g. Anvil, MacMillan Pass and Howards Pass), only those deposits of the Anvil district have been mined, however, all three have potential for significant new discoveries. Other areas of Yukon have potential for SEDEX-type mineralization, but have not received nearly the same level of exploration as Selwyn Basin. These include Selwyn Basin-equivalent rocks of the Cassiar Terrane, and the Nasina Assemblage of the Yukon-Tanana Terrane. In the Yukon-Tanana Terrane, the mineral potential is highlighted by the discovery of massive sulphide mineralization in the Forty Mile district of Alaska, across the Canada-United States border.

Figure 26. *Diamond drilling on the XY deposit at the Selwyn Project (Howards Pass). The XY exploration camp and airstrip are visible in the background.*

The largest exploration program in Yukon was by Pacifica Resources Ltd. (*www.pacificaresources.com*) on their **Selwyn** Project. The Selwyn Project covers an area of over 300 km^2 that encompasses the bulk of the Howards Pass district (Yukon MINFILE 105I 12, 37 and 38). The approximately $14-million exploration program included diamond drilling (Fig. 26), geological mapping and prospecting, geochemical surveys, continuing metallurgical analysis and dense media separation testing, and commencement of baseline environmental and engineering studies. Drilling in 2006 resulted in the discovery of the HC, HC West, OP 17 and Pelly North zones. All mineralization zones discovered to date within the district have been in a single defined stratigraphic horizon named the 'Active Member'. All drillholes that have intersected the Active Member have been mineralized. Pacifica's drilling in 2006 tested approximately 37 km of strike length of the Active Member, which demonstrates the incredible size of the mineralizing system at the Selwyn Project.

Table 2. *Selected drill results from the 2006 drilling program at the Selwyn Poject.*

Drillhole	Thickness (m)	Zn (%)	Pb (%)
XY high-grade underground target			
XY-150	29.35 (true)	5.8	2.12
including	2.4	18.8	9.12
XY-141	24.72 (true)	8.64	2.26
including	2.85	26.56	4.91
Anniv deposit			
ANC-153	8.7 (true)	6.97	3.57
including	1.67	16.37	13.07
Don Valley-HC West open-pit target area			
DON-22	8.10 (true)	6.02	1.73
including	2.67 (true)	12.33	3.07
Don Valley-Don zone			
DON-42	16.33	6.92	2.62
including	3.88	12.98	6.95

Mineral resources at the Selwyn Project are contained in three deposit areas: the XY, Anniv and Brodel. Resources at the Selwyn Project are 43-101 compliant and consist of 33.50 million tonnes grading 5.52% Zn and 2.10% Pb in the Indicated category, and 112.91 million tonnes grading 5.40% Zn and 2.14% Pb in the Inferred category. These resources include results from 2005 drilling, and will be updated with the over 40 000 m of drilling that was completed in 2006. Drilling in 2006 was directed at upgrading the resource categories in the known deposits, expanding high-grade underground resources, defining resources in the new discovery areas made in 2005, testing the Active Member on a district scale, and defining resources in any additional discovery areas. Drilling in 2006 was also aimed at refining the geologic model of the district to include the physical distribution of the deposits, grade distribution within the deposits, and the ultimate potential of the district. The program was successful in achieving all of the above-mentioned goals.

A few highlights from the vast amount of exploration results are included in Table 2. These results highlight some of the broad intersections of mineralized Active Member and some of the higher grade intersections (Fig. 27) that are being discovered. The company has also conducted gravity separation testwork that indicates that the stratiform nature of the mineralization allows for the separation of dense mineralized beds from barren waste beds. This feature would permit a pre-concentration of the run-of-mine material before it would enter a concentrator. Simply put, removal of waste material in a gravity separation circuit is much less expensive than milling it, and results in an increase in the grade of material entering a milling facility and lower processing costs.

Yukon Zinc Corporation (*www.yukonzinc.com*) acquired 100% of the **Swift** property (Yukon MINFILE 105B 026 and 27) in southern Yukon and conducted an airborne gravity survey over the property in 2006. The property hosts skarn-type zinc and copper mineralization. Numerous theories have been put forth as to the origin of the mineralization. Yukon Zinc is designing an exploration program on the property that is modelled on stratabound-type mineralization undergoing later contact metamorphism which resulted in the skarn mineral assemblages of the existing occurences.

Figure 27. *High-grade, laminated, low-iron sphalerite (grey) from the XY deposit at the Selwyn Project.*

VOLCANIC

Exploration for volcanic-hosted massive sulphide (VHMS) deposits occurred within variably metamorphosed Upper Paleozoic sedimentary and volcanic rocks of the Yukon-Tanana Terrane, and a belt of Mississippian felsic volcanic and sedimentary rocks of the Pelly Mountain volcanic belt. Rocks of the Yukon-Tanana Terrane are within the Selwyn Basin, a predominantly off-shelf metasedimentary and metavolcanic sequence deposited west of ancestral North America, while rocks of the Pelly Mountain volcanic belt are within the Pelly-Cassiar platform, a miogeoclinal sequence thought to be part of ancestral North America.

Figure 28. *Portal entrance to the Wolverine deposit.*

Yukon Zinc Corporation completed a feasibility study on the **Wolverine** deposit (Yukon MINFILE 105G 072) in May, 2006 by Hatch Associates Ltd. Yukon Zinc subsequently initiated a review and optimization study to evaluate opportunities for reduction of operating and capital costs, and identify operating improvements to increase cashflow for the proposed operations. The Measured and Indicated resources at Wolverine are 4.46 million tonnes grading 12.14% Zn, 354.8 g/t Ag, 1.16% Cu, 1.69 g/t Au and 1.58% Pb. Inferred resources are 1.69 million tonnes containing 12.16% Zn, 385.4 g/t Ag, 1.23% Cu, 1.71 g/t Au and 1.74% Pb. In December, 2006, Yukon Zinc received its Quartz mining license for development of the Wolverine mine (Fig. 28). The Quartz license is required

Figure 29. *Magnetite in drill core from the Magnum project, a volcanic-hosted massive sulphide target in the Dawson mining district.*

to proceed with mine development activities, such as construction of the main access road and earthworks for foundations. The company has applied for a Type A water license that is required for water use and waste deposition during the later phase of construction and operations.

The **Magnum** property (Yukon MINFILE 116C 118), located northwest of Dawson City, was optioned by Klondike Silver Corp. (*www.klondikesilver.com*) from Strategic Metals Ltd. (*www.strategicmetalsltd.com*). The property is underlain by volcanic and sedimentary rocks of the Finlayson assemblage, Yukon-Tanana Terrane (Colpron *et al.*, 2006). These rocks were adjacent to the Finlayson Lake volcanogenic-massive-sulphide district prior to the approximately 430 km of post-Late Cretaceous displacement along the Tintina Fault. Magnetic surveys successfully delineated a magnetite-rich horizon (Fig. 29) on the property that may represent an exhalative iron formation, similar to that found in the Finlayson district. Airborne VTEM surveys were flown on the property. Follow-up to the airborne survey included the completion of a 2-hole, 368.8-m, diamond-drill program in the fall. Results from the program were pending at year-end.

Figure 30. *Nick Mitchell, geologist with Archer, Cathro and Associates (1981) Ltd., at the Marg volcanogenic-massive sulphide deposit.*

Yukon Gold Corporation (*www.yukongoldcorp.com*) explored the **Marg** copper-lead-zinc-silver-gold deposit (Yukon MINFILE 106D 009) with an airborne geophysical survey (VTEM) and a diamond-drill program (Fig. 30). The Marg deposit is located approximately 80 km northeast of Mayo in central Yukon and is hosted in Devonian to Mississippian Earn Group volcaniclastic and sedimentary rocks of the Selwyn Basin. Drilling is directed at expanding the Indicated resources of 4 646 200 tonnes grading 1.80% Cu, 2.57% Pb, 4.77% Zn, 65 g/t Ag and 0.99 g/t Au, and an Inferred resource of 880 800 tonnes grading 1.55% Cu, 1.90% Pb, 3.75% Zn, 50.4 g/t Ag and 0.95 g/t Au. All drillholes intersected mineralization. Some highlights from drilling include drillhole 93 that intersected 2.38 m of mineralization grading 11.29% Zn, 3.45% Cu, 4.54% Pb, 1.41 g/t Au and 102.1 g/t Ag.

In the Pelly Mountain volcanic belt, Eagle Plains Resources (*www.eagleplains.com*) explored the **MM, Fire** and **Ice** properties (Yukon MINFILE 105F 012, 71 and 73) and conducted an airborne geophysical survey (VTEM), geological mapping and prospecting.

Figure 31. Geologists of Eagle Plains Resources examine the discovery outcrop at the Blende zinc-lead-silver deposit.

VEIN/BRECCIA

Blind Creek Resources and Eagle Plains Resources conducted a diamond-drill program on the **Blende** deposit (Yukon MINFILE 106D 064) in central Yukon. The Blende is a structurally controlled, carbonate-hosted zinc-lead-silver deposit (Fig. 31). The project commenced with the construction of a winter road into the property in March, 2006, followed by a 23-hole, 4230-m drill program. The Blende hosts an Inferred resource of 19.6 million tonnes grading 3.04% Zn, 2.8% Pb and 56 g/t Ag. The 2006 drill program was aimed at upgrading and expanding the existing resource. The company also performed regional- and property-scale geological mapping, geochemistry and prospecting. In addition, the company supported Mike Moroskat of the University of Alberta, who is currently working on a Master of Science thesis. Results were not available at year-end.

Yukon Zinc Corporation conducted an airborne gravity survey on their **Logan** deposit (Yukon MINFILE 105B 99). The Logan deposit is a structurally controlled vein and breccia zone within the mid-Cretaceous Marker Lake Batholith, and hosts a historical resource of 12 300 000 tonnes grading 6.17% Zn and 26.4 g/t Ag. The deposit is open at depth.

BASE METALS – COPPER

Exploration for copper in Yukon was directed at a wide range of deposit models. Porphyry-related systems were the main target of exploration. Interest in this style of copper mineralization was generated by the successful exploration and development of several mineral occurrences such as the Jurassic Minto deposit in the Dawson Range, Cretaceous intrusive rocks near the Alaska/Yukon border, and Devonian to Mississippian meta-igneous intrusions to the south of Dawson City in the Stewart River map area. Iron oxide-copper-gold (IOCG) deposits continue to be evaluated for their copper potential in northern Yukon. In the Whitehorse Copper Belt and other areas, skarn mineralization was the target for several exploration programs.

PORPHYRY/SHEETED VEIN

The **Carmacks Copper** deposit (Yukon MINFILE 115I 008) of Western Copper Corporation (*www.westerncoppercorp.com*) is located approximately 40 km southeast of the Minto deposit. Western Copper completed approximately 7200 m of drilling in 34 holes in order to infill, upgrade and expand existing oxide resources in the No. 1 zone (Fig. 32). Western Copper conducted additional drilling on other known zones in the deposit area. The company will use the new drilling data to update the historical oxide resource of 13.28 Mt of 0.97% Cu to meet 43-101 standards, as well as update a feasibility study that was completed in 1997. The Minto and Carmacks deposits are both hosted in Jurassic granodiorite. Both deposits bear similarities to porphyry and iron oxide-copper-gold deposits, however, the origin of the deposits is still subject to debate. Partial results from drilling of the No. 1 zone were received at year-end. Highlights include drillhole WC06-07 that intersected 16 m of remobilized mineralization in the hanging wall of the zone, which assayed 0.52% total Cu (0.46% non-sulphide Cu) and 0.22 g/t Au, in addition to 37 m of 2.29% total Cu (2.00% non-sulphide Cu) and 1.54 g/t Au. These grades are higher than those that were determined in adjacent, historical drillholes. The company also drilled the deposit to depth below the oxide resources and intersected sulphide mineralization. The No. 13 zone, located 1 km south of the No. 1 zone (Fig. 33), was tested with 10 drillholes, of which seven of those intersected oxide and sulphide mineralization, in addition to native copper. Assay results from these drillholes were not available at year-end.

Figure 32. *High-grade oxide copper (malachite) in core drilled in the No. 1 zone at the Carmacks Copper deposit.*

Copper Ridge Exploration (*www.copper-ridge.com*) explored their **Lucky Joe** property and completed a program that included soil geochemistry, geophysics (IP) and diamond drilling. The planned 2000-m drill program was terminated early due to drill breakdowns, complicated drilling, difficulty securing a drilling contractor, and the onset of winter conditions. A total of 780 m of drilling in three holes was completed. Two targets were tested: the Bear Cub anomaly and the Ryan's Creek trend anomaly. The Bear Cub anomaly is defined by an 11.3-km-long trend of elevated copper and gold soil geochemical values, and coincident IP chargeability anomalies. The Ryan's Creek trend anomaly is parallel to, and 4 km east of, the Bear Cub anomaly; it is defined by a 7.2-km trend of similar copper values, but stronger gold soil geochemical values and coincident IP chargeabilty anomalies. The claims cover an area that contains an assemblage of metasedimentary and meta-igneous rocks of the Yukon-Tanana Terrane.

Partial results were available by year-end. One of the two holes from the Bear Cub drill program intersected good alteration and anomalous results from meta-igneous rocks, however, the hole was terminated before reaching its target depth. A single hole completed on the Ryan's Creek trend intersected moderately to strongly altered schist containing up to 2% pyrite and chalcopyrite. Within this zone, a 12-m intersection of mineralized rock was assayed at 0.36% Cu and 0.80 g/t Au, including 3.0 m of 0.23% Cu and 2.90 g/t Au. The hole was drilled on the southern end of the anomalous trend and the majority of the zone remains untested by drilling.

Figure 33. *View of the stripped No. 1 zone looking north from the No. 13 zone at the Carmacks Copper deposit.*

Atac Resources Ltd. (*www.atacresources.com*) conducted an exploration program of geochemistry, prospecting, geological mapping and airborne geophysics (VTEM) on the **Nikki** property (Yukon MINFILE 115K 082), which is optioned to a private company. Interbedded, pyritic volcanic and sedimentary rocks are cut by a diorite stock, the core of which is composed of porphyritic monzonite to granodiorite. The porphyritic monzonite is weakly pyritic, and moderately chloritized and sericitized. Historical drilling from the early 1970s reportedly intersected mineralized rock grading about 0.13% Cu and 0.005% MoS_2.

Strategic Metals Ltd. (*www.strategicmetalsltd.com*) completed an exploration program on the **Hopper** property (Yukon MINFILE 115H 018 and 019) that included geochemistry, geological mapping and prospecting. Historical work on the property has been directed at copper-gold skarn mineralization associated with an Early Tertiary hornblende-biotite granodiorite stock, but Strategic Metals is investigating the potential for porphyry-style mineralization.

Figure 34. *Spring drilling on the Grafter copper-skarn deposit in the Whitehorse Copper Belt.*

H. Coyne and Sons, a private Whitehorse-based company, holds numerous mining claims and leases in the Whitehorse Copper Belt. The company conducted drilling on the **Hat** claims (Yukon MINFILE 105D 054) and in the **Best Chance/Grafter** areas (Héon, 2004; Fig. 34). On the Hat claims, previous drilling by the company has intersected high-grade, bornite-chalcopyrite skarn mineralization (4.99% Cu, 1.05 g/t Au and 40.3 g/t Ag over 10.6 m) and porphyry-style, sheeted quartz-bornite-chalcopyrite-molybdenite veins in granodiorite. Drilling in 2006 was directed at the porphyry-style mineralization, and additional vein and disseminated copper-molybdenum mineralization were discovered. Drilling at the Best Chance/Grafter intersected bornite-chalcopyrite skarn mineralization. Assay results were not available by year-end.

Arcturus Ventures Inc. (*www.arcturusventuresinc.com*) has staked claims in the **Lewes River** project area (Yukon MINFILE 105D 022), in the southern portion of the Whitehorse Copper Belt. The company conducted prospecting on porphyry and skarn targets.

SKARN

Manson Creek Resources (*www.manson.ca*) conducted an exploration program of soil geochemistry and magnetic surveying on their **Cuprum** property (Yukon MINFILE 105E 008), located 50 km north of Whitehorse. The work by Manson Creek has outlined a coincident magnetic and copper-lead-zinc-silver geochemical anomaly that they plan on drill testing in 2007. Skarn mineralization on the property contains magnetite, and minor bornite and chalcopyrite, and was discovered in two areas. The skarn is associated with marble in deformed volcanic rocks that are in contact with biotite granite belonging to the Late Cretaceous Annie Ned pluton.

WERNECKE BRECCIA

At least 65 iron oxide-copper-gold ± uranium ± cobalt (IOCG) prospects are associated with a large-scale Proterozoic breccia system in north-central Yukon. The breccia system, known as Wernecke Breccia, consists of numerous individual breccia bodies that occur in the Early Proterozoic Wernecke Supergroup, an approximately 13-km-thick deformed and weakly metamorphosed sequence of sedimentary rocks.

International KRL Resources Corp. (*www.krl.net*) planned on a 15 000-m drill program, but was only able to complete a 9-hole, 1600-m drill program on the **Nor** property (Yukon MINFILE 106L 061). The property covers an area that encompasses a heterolithic, diatreme breccia body intruded into a fault-bounded outlier of Middle Proterozoic limy siltstone and argillite. The outlier is exposed through Cambrian limestone that unconformably overlies it. Drilling targeted a linear magnetic anomaly, outlined in 2005 on the Nor ridge, that has a coincident copper-uranium soil anomaly. Six of the nine holes intersected copper mineralization, of which the most significant mineral assay included 20 m of 0.25% Cu.

Copper Ridge Exploration (*www.copper-ridge.com*) conducted an exploration program on their **Yukon Olympic** property (Yukon MINFILE 116G 082) and completed a magnetic, induced polarization and gravity survey to better define the existing circular magnetic and partially overlapping gravity anomaly identified in previous surveys. Furthermore, the company hoped to identify any near-surface sources of metallic mineralization. The survey defined three anomalous areas that warrant drilling.

Copper Ridge Exploration also conducted a program of geophysics including induced polarization and horizontal loop electromagnetics over a previously defined 4.5-mgal gravity anomaly on their **Ironman** property (Yukon MINFILE 116A 017). The surveys defined a zone of low resistivity and high conductivity underlying the gravity anomaly. The property hosts several zones of copper- and gold-bearing hematite breccias around the periphery of the anomaly. The anomaly is covered by younger carbonate rocks.

SEDIMENTARY

An interesting new occurrence is the **Tidd** property (Yukon MINFILE 105J 029) of Strategic Metals Ltd. (*www.strategicmetalsltd.com*) that has been optioned by Sedex Mining Corp. (*www.sedexmining.com*). The property is underlain by gently dipping sedimentary rocks identified by the company as the Cambrian to Ordovician Vangorda and Lower Cambrian Mt. Mye formations, the same stratigraphy that hosts the Faro sedimentary-exhalative deposits. The company performed a program of geochemistry, geophysics (airborne VTEM, ground magnetics), geological mapping, prospecting and diamond drilling in 2006. Mineralization is hosted within moderately to strongly brecciated, chlorite-sericite-altered and silicified sedimentary rocks and float samples. Samples from a 3000-m-long corridor of mineralized rock contain mineral assay values of up to 6.85% Cu, 411 g/t Ag, 0.34% Bi, 157 g/t In, 3.61% Pb and 2.39% Zn. Sawn channel sampling completed across the main showing included a mineral assay of 1.08% Cu, 68.53 g/t Ag, 46 g/t In and 0.02% Bi over 10.5 m. Results from the drilling program were not available by year-end.

BASE METALS – NICKEL ± PLATINUM GROUP ELEMENTS (PGE)

Exploration for nickel was largely directed in the Kluane mafic-ultramafic belt in western Yukon. The Kluane region is within the Insular Superterrane, which is largely composed of Devonian to Triassic island arc and ocean floor volcanic rocks, and thick assemblages of overlying sedimentary rocks.

MAFIC/ULTRAMAFIC

Coronation Minerals Inc. (*www.coronationminerals.com*) has an agreement to purchase the **Wellgreen** deposit (Yukon MINFILE 115G 024) from Northern Platinum Ltd. The Wellgreen deposit hosts a historical resource of 50 million tonnes grading 0.36% Ni, 0.35% Cu, 0.54 g/t Pt and 0.34 g/t Pd. This company initiated a program of diamond drilling that was designed to twin historical drilling, as well as to upgrade the resource to comply with National Instrument 43-101 standards. Partial drill results were available at year-end and included hole WS06-149 that intersected 92.17 m of mineralized rock grading 0.26% Ni, 0.38% Cu, 0.61 g/t Pt, 0.40 g/t Pd, 0.11 g/t Au and 177 ppm Co, including 21.36 m grading 0.23% Ni, 0.62% Cu, 1.01 g/t Pt, 0.54 g/t Pd, 0.22 g/t Au and 180 ppm Co. Hole WS06-153 was drilled to test a historical hole; mineral assay results from the new hole were similar to historical results. Drillhole WS06-153 was extended to a far greater depth (480 m) compared to the historical drillhole when it was discovered that the ultramafic rocks continued to depth. Mineral assay results from the deeper ultramafic intersection were not available at year-end.

Golden Chalice Resources (*www.goldenchaliceresources.com*) optioned the **Burwash** property (Yukon MINFILE 115G 100) from Strategic Metals Ltd. and performed an exploratory program of airborne geophysics (VTEM), geological mapping, prospecting and soil sampling. The property is located adjacent to the

Wellgreen property. The Burwash property hosts similar mineralization and grades to those that have been discovered on the Wellgreen property during previous drill programs.

The **Canalask** property (Yukon MINFILE 115F 045) was optioned from StrataGold Corporation (*www.stratagold.com*) by Falconbridge Ltd. (now Xstrata). The property is located in the Kluane mafic-ultramafic belt and has a small historical resource of 390 235 tonnes grading 1.35% Ni. The company staked claims to the northwest and southeast along the belt. Airborne geophysics, prospecting and geological mapping were completed in the 2006 program.

A new nickel occurrence was discovered in 2004 by True North Gems (*www.truenorthgems.com*) while exploring for gemstones. The **Bandito** property (Yukon MINFILE 95C 051) has previously been explored for uranium and rare-earth elements. The claims cover an area that encompasses a syenitic stock of probable Cretaceous age. The syenitic stock intrudes Proterozoic green argillite and quartzite that is unconformably overlain by Cambrian or younger boulder conglomerate. True North Gems completed a program of airborne geophysics (time-domain electromagnetics and magnetometer), geological mapping, geochemistry, prospecting and sampling on the property in 2006. Geochemical sampling outlined an area 750 m by 600 m that contains up to 2860 ppm Ni, 4740 ppm Cu, 4670 ppm Pb, 2150 ppm Zn, 346 ppm Co, 277 ppm Bi and 736 ppm As. Float samples collected on the property have been assayed and have values in the range of 7.08% to 15.85% Ni. The predominant minerals are within oxide-cemented breccias and veins, and include abundant green annabergite (also known as nickel bloom), malachite, azurite, pyrite and chalcopyrite.

BASE METALS – TUNGSTEN ± MOLYBDENUM

Yukon and the adjacent Northwest Territories are known to have a high number of tungsten occurrences and deposits. Exploration for tungsten focused on scheelite-bearing skarn deposits developed in Paleozoic carbonate rocks of the Selwyn Basin at, or near, their contact with felsic intrusions of the mid-Cretaceous Tungsten or Tombstone plutonic suites. Exploration for tungsten also targeted scheelite and wolframite-bearing quartz-molybdenite stockwork and veins developed in, or near, Late Cretaceous/Early Tertiary felsic intrusions of the Cassiar suite.

SKARN

North American Tungsten (*www.natungsten.com*) continued with environmental baseline studies at their **MacTung** deposit (Yukon MINFILE 105 002), one of the largest tungsten deposits in the world. The company is in the process of updating the historical resource of 30 million tonnes of 0.94% WO_3. Results from drilling in 2005 will conform to National Instrument 43-101 standards. The new resource will allow the company to update previous technical and feasibility work completed on the MacTung deposit.

Playfair Mining Ltd. (*www.playfairmining.com*) conducted a 6-hole, 755-m drill program on the **Risby** deposit (Yukon MINFILE 105F 034) in south-central Yukon. Garnet-diopside-pyrrhotite-scheelite skarn occurs in Cambrian carbonate rocks intruded by a mid-Cretaceous quartz monzonite pluton of the Cassiar Suite. Drilling was completed in the area where a historical resource of 2.7 Mt grading

0.81% WO_3 was outlined by Hudson Bay Mining and Smelting in 1982. Four drillholes were completed and intersected significant mineralization, highlighted by intersections such as that found in drillhole RT06-05 containing a mineral assay of 6.49 m grading 1.09% WO_3. Two drillholes were not completed and thus did not intersect the target mineralization.

Figure 35. *Molybdenum on a fracture in core from the Logtung deposit.*

PORPHYRY/SHEETED VEIN

Largo Resources (*www.largoresources.com*) optioned the **Logtung** deposit (Yukon MINFILE 105B 039) from Strategic Metals Ltd., and refers to the project as the **Northern Dancer.** The Logtung deposit is the world's largest intrusion-hosted tungsten deposit. The Logtung deposit has scheelite- and molybdenite-bearing quartz veins hosted in a high-level felsic intrusion of the Cassiar Suite. The company completed a 17-hole, 3945-m diamond drill program that was designed to upgrade the historical resource of 162 Mt grading 0.13% WO_3 and 0.052% Mo to meet National Instrument 43-101 standards. The drilling was also completed in order to determine if a higher grade core of tungsten and/or molybdenum mineralization could be defined. The deposit contains numerous stages of veining. Current drill results suggest that a late-stage, near vertical, sheeted-quartz-vein array may not have been adequately tested by historical drilling, and that a higher-grade tungsten core may exist within the deposit. Highlights from drilling include better-than-average molybdenum grades that consist of 134.51 m of 0.13% MoS_2 and 0.04% WO_3 in drillhole LT06-70, and 52.00 m of 0.14% MoS_2 and 0.07% WO_3 in drillhole LT-06-63. Significant tungsten-rich (Fig. 35) mineralized intersections in drillholes include the following: 114.95 m grading 0.16% WO_3 and 0.08% MoS_2, including 12.22 m grading 0.54% WO_3 and 0.19% MoS_2 in drillhole LT-06-66; and 83.89 m grading 0.20% WO_3 and 0.04% MoS_2 in drillhole LT-06-68 (Fig. 36). The upgraded resource

Figure 36. *Fluorescent scheelite in core under ultraviolet light from the Logtung deposit.*

Figure 37. Drilling at the Tootsee River tungsten-molybdenum project.

calculation will be used in a scoping study on the deposit. Drilling in 2007 will test the higher grade tungsten core of the deposit.

The **Tootsee River** project (Yukon MINFILE 105B 089) was optioned by Cumberland Resources (*www.cumberlandresources.com*) from North American Tungsten Corporation. The company performed an airborne geophysical survey (magnetometer) and a diamond-drill program (Fig. 37) of three holes totaling 1496 m. Historical drilling in the early 1980s identified scheelite and molybdenite mineralization in stockwork. Scheelite and molybdenite were also identified in green calc-silicate hornfels near small dykes and porphyry bodies related to the Cretaceous Cassiar Batholith. Results from the program were not available at year-end.

BASE METALS – MOLYBDENUM

PORPHYRY/SHEETED VEIN

Tintina Mines Ltd. (*www.tintinamines.com*) conducted environmental and geotechnical studies on their **Red Mountain** project (Yukon MINFILE 105C 009). Red Mountain contains a historical resource (non 43-101 compliant) of 187 Mt grading 0.167% Mo, and a higher grade core of 21.3 Mt grading 0.293% Mo. The company conducted geotechnical studies, and cleared along the existing and proposed access and haulage route into the deposit. In addition, the company performed geotechnical, engineering, geological, environmental and hydrological studies required to test the potential portal and infrastructure sites associated with the deposit.

BASE METALS – TIN

SKARN

Brett Resources Inc. (*www.brettresources.com*) explored the **JC** tin deposit (Yukon MINFILE 105B 040) and completed an exploration program of geological mapping and sampling, and ground-based magnetometer surveying. The tin-bearing, calc-silicate skarn mineralization occurs along the western margin of the Cretaceous Seagull Batholith. Mineral assay values from trenching include one interval of 3 m of 0.87% Sn in one trench, and another trench containing 1.5 m of 0.93% Sn, including 0.15 m of 4.04% Sn.

URANIUM

Uranium exploration in Yukon peaked in the early 1980s. Until recently, no new exploration or research had been undertaken for over 20 years. Renewed interest in uranium is slowly filling in the knowledge gap. A flurry of uranium exploration activity occurred in the past year. Roughly $12 million was spent on uranium targets in 2006. Yukon is highly prospective for uranium. Four main deposit types were explored this past season and include Wernecke Breccia-associated (iron oxide-copper-gold + uranium-type), fault/shear-associated (possible unconformity-related), intrusion-related, and volcanic-related uranium deposits.

The Wernecke Mountains, north of Mayo, was the main area targeted for uranium exploration. Areas of exposure of Wernecke Breccia have been explored in recent years, mainly for their copper-gold content, however, in the last year, a significant amount of claim-staking has occurred based on the uranium potential of these breccia bodies. Unconformity-related uranium potential has also been recognized within Wernecke Supergroup (Hunt, 2006). All the companies active in the Wernecke Mountains have recognized this potential, and future exploration programs may include the drilling of potential unconformity-related targets.

WERNECKE BRECCIA

Cash Minerals Ltd. (*www.cashminerals.com*) and Twenty Seven Capital Corp. (*www.27capitalcorp.com*) formed a joint venture called the Yukon Uranium Project (YUP) in order to conduct several exploration programs on properties in the Wernecke Mountains area. A 19-hole, 3004-m diamond drill program was completed on the **Igor** property (Yukon MINFILE 106E 009) in 2006. Results from this drill program were not available at year-end. Exploration drilling at Igor in 2005 included a 74.44-m drillhole intersection, which averaged 0.069% U_3O_8 (1.4 pounds-per-ton U_3O_8) and 1.88% Cu in an iron oxide-copper-gold (IOCG) breccia. Cash Minerals has also retained Dr. Geordie Mark, an IOCG geological specialist from Australia, who is conducting mapping, core evaluation, magnetic survey analysis and the construction of geological models associated with Olympic Dam-type characteristics on the Igor and other Wernecke Breccia-related properties being explored by the YUP (Fig. 38).

Other work completed by YUP in 2006 included 2340 m of diamond drilling in 10 holes at other properties in the Wernecke Mountains, structural and stratigraphic mapping, ground and helicopter-borne radiometric and gravity surveys, and airborne magnetic surveys. This extensive regional exploration program led to the claim staking of approximately 80 000 hectares in 2006. Yukon Uranium Project now holds 19 properties in the Wernecke Mountains.

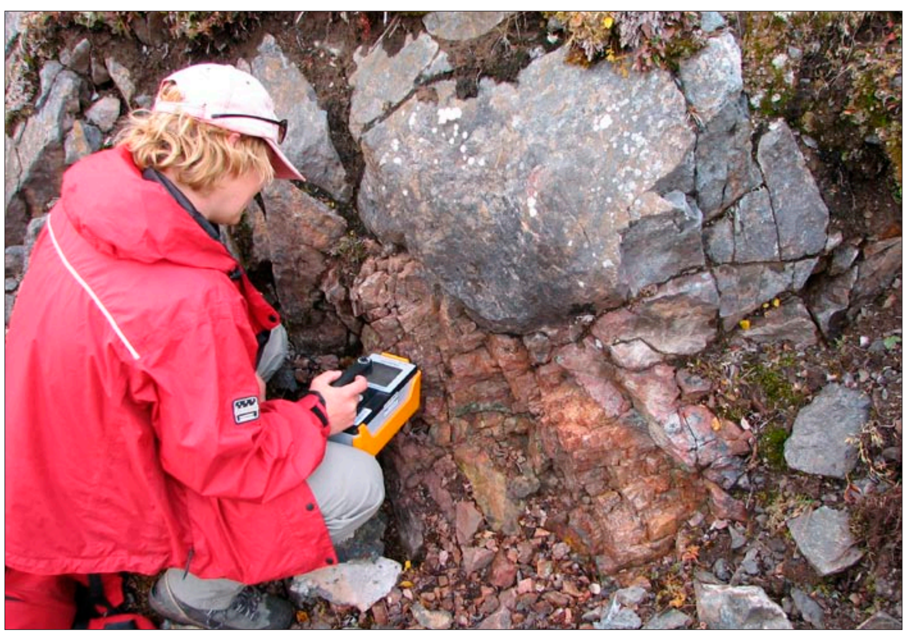

Figure 38. *Lara Lewis of Yukon Geological Survey examines a uranium-bearing outcrop in Wernecke Breccia on the Igor property.*

Figure 39. Geologists examine a uranium-bearing outcrop on Slab Mountain.

Fronteer Development Group Inc. (*www.fronteergroup.com*) and Rimfire Minerals Corporation (*www.rimfire.bc.ca*) formed a joint venture from Newmont Exploration Canada Ltd. and NVI Mining Ltd., a subsidiary of Breakwater Resources Ltd. The joint-venture companies acquired mineral claims and a proprietary geoscience dataset covering a large region of the northern Yukon that includes the Wernecke Breccias. The dataset covers 5000 km^2 and includes airborne radiometric and magnetic surveys, geological and geochemical surface sample data, as well as geological data from 14 600 m of drilling. During the 2006 field season, the companies investigated 48 target areas, conducted geological mapping, geochemical sampling and prospecting, and completed a 9750-line-km airborne gravity survey. The companies also carried out additional claim staking and increased their landholdings in the district to encompass 24 properties, an area of approximately 40 000 hectares. The exploration was staged from the **Slab** (Fig. 39) property (Yukon MINFILE 106D 070).

The program resulted in the discovery of several new areas of mineralization. The **Thunder Mountain** property is a new gold-uranium-copper discovery. A total of 25 samples were collected over an area of approximately 400 m by 550 m. Carbonate-iron oxide-potassium feldspar-altered heterolithic (siltstone, dolostone) breccia boulders assayed up to a spectacular 99.2 g/t Au, 0.57% U_3O_8 and 5.1 g/t Ag. Copper-bearing breccia in the same area assayed up to 6.88% Cu, 13 g/t Ag and 1.1 g/t Au. The **Fireweed** prospect is a new uranium occurrence. Ninety-three boulders of iron oxide-potassium feldspar-silica-altered chlorite schist (Fig. 40) were collected over a 200-m by 400-m area and averaged 0.22% U_3O_8. Twenty-two samples assayed in excess of 0.14% U_3O_8, up to a maximum value of 5.55% U_3O_8. Five select grab samples were collected in the same area, one of which assayed 0.854 g/t Au and another assayed 1.53% Cu. The **Hail** prospect is defined by uranium-bearing boulders that occur over an area measuring at least 160 m by 60 m. Seventeen boulders were sampled and have an average grade of 0.15% U_3O_8, and a maximum value of 0.30% U_3O_8. At the Hail West copper-gold-silver prospect, mineralized rock was sampled in outcrop over an area 200 m in length. One select sample, taken from an outcropping chalcopyrite-bearing vein approximately 30 cm wide, assayed 24.5% Cu, 2.45 g/t Au and 62.50 g/t Ag. Three other grab samples taken from outcropping veins ranged from 0.02 to 4.12 g/t Au and 0.16 to 7.18% Cu. The **Pagisteel fault** prospect is a regional-scale structure that follows a broad, northeast-trending valley that has no outcrop, but extensive soil development. A soil geochemical survey was carried out over a 2.5-km-long section of this fault. Twenty-six float samples were collected within the soil grid area and they showed elevated copper and gold values. One of these samples was assayed at 5.75% Cu, 1.24 g/t Au and 5.75 g/t Ag.

Figure 40. Iron oxide-potassium feldspar-silica-altered chlorite schist from the newly discovered Fireweed prospect in the Wernecke Mountains.

FAULT/SHEAR-ASSOCIATED

The Yukon Uranium Project of Cash Minerals Ltd. and Twenty Seven Capital Corp. conducted a drill program on the **Lumina** project (Yukon MINFILE 106C 069). Fourteen of the nineteen drillholes (Fig. 41) from the Lumina project (Jack Flash showing) intersected uraniferous intervals within variably brecciated and altered siltstone-dominant strata. The altered siltstone was mapped by the company as Lower Proterozoic Fairchild Lake Group. The most radioactive material was localized at what has been interpreted to be a redox interface, where uranium mineralization within hydrothermal water has concentrated in fracture zones (Fig. 42). Strongly brecciated strata that underlie the mineralization are bleached and commonly hematite-bearing, while the overlying, less-brecciated strata are relatively unaltered. Regional mapping has identified a

Figure 41. Helicopter supported, low-impact drillings on Lumina property.

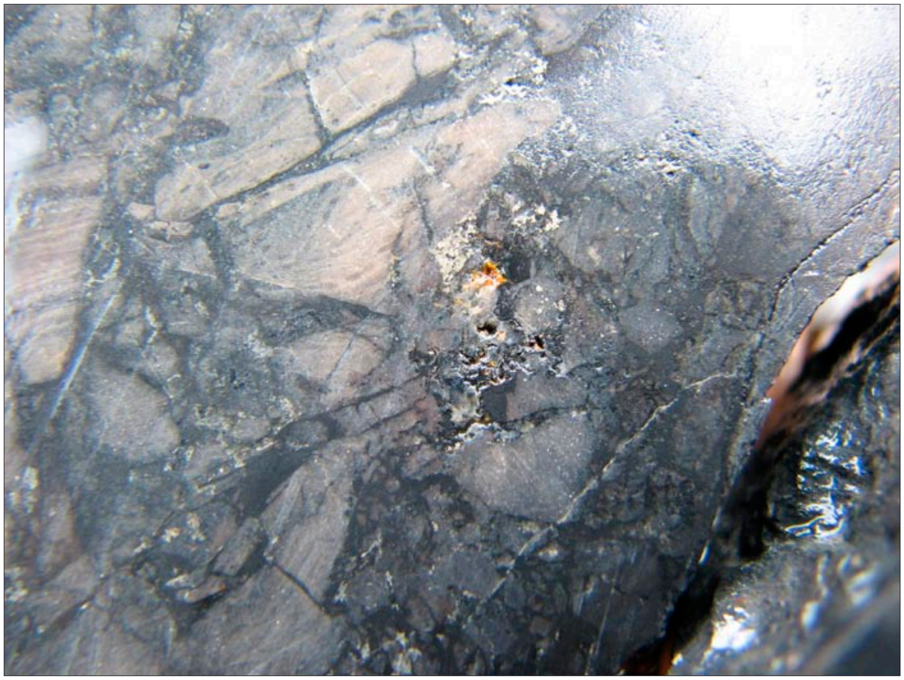

Figure 42. High-grade uranium mineralization within brecciated siltstone in core from the Lumina property.

structural corridor which controls the mineralization at the Jack Flash and other showings on the property. The uranium mineralization associated with the controlling structures may have been remobilized and is related to a potential unconformity-related source at depth. Highlights from drilling include drillhole L06-07 containing 27.01 m grading 0.203% U_3O_8, including 17.04 m grading 0.290% U_3O_8; drillhole L06-09 containing 0.030% U_3O_8 over 21.71 m, including 0.161% U_3O_8 over 1.48 m; and drillhole L06-11 containing 0.287% U_3O_8 over 2.15 m. In addition, surface samples from outcrops, subcrops and boulders were collected over an area of about 50 km^2 in the central and northern part of the Lumina property. These samples were assayed and contained up to 1.82% U_3O_8. The joint venture companies also flew an airborne radiometric survey of 1178-line-km that has identified over 90 new radiometric anomalies at the Lumina property.

Signet Minerals (*www.signetminerals.ca*) completed an exploration program of geological mapping, sampling, prospecting, kubota trenching, airborne geophysics (magnetometer, electromagnetics and radiometrics) and a ground-based gravity survey on the **Curie** project. Based on the airborne surveys, the company carried out additional claim staking in the region, bringing their total landholdings in the district to 25 000 ha. The property encompasses many known uranium occurrences (Yukon MINFILE 106E 003, 006, 011, 022, 026, 027, 028, 029, 030, 031 and 040) that were re-sampled, confirming historical uranium and copper-gold mineralization. An airborne geophysical survey has identified a 20-km-long, regional-scale, linear magnetic anomaly that is associated with several of the known uranium showings on the property. Kubota trenching was completed at the **Deer** showing (Yukon MINFILE 106E 031), where previous grab samples assayed up to 54.3% U_3O_8. The trenching revealed a highly tectonized mineralized zone composed of a hanging-wall sequence of pink, potassic-altered siltstones, a central, 1- to 2-m-wide chloritic shear

Figure 43. The excavated Deer showing at the Curie project in the Wernecke Mountains.

zone, and a footwall sequence of bleached and sericitized siltstones with radioactive stringers and veins (1-10 cm). Limited chip samples of the zone were assayed at up to 0.84% U_3O_8 over 1.0 m (Fig. 43). The Deer showing is interpreted as a potential leakage zone from unconformity-related mineralization, or an unexposed Wernecke Breccia (iron oxide-copper-gold target) at depth.

INTRUSION-RELATED

The **Murphy** project (Yukon MINFILE 105F 079) is located approximately 85 km northeast of Whitehorse. Signet Minerals optioned the property from Twenty Seven Capital Corp. (*www.27capitalcorp.com*) and completed an exploration program on the property that included an airborne radiometrics survey and ground-based magnetic and electromagnetic surveys, followed by diamond drilling. The property is underlain by a Cretaceous granitic batholith of the Cassiar Suite. Previous work had found anomalous uranium (up to 0.23% U_3O_8) associated with more biotite-rich phases of the intrusion. The drilling program began in October and was suspended due to weather conditions after completing approximately 1/3rd of the planned 1000-m drill program. Results were not available at year-end.

Cash Minerals Ltd. and joint venture partner, Twenty Seven Capital Corp., explored the **Pedlar** property (Yukon MINFILE 115J 092) in central Yukon and completed a program of reverse-circulation drilling. The claims cover an area encompassing quartzite and schist cut by a small, unmapped body of Cretaceous Coffee Creek granite. Uranium values up to 304 ppb were obtained from water in the main stream draining the property. Results from the drill program were reported to be unsatisfactory.

VOLCANIC-RELATED

Cash Minerals Ltd. and joint venture partner, Twenty Seven Capital Corp., also explored the **Hot Dog** property (Yukon MINFILE 115H 014) and completed a radon gas survey and diamond drill program. The drilling was directed toward a radioactive zone in a regolith, which formed at the contact between an Early Jurassic granodiorite and overlying Eocene volcanic flows. Results of the drilling were not available at year-end.

GEMSTONES

VEIN/BRECCIA-ASSOCIATED

True North Gems Inc. (*www.truenorthgems.com*) completed a program of detailed geological and structural mapping, accompanied by trenching, on several existing and newly discovered emerald-bearing zones on the **Tsa Da Glisza** property (Yukon MINFILE 105G 147). The focus of the program was to collect enough data on the Summit zone to support an independent resource calculation and pre-feasibility study. Re-logging and a petrographic analysis of previous drill core were also completed in order to better define structural relationships and alteration patterns. Exploration in 2005 resulted in the discovery of new emerald-bearing veins in the Summit and Far West zones, and better delineation of the geochemical anomalies (Be, Sn, W, Cs, Bi, Cu) that reflect emerald potential. The largest and strongest geochemical response was in the Otter zone, an area to the north of the known emerald occurrences in the Summit and Shadow zones, which has a similar,

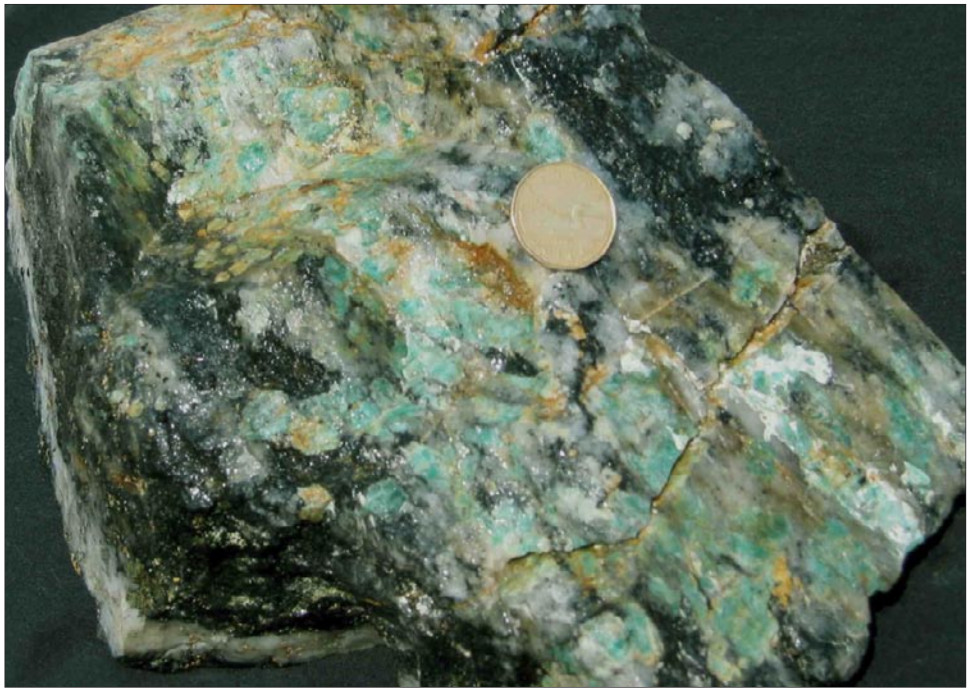

Figure 44. *Emerald-bearing boulder from the Shadow zone at the Tsa da Glisza project.*

but weaker, geochemical response. The company also announced their 2005 exploration results that included the recovery of emeralds measuring up to 15 mm by 50 mm in the Southwest vein. Results from the processing of the 2005-mined and 2002-2004-stockpiled material produced 763.77 g of gem-, 6348.09 g of near-gem-, and 3648.29 g of non-gem-grade emeralds, a significant increase in the proportion of gem and near-gem material over previous sampling. A total of 9402 g of gem and near-gem emerald rough were shipped for cutting (Fig. 44).

COAL

Cash Minerals Ltd. completed a feasibility study on the **Division Mountain Coal** project (Yukon MINFILE 115H 013) that is located 20 km west of Highway 2 and Yukon's main power grid, and 300 km from the closest tidewater port at Skagway, Alaska. The feasibility study concluded that current conditions do not support the development of a mine to serve the export coal market, however, it does identify the upside potential of the Division Mountain Coal project. Potential developments which could lead to an increased project value may include:

- more cost-effective operations as a result of more detailed resource information and detailed mine planning;
- increase in potential production to meet increased industrial demand in the region; and
- discovery of further reserves of PCI- (Pulverized Coal Injection) and/or metallurgical-grade coal. This could lead to additional markets.

The feasibility study confirmed that it is technically and economically feasible to develop an open-pit mine that will produce 240 000 tonnes of unwashed coal per year over a 20-year period. The product would be sold to a potential 50-megawatt (net) mine-mouth power station located adjacent to the Division Mountain property. The mine feasibility study was completed by Norwest Corporation, a leading North American coal and energy engineering consultancy based in Salt Lake City, Utah. In conjunction with the Division Mountain mine feasibility study, Cash Minerals also commissioned a preliminary pre-feasibility study on the potential mine-mouth coal-fired electricity generating plant located adjacent to the mine. The study estimates an operating cost of 12.2 cents per kilowatt hour (2006 cost basis).

Figure 45. Coal seam in core from the Corduroy Mountain property near Division Mountain.

Measured coal resources at Division Mountain from the 2005 National Instrument 43-101 report by Norwest Corporation are 52.5 mT. In 2006, exploration drilling was completed on a number of targets in this area. Coal-bearing stratigraphy was confirmed at Cub Mountain (adjacent to Division Mountain) and Tantalus Butte (northeast of Carmacks). A number of very encouraging coal intersections were achieved at the Corduroy Mountain property, which is located 10 km east of Division Mountain. Four holes were completed, with all holes intersecting multiple seams, ranging from 0.50 m to 5.65 m (Fig. 45). The 5.65-m-intersection was found in drillhole 06-99. Coal-quality analyses from the four coal intersections from this hole are reported in Table 3.

Santoy Resources Ltd. and 50/50 partner Almaden Minerals Ltd. conducted a 2-hole, 888-m drill program on the **Rock River** coal project (Yukon MINFILE 95D 026) in southeastern Yukon. The project encompasses a Tertiary coal deposit which ranges from lignite A- to sub-bituminous C-rank based on limited historical work. The objective of the program was to drill deeper into the basin in order to test for continuity of the previously discovered thermal coal. Results were not available by year-end.

Table 3. Data from Hole 06-99, Corduroy Mountain.

Intersection from (m)		Width (m)	Ash AD*%	Fixed carbon AD%	Moisture AD%	Moisture Total%	Sulphur AD%	Volatile matter AD%	Kcal/Kg AD%
74.42	75.83	1.41	19.02	49.27	0.99	3.43	0.49	29.24	5959
76.02	77.43	1.41	24.54	45.57	1.15	3.51	0.42	27.50	5464
96.26	101.91	5.65	23.13	44.09	0.58	2.67	0.54	30.67	5608
105.16	109.50	4.34	18.93	49.83	0.56	2.49	0.48	29.29	6026

*AD is air dried

ACKNOWLEDGEMENTS

This report is based on public information gathered from a variety of sources. It also includes information provided by companies through press releases, personal communications, and property visits conducted during the 2006 field season. The cooperation of companies and individuals in providing information, as well as their hospitality, time, and access to properties during field tours, is gratefully acknowledged.

REFERENCES

Canadian Securities Administrators, 2001. National Instrument 43-101: Standards of Disclosure for Mineral Projects (Amended NI 43-1-1 or NI 43-101).

Colpron, M., Nelson, J.L. and Murphy, D.C., 2006. A tectonostratigraphic framework for the pericratonic terranes of the northern Cordillera. *In:* Paleozoic Evolution and Metallogeny of Pericratonic Terranes at the Ancient Pacific Margin of North America, Canadian and Alaskan Cordillera, M. Colpron and J.L. Nelson (eds.), Geological Association of Canada, Special Paper 45, p. 1-23.

Deklerk, R. and Traynor, S., 2005. Yukon MINFILE – A database of mineral occurrences. Yukon Geological Survey, CD-ROM.

Hart, C.J.R. and Lewis, L.L., 2006. Gold mineralization in the upper Hyland River area: A nonmagmatic origin. *In:* Yukon Exploration and Geology 2005, D.S. Emond, G.D. Bradshaw, L.L. Lewis and L.H. Weston (eds.), Yukon Geological Survey, p. 109-125.

Héon, D., 2004. The Whitehorse Copper Belt, Yukon. An Annotated Geology Map. Yukon Geological Survey, Open File 2004-15.

Hunt, J.A., Abbott, J.G. and Thorkelson, D.J., 2006. Unconformity-related uranium potential: Clues from Wernecke Breccia, Yukon. *In:* Yukon Exploration and Geology 2005, D.S. Emond, G.D. Bradshaw, L.L. Lewis and L.H. Weston (eds.), Yukon Geological Survey, p. 127-137.

Soloviev, S.G, 2007 (this volume). New data on the geology and mineralization of the Skukum Creek gold-silver deposit, southern Yukon (NTS 105D/3). *In:* Yukon Exploration and Geology 2006, D.S. Emond, L.L. Lewis and L.H. Weston(eds.), Yukon Geological Survey, p. 253-268.

Traynor, S., 2007 (this volume). Yukon Mining Incentives Program Overview 2006. *In:* Yukon Exploration and Geology 2006, D.S. Emond, L.L. Lewis and L.H. Weston (eds.), Yukon Geological Survey, p. 53-54.

APPENDIX 1: 2006 EXPLORATION PROJECTS

Project name	Company	Minfile no.	NTS	Work type	Primary commodity	Deposit
PRECIOUS METALS – GOLD						
Ketza River	YGC Resources Ltd.	105F 019		P,G,GC,T,DD,PF	Au	skarn/ replacement
Skukum Creek	Tagish Lake Gold Corp.	105D 022A		G,DD,UG,PF	Au	vein/breccia
Lone Star	Klondike Star Mineral Corp.	115O 072		P,G,GP,GC,T,DD,BS	Au	vein/breccia
Dublin Gulch	StrataGold Corp.	106D 025		P,G,GC,T,DD	Au	porphyry/ sheeted vein
Golden Revenue	Northern Freegold Resources/ Atac Resources	115I 042		P,G,AGP,DD	Au	porphyry/ sheeted vein
Sonora Gulch	Firestone Ventures Inc.	115J 008		P,G,AGP,GC,DD	Au	porphyry/ sheeted vein
Mike Lake	Dynamite Resources Ltd.	116A 012A		G,AGP,GC,DD	Au	porphyry/ sheeted vein
Brewery Creek	Alexco Resource Corp.	116B 160		G,DD	Au	porphyry/ sheeted vein
Red Mountain Gold	Regent Ventures Ltd.	115P 006		G,AGP,DD	Au	porphyry/ sheeted vein
Shell Creek	Logan Resources Ltd.	116C 029		G,GP,GC,DD	Au	vein/breccia
Idaho Creek	Klondike Silver Corp./ Atac Resouces	115J 099		P,G,GP,DD	Au	vein/breccia
Moosehorn	Mountain Rio Resources	115N 024		P,G,GC,T,DD	Au	vein/breccia
Heidi	Logan Resources Ltd.	116A 037		G,DD	Au	porphyry/ sheeted vein
Dominion	Klondike Star Mineral Corp.	115O 066		P,G,GC,T,BS	Au	vein/breccia
Mount Hinton	Yukon Gold Corp.	105M 052		P,G,GC,RC	Au	vein/breccia
Scheelite Dome	Copper Ridge Exploration Inc.	115P 004		P,G,GP,GC,T	Au	skarn/ replacement
Eureka	Strategic Metals Ltd.	115O 057		G,T,DD	Au	vein/breccia
Grew Creek	Freegold Ventures Ltd.	105K 009		G,DD	Au	vein/breccia
Cheyenne	Logan Resources Ltd.	116B 096		P,G,GC,	Au	skarn/ replacement
Arn	Golden Reign Resources Ltd./ Atac Resources	115F 048		P,G,AGP,GC	Au	skarn/ replacement
Panorama	Atac Resources Ltd.	116A 031		P,G,AGP,GC,T	Au	porphyry/ sheeted vein
Crown Jewel	International Gold Resources Inc.	115O 139		P,G,GC	Au	vein/breccia
Klaza	Bannockburn Resources Ltd./ Atac Resources	115I 067		P,G	Au	vein/breccia

Abbreviations

AGP – airborne geophysics
BS – bulk sample
D – development
DD – diamond drilling
F – feasibility
G – geology
GC – geochemistry
GP – geophysics
M – mining
P – prospecting
PD – percussion drilling
PF – prefeasibility
R – reconnaissance
RC – reverse circulation drilling
T – trenching
U/GD – underground development

Appendix 1 (continued): 2006 EXPLORATION PROJECTS

Project name	Company	Minfile no.	NTS	Work type	Primary commodity	Deposit
Clear Creek	StrataGold Corp.	115P 023		P,G,GC,T	Au	porphyry/ sheeted vein
Spice	Klondike Gold Corp./ Tanana Exploration Inc.	105G 150		P,G,GC	Au	vein/breccia
Mahtin	International Gold Resources Inc.	115P 007		AGP	Au	porphyry/ sheeted vein
Bonanza	International Gold Resources Inc.	115 080		P,GC	Au	vein/breccia
Tinta Hill	Northern Freegold Resources	115I 058		P,G,GC	Au	vein/breccia
Hartless Joe	New Shoshoni Ventures Ltd./ Atac Resources	105D 203		P,AGP	Au	vein/breccia
Byng	New Shoshoni Ventures Ltd./ Atac Resources	105D 184		P,AGP	Au	vein/breccia
Horn	Ryanwood Explorations	New	105H/15	P,GP,GC	Au	vein/breccia
King Solomon Dome	Klondike Star Mineral Corp./ JAE Resources Inc.	115O 068		P,G,GC,T	Au	vein/breccia
Typhoon	Curlew Lake Resources Inc.	115P 060		G,GP,GC	Au	porphyry/ sheeted vein
Sey	Northern Freegold Resources/ Atac Resources	115I 121		P,G,GC	Au	vein/breccia
Goldy	Northern Freegold Resources	115I 112		AGP	Au	vein/breccia
Goldstar	Northern Freegold Resources	115I 053		AGP	Au	skarn/ replacement
Glen	Northern Freegold Resources	115I 120		AGP	Au	vein/breccia
Happy	Northern Freegold Resources	115I 106		P,G	Au	vein/breccia
Nitro	Northern Freegold Resources	115I 038		P,G	Au	porphyry/ sheeted vein
PRECIOUS METALS – SILVER						
Keno Hill	Alexco Resource Corp.	105M 001		P,G,AGP,T,DD	Ag	vein/breccia
CMC Silver (Silver Hart)	CMC Metals Ltd.	105B 021		P,G,T,DD	Ag	vein/breccia
Touchdown	Valencia Ventures Inc./ Strategic Metals	105B 022		P,G,GC,T	Ag	skarn/ replacement
Blue Heaven	Valencia Ventures Inc./ Strategic Metals	105B 020		P,G,GC,T,DD	Ag	vein/breccia
Qb	Valencia Ventures Inc./ Strategic Metals	105B 098		P,G,T	Ag	vein/breccia
Stump	Klondike Silver Corp.	105F 056		P,G	Ag	vein/breccia
Connaught	Klondike Silver Corp./ Atac Resources	115N 040		P,GP,GC,T,RC	Ag	vein/breccia

Abbreviations

AGP – airborne geophysics
BS – bulk sample
D – development
DD – diamond drilling
F – feasibility
G – geology
GC – geochemistry
GP – geophysics
M – mining
P – prospecting
PD – percussion drilling
PF – prefeasibility
R – reconnaissance
RC – reverse circulation drilling
T – trenching
U/GD – underground development

Appendix 1 (continued): 2006 EXPLORATION PROJECTS

Project name	Company	Minfile no.	NTS	Work type	Primary commodity	Deposit
Clark-Cameron	CMC Metals Ltd./ Tanana Exploration Inc.	106D 011		AGP	Ag	vein/breccia
Logjam	CMC Metals Ltd.	105B 038		P,G,GC	Ag	vein/breccia
End Zone	Valencia Ventures Inc./ Strategic Metals	105B 101		P,G,GC	Ag	skarn/ replacement
Pigskin	Valencia Ventures Inc./ Strategic Metals	105B 107		P,G	Ag	vein/breccia
BASE METALS – ZINC-LEAD						
Selwyn Project	Pacifica Resources Ltd.	105I 012		P,G,GC,DD	Zn-Pb	sediment associated
Blende	Eagle Plains Resources Ltd./ Blind Creek Resources	106D 064		P,G,GC	Zn-Pb	vein/breccia
Marg	Yukon Gold Corp. Inc.	106D 009		G,AGP,DD	Zn-Pb	volcanic associated
Wolverine	Yukon Zinc Corp.	105G 072		F	Zn-Pb	volcanic associated
Magnum	Klondike Silver/ Strategic Metals Ltd.	116C 118		G,AGP,DD	Zn-Pb	volcanic associated
Ultra	Klondike Star Mineral Corp.	115B 008		P,G,GC	Zn-Pb	volcanic associated
Swift	Yukon Zinc Corp.	105B 027		AGP	Zn-Pb	sediment associated
Pelly Mountain VMS	Eagle Plains Resources Ltd.	105F 012		P,G,AGP,GC,T	Zn-Pb	volcanic associated
Logan	Yukon Zinc Corp.	105B 099		AGP	Zn-Pb	vein/breccia
BASE METALS – COPPER						
Minto	Sherwood Copper Corp.	115I 021		G,GP,GC,T, DD,RC,PF,D	Cu	porphyry/ sheeted vein
Carmacks Copper	Western Copper Corp.	115I 008		G,DD	Cu	porphyry/ sheeted vein
Nor	International KRL Resources Corp.	106L 061		P,G,DD	Cu	Wernecke Breccia
Tidd	Sedex Mining Corp./ Strategic Metal	105J 029		P,G,AGP,GP, GC,T,DD	Cu	sediment associated
Lucky Joe	Copper Ridge Exploration Inc.	115O 051		G,GP,DD	Cu	porphyry/ sheeted vein
Nikki	ATAC Resources Ltd.	115K 082		P,G,AGP,GC,T	Cu	porphyry/ sheeted vein
Ironman	Copper Ridge Exploration Inc.	116A 017		G,GP,GC	Cu	Wernecke Breccia

Abbreviations

AGP – airborne geophysics
BS – bulk sample
D – development
DD – diamond drilling
F – feasibility
G – geology
GC – geochemistry
GP – geophysics
M – mining
P – prospecting
PD – percussion drilling
PF – prefeasibility
R – reconnaissance
RC – reverse circulation drilling
T – trenching
U/GD – underground development

Appendix 1 (continued): 2006 EXPLORATION PROJECTS

Project name	Company	Minfile no.	NTS	Work type	Primary commodity	Deposit
Hat	H. Coyne and Sons	105D 125		P,G,DD	Cu	skarn/ replacement
Yukon Olympic	Copper Ridge Exploration Inc.	116G 082		G,GP	Cu	Wernecke Breccia
Hopper	Strategic Metals Ltd.	115H 019		P,G	Cu	porphyry/ sheeted vein
Cuprum	Manson Creek Resources Ltd.	105E 008		P,G,GP,GC	Cu	skarn/ replacement
BASE METALS – NICKEL ± PLATINUM GROUP ELEMENTS						
Bandito	True North Gems Inc.	095C 051		P,G,AGP,GC,T,	Ni	skarn/ replacement
Wellgreen	Coronation Minerals/ Northern Platinum	115G 024		G,T,DD	Ni/PGE	mafic/ ultramafic associated
Canalask	Falconbridge Ltd./ StrataGold Corp.	115F 045		G,AGP,GP,GC	Ni/PGE	mafic/ ultramafic associated
Burwash	Golden Chalice Resources Inc./Strategic Metals	115G 100		P,G	Ni/PGE	mafic/ ultramafic associated
BASE METALS – TUNGSTEN						
Logtung (Northern Dancer)	Largo Resources Ltd./ Stategic Metals	105B 039		P,G,DD	W	porphyry/ sheeted vein
Tootsee	Cumberland Resources Ltd./ North American Tungsten	105B 089		P,G,AGP,DD	W	porphyry/ sheeted vein
Risby	Playfair Mining Ltd.	105F 034		G,DD	W	skarn/ replacement
MacTung	North American Tungsten	105O 002		F	W	skarn/ replacement
BASE METALS – MOLYBDENUM						
Red Mountain	Tintina Mines Ltd.	105C 009		G,DD,RC,PF	Mo	porphyry/ sheeted vein
BASE METALS – TIN						
Tin (JC)	Brett Resources Ltd.	105B 040		P,G,GP	Sn	skarn/ replacement

Abbreviations

AGP – airborne geophysics
BS – bulk sample
D – development
DD – diamond drilling
F – feasibility
G – geology
GC – geochemistry
GP – geophysics
M – mining
P – prospecting
PD – percussion drilling
PF – prefeasibility
R – reconnaissance
RC – reverse circulation drilling
T – trenching
U/GD – underground development

Appendix 1 (continued): 2006 EXPLORATION PROJECTS

Project name	Company	Minfile no.	NTS	Work type	Primary commodity	Deposit
BASE METALS – URANIUM						
Igor	Cash Minerals Ltd./ Twenty Seven Capital Corp.	106E 009		P,G,GC,DD	U	Wernecke Breccia
Slab	Fronteer Development Group Inc./Rimfire Minerals	106D 070		P,G,AGP,GC	U	Wernecke Breccia
Lumina	Cash Minerals Ltd./ Twenty Seven Capital Corp.	106C 069		P,G,AGP,GC,DD	U	Wernecke Breccia
Curie	Signet Minerals Inc.	106E 031		P,G,AGP,GC	U	Wernecke Breccia
Hot Dog	Cash Minerals Ltd./ Twenty Seven Capital Corp.	115H 014		P,G,DD	U	volcanic associated
Pedlar	Cash Minerals Ltd./ Twenty Seven Capital Corp.	115J 092		P,G,DD	U	porphyry/ sheeted vein
Murphy	Signet Minerals Inc./ Twenty Seven Capital Corp.	105F 079		G,AGP,DD	U	porphyry/ sheeted vein
Steel	Cash Minerals Ltd./ Twenty Seven Capital Corp.	106D 049		P,G,DD	U	Wernecke Breccia
Vic	Cash Minerals Ltd./ Twenty Seven Capital Corp.	106D 072		P,G,AGP,GC,T,DD	U	Wernecke Breccia
Bonnie	Cash Minerals Ltd./ Twenty Seven Capital Corp.	new	106C/13	P,G,AGP,T,GC,DD	U	Wernecke Breccia
Angel	Cash Minerals Ltd./ Twenty Seven Capital Corp.	new	106D/15	P,G,AGP,GC,T,DD	U	Wernecke Breccia
Dolores	Cash Minerals Ltd./ Twenty Seven Capital Corp.	106C 013		P,G,AGP	U	Wernecke Breccia
Pike	Signet Minerals Inc./ Twenty Seven Capital Corp.	106E 040		P,G,AGP	U	Wernecke Breccia
Bond	Cash Minerals Ltd./ Twenty Seven Capital Corp.	106D 065		P,G,AGP	U	Wernecke Breccia
Alle	Cash Minerals Ltd./ Twenty Seven Capital Corp.	105B 126		P,G,AGP	U	porphyry/ sheeted vein
GEMSTONES						
Tsa da Glizsa	True North Gems Inc.	105G 147		P,G,T,BS	gemstones	gemstones
COAL						
Division Mountain	Cash Minerals Ltd.	115H 013		G,DD	coal	industrial minerals
Rock River Coal	Almaden Minerals Ltd./ Santoy Resources	095D 026		G,DD	coal	industrial minerals
Tantalus Butte	Cash Minerals Ltd.	115I 003		G,DD	coal	industrial minerals

Abbreviations

AGP – airborne geophysics
BS – bulk sample
D – development
DD – diamond drilling
F – feasibility
G – geology
GC – geochemistry
GP – geophysics
M – mining
P – prospecting
PD – percussion drilling
PF – prefeasibility
R – reconnaissance
RC – reverse circulation drilling
T – trenching
U/GD – underground development

APPENDIX 2: 2006 DRILLING STATISTICS

Company	Property	# drill holes	Diamond drilling (m)	Percussion/ reverse circulation (m)
Alexco Resource Corp.	Brewery Creek	9	1184	
Alexco Resource Corp.	Keno Hill	42	11 500	
Almaden Minerals Ltd./Santoy Resources Ltd.	Rock River Coal	2	888	
Cash Minerals Ltd./Twenty Seven Capital Corp.	Angel	2	300	
Cash Minerals Ltd./Twenty Seven Capital Corp.	Vic	3	652	
Cash Minerals Ltd./Twenty Seven Capital Corp.	Bonnie	3	490	
Cash Minerals Ltd./Twenty Seven Capital Corp.	Lumina	22	2600	
Cash Minerals Ltd./Twenty Seven Capital Corp.	Pedlar	5		733
Cash Minerals Ltd./Twenty Seven Capital Corp.	Steel	2	900	
Cash Minerals Ltd./Twenty Seven Capital Corp.	Hot Dog	8	433	
Cash Minerals Ltd./Twenty Seven Capital Corp.	Igor	23	3000	
Cash Minerals Ltd.	Division Mountain	7	667	806
Cash Minerals Ltd.	Tantalus Butte	7	942	
CMC Metals Ltd.	CMC Silver (Silver Hart)	10	725	
Copper Ridge Exploration Inc.	Lucky Joe	3	780	
Coronation Minerals Inc./Northern Platinum Ltd.	Wellgreen	11	1936	
Cumberland Resources Ltd./North American Tungsten	Tootsee	3	1496	
Dynamite Resources Ltd.	Mike Lake	10	1698	
Eagle Plains Resources Ltd./Blind Creek Resources	Blende	23	4230	
Firestone Ventures Inc.	Sonora Gulch	12	1821	
International KRL Resources Corp.	Nor	9	1600	
Klondike Silver Corp./Atac Resources	Idaho Creek	5		555
Klondike Star Mineral Corp.	Lone Star	23	2892	
Largo Resources Ltd./Stategic Metals	Logtung (Northern Dancer)	17	3945	
Logan Resources Ltd.	Heidi	3	427	
Logan Resources Ltd.	Shell Creek	3	400	
Mountain Rio Resources	Moosehorn	24	2250	
Northern Freegold Resources/Atac Resources	Golden Revenue	26	4798	2165
Pacifica Resources Ltd.	Howards Pass	191	39 900	
Playfair Mining Ltd.	Risby	4	1000	
Regent Ventures Ltd.	Red Mountain Gold	5	1162	
Sedex Mining Corp./Strategic Metals	Tidd	16	1887	
Sherwood Copper Corp.	Minto	119	24 252	
Signet Minerals Inc.	Murphy	4	384	
StrataGold Corp.	Dublin Gulch	10	4280	
Strategic Metals Ltd.	Eureka	10		830
Klondike Silver Corp./Strategic Metals	Magnum	2	338	
Tagish Lake Gold Corp.	Skukum Creek	72	6452	

Appendix 2 (continued): 2006 DRILLING STATISTICS

Company	Property	# drill holes	Diamond drilling (m)	Percussion/ reverse circulation (m)
Tintina Mines Ltd.	Red Mountain	2	173	
Valencia Ventures Inc./Strategic Metals	Blue Heaven	4	517	
Western Copper Corp.	Carmacks Copper	34	7204	742
YGC Resources Ltd.	Ketza River	238	29 500	
Yukon Gold Corp./Atna Resources	Marg	9	2987	
TOTAL			**172 590**	**5831**

Yukon Placer Mining Overview 2006

***William LeBarge*[1]**
Yukon Geological Survey

LeBarge, W., 2006. Yukon Placer Mining Overview 2006. *In:* Yukon Exploration and Geology 2007, D.S. Emond, L.L. Lewis and L.H. Weston (eds.), Yukon Geological Survey, p. 49-52.

PLACER MINING

Today, more than 100 years after the discovery of gold in the Yukon, placer mining is still an important sector in the Yukon's economy. Over 16.6 million crude ounces (518 tonnes) of placer gold have been produced to date in the Yukon — at today's prices that would be worth more than $9 billion.

Approximately 350 people were directly employed at 115 placer mines in 2006 — and several hundred more were employed in businesses and industries that serve the placer mining industry. Most of the placer operations were small and family-run, with an average of three or four employees.

A cold spring and the resulting remnant ground frost created a delay in the start of mining for many operations, but a warm autumn allowed several mines to continue sluicing late in the season. Many mine operators had difficulty obtaining skilled workers, and this affected their operations as they were forced to eliminate a shift or decrease operating hours.

The majority of active placer mining operations were in the Dawson Mining District, followed by the Whitehorse Mining District and the Mayo Mining District. No placer mines were active in the Watson Lake Mining District.

The total Yukon placer gold production in 2006 was 58,294 crude ounces (1 813 147 g), compared to 70,322 crude ounces (2 187 260 g) in 2005. The value of this 2006 gold production was $31.8 million.

Approximately 87% of the Yukon's placer gold was produced in the Dawson Mining District, which includes the unglaciated drainages of Klondike River, Indian River, west Yukon (Fortymile and Sixtymile rivers) and the lower Stewart River (Fig. 1). The remaining gold came from the unglaciated Moosehorn Range in the Whitehorse Mining District, and other placer districts in the glaciated Mayo and Whitehorse mining districts which include Clear Creek, Mayo, Dawson Range, Kluane, Livingstone and Whitehorse South.

Reported placer gold production from Indian River drainages in 2006 dropped from 2005, from 26,473 crude ounces (823 403 g) to 18,008 crude ounces (560 111 g). Decreases were seen in all drainages but the largest shortfalls were from Indian River and Dominion and Sulphur creeks.

In Klondike-area drainages, production increased to 15,442 crude ounces (480 300 g) from 12,627 crude ounces (392 744 g) in 2005. Notable increases were seen on Klondike River, Bear Creek and Paradise Hill on Hunker Creek.

[1]*bill.lebarge@gov.yk.ca*

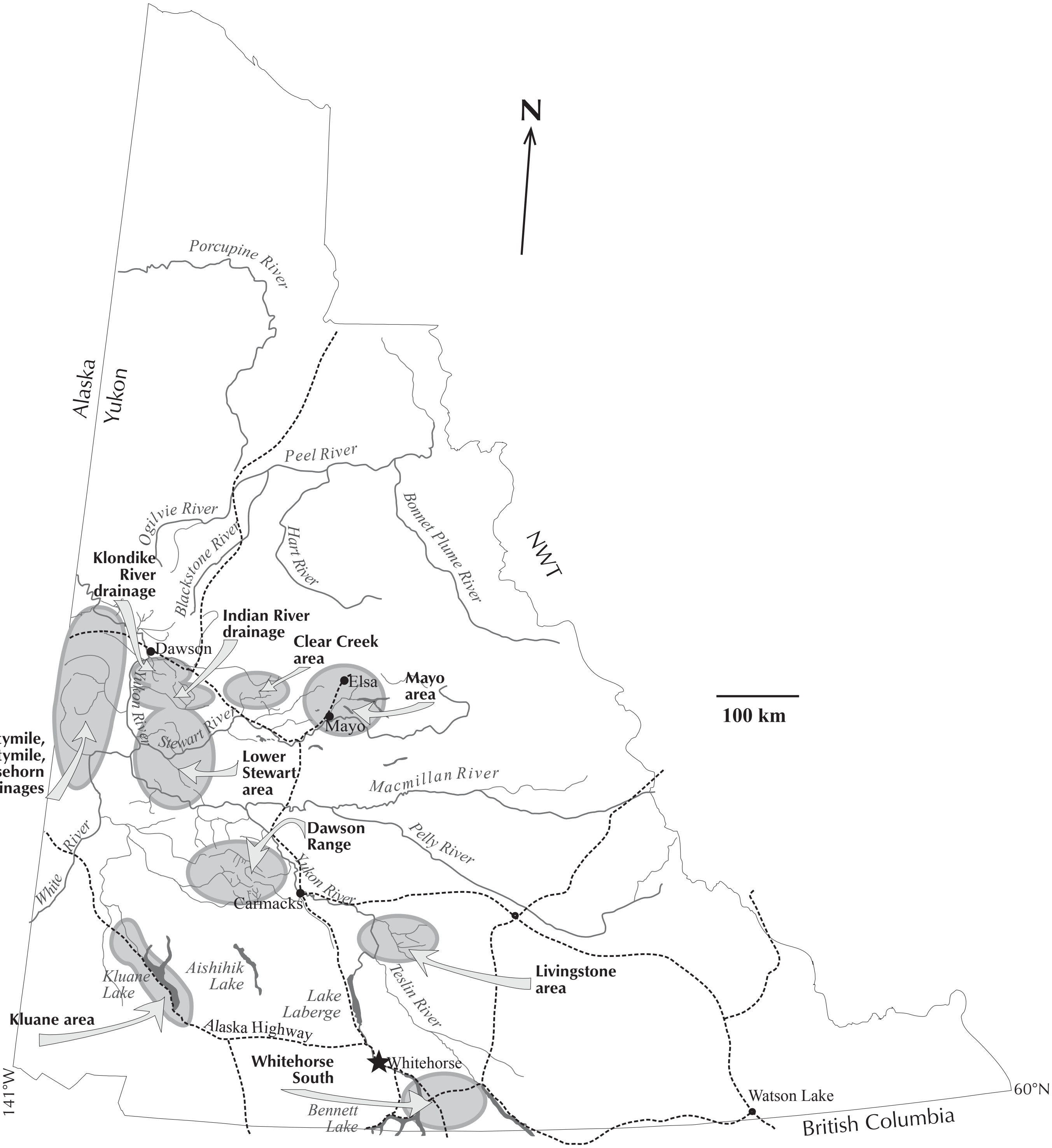

Figure 1. Yukon placer mining areas.

West Yukon (Sixtymile, Fortymile and Moosehorn Range) placer gold production decreased from 12,314 crude ounces (383 008 g) in 2005 to 9333 crude ounces (290 289 g) in 2006. The largest drop was from Sixtymile River, while Matson Creek and Ten Mile Creek saw slight increases.

Reported production from operations in the Lower Stewart drainages was also down in 2006, to a total of 7884 crude ounces (245 220 g) from 9572 crude ounces (297 722 g) the previous year. All operations reported less gold with the exception of Henderson Creek, which increased substantially.

As usual, little gold was reported from Clear Creek drainages although several operations were active in 2006. The total reported gold from royalties decreased slightly from 255 crude ounces (7931 g) to 232 crude ounces (7216 g).

In the Dawson Range area, reported placer gold production dropped to less than half of the 2005 total, from 1545 crude ounces (48 054 g) to 735 crude ounces (22 861 g).

In the Mayo area, gold production decreased from 2340 crude ounces (72 782 g) to 1471 crude ounces (45 753 g).

In the Kluane area, reported placer gold production dropped from 2667 crude ounces (82 953 g) to 2260 crude ounces (70 294 g).

The Livingstone area remained inactive, although 64 crude ounces (1991 g) of gold were reported.

In the Whitehorse South area, Iron Creek produced 24.8 crude ounces (771 g), roughly the same as the 2005 total of 27.4 crude ounces (852 g).

PLACER EXPLORATION

Placer miners throughout the Yukon continue to explore for new deposits, using traditional methods such as auger, reverse circulation and churn drilling, and more recent innovations including ground-penetrating radar and magnetometer surveys. Trenching and bulk sampling also continue to be well-used methods of testing placer ground.

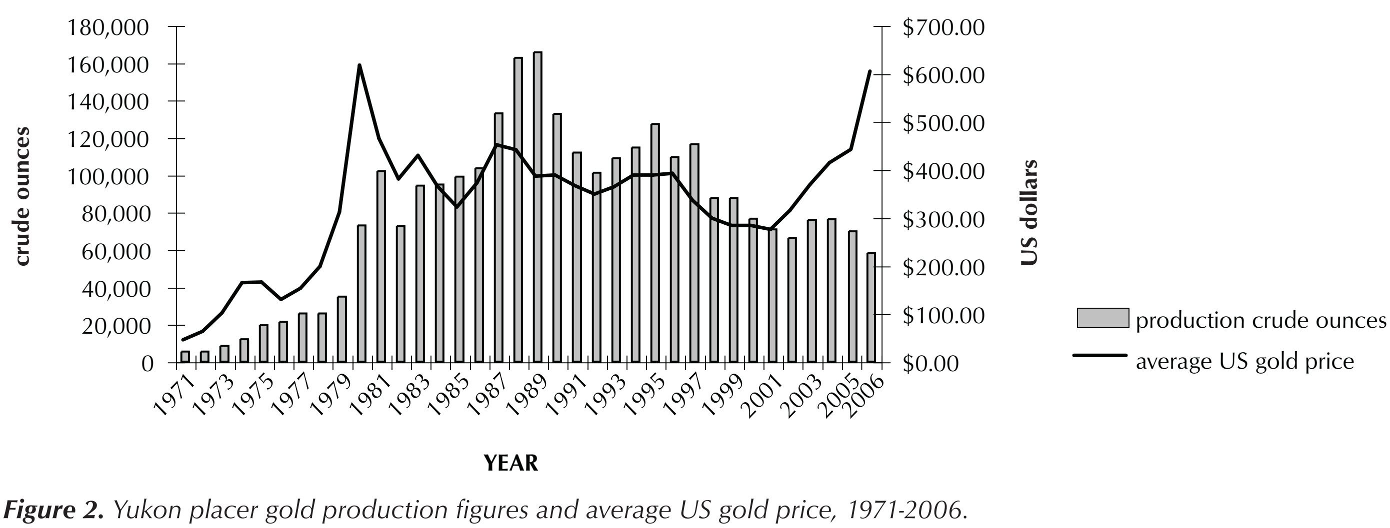

Figure 2. *Yukon placer gold production figures and average US gold price, 1971-2006.*

Several large mining operations were relocated to new ground in 2006, the result of both favourable exploration results in new areas and diminishing or exhausted reserves in extensively mined areas. This appears to have had a negative effect on the amount of gold produced as operators expended time, effort and money towards setting up new mines instead of sluicing gravel at established properties.

One of the exploration highlights of 2006 was the extensive development of the lower Sixtymile River drainage between the mouth of Ten Mile Creek and the confluence of Sixtymile River and Yukon River. In addition to testing and mining of several areas in the main valley and adjacent benches, several kilometres of road and an airstrip were constructed. This improved access is favourable for increased development and testing of nearby drainages such as Twenty Mile Creek and Thirteen Mile Creek, as well as the upstream reaches of the Sixtymile River.

The staff at the Yukon Geological Survey and the Client Services and Inspection Division (Department of Energy, Mines and Resources, Yukon government) can provide information and advice regarding placer mining in the Yukon. Publications on placer mining in the Yukon are available through the Yukon Geological Survey office at Room 102, Elijah Smith Building, 300 Main St., Whitehorse, Yukon. Many recent publications and maps can be downloaded for free from our website at *www.geology.gov.yk.ca,*

APERÇU

Aujourd'hui, plus de cent ans après la découverte des premiers gisements d'or dans le Yukon, l'exploitation des placers reste un important secteur de l'économie du Yukon. Plus de 16,6 millions d'onces brutes (518 tonnes) d'or placérien ont été produites à ce jour au Yukon, ce qui représente plus de 9 milliards $ au prix actuel de l'or.

Près de 350 personnes étaient employées directement sur des placers en 2006 et plusieurs centaines d'autres étaient employées dans des entreprises et des industries au service de l'industrie des placers. La plupart des placers sont de petites entreprises familiales qui emploient en moyenne trois à quatre employés.

La majorité des placers encore actifs sont situés dans le district minier de Dawson, le restant se trouvant dans les districts miniers de Whitehorse et de Mayo. Il n'y a présentement aucune mine active dans le district minier de Watson Lake.

La production d'or dans les placers du Yukon a totalisé 58 294 d'onces brutes (1 813 147 g) en 2006 alors qu'elle s'élevait à 70 322 onces brutes (2 187 260 g) en 2005. La production d'or en 2006 est évaluée à 31,8 millions $.

Approximativement 87 % de l'or placérien du Yukon a été produit dans le district minier de Dawson qui inclut les drainages non englacés de la rivière Klondike, de la rivière Indian, de l'Ouest du Yukon (rivières Fortymile et Sixtymile) et le cours inférieur de la rivière Stewart. Le reste de l'or a été extrait de la chaîne non englacée Moosehorn dans le district minier de Whitehorse et d'autres districts placériens dans les districts miniers englacés de Mayo et de Whitehorse qui comprennent Clear Creek, Mayo, la chaîne Dawson, Kluane, Livingstone et Whitehorse Sud.

Yukon Mining Incentives Program Overview 2006

***Steve Traynor*[1]**
Yukon Geological Survey

Traynor, S., 2007. Yukon Mining Incentives Program Overview 2006. *In:* Yukon Exploration and Geology 2006, D.S. Emond, L.L. Lewis and L.H. Weston (eds.), Yukon Geological Survey, p. 53-54.

The Yukon Mining Incentives Program (YMIP) received 62 applications for funding by the March 1, 2006 submission deadline. Contribution agreements totaling $880 600 were subsequently issued to 53 successful applicants. Proposals approved for funding included 5 under the Grassroots-Prospecting module, 17 under the Focused Regional module and 31 under the Target Evaluation module.

Gold continued to be the main commodity of exploration interest and was the focus of 34 of the projects which received approval for YMIP funding. Projects targeting copper and zinc-lead accounted for nine and six projects, respectively. While four other applicants explored for gemstones (2), molybdenum (1) and uranium (1). This year saw an increase in approved applicants proposing placer-related projects, with over 25% of the successful applicants undertaking placer exploration and testing programs.

Feedback, requested this year in the form of a survey, revealed that almost half of those responding would not have undertaken many of the exploration projects carried out in the Yukon in the past five years had YMIP funding not been available. Most of this group of respondents includes local private companies and/or aggressive and experienced prospectors who are currently attracting significant amounts of junior exploration capital to the Territory.

The program is achieving its goal of stimulating grassroots exploration, which is critical in maintaining a supply of projects with potential for new discoveries and advanced exploration. In fact, half of the 140 projects active in 2006 in the Yukon are either currently receiving YMIP funding or are projects that have been optioned off to listed junior companies following their initial discovery through past YMIP-funded projects.

In the process of stimulating exploration for new grassroots targets, programs such as the Yukon Mining Incentives Program continue to encourage new mining industry spending and contribute to activities that may lead to the development of new mines. Widely acclaimed by prospectors and industry alike, these programs are the cornerstones of healthy mining industries in jurisdictions which promote and support their existence through continued and stable levels of funding.

RÉSUMÉ

Soixante deux demandes de financement ont été déposées dans le cadre du Programme d'encouragement des activités minières au Yukon (PEAMY) avant la date limite de présentation des demandes (1er mars 2006). Des accords de contribution, d'une valeur totale de 880 600 $, ont par la suite été paraphés avec 53 demandeurs. Les propositions dont le financement a été approuvé comprennent 5 projets d'exploration primaire et de prospection, 17 projets dans des régions sous-

[1]*steve.traynor@gov.yk.ca*

explorées et 31 projets visant à faciliter l'évaluation de cibles.

L'or demeure le produit suscitant le plus d'intérêt dans le domaine de l'exploration et il est le point de mire de 34 des projets financés par le PEAMY. Neuf projets approuvés portent sur le cuivre et six sur le plomb zinc. Quatre autres projets sont axés sur des activités d'exploration à la recherche de gemmes (2), de molybdène (1) et d'uranium (1). Cette année a été marquée par une hausse du nombre de projets centrés sur des placers qui ont été approuvés, plus de 25 % des projets approuvés consistant en des programmes d'essai et d'exploration de placers.

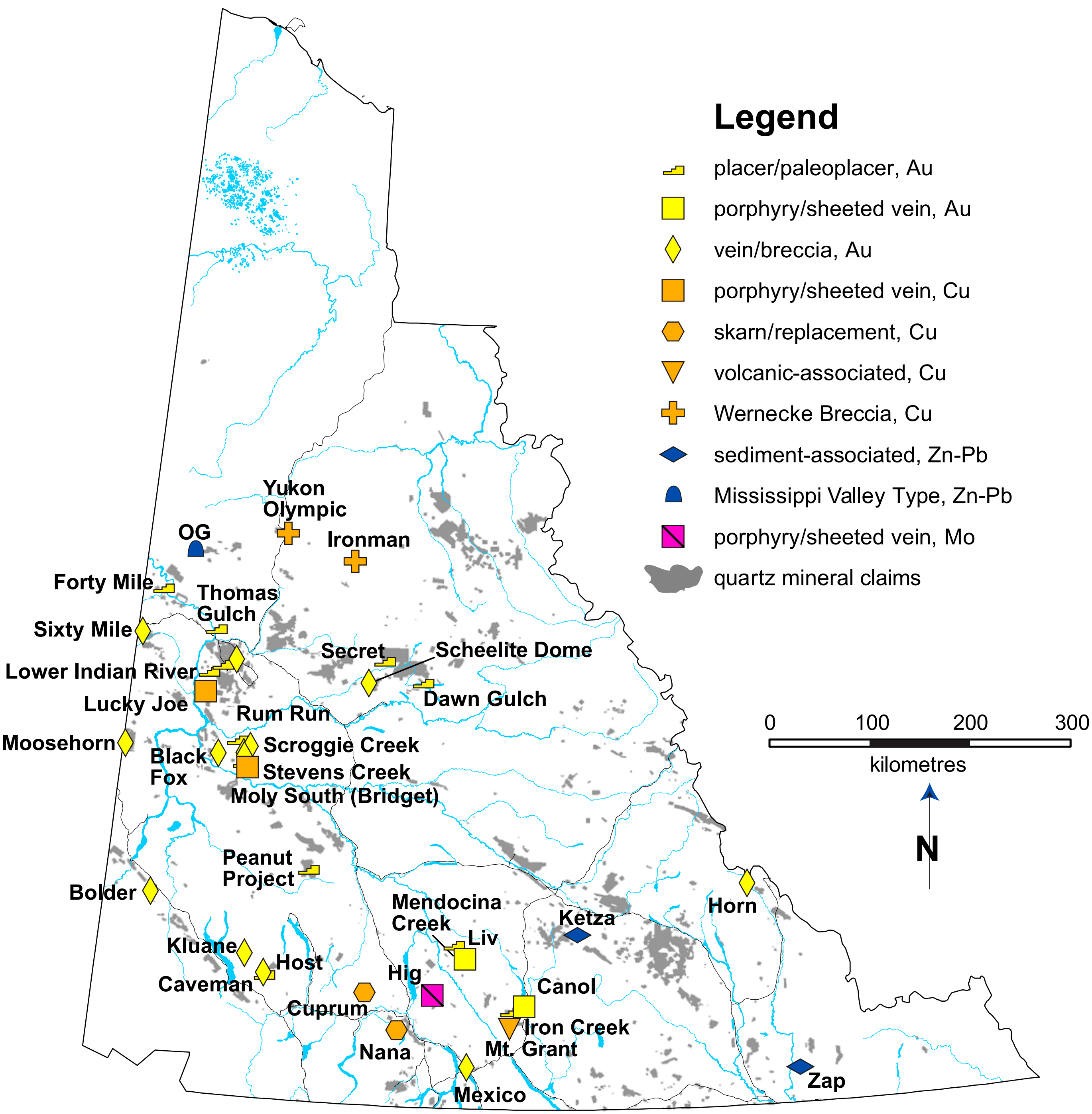

Figure 1. *2006 Yukon Mining Incentives Program project locations.*

GOVERNMENT

Yukon Geological Survey

Grant Abbott and staff
Yukon Geological Survey

Overview 57
Projects 58
Programs 62
Information management and distribution 63
2006 publications and maps 66

La Commission géologique du Yukon

Grant Abbott et Maurice Colpron
La Commission géologique du Yukon

Sommaire d'activités 73
Travaux sur le terrain 73
Diffusion de l'information 76

Robert E. Leckie Awards for Outstanding Reclamation Practices

Judy St. Amand
Mining Lands, Energy, Mines and Resources

Outstanding Quartz Reclamation 77
Outstanding Placer Reclamation 78

Yukon Geological Survey

Grant Abbott[1] and staff

Abbott, J.G. and staff, 2007. Yukon Geological Survey. *In:* Yukon Exploration and Geology 2006, D.S. Emond, L.L. Lewis and L.H. Weston (eds.), Yukon Geological Survey, p. 57-71.

OVERVIEW

The Yukon Geological Survey (YGS; Fig. 1) is recovering from the tragic loss of Geoff Bradshaw, our Mineral Assessment Geologist, in a helicopter accident over the summer. We thank so many of our colleagues in the geological and mining communities for their tremendous sympathy and support. We are also adjusting to the departure of geologists Craig Hart and Julie Hunt to the sunny climes of Australia. We wish them well, and thank them for their significant contributions to Yukon geology. We welcome three new staff: Carrie Labonte took over from Monique Raitchey in March as office manager; Aubrey Sicotte came on board in January 2007 as spatial data administrator; and Yana Fedortchouk joined us for six months as a project geologist.

YGS has a new organizational structure (Fig. 2) with four main subdivisions. New responsibilities go to Mike Burke as Acting Head of Mineral Services; Diane Emond as Acting Head of Technical

Figure 1. *Yukon Geological Survey staff from left to right: Grant Abbott, Tiffani Fraser, Don Murphy, Charlie Roots, Tammy Allen, Mike Burke, Lee Pigage, Karen Pelletier, Carrie Labonte, Lara Lewis, Jeff Bond, Olwyn Bruce, Leyla Weston, Panya Lipovsky, Diane Emond, Steve Israel, Ali Wagner, Maurice Colpron, Steve Traynor, Bill LeBarge, Rod Hill, Robert Deklerk. Absent: Grant Lowey, Yana Fedortchouk.*

[1]grant.abbott@gov.yk.ca

Services; Don Murphy as Acting Head of Regional Geology; and Lee Pigage as Acting Head of Resource Assessments and Outreach.

YGS continued to enjoy stable core funding, and also benefited significantly from the DIAND Targeted Investment Program under the Strategic Investments in Northern Economic Development (SINED) Fund. SINED funding enabled us to undertake large geochemical and geophysical surveys that would not have otherwise been possible.

The Technical Liaison Committee to the YGS reviews our program twice a year. We are grateful to Chair Gerry Carlson and the committee for their valuable support and constructive advice. This year Greg Lynch from Shell Canada joined the committee to represent Oil and Gas interests. Other members are Rob Carne, Shawn Ryan, Al Doherty, Jean Pautler, Forest Pearson, Jim Mortensen and Jim Christie.

PROJECTS

The YGS completed or supported 24 field projects in 2006. They are listed on the following pages. This year included a diversity of work that reflects our mandate to support hydrocarbon development and to meet increased demands for baseline data to address environmental and development issues, while continuing to support our primary client, the mineral industry. Projects included 1:50 000-scale bedrock mapping, mineral deposit studies, surficial studies and mapping, regional stream sediment geochemistry, an aeromagnetic survey and topical geology studies. However, with the tragic events of the summer, and departure of key staff, our capacity to undertake mineral deposits studies has been significantly diminished.

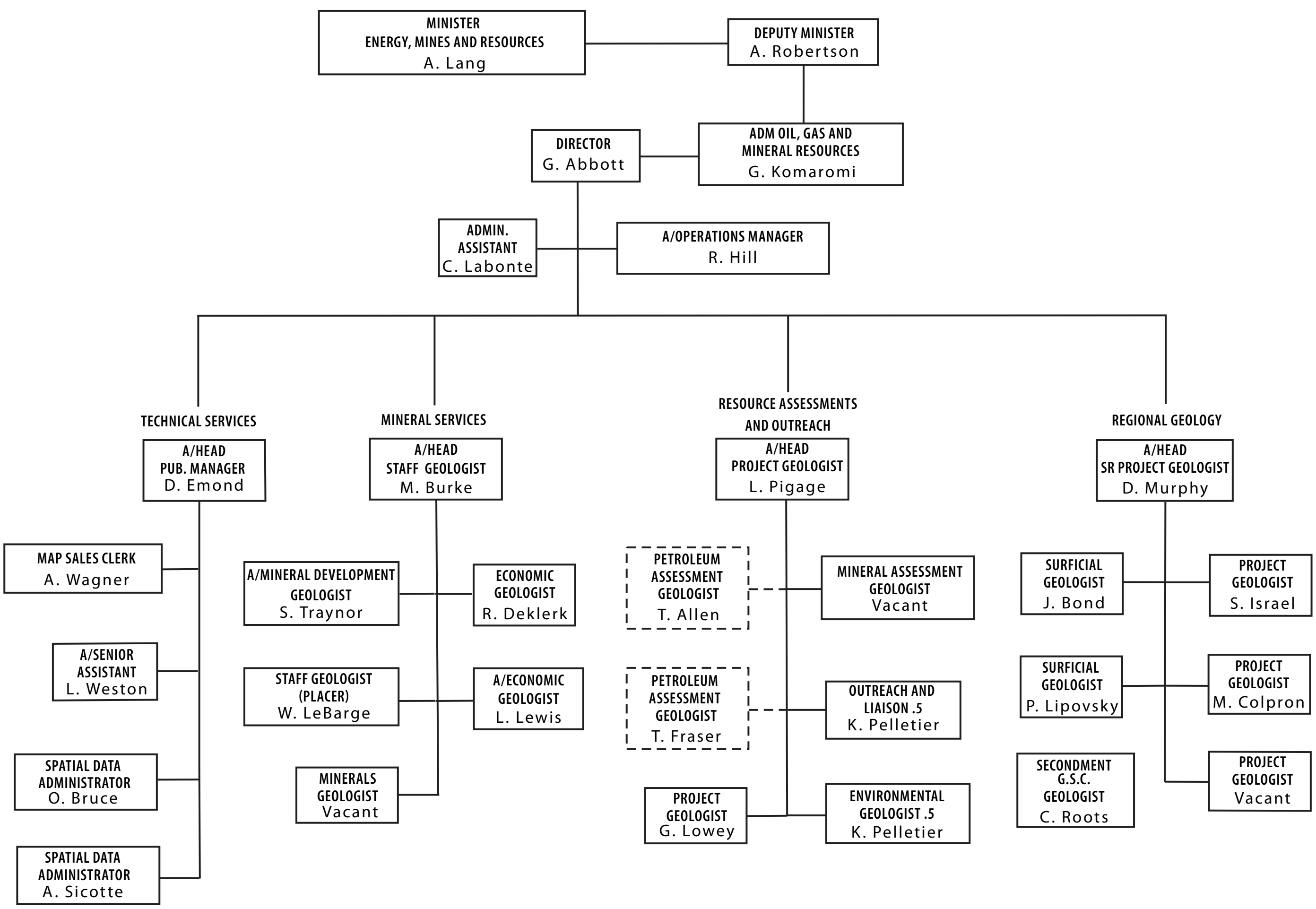

Figure 2. *Yukon Geological Survey organization chart.*

BEDROCK MAPPING

1. **Maurice Colpron** teamed up with **Steve Gordey** (Geological Survey of Canada [GSC]), **Grant Lowey, Steve Piercey** (Laurentian University) and **Don Murphy** to map the northwestern portion of Whitehorse Trough. This map provides ground control of the bedrock geology along the western portion of the seismic survey acquired in 2004 by GSC/YGS. Compilation and interpretation of the various geoscience datasets is underway and will provide the basis for reassessing the oil and gas potential of northern Whitehorse Trough.

2. **Lee Pigage** began a mapping project in the Otter Creek area (NTS 95D/6) of southeast Yukon. This project is a continuation of his earlier work in the Pool Creek and Toobally Lakes areas, and will improve our understanding of structure, stratigraphy and mineral potential of the southeast margin of Selwyn Basin.

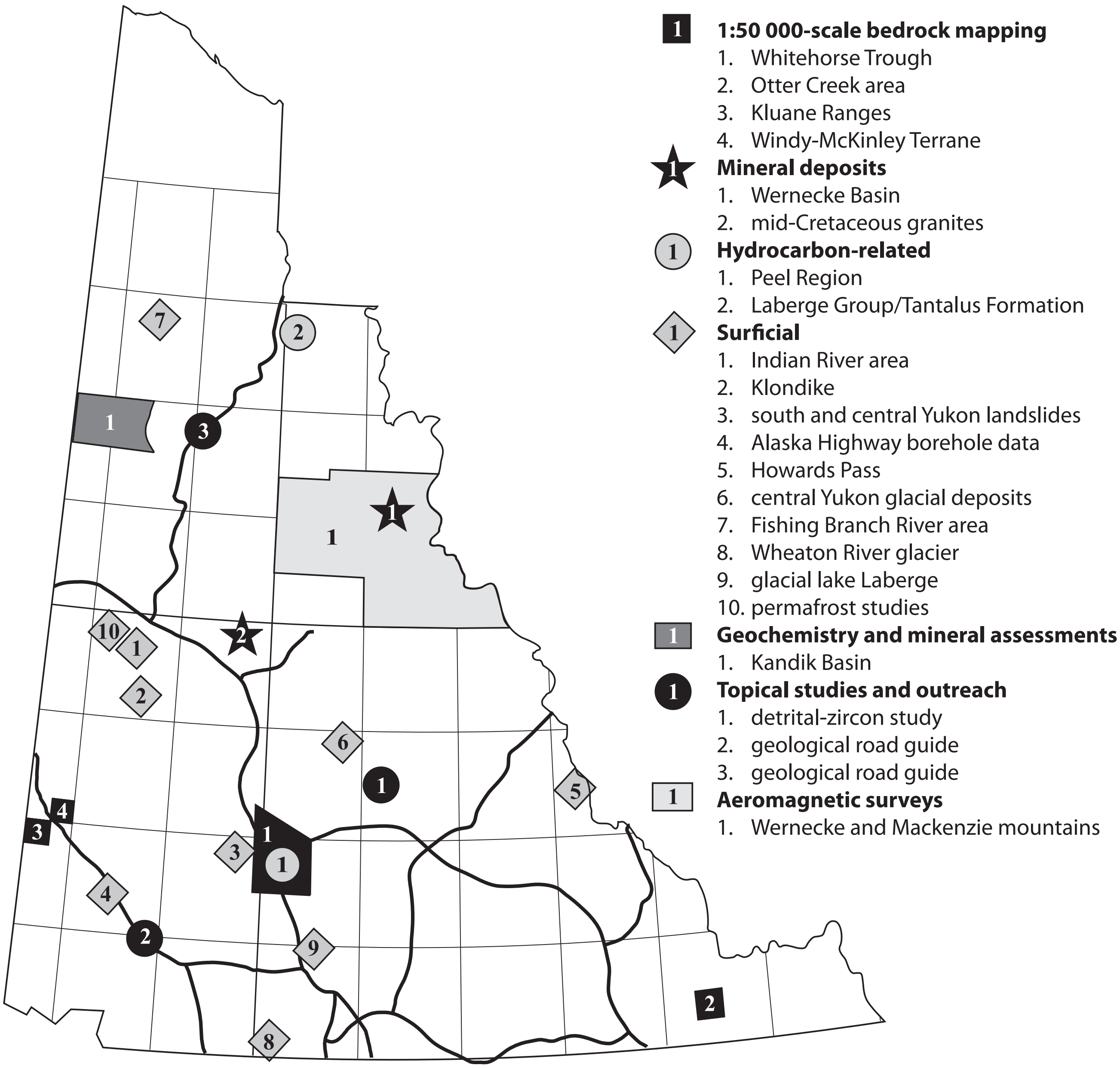

Figure 3. *Field projects carried out or sponsored by the Yukon Geological Survey in 2006.*

3. **Steve Israel** continued mapping in the Kluane Ranges, focusing on Late Paleozoic strata of the Skolai Group east of the White River where it is host to Triassic mafic-ultramafic intrusions that host nickel, copper and platinum-group-element mineralization. In conjunction with **Jim Mortensen** of the University of British Columbia (UBC), this project is also examining the provenance of Wrangell Terrane through detrital-zircon studies of Middle Triassic and Late Paleozoic sedimentary deposits. Studies of the young deformation associated with the Denali Fault are also taking place in collaboration with **Don Murphy** (YGS) and workers from the USGS in Alaska.
4. **Don Murphy** conducted a reconnaissance of the poorly exposed, poorly understood Windy-McKinley Terrane. As originally defined in central Alaska, the Windy and McKinley terranes comprise ophiolitic rocks of unknown age, and mélange and flysch of Mesozoic age. Little is known about the original relationships, if any, between these components and adjacent rocks of Yukon-Tanana Terrane. Don's work will document the nature of these assemblages in Yukon, thereby providing a basis for mineral exploration decisions and land-use planning in the area.

MINERAL DEPOSIT STUDIES

1. **Lara Lewis** gathered data on intrusion-related and Wernecke Breccia uranium occurrences for a compilation on uranium exploration in Yukon. She is studying the enigmatic uranium occurrences associated with Wernecke Breccia. New U-Pb dates for uranium mineralization are expected to provide constraints on timing of mineralizing events.
2. **Jake Hanley** and **Ed Spooner** (University of Toronto) are continuing a post-doctoral study of the evolution and generation of magmatic fluids in mid-Cretaceous granites in Yukon and their relationship to gold mineralization.

HYDROCARBON-RELATED STUDIES

1. **Tammy Allen** and **Tiffani Fraser** began a four-year project assessing the hydrocarbon potential of the Peel Region in northeastern Yukon. The study involves collaboration with the GSC, the Northwest Territories Geoscience Office, industry and university affiliates. The focus this year is the Upper Devonian – Lower Carboniferous Tuttle Formation. A major objective of this project is to assess the Tuttle as a potential petroleum reservoir, and to examine neighbouring units as petroleum sources. Another objective is to clarify stratigraphic relationships and sedimentology of Upper Paleozoic strata.
2. **Grant Lowey** continued studies of the sedimentology, stratigraphy and hydrocarbon potential of the Laberge Group and Tantalus Formation in the Whitehorse Trough, where studies last year discovered petroleum fluid inclusions and identified two potential petroleum source rocks. He also assisted M. Colpron in 1:50 000-scale bedrock mapping of the northern part of this frontier petroleum basin.

SURFICIAL STUDIES

1. Yukon Geological Survey placer geologist **William LeBarge, Dr. Vladimir Naumov** (Perm University, Russia) and **Dr. Rob Chapman** (University of Leeds, United Kingdom) are studying the sedimentology, stratigraphy and gold characteristics of gravel and conglomerate deposits in the Indian River area. These gravel terraces and the underlying conglomerates are currently the focus of exploration by Boulder Mining Corporation and Klondike Star. New interpretations of geology and data from this study will further characterize the nature of the placer gold distribution in the Indian River drainage and may help to identify new placer reserves, locally, and in nearby drainages. This research complements a study by **Dr. Jim Mortensen** at UBC, focusing on the trace-element characteristics of placer gold in the Klondike, which may help to reveal potential undiscovered lode gold sources.

2. **Jeff Bond,** in partnership with **Paul Sanborn** and **Scott Smith**, continued their studies of the unglaciated soils in the Klondike. This year, Jeff undertook a geochemical investigation of the soils at the original Boulder Lode mine site on the Lone Star property. In addition, upland cryosols (permafrost-affected soils) were studied on the Lone Star property. Assisting with this investigation is **Kathryn Denommee** from the University of Waterloo. Her undergraduate thesis involves mapping the surficial materials on a typical north-facing unglaciated slope from the Lone Star property.

3. **Panya Lipovsky** continued work monitoring permafrost-thaw-related landslides in south and central Yukon. In collaboration with C-CORE and the European Space Agency, InSAR, remote sensing technology and high-precision GPS surveys were used to monitor small-scale ground movements at five landslide sites near Beaver Creek, Carmacks and Little Salmon Lake. A reconnaissance inventory of landslides in the Pelly River watershed was also undertaken.

4. **Erin Trochim** and **Panya Lipovsky** continued their compilation of Yukon Department of Highways borehole data to capture detailed geotechnical and permafrost information. Their work has extended the data set to cover the Alaska Highway from Beaver Creek to east of Haines Junction.

5. **Derek Turner** and **Brent Ward** (Simon Fraser University), and **Jeff Bond** began a study looking at the glacial history of the Howards Pass property in the Selwyn Mountains. The work is being completed through Derek Turner's MSc thesis. His project involves reconstructing the late glacial history of the Selwyn Lobe of the Cordilleran ice sheet, mapping the surficial geology of Pacifica Resources' property and conducting a mobile metal ion geochemistry case study across the SEDEX deposit.

6. ***Brent Ward*** and **Jeff Bond** continued their investigation into the age of Reid glacial deposits in central Yukon. This involved sampling for cosmogenic dating and tephra chronology in the Pelly River area.

7. **Nicholas Utting** and **Ian Clark** (University of Ottawa), in cooperation with YGS, conducted a study on the water chemistry and noble gases in perennial springs at Bear Cave Mountain, Fishing Branch River area. This work is to address First Nation concerns about potential disturbance of groundwater during hydrocarbon exploration.

8. **Monica Bruckner, Mark Skidmore** and **Jeff Bond —** Monica conducted her Master's thesis field research (Montana State University) on one of the Wheaton River glaciers this past summer. She is investigating the biogeochemical characteristics of meltwater in a deglaciating basin.

9. **Stephen Horton** (University of Victoria), **Jeff Bond** and **Peter Von Gaza** (Geomatics Yukon) — Stephen's undergraduate research involves reconstructing the paleogeography of glacial lake Laberge.

10. **Dr. Antoni Lewkowicz** and graduate students from the University of Ottawa continued with a number of permafrost studies around the Territory. They have been documenting the effects of the 2004 forest fires near Dawson on slope stability and sedimentation into watercourses, investigating the origin and dynamics of thermokarst lakes and palsas in the Wolf Creek watershed near Whitehorse, and developing regional permafrost modelling/mapping techniques. Geophysical investigations of permafrost landforms and recent landslides were also carried out in collaboration with **Bernd Etzelmüller** (University of Oslo, Norway) and YGS personnel.

11. **Panya Lipovsky** and **Jeff Bond** are compiling a digital surficial geology map for the entire Yukon, with funding from DIAND under the Strategic Initiatives for Northern Economic Development Program (SINED).

TOPICAL STUDIES AND OUTREACH

1. **Luke Beranek**, a UBC PhD candidate with **Jim Mortensen**, has been steadily adding to the detrital-zircon database for Late Paleozoic and Triassic rocks on both sides of the boundary between the North American continental margin sequence and Slide Mountain and Yukon-Tanana terranes. Luke's 2005 work showed that the terranes were already shedding debris into North America by the Early Triassic, substantially earlier than previously thought. This season, Luke collected samples from occurrences of Triassic rocks in the Pelly, Selwyn and Ogilvie mountains.

2,3. **Karen Pelletier** and **Charlie Roots** (GSC) began work on a Yukon geological road guide this summer by scouting appropriate geological stops of interest along most roadways in Yukon. Charlie, along with **Tiffani Fraser** and **Tammy Allen**, also contributed to the Dempster Highway Log being prepared jointly with GSC/NWT. A draft of the guide, entitled *Roadside Geology of the Dempster Highway, Northwest Territories and Yukon: A traveller's guide to the Geology of Canada's most northwestern road link*, will be available for use by tourists for spring 2007, along with accompanying road brochures for designated highway segments. The final product is projected to be complete by spring 2008.

REGIONAL GEOCHEMISTRY AND MINERAL ASSESSMENTS

1. GSC, in collaboration with **Geoff Bradshaw,** completed a stream geochemical survey of an area covering the Kandik Basin in northcentral Yukon, south of Fishing Branch Territorial Park. Funding for the survey was provided by DIAND through SINED. Results will be released in late spring 2007.

AEROMAGNETIC SURVEYS

1. GSC, in collaboration with YGS, began an extensive aeromagnetic survey in the Wernecke and Mackenzie mountains. Funding was provided by DIAND under SINED. Inclement weather during the summer prevented completion of the survey. Completion is now expected in early 2007, with results released in late summer.

PROGRAMS

MINING AND PETROLEUM ENVIRONMENT RESEARCH GROUP (MPERG)

MPERG is a cooperative working group made up of government agencies, environmental, mining and petroleum resource companies, Yukon First Nations and Non-Government Organizations (NGOs). It was established to promote research into environmental issues for mining and petroleum development in the Yukon. Participants bring together their resources and knowledge to work cooperatively on industry-related environmental issues and projects. MPERG creates a favourable environment to facilitate finding solutions before environmental problems arise. The group is funded by YGS and chaired by Grant Abbott, with administrative support from Karen Pelletier.

Five studies were approved for funding for 2006/07:

- John L. Bailey: Yukon River Basin Stream Bioassessment Modeling and Placer Mining Stream Gradient Analysis
- The Yukon Government Oil and Gas Management Branch: Preliminary Investigation of Seismic Lines and associated disturbances in the Eagle Plains and Peel Plateau regions of North Yukon
- EDI Environmental Dynamics Inc in partnership with Devon Energy Corp., Environment Canada, and the Yukon Department of Transportation and Engineering: Regeneration effects of Linear Development Subject to Wildfires in Continuous Permafrost Zones
- Gartner Lee Ltd.: Regional Water Quality Assessment of the South Macmillan River Watershed
- Laberge Environmental Services: Follow-up monitoring: Pilot Sale Erosion Control at Gold Run Creek and Shrub Trial Plots at Brewery Creek Mine

YUKON MINING INCENTIVES PROGRAM

The Yukon Mining Incentives Program (YMIP) is currently administered by Steve Traynor. This year, funding was offered to 53 of 62 applicants, for a total of $880 600. Proposals approved for funding included 5 under the Grassroots-Prospecting module, 17 under the Focused Regional module, and 31 under the Target Evaluation module.

Gold continued to be the main commodity of exploration interest and was the focus of 34 of the projects which received approval for YMIP funding. Projects targeting copper and zinc-lead accounted for nine and six projects, respectively. Two applicants explored for gemstones; one applicant explored for molybdenum and another for uranium. This year saw an increase in approved applicants proposing placer-related projects, with over 25% of the successful applicants undertaking placer exploration and testing programs.

LIAISON TO INDUSTRY, FIRST NATIONS AND THE PUBLIC

The YGS recognizes the importance of effectively communicating information on the geology and mineral and energy resources of the Yukon to a broad audience that includes industry, resource managers, First Nations and the general public. We are continuing to focus more attention on developing strategies and products that meet these needs.

Mike Burke and Bill LeBarge, our main links to the exploration industry, continued to monitor Yukon hard-rock and placer mining and mineral exploration activity, visit active properties, review reports for assessment credit, and maintain the assessment report library.

Karen Pelletier, Charlie Roots and other YGS staff continue to make presentations in the schools and conduct field trips in the communities. Products developed this year to increase public awareness of the geology and mineral resources of the Yukon include new commodity and mineral potential brochures. Upgrades to our websites will be in place by the end of March.

Karen Pelletier also reviews Mining Land Use and Water License applications, and monitors reclaimed sites to document the effectiveness of mitigation practices. As well, she represents the YGS on several committees which sponsor environmental research involving geology. Karen has also been involved in developing a best-practices guide for reclamation of placer mines.

INFORMATION MANAGEMENT AND DISTRIBUTION

With the increasing volume of information generated by the YGS and others, and rapidly evolving digital technology, the Survey continues to put significant resources into making geological information more accessible. Our website and Map Gallery are both undergoing substantial revisions that will make them easier to use and provide greater online functionality to the MINFILE and publications databases. A large part of our effort has gone into developing and maintaining key databases and making all of our information internet-accessible. Ongoing activities include support for the H.S. Bostock Core Library and the Energy, Mines and Resources (EMR) library (Elijah Smith Building) in Whitehorse.

DATABASES

Yukon MINFILE is a database containing over 2600 records on Yukon's mineral occurrences. It is maintained by Robert Deklerk and Lara Lewis. Recent efforts have gone toward making the database fully searchable online. As a result, the most current CD-ROM release dates back to November 2005, and will likely be the last CD-ROM of the database we release. Online searching of the database will allow the user to access the most complete and up-to-date data, as it will link to a non-static dataset. This new direction has required conversion of the database from Access to Oracle and the standardization of data and data fields. The online search is expected to be completed in mid-2007.

The Yukon Placer Database, compiled by Bill LeBarge, was updated and a new version was released in May, 2006. The database is in Microsoft Access 2000 format and is a comprehensive record of the geology and history of Yukon placer mining. The database contains descriptions of 457 streams and rivers, and 1443 associated placer occurrences, of which 130 were updated for this version. It also includes location maps in Portable Document Format (PDF). A new release is planned for spring 2007, which will include detailed updated information from placer mining activity between 2003 and 2006.

YGS, in partnership with the GSC, is in the process of updating the Yukon Digital Geology compilation, which was last revised in 2003. The revised database will not only incorporate recent maps, but will also conform to the North American Data Model. This standard, which is slowly being adopted by geological surveys across North America, allows users to generate a seamless map from more than one source (i.e., two or more jurisdictions). The model will allow the selection of subsets of data to generate maps defined by lithology, age or map unit. It will also be possible to create generalized maps through a hierarchy of attributes (i.e., Group *versus* Formation or Paleozoic *versus* Devonian). The new map database is expected to be available online by April, 2007.

Jeff Bond and Panya Lipovsky began development of a Digital Surficial Geology Map of the Yukon, in partnership with the GSC, and with SINED funding. The map database will have the same functionality as the bedrock database. The release is planned for early 2008.

The Yukon Regional Geochemical Database 2003, compiled by Danièle Héon, contains all of the available digital data for regional stream sediment surveys that have been gathered in the Yukon under the Geological Survey of Canada's National Geochemical Reconnaissance Program. It can be viewed online through the Map Gallery and is available on CD-ROM in Microsoft Excel 2000 format and in ESRI ArcView Shapefile format.

The YukonAge Database, compiled by Katrin Breitsprecher and Jim Mortensen at the University of British Columbia, with funding from the YGS, was

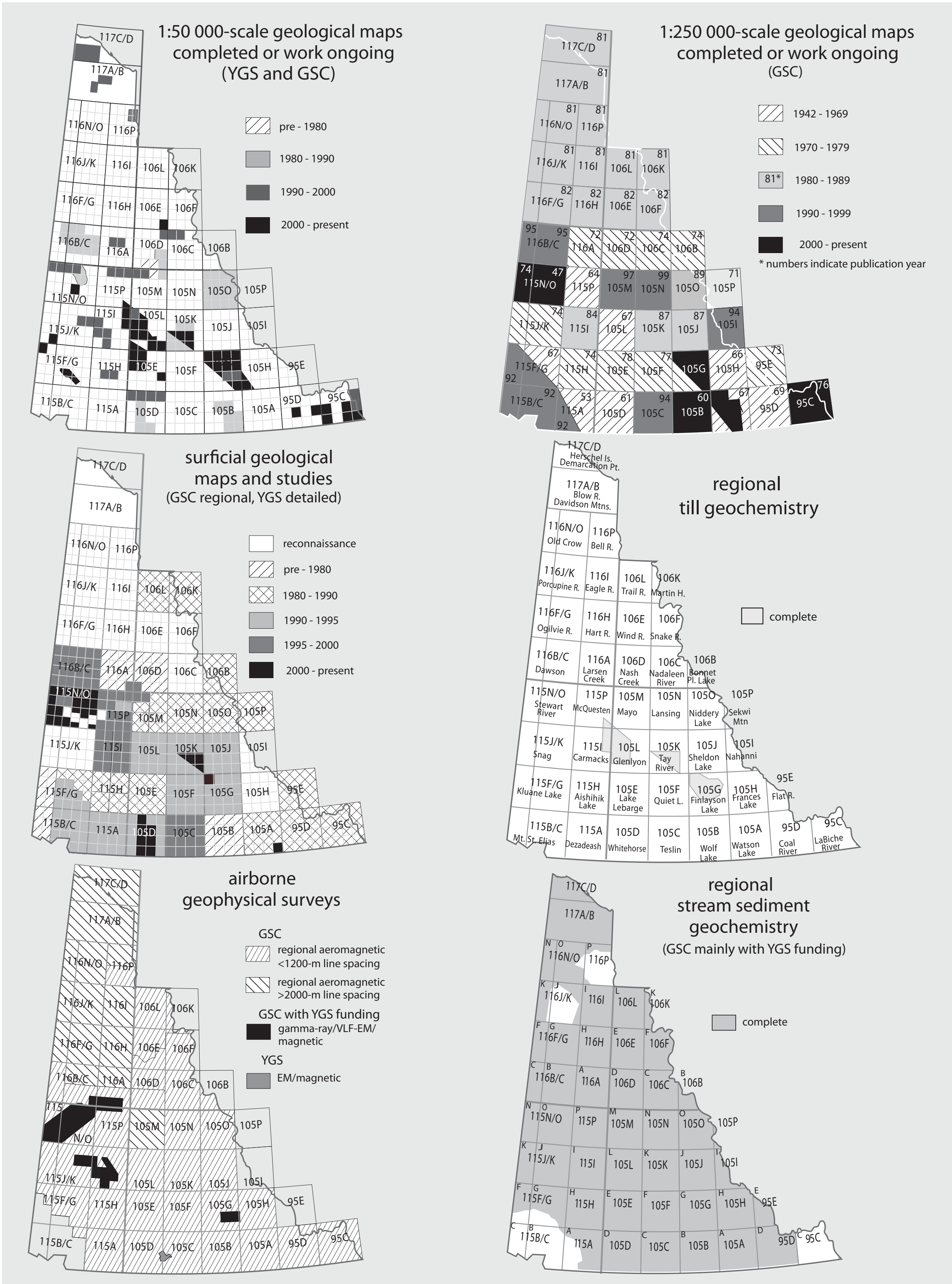

Figure 4. *Summary of available geological maps, and regional geochemical and geophysical surveys in the Yukon.*

updated in 2004. It can be viewed on the YGS Map Gallery in a version modified by Mike Villeneuve and Linda Richard of the Geological Survey of Canada. The database now contains 1556 age determinations derived from 1166 rock samples from the Yukon Territory. It is available in both Microsoft Access 2000 format and as a flat file in Microsoft Excel 2000 format so that the data may be viewed without Microsoft Access.

The Yukon Geoscience Publications Database is available online. It is current and contains almost 8000 references to papers on Yukon geology and mineral deposits, including YGS publications.

All open assessment reports (more than 5000) are now in PDF format and accessible over the internet through the EMR library website. In the Yukon, reports remain confidential for five years. In addition, we have acquired exploration records from the various companies that owned the Faro District. This acquisition includes both records of the Faro District as well as outside projects. Most of the records are now available for viewing.

H.S. BOSTOCK CORE LIBRARY

Mike Burke maintains the H.S. Bostock Core Library. The facility contains about 128 000 m of diamond drill core from about 200 Yukon mineral occurrences. Confidentiality of material is determined on the same basis as mineral assessment reports. Confidential core can be viewed with a letter of release from the owner. Rock saws and other rock preparation equipment are available to the public.

EMR LIBRARY

The Yukon Energy, Mines and Resources Library is the Yukon's largest scientific library and an invaluable resource. It is located in Room 335 of the Elijah Smith Building and is open to the public. The Library provides access to Yukon Mining Assessment reports, maps (geology, topographic and aeromagnetic), and aerial photographs. It holds many geology journals and a good selection of materials on general geology, Yukon geology and economic geology. The Library is also the access point for Faro exploration records. In addition to geological information, the Library has books, reports, and journals in other areas: oil and gas, forestry, agriculture and energy, as well as a very comprehensive collection of Yukon publications.

INFORMATION DISTRIBUTION

The YGS distributes information in three formats: 1) paper maps and reports are sold and distributed through our Geoscience Information and Sales Office; 2) many recent publications and databases are available in digital format at much lower prices than for paper copies; and, 3) most of our publications are available as PDF files on our website (www.geology.gov.yk.ca), free of charge. A catalogue of assessment reports is also available online (*www.emr.gov.yk.ca/library*).

We are pleased to make spatial data available through our interactive map server, the Map Gallery, which can be accessed through the YGS website. We are continuing to improve the Map Gallery and users are encouraged to provide feedback and suggest improvements.

Hard copies of YGS publications are available at the following address:

Geoscience Information and Sales
c/o Whitehorse Mining Recorder
102-300 Main Street (Elijah Smith Building)
P.O. Box 2703 (K102)
Whitehorse, Yukon Y1A 2C6

Ph. (867) 667-5200
Fax (867) 667-5150
E-mail: geosales@gov.yk.ca

To access publications and to learn more about the Yukon Geological Survey visit our website at *geology.gov.yk.ca,* or contact us directly:

Grant Abbott, A/Director
Yukon Geological Survey
2099 Second Avenue
P.O. Box 2703 (K10)
Whitehorse, Yukon Y1A 2C6
Ph. (867) 667-3200
E-mail: grant.abbott@gov.yk.ca

Rod Hill, A/Manager
Yukon Geological Survey
2099 Second Avenue
P.O. Box 2703 (K10)
Whitehorse, Yukon Y1A 2C6
Ph. (867) 667-5384
E-mail: rod.hill@gov.yk.ca

To access the EMR Library:
Website: *www.emr.gov.yk.ca/library*
Ph. (867) 667-3111
E-mail: emrlibrary@gov.yk.ca

2006 PUBLICATIONS AND MAPS

YGS ANNUAL REPORTS

Emond, D.S., Bradshaw, G.D., Lewis, L.L. and Weston, L.H. (eds.), 2006. Yukon Exploration and Geology 2005, Yukon Geological Survey, 339 p.

Burke, M., LeBarge, W., Traynor, S., Abbott, G., Colpron, M. and St. Amand, J., 2006. Yukon Mining, Development and Exploration Overview 2005, Yukon Geological Survey, 75 p.

Traynor, S. (compiler), 2006. Yukon Mineral Deposits 2006, Yukon Geological Survey, 14 p.

YGS DATABASES

Deklerk, R. and Traynor, S. (compilers), 2005. Yukon MINFILE 2005 – A database of mineral occurrences, Yukon Geological Survey, CD-ROM.

LeBarge, W.P. (compilers), 2006. Yukon Placer Database 2006 – Geology and mining activity of placer occurrences, Yukon Geological Survey, CD-ROM.

YGS OPEN FILES

Bond, J.D. and Sanborn, P.T., 2006. Morphology and geochemistry of soils formed on colluviated weathered bedrock: Case studies from unglaciated upland slopes in west-central Yukon, Yukon Geological Survey, YGS Open File 2006-19.

Bond, J.D. and Church, A., 2006. McConnell ice-flow and placer activity map, Big Salmon Range, Yukon (1:100 000 scale), Yukon Geological Survey, YGS Open File 2006-20.

Colpron, M. (compiler), 2006. Tectonic assemblage map of Yukon-Tanana and related terranes in Yukon and Northern British Columbia (1:1 000 000 scale), Yukon Geological Survey, YGS Open File 2006-1.

Friske, P.W.B., McNeil, R.J., McCurdy, M.W., Wilson, R.S. and Day, S.J.A., 2006. Geochemical Data from a National Geochemical Reconnaissance Stream Sediment and Water Survey in the Yukon Portion of the Flat River Map Area, Southeast Yukon Territory (Part of NTS 95E), Yukon Geological Survey, YGS Open File 2006-18/GSC Open File 5329, CD-ROM.

Friske, P.W.B., McNeil, R.J., McCurdy, M.W., Wilson, R.S. and Day, S.J.A., 2006. Geochemical Data from a National Geochemical Reconnaissance Stream Sediment and Water Survey in the Area of Old Crow, Northern Yukon Territory (Parts of 116J, 116K, 116N, 116O, 116P, 117A, 117B), Yukon Geological Survey, YGS Open File 2006-17/GSC Open File 5319, CD-ROM.

YGS MINERAL ASSESSMENT OPEN FILES

These have been worked on over the last 10 years and were released in 2006.

Fonseca, A., 2006. Mineral Assessment of the Ddhaw Ghro Habitat Protection Area, Yukon, Yukon Geological Survey, YGS Open File 2006-5.

Fonseca, A., 2006. Mineral Assessment of the proposed Frances Lake Special Management Area, Yukon, Yukon Geological Survey, YGS Open File 2006-6.

Fonseca, A., 2006. Protected Areas in Canada, Yukon Geological Survey, YGS Open File 2006-14.

Héon, D., 2006. Mineral Assessment of the Tombstone Study Area, Yukon, Yukon Geological Survey, YGS Open File 2006-2.

Héon, D., 2006. Mineral Assessment of the Eagle Plain Study Area, Yukon, Yukon Geological Survey, YGS Open File 2006-3.

Héon, D., 2006. Mineral Assessment of the Northern Kluane Wildlife Sanctuary, Yukon, Yukon Geological Survey, YGS Open File 2006-4.

Héon, D., 2006. Isotope dating of lead-zinc occurrences in the Bonnet Plume area, Preliminary report, Yukon Geological Survey, YGS Open File 2006-16.

Héon, D. and Sax, K., 2006. Investigations of 2000 RGS survey, Northern Yukon, Eagle Plains Ecoregion, Yukon Geological Survey, YGS Open File 2006-15.

Hulstein, R., 2006. Report on the Detailed Mineral Assessment of the Proposed Kusawa Natural Environment Park Special Management Area, Yukon, Yukon Geological Survey, YGS Open File 2006-7.

Hulstein, R., vanRanden, J., Stroshein, R. and Andersen, F., 2006. Report on 2002 Geochemical Procedures used during Mineral Resource Assessments, Yukon Geological Survey, YGS Open File 2006-13.

Stroshein, R., 2006. Report on the Detailed Mineral Assessment of the Proposed Lewes Marsh/ McClintock Bay and Tagish River Special Management Areas, Yukon, Yukon Geological Survey, YGS Open File 2006-9.

Stroshein, R., 2006. Report on the Detailed Mineral Assessment of the Proposed Scottie Creek Special Management Area, Yukon, Yukon Geological Survey, YGS Open File 2006-12.

Stroshein, R. and Hulstein, R., 2006. Report on the Detailed Mineral Assessment of the Proposed Pickhandle Lakes Special Management Area, Yukon, Yukon Geological Survey, YGS Open File 2006-10.

Stroshein, R. and Hulstein, R., 2006. Report on the Detailed Mineral Assessment of the Proposed Wellesley Lake Special Management Area, Yukon, Yukon Geological Survey, YGS Open File 2006-11.

vanRanden, J., 2006. Report on the Detailed Mineral Assessment of the Proposed Snafu/Tarfu Natural Environment Park Special Management Area, Yukon, Yukon Geological Survey, YGS Open File 2006-8.

YGS CONTRIBUTIONS TO OUTSIDE PUBLICATIONS

Colpron, M., 2006. Contexte géodynamique du terrane de Yukon-Tanana, Cordillère canadienne: Faculté des Sciences et Techniques de Marrakech, Deuxièmes Journées De Launay, Marrakech, Morocco, p. 18-19.

Buffett, G., White, D., Roberts, B. and **Colpron, M.**, 2006. Preliminary results from the Whitehorse Trough seismic survey, Yukon Territory. Geological Survey of Canada, Current Research, 2006-A2, 9 p.

Colpron, M. and Nelson, J. (eds.), 2006. Paleozoic Evolution and Metallogeny of Pericratonic Terranes at the Ancient Pacific Margin of North America, Canadian and Alaskan Cordillera. Geological Association of Canada, Special Paper 45, 523 p.

Gabrielse, H., **Murphy, D.C**. and Mortensen, J.K., 2006. Cretaceous and Cenozoic dextral orogen-parallel displacements, magmatism, and paleogeography, north-central Canadian Cordillera. *In:* Paleogeography of the North American Cordilera: Evidence For and Against Large-Scale Displacements, J.W. Haggart, R.J. Enkin and J.W.H. Monger (eds.), Geological Association of Canada, Special Paper 46, p. 255-276.

Israel, S., Kennedy, L.A., Schiarizza, P., Friedman, R.M. and Villeneuve, M.E., 2006. Evidence for Early to Late Cretaceous, sinistral deformation in the Tchaikazan River area, southwestern British Columbia: Implications for the tectonic evolution of the southern Coast Belt. *In:* Paleogeography of western North American Cordillera, J.W. Haggart, R.J. Enkin and J.W.H. Monger (eds.), Geological Association of Canada, Special Paper 46, p. 331-350.

Israel, S. and van der Heyden, P., 2006. Geology, Atnarko (93C/05), British Columbia. Geological Survey of Canada, 1:50 000-scale map.

Israel, S., van der Heyden, P., Haggart, J. and Woodsworth, G.J., 2006. Geology, Junker Lake and part of Knot Lakes (93C/04 and 92N/13), British Columbia. Geological Survey of Canada, 1:50 000-scale map.

Kennedy, L.A. and **Israel, S.**, 2006. Rheological contrasts in folded migmatites: An example from the Atnarko Metamorphic Complex, Central west British Columbia. Tectonic Studies Group, Annual General Meeting, University of Manchester, Manchester England, Abstract volume.

Lowey, G.W., 2006. The origin and evolution of the Klondike goldfields, Yukon, Canada. Ore Geology Reviews, vol. 28, p. 431-450.

YGS ABSTRACTS

Colpron, M., 2006. Tectonostratigraphic framework and Paleozoic evolution of pericratonic terranes in the northern Cordillera, Geological Society of America, Cordilleran Section, Anchorage, Alaska, Abstracts with Programs vol. 38, no. 5, p. 5.

Dusel-Bacon, C., Paradis, S., **Murphy, D.C.**, Piercey, S.J. and Dashevsky, S., 2006. Volcanic-hosted massive sulphide deposits of the Northern Cordillera: Diverse expressions of extension and subduction along the Paleozoic North American continental margin. Geological Society of America, Programs with Abstracts, vol. 38, no. 5, abstract 25-1, p. 69.

Fraser, T.A. and **Allen, T.L.**, 2006. Preliminary Investigations of the Upper Devonian to Lower Carboniferous Tuttle Formation, East Richardson Mountains, Yukon. *In:* 34th Annual Yellowknife Geoscience Forum Abstracts, A.L. Jones and D. Irwin (compilers), Northwest Territories Geoscience Office, Yellowknife, NT, p. 24.

Kennedy, L.A. and **Israel, S.**, 2006. Constraints on the rheological behaviour of migmatites: Preliminary work from the Atnarko metamorphic complex, BC. Canadian Tectonics Group, 26th Annual meeting Crowsnest Pass, Program with Abstracts, p. 7.

Lowey, G.W., 2006. Reassembling the Nutzotin-Dezadeash basin: new evidence from the Dezadeash Formation, Yukon. AAPG-GSA-SPE Joint Meeting, Anchorage, May 6-11, 2006. Geological Society of America, 2005 annual meeting, Abstracts with Programs, vol. 38, no. 5, p. 80

Lowey, G.W., Long, D.G.F., Fowler, M.G., Stasiuk, V.D. and Sweet, A.R., 2006. Hydrocarbon source rock potential of the Whitehorse Trough, a frontier basin in southern Yukon. CSPG-CSEG-CWLS Joint Conference, Calgary, May 15-18, 2006, abstract, p. 116.

Mortensen, J.K., Gordey, S.P., **Murphy, D.C.** and Abbott, J.G., 2006. Late Devonian-Early Mississippian felsic magmatism in the Selwyn Basin and Cassiar Platform, Yukon, and implications for the nature of the Northern Cordilleran margin in the mid-Paleozoic. Geological Society of America, 2005 annual meeting, Abstracts with Programs, vol. 38, no. 5, abstract 3-6, p. 6.

Mortensen, J.K. and **Israel, S**., 2006. Is the Windy-McKinley terrane a displaced fragment of Wrangellia? Evidence from new geological, geochemical and geochronological studies in western Yukon. Geological Society of America, 2005 annual meeting, Abstracts with Programs, vol. 38, no. 5, abstract 43-10.

Murphy, D.C., 2006. Late Paleozoic evolution of Yukon-Tanana and Slide Mountain terranes, Finlayson Lake district, southeastern Yukon, Canada. Geological Society of America, 2005 annual meeting, Abstracts with Programs, vol. 38, no. 5, abstract 3-2, p. 5.

Piercey, S.J. and **Colpron, M.**, 2006. Geochemistry, Nd-Hf isotopic composition and detrital zircon geochronology of the Snowcap assemblage, Yukon: Insights into the provenance and composition of the basement to Yukon-Tanana terrane, Geological Society of America, Cordilleran Section Meeting, Anchorage, Alaska, Abstracts with Programs vol. 38, no. 5, p. 5.

Pyle, L.J., Gal, L.P., Hadlari, T., Jones, A.L., Lemieux, Y., Zantvoort, W.G., **Allen, T.L.** and **Fraser, T.A.**, 2006. Regional Geoscience studies and Petroleum potential, Peel Plateau and Plain: Lower to Middle Paleozoic Mackenzie-Peel Shelf. *In:* 34th Annual Yellowknife Geoscience Forum Abstracts, A.L. Jones and D. Irwin (compilers), Northwest Territories Geoscience Office, Yellowknife, NWT, p. 45.

Ward, B.C., **Bond, J.D.** and Gosse, J.C., 2006. Dichotomy Between the age of the Penultimate Glaciation for Different Source Areas of the Northern Cordilleran Ice Sheet, Yukon Territory, Canada. American Geophysical Union, Fall Meeting, San Fransisco, United States, abstract PP54A-07.

YUKON GEOLOGICAL PAPERS OF INTEREST

Aerts, J., Renssen, H., Ward, P.J., de Moel, H., Odada, E., Bouwer, L.M. and Goosse, H., 2006. Sensitivity of global river discharges under Holocene and future climate conditions. Geophysical Research Letters, vol. 33, No. 19, L19401, doi: 10.1029/2006GL027493.

Anderson, L., Abbott, M.B., Finney, B.P. and Burns, S.J., 2006. Regional atmospheric circulation change in the North Pacific during the Holocene inferred from lacustrine carbonate oxygen isotopes, Yukon Territory, Canada. Quaternary Research, vol. 65, p. 350-351.

Baker, T., Ebert, S., Rombach, C. and Ryan, C.G., 2006. Chemical compositions of fluid inclusions in intrusion-related gold systems, Alaska and Yukon, using PIXE microanalysis. Economic Geology and the Bulletin of the Society of Economic Geologists, vol. 101, no. 2, p. 311-327.

Canil, D., Johnston, S.T. and Mihalynuk, M., 2006. Mantle redox in Cordilleran ophiolites as a record of oxygen fugacity during partial melting and the lifetime of mantle lithosphere. Earth and Planetary Science Letters, vol. 248, p. 106-117.

Canil, D., Mihalynuk, M. and Charnell, C., 2006. Sedimentary record for exhumation of ultrahigh pressure (UHP) rocks in the northern Cordillera, British Columbia, Canada. Geological Society of America Bulletin, vol. 118, no. 9-10, p. 1171-1184.

Chapman, R.J. and Mortensen, J.K., 2006. Application of microchemical characterization of placer gold grains to exploration for epithermal gold mineralization in regions of poor exposure. Journal of Geochemical Exploration, vol. 91, p. 1-26.

Clague, J.J., Luckman, B.H., Van Dorp, R.D., Gilbert, R., Froese, D., Jensen, B.J.L. and Reyes, A.V., 2006. Rapid changes in the level of Kluane Lake in Yukon Territory over the last millennium. Quaternary Research, vol. 66, p. 342-355.

Cook, R.B., 2006. Polybasite, Husky Mine, Elsa, Yukon Territory, Canada. Rocks and Minerals. Gems and Minerals of Canada, vol. 81, no. 1, p. 44-48.

Dore, G., Beaulac, I. and Gassen, W.V., 2006. Performance of the Beaver Creek section of the Alaska Highway. Cold Regions Engineering 2006: Current practices in cold regions engineering. Proceedings of the 13th International Conference on Cold Regions Engineering, 12 p.

Frappart, F., Ramillien, G., Biancamaria, S., Mognard, N.M. and Cazenave, A., 2006. Evolution of high-latitude snow mass derived from the GRACE gravimetry mission (2002-2004). Geophysical Research Letters, vol. 33, L02501.

Froese, D.G., Zazula, G.D. and Reyes, A.V., 2006. Seasonality of the late Pleistocene Dawson tephra and exceptional preservation of a buried riparian surface in central Yukon Territory, Canada. Quaternary Science Reviews, vol. 25, p. 1542-1551.

Gilbert, R. and Desloges, J.R., 2005. The record of glacial Lake Champagne in Kusawa Lake, southwestern Yukon Territory. Canadian Journal of Earth Sciences, vol. 42, no. 12, p. 2127-2140.

Gueguen, C., Guo, L.D., Wang, D., Tanaka, N. and Hung, C.C., 2006. Chemical characteristics and origin of dissolved organic matter in the Yukon River. Biogeochemistry, vol. 77, p. 139-155.

Guo, L.D. and Macdonald, R.W., 2006. Source and transport of terrigenous organic matter in the upper Yukon River: Evidence from isotope (delta C-13, Delta C-14, and delta N-15) composition of dissolved, colloidal, and particulate phases. Global Biogeochemical Cycles, vol. 20, no. 2, DOI 10.1029/2005GB002593.

Huscroft, C.A., Ward, B.C., Jackson, L.E. and Tarnocai, C.E., 2006. Investigation of high-level glaciofluvial terraces and re-evaluation of established soil stratigraphy for early and middle Pleistocene surfaces, central Yukon, Canada. Boreas, vol. 35, no. 1, p. 96-105.

Kavanaugh, J.L. and Clarke, G.K.C., 2006. Discrimination of the flow law for subglacial sediment using in situ measurements and an interpretation model. Journal of Geophysical Research-Earth Surface, vol. 111, F01002, doi:10.1029/2005JF000346.

Kinnard, C. and Lewkowicz, A.G., 2006. Frontal advance of turf-banked solifluction lobes, Kluane Range, Yukon Territory, Canada. Geomorphology, vol. 73, p. 261-276.

Lacelle, D., Lauriol, B. and Clark, I.D., 2006. Effect of chemical composition of water on the oxygen-18 and carbon-13 signature preserved in cryogenic carbonates, Arctic Canada: Implications in paleoclimatic studies. Chemical Geology, vol. 234, p. 1-16.

Lauriol, B., Lamirande, I. and Lalonde, A.E., 2006. The giant steps of Bug Creek, Richardson Mountains, NWT. Canada Permafrost and Periglacial Processes, vol. 17, no. 3, p. 267-275.

Mair, J.L., Goldfarb, R.J., Johnson, C.A., Hart, C.J.R. and Marsh, E.E., 2006. Geochemical Constraints on the Genesis of the Scheelite Dome Intrusion-Related Gold Deposit, Tombstone Gold Belt, Yukon, Canada. Economic Geology, vol. 101, no. 3, p. 523-553.

Mair, J.L., Hart, C.J.R. and Stephens, J.R., 2006. Deformation history of the northwestern Selwyn Basin, Yukon, Canada: Implications for orogen evolution and mid-Cretaceous magmatism. Geological Society of America Bulletin, vol. 118, p. 304-323.

McCartney, S.E., Carey, S.K. and Pomeroy, J.W., 2006. Intra-basin variability of snowmelt water balance calculations in a subarctic catchment. Hydrological Processes. Special Volume: Eastern Snow Conference/Western Snow Conference, vol. 2, no. 4, p. 1001-1016.

McCausland, P.J.A., Symons, D.T.A. and Hart, C.J.R., 2005. Rethinking “Yellowstone in Yukon” and Baja British Columbia: Paleomagnetism of the Late Cretaceous Swede Dome stock, northern Canadian Cordillera. Journal of Geophysical Research-Solid Earth, vol. 110, B12107, doi:10.1029/2005JB003742.

Miskovic, A. and Francis, D., 2006. Interaction between mantle-derived and crustal calc-alkaline magmas in the petrogenesis of the Paleocene Sifton Range volcanic complex, Yukon, Canada. Lithos, vol. 87, p. 104-134.

Nishikawa, O., Okrugin, V., Belkova, N., Saji, I., Shiraki, K. and Tazaki, K., 2006. Crystal symmetry and chemical composition of yukonite: TEM study of specimens collected from Nalychevskie hot springs, Kamchatka, Russia and from Venus Mine, Yukon Territory. Canada Mineralogical Magazine, vol. 70, p. 73-81.

Pilkington, M., Snyder, D.B. and Hemant, K., 2006. Weakly magnetic crust in the Canadian cordillera. Earth and Planetary Science Letters, vol. 248, p. 476-485.

Quinton, W.L., Shirazi, T., Carey, S.K. and Pomeroy, J.W., 2005. Soil water storage and active-layer development in a sub-alpine tundra hillslope, southern Yukon Territory. Canada Permafrost and Periglacial Processes, vol. 16, no. 4, p. 369-382.

Reyes, A.V., Luckman, B.H., Smith, D.J., Clague, J.J. and Van Dorp, R.D., 2006. Tree-ring dates for the maximum Little Ice Age advance of Kaskawulsh Glacier, St. Elias Mountains, Canada. Arctic, vol. 59, no. 1, p. 14-20.

Ruks, T.W., Piercey, S.J., Ryan, J.J., Villeneuve, M.E. and Creaser, R.A., 2006. Mid- to late Paleozoic K-feldspar augen granitoids of the Yukon-Tanana Terrane, Yukon, Canada; implications for crustal growth and tectonic evolution of the northern Cordillera. Geological Society of America Bulletin, vol. 118, no. 9-10, p. 1212-1231.

Sanborn, P.T., Smith, C.A.S., Froese, D.G., Zazula, G.D. and Westgate, J.A., 2006. Full-glacial paleosols in perennially frozen loess sequences, Klondike Goldfields, Yukon Territory, Canada. Quaternary Research, vol. 66, no. 1, p. 147-157.

Symons, D.T.A. and McCausland, P.J.A., 2006. Paleomagnetism of the Fort Knox Stock, Alaska, and rotation of the Yukon-Tanana terrane after 92.5 Ma. Tectonophysics, vol. 419, p. 13-26.

Truffer, M. and Harrison, W.D., 2006. In situ measurements of till deformation and water pressure. Journal of Glaciology, vol. 52, p. 175-182.

Wilson, S.A., Raudsepp, M. and Dipple, G.M., 2006. Verifying and quantifying carbon fixation in minerals from serpentine-rich mine tailings using the Rietveld method with X-ray powder diffraction data. American Mineralogist, vol. 91, p. 1331-1341.

Woo, M.-K. and Thorne, R., 2006. Snowmelt contribution to discharge from a large mountainous catchment in subarctic Canada. Hydrological Processes, vol. 20, no. 10, p. 2129-2139.

Yalcin, K., Wake, C.P., Kreutz, K.J., Germani, M.S. and Whitlow, S.I., 2006. Ice core evidence for a second volcanic eruption around 1809 in the Northern Hemisphere. Geophysical Research Letters, vol. 33, L14706, doi:10.1029/2006GL026013.

Zdanowicz, C., Hall, G., Vaive, J., Amelin, Y., Percival, J., Girard, I., Biscaye, P. and Bory, A., 2006. Asian dustfall in the St. Elias Mountains, Yukon, Canada. Geochimica Et Cosmochimica Acta, vol. 70, p. 3493-3507.

Zazula, G.D., Schweger, C.E., Beaudoin, A.B. and McCourt, G.H., 2006. Macrofossil and pollen evidence for full-glacial steppe within an ecological mosaic along the Bluefish River, eastern Beringia. Quaternary International. Special Issue: Third international Mammoth Conference, Dawson, Yukon, May 24-29, 2003, J.E. Storer (ed.), issue 142-143, p. 2-19.

Zou, L., Sun, M.Y. and Guo, L.D., 2006. Temporal variations of organic carbon inputs into the upper Yukon River: Evidence from fatty acids and their stable carbon isotopic compositions in dissolved, colloidal and particulate phases. Organic Geochemistry, vol. 37, p. 944-956.

YUKON THESES

Brideau, M.-A., 2006. The influence of tectonic structures on rock mass quality and implications for rock slope stability. Unpublished MSc thesis, Simon Fraser University, Burnaby, B.C., 198 p.

Lyle, R.R., 2006. Landslide susceptibility mapping in discontinuous permafrost: Little Salmon Lake, central Yukon. Unpublished MSc thesis, Queen's University, Kingston, Ontario. 351 p.

Simard, R.-L., 2005. Volcanology, geochemistry, and tectonic setting of late Paleozoic volcanic formations in the northern Canadian Cordillera: A key to understanding the evolution of pericratonic terranes. Unpublished PhD thesis, Dalhousie University, Halifax, Nova Scotia, 184 p.

YUKON GEOLOGICAL ABSTRACTS OF INTEREST

Barley, E.M., Walker, I.R. and Stepanovic, L.C., 2005. Midge derived paleotemperature reconstructions for three sites from Yukon, Canada and Alaska, U.S.A. Geological Society of America, 2005 annual meeting, Abstracts with Programs, vol. 37, no. 7, p. 120.

Groat, L.A., 2006. Recent gem discoveries in Canada. Abstracts of the 27th annual FM-MSA-TGMS, Tucson Mineralogical Symposium. The Mineralogical Record, vol. 37, no. 1, p. 67.

Kortlever, B., McKenney, R., Apgar, J. and Ramage, J., 2005. Investigating the use of gage data and vegetation mapping to determine the rate and style of channel change on the Wheaton River, Yukon Territory, Canada. Geological Society of America, 2005 annual meeting, Abstracts with Programs, vol. 37, no. 7, p. 302.

Lewkowicz, A.G., Bonnaventure, P., Schultz, E. and Etzelmuller, B., 2006. Mountain Permafrost in the Yukon Territory, Canada: Mapping and Modelling. Eos, Transactions, American Geophysical Union, vol. 87, no. 52, fall meeting supplement, abstract C42A-04.

Mauthner, M., 2006. Minerals of the Silver Trail, Yukon Territory, Canada. Abstracts of the 27th annual FM-MSA-TGMS meeting, Tucson Mineralogical Symposium. The Mineralogical Record, vol. 37, no. 1, p. 67.

McKenney, R., Payne, J.F., Ramage, J., Kortlever, B. and Apgar, J., 2005. Sub-arctic climate variability indicated by patterns of channel change in the upper Yukon Basin, Yukon Territory, Canada. Geological Society of America, 2005 annual meeting, Abstracts with Programs, vol. 37, no. 7, p. 224.

Ramage, J.M. and McKenney, R., 2005. Remote sensing of interannual snowmelt variability, Yukon River basin, Yukon Territory, Canada Geological Society of America, 2005 annual meeting, Abstracts with Programs, vol. 37, no. 7, p. 224.

Reyes, A.V., 2006. Degradation and Local Survival of Permafrost Through the Last Interglaciation in Interior Alaska and Yukon Territory. Eos, Transactions, American Geophysical Union, vol. 87, no. 52, fall meeting supplement, abstract.

Walvoord, M.A. and Striegl, R.G., 2005. Climate-driven response of groundwater input to the Yukon River. Geological Society of America, 2005 annual meeting. Abstracts with Programs, vol. 37, no. 7, p. 372.

GSC CONTRIBUTIONS TO YUKON GEOLOGY

Friske, P.W.B., McNeil, R.J., McCurdy, M.W., Wilson, R.S. and Day, S.J.A., 2006. Geochemical Data from a National Geochemical Reconnaissance Stream Sediment and Water Survey in the Yukon Portion of the Flat River Map Area, Southeast Yukon Territory (Part of NTS 95E). Yukon Geological Survey and Geological Survey of Canada, YGS Open File 2006-18/GSC Open File 5329, CD-ROM.

Friske, P.W.B., McNeil, R.J., McCurdy, M.W., Wilson, R.S. and Day, S.J.A., 2006. Geochemical Data from a National Geochemical Reconnaissance Stream Sediment and Water Survey in the Area of Old Crow, Northern Yukon Territory (Parts of 116J, 116K, 116N, 116O, 116P, 117A, 117B). Yukon Geological Survey and Geological Survey of Canada, YGS Open File 2006-17/GSC Open File 5319, CD-ROM.

Gordey, S.P., Williams, S.P., Cocking, R.B. and Ryan, J.J., 2006. Digital geology, Stewart River area, Yukon. Geological Survey of Canada, GSC Open File 5122, 12 maps, DVD.

Khudoley, A.K. and Fallas, K.M., 2006. Geology, Brown Lake, Yukon Territory. Geological Survey of Canada, "A" Series Map 2083A, 1:50 000 map sheet.

Madsen, J.K., Breitsprecher, K. and Anderson, R.G., 2006. CordMinAge2005 - isotopic ages for significant mineral deposits of the Canadian Cordillera. Geological Survey of Canada, Open File 4969.

La Commission géologique du Yukon

Grant Abbott[1] et Maurice Colpron[2]
Le Service de géologie du Yukon

Abbott, J.G. et Colpron, M., 2007. La Commission géologique du Yukon. *Dans :* Yukon Exploration and Geology 2006, D.S. Emond, L.L. Lewis et L.H. Weston (réds.), la Commission géologique du Yukon, p. 73-76.

SOMMAIRE D'ACTIVITÉS

La commission géologique du Yukon (CGY) se remet de la perte tragique de notre géologue d'évaluation des ressources minérales, Geoff Bradshaw, dans un accident d'hélicoptère au cours de l'été dernier. Nous remerçions les nombreux collègues et amis des communautés géologique et minière pour leur incroyable support. Nous nous ajustons aussi aux départs de deux de nos géologues, Craig Hart et Julie Hunt; nous leur souhaitons du succès sous le soleil d'Australie et les remerçions pour leurs importantes contributions à la géologie du Yukon. Toutefois, jusqu'à leur remplacement, notre capacité de conduire des études de gîtes minéraux en sera réduite.

La CGY opère maintenant selon un nouvel organigramme comprenant quatre services. Les responsabilités de gérance des Services minéraux revient maintenant à Mike Burke en tant que chef intérimaire; alors que Diane Emond est chef des Services techniques, Don Murphy est chef du Service de géologie régionale, et Lee Pigage est chef du Service d'évaluation des ressources et des relations publiques.

TRAVAUX SUR LE TERRAIN

CARTOGRAPHIE DU SUBSTRATUM ROCHEUX

1. **Maurice Colpron** a collaboré avec **Steve Gordey** (commission géologique du Canada [CGC]), **Grant Lowey, Steve Piercey** (université Laurentienne) et **Don Murphy** pour cartographier la partie nord-ouest de la fausse de Whitehorse. Cette cartographie complète les contôles de surface de la géologie le long de la partie ouest du relevé sismique acquit en 2004 par la CGY et la CGC. La compilation et l'interprétation des diverses données géoscientifiques sont en cours; elles formeront la base d'une réévaluation du potentiel pétrolier de la fausse de Whitehorse septentrionale.

2. **Lee Pigage** a entammé la cartographie de la région d'Otter Creek (STN 95D/6) dans le sud-est du Yukon. Ce projet continue ses travaux antérieurs dans les régions de Pool Creek et de Toobally Lakes. Il permettra d'améliorer nos connaissances de la stratigraphie, la structure, et le potentiel minéral à la limite sud-est du bassin de Selwyn.

[1]grant.abbott@gov.yk.ca
[2]maurice.colpron@gov.yk.ca

3. **Steve Israel** a continué la cartographie des monts Kluane, se concentrant cette année sur les strates Paléozoïques tardive du Groupe de Skolai à l'est de la rivière White. Dans cette région, ces strates contiennent des intrusifs mafiques à ultramafiques du Trias minéralisés en nickel-cuivre et éléments du groupe du platine. Ce projet examine aussi la provenance des strates sédimentaires du Paléozoique tardif et du Trias moyen du terrane de Wrangel, à l'aide des zircon détritiques et en collaboration avec **Jim Mortensen** (université de Colombie-Britannique). L'étude de la déformation récente le long de la faille de Denali est aussi en cours en collaboration avec **Don Murphy** et des collègues du USGS en Alaska.

4. **Don Murphy** a conduit une cartographie de reconnaissance du terrane de Windy-McKinley : une région avec peu d'affleurements, donc peu connue. Tels que définis dans le centre de l'Alaska, les terranes de Windy et de McKinley comprennent des roches ophiolitiques d'âge inconnu, et du mélange et du flysch du Mésozoïque. On en sait peu sur les relations originelles entre ces diverses composantes, et entre celles-ci et le terrane de Yukon-Tanana. Les travaux de Don permettrons d'établir la nature de ces assemblages au Yukon, et d'assiter l'exploration minérale et la planification d'usage des terres dans la région.

ÉTUDES DE GÎTES MINÉRAUX

1. **Lara Lewis** a recueillie des données de terrain sur les indices d'uranium assoçiés aux brèches de Wernecke et reliés aux intrusions, dans le cardre d'une compilation portant sur l'exploration pour l'uranium au Yukon. De nouvelles datations de la minéralisation en uranium devraient établir la chronolgie des événements minéralisateurs.

2. **Jake Hanley** et **Ed Spooner** (université de Toronto) poursuivent une étude post-doctorale portant sur l'origine et l'évolution des fluides magmatiques, et leurs relations à la minéralisation aurifère dans les granits du Crétacé moyen au Yukon.

ÉTUDES PORTANT SUR LES HYDROCARBURES

1. **Tammy Allen** et **Tiffani Fraser** ont entammées une étude de quatre ans portant sur l'évaluation du potentiel en hydrocarbures de la région de Peel, dans le nord-est yukonnais. Ce projet est une collaboration de la CGY avec la CGC, le centre géoscientifique des Territoires du Nord-Ouest, et des partenaires industriels et universitaires. Cette année, Tammy et Tiffani ont concentrées leurs efforts sur la Formation de Tuttle, d'âge Dévonien tardif à Mississipien précoce. Les principaux objectifs de ce projet sont : a) d'évaluer le potentiel de la Formation de Tuttle en tant que réservoir pétrolier ; b) d'examiner les unités avoisinantes en tant que sources possible de pétrole ; et c) d'éclaircir les relations stratigraphiques et sédimentologiques entre les strates Paléozoïques supérieures de la région.

2. **Grant Lowey** a poursuivit ses études de la sédimentologie, la stratigraphie, et le potentiel en hydrocarbures du Groupe de Laberge et de la Formation de Tantalus dans la fausse de Whitehorse. Ses études antérieures ont révélées la présence d'inclusions fluides de pétrole et ont identifiées deux unités comme étant des roches sources possibles. Grant a aussi participé à la cartographie géologique de la partie septentrionale de ce bassin inexploré avec Maurice Colpron.

ÉTUDES DES DÉPÔTS MEUBLES

1. **William LeBarge**, le géologue des placers de la CGY, **Valdimir Naumov** (université de Perm en Russie), et **Rob Chapman** (université de Leeds aux Royaumes Unis) étudient la sédimentologie, la stratigraphie et les caractéristiques de l'or dans les dépôts de graviers et de conglomérats de la région de la rivière Indian. Ces graviers de terrace, de même que les conglomérats sous-jacents, font présentemment l'objet de travaux d'exploration des sociétés de Boulder Mining Corporation et de Klondike Star Ltd. Cette étude devrait engendrée de nouvelles interprétations de la géologie permettants de mieux caractériser la distribution de l'or placérien dans le bassin versant de la rivière Indian et on espère d'identifier de nouvelles ressources en placers dans la région immédiate et dans les ruisseaux avoisinants. Ce projet complémente l'étude de **Jim Mortensen** (université de Colombie-Britannique) portant sur la composition en éléments traces de l'or placérien du Klondike ; étude qui pourrait révéler de nouvelles sources d'or filonien.

2. **Jeff Bond** a continué son étude des sols dans les terrains non-glaciaires du Klondike en collaboration avec **Paul Sanborn** et **Scott Smith**. Cette année, Jeff a complété une étude géochimique des sols au site original de la mine Boulder Lode, sur la propriété Lone Star. Il a aussi étudié les sols gelés de plateau de la propriété Lone Star avec l'assistance de **Kathryn Denomme** de l'université de Waterloo. La thèse de baccalauréat de Kathryn porte sur la cartographie des dépôts meubles le long d'une pente d'aspect typique vers le nord sur la propriété Lone Star.
3. **Panya Lipovsky** a continuée la surveillance des glissements de terrain reliés à la fonte du pergélisol dans le sud et le centre du Yukon. Grace aux collaborations de C-CORE et d'InSAR, l'agence spatiale européenne, on a mesuré des mouvements de terrain de petite échelle à l'aide de techniques de télédétection et de rélevés SPG de haute précision à cinq endroits près de Beaver Creek, de Carmacks et du lac Little Salmon. Un inventaire des glissements de terrain dans le bassin versant de la rivière Pelly a aussi été entammé.
4. **Erin Trochim** et **Panya Lipovsky** ont continuées leur compilation des données de forages du ministère des routes du Yukon afin d'en capturer des informations détaillées sur la géotechnique et le pergélisol. Ces travaux ont permis d'augmenter la banque de données telle que la route de l'Alaska est maintenant couverte de Beaver Creek jusqu'à l'est de Haines Junction.
5. **Derek Turner** et **Brent Ward** (université Simon Fraser) ont entammés en collaboration avec **Jeff Bond** une étude de l'histoire glaciaire de la propriété d'Howards Pass dans les monts Selwyn. Ces travaux forment la base de la thèse de maîtrise de Derek. Son étude comprend l'évolution tardi-glaciaire du lobe Selwyn de la couverture glaciaire de la cordillère, la cartographie des dépôts meubles sur la propriété de Pacifica Resources, et une étude géochimique des ions métalliques mobiles au travers de ce gisement de type SEDEX.
6. **Brent Ward** et **Jeff Bond** ont poursuivis leur étude portant sur l'âge de dépôts glaciaires de Reid dans le centre du Yukon. La région de la rivière Pelly fût le sujet d'échantillonage pour des datations cosmogéniques et des téphras.
7. **Nicholas Utting** et **Ian Clark** (université d'Ottawa) étudient, en collaboration avec la CGY, la composition chimique et en gaz nobles des eaux de sources annuelles de la montagne Bear Cave, dans la région de la rivière Fishing Branch. Ces travaux répondent aux inquiètudes des premières nations vis-à-vis les effets possibles de l'exploration pour les hydrocarbures sur les eaux souterraines.
8. **Monica Bruckner** (université de l'État du Montana) a poursuivie une étude de terrain d'un des glaciers à la source de la rivière Wheaton dans le cardre de sa maîtrise sous la tutelle de **Mark Skidmore** et **Jeff Bond.** Elle étudie les caractéristiques biogéochimiques des eaux de fonte dans un bassin périglaciaire.
9. **Stephen Horton** (université de Victoria) poursuit une étude de baccalauréat portant sur la paléogéographie du lac glaciaire de Laberge avec l'aide de **Jeff Bond** et **Peter Von Gaza** (géomatique Yukon).
10. **Antoni Lewkowicz** et ses étudiants gradués de l'université d'Ottawa ont poursuivient de nombreuses études du pergélisol à travers le territoire. En autre : a) ils enregistrent les conséquences des feux de forêt de 2004 sur la stabilité des pentes et l'accumulation de sédiments dans les ruisseaux ; b) ils étudient l'origine et la dynamique des lacs thermokastiques et des palses dans le bassin du ruisseau Wolf près de Whitehorse ; et c) ils développent des méthodes de cartographie régionale et de modélisation du pergélisol. Des études géophysiques du pergélisol et de glissements de terrain récents ont aussi été conduitent en collaboration avec **Bernd Etzelmüller** (université d'Oslo, la Norwège) et les employés de la CGY.
11. **Panya Liposky** et **Jeff Bond** compilent une carte des dépôts meubles pour l'ensemble du territoire, à l'aide d'un financement du ministère des affaires indiennes et du nord canadien (MAINC) dans le cardre du programme de dévellopement économique du Nord.

ÉTUDES DÉTAILLÉES ET RELATIONS PUBLIQUES

1. **Luke Beranek** continue d'augmenter le nombre d'analyses des zircons détritiques dans les roches Paléozoïques tardives et du Trias de part et d'autre de la limite entre la marge continentale nord-américaine et les terranes de Slide Mountain et Yukon-Tanana. Cette étude forme la base de sa thèse de doctorat à l'université de Colombie-Britannique sous la tutelle de **Jim Mortensen**. En 2005, Luke a démontré que des débris provenant des terranes s'accumulaient sur la marge nord-américaine dès le Trias précoce, beaucoup plus tôt que l'on le croyait auparavant. La saison dernière, il a étendu son échantillonage aux roches triassiques des monts Pelly, Selwyn et Ogilvies.
2. **Karen Pelletier** et **Charlie Roots** (CGC) ont entammés un guide géologique des routes yukonaises en visitant les sites géologiques d'intérêts le long de la plupart des routes du Yukon. Charlie s'est joint à **Tiffani Fraser** et **Tammy Allen** pour la préparation d'un guide de la route Dempster en collaboration avec la CGC et les Territoires du Nord-Ouest ; une version préliminaire de ce guide, de même que d'autres brochures couvrant certains segments des autres routes du Yukon devraient être disponible au publique au printemps 2007. Nous espérons compléter l'ensemble de ce projet pour le printemps 2008.

GÉOCHIMIE ET ÉVALUATION DU POTENTIEL MINÉRAL

1. La CGC, en collaboration avec **Geoff Bradshaw**, ont complétés un relevé géochimique des ruisseaux pour une région couvrant le bassin de Kandik dans le centre-nord du Yukon, au sud du parc territorial de Fishing Branch. Le financement pour ce relevé provient du programme de dévellopement économique du Nord du MAINC.

RELEVÉS AÉROMAGNÉTIQUES

1. La CGC, en collaboration avec la CGY, ont débutées un programme majeur de relevés aéromagnétiques des monts Wernecke et Mackenzie. Le financement provient du programme de dévellopement économique du Nord du MAINC. Toutefois, les pauvres conditions météorologiques au cours de l'été dernier ont empêcher la finalisation de ces relevés. On espère maintenant compléter ces relevés au début de 2007 et de publier les résultats vers la fin de l'été.

DIFFUSION DE L'INFORMATION

La Commission géologique du Yukon diffuse de l'information en trois formats : 1) les cartes et rapports sur papier sont vendus par le Bureau d'information et des ventes en géoscience ; 2) la plupart de nos publications et bases de données récentes sont disponibles en format numérique à prix réduit ; et 3) plusieurs de nos publications sont disponibles sans frais sous format PDF sur notre site internet (*www.geology.gov.yk.ca*). La liste des rapports d'évaluation de propriétés minières disponibles en format numérique est maintenant aussi offerte par internet (*www.emr.gov.yk.ca/library*).

Nous sommes fier de diffuser de l'information géospatialle par l'entremise de notre service de carte interactive ('Map Gallery'), que l'on accède par le site internet de la CGY. Ce site de carte interactive est continuellement le sujet d'améliorations ; nous apprécions les commentaires des usagers.

Les publications de la Commission géologique du Yukon sont diffusées par le Bureau d'information et des ventes en géoscience. Elles sont disponible à l'addresse suivante :

Bureau d'information et des ventes en géosciences
a/s Conservateur des registres miniers
le ministère de l'Énergie, des Mines et des Ressources
le gouvernement du Yukon

300, rue Main - bur. 102
C.P. 2703 (K102)
Whitehorse (Yukon) Y1A 2C6
Téléphone : (867) 667-5200
Télécopieur : (867) 667-5150
Courriel : geosales@gov.yk.ca

Pour en savoir plus sur la Commission géologique du Yukon, visitez notre page d'accueil à *www.geology.gov.yk.ca* ou communiquez directement avec :

Grant Abbott, Directeur
Commission géologique du Yukon
2099, 2ème Avenue
C.P. 2703 (K10), Whitehorse (Yukon) Y1A 2C6
Téléphone : (867) 667-3200
Courriel : grant.abbott@gov.yk.ca

Rod Hill, Gestionnaire
Commission géologique du Yukon
2099, 2ème Avenue
C.P. 2703 (K10), Whitehorse (Yukon) Y1A 2C6
Téléphone : (867) 667-5384
Courriel : rod.hill@gov.yk.ca

Robert E. Leckie Award for Outstanding Reclamation Practices

***Judy St. Amand*[1]**
Mining Lands, Energy Mines and Resources

St. Amand, J., 2007. Robert E. Leckie Awards for Outstanding Reclamation Practices. *In:* Yukon Exploration and Geology 2006, D.S. Emond, L.L. Lewis and L.H. Weston (eds.), Yukon Geological Survey, p. 77-79.

OUTSTANDING QUARTZ RECLAMATION

DYNAMITE RESOURCES LTD.

Dynamite Resources Ltd. is a junior mining company that is exploring the highly prospective Mike Lake project. The claims are located about 80 km east-northeast of Dawson City and are accessible only by air.

During initial exploration, the company discovered an abandoned camp on a nearby property (Fig. 1). Over the next month, the operator returned the area to its original pristine environment. The camp was dismantled and all material disposed of or incinerated.

The company has followed every recommended best practice at its camp, drill sites, fuel and core storage areas, as well as preparation for seasonal closure (Fig. 2). This company has gone beyond the requirements of legislation by reclaiming an area where there was no requirement for it to do so.

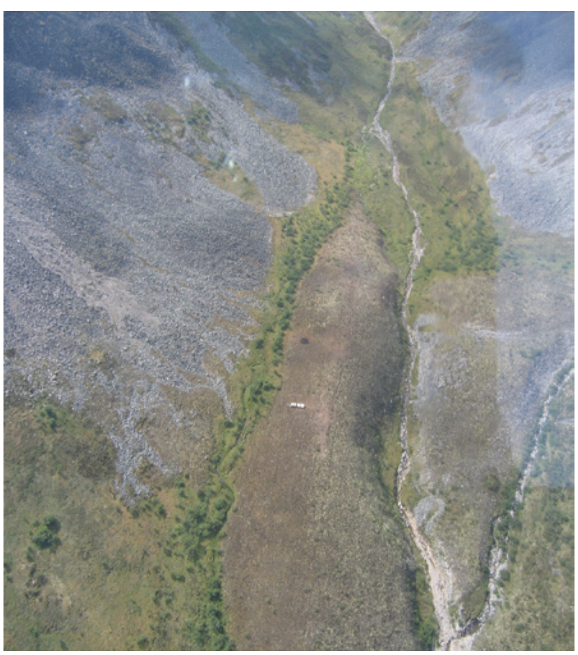

Figure 1. *Abandoned camp reclaimed in Mike Lake area.*

Figure 2. *Seasonal closure, Mike Lake project.*

[1]*judy.stamand@gov.yk.ca*

Honourable mention: Deloitte & Touche are the court-appointed receiver for Anvil Range Mining Corp. at Faro. Although revegetation of this site was required as part of a water use license, the work undertaken to reclaim the fresh-water reservoir and supply dam is commendable (Fig. 3).

For the revegetation program, indigenous flora was solely used. Seeds were manually broadcast using pouch-style seeders, and integrated into the soil substrate with hand rakes, as well as with harrows pulled by an ATV for selected areas. Due to this site's geographical features, hands-on seeding was needed, which was consequently very labour intensive.

Additionally, subsequent monitoring of plant growth and establishment has shown excellent results, which can be attributed to the diligence of the reclamation practices.

OUTSTANDING PLACER RECLAMATION

365334 ALBERTA LTD.

365334 Alberta Limited, operating as A-1 Cats, has mined on Dominion Creek in the Dawson Mining district since 2002 (Fig. 4).

A-1 Cats management continues to address land-based reclamation on an ongoing basis. Reclamation is timely and economical by minimizing movement of material. Use of organic material has expedited natural revegetation, and although seeding is not a requirement in areas where revegetation naturally occurs, the company has experimented in some areas with spectacular results.

Their desire to enhance old workings has resulted in low-relief topography, which is not only aesthetically pleasing but a safer environment for people and wildlife.

The entire property, including areas that were disturbed prior to their arrival, is being reclaimed to present day standards. The company's Best Management Practices are a credit to the placer industry.

Figure 3. *Reclamation of fresh water reservoir and supply dam, Faro, Yukon.*

Honourable mention: Bardusan Placers operate in the Mayo Mining District in a narrow valley with intermittent permafrost, vast quantities of slide rock, and extensive hard rock workings from past United Keno Hill Mines activities in the area. Bardusan Placers is working upstream on Lightning Creek using systematic mining practices and long-term planning (Fig. 5). They accomplish efficient and prompt reclamation of the previous year's mining cut by using the stripping/wastes from the following year's mining.

Rather than use the creek as a conduit, which is common in narrow valleys, the Barchens, in an innovative and forward-thinking fashion, transport water to their settling ponds via an underground culvert system.

The Barchen family has responded to the environmental challenges of the regulatory era by meeting and exceeding government expectations for operational considerations, discharge standards and final reclamation of the mined properties.

Figure 4. *A-1 Cats' ongoing reclamation, placer mining at Dominion Creek.*

Figure 5. *Natural revegetation on Lightning Creek.*

GEOLOGICAL FIELDWORK

Investigating a Triassic overlap assemblage in Yukon: On-going field studies and preliminary detrital-zircon age data
L.P. Beranek and J.K. Mortensen 83

Evaluation of the origins of gold hosted by the conglomerates of the Indian River formation, Yukon, using a combined sedimentological and mineralogical approach
D.P.G. Bond and R.J. Chapman 93

Late Wisconsinan McConnell glaciation of the Big Salmon Range, Yukon
J.D. Bond 105

The Dawson City landslide (Dawson map area, NTS 116B/3), central Yukon
M.A. Brideau, D. Stead, V. Stevens, C. Roots, P. Lipovsky and P. VonGaza 123

Developing a new method to identify previously unrecognized geochemical and morphological complexity in placer gold deposits in western Yukon
E.C. Crawford, R.K. Chapman, W.P. LeBarge and J.K. Mortensen 139

Micropetrology and mineral geochemistry of the Tombstone and Deadman plutons, Tombstone Plutonic Suite, central Yukon
A.M. Flanders, M.J. Harris, L. Kearns and C.J.R. Hart 149

Field investigations of the Upper Devonian to Lower Carboniferous Tuttle Formation, eastern Richardson Mountains, Yukon
T.A. Fraser and T.L. Allen 157

Are mafic dykes in the Nor and Hart River areas of the Yukon correlative to the Bonnet Plume River Intrusions? Constraints from geochemistry
J. Hunt and D. Thorkelson 175

A reconnaissance inventory of permafrost-related landslides in the Pelly River watershed, central Yukon
P.S. Lipovsky and C. Huscroft 181

Structure of schist in the vicinity of the Klondike goldfield, Yukon
D. MacKenzie, D. Craw, J.K. Mortensen and T. Liverton 197

Laser ablation ICP-MS U-Pb zircon ages for Cretaceous plutonic rocks in the Logtung and Thirtymile Range areas of southern Yukon
J.K. Mortensen, A. Brand and T. Liverton 213

The three 'Windy McKinley' terranes of Stevenson Ridge (115JK), western Yukon
D.C. Murphy 223

Morphological and compositional analysis of placer gold in the South Nahanni River drainage, Northwest Territories
K.L. Rasmussen, J.K. Mortensen and H. Falck 237

Investigating a Triassic overlap assemblage in Yukon: On-going field studies and preliminary detrital-zircon age data

***Luke P. Beranek*[1] *and James K. Mortensen*[2]**
Pacific Centre for Isotopic and Geochemical Research,
Department of Earth and Ocean Sciences, University of British Columbia

Beranek, L.P. and Mortensen, J.K., 2007. Investigating a Triassic overlap assemblage in Yukon: On-going field studies and preliminary detrital-zircon age data. *In:* Yukon Exploration and Geology 2006, D.S. Emond, L.L. Lewis and L.H. Weston (eds.), Yukon Geological Survey, p. 83-92.

ABSTRACT

New field and detrital-zircon age data from the Selwyn Basin indicate the Yukon-Tanana Terrane (YTT) was a source region for Triassic sediments (Smithian – Norian; conodont ages) that were deposited along the ancestral margin of North America (NAM). Triassic rocks of the NAM contain middle to late Paleozoic detrital-zircon and geochemical signatures which are unique to the YTT and absent from the NAM, demonstrating that the Triassic rocks represent the earliest observed overlap assemblage linking allochthonous terranes to the NAM in the northern Cordillera. New provenance data also defines and characterizes Jurassic assemblages. Terrane accretion in the northern Cordillera was previously thought to have commenced in Early to Middle Jurassic time; however, the presence of a 40-50 m.y. older Triassic overlap assemblage requires that Triassic rocks were deposited in a collision-related foreland basin setting rather than a stable continental terrace and rise.

RÉSUMÉ

De nouvelles données géochimiques et de datation de zircons détritiques recueillies dans le bassin de Selwyn indiquent que le terrane de Yukon-Tanana (TYT) a constitué une région source de sédiments du Trias (conodontes des Smithien – Norien), qui ont été déposés le long de l'ancestrale marge de l'Amérique du Nord (AMA). Les roches du Trias de l'AMA renferment des zircons détritiques datant du Paléozoïque moyen à tardif et présentent des signatures géochimiques uniques au TYT et absentes de l'AMA, ce qui démontre que ces roches représentent l'assemblage chevauchant le plus précoce observé reliant les terranes allochtones à l'AMA dans la Cordillère septentrionale. De nouvelles données sur la provenance permettent en outre de définir et de caractériser les assemblages du Permien et du Jurassique. On pensait antérieurement que l'accrétion des terranes dans le nord de la Cordillère avait commencé au Jurassique précoce à moyen; cependant, la présence d'un assemblage chevauchant du Trias de 40 à 50 Ma plus ancien exige que les roches du Trias aient été déposées dans un cadre de bassin d'avant pays associé à une collision plutôt que dans un cadre de terrasse et de glacis continentaux stables.

[1]*lberanek@eos.ubc.ca*
[2]*jmortensen@eos.ubc.ca*

INTRODUCTION

Triassic sedimentary rocks of the Yukon are generally characterized as fine-grained, siliciclastic marine deposits of the Cordilleran miogeocline reflecting passive-margin sedimentation along the western fringe of ancestral North America (Gordey and Anderson, 1993). In eastern and north-central Yukon, Triassic rocks unconformably overlie middle to late Paleozoic sedimentary units of the Selwyn Basin, the distal portion of the passive-margin sequence in the northern Canadian Cordillera. Triassic rocks are also known to be in depositional contact with Paleozoic assemblages of the pericratonic Yukon-Tanana and Slide Mountain terranes, which are located outboard of the Selwyn Basin (Colpron *et al.*, 2006).

Recent geologic investigations demonstrate that the depositional framework of Triassic sedimentary rocks and their relationship with pericratonic terranes in the northern Cordillera is unclear (e.g., Nelson *et al.*, 2006). For example, conspicuous detrital muscovite and local feldspar in Triassic rocks assigned to the Cordilleran passive margin (minerals largely absent in the underlying Paleozoic stratigraphy) may reflect uplift and east-directed sedimentation sourced from terranes to the west (Ross *et al.*, 1997). However, regional studies of the miogeocline in Alberta determined no western or oceanward source has supplied sediment to Triassic marginal basins (Gibson and Barclay, 1989; Davies, 1997).

Lithologically similar packages of Triassic rocks were deposited in the Selwyn Basin and on the Yukon-Tanana and Slide Mountain terranes; hence, these similar successions may record the presence of a sedimentary overlap assemblage defining the first linkage of allochthonous terranes with North America (Murphy *et al.*, 2006). The Yukon-Tanana, with the intervening Slide Mountain, represents the first terrane found west of the North American margin in the northern Cordillera; therefore the style and timing of its accretion is paramount in understanding the fundamentals of Mesozoic Cordilleran tectonics and crustal growth of Laurentia. The implications of a Triassic overlap assemblage extend beyond the Yukon, as similar rocks are found in northern British Columbia and Alaska (Nelson, 1993; Dusel-Bacon and Harris, 2003). Additionally, the interpreted timing of accretion of well known Cordilleran terranes may require revision. For example, the Yukon-Tanana Terrane is interpreted to have late Paleozoic to early Mesozoic links with Quesnellia and Stikinia (Simard *et al.*, 2003; Colpron *et al.*, 2006). Terrane accretion was previously presumed to have commenced in the Early to Middle Jurassic (Gabrielse and Yorath, 1991), therefore the presence of a Triassic overlap assemblage some 40-50 million years earlier requires Triassic rocks to be deposited within a collision-related peripheral foreland basin instead of a stable continental terrace and rise.

This paper mainly highlights results of new field work and preliminary U-Pb detrital-zircon dating of Triassic sedimentary rocks collected during the summer of 2006. We examine the provenance for passive margin sediments of the Selwyn Basin and parautochthonous Cassiar Terrane, along with Triassic units of the outboard Yukon-Tanana and Slide Mountain terranes. Provenance data from unstudied and newly discovered Jurassic sedimentary assemblages of the Yukon are also included. Preliminary provenance data suggest Triassic sedimentary rocks of the Selwyn Basin contain detritus from Yukon-Tanana and Slide Mountain terranes. From these data, we conclude that the Yukon-Tanana Terrane was linked to North America by the Early Triassic. The direct implication is that Yukon-Tanana Terrane overrode the North American margin by Early Triassic time, creating a peripheral foreland basin on the lower plate. Early to Middle Triassic rocks of the Selwyn Basin represent primary and reworked deposits of this pro-foreland assemblage. The oldest preserved Triassic rocks of Yukon-Tanana and Slide Mountain terranes, recording the earliest presence of the second sedimentary phase, the overlap assemblage, are Middle Triassic in age (Teh clastic unit of Roots *et al.*, 2002; Big Campbell window of Murphy *et al.*, 2006).

PREVIOUS WORK

Field and laboratory studies carried out in 2005 (summarized in Beranek and Mortensen, 2006) included examination of the type section of the Early Triassic Jones Lake Formation in the Little Nahanni map area (NTS 105I/13), which is the only formally described Triassic stratigraphic section in the Selwyn Basin (Gordey and Anderson, 1993). The Jones Lake Formation type section, exposed in the core of the Wilson syncline, comprises >750 m of orange-tan weathering, ripple cross-laminated calcareous siltstone and carbonaceous shale with subordinate limestone. Detrital muscovite is pervasive and locally abundant along shaley bedding planes. Paleocurrent information suggests east to southeasterly flow in a dominantly nearshore environment. New biostratigraphic control based on conodont faunas constrain the entire Jones Lake Formation type section as Early Triassic (Smithian) and the top of underlying Mount Christie Formation as Early Permian (early Artinskian). Whole-rock shale geochemical analyses of the Mount Christie and Jones Lake formations suggest a source that is dominantly granitic and evolved; however, the Jones Lake Formation contains geochemical signatures that suggest partial derivation from a mafic, juvenile source terrain (Beranek and Mortensen, 2006).

Various geologic compilations and bedrock mapping campaigns across the Yukon have constrained the age of Triassic sedimentary rocks and their association with the Cordilleran passive margin (Abbott, 1977; Gordey, 1981; Murphy *et al.*, 2006), Yukon-Tanana Terrane (Roots *et al.*, 2002; Pigage, 2004; Colpron *et al.*, 2005), and Slide Mountain Terrane (Murphy *et al.*, 2006). In two related studies, Colpron *et al.* (2005) reported detrital-zircon age data within a Triassic conglomerate in the Glenlyon map area of central Yukon, and Creaser and Harms (1998) used Nd isotope geochemistry to characterize Triassic sandstones overlying the Klinkit Group near the Yukon-British Columbia border. However, no previous studies have tested possible correlations of Triassic rocks across the Yukon or attempted to determine their provenance in order to evaluate whether the Triassic sequence comprises an overlap assemblage.

FIELD SITES AND PRELIMINARY DETRITAL-ZIRCON DATA

In the following section, we discuss U-Pb detrital-zircon provenance data from seven field sites in Yukon. These data are preliminary in nature and will be used for detailed, site-specific studies in forthcoming publications; U-Pb ages are put into populations according to the time scale of Okulitch (2002). All detrital zircon was analysed by the lead author using laser-ablation ICP-MS methods at the Pacific Centre for Isotopic and Geochemical Research at the University of British Columbia.

SELWYN BASIN

Little Nahanni map area

The type section of the Early Triassic (Smithian) Jones Lake Formation is located in the easternmost Selwyn Basin, south of MacMillian Pass (Location 1 on Fig. 1). It is in disconformable contact with the underlying Late(?) Mississippian-Early Permian Mount Christie Formation, which itself unconformably overlies the Early to mid-Mississippian Tsichu formation. Gordey and Anderson (1993) document a significant sub-Triassic regional unconformity in the Nahanni map area, as the Jones Lake Formation is known to sit on rocks as old as the Devono-Mississippian Earn Group. Notably, Orchard (2006) described Griesbachian and Dienerian (earliest Triassic) reworked conodont faunas in the type section of the Jones Lake Formation and interpreted a regional Smithian depositional event.

In 2005, the type sections of the Mount Christie and Jones Lake formations were measured and sampled to determine their provenance, depositional age and lithofacies associations (Beranek and Mortensen, 2006). The Tsichu formation was also sampled. Measuring and sampling a complete Mississippian to Triassic stratigraphic succession makes it possible to observe any systematic changes in sediment character or provenance through time.

Preliminary detrital-zircon age data from Tsichu formation quartz sandstone yielded many Paleozoic and Precambrian age populations (n=102 grains): Late to Middle Devonian (*ca.* 360-390 Ma), Early Devonian (*ca.* 400 Ma), Silurian to Cambrian (425-530 Ma), early Neoproterozoic to middle Mesoproterozoic (*ca.* 950-1300 Ma), late to middle Paleoproterozoic (1600-1800 Ma), middle to early Paleoproterozoic (1800-2000 Ma), early Paleoproterozoic (2000-2400 Ma), and Late Archean (2500-2900 Ma). Proterozoic and Archean ages compare favourably with known U-Pb zircon ages of sandy miogeoclinal rocks in the Cordillera and Precambrian basement complexes of Laurentia (Gehrels, 2000; Link *et al.*, 2005). Early to middle Paleozoic ages (Cambrian-Early Devonian) may be sourced from undated volcaniclastic units of the Selwyn Basin (Goodfellow *et al.*, 1995; Gordey and Anderson, 1993) or recycled through early Paleozoic rocks from Arctic Canada (Ross *et al.*, 1997; Miller *et al.*, 2006). Late to Middle Devonian ages correspond to the Ecstall and Finlayson magmatic cycles, generated by the rifting of Yukon-Tanana Terrane from the North American autochthon (Piercey *et al.*, 2006). It is noteworthy that the Early to mid-Mississippian (*ca.* 330 Ma) Tsichu formation contains no detrital zircons younger than *ca.* 360 Ma, suggesting magmatism along the rifted margin ceased by the Late Devonian.

Preliminary detrital-zircon age data from micaceous sandstone of the Jones Lake Formation contain the following age populations (n=98 grains): late Early Mississippian (*ca.* 345 Ma), Late to Middle Devonian (360-380 Ma), Early Devonian to Silurian (400-440 Ma), Ordovician-Cambrian (450-540 Ma), late to middle Neoproterozoic (570-750 Ma), and early Neoproterozoic to Late Archean (*ca.* 1000-3000 Ma). U-Pb ages are similar to the underlying Tsichu formation, however, the type section of the Jones Lake Formation contains late Early Mississippian detrital zircons, whose signature is known to be region- and age-specific to the Yukon-Tanana Terrane to the west (Wolverine Cycle, Piercey *et al.*, 2006) and absent from the ancestral margin of North America. This suggests the Yukon-Tanana Terrane was proximal or linked to the ancient Pacific margin by the Early Triassic.

Frances Lake and Watson Lake map areas

During July, 2005, several Triassic localities were investigated in the Frances Lake and Sa Dena Hes mine road areas of southeastern Yukon (Location 2 on Fig. 1). All sites are interpreted to be in depositional contact with Paleozoic units of the Selwyn Basin (Murphy *et al.*, 2006). Two new conodont collections along the new Sa Dena Hes mine road contained Middle Triassic (late Ladinian) fauna, consistent with previous sampling of the region (Murphy *et al.*, 2006; Orchard, 2006). Light grey weathering, parallel-laminated siltstone and sandstone of this area contain appreciable amounts of muscovite and feldspar. In the Mt. Hundere area, Abbott (1977) located cross-bedding in outcrop and observed current directions suggesting dominantly eastward transport.

Preliminary detrital-zircon age data for Middle Triassic rocks from three localities in southeastern Yukon have main age populations (n=219 grains) that are early Late Triassic (222 Ma), Middle to Early Triassic (233-246 Ma), Early Triassic to mid-Permian (250-269 Ma), mid-Permian to Early Pennsylvanian (269-312 Ma), Late to mid-Mississippian (320-337 Ma), Early Mississippian (350-

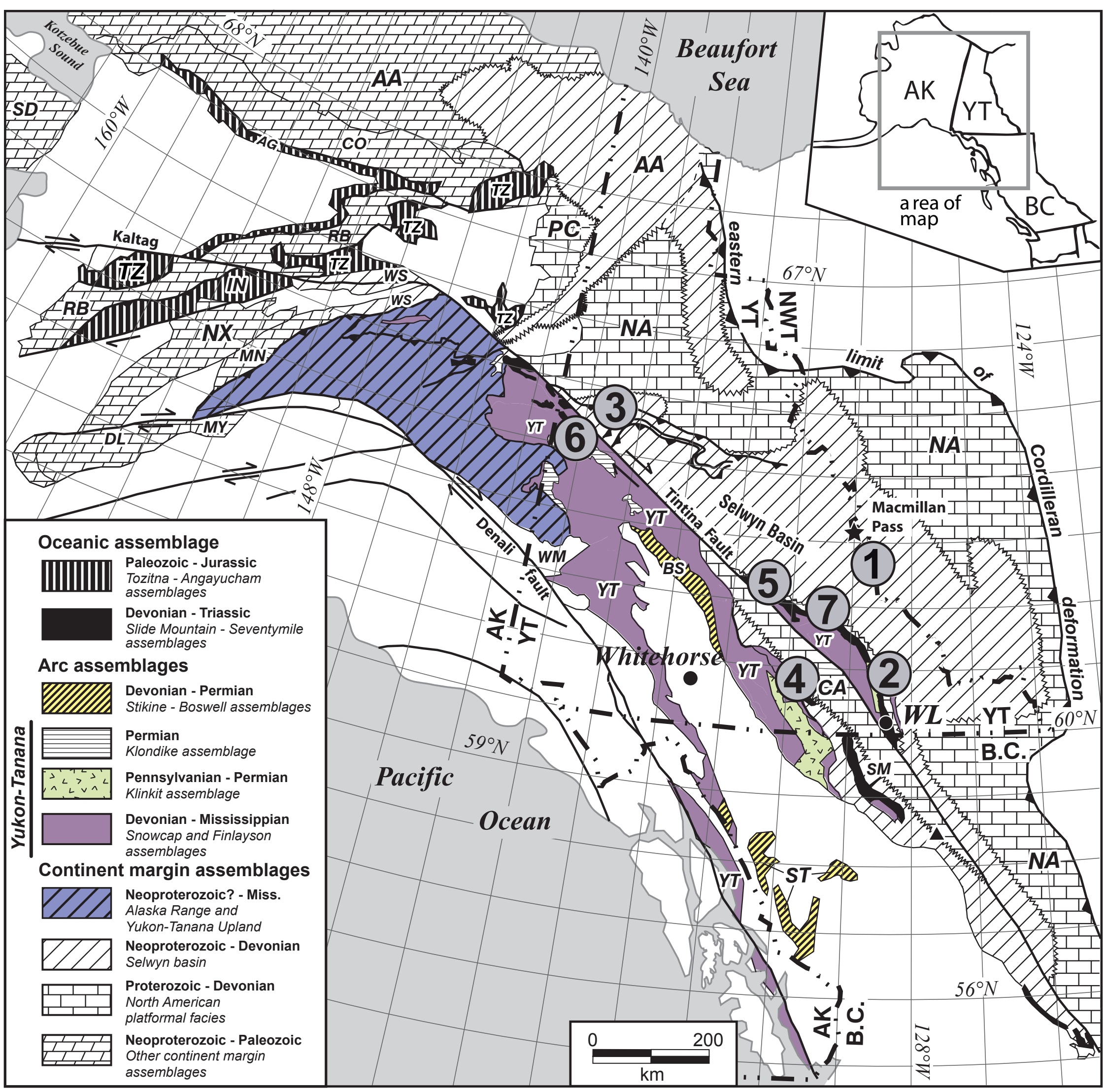

Figure 1. *Tectonic assemblage map of the northern Cordillera. Numbered circles indicate Triassic successions of this study. Modified from Colpron et al. (2006).*

355 Ma), Late to Middle Devonian (358-391 Ma), Early Devonian (400-416 Ma), Silurian-Ordovician (435-476 Ma), Cambrian (490-543 Ma), late Neoproterozoic (543- *ca.* 590 Ma), late to middle Neoproterozoic (600-*ca.* 700 Ma), and early Neoproterozoic to Late Archean (1000-3000 Ma). These populations represent the composite Yukon-Tanana signature, as all middle to late Paleozoic magmatic cycles are represented (*cf.* Piercey *et al.*, 2006). Interestingly, the 300-312 Ma age peak recorded in these sedimentary rocks coincides with a known lull in felsic magmatism in Yukon-Tanana (Colpron *et al.*, 2006); we interpret these zircons to be recycled through the Boswell assemblage (Stikinia/Yukon-Tanana overlap). Pennsylvanian detrital zircons are known to be in Middle(?) Triassic conglomerate of the Glenlyon map area, and Colpron *et al.* (2005) interpreted detrital zircon therein to be recycled through the Boswell assemblage. Early Late Triassic zircon (222 Ma; 3 grains) is present in one sample, a micaceous sandstone from 99 Mile Creek just south of Frances Lake, and suggests some rocks of this region extend beyond the Ladinian. However, Triassic samples from this area contain detrital zircon with concordant analyses of 238 and 240 Ma (Ladinian), suggesting syn-depositional magmatism, previously undocumented. Colpron *et al.* (2005) documented a single 239 Ma detrital-zircon age in Middle(?) Triassic conglomerate of the Glenlyon map area.

Dawson map area

In the upper Klondike River area north of Dawson, calcareous siltstone, feldspathic sandstone, and fossiliferous limestone of unknown Triassic age unconformably overlie Permian siliceous shale and are overlain by Middle Jurassic carbonaceous shale and feldspathic grit (Location 3 on Fig. 1; Fig. 2).

Coarse-grained feldspathic arenite and medium-grained feldspathic wacke from the upper member of the Triassic section (Middle to Late Triassic?) yielded preliminary U-Pb detrital-zircon age distributions that are similar to the previously discussed samples. Major detrital-zircon age populations (n=165) are Early Mississippian (331-334 Ma), Middle Devonian (380-390 Ma), Early Devonian (400-410 Ma), Silurian (420-440 Ma), Early Ordovician (*ca.* 470-490 Ma), Cambrian (506-543 Ma), late to middle Neoproterozoic (550-700 Ma), and early Neoproterozoic to Late Archean (1000-3100 Ma). The presence of late Early Mississippian (*ca.* 330 Ma) detrital zircons suggests that during the Triassic, the North American margin of this region was proximal to the Yukon-Tanana Terrane.

Jurassic carbonaceous shale and feldspathic grit known as the Lower Schist Division sit on top of the Triassic rocks. Contacts with underlying rock units are covered, and conodont age determinations for the Triassic section are still in progess. Poulton and Tempelman-Kluit (1982) assigned an early Late Jurassic (Late Oxfordian) age to the Lower Schist Division succession based on the presence of Buchia and Cardioceras. One detrital-zircon sample,

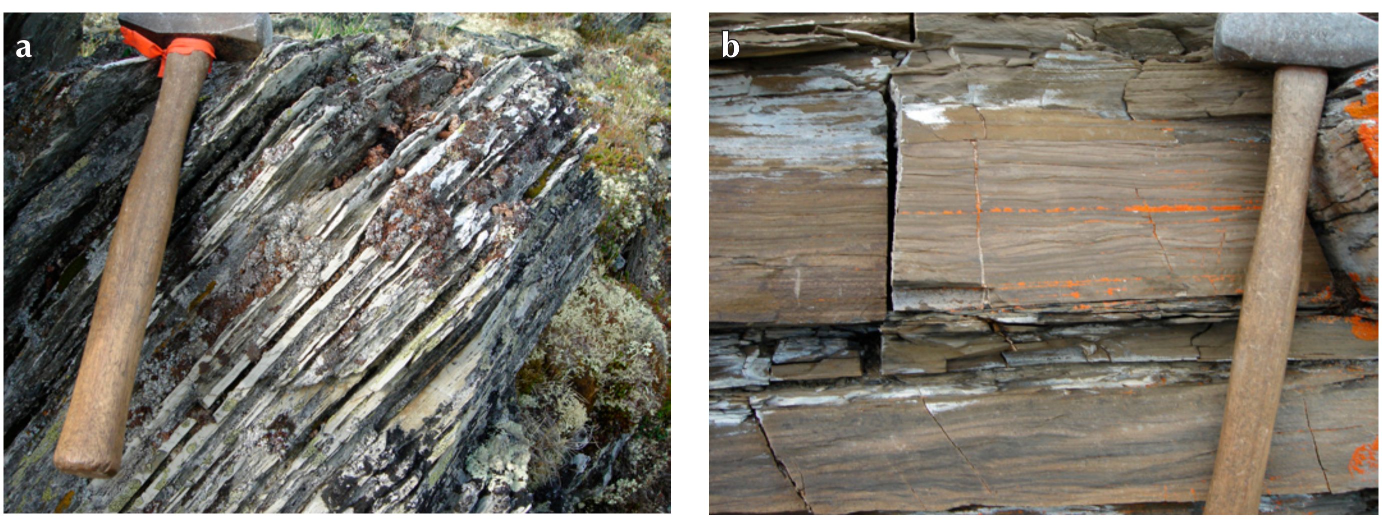

Figure 2. (a) *Typical outcrop view of white-green weathering, grey thinly bedded, siliceous Permian shale that underlies Triassic rocks east of Mt. Robert Service, upper Klondike River area.* ***(b)*** *Wavy-laminated calcareous siltstone and sandstone of the lower Triassic succession east of Mt. Robert Service. Detrital mica is pervasive, especially along shale partings.*

from a 1-m-thick feldspathic grit, yielded the following preliminary age populations (n=73 grains): Middle Jurassic (Bajocian) to Early Jurassic (170-190 Ma), Late Permian (258 Ma), Pennsylvanian to latest Devonian (312-360 Ma), Early Paleozoic to middle Neoproterozoic (420-717 Ma), and early Neoproterozoic to Late Archean (1000-2700 Ma). Jurassic sedimentary rocks of the Selwyn Basin may essentially define a middle Mesozoic overlap assemblage linking an outboard terrane(s) to the composite Yukon-Tanana/North America block. While Early Jurassic plutons are common in Yukon-Tanana, ages younger than *ca.* 180 Ma are scarce; this could reflect sourcing from an outboard terrane, such as Stikinia.

CASSIAR TERRANE

Finlayson Lake map area

Triassic rocks in the Pelly Mountains of southeastern Yukon overlie Devonian-Permian(?) black shale and chert of the parautochthonous Cassiar Terrane, a miogeoclinal block displaced along the margin due to dextral translation of the Tintina Fault (Location 4 on Fig. 1). In several localities around southeastern Yukon, rocks of the miogeocline (Triassic and older) are overlain by immature sedimentary rocks, which are structurally overlain by allochthons; these have been regarded by Tempelman-Kluit (1979) as synorogenic clastic and cataclastic rocks, respectively. Gordey (1981) produced a geologic map of the Indigo Lake area in the Pelly Mountains, which outlined the extent and nature of the McNeil Klippe (cataclastic rocks; siliceous mylonite), which in this area overlies a section of Jura-Cretaceous greywacke (synorogenic clastics) and Triassic and Paleozoic miogeoclinal rocks. Field work during 2006 and detrital-zircon dating suggest a reinterpretation for the McNeil Klippe region is necessary. Middle to Late Triassic rocks are overlain by two successions of rocks: a lower one we interpret to comprise Late Permian to Early Triassic sedimentary and volcanic rocks that are tentatively considered to be equivalent to portions of the Simpson Lake group (Permian-Triassic forearc assemblage) in southeastern Yukon; and an upper package which comprises highly deformed chert and calc-silicate rock, which is interpreted to be the Mississippian to Permian(?) Fortin Creek group (Slide Mountain Terrane).

Limited exposure in the Triassic section under the McNeil Klippe did not allow measurement of the succession; however, Gordey (1981) interpreted a thickness of 500 to 750 m. Our new work delimits three separate 30-m sections, each representing the average character for a lower, middle and upper 'member' of the Triassic. The lower member is typified by 2- to 4-cm-thick beds of parallel laminated, brown-weathering, micaceous, silty shale intercalated with 1- to 5-cm-thick, wispy to parallel-laminated, brown-orange-weathering limy siltstone to silty limestone (Fig. 3a). The middle member contains thinly laminated, grey-brown-weathering, carbonaceous shale and parallel-laminated silty shale that grades up-section into silty shale with distinctive lenticular bodies of brown-orange-weathering calcareous material (Fig. 3b). The upper member comprises 1- to 2-cm-thick beds of distinctive wavy laminated, grey siltstone to silty shale with wisps (1-5 mm) of brown-orange-weathering limy silt which thicken up-section into 4-cm couplets with dark grey shale (Fig. 3c). Above the upper member, exposure is limited, but limestone, carbonaceous shale and coarse-grained micaceous sandstone make up the stratigraphy.

Preliminary detrital-zircon data from the Triassic section underlying the McNeil Klippe, and probable allochthon of feldspathic grit, is derived from a composite of coarse-grained, micaceous sandstone and a fine-grained, calcareous siltstone (conodont ages in progress). The major age populations are (n=76 grains) Late to Middle Triassic (212-232 Ma), Early Triassic to Late Permian (248-255 Ma), Late Mississippian (319-322 Ma), Early Mississippian to latest Devonian (354-361), Late to mid-Devonian (375-390 Ma), early Paleozoic (430-512 Ma), late to middle Neoproterozoic (542-762 Ma), and early Neoproterozoic to Lake Archean (1000-2700 Ma).

Preliminary U-Pb detrital-zircon age populations (n=62 grains) from feldspathic grit mapped by Gordey (1981) as synorogenic clastic rocks (our interpreted Simpson Lake group equivalent) overlying North American Triassic rocks are Middle to Early Triassic (237-245 Ma), Early Triassic (246-253 Ma), Late to mid-Permian (254-268 Ma), and Early Permian (280 Ma). These ages contain a high amount of Klondike Cycle-aged zircons (Piercey *et al.*, 2006). As in the case of the Middle Triassic samples from the Finlayson Lake map area, it is unclear where the 237-253 Ma zircons are being derived from, since Early to early Late Triassic magmatism has not been recognized thus far in the Yukon.

YUKON-TANANA TERRANE

Tay River map area

Massive pebble to cobble conglomerate and intercalated sandstone, chert and basalt sit unconformably on rocks of

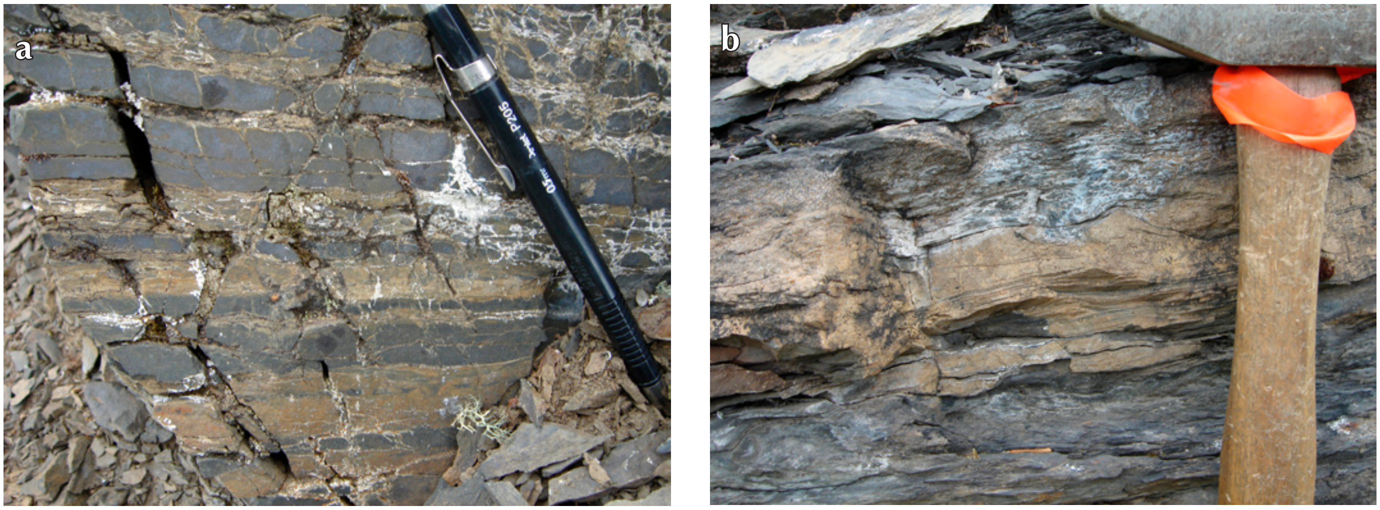

Figure 3. (a) *Triassic silty shale with wispy calcareous material, lower member, McNeil Lake area.* ***(b)*** *Triassic silty shale with lenticular silty limestone bodies, middle member, McNeil Lake area.* ***(c)*** *Triassic couplets of limy siltstone and carbonaceous shale, upper member, McNeil Lake area.*

the Yukon-Tanana Terrane north of the Tintina Fault, near Faro (Location 5 on Fig. 1; Fig. 4). Pigage (2004) informally named this succession the Faro Peak formation. Carnian and Norian conodont faunas were collected from limestone clasts within Faro Peak formation conglomerate and Pigage (2004) assigned this unit a Late Triassic age. The Faro Peak formation conglomerates also contain clasts of metaclastic rocks, chert, and mafic to intermediate volcanic rocks.

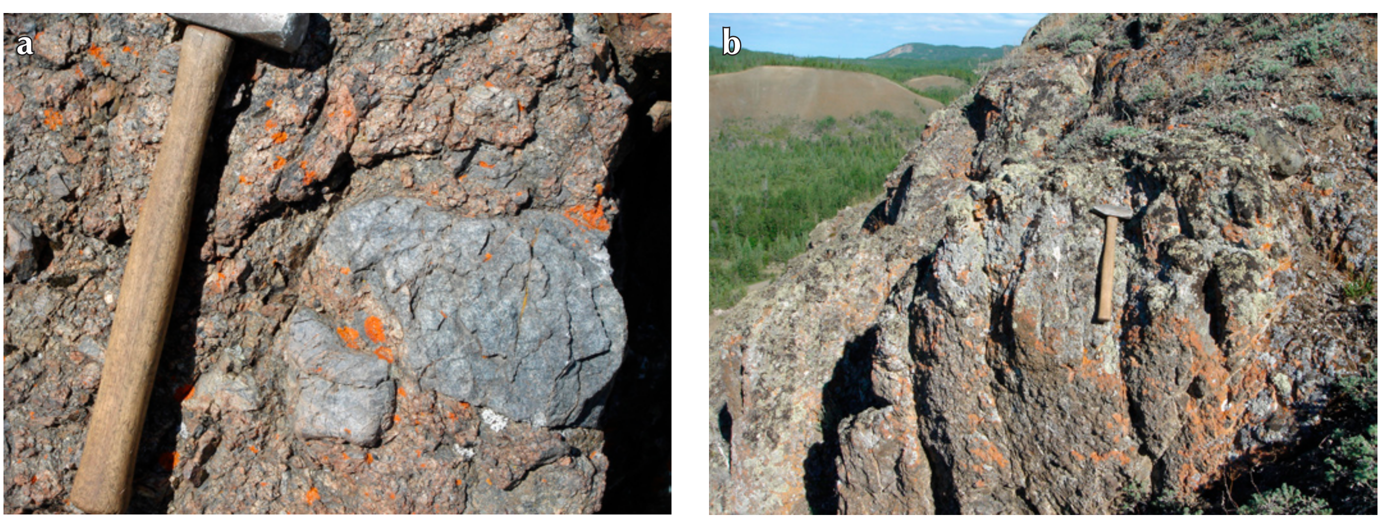

Figure 4. (a) *View of pebble to cobble conglomerate of the Faro Peak formation, north of Faro townsite. Cobble to right of hammer is a micaceous metaclastic rock.* ***(b)*** *Typical view of massive, granule to pebble conglomerate of the Faro Peak formation, east of Faro townsite.*

Results of detrital-zircon dating of Faro Peak samples collected during 2006 indicate that the depositional age of this unit is not Late Triassic as previously believed. Preliminary detrital-zircon age dating shows major age populations (n=89 grains) from two Faro Peak conglomerate samples are Middle Jurassic (167-176 Ma), Early Jurassic (178-200 Ma), Late Triassic (202-235 Ma), Permian (250-278 Ma), Pennsylvanian to Late Mississippian (306-319 Ma), and Proterozoic (1000-1900 Ma). These data require that the depositional age of the Faro Peak formation can be no older than Middle Jurassic. This is, in general terms, age-correlative with rocks of the Lower Schist Division in the upper Klondike River area, north of Dawson. More importantly, the Jurassic detrital zircons of the Faro Peak formation may separate it from the synorogenic clastic rocks of Tempelman-Kluit (1979), which we interpret to be mainly Permian to Early Triassic in age.

SLIDE MOUNTAIN TERRANE

Dawson map area

Triassic rocks exposed in the vicinity of the Clinton Creek mine, northwest of Dawson, are spatially associated with greenstone and ultramafic units of the Slide Mountain Terrane (Location 6 on Fig. 1). Contact relationships are faulted, and it is unclear if Triassic sedimentary packages of the region were originally deposited on Slide Mountain Terrane or Yukon-Tanana Terrane. Four new conodont collections confirm these rocks are Late Triassic (early Norian) in age.

Preliminary detrital-zircon age populations (n=173 grains) from three grouped samples are Late Triassic (*ca.* 221 Ma), mid- to Early Permian (260-300 Ma), Late Mississippian (321-343 Ma), Early Mississippian (346-357 Ma), Late to mid-Devonian (363-394 Ma), early Paleozoic (400-*ca.* 540 Ma), late to middle Neoproterozoic (555-772 Ma), and early Neoproterozoic to early Paleoproterozoic (1000-1900 Ma). Regardless of whether these Triassic rocks were originally part of the Slide Mountain Terrane or the Yukon-Tanana Terrane, they definitely received sedimentary input from the Yukon-Tanana Terrane, as shown by the composite Permian-Early Mississippian age groupings present (Klondike-Wolverine cycles; Piercey *et al.*, 2006).

Finlayson Lake map area

Triassic rocks in the northern Finlayson Lake District (Location 7 on Fig. 1) comprise sandy bioclastic limestone and shale that lie in angular unconformity with the underlying Fortin Creek group (Slide Mountain Terrane). These rocks are all in the hanging wall of the Inconnu thrust, a regional thrust fault placing outboard rocks in contact with the North American margin (Murphy *et al.*, 2006). Overlying the Late Triassic package is an allochthon containing tan-grey chert-pebble conglomerate, lithic sandstone, and grey limestone which we interpret to be equivalent to the Permo-Triassic Simpson Lake group. The sandy bioclastic limestone unit has been assigned an early Norian age, and conodont fauna therein are unknown in rocks of the Western Canada Sedimentary Basin (Orchard, 2006). However, these fauna are present in early Norian Eurasian (Tethyan) successions observed further outboard (i.e., Cache Creek Terrane, Wrangellia).

Preliminary detrital-zircon age populations from the Late Triassic sandy bioclastic limestone (n=78 grains) are Pennsylvanian to Late Mississippian (312-330 Ma), Late to Middle Devonian (357-386 Ma), Early Devonian to Cambrian (399-539 Ma), late Neoproterozoic (575-657 Ma), and early Neoproterozoic to Late Archean (1000-2800 Ma). The presence of specific Proterozoic and middle to late Paleozoic age populations suggest this package was formed in proximity to the Laurentian margin, as those ages are observed in other studied Devonian to Triassic samples of the Selwyn Basin. The presence of Eurasian conodont faunas may simply call for Late Triassic rocks of Slide Mountain Terrane to have formed in a lower paleolatitude, rather than in outboard Tethyan realms.

Chert-pebble conglomerate and lithic sandstone in the allochthon structurally overlying the composite Late Triassic section contains the following preliminary detrital-zircon age populations (n=157 grains): Middle Triassic (235-244 Ma), Early Triassic (245-253 Ma), Permian (254-*ca.* 300 Ma), and Precambrian (1452-2470 Ma). The abundance of Triassic and mid- to Late Permian detrital zircons correlates well with the feldspathic grit (Simpson Lake group?) overlying Triassic rocks in the McNeil Klippe area.

SUMMARY

Preliminary provenance data indicate Triassic rocks of the Cordilleran margin contain abundant Paleozoic and early Mesozoic detrital zircons. The presence of early Paleozoic detrital zircons can be explained by an influx of sediment from the Arctic. The presence of Mississippian to Triassic detrital zircon, however, requires that the Yukon-Tanana

Terrane was proximal to the North American margin by at least Early Triassic time.

Although still a work in progress, the simplest tectonic model to explain these signatures is that Triassic rocks of the Yukon form a two-part sedimentary succession: (1) an early phase (Permo-Triassic to Middle? Triassic) peripheral foreland basin assemblage superimposed on the Selwyn Basin (North America); and (2) a post-orogenic, or molasse, phase producing a sedimentary overlap assemblage overlying all tectonic elements of the northern Cordillera. Whether the accretion of Yukon-Tanana Terrane was a 'passive' docking, or a dramatic collisional event, the collider would have created an uplifted hinterland, shedding sediment downslope, in this case to the east, onto the overridden Selywn Basin. Geodynamically, the Triassic basin would be designated as a peripheral foreland basin, a depocentre controlled by the tectonic loading of the collider. Similar in nature to the retro-arc foreland basin of fold and thrust belts, a peripheral foreland basin is genetically different, as basin formation is primarily within the lower, overridden plate (North America). This model is simplistic, as convergence of Yukon-Tanana Terrane with North America was assuredly oblique; strike-slip motion may have produced additional accommodation space within the flexed Selwyn Basin.

New U-Pb detrital-zircon geochronology has also expanded our knowledge base of Jurassic sedimentary assemblages in Yukon, and further constrained the sources for immature clastic rocks associated with allochthons of Slide Mountain Terrane in the Finalyson Lake map area.

ACKNOWLEDGMENTS

All field expenses and conodont age determinations related to this project are funded by the Yukon Geological Survey, and analytical work is funded by a NSERC Discovery Grant to J.K. Mortensen. Dr. Michael Orchard of the Geological Survey of Canada in Vancouver conducted all conodont age determinations. We thank Don Murphy for his thorough review of this manuscript.

REFERENCES

Abbott, J.G., 1997. Structure and stratigraphy of the Mt. Hundere area, southeastern Yukon. Unpublished M.Sc. thesis, Queen's University, Kingston, Ontario, Canada, 111 p.

Beranek, L.P. and Mortensen, J.K., 2006. Triassic overlap assemblages in the northern Cordillera: Preliminary results from the type section of the Jones Lake Formation, Yukon and Northwest Territories (NTS 105I/13). *In:* Yukon Exploration and Geology 2005, D.S. Emond, G.D. Bradshaw, L.L. Lewis and L.H. Weston (eds.), Yukon Geological Survey, p. 79-91.

Colpron, M., Gladwin, K., Johnston, S.T., Mortensen, J.K. and Gehrels, G.E., 2005. Geology and juxtaposition history of Yukon-Tanana, Slide Mountain and Cassiar terranes in the Glenlyon area of central Yukon. Canadian Journal of Earth Sciences, vol. 42, p. 1431-1448.

Colpron, M., Nelson, J.L. and Murphy, D.C., 2006. A tectonostratigraphic framework for the pericratonic terranes of the northern Canadian Cordillera. *In:* Paleozoic Evolution and Metallogeny of Pericratonic Terranes at the Ancient Pacific Margin of North America, Canadian and Alaskan Cordillera, M. Colpron and J.L. Nelson (eds.), Geological Association of Canada, Special Paper 45, p. 1-23.

Creaser, R.A. and Harms, T.A., 1998. Lithological, geochemical, and isotopic characterization of clastic units in the Klinkit and Swift River assemblages, northern British Columbia. SNORCLE and Cordilleran Tectonics Workshop, LITHOPROBE Report No. 69, p. 239-241.

Davies, G.R., 1997. The Triassic of the Western Canada Sedimentary Basin: tectonic and stratigraphic framework, paleogeography, paleoclimate, and biota. Bulletin of Canadian Petroleum Geology, vol. 45, p. 434-460.

Dusel-Bacon, C. and Harris, A.G., 2003. New occurrences of late Paleozoic and Triassic fossils from the Seventymile and Yukon-Tanana terranes, east-central Alaska, with comments on previously published occurrences in the same area. *In:* Studies in Alaska by the U.S. Geological Survey during 2001, J.P. Galloway (ed.), U.S. Geological Survey Professional Paper 1678, p. 5-30.

Gabrielse, H. and Yorath, C.J., 1991. Tectonic synthesis, Chapter 18. *In:* Geology of the Cordilleran orogen in Canada, H. Gabrielse and C.J. Yorath (eds.), Geological Survey of Canada, Geology of Canada, no. 4, p. 667-705.

Gehrels, G.E., 2000. Introduction to detrital-zircon studies of Paleozoic and Triassic strata in western Nevada and northern California. *In:* Paleozoic and Triassic Paleogeography and Tectonics of Western Nevada and Northern California, M.J. Soreghan and G.E. Gehrels (eds.), Geological Society of America Special Paper 347, p. 1-17.

Gibson, D.W. and Barclay, J.E., 1989. Middle Absaroka Sequence- the Triassic stable craton. *In:* Western Canada Sedimentary Basin - A Case History, B. Ricketts(ed.), Canadian Society of Petroleum Geologists, Special Publication No. 30, p. 219-233.

Goodfellow, W.D., Cecile, M.P. and Leybourne, M.I., 1995. Geochemistry, petrogenesis, and tectonic setting of lower Paleozoic alkalic and potassic volcanic rocks, Northern Canadian Cordilleran Miogeocline. Canadian Journal of Earth Sciences, vol. 32, p. 1236-1254.

Gordey, S.P. and Anderson, R.G., 1993. Evolution of the northern Cordilleran Miogeocline, Nahanni Map Area (105I), Yukon and Northwest Territories. Geological Survey of Canada, Memoir 428, 214 p.

Gordey, S.P., 1981. Stratigraphy, structure and tectonic evolution of southern Pelly Mountains in the Indigo Lake area, Yukon Territory. Geological Survey of Canada, Bulletin 318, 44 p.

Link, P.K., Fanning, C.M. and Beranek, L.P., 2005. Reliability and longitudinal change of detrital-zircon age spectra in the Snake River system, Idaho and Wyoming: An example of reproducing the bumpy barcode. Sedimentary Geology, vol. 182, p. 101-142.

Miller, E.L., Toro, J., Gehrels, G.E., Amato, J.M., Prokopiev, A., Tuchkova, M.I., Akinin, V.V., Dumitru, T.A., Moore, T.E. and Cecile, M.P., 2006. New insights into Arctic paleogeography and tectonics from U-Pb detrital-zircon geochronology. Tectonics, vol. 25, p. 1-19.

Murphy, D.C., Mortensen, J.K., Piercey, S.J., Orchard, M.J. and Gehrels, G.E., 2006. Mid-Paleozoic to early Mesozoic tectonostratigraphic evolution of Yukon-Tanana and Slide Mountain terranes and affiliated overlap assemblages, Finlayson Lake massive sulphide district, southeastern Yukon. *In:* Paleozoic Evolution and Metallogeny of Pericratonic Terranes at the Ancient Pacific Margin of North America, Canadian and Alaskan Cordillera, M. Colpron and J.L. Nelson (eds.), Geological Association of Canada, Special Paper 45, p. 75-105.

Nelson, J.L, Colpron, M., Piercey, S.J., Dusel-Bacon, C., Murphy, D.C. and Roots, C.F., 2006. Paleozoic tectonic and metallogenic evolution of the pericratonic terranes in Yukon, northern British Columbia and eastern Alaska. *In:* Paleozoic Evolution and Metallogeny of Pericratonic Terranes at the Ancient Pacific Margin of North America, Canadian and Alaskan Cordillera, M. Colpron and J.L. Nelson (eds.), Geological Association of Canada, Special Paper 45, p. 323-360.

Okulitch, A.V., 2002. Geological time chart, 2002. Geological Survey of Canada, Open File 3040.

Orchard, M.J., 2006. Late Paleozoic and Triassic conodont faunas of Yukon and northern British Columbia and implications for the evolution of the Yukon-Tanana terrane. *In:* Paleozoic Evolution and Metallogeny of Pericratonic Terranes at the Ancient Pacific Margin of North America, Canadian and Alaskan Cordillera, M. Colpron and J.L. Nelson (eds.), Geological Association of Canada, Special Paper 45, p. 229-260.

Piercey, S.J., Nelson, J.L., Colpron, M., Dusel-Bacon, C., Roots, C.F. and Simard, R.-L, 2006. Paleozoic magmatism and crustal recycling along the ancient Pacific margin of North America, northern Cordillera. *In:* Paleozoic Evolution and Metallogeny of Pericratonic Terranes at the Ancient Pacific Margin of North America, Canadian and Alaskan Cordillera, M. Colpron and J.L. Nelson (eds.), Geological Association of Canada, Special Paper 45, p. 281-322.

Pigage, L.C., 2004. Bedrock geology compilation of the Anvil District (parts of NTS 105K/2, 3, 4, 5, 6, 7, and 11), central Yukon. Yukon Geological Survey, Bulletin 15, 103 p.

Poulton, T.P. and Tempelman-Kluit, D.J., 1982. Recent discoveries of Jurassic fossils in the Lower Schist Division of central Yukon. Geological Survey of Canada, Current Research, Part C, Paper 82-1C, p. 91-94.

Roots, C.F., Harms, T.A., Simard, R., Orchard, M.J. and Heaman, L., 2002. Constraints on the age of the Klinkit assemblage east of Teslin Lake, northern British Columbia. Current Research, Part A, Geological Survey of Canada, Paper 2002- A7, p. 1-11.

Ross, G.M., Gehrels, G.E. and Patchett, J.P., 1997. Provenance of Triassic strata in the Cordilleran miogeocline, western Canada. Bulletin of Canadian Petroleum Geology, vol. 45, no. 4, p. 461-473.

Simard, R.-L., 2003. Geological map of southern Semenof Hills (part of NTS 105E/1, 7, 8), south-central Yukon (1: 50 000 scale). Yukon Geological Survey, Open File 2003-12.

Tempelman-Kluit, D.J., 1979. Five occurrences of transported synorogenic clastic rocks in Yukon Territory. Geological Survey of Canada, Current Research, Part A, Paper 79-1A, p. 1-12.

Evaluation of the origins of gold hosted by the conglomerates of the Indian River formation, Yukon, using a combined sedimentological and mineralogical approach

David P.G. Bond and Robert J. Chapman
School of Earth and Environment, University of Leeds[1]

Bond, D.P.G. and Chapman, R.J., 2007. Evaluation of the origins of gold hosted by the conglomerates of the Indian River formation, Yukon, using a combined sedimentological and mineralogical approach. *In:* Yukon Exploration and Geology 2006, D.S. Emond, L.L. Lewis and L.H. Weston (eds.), Yukon Geological Survey, p. 93-103.

ABSTRACT

Conglomerates belonging to the Indian River formation (IRF), south of the Klondike goldfield, have recently become the focus of exploration activity owing to their potential as hosts for paleoplacer gold derived from the Klondike. However, textures within the conglomerate have been interpreted as indicative of hydrothermal activity, and the possibility exists of *in situ* epithermal gold.

Paleocurrents in conglomerates indicate dominant transport from the southeast, incompatible with gold transport from the Klondike. Gold grains from unconsolidated conglomerate at Montana Creek reveal an epithermal signature (20-50% Ag, 0.3 to 3% Hg and opaque inclusion suite containing complex polymetallic sulphotellurides and sulphosalts), distinct from the signature of placer and lode sources in the central and southern Klondike (12-20% Ag, Hg absent and opaque inclusion suite of simple base metal sulphides). Gold grain morphology and alteration textures within unconsolidated conglomerates suggests that Montana Creek gold is derived from *in situ* epithermal mineralization related to that previously reported at Eureka Dome.

RÉSUMÉ

Les conglomérats de la formation d'Indian River du Crétacé tardif, au sud du champ aurifère du Klondike, sont récemment devenus le point de mire des activités d'exploration en raison de leur potentiel comme sources d'or de paléoplacers dérivé du Klondike. Cependant, la texture des conglomérats a été considérée comme un indice d'activité hydrothermale, et il est possible que de l'or épithermal soit présent in situ.

Les paléocourants dans les conglomérats indiquent que le transport s'est principalement effectué depuis le sud est, ce qui est incompatible avec l'hypothèse du transport de l'or à partir du Klondike. Les grains d'or de conglomérats non consolidés au ruisseau Montana révèlent une signature épithermale (Ag [de 20 à 50 %], Hg [de 0,3 à 3 %], cortège d'inclusions opaques composées de sulfotellurures et de sulfosels polymétalliques complexes) distincte de celle des sources filoniennes et placériennes du centre et du sud du Klondike (Ag [de 12 à 20 %], Hg absent, cortège d'inclusions opaques composées de sulfures simples de métaux communs). La morphologie des grains d'or et les textures d'altération dans les conglomérats non consolidés suggèrent que l'or du ruisseau Montana est le produit d'une minéralisation épithermale in situ semblable à celle déjà signalée au dôme d'Eureka.

[1]*School of Earth and Environment, University of Leeds, Leeds, LS2 9JT, UK*

INTRODUCTION

The Indian River drains the southern Klondike goldfield (Fig. 1), and continues to be a major producer of placer gold in the region. In addition to the exploitation of placer gold in recent gravel deposits, several attempts have been made to recover gold from the Indian River formation (IRF), a Cretaceous sedimentary sequence (Albian, *ca.* 100 Ma), which outcrops to the south of the Indian River in several north-draining tributaries. The McKinnon conglomerate bed of the IRF was mined as early as 1899 at McKinnon Creek, although the auriferous potential of the conglomerate at other localities remains unproven. Recently, interest in the IRF has been renewed during exploration by Boulder Mining (2004), and Klondike Star Mineral Corporation (2005). An improved understanding of the relationship between the auriferous conglomerate and the other known gold sources in the region would aid future exploration in the area, both in terms of recent placer, as well as paleoplacer deposits. This report discusses sedimentological data collected from several conglomerate exposures, together with other units of the IRF. In addition to fieldwork, several drill core samples from McKinnon Creek (stored at the Bostock Core Library in Whitehorse) were also re-examined. Finally, gold grains collected from an exposure of conglomerate at Montana Creek have been analysed by scanning electron microscope (SEM) methods to permit comparison with other signatures of placer gold grains throughout the region.

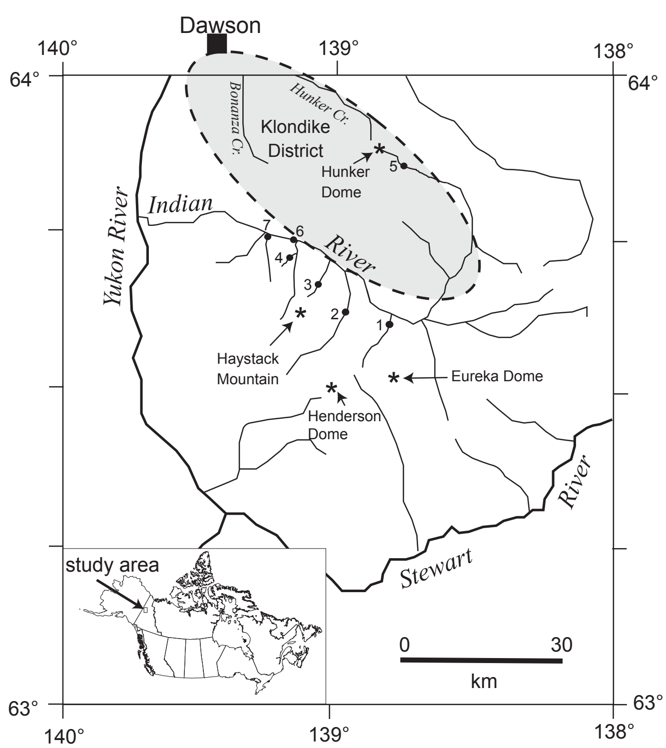

Figure 1. *Location map of study area (adapted from Chapman and Mortensen 2006). 1 = Eureka Creek; 2 = Montana Creek; 3 = McKinnon Creek; 4 = Diversion Creek; 5 = Upper Dominion Creek; 6 = road-cut near Arkenstall's camp; 7 = Boulder Mining pits. Klondike District is within dashed outline area.*

STRATIGRAPHY

The IRF has received little attention to date, and the most thorough investigation of the formation remains the PhD thesis of Grant Lowey (1984). Lowey (1984) presented a large amount of data which demonstrated the IRF to be a >500-m-thick, interbedded sequence of sandstone, shale, conglomerate and minor coal, deposited in a marginal marine basin by a southward-prograding fan-delta complex, during the Middle Albian (early Cretaceous). Lowey (1984) principally examined drill core samples collected during the 1970s and 1980s; these included cores 137-2 and 137-3 of Dome Exploration (also known as Yukon Revenue Mines), which are now stored in the Bostock Core Library, Whitehorse. Other drill core (e.g., IR-80-2) were examined and remain on site in the Indian River area. Outcrops were also studied by Lowey (1984), however, due to the nature of the terrain, outcrop exposures are of limited extent. One of the aims of the current project was to further identify exposures of outcrop with the help of local placer miners.

The IRF is in unconformable contact with a basement of Proterozoic/Paleozoic igneous and metamorphic rocks (including gneiss, schists and quartzite), and is locally intruded by, and overlain by, volcanic rocks belonging to the Haystack andesite and Carmacks Group (Fig. 2). It is bound to the north by the Indian River fault and to the west by the Ruby Creek fault. Documented outcrop exposures extend as far south as Henderson Dome and as far east as Eureka Dome (Fig. 2). At many localities, the IRF is overlain by recent gravel deposits and the contact may be indistinct where the conglomerate is unconsolidated.

The IRF consists of the following geologic units:

- Reindeer chert member (core 137-2 of Dome Exploration Ltd., depth 410.25-463 m; not observed in outcrop)
- Ruby quartz member (core 137-2 of Dome Exploration Ltd., depth 0-410.25 m)

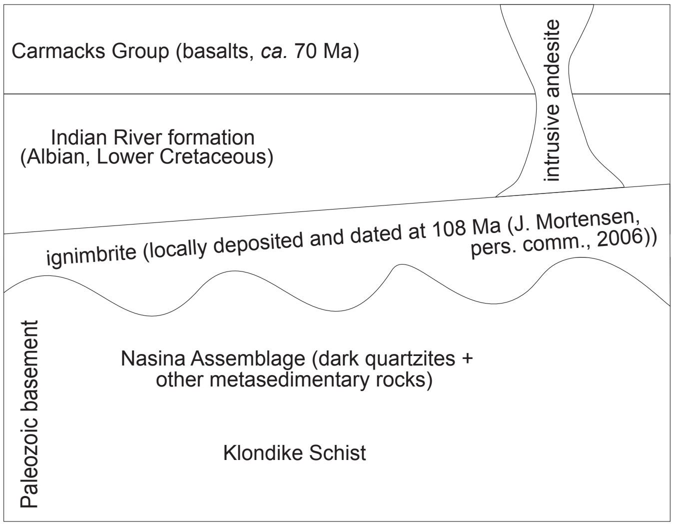

Figure 2. *Schematic diagram of stratigraphic relationships within the study area.*

- McKinnon conglomerate bed (part of the Ruby quartz member; outcrops along McKinnon Creek). Borehole P-75-1 of Dome Exploration Ltd. intersected at least 20 m of this unit.

The stratotype for the formation is the Dome Exploration drill core 137-2.

The McKinnon conglomerate bed is thought to be the regional equivalent of conglomerates of the Sixty Mile formation which outcrops to the north and northwest of Dawson, which suggests that they were deposited over a large area (Lowey, 1984). Conglomerates in the Indian River area are variable in terms of clast size, composition and degree of consolidation. In places, the conglomerate unit is highly silicified and consolidated, whereas elsewhere, it is poorly consolidated and breaks apart readily. In some instances, the boundary between these conglomerates and overlying, recent gravel deposits is diffuse, and difficult to identify.

POSSIBLE ORIGINS OF GOLD WITHIN THE CONGLOMERATE OF THE IRF

Relatively little information is available regarding the occurrence and nature of gold within the conglomerate. There are several possibilities for the origins of the gold, which are summarized as follows:

a) The gold resulted from *in situ* epithermal mineralization, related to the Carmacks volcanism (*ca.* 70 Ma).

b) The gold is detrital in origin and was transported from the Klondike goldfield located to the north and redeposited, together with other sediments, forming the conglomerate unit.

c) The gold is detrital in origin and was originally deposited in Quaternary placer gold deposits and was subsequently reworked into the underlying unconsolidated conglomerates of the IRF. The origin of the detrital gold may or may not be the Klondike goldfield.

In order to evaluate these possibilities, a combined sedimentological and mineralogical approach was adopted which involved inspection of outcrops for any textures indicative of post-depositional hydrothermal activity, reconstruction of paleocurrent directions, observations of the relationships of clasts to local and regional bedrock types, and comparison of the microchemical signatures of gold grains obtained from the study area to those of placer gold from Eureka Creek and the Klondike placer area.

SEDIMENTOLOGICAL INVESTIGATIONS

Exposures of the IRF conglomerate are rare, and where present, difficult to access. Outcrop exposures were identified at Boulder Mining's pits along the Indian River, McKinnon Creek, Montana Creek and Diversion Creek, as well as at a road-cut exposure 2 km east of Arkenstall's camp on the Indian River (Fig. 1). Drill core from the Indian River area were examined at the Bostock Core Library, Whitehorse. Although the drill core have sedimentary rocks that are cross-bedded, they do not provide paleocurrent data since the orientation of the drill core cannot be determined.

BOULDER MINING PIT

The IRF unconformably overlies Klondike Schist in Boulder Mining pit 2. In a poorly exposed section, a thin coal bed overlies the schist. The section is incomplete and most beds have been destroyed by mining activity. However, in places, 10-30-cm-thick beds of sandstone, and thin (<5 cm) beds of shale and pebbly sandstone are observed. No conglomerate beds are observed at this locality. This series of rocks is incised and overlain by recent gravel and sand deposits. Bedding appears to be sub-horizontal. The IRF in this section has largely been eroded and the total thickness of IRF is probably only a few metres. In the nearby Boulder Mining pit 1, the IRF is not observed and the Klondike Schist is overlain by recent gravel and sand deposits, which incise the schists and reflect a series of channel fills.

It is apparent from this location and others in the area, that where the IRF is not overlain by volcanic rocks of the Carmacks Group, it has been almost, or entirely eroded away.

MCKINNON CREEK

A section of the IRF is exposed from the old Brittania shaft (NAD 83, Zone 7, 0591630E, 7065083N), and extends northeastwards for 2 km. This shaft is now flooded, although the old workings include one of the best exposures of conglomerate in the area.

Previous work along McKinnon Creek

The McKinnon brothers discovered gold in conglomerate at McKinnon Creek in 1899 while establishing a winter route to the Klondike from the south. This unit is now known as the McKinnon conglomerate bed. The brothers continued investigation of the conglomerate for the remainder of their lives (T. Liverton, pers. comm., 2006). A 2.5-ton (2.3 tonnes) bulk sample from the 60-foot (18-m) level in the Britannia shaft on McKinnon Creek is quoted as yielding a grade of 0.69 g/t (0.02 oz/ton) by amalgamation of the stamp-mill product. This original work by the McKinnon brothers represents the only bulk sampling of subsurface conglomerate horizons; all other samples taken of the conglomerate unit were surface grab samples and core assays. Several other exploration programs have since been carried out and resulting grades from sampled ore are summarized in Table 1.

Comparison of these data concluded that the highest grades were obtained from the subsurface conglomerate samples.

Field observations

The area surrounding the shaft provides the best exposure of the McKinnon conglomerate bed. The conglomerate is clast supported. Clasts are predominantly vein quartz pebbles and fewer black quartzite clasts belonging to the basement Nasina Assemblage (Fig. 3). The matrix is a poorly sorted, fine to coarse sand. In places, the matrix is poorly consolidated, while elsewhere, it is much better consolidated and has been extensively silicified.

Bedding in the conglomerate can be difficult to identify. Bedrock faces that are exposed in an adit approximately 5 m from the Britannia shaft have strike and dip measurements of 010°/40° W and 012°/26° W. These may be localized dips due to faulting of the sequence, given that the large-scale geometry (according to the mapping of Bostock (1942) and the study of Lowey (1984)) suggests only very shallow dips for the IRF. Imbrication was not observed in the conglomerate.

A short distance downstream from the Britannia shaft (NAD 83, Zone 7, 0591794E, 7065282N), the conglomerate has a striking black appearance (Fig. 4), where the matrix is derived almost entirely from weathered Nasina quartzite. Intriguingly, the clasts have a bimodal size distribution: common, angular clasts of vein quartz measuring 0-2 cm along the long axis, and

Table 1. *Summary of gold grades reported from McKinnon Creek area.*

Exploration	Method/target	Au grade (g/t)
McKinnon brothers (Tough, 1987)	2.5-ton (2.3-tonne) bulk sample at 60-ft (18-m) level in Britannia shaft	0.69
Lisle, 1974	surface soil geochemistry	<0.01, with isolated anomalies of 0.01 – 0.25
Dome Exploration Ltd., 1979	assay of diamond drill core from McKinnon Creek road	values reported as 0.01
	assay of diamond drill core from McKinnon Creek road (935 to 939 ft [285 to 286 m] depth in hole 137-2)	0.18
Tough, 1987	cyanidation (60-ft level [18-m], Britannia shaft)	5.0 – 10.9
Davidson, 1994	assay of split core samples; drilled by Volcano Resources (43.5 to 48.5 ft [13.3 to 14.8 m] depth)	1.47
	assay of split core samples; drilled by Volcano Resources (73 to 76 ft [22 to 23 m] depth)	4.03
	bulk samples (500 kg) of conglomerate	0.04 – 0.118

Figure 3. *McKinnon conglomerate, exposed by the Britannia shaft. The conglomerate has a consolidated matrix containing vein quartz and minor basement clasts.*

Figure 4. *Striking black matrix and weak bedding in the McKinnon conglomerate, downstream of the Britannia shaft (notebook for scale).*

probably sourced locally; and rarer, large clasts (up to 10 cm along the long axis) of well rounded quartz, which presumably have been transported over a greater distance. Bedding at this location has a strike and dip of 005°/05° W, more in keeping with the regional dip.

The poorly exposed section of IRF can be observed northeastwards from the Britannia shaft, along the east bank of McKinnon Creek. The section is composed of conglomerate at the shaft and progresses into a sequence of volcanic rock (dacite), black conglomerate (as described above), andesite, mudstone, shale and sandstone (presumably IRF, but very poorly exposed), and finally a thick, andesite flow. The andesite flow is exposed for several hundred metres until the end of the section where the exposed bedrock intersects a ford in the creek. The precise relationship between the IRF and the volcanic rocks is not apparent, but it is probable that the volcanic rocks intruded the sediment locally.

MONTANA CREEK

A 3-m section of sedimentary rocks is exposed above Montana Creek (NAD 83, Zone 7, 0598575E 7054875N) and consists of pale-grey, coarse-granule conglomerate, interbedded with medium-grained sandstone. The granule conglomerate is poorly sorted and contains clasts of white quartz up to 2 mm in diameter. Several beds are cross-laminated, or cross-bedded. Talus near the outcrop has clearly defined, long tool marks and flute casts, however, these were not found *in situ* and thus can not be used to provide paleocurrent data. There is also a significant amount of organic material present, mostly as <1-cm fragments of coal and wood. Pyritic nodules up to 2 cm in diameter are also present. Strike and dip measurements of the sandstone beds are as follows: 128°/28° NE, 155°/32° NE and 155°/17° NE.

Lower down in the Montana Creek valley (NAD 83, Zone 7, 0598151E, 7055885N), recent placer mining activity has focussed on unconsolidated, Quaternary gravel deposits. The recent gravel deposits have been extensively mined, and it is possible that mining activity may have extended down into the uppermost portions of bedrock, that is, the underlying conglomerate of the IRF. It is very difficult to discern the contact between recent, Quaternary gravel deposits and the conglomerate of the Cretaceous IRF.

At Montana Creek, mine tailings are composed of large boulders (up to 1 m) of predominantly black Nasina quartzite, and lesser amounts of orthogneiss. These are

Figure 5. *Fractured and healed boulder of Nasina quartzite, from conglomerate at Montana Creek.*

extremely well rounded and polished, and many have fractures which have been subsequently healed by quartz (Fig. 5). Some blocks of consolidated conglomerate are also present and have a micaceous, sandy matrix, which is not silicified.

DIVERSION CREEK

Bedrock exposures of sand and gravel are located along the banks of Diversion Creek (NAD 83, Zone 7, 0584877E, 7070584N) and are overlain by recent, gold-bearing gravel deposits (Fig. 6). Based on composition and the presence of bedding and cross-bedding, this bedrock exposure has been identified as IRF. It is a poorly consolidated, clast-supported conglomerate, in a matrix of coarse, granular sand. Clasts vary in size from 1 mm to 4 cm across, and are generally sub-angular to sub-rounded. The composition is dominated by quartz, dark grey Nasina quartzite and weathered sandstone. The pure white vein quartz that characterizes the conglomerate at McKinnon Creek appears to be absent at this location.

Two hundred metres downstream of the above-mentioned outcrop, the conglomerate unit is a thick bed with much larger clasts, up to 30 cm across, in a matrix of medium sand. This conglomerate is composed of Nasina quartzite, vein quartz, schist, gneiss, kyanite and volcanic rocks of rhyolite. This composition, together with the notable absence of Carmacks basalts, suggests that this conglomerate belongs to the IRF.

Where the conglomerate is texturally finer (at the locality discussed above), bedding and cross-bedding are observed (Figs. 6, 7 and 8). Strike and dip measurements of the thinly bedded conglomerate at this location are as follows: 044°/05° NW, 050°/06° NW and 070°/04° NW. These shallow dips are consistent with the regional dip of the IRF.

The cross-bedding in finer grained gravel deposits has dips of 30° towards 320°, 34° towards 000°, and 24° towards 340°. The excavated cross-bedding plane revealed a strike and dip of 045°/30° NW (Fig. 8). All of these values are consistent with paleocurrents from the southeast.

Figure 6. *Exposure at Diversion Creek of thinly bedded, near-horizontal conglomerate overlain by recent gravel deposits.*

Figure 7. *Cross-bedding defined by lags of coarse-grained material within thinly bedded conglomerate at Diversion Creek.*

Figure 8. *Weak cross-bedding at Diversion Creek; pen in photo is parallel to cross-bedding. This face was excavated in order to obtain a strike and dip of cross-bedding.*

ROAD-CUT NEAR ARKENSTALL'S CAMP

Sandstone of the IRF are exposed in a road-cut on the north side of Indian River, 2 km east of Kam Arkenstall's camp (NAD 83, Zone 7, 0584094E, 7072601N). Outcrop in this section consists of a blocky, medium-grained, pale grey sandstone, unconformably overlying the metamorphic basement (Fig. 9). The sandstone contains dark flecks (coal?), is micaceous and well consolidated. Some blocks have wavy lamination, and in places, millimetre-scale cross-bedding. The sandstone beds have strike and dip measurements of 072°/22° N and 080°/20° N.

Two sets of cross-bedding were measured in different sandstone beds that are 20 m apart. The first set has an apparent dip of 32° towards 280°, implying paleocurrent from the southeast (Fig. 10). The second set has an apparent dip (planes are not visible) of 14° towards 120°, i.e., implying a paleocurrent from the northwest (Fig. 11). The former is consistent with that recorded at Diversion Creek. The latter is the opposite paleocurrent direction to that recorded at Diversion Creek. It should be noted that this data is in part consistent with some paleocurrent directions suggested by Lowey (1984), who indicates both southwest- and northwest-oriented transport directions for different parts of the IRF. It is clear that further study of paleocurrent directions is required, but this is largely hindered by the lack of suitable outcrop exposure.

Figure 9. *Contact (dashed line) between the metamorphic basement and the overlying sandstone of the IRF, at the Indian River road-cut. Approximately 6 m of section is exposed.*

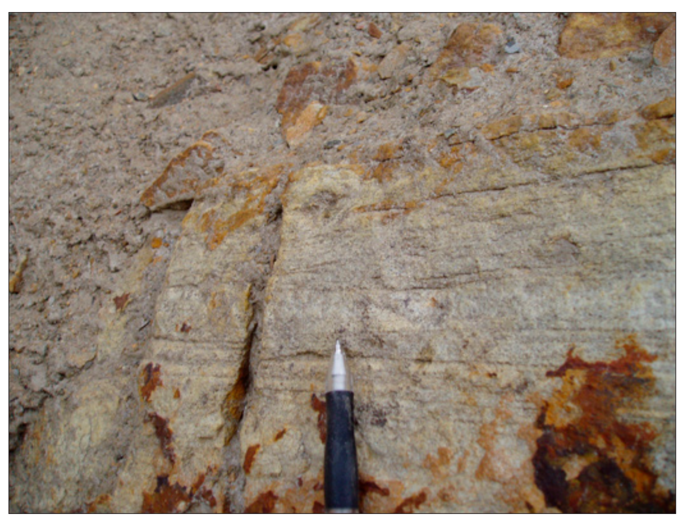

Figure 10. *Set of northwest-trending, millimetre-scale cross-beds at the Indian River road-cut.*

Figure 11. *Set of larger, southeast-trending cross-beds at the Indian River road-cut.*

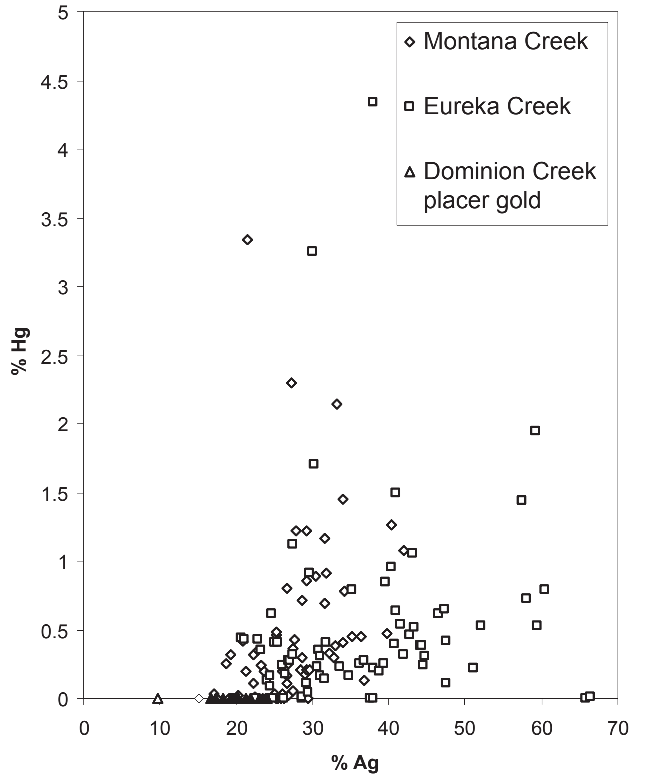

Figure 12. *Compositional variation in populations of placer gold from Montana Creek, Eureka Creek and Upper Dominion Creek. Orogenic gold from the south of the Klondike, typified by that from Upper Dominion Creek, has a relatively tight compositional field on the % Ag axis.*

MICROCHEMICAL ANALYSIS OF GOLD GRAINS

Populations of placer grains may be characterized in terms of the alloy compositions, internal textures and suites of opaque and transparent mineral inclusions. These data may be combined to provide a 'microchemical signature' which can be related to the style of source mineralization and also used to differentiate between placer gold grains derived from distinct sources.

Alloy compositions of gold from the Klondike have been reported by Knight *et al.*, (1999) and Mortensen *et al.*, (2004). The lode gold occurrences on Hunker Dome have been described as the orogenic type, and have a relatively simple mineralogy of gold (containing between 12% and 20% by mass Ag) and base metal sulphides (Table 2). This signature is also prevalent in placer gold from a drainage to the south of this lode occurrence (Knight *et al.*, 1999; Chapman and Mortensen, 2006). Study of placer gold grains from Eureka Creek and some grains from alluvium on Eureka Dome (Fig. 12) revealed a completely different chemical and mineralogical signature, and was interpreted as having an epithermal origin (Dumula and Mortensen, 2002). Further detailed studies of the mineralogy of the opaque inclusion suite by Chapman and Mortensen (2006) concluded that the source mineralization was of the low-sulphidation epithermal type and a temperature

Table 2. *Gold grain inclusion assemblages from Hunker Dome lode deposit, Eureka Creek placer deposit, and Montana Creek conglomerate. Py = pyrite, Ga = galena, Sph = sphalerite, Cpy = chalcopyrite, Arg = argentite, AgCuS = unidentified Cu-Ag sulphide, Asp = arsenopyrite, Hs = hessite, Tet = tetrahedrite, Cer = cervelleite, CuAgSbS = unknown Cu-Ag sulphosalt.*

		Number of grains containing inclusions of...										
	No. of grains	**Py**	**Ga**	**Sph**	**Cpy**	**Arg**	**AgCuS**	**Asp**	**Hs**	**Tet**	**Cer**	**CuAgSbS**
Hunker Dome lode	132	47	1	1	8	1	0	0	0	0	0	0
Eureka Creek placer	98	10	1	5	8	9	5	1	12	2	6	0
Montana Creek conglomerate	67	10	3		1	1	1	0	1	1	3	2

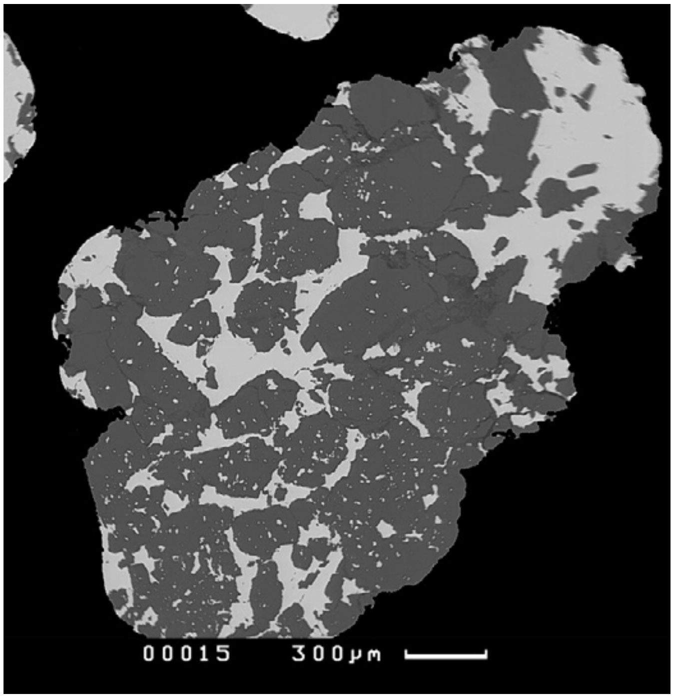

Figure 13. *Backscattered electron (BSE) image of a polished section of a composite gold-quartz grain from Montana Creek.*

of emplacement of around 200°C. These gold grains were characterized by elevated levels of Hg in the alloy (Fig. 12) and an opaque inclusion suite containing complex polymetallic tellurides, sulphotellurides and sulphosalts (Table 2). The opaque inclusions frequently occurred as tiny intergrowths (5 microns), a texture suggestive of post-depositional equilibration.

A sample of relatively coarse gold grains (0.5-3 mm) was obtained from an exploratory pit dug in unconsolidated conglomerate by Klondike Star in 2005 at NAD 83, Zone 7, 0598064E, 7055855N (V. Matkovitch, pers. comm., 2006). The grains are angular and many grains contain a large proportion of quartz; this was observed while examining polished sections by Scanning Electron Microscope (SEM) (Fig. 13). The results of microchemical characterization of these grains are included in the Montana Creek sample population (Fig. 12; alloy compositions) and Table 2 (opaque inclusion suite). The signature of the population is similar to that previously obtained for gold from Eureka Creek (Chapman and Mortensen, 2006); an epithermal origin is inferred.

DISCUSSION

Paleocurrent data were interpreted and transport is believed to have been towards the northwest in the conglomerate at Diversion Creek and within sandstone at the Indian River road-cut. This is consistent with data presented by Lowey (1984). Cross-bedding measured in another sandstone bed at the Indian River road-cut was interpreted as having a paleocurrent direction flowing to the southeast. Although unusual, it is not impossible that channels could flow in opposite directions from one time to another. Lowey (1984) also records southwestward transport for the IRF. Paleocurrent directions cannot be reconstructed from drill core because the orientation of these is unknown. The clasts observed in the conglomerates are all representative of local lithologies, some of which are present in the Klondike area. The clasts present are not indicative of any particular source area.

Present knowledge of the distribution of gold within the conglomerate (both in terms of geographical extent and depth in the unit) is insufficient to draw any firm conclusions regarding potential transport by fluvial action. However, far more information is available from the study of the gold grains themselves. This work has demonstrated that the gold obtained from the conglomerate at Montana Creek is not derived from the Klondike, but from epithermal mineralization, presumably associated with Carmacks Group volcanism.

The timing of the generation of the textures observed within the conglomerate and the large quartzite boulders contained therein at Montana Creek is unknown. It is possible that quartz veins were already present within the boulders prior to deposition of the conglomerate and that these quartz veins are related to the white vein quartz clasts within the conglomerate. If alteration occurred following deposition of the conglomerate, it can be explained by the following model:

a) long-range fluvial transport by a powerful flow, generating large, rounded boulders;

b) conglomerate deposition followed by matrix silicification, resulting in a competent rock;

c) fracturing of boulders during tectonism;

d) healing of fractured boulders by hydrothermal activity; and

e) subsequent partial degredation of the conglomerate cement during further hydrothermal activity.

However, hydrothermal fluids flowing through silicate rocks cool below about 400°C, and they become oversaturated in silica and precipitate quartz. Quartz dissolution requires either a pressure increase (unlikely for a fluid flowing through a conglomerate), or a high pH. Fluid buffered by silicate rocks, however, tends to be near-neutral to mildly acidic. Thus, the origins of the features described above remain problematic.

Lowey (1985) considered the extent of clay and quartz cementation of the conglomerate to be indicative of epithermal mineralization, but to date, there has been no reliable detections of gold within consolidated conglomerates. If this is indeed the case, it suggests that the most important gold values would be associated with the unconsolidated conglomerates belonging to the IRF, which are revealed only as a consequence of placer mining.

The texture of the gold grains from the conglomerate at Montana Creek is indicative of very limited fluvial transport. The angular morphology of the gold grains and the large amount of associated quartz is suggestive of transport distances of < 50 m (Townley *et al.*, 2003), however, the model of erosion from an epithermal source followed by rapid burial and fluvial reworking into the underlying conglomerate demands a proximal significant source, which has been completely eroded. Furthermore, although gold is capable of a significant amount of settling in unconsolidated sediments, this process is controlled by differential density; many of the gold particle grains studied here exhibit a low bulk density as a consequence of the amount of associated quartz (Fig. 13). The observations mentioned above lend further support to the possibility that the gold present in these sediments may have formed from *in situ* epithermal mineralization.

CONCLUSION AND FURTHER WORK

It is unlikely that gold found in the IRF originated from the Klondike area as is indicated by paleocurrent data. Furthermore, the chemical and mineralogical signature of gold grains extracted from unconsolidated conglomerate at Montana Creek is distinct from that of gold grains derived from orogenic lode sources in the Klondike goldfield. However, the chemical and mineral signature is consistent with that of gold grains obtained from Eureka Creek, which were previously characterized as low-sulphidation epithermal. The current hypothesis that unconsolidated conglomerates of the IRF host low-temperature epithermal mineralization can only be proven by the identification of gold-bearing mineralization *in situ*, and further work is currently ongoing to study the textures and mineralogy of conglomerates from various localities, as well as the signatures of populations of placer gold grains throughout the Indian River drainage.

ACKNOWLEDGEMENTS

Fieldwork was supported by a grant from the Yukon Geological Survey and Klondike Star Mineral Corporation. Klondike Star provided logistical support. Informal discussions with Vern Matkovitch and Tim Liverton provided much valuable information regarding areas of outcrop exposure, as well as the history of the area. Professor Jim Mortensen of the University of British Columbia is thanked for his unfailing energy and optimism. Evan Crawford and Simon Lloyd provided valuable assistance in the field. Robert Marshall and Dr. Eric Condliffe of the University of Leeds are thanked for their expert polishing of gold grains, and assistance with analyses of gold grains, respectively. Dr. Murray Allan of the University of Leeds is thanked for his helpful review of this manuscript.

REFERENCES

Bostock, H.S., 1942. Ogilvie, Yukon Territory. Geological Survey of Canada, "A" Series Map , 711A, 1:253 440 scale (1 in to 4 mi).

Chapman, R.J. and Mortensen, J.K., 2006. Application of microchemical characterization of placer gold grains to exploration for epithermal gold mineralization in regions of poor exposure. Journal of Geochemical Exploration, vol. 91, no. 1, p. 1-26.

Davidson, G.S., 1994. Exploration report on the McKinnon Creek project, Indian River, Dawson Mining District. Energy, Mines and Resources, Government of Yukon, Assessment Report 093167 for Richlode Investments Corp.

Dome Exploration (Canada) Ltd., 1979. Drill logs for holes 137-1 to 137-4. Energy, Mines and Resources, Government of Yukon, Assessment Report 091354.

Dumula, M.R. and Mortensen, J.K., 2002. Composition of placer and lode gold as an exploration tool in the Stewart River map area, western Yukon. *In:* Yukon Exploration and Geology 2002, C.F. Roots and D.S. Emond (eds.), Exploration and Geological Services Division, Yukon Region, Indian and Northern Affairs Canada, p. 1-16.

Knight, J.B., Mortensen, J.K. and Morison, S.R., 1999. Lode and placer gold composition in the Klondike district, Yukon Territory, Canada: Implications for the nature and genesis of Klondike placer and lode gold. Economic Geology, vol. 94, p. 649-664.

Lisle, T.E., 1974. Preliminary geological report on the Mac, Ray and Tom mineral claims approximately 25 miles southeast of Dawson City. Energy, Mines and Resources, Government of Yukon, Assessment Report 060902 for Andac Resources Ltd.

Lowey, G.W., 1984. The stratigraphy and sedimentology of siliciclastic rocks, west-central Yukon, and their tectonic implications. Unpublished PhD thesis, University of Calgary, Alberta, Canada, 310 p.

Lowey, G.W., 1985. Auriferous conglomerates at McKinnon Creek, west-central Yukon (115O/11): paleoplacer or epithermal mineralization? *In:* Yukon Exploration and Geology 1983, K.J. Grapes and J.A. Morin (eds.), Exploration and Geological Services Division, Yukon Region, Indian and Northern Affairs Canada, p. 69-78.

Mortensen, J.K., Chapman, R.J., LeBarge, W. and Jackson. L., 2004. Application of placer and lode gold geochemistry to gold exploration in the western Yukon. *In:* Yukon Exploration and Geology 2004, D.S. Emond, L.L. Lewis and G.D. Bradshaw (eds.), Yukon Geological Survey, p. 205-212.

Tough, T.R., 1987. Preliminary geological report on the McKinnon Creek property. Energy, Mines and Resources, Government of Yukon, Assessment Report 092156 for Volcano Resources Corp.

Townley, B.K., Herail, G., Maksaev, V., Palacios, C., de Parseval, P., Sepuldeva, F., Orellana, R., Rivas, P. and Ulloa, C., 2003. Gold grain morphology and composition as an exploration tool: application to gold exploration in covered areas. Geochemistry, Exploration, Environment, Analysis, vol. 3, 29-38.

Late Wisconsinan McConnell glaciation of the Big Salmon Range, Yukon

Jeffrey D. Bond[1]
Yukon Geological Survey

Bond, J.D., 2007. Late Wisconsinan McConnell glaciation of the Big Salmon Range, Yukon. *In:* Yukon Exploration and Geology 2006, D.S. Emond, L.L. Lewis and L.H. Weston (eds.), Yukon Geological Survey, p. 105-122.

ABSTRACT

The late Wisconsinan McConnell glaciation of the Big Salmon Range in the Pelly Mountains consisted of a four-phase ice-flow history. Phase 1 ice-flow consisted of local alpine glaciers advancing to the mountain front. During phase 2, or glacial maximum, the Cassiar lobe of the Cordilleran ice sheet advanced to the northwest and overtopped the range. Retreat of the Cassiar lobe during phase 3 of the glaciation resulted in ponding of meltwater in eastern drainage basins. The meltwater spilled over into western basins and caused significant erosion of surficial sediments. Phase 4 of the glaciation is marked by a limited late-glacial readvance of local alpine glaciers. This glacial history has several important implications for mineral and placer exploration in the area.

RÉSUMÉ

La glaciation de McConnell au Wisconsinien tardif dans la chaîne Big Salmon des monts Pelly a consisté en quatre phases d'écoulement glaciaire. Pendant la phase 1 des glaciers alpins locaux se sont avancés jusqu'à la marge de la chaîne de montagnes. Pendant la phase 2, ou maximum glaciaire, le lobe de Cassiar de l'inlandsis de la Cordillère s'est avancé vers le nord-ouest pour déborder la chaîne de montagnes. Le recul du lobe de Cassiar pendant la phase 3 de la glaciation a entraîné l'accumulation d'eau de fonte dans les bassins versants orientaux qui ont débordé dans les bassins occidentaux engendrant une importante érosion des sédiments de surface. La phase 4 de la glaciation a été une nouvelle avancée glaciaire tardive restreinte des glaciers alpins locaux.

Des études des minéraux lourds ont été effectuées afin d'évaluer les ruisseaux à placers éloignés dans la chaîne Big Salmon. Les faits saillants relevés dans les données sont des concentrations anormales en arsénopyrite dans un tributaire sans nom du lac Quiet et en ilménite dans le ruisseau Iron, qui présente une géochimie favorable pour les indicateurs de diamants.

[1]*jeff.bond@gov.yk.ca*

INTRODUCTION

During the last glaciation, southern Yukon was covered both by ice-cap complexes and the northern component of the Cordilleran ice sheet (Jackson and Mackay, 1991). The Cordilleran ice sheet consisted of an assemblage of semi-autonomous ice lobes that originated from distinct upland source areas, such as the Selwyn, Cassiar and eastern Coast mountains (Hughes *et al.*, 1969; Jackson and Mackay, 1991). Not all uplands in southern Yukon acted as accumulation zones for ice lobes, perhaps due to the nature of precipitation patterns (Ward and Jackson, 1992; Bond and Kennedy, 2005). Previous glacial history studies in the Pelly Mountains have shown that after a period of local alpine ice advance at the onset of the last glaciation, the upland was invaded by the Cassiar lobe of the Cordilleran ice sheet (Fig. 1; Kennedy and Bond, 2004; Bond and Kennedy, 2005). The result was an effective reversal of ice-flow in mountain valleys and a complete change in the style of glaciation for that area.

In 2005, a glacial history study was completed for the Big Salmon Range, which forms the southwest extension of the Pelly Mountains (Fig. 1). While a multi-phase glacial history was anticipated for the range, it was uncertain how the glaciation may have impacted valley bottom sediments, which are of particular interest due to the placer potential of the area. This paper characterizes the glacial history for the Big Salmon Range and addresses implications for mineral and placer exploration.

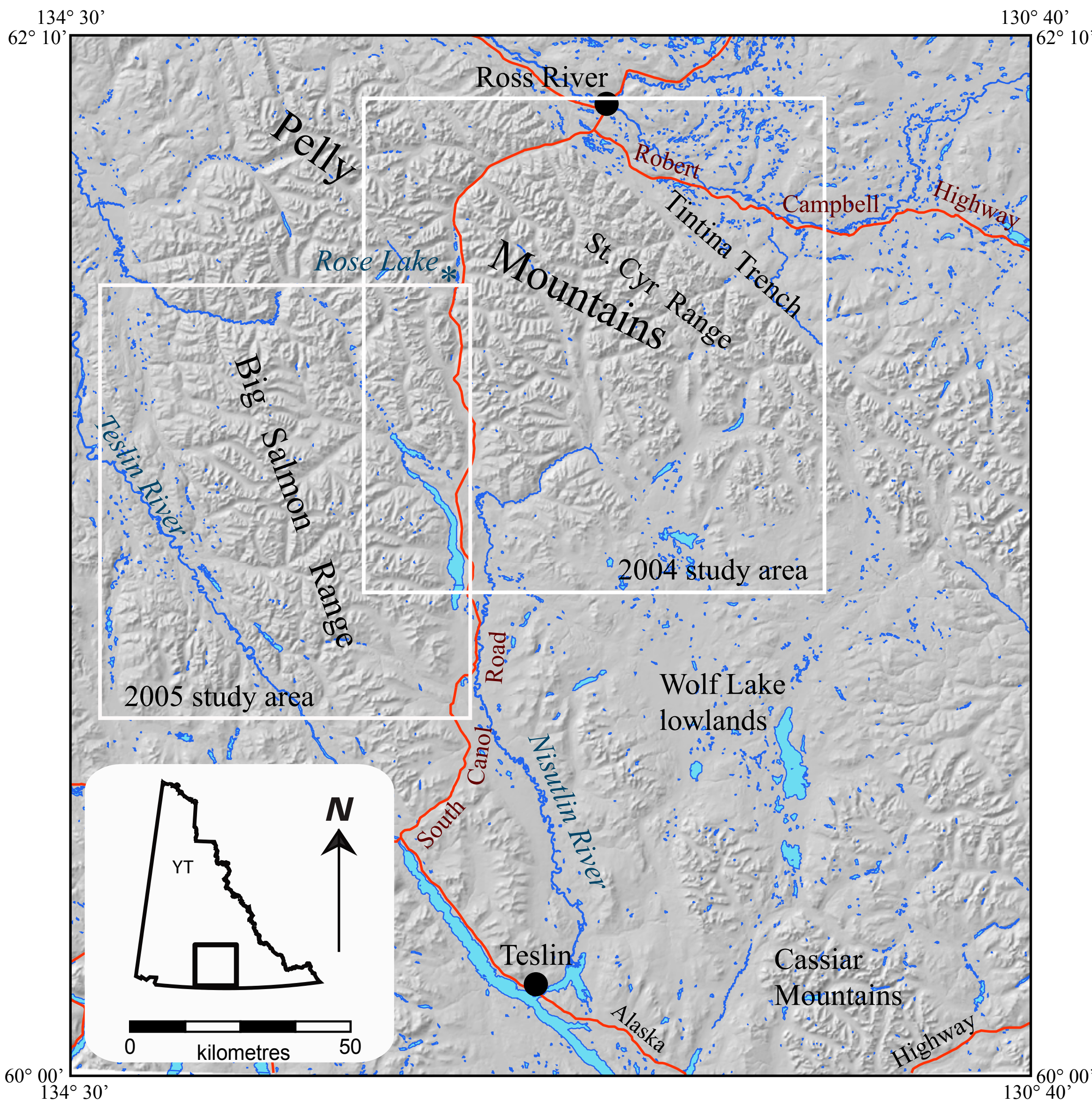

Figure 1. *Regional location map of the 2004 Pelly Mountain study area and the 2005 Big Salmon Range study area.*

PHYSIOGRAPHY, DRAINAGE AND BEDROCK GEOLOGY

The Big Salmon Range is bounded to the west by the Teslin River and to the east by the Wolf Lake lowlands and main ranges of the Pelly Mountains (Figs. 1 and 2). The main drainage divide within the range trends to the north-northwest and contains summits that reach up to 2174 m (7134 ft). Mountains and ridges near the fringe of the range typically reach elevations of around 1800 m (6000 ft). Streams draining to the east in the Big Salmon Range flow into the Nisutlin River, Quiet Lake, or the Big Salmon River; streams draining to the west flow into the South Big Salmon River, Boswell River, or directly into the Teslin River (Figs. 1 and 2).

The geology of the Big Salmon Range can be divided into two general groups: Yukon-Tanana Terrane and mid-Cretaceous intrusive rocks. Yukon-Tanana Terrane in this area consists of metasedimentary rocks belonging to the Snow Cap and Finlayson assemblages (Colpron, 2006a). The Snow Cap assemblage is largely composed of upper Devonian and older siliciclastic rocks, whereas the Finlayson assemblage in the Big Salmon Range consists of upper Devonian to lower Mississippian carbonaceous rocks (Colpron, 2006a). These assemblages have been intruded by the mid-Cretaceous Quiet Lake Batholith, which forms the core of the Big Salmon Range (Gordey and Makepeace, 2003).

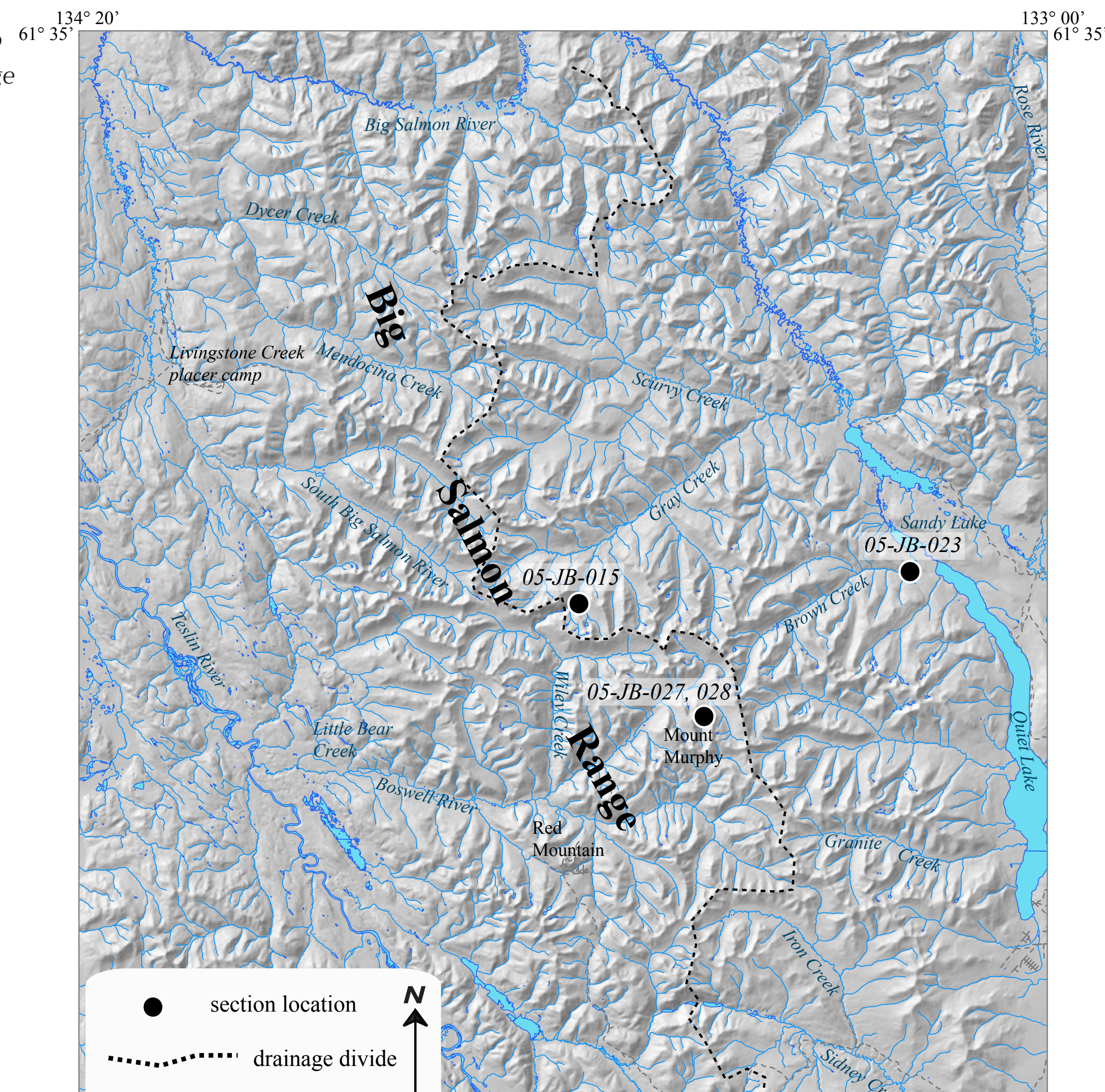

Figure 2. *Location map of the Big Salmon Range study area.*

MINERALIZATION

The Livingstone Creek placer district has produced an estimated 50,000 ounces of gold (1.6 million grams) since its discovery in 1898 (Fig. 2; Lebarge, 2006). The source of the Livingstone placer gold is uncertain, however it is thought to be attributed to skarn mineralization associated with an Early Mississippian metatonalite body that intrudes metasedimentary rocks of the Yukon-Tanana Terrane Snowcap assemblage (Colpron, 2006b). Other known placer gold-bearing streams in the Big Salmon Range include: Dycer, Little Bear, Brown, Iron and Evelyn creeks (Fig. 2; Bond and Church, 2006).

Significant hardrock mineralization in the Big Salmon Range includes the Red Mountain porphyry molybdenum deposit. Molybdenite is found in quartz stockwork that cuts a Late Cretaceous quartz-monzonite porphyry stock (Mortensen, 1992). The inferred resource consists of 187 million tonnes, grading 0.167% MoS_2 (Deklerk and Traynor, 2005).

REGIONAL QUATERNARY GEOLOGY

Yukon has been glaciated numerous times since the late Pliocene (Froese *et al.*, 2000; Duk-Rodkin and Barendregt, 1997; Duk-Rodkin *et al.*, 2001; Jackson *et al.*, 1991). Centres of ice accumulation have included: the St. Elias, interior Coast and Cassiar mountains in southern Yukon; the Selwyn Mountains in eastern Yukon; and the Ogilvie and Wernecke mountains in central Yukon. Ice from each of these accumulation zones flowed radially outward into lowland areas. Thickening ice masses on the landscape developed into separate ice lobes that eventually merged to form a continuous carapace of ice across southern and eastern Yukon (Fig. 3; Jackson *et al.*, 1991). This ice mass formed the northern component of the Cordilleran ice sheet (Fulton, 1991). The limited ice extent in central Yukon was likely a function of aridity (Ward and Jackson, 1992).

The chronology of the last (McConnell) glaciation in Yukon is pieced together from a variety of locations throughout south and central Yukon. Where pre-McConnell organic material has been identified, pollen assemblages suggest that a cooler climate was associated with the onset of glaciation approximately 29 600 years BP (Matthews *et al.*, 1990). In the Tintina Trench, at the foot of the Pelly Mountains, bone-bearing gravel beneath McConnell till was dated at 26 350 ± 280 BP, suggesting ice had not yet extended out of the Pelly Mountains by this date (Jackson and Harington, 1991). Similarly, twig fragments found in a silt unit beneath McConnell till near Watson Lake imply that McConnell glaciers had not yet reached southeast Yukon by 23 900 ± 1140 BP (GSC-2811; Klassen, 1987). The retreat of ice from glacial maximum had begun by 13 660 ± 180 BP as indicated by a radiocarbon age obtained near the terminus of the St. Elias Mountains piedmont lobe complex (GSC-1110; Rampton, 1971). Radiocarbon-dated macrofossils in Marcella Lake (Kettlehole pond) suggest ice-free conditions in southern Yukon by 10 700 BP (Anderson *et al.*, 2002).

Evidence of prior glaciations and interglaciations in the Big Salmon Range is limited. Previous sedimentological investigations by Levson (1992) identified buried pre-Wisconsinan gravel in the Livingstone Creek area. No dates have been published from the Big Salmon Range that constrain the Quaternary chronology specific to this area. A companion open-file map to this report was published for the Big Salmon Range and describes the ice-flow and placer activity history (Bond and Church, 2006).

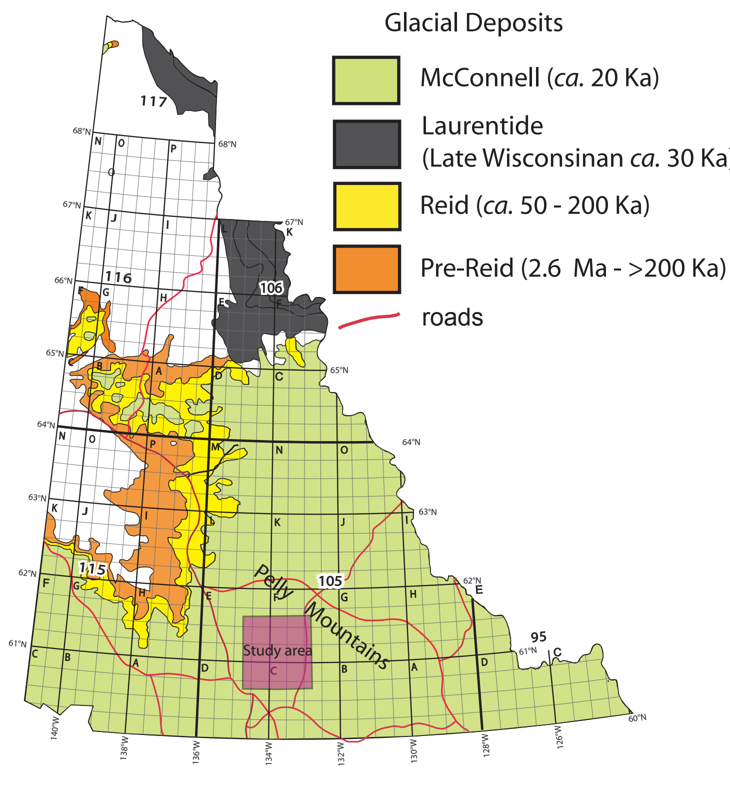

Figure 3. *Glacial limits map of the Yukon (after Duk-Rodkin, 1999).*

METHODS

GEOMORPHOLOGY

The reconstruction of ice-flow for the study area was achieved by examining surficial maps by Jackson (1993), Klassen and Morison (1987), Morison and Klassen (1997), and from new air photo interpretation (Bond and Church, 2006). Morphological attributes of specific glacial landforms contain information that can be used to interpret ice-flow and relative ice thicknesses. This study identified meltwater channels and moraines in order to reconstruct ice-flow during deglaciation, whereas high-elevation aligned landforms provided evidence used to reconstruct ice-flow at glacial maximum.

Meltwater channels

Meltwater channels represent the most common landform that was identified in order to resconstruct the glacial history in the Big Salmon Range. Their relative adundance compared to other glacial landforms is attributed to their erosional nature, particularly when they cut into bedrock as opposed to sediments, in which case they are more resistant to weathering. Meltwater channels that form adjacent to a glacier are called ice-marginal channels, and these commonly occur in clusters where structural and physical characteristics of the bedrock promote enhanced erosion. The dip of an ice-marginal channel reflects the former dip of the glacier and therefore indicates a general ice-flow direction (Fig. 4). A second type of meltwater channel is called a proglacial channel. These channels are commonly found originating at drainage divides where glacier meltwater was impounded on one side of a mountain pass and forced to drain into a lesser glaciated opposing basin (Fig. 5). These channels may erode their base for many kilometres away from the glacier source, depending on valley gradients and ice dams. The presence of these channels helps reconstruct relative ice distributions between neighbouring valleys.

Figure 4. *Lateral meltwater channels cut into bedrock on the flanks of Gray Creek valley. The channels dip in the up-valley direction and reflect the former profile of a receding glacier. View is to the southeast.*

Figure 5. *Proglacial meltwater channels in a tributary to Brown Creek. These channels flow away from a former ice margin and cut across a drainage divide into Gray Creek. View is to the north.*

Moraines

All of the moraines that were mapped represent recessional features and are therefore remnants from deglaciation. Lateral and end moraines reflect the profile of the former glacier margin, and from that, relative ice distribution and ice-flow can be determined (Fig. 6). Where moraines are present on valley sides, caution must be used to ensure that post-depositional mass movements have not occurred to alter the original dip of the landforms.

Aligned landforms

Aligned landforms are the most direct indicators of ice-flow, but they are the least abundant in the study area. In the Big Salmon Range, the only types of aligned landforms found are bedrock ridges that are oriented in the direction of ice-flow (Fig. 7). The combination of glacial erosion and bedrock attributes produce elongate ridges aligned in the direction of ice-flow. Where the ice-flow is parallel with bedding or foliation in bedrock, the aligned ridges are commonly more abundant and better accentuated. Aligned landforms are typically preserved at higher elevations on flat to gently sloping terrain. Their position near mountain summits makes them useful for understanding ice-flow that occurred at, or near, glacial maximum.

STRATIGRAPHY

The stratigraphy of Quaternary sediments was compiled to advance our understanding of the McConnell ice-flow history in the Big Salmon Range. Emphasis was placed on exposures that could potentially help understand ice accumulations prior to glacial maximum; landforms formed during glacial maximum are generally eroded or buried during later phases of glaciation.

Figure 6. *An end moraine in an unnamed alpine valley in the Big Salmon Range. This moraine was deposited by a late deglacial readvance of a local cirque glacier.*

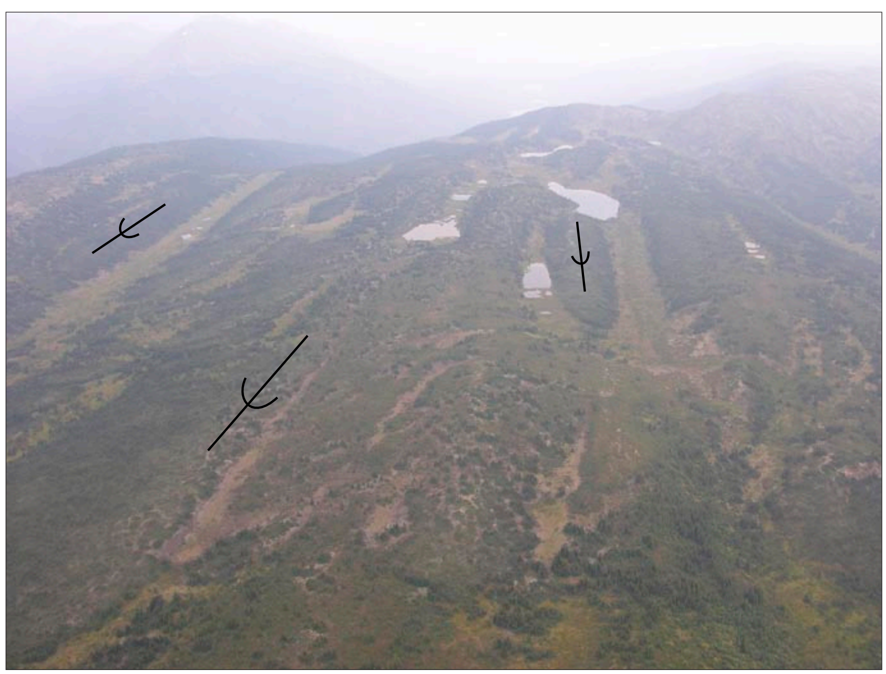

Figure 7. *Aligned till and bedrock landforms west of Livingstone Creek in the Semenof Hills. These landforms are evidence of paleo ice-flow in a northerly direction.*

Exposures of glacial deposits were examined in order to collect the following data: texture, thickness, colour, cohesion, structure and till fabric. Till fabric analysis measures the long-axis orientation of clasts in subglacial till in order to determine the ice-flow direction at the time of deposition. A minimum of 50 clasts are measured during till fabric analysis. The mean orientation of the clasts was also determined for each population, providing an indication of dominant ice-flow direction.

RESULTS

GEOMORPHOLOGY

The oldest landforms from the McConnell glaciation are associated with unconstrained ice-flow across the Big Salmon Range (Bond and Church, 2006). Aligned bedrock landforms were mapped on ridges at elevations up to 1676 m (5500 ft). These landforms record a northwesterly ice-flow direction across the range, and in many areas, they crosscut the topographic trend of the local valleys and ridges. Additional evidence is provided by glacial erratics on Mount Murphy, near the Boswell River. Boulders as tall as 1 m are found at elevations up to 2000 m (6561 ft). The direction of transport of this erratic train is uncertain, however, its elevation indicates ice thicknesses likely exceeded the mountain peaks in this area. Similar landforms were mapped further east near Rose Lake at 1524 m (5200 ft) and they record a northwesterly ice-flow across the Pelly Mountains (Fig. 1; Bond and Kennedy, 2005).

Abundant moraines and meltwater channels below 1676 m (5500 ft) of elevation record topographically controlled easterly to westerly ice-flow in the Big Salmon Range (Bond and Church, 2006). Easterly draining valleys experienced up-valley ice-flow, whereas westerly draining valleys experienced down-valley ice-flow. Evidence of this is provided by up-valley trending end moraines and meltwater channels preserved in Scurvy, Gray, Granite and Iron creek drainages (Fig. 2). On the fringes of the range, the ice flowed parallel to major bounding valleys such as the Teslin and Big Salmon river valleys. As a result, tributaries located on the periphery of these major bounding valleys were commonly glaciated by ice-flow moving perpendicular to the topography.

Up-valley flowing glaciers on the eastern side of the Big Salmon Range forced meltwater to breach mountain passes and descend into the western drainages. In doing so, the meltwater cut deep channels that extended several kilometres (Fig. 8).

Figure 8. *An incised meltwater channel near the headwaters of Mendocina Creek. The depth of incision into the valley bottom is approximately 30 m. The channel extends for 35 km down to the South Big Salmon River. View is to the east.*

QUATERNARY STRATIGRAPHY

05-JB-023: Brown Creek

Brown Creek drains the eastern side of the Big Salmon Range and is a tributary to Sandy Lake (Fig. 2). The exposure is located at the intersection where Brown Creek flows out of the Big Salmon Range and enters the Quiet Lake valley. The section is illustrated in Figure 9 and consists of boulder-dominated gravel/diamicton (Unit 1) at the base, overlain by a compact grey till (Unit 2), and capped by a sorted sandy gravel (Unit 3).

Unit 1 is a coarse, poorly sorted gravel containing a matrix of muddy sand. The cobbles and boulders are mainly granitic in composition and have a crude imbrication suggestive of a paleo-flow that is concurrent with the modern Brown Creek. Unit 1 is interpreted as an ice-proximal, advance outwash gravel originating from a local alpine glacier in Brown Creek.

Unit 2 is a cohesive, matrix-supported, grey diamict with abundant jointing and an abrupt lower contact. The mean orientation of the clast fabric within the unit is 309°. Unit 2 is interpreted as a basal lodgement till derived from a Cordilleran/regional glacier flowing to the northwest in the Quiet Lake valley.

Unit 3 consists of >13 m of bedded sand and gravel. This unit was deposited by fluvial processes, however, no paleo-current information was obtained from this unit. Its stratigraphic position above the basal lodgement till

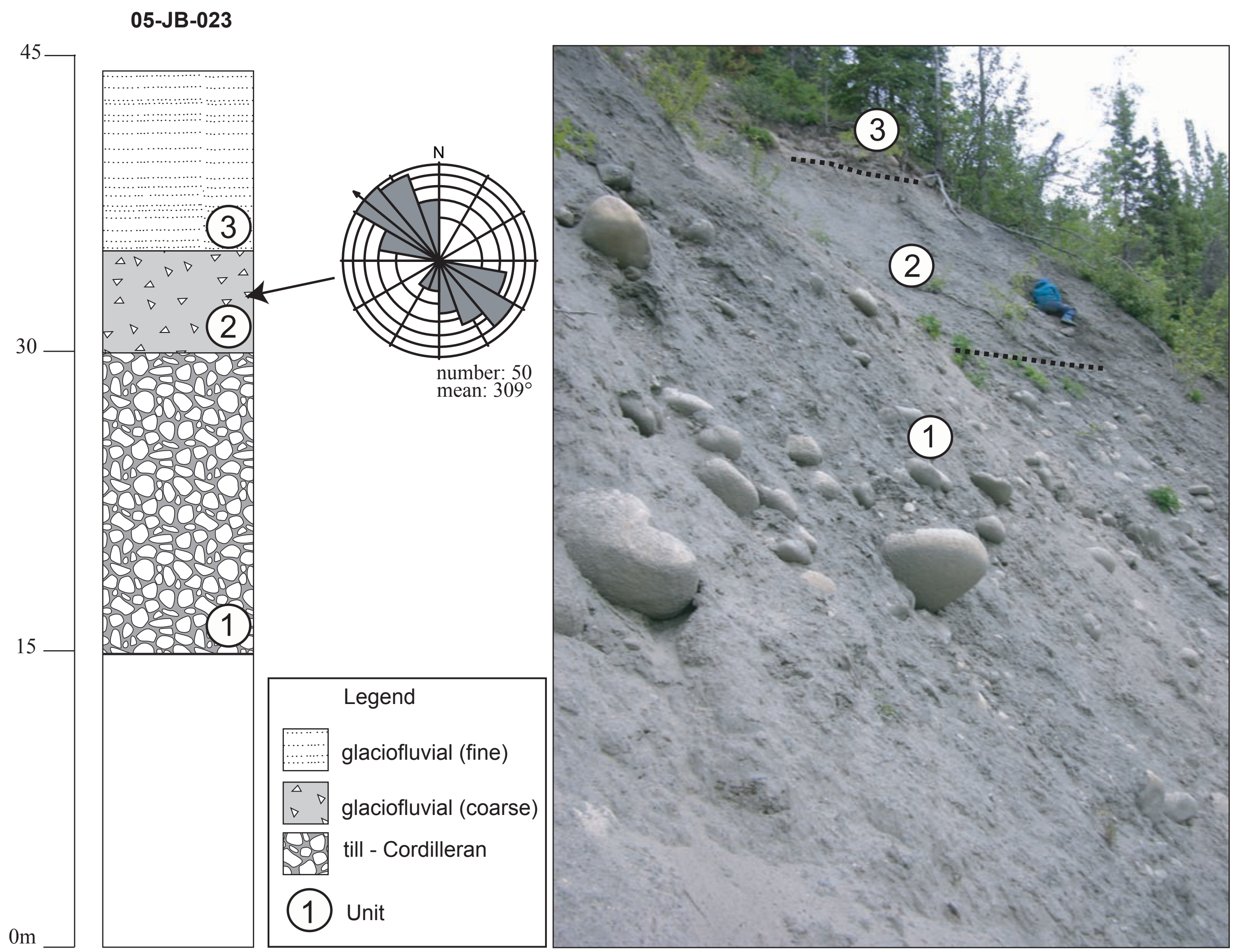

Figure 9. *Stratigraphic section 05-JB-023 consists of a sequence of glacial deposits from at least three phases of the last glaciation. The exposure is located near the mouth of Brown Creek.*

suggests it is an ice marginal, post-glacial outwash associated with the retreating Cordilleran ice sheet.

05-JB-027 and 028: Mount Murphy

A stream-cut exposure was investigated on an unnamed tributary in the headwaters of the Boswell River. The stream originates from a northeast-facing cirque on Mount Murphy (Fig. 2). The stratigraphy from the exposure is illustrated in Figure 10. The unit descriptions and correlations were acquired from a number of exposures within the valley, so the stratigraphy represents a composite reconstruction.

Unit 1 is an olive-brown diamict consisting of equal parts fine and coarse clastic fractions. Clasts are angular and the dominant lithology is intrusive. Bedded sand and washed granule deposits are present within the matrix component and jointing was also observed in less-sorted components of the deposit. The clast fabric analysis yielded two apparent ice-flow directions: the dominant fabric suggests an ice-flow toward the northeast and a secondary fabric records a northwesterly ice-flow. Unit 1 is interpreted as a basal melt-out till that was deposited from a local alpine glacier originating on Mount Murphy.

Unit 2 is a moderately cohesive and jointed olive-grey diamict. The diamict is matrix supported and contains

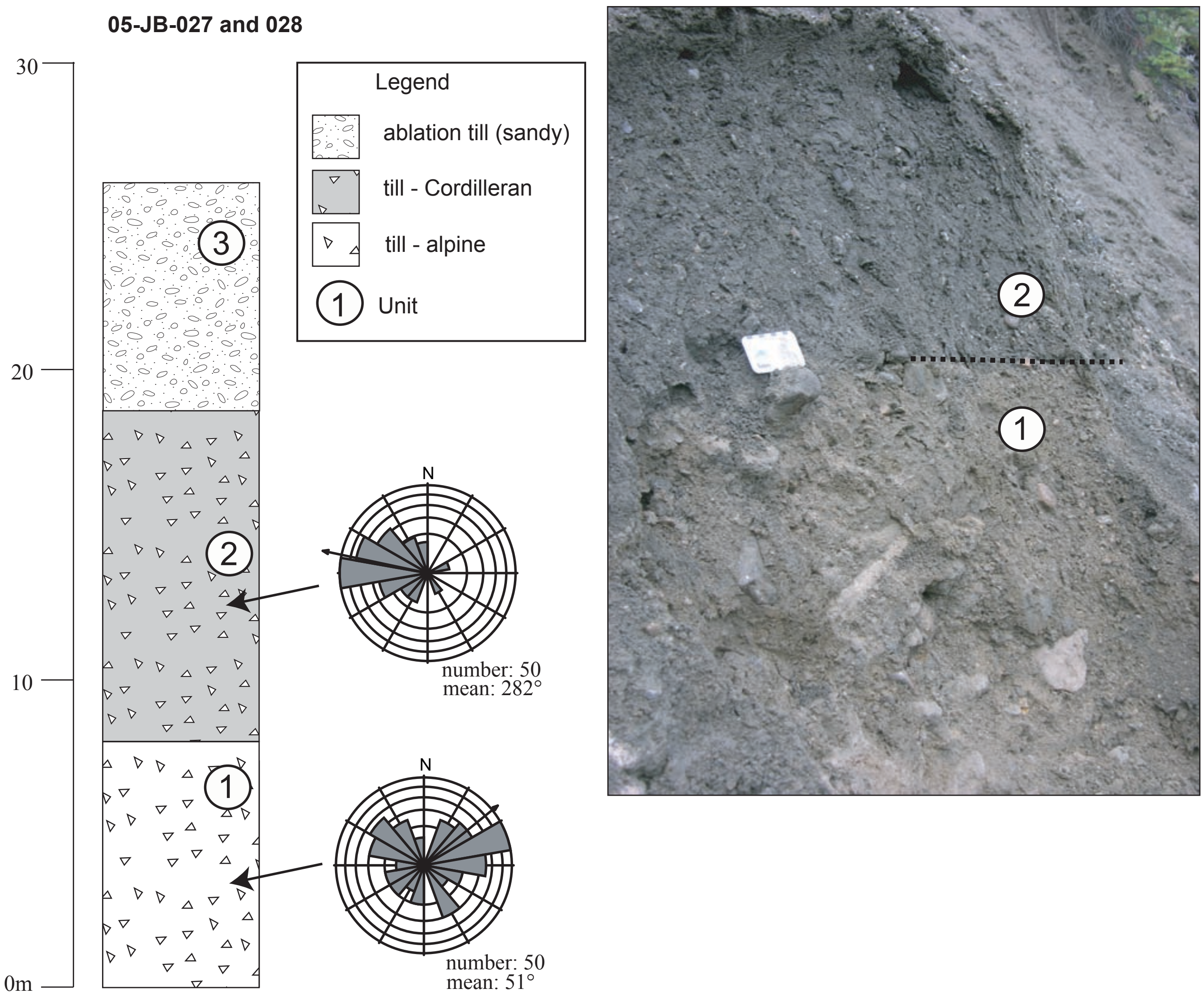

Figure 10. *A composite stratigraphic section from 05-JB-027 and 028 includes multiple tills exposed in a stream-cut near Mount Murphy. Photo is of till deposits exposed at station 05-JB-027.*

smaller clast sizes than observed in unit 1. The clast fabric within this unit reflects a consistent paleo ice-flow direction to the west (mean 282°). Unit 2 is interpreted as a basal lodgement till originating from a large Cordilleran valley glacier or ice sheet flowing to the west.

Unit 3 is a loosely consolidated, sandy-brown diamict that contains numerous boulders. The deposit is poorly exposed and likely correlates with an erratic train located above the section on the edge of the valley. Unit 3 is interpreted as an ablation till associated with retreat of the same Cordilleran ice sheet/glacier that deposited unit 2.

05-JB-015: near divide between Gray and Wiley creeks

A stream-cut exposure was examined on an unnamed tributary at the headwaters of Gray Creek (Fig. 2). The stream originates within a cirque located approximately 3 km to the southeast. The deposit consists of a succession of glacial diamicts of local and regional origins (Fig. 11).

Unit 1 is a coarse, clast-supported diamict consisting of angular granitic boulders. This unit is in contact with bedrock of the Quiet Lake Batholith. Unit 1 is interpreted as local alpine till. No fabric analysis was completed on this unit.

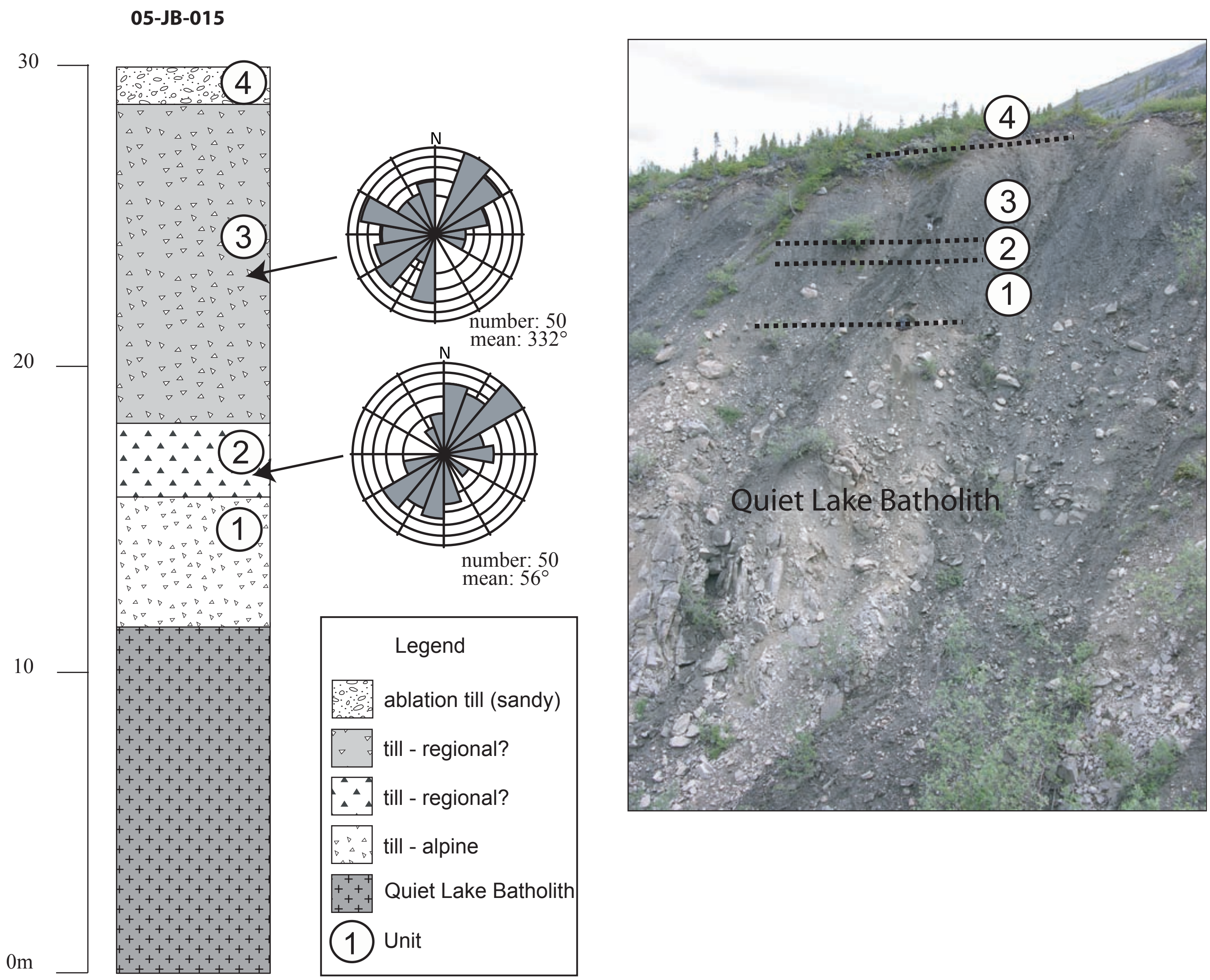

Figure 11. *Stratigraphic section 05-JB-015 consists of a sequence of glacial diamicts. The exposure is located near the divide between Gray and Wiley creeks.*

Unit 2 is a grey-brown cohesive, oxidized till. Equal amounts of clasts and matrix are present and minor jointing was observed. Polished and striated clasts were also present. The prominent mean orientation of clast fabric within this unit is 56°, or northeast. This unit is interpreted as a basal lodgement till, possibly originating from the Cordilleran ice sheet.

Unit 3 is a dark-grey, matrix-supported cohesive diamict. Jointing is present within the deposit and few boulders were visible. The clast fabric for this unit has a strong northeast, as well as southwest orientation. Westward, or up-valley-trending moraines noted in the local area likely correlate with this diamict unit and therefore the fabric likely suggests a southwesterly ice-flow.

Unit 4 consists of a veneer of sandy gravel, interpreted as an ablation deposit associated with unit 3.

DISCUSSION

The late Wisconsinan McConnell glacial history of the Big Salmon Range can be separated into four phases. McConnell ice originated from both local and regional sources.

McConnell advance: Phase 1

Evidence for the regional extent of this phase is limited to sporadic stratigraphic exposures. A more comprehensive reconstruction would require glacier modeling and additional Quaternary stratigraphic research.

Local alpine glaciers within the Big Salmon Range advanced from cirque accumulation zones with onset of the last glaciation and global cooling (Fig. 12a; Bond and Church, 2006). Stratigraphic evidence from Mount Murphy and upper Gray Creek indicate that local glaciers advanced at least 3 km from their source areas. However, stratigraphy from Brown Creek suggests that local alpine glaciers likely extended up to 16 km down-valley. A proglacial outwash deposit at the mouth of Brown Creek (Fig. 9, Unit 1) implies that a local alpine glacier had advanced near to the mountain front. No alpine till was observed at this site, so it is unlikely that the glacier extended into the Quiet Lake valley. This contrasts with the Pelly Mountains further east, where alpine glaciers advanced beyond the mountain front at the onset of the last glaciation (Bond and Kennedy, 2005).

McConnell glacial maximum: Phase 2

At glacial maximum, the Cassiar lobe of the Cordilleran ice sheet overtopped the Big Salmon Range (Bond and Church, 2006). This is supported by the presence of high-elevation, glacially aligned bedrock that records a west-northwest ice-flow direction throughout much of the range (Fig. 12b). This ice-flow trajectory shifts to a north-northwest direction upon converging with ice in the Teslin River valley on the west side of the range (Fig. 12b). A similar glacial history was interpreted for the Pelly Mountains to the east where the Cassiar lobe of the Cordilleran ice sheet advanced from the south and invaded the upland (Bond and Kennedy, 2005). The thickness of the ice sheet over the Big Salmon Range was sufficient enough to permit ice to flow over the range without being influenced and directed by the underlying topography. Erratics observed on Mount Murphy indicate a minimum ice sheet thickness of 760 m in the central part of the range, however, the actual thickness was likely much greater.

McConnell early deglaciation: Phase 3

The Cassiar lobe began to thin over the Big Salmon Range due to a warmer climate following glacial maximum. This reduction in ice thickness resulted in ice movement shifting more towards the west due to the greater influence of the underlying, local topography (Fig. 12c). As the Cassiar lobe retreated to the southeast, its ice-front eventually reached the Teslin River valley. Westward-flowing ice out of the Big Salmon Range would have resembled a system of converging valley glaciers. These glaciers were being fed by thicker accumulations of the Cassiar lobe on the eastern side of the range, where ice-flow was partially restricted by the topographic divide.

Retreat of the Cassiar lobe valley glaciers to the east of the drainage divide signified another change in the deglacial history. The up-valley ice-flow on the eastern side of the range resulted in the formation of proglacial lakes against the ice front. The accumulating meltwater was forced to drain over the divide into the western valleys. Glaciolacustrine and glaciodeltaic deposits at the headwaters of Gray Creek provide good evidence for this part of the glacial history, as do many channels that cut across the passes within the Big Salmon Range (Bond and Church, 2006). Erosion by the meltwater streams was significant enough in some western drainages (e.g., Mendocina Creek) to completely erode morainal deposits from the valley bottoms. In addition, the meltwater erosion created canyons in the valley floors; these are still present today and continue to control the modern floodplain morphology (Fig. 13).

With the development of proglacial lakes in the eastern drainages, the retreat of the Cassiar lobe may have been more rapid due to the process of calving at the ice front. Glaciolacustrine deposits were not observed in any of the eastern drainages with the exception of a small exposure at the headwaters of Gray Creek. Glaciolacustrine deposits would be expected in these eastern drainages had a consistent rate of ice retreat been maintained. Instead, morainal and glaciofluvial sediments appear to dominate the lower valleys (Jackson, 1993; Morison and Klassen, 1997) of the eastern drainages. The lack of glaciolacustrine sediment can only be explained by two processes: either rapid ice-retreat, or a change from

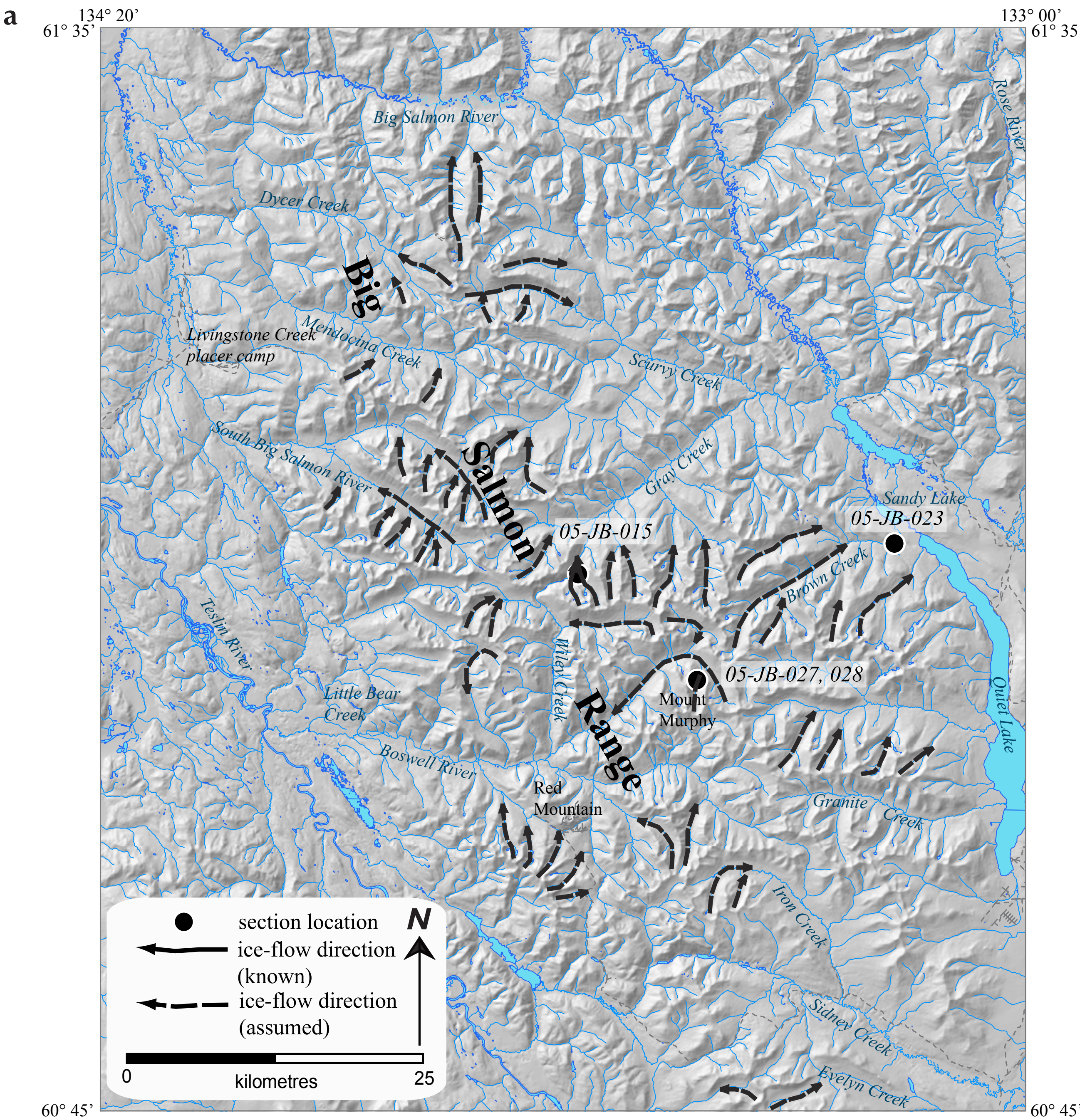

Figure 12(a). *Phases of the McConnell glaciation in the Big Salmon Range (after Bond and Church, 2006). Phase 1: glacial onset characterized by local ice-flow.*

ponded to unponded conditions at the ice margin. An increased rate of retreat could be explained by the process of glacial calving into the proglacial lakes. A change from ponded to unponded conditions could only occur if subglacial drainages were established that allowed water to flow down-valley against the ice-flow. At present, the mechanism of ice retreat in the eastern valleys remains uncertain.

b

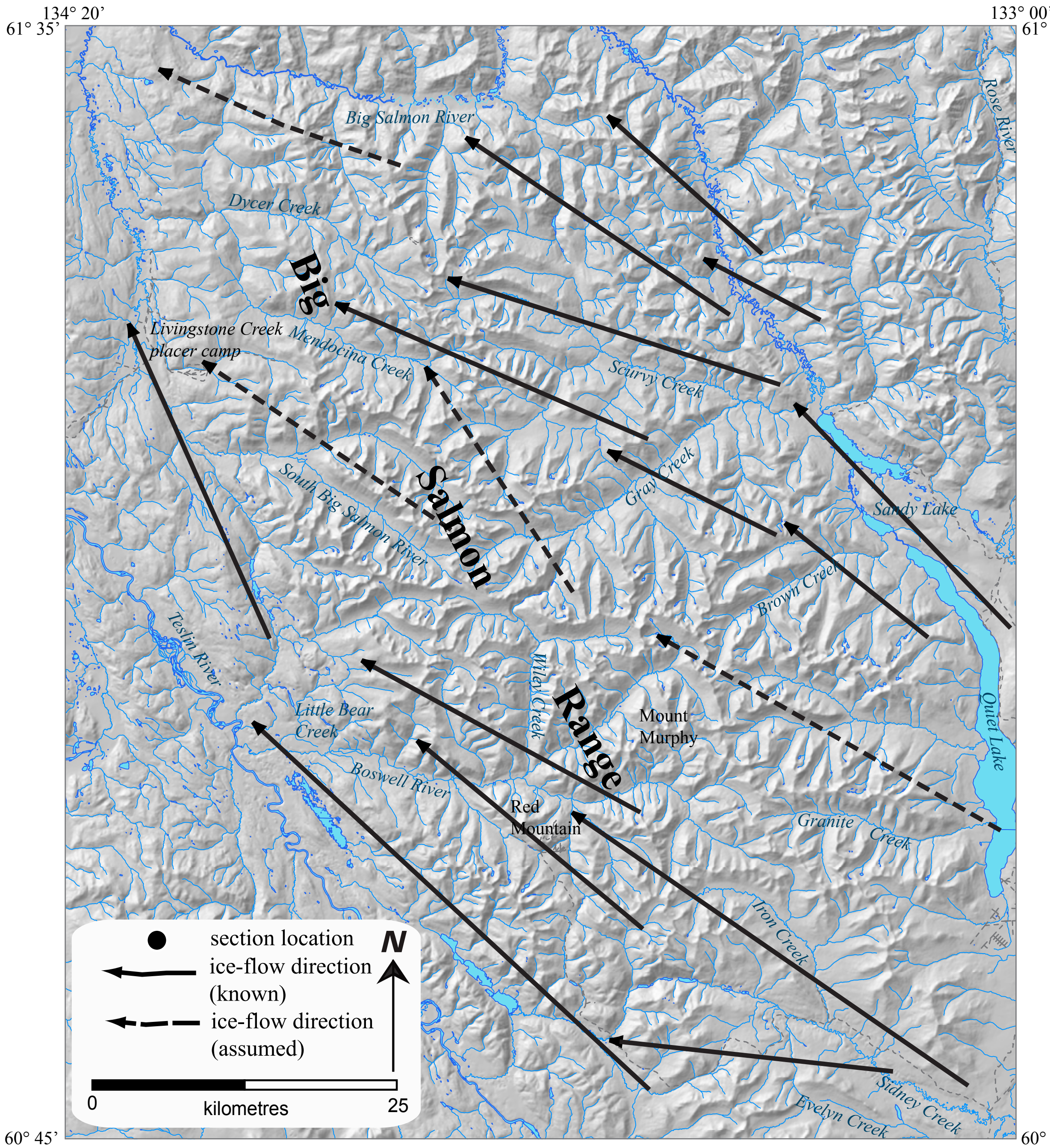

Figure 12(b). *Phases of the McConnell glaciation in the Big Salmon Range (after Bond and Church, 2006). Phase 2: glacial maximum ice-flow reconstruction; ice-flow is to the west-northwest and originates from the Cassiar lobe of the Cordilleran ice sheet.*

McConnell late deglaciation (local readvance): Phase 4

As the Cassiar lobe continued to retreat, a reactivation of local alpine glaciers occurred (Fig. 6; Bond and Church, 2006). End moraines preserved from this phase provide evidence that ice generally advanced less than 3 km from their source areas. The timing of this readvance during the deglacial period has not been determined. A similar readvance was noted in the Pelly Mountains to the east, however, it was much more extensive than in the Big Salmon Range (Bond and Kennedy, 2005). One reason for this could be attributed to the presence of larger cirque complexes in the main part of the Pelly Mountains. Larger upland basins would have had the ability to preserve

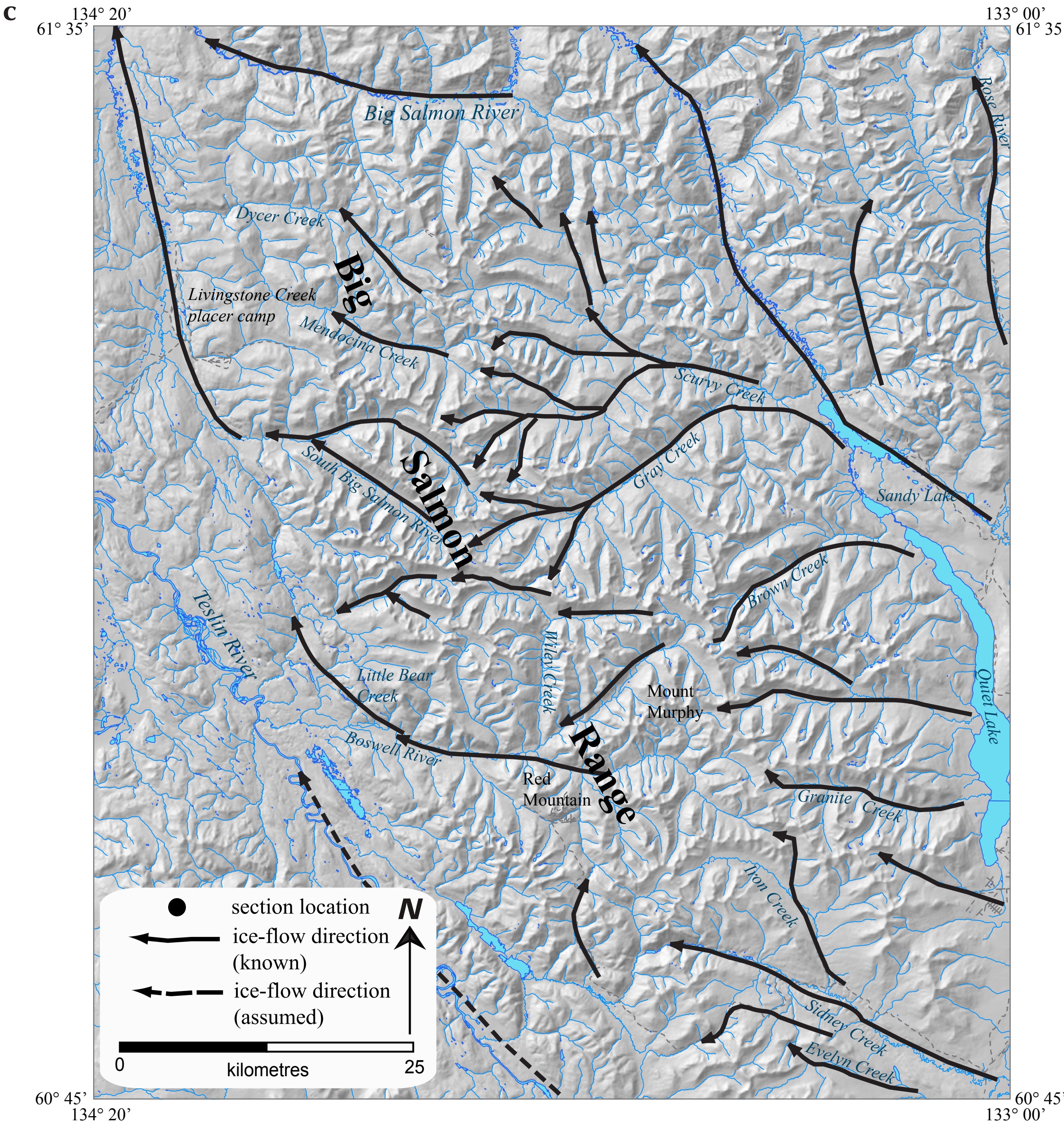

Figure 12(c). *Phases of the McConnell glaciation in the Big Salmon Range (after Bond and Church, 2006). Phase 3: early deglaciation characterized by the retreat of the Cassiar lobe.*

Figure 13. *A canyon located near the middle reaches of Mendocina Creek. The entire length of Mendocina Creek has been altered by the effects of glacial meltwater erosion. The canyon walls are approximately 10 m high.*

remnant ice bodies from the Cassiar lobe. These ice caps would then have the capacity to respond quickly to periods of cooler and wetter climatic conditions if they were to arise during deglaciation. Remnant ice bodies likely existed in the Big Salmon Range as well; however, they were probably less extensive and more isolated. Furthermore, differences between remnant ice bodies in the Big Salmon Range and the Pelly Mountains may be related to regional precipitation variations. This phase of late deglaciation is not illustrated in the Figure 12 compilation because of its limited nature.

IMPLICATIONS FOR MINERAL AND PLACER EXPLORATION

Understanding the glacial history of a region is critical for determining transport directions and provenance of erratic trains and soils derived from till. In addition, it provides invaluable details regarding the erosional and depositional history that has impacted a specific area. The multi-phase ice-flow history proposed for the Big Salmon Range highlights several implications that are important for exploration projects which utilize float, soil and stream geochemistry sampling methods.

MINERAL EXPLORATION

Ice-flow directions for the individual phases of the glacial history have been discussed in the previous section; however, the relative significance of these phases, in terms of drift transport, has not been discussed. As a general rule, the most recent ice-flow phase is the most significant transport direction to consider when tracing the origin of till and erratics. For example, upper drainages that were glaciated by the phase 4 alpine readvance are likely blanketed by surficial materials that are largely derived from the source cirque and surrounding valley walls. A component of foreign drift from a previous transport phase will also be present within the deposit, but will likely account for a smaller percentage of the total drift composition. Despite this general rule of thumb, it is of critical importance that the entire glacial history be taken into account when assessing the origin of soil and erratics. This was demonstrated at the mouth of Brown Creek, where phase 1 alpine glaciofluvial deposits were preserved under phase 2 and 3 till deposits. If anomalous float boulders were found in the modern floodplain of Brown Creek, all three phases would need to be considered in order to determine an origin for the clasts.

The transportation of drift by the Cassiar lobe at glacial maximum is difficult to quantify in the study area. Most of the ice-flow indicators for this phase are found on ridge and plateau summits that were susceptible to basal erosion by the ice sheet. The transport directions on these summit surfaces should parallel the ice-flow directions outlined for glacial maximum. The significance of this phase on sediment transport in mountain valleys is likely less important, due to the active deglacial processes that occurred in the lower areas.

The most widespread surficial materials in the Big Salmon Range are attributed to drift deposits from phase 3 of the glaciation. For most of the valleys, this was the last

Figure 14. *A boulder-dominated placer gold-bearing alluvium deposit observed near the mouth of Brown Creek. This deposit likely represents an alluvial lag deposited during post-glacial incision of Brown Creek. The pogo stick is divided into 25-cm intervals.*

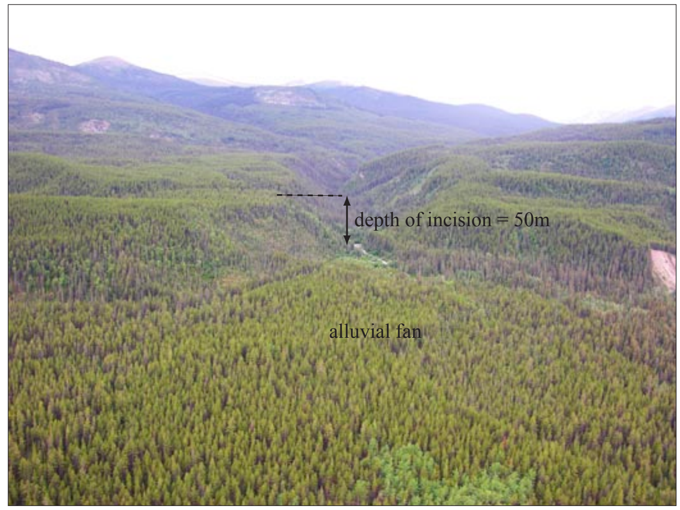

Figure 15. *A view to the west of the mouth of Brown Creek where it exits the Big Salmon Range. In the foreground is an alluvial fan that was deposited as Brown Creek incised into the underlying glacial deposits and bedrock during the early Holocene. The incision occurred in response to base-level change of the Quiet Lake valley.*

phase of the glaciation to erode and deposit material. The processes of erosion and deposition would have been enhanced because the ice was thinner and more easily directed by the underlying topography. The glacier dynamics may have also varied on either side of the Big Salmon Range. On the east side of the range, the ice was flowing up-valley and therefore may have flowed with less energy compared to the western valleys that contained down-valley flowing glaciers. The more vigorous ice-flow in the western valleys likely increased erosion of the bedrock. However, the increased flow would also have reduced the thickness of the glaciers, and therefore the area exposed to erosion. The slower ice-flow on the eastern side of the range may have increased glacial deposition in this area, resulting in greater drift thicknesses.

PLACER EXPLORATION

The Big Salmon Range contains a number of placer gold-bearing streams (Bond and Church, 2006). The Livingstone Creek placer camp contained the most significant deposits, which produced $1 million in gold in the first forty years of activity (Bostock and Lees, 1938). Previous geological research by Levson (1992) in the Livingstone camp area concluded that small tributaries oriented transverse to the former direction of ice-flow were dominated by glacial deposition rather than erosion. This permitted the preservation of pre-glacial placer deposits. Similar settings for placer gold were also noted in glaciated areas near Mayo (LeBarge *et al.*, 2002). These cases highlight the significance of this setting as a potential exploration target for placer gold deposits.

While stream orientation with respect to paleo ice-flow played a significant role in the Livingstone camp, other known placer streams in the Big Salmon Range were affected by ice-flow parallel to valleys. These include Dycer, Iron, Evelyn and Brown creeks (Bond and Church, 2006). The stratigraphy presented earlier for Brown Creek provides evidence that the drainage contained a local alpine glacier during phase 1 of glaciation. Despite the active glacial processes in this drainage, a potentially economic placer deposit has been identified near the mouth of the creek. The placer gold-bearing unit at Brown Creek is not a pre-glacial deposit, but rather a boulder-dominated alluvium that was deposited in response to significant down-cutting following the glaciation (Fig. 14). This local erosion, or base-level change, occurred in response to fluvial/glacial erosion that occurred in the Quiet Lake valley (Fig. 15). Similarly, a drop in base-level in Sidney Creek caused Iron Creek to cut a canyon at its mouth through thick glacial drift in the valley bottom. This undoubtedly contributed to the value of the placer deposit by reconcentrating placer gold onto a new bedrock surface. Future placer discoveries on the east side of the Big Salmon Range may occur where similar post-glacial erosion has taken place.

Streams draining the west side of the Big Salmon Range were more likely to have been affected by meltwater erosion rather than glacial deposition. As was described for phase 3 of the glaciation, meltwater that ponded in the eastern basins drained to the west over low passes. The streambed erosion associated with these meltwater channels was significant and may have eroded or redistributed any previously existing placer deposits (Fig. 13). Areas affected by meltwater erosion are easily identified by the abundant bedrock canyons in the valley bottoms. Basins that escaped the meltwater erosion should have a component of the glacial stratigraphy preserved in the valley bottom. A stratigraphy similar to that described by Levson (1992) for the Livingstone placer camp would be of particular significance for potential placer exploration.

CONCLUSIONS

A four-phase glacial history has been described for the Big Salmon Range. Local ice accumulations early in the glaciation were insufficient to redirect the Cassiar lobe that invaded the range from the southeast. By glacial maximum, the Cassiar lobe had overtopped the upland. During deglaciation, the retreat of the Cassiar lobe differed between the western and eastern drainages. The down-valley ice-flow, as well as high meltwater flow on the west side of the Big Salmon Range, resulted in the dominance of erosional processes. In contrast, the up-valley ice-flow on the eastern side of the Big Salmon Range caused depositional processes to dominate. The surficial geology throughout most of the Big Salmon Range is remnant from this phase of the glacial history.

While conducting mineral and placer exploration in the Big Salmon Range, one needs to consider all phases of the last glaciation to properly assess the genesis of the surficial materials. For example, it is important to be aware that ice-flow directions shifted during the glaciation, causing upland flow directions to possibly contrast with lowland flow directions in the same general area. Likewise, the preservation of a placer deposit is dependant on the degree of erosion that has occurred in the drainage. This is commonly a function of a valley's orientation relative to the paleo-ice flow. In addition, the placer economics of an area are significantly enhanced by post-glacial fluvial incision.

ACKNOWLEDGEMENTS

Funding for this project was provided by the Yukon Geological Survey. Special thanks are owed to Amber Church for her field assistance. Safe and reliable helicopter transport was provided by Heli Dynamics Ltd. of Whitehorse. A review of this paper was completed by Panya Lipovsky, and Leyla Weston provided excellent editing improvements.

REFERENCES

Anderson, L., Abbott, M., Finney, B. and Edwards, M.E., 2002. The Holocene lake-level history of Marcella Lake, southern Yukon Territory, Canada. *In:* The Geological Society of America Northeastern Section – 37th Annual Meeting, Springfield, Massachusetts, Session No. 19 Program Abstract.

Bond, J.D. and Church, A., 2006. McConnell ice-flow and placer activity map, Big Salmon Range, Yukon. Yukon Geological Survey, Open file 2006-20, 1:100 000 scale.

Bond, J.D. and Kennedy, K.E., 2005. Late Wisconsinan McConnell ice-flow and sediment distribution patterns in the Pelly Mountains, Yukon. *In:* Yukon Exploration and Geology 2004, D.S. Emond, L.L. Lewis and G.D. Bradshaw (eds.), Yukon Geological Survey, p. 67-82.

Bostock, H.S. and Lees, E.J., 1938. Laberge map area, Yukon. Geological Survey of Canada, Memoir 217.

Colpron, M. (compiler), 2006a. Tectonic assemblage map of Yukon-Tanana and related terranes in Yukon and northern British Columbia (1:1 000 000 scale). Yukon Geological Survey, Open File 2006-1.

Colpron, M., 2006b. Geology and mineral potential of Yukon-Tanana Terrane in the Livingstone Creek area (NTS 105E/8), south-central Yukon. *In:* Yukon Exploration and Geology 2005, D.S. Emond, G.D. Bradshaw, L.L. Lewis and L.H. Weston (eds.), Yukon Geological Survey, p. 93-107.

Deklerk, R. and Traynor, S. (compilers), 2005. Yukon MINFILE 2005 – A database of mineral occurrences. Yukon Geological Survey, CD-ROM.

Duk-Rodkin, A. and Barendregt, R.W., 1997. Glaciation of Gauss and Matuyama age, Tintina Trench, Dawson area, Yukon. Canadian Quaternary Association Biannual Meeting May 22-24, 1997: Université de Québec à Montréal, Montréal, Québec.

Duk-Rodkin, A., 1999. Glacial limits map of Yukon Territory. Geological Survey of Canada, Open File 3694; Exploration and Geological Services Division, Yukon Region, Indian and Northern Affairs Canada, Geoscience Map 1999-2, scale 1:1 000 000.

Duk-Rodkin, A., Barendregt, R.W., White, J.M. and Singhroy, V.H., 2001. Geologic evolution of the Yukon River: Implications for placer gold. Quaternary International, vol. 82, p. 5-31.

Froese, D.G., Barendregt, R.W., Enkin, R.J. and Baker, J., 2000. Paleomagnetic evidence for multiple late Pliocene-early Pleistocene glaciations in the Klondike area, Yukon Territory. Canadian Journal of Earth Sciences, vol. 37, p. 863-877.

Fulton, R.J., 1991. A conceptual model for growth and decay of the Cordilleran Ice Sheet. Géographie physique et Quaternaire, vol. 45, no. 3, p. 281-286.

Gordey, S.P. and Makepeace, A.J. (compilers), 2003. Yukon digital geology, version 2. Geological Survey of Canada Open File 1749; Yukon Geological Survey Open File 2003-9(D), 2 CD-ROMS.

Hughes, O.L., Campbell, R.B., Muller, J.E. and Wheeler, J.O., 1969. Glacial limits and flow patterns, Yukon Territory, south of 65 degrees north latitude; Geological Survey of Canada, Paper 68-34, 9 p.

Jackson, L.E., Jr. and Mackay, T.D., 1991. Glacial limits and ice-flow directions of the last Cordilleran Ice Sheet between 60 and 63 degrees north. Geological Survey of Canada Open File 2329, 1:1 000 000 scale.

Jackson, L.E., Jr. and Harington, C.R., 1991. Pleistocene mammals, stratigraphy, and sedimentology at the Ketza River site, Yukon Territory. Géographie physique et Quaternaire, vol. 45, p. 69-77.

Jackson, L.E., Jr., Ward, B., Duk-Rodkin, A. and Hughes, O.L., 1991. The last Cordilleran ice sheet in southern Yukon. Géographie physique et Quaternaire, vol. 45, p. 341-354.

Jackson, L.E., Jr., 1993. Surficial Geology, Gray Creek, Yukon Territory. Geological Survey of Canada, Map 1792A, scale 1:100 000.

Kennedy, K.E. and Bond, J.D., 2004. Evidence for a late-McConnell re-advance of the Cassiar lobe in Seagull Creek, Pelly Mountains, central Yukon. *In:* Yukon Exploration and Geology 2003, D.S. Emond and L.L. Lewis (eds.), Yukon Geological Survey, p. 121-128.

Klassen, R.W., 1987. The Tertiary-Pleistocene stratigraphy of the Liard Plain, southeastern Yukon Territory. Geological Survey of Canada, Paper 86-17, 16 p.

Klassen, R.W. and Morison, S.R., 1987. Surficial geology, Laberge, Yukon Territory, Geological Survey of Canada, Map 8-1985, scale 1:250 000.

LeBarge, W.P. (compiler), 2006. Yukon Placer Database 2004 – Geology and mining acitivity of placer occurrences. Yukon Geological Survey, CD-Rom.

LeBarge, W.P., Bond, J.D. and Hein, F.J., 2002. Placer gold deposits of the Mayo area, central Yukon. Exploration and Geological Services Division, Yukon Region, Indian and Northern Affairs Canada, Bulletin 13, 209 p.

Levson, V., 1992. The sedimentology of Pleistocene deposits associated with placer gold bearing gravels in the Livingstone Creek area, Yukon Territory. *In:* Yukon Geology, Vol. 3; Exploration and Geological Services Division, Yukon Region, Indian and Northern Affairs Canada, p. 99-132.

Matthews, J.V., Schweger, C.E. and Hughes, O.L., 1990. Plant and insect fossils from the Mayo Indian Village section (central Yukon): New data on middle Wisconsinan environments and glaciation. Géographie physique et Quaternaire, vol. 44, p. 15-26.

Morison, S.R. and Klassen, R.W., 1997. Surficial geology, Teslin, Yukon Territory, Geological Survey of Canada, 1891A, scale 1:125 000.

Mortensen, J.K., 1992. Pre-mid-Mesozoic tectonic evolution of the Yukon-Tanana terrane,Yukon and Alaska. Tectonics, vol. 11, no. 4, p. 836-853.

Rampton, V.N., 1971. Late Quaternary vegetational and climatic history of the Snag-Klutlin area, Yukon Territory, Canada. Geological Society of America Bulletin, vol. 82, p. 959-978.

Ward, B.C. and Jackson, L.E., Jr. 1992. Late Wisconsinan glaciation of the Glenlyon Range, Pelly Mountains, Yukon Territory, Canada. Canadian Journal of Earth Sciences – Journal Canadien des Sciences de la Terre, 29 (9), p. 2007-2012.

The Dawson City landslide (Dawson map area, NTS 116B/3), central Yukon

Marc-André Brideau
Doug Stead
Victoria Stevens
Department of Earth Sciences, Simon Fraser University[1]

Charlie Roots
Geological Survey of Canada[2]

Panya Lipovsky
Yukon Geological Survey

Peter VonGaza
Yukon Geomatics

Brideau, M.-A., Stead, D., Stevens, V., Roots, C., Lipovsky, P. and VonGaza, P., 2007. The Dawson City landslide (Dawson map area, NTS 116B/3), central Yukon. *In:* Yukon Exploration and Geology 2006, D.S. Emond, L.L. Lewis and L.H. Weston (eds.), Yukon Geological Survey, p. 123-137.

ABSTRACT

A pre-historic pseudo-circular rock-slope failure at the northern edge of Dawson City, Yukon occurs in altered ultramafic rocks. The middle section of the landslide debris continues to move down-slope, as is evident from sheared trenches, stretched roots and split trees along its edges, and a steep snout exposing fresh material. Dendrochronological analysis demonstrated that the split trunk of one tree has displaced over the last 40 to 45 years at an average movement rate of 4.5 cm/year. This moving section of the debris could be characterized as a rock glacier or as an earth flow, although our present observations and measurements do not confirm either mechanism. A block upslope from the headscarp of the landslide exhibits signs of recent movement. To assess the movement rate of the different sections of the landslide in the future, a monitoring array was set up and an initial set of measurements was taken in July, 2006.

RÉSUMÉ

Une rupture pseudo-circulaire préhistorique de talus rocheux s'est produite dans les matériaux ultramafique à la limite nord de Dawson City, au Yukon. La section du milieu des débris d'éboulement continue à se déplacer vers le bas de la pente, comme le font fois des tranchés cisaillées, des racines étirées, et des arbres fendus le long de leurs limites, et le nez de cette section qui expose des matériaux de débris frais. Une analyse dendrochronologique a démontré qu'un tronc d'arbre déchiré s'est déplacé pendant les 40-45 dernières années avec un taux moyen de mouvement de 4.5 cm/a. Cette section des débris pourrait être considérée comme un glacier de roche ou une coulée de terre malgré que nos observations à se stade-ci ne nous permettent pas de confirmer l'un ou l'autre de ces mécanismes. Un système de monument de levé a été mis en place et un relevé initial fut effectué en juillet, 2006 pour évaluer les taux de déplacement des différentes sections du glissement dans le future.

[1]*8888 University Drive, Burnaby, British Columbia, Canada V5S 1S6, mbrideau@sfu.ca*
[2]*co-located with Yukon Geological Survey, Whitehorse, Yukon, Canada, charlie.roots@gov.yk.ca*

INTRODUCTION

The Dawson City landslide (also known as the Moosehide slide) is a dominant feature of Dawson's city-scape (Fig. 1). Due to its close proximity to the north edge of the town (Fig. 2), a variety of human land use activities have periodically taken place on the landslide debris. During the goldrush-era housing shortage (Brand, 2002), the landslide deposit and its flanks were temporarily occupied. In about 1908 (see Tyrrell, 1910), a flume was built across the upper talus to carry water to the town from Moosehide Creek; its foundation remains to this day. In the late 1970s, the lower third of the landslide deposit was quarried for coarse fill and rip-rap, and was subsequently re-contoured. During the 1990s, this area has been used as a temporary campground. High above this activity, the rock cliffs (hereafter called the headscarp) spawn occasional rockfall, which has accumulated at the base of the headscarp in a deposit (hereafter called the 'landslide debris deposit') with a furrowed character. A trail popular with summer hikers crosses the debris train below the headscarp. The surface of the landslide debris deposit slopes, steeply at intervals, down to the uppermost streets at the north edge of the town, where it terminates in a steep-sided front. Local inhabitants have wondered whether another catastrophic slide will ever occur and whether the debris will continue to encroach on their property. At the same time, earth scientists have long speculated about how the slide initiated and what the present mechanism of movement is.

The observations in this article reflect fieldwork performed primarily by the first author and his assistants during the summers of 2005 and 2006, as well as discussions among the other authors. Statistical and laboratory analysis of rocks (first author) and organic material (third author) reflect thesis-related research. A second phase of the study was initiated in 2006 when survey pins were inserted in the debris train and on opposite sides of an expanding tension crack above the headscarp. By periodically and precisely remeasuring their positions, we hope to be able to detect and monitor small ground movements in the future. This monitoring will provide a better understanding of the magnitude and direction of displacement, and therefore the mechanism of movement.

REGIONAL GEOGRAPHIC AND CLIMATIC SETTING

The townsite of Dawson City is located on fluvial terrace on the east bank of the Yukon River (elevation 308 m). East of 8th Avenue (the highest street and furthest east of the river), the slope steepens and rises to a rounded summit known as Midnight Dome (elevation 850 m). This feature is a relatively small mountain in the Klondike

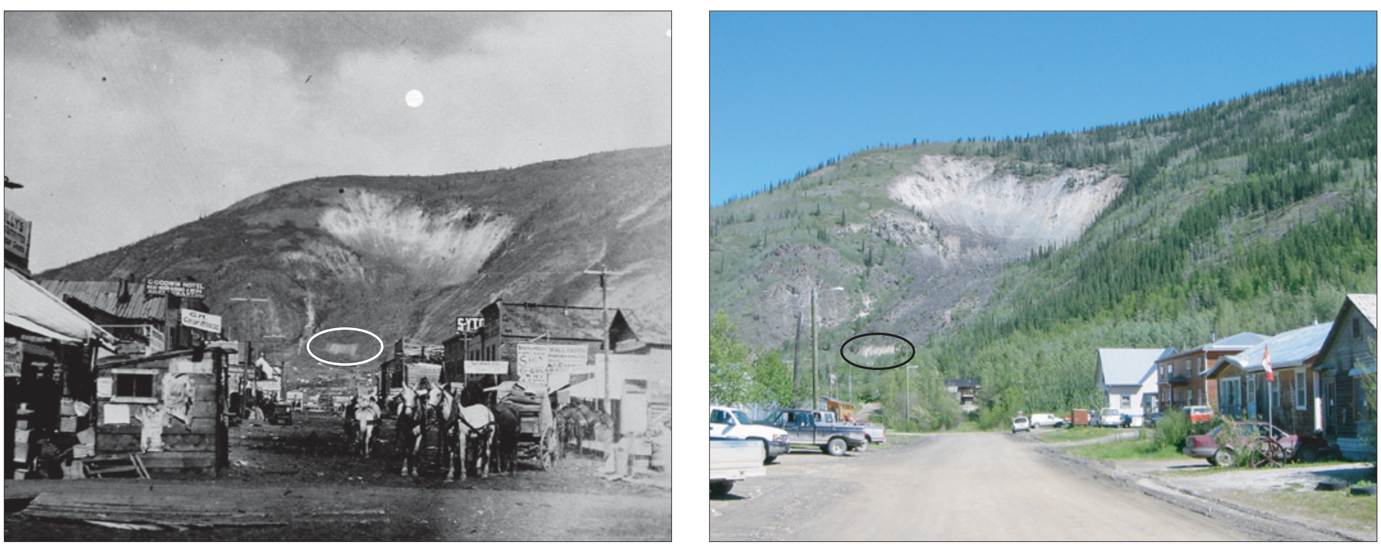

View down 2nd Avenue, *ca.* 1900. **View down 3rd Avenue, 2005.**

Figure 1. *Northward view of the landslide in ca. 1900 and in 2005, showing little change in the headscarp. Note that the pale snout (circled on the figure) of the middle to lower section of the debris has moved downslope. The historical photograph was obtained from the archive at the Dawson City Museum and is part of the collection of Mrs. Ellen Northrop Shannon.*

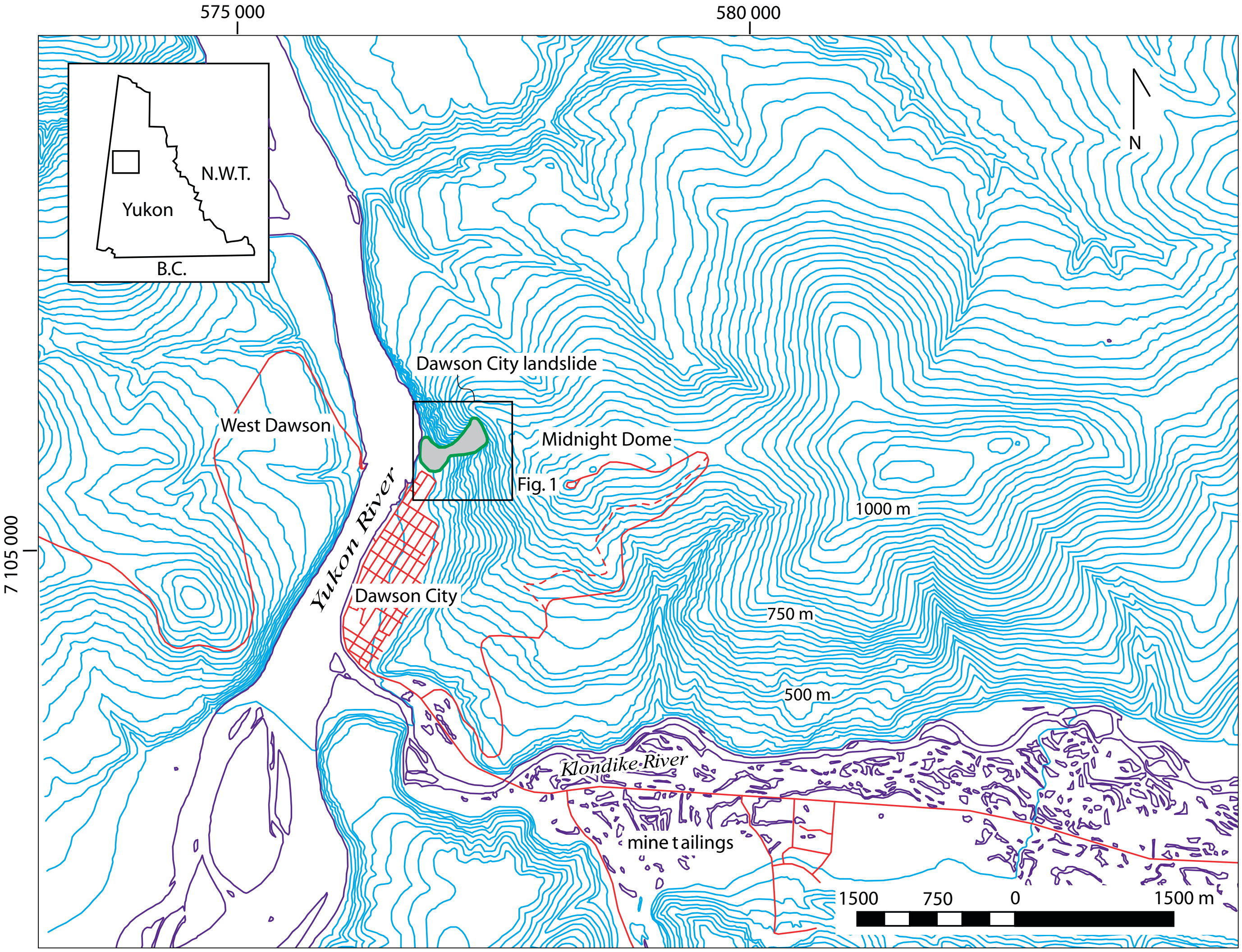

Figure 2. *Location map of the Dawson City landslide at the northern edge of town (modified from Brideau et al., in press).*

Plateau physiographic region. The region is unglaciated and part of eastern Beringia (Froese *et al*., 2000, 2001), so upper slopes are typically deeply weathered and outcrop is rare (Duk-Rodkin, 1996).

The present continental climate consists of warm summers and cold winters. Weather records yield an annual average air temperature of about -5°C (Wahl *et al*., 1987), but during the last decade this average has increased by several degrees (Environment Canada[3]) to the detriment of permafrost and other periglacial features. Winter snowfall ranges from 50-80 cm (some recent years had snowfalls at the top of this range), but snow melts quickly from west- and south-facing slopes in April. During most summers, the forest floor barely dries out between rainstorms, although some summers are very dry which makes them more prone to forest fires. Stable rock surfaces support thick lichen (although some ultramafic substrates are nutrient-poor for plant growth), and dense mixed (spruce-birch) second-growth forest occurs on thin soils, several tens of centimetres thick. Soils are composed of colluvium generally derived from local weathered bedrock intermixed with silty aeolian deposits (loess) and organic matter (Bond and Sanborn, 2006), and they are commonly modified by cryoturbation.

The Klondike Plateau lies within the zone of widespread but discontinuous permafrost (Yukon Ecoregions Working Group, 2004).

The Dawson City landslide involves two rock types: metasedimentary rock from the Yukon-Tanana Terrane and ultramafic rock of the Slide Mountain Terrane. These units are interpreted as a volcanic-arc assemblage overthrust by a sliver of oceanic crust, respectively (Mortensen, 1988a; Colpron, 2006).

[3]*http://www.climate.weatheroffice.ec.gc.ca/climate_normals/index_e.html*

FIELD OBSERVATIONS AND MEASUREMENTS

The Yukon River cuts into the northwest-trending spur of Midnight Dome; the headscarp of the Dawson City landslide forms a southwest-facing bowl on the south side of that spur (Fig. 2). The landslide debris extends out of this bowl and downward, south of a rock buttress to the river, forming the northern boundary of the town. The rectangular headscarp is approximately 300 m wide and 100 m high. Directly below the headscarp a talus apron slope extends about 80 m in length, grading from sand near the top to boulder-sized particles at its base. Coarse debris extends below the talus for up to 550 m, dropping about 200 m in elevation. The landslide debris deposit begins as a gently sloping boulder field, becoming steeper in several locations where rock outcrops constrict the mid-section. It then widens and flattens toward the toe of the debris and terminates in a steeply sloping face that exhibits freshly exposed sediment. Linear extensional features such as tension cracks and trenches surround the headscarp and the margins of the landslide debris deposit.

From the lobate shape of the debris deposit and the abundance of very coarse blocks, we believe the initial slope failure event was a catastrophic rock slide. The upper part of the debris has been subsequently buried by ongoing piecemeal rockfall, which still continues today. Since the initial failure, the upper half of the debris has continued to move slowly downslope, as indicated by its wrinkled and furrowed surface, and trees growing on or adjacent to the debris with split or curved trunks. We address several possible failure mechanisms following descriptions of the landslide's morphological components.

HEADSCARP

The headscarp of the Dawson City landslide consists of abundantly fractured rock with an average slope angle of 60° and some nearly vertical faces up to 20 m high. Small amounts of rockfall have been observed after human disturbance, heavy rains or during freeze-thaw cycles. However, only small-magnitude mass movement has occurred at the headscarp during the past century because neither the stone flume located immediately below the headscarp, nor the footpath located at the base of slope, have been obliterated.

The headscarp is composed of altered ultramafic rocks. Serpentinite predominates (70-90%) with hornblende pyroxenite, gabbro and calcite also being present in variable amounts. Mottled green-black and orange rock surfaces with belt-buckle texture indicate alteration of original olivine to iddingsite; thin sections of this rock also revealed minor calcite (~5%), chlorite (~5%), pyroxene (0-5%) and magnetite (~1%). The ultramafic rock is laced with incipient and open fractures. Fresh surfaces of the rock are difficult to obtain and most faces are fracture surfaces coated with serpentine. We believe the gabbroic rock is medium crystalline, with no evidence of ductile strain.

Several types of linear features were observed upslope from the headscarp. These include tension cracks (bounded by discontinuities in the bedrock), trenches (distinct lows in the topography), antislope (uphill-facing) scarps and ridges (Fig. 3). The length of the linear features varies between 5-100 m, their width between 0.5-8 m, and their observed depth between 0.2-3 m. Circular and rectangular depressions (length x width x depth: about 0.5 x 1.0 x 0.75 m) were observed behind the headscarps. These may be anthropogenic features (prospecting pits, caches, or dwelling structures) because they lack structural orientation and are close to the existing trail. Similar features were previously described in archeological reports of the area surrounding Dawson City (Brand, 2002; Thomas Heritage Consulting, 2005).

A tension crack outlining a potentially unstable block is located above the central portion of the headscarp. The location of this block is conceptually represented in Figure 4 and is shown on the map of linear features in Figure 3. Disturbed vegetation, exposed soil horizons, stretched roots and split trees were interpreted as indications of recent movement along the tension crack.

SIDEWALLS AND ADJACENT SLOPES

Directly beneath the headscarp, bedrock outcrop is obscured by talus and landslide debris, but a promontory on the north side and sidescarp on both sides of the landslide consists of brown to dark grey carbonaceous phyllite, amphibolite schist and minor quartzite. These rocks contain quartz (25-70%), mica (muscovite and biotite; 5-30%), chlorite (0-20%) and calcite (0-20%); thin sections also show minor amounts of opaque minerals (0-5%), epidote (1%) and zircon (1%). These rocks are more coherent than the ultramafic rock higher up and reveal discrete zones of high strain with oriented platy minerals and thin planes of mylonite. In places the strain zones have been folded (Fig. 5).

The contact between the ultramafic and underlying metasedimentary rocks was mapped on a regional scale

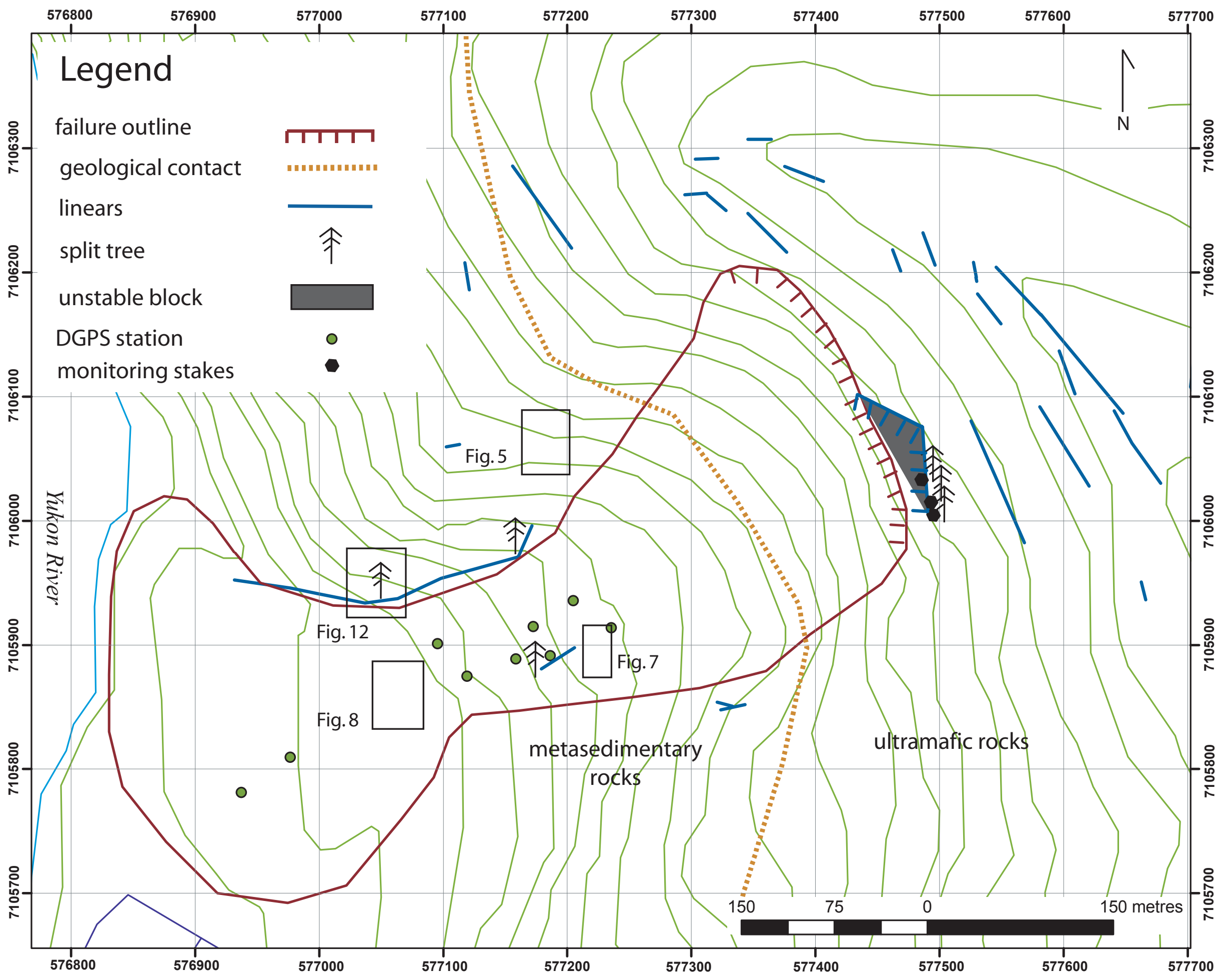

Figure 3. Distribution of measured linear features, showing their orientation and length (modified from Brideau et al., in press).

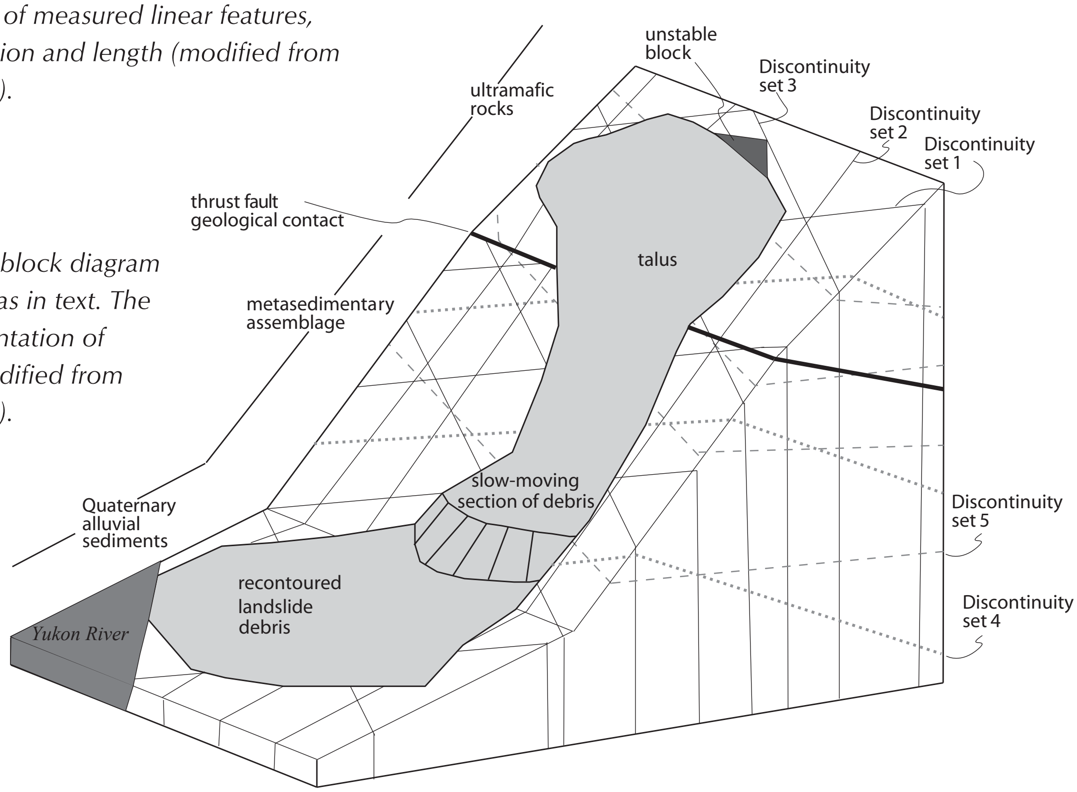

Figure 4. Conceptual block diagram with features labeled as in text. The lines indicate the orientation of discontinuity sets (modified from Brideau et al., in press).

by Green (1972) and deduced to be a horizontal to southerly shallow-dipping brittle shear zone (Mortensen, 1988a,b). Mortensen (1990) interpreted the ultramafic rock to be a tabular sliver thrust from the west or southwest over the metasedimentary-metavolcanic rocks.

Beneath the headscarp, the contact is covered by debris, but on either side of the headscarp, the contact is constrained to within a few metres by outcrops of contrasting lithology. We did not observe any brittle or ductile features attributable to movement on this contact, except that the underlying rock is pervasively strained as described above.

Discontinuity patterns and rock-mass quality was examined and described by Brideau *et al.* (in press). Measurements were made on accessible surfaces facing southwest and south. Five dominant and two subordinate discontinuity sets were recognized in the headscarp (Fig. 6, Table 1,). Discontinuity sets 1, 2 and 3 steeply dip to the southeast, southwest and west, respectively. Discontinuity set 4 dips 40-50° to the northwest. Discontinuity set 5 dips to the southeast at 30-40°, roughly parallel to composition banding in the ultramafic rocks. Discontinuity set 6 dips to the southwest at 60-80°. Discontinuity set 7 is sub-horizontal and therefore has a wide range of dip directions. Figure 4 conceptually illustrates the relationships between the geomorphology, bedrock geology, tectonic contact and orientation of the major discontinuity sets present at the Dawson City landslide.

TALUS

The upper section of the debris (Fig. 4) consists of an 80-m-long talus cone, with a steep slope (at the angle of repose). The talus particle sizes grade from sand and gravel at the top (near the contact with the weathered bedrock headscarp), to boulders up to 50 cm wide at its base. Here the slope gradient becomes gentler and the landslide debris deposit is first evident (i.e., boulders have been in place for a long period based on their lichen cover). Tension cracks 30-40 cm long and 10-20 cm deep are parallel to the contour lines and observed locally in the upper parts of the talus.

LANDSLIDE DEBRIS DEPOSIT

The landslide debris deposit is constricted in the mid-section by rock abutments spaced 100 m apart. The narrow passage provides a 'choke' on downslope movement, separating the 'upper' debris (a rubble field

Figure 5. *Folded metasedimentary rock on the western side of the landslide. See Figure 3 for location.*

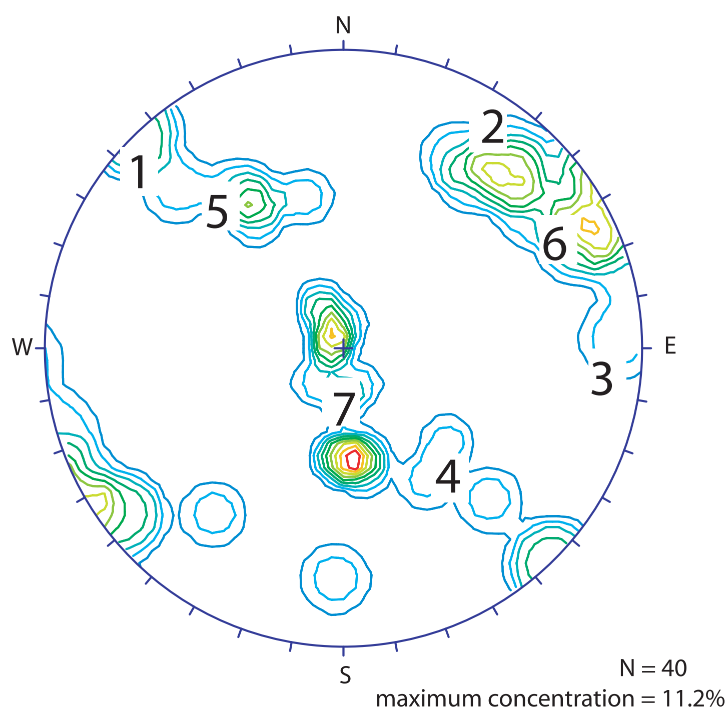

Figure 6. *Contoured stereonet of poles to discontinuity planes in the headscarp. The numbers refer to discontinuity sets discussed in the text (and Table 1 and Fig. 4) and N refers to the number of measurements included in this figure.*

Table 1. Summary orientation and roughness characteristics of discontinuity sets (see text for explanation; from Brideau et al., in press).

Discontinuity set	Dip (°)	Dip direction(°)	Primary roughness	Secondary roughness
1	80-90	130-140	planar	rough
2	80-90	220-230	planar	rough
3	70-80	260-270	planar	rough
4	40-50	330-340	undulating	rough (dominant) smooth (subordinate)
5	30-40	130-140	undulating	smooth
6	60-80	230-240	planar	rough
7	10-30	020-070	planar	smooth

above the constriction) from the 'lower' debris and wider spill area below. The middle to lower section of the landslide deposit consists predominantly of lichen-covered altered ultramafic boulders with an average size of 0.3 x 0.3 x 0.3 m and a maximum size of approximately 1.5 x 1.5 x 1.0 m. The tongue-shaped lower section is characterized by subtle transverse arcuate ridges and longitudinally sheared trenches about 100 m long with stretched roots and split trees spanning them. Localized pockets within the central portion of the middle to lower section of debris expose loose fresh soil. Although tree and shrub cover is sparse on the deposit, their spatial distribution commonly follows geomorphic features such as furrows and trenches (Fig. 7). The snout of this section of the landslide debris is composed of a steep (~40°) face of tan-coloured, less-weathered finer material (sand to gravel-sized) that is actively sloughing (Fig. 8). The steep

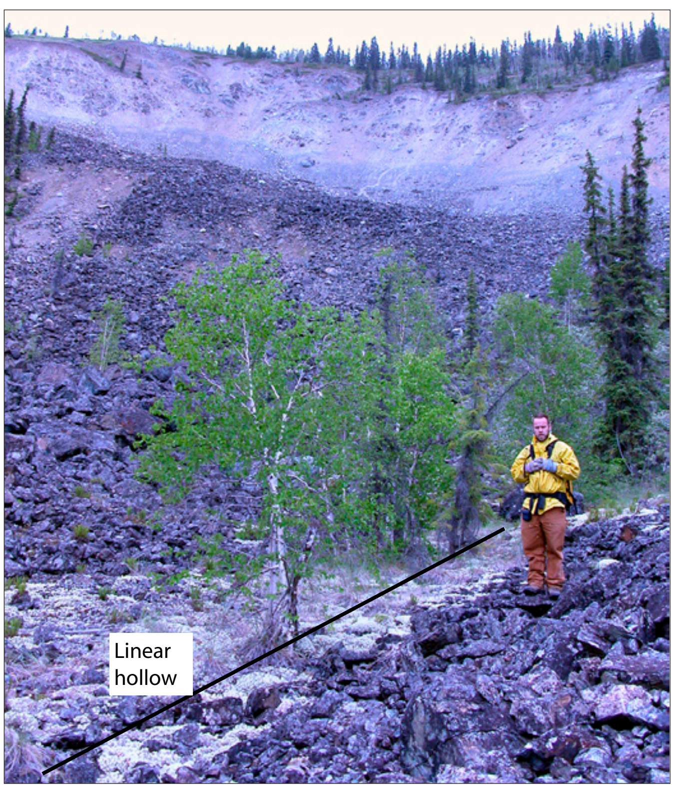

***Figure 7.** View of the eastern edge of the moving section of debris. Note that the trees are preferentially growing in a linear hollow. See location on Figure 3.*

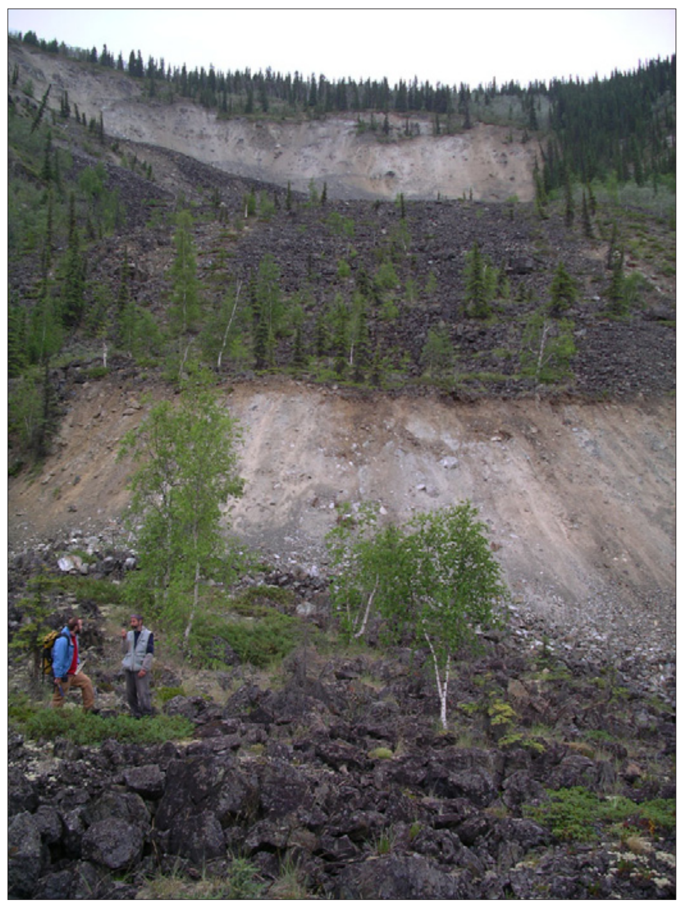

***Figure 8.** Steep snout of the moving section of the landslide debris. It exposes ultramafic gravel and cobbles. Boulder fields above and below have thick lichen cover.*

fresh snout along with the sheared trenches, splitting trees and stretched roots indicate differential motion within the landslide debris (Fig. 4).

The lower section of the landslide debris is accessible from the north end of Front Street. From about 1906 until the 1940s, a level area provided the foundation for the Sisters of St. Ann's Mission, an impressive three-story wooden hospital. During the late 1970s, the back of this level area was excavated to fill in low-lying properties and supply rip-rap for the dyke that protects Dawson City from the Yukon River. The wisdom of increasing the slope of an unstable deposit by excavating the toe was questioned, and the City of Dawson subsequently recontoured the area. The original lobate morphology of this section of debris consisted of concentric compression ridges, as observed in pre-1970 aerial photographs. Further downslope, below the contoured area, the landslide deposit is overgrown with long grass and alder thickets, and the land surface drops steeply into the Yukon River.

LABORATORY TESTS AND ANALYSES

Rock strength

The rock-mass quality was estimated using the Geological Strength Index (GSI) (Hoek and Brown, 1997). The GSI is a quantitative measure of the structure (discontinuities, bedding and schistosity) and surface conditions (roughness, weathering and infillings) of a rock mass (Marinos and Hoek, 2000; Marinos *et al*., 2005). At the Dawson City landslide, 51 GSI estimates were obtained primarily from the headscarp and sidescarp, but also from outcrops on either side of the slope failure. The range of determinations, for both metasedimentary and ultramafic rocks, are encompassed in the shaded areas on Figure 9. The ultramafic rocks exhibit a large variability in rock-mass quality from disintegrated (GSI of 10-20) to very blocky (GSI of 60-70). Recent use of the GSI chart to characterize ultramafic rocks elsewhere in the world also demonstrated large variability in rock-mass quality (Marinos *et al*., 2006). While the discontinuity pattern for both the metasedimentary and ultramafic lithologies are similar, the higher discontinuity intensity and the poorer discontinuity surface conditions of the ultramafic rock result in the lower rock-mass quality values.

Intact rock strength was estimated by performing point load tests on hand samples collected in 2005 and 2006. The samples were cut using a rock saw to the standards outlined by the International Society for Rock Mechanics for the testing of irregular blocks (ISRM, 1985). The results of these tests are presented in Table 2 and compared with published unconfined compressive strength (UCS) values.

Table 2. *Point-load index values and corresponding uniaxial compressive strength estimates obtained from samples collected at the Dawson City landslide and previously published values for serpentinite (UCS = unconfined compressive strength; modified from Brideau et al., in press).*

Lithology	UCS minimum (MPa)	UCS average (MPa)	UCS maximum (MPa)	Reference	Test method
serpentinite	56 (I_{s50} 2.5)	195 (I_{s50} 8.9)	340 (I_{s50} 15.4)	this study	point load
altered serpentinite	NA	45	139	Coumantakis, 1982	uniaxial
fresh serpentinite	NA	95	268	Coumantakis, 1982	uniaxial
serpentinite	17	68	128	Kilic, 1995	uniaxial
serpentinite	34	78	127	Paventi *et al*., 1996	triaxial
serpentinite	17	149	295	Kilic *et al*., 1998	uniaxial
dunite (9% serpentinite)	147	NA	151	Escartin *et al*., 2001	triaxial
serpentinite	NA	66.5	NA	Glawe and Linard, 2003	uniaxial
serpentinite	NA	90 (I_{s50} 4.1)	NA	Glawe and Linard, 2003	point load
serpentinite	74	NA	166	Grasselli, 2006	NA

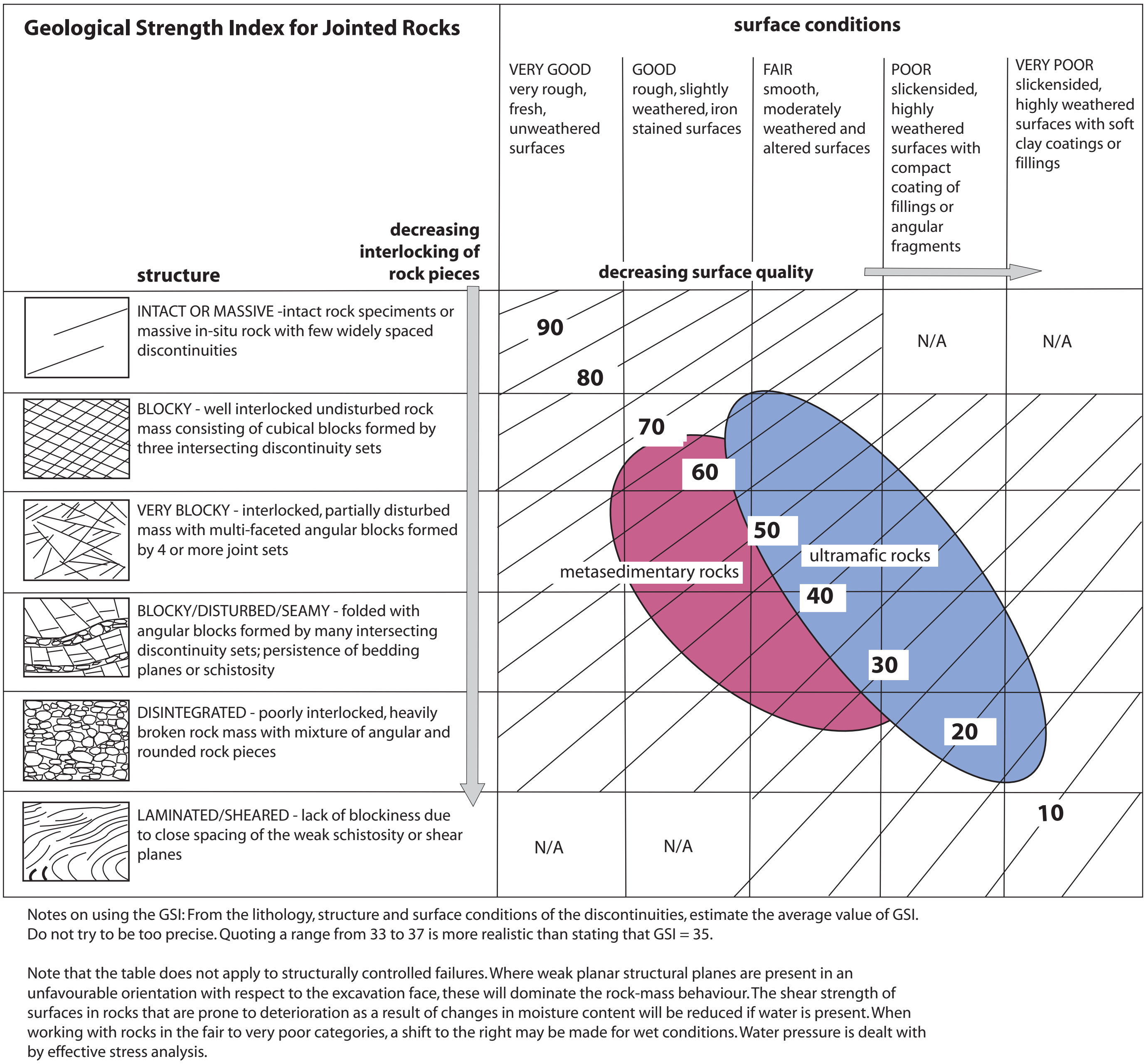

Figure 9. *Range of Geological Strength Index values observed at the Dawson City landslide for the metasedimentary and ultramafic rocks (from Brideau et al., in press).*

Soil material testing

Two samples were collected for preliminary analysis to determine the physical characteristics of the material making up the slow-moving feature. The samples were first sieved to determine the grain-size distribution (Fig. 10). The two samples consisted of 75 and 90% gravel (size range 2-4 cm), respectively, and their grain-size distribution is considered to be within the range of well graded gravel, but close to the boundary of poorly graded gravel (following accepted standards as outlined in Craig, 2004 and British Standard Institute, 1981).

The consistency of the two soil samples was then investigated by determining the liquid and plastic limits of the fine portion which passes through sieve #40 (425 μm) (according to ASTM, 2006). The consistency of remoulded soil varies in proportion to its water content. With high water content, the soil-water mixture behaves as a liquid, while with lower water content it behaves

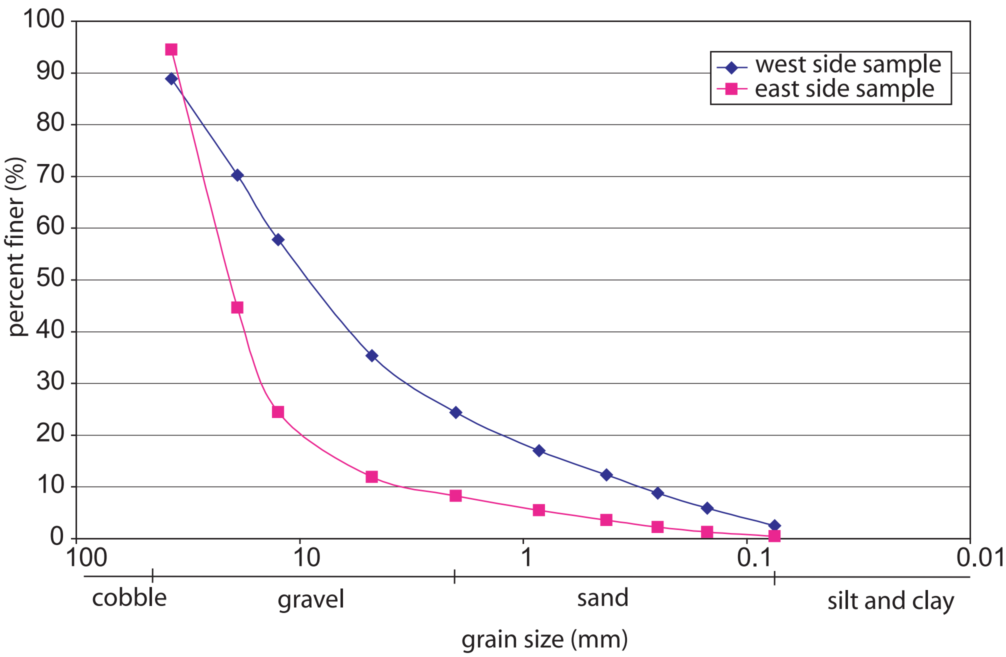

Figure 10. *Grain-size distribution curves of two samples collected from steep snout (see Fig. 6) of the moving landslide debris.*

plastically. With still lower water content, the soil behaves as a semi-solid to solid. The liquid limit is the water content at the boundary between liquid and plastic behaviour of a soil; the plastic limit is the water content at the boundary between plastic and semi-solid behaviour.

For this project, plastic limits of 35.7% (eastern sample) and 37.2% water (western sample) were determined using a standard test (ASTM, 2006), where a thread of soil is rolled on a glass plate. Liquid limits of 79.1% (eastern sample) and 65.7% water (western sample) were determined using the cone penetrometer test. Figure 11 shows plasticity index (liquid limit – plastic limit) versus liquid limits for the two samples as compared to previously published values for earth flows in southern British Columbia (Bovis, 1985).

Such high plastic and liquid limit values are usually associated with smectite clays (the clay mineral group that is composed of pyrophyllite, talc, vermiculite, sauconite, saponite, nontronite and montmorillonite). The weathering of ultramafic rocks, however, commonly produces montmorillonite clay (Wildman *et al*., 1968; Paradis and Simandl, 1996; Yagi *et al*., 1996). Soil moisture has also been found to be important in the weathering of soils derived from serpentinite.

DENDROCHRONOLOGY

Split trees can occur on landslides where a tension crack in the soil underneath or proximal to a tree forces the trunk to split. Roots and trees also continue to grow and compensate for on-going slope deformation; trees tilted

Figure 11. *Plasticity index vs. liquid limit plot for the soil samples collected from the snout of the moving debris at the Dawson City landslide compared with previously published values from Bovis (1985). Soil samples which plot above the A-line have mechanical behaviours dominated by clay while samples that plot below it have mechanical behaviours dominated by silt (British Standard Institute, 1981).*

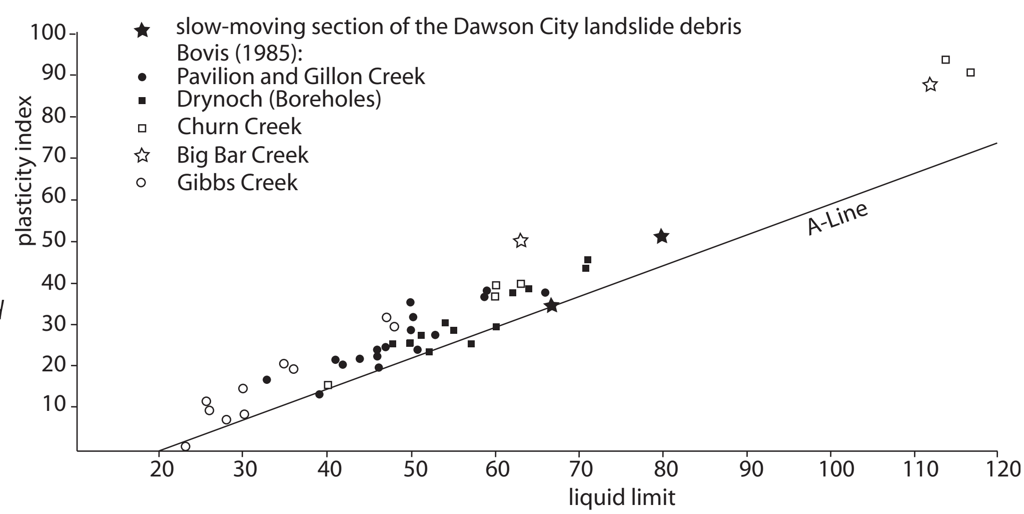

by slope movements produce reaction wood on their downslope side in order to bend vertically again. Since this damage reflects slow and incremental movement (Wilford *et al*., 2005), the study of tree rings may be useful for constraining the age of a mass movement and can also indicate the progression of movement through an area.

Four split trees were examined to determine current movement rates of different portions of the Dawson City landslide. Split trees occur along sheared trenches, parallel to the edge of the middle to lower landslide deposit and above the active headscarp. These trees were cored in July, 2006 and are being examined as part of a larger dendrogeomorphology study on split trees. Tension cracks and trenches were also observed throughout the landslide site. In areas with thick organic soil, stretched roots spanned several tension cracks.

A small birch tree growing near the western margin of the moving section of the landslide debris is of particular interest (Fig. 3). A large root from this tree has been sheared from the trunk, which is now growing 1.9 m downslope of the sheared root (Fig. 12). A core was taken from the tree and indicates that the tree is between 40-45 years old. From this date, it can be interpreted that this portion of the northeast lateral tension crack has moved at least 1.9 m in less than 40 years. This suggests that the moving section of the debris has a minimum average differential movement rate of 4.5 ± 0.25 cm/yr.

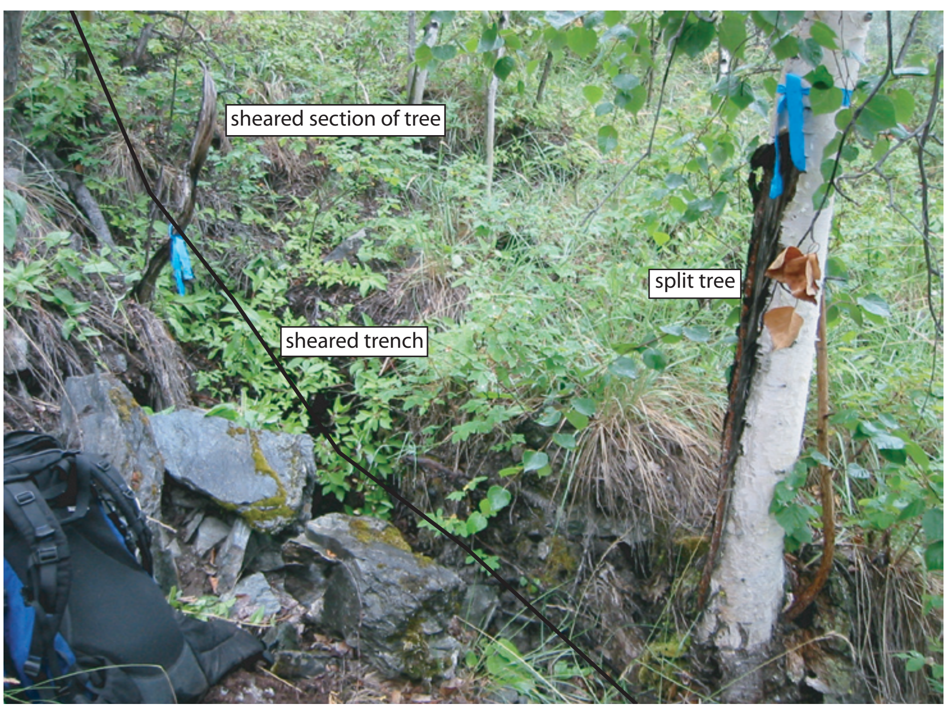

Figure 12. *Split tree that was cored along the western edge of the moving section of the landslide debris.*

MONITORING PROGRAM INITIATED

Several techniques are being attempted to monitor movement rates of the different sections of the Dawson City landslide. Three arrays of stakes (two on the 'stable' side and one on the 'unstable' side) were installed along the tension crack outlining a potentially unstable block above the central portion of the headscarp. A tape measure will be used to periodically measure the distance between the stakes on either side of the tension crack (Fig. 3). This approach should allow estimates of movement rate and direction with a precision of about 1 cm.

On the lower and middle portion of the landslide debris, nine steel survey pins were installed in July, 2006. Their precise locations were measured using a Thales ProMar3-differential Global Positioning System (DGPS), with a field precision of <1 cm. The pins will be resurveyed annually (or more frequently if significant movement is detected) in order to characterize the movement rates and directions of the landslide debris. The locations of the survey pins are shown on Figure 3 and their locations are given in the Appendix 1. As described in the previous section, tree coring of split and bent trees is also being used to estimate movement ages and rates for both the lower landslide debris and the potentially unstable block above the headscarp.

DISCUSSIONS

LANDSLIDE FAILURE MECHANISM

Brideau *et al*. (in press) evaluated the kinematic feasibility of translational sliding, toppling or wedge failure. Our studies found that toppling and sliding are only marginally feasible, and neither of these simple failure modes can explain the geomorphic features and rock-mass characteristics observed at the site. While the intact rock strength of the material varied considerably (as estimated by the point load tests), it is the highly fractured nature of the outcrops (five major and two subordinate discontinuity sets) that results in a weak rock-mass strength. A pseudo-circular failure mechanism is therefore proposed to explain the failure mechanism similar to those generally described in soil slope failure. Numerical modeling using limit equilibrium and finite difference codes suggests that this type of circular failure is only possible with high pore-water pressures, and seismic acceleration.

MECHANISM OF SLOW MOVEMENT IN LANDSLIDE DEBRIS

The question of whether the slowly moving landslide debris should be considered an earth flow or a rock glacier is a challenging one. While several key characteristics that define earth flows and rock glaciers are exhibited in the Dawson City landslide, several others are lacking and there is no intermediate terminology to better describe the movement behaviour.

Rock glaciers are defined by Haeberli *et al*. (2006, p. 190) as "steadily creeping and perennially frozen ice-rich debris on a non-glacierised mountain slope". They usually have a lobate or tongue-shaped appearance extending outwards and downslope from talus cones or from glaciers (Martin and Whalley, 1987; Giardino *et al*., 1987). The fundamental dynamic process of rock glaciers is creep within permafrost (Haeberli *et al*., 2006). Rock glaciers can be talus-fed with further episodic inputs of re-worked clastic material from small debris flow/avalanches (Barsch, 1996).

Earth flows are defined by Hungr *et al*. (2001) as intermittent flow-like movement of plastic clayey earth. A ternary diagram of material making up earth flows presented by those authors reveals that up to 40% per weight can be composed of gravel-sized material. Earth flows in weathered fine-grained sedimentary material (siltstone and shale) and volcanic rocks have been described in southern British Columbia by Bovis (1985) and VanDine (1980). Hungr *et al*. (2001) suggest that a balance exists between material supply (from headscarp retrogression via slumps or falls) and material removal at the toe (from fluvial erosion or by anthropogenic action). They also suggest that pore pressure controls the rate of movement of earth flows.

Table 3 summarizes the key characteristics that are generally associated with earth flows and rock glaciers, and indicates which of them are found at the Dawson City landslide. Several characteristics of the middle to lower section of the debris at the Dawson City landslide are common to both rock glaciers and earth flows, including its elongated lobate shape and presence of sheared trenches and split trees. The presence of the steep snout at the terminus, a boulderly 'carapace'

Table 3. *Summary of characteristics of rock glaciers and earth flows, and evidence for their presence in the moving section of the Dawson City landslide debris (X indicates characteristic feature).*

Characteristics	Rock glacier	Earth flow	Observed in moving section of the landslide deposit in Dawson City
elongated shape with lobate terminus in plan view	X	X	yes
sheared trenches along edge of moving section	X	X	yes
split trees an indication of current state of activity	X	X	yes
ice-rich core	X		no
steep snout at terminus	X		yes
seepage in terminus zone	X		no
boulder 'carapace' overlying gravely diamicton	X		yes
occurrence at low elevation above sea-level		X	yes
occurrence on south-facing slopes	rare	X	yes
grain-size distribution dominated by gravel-size and larger material	X		yes
high plasticity index of fine material	unknown	X	yes

overlying gravelly diamicton, and a grain-size distribution dominated by gravel-size and larger material supports the rock glacier classification. However, the lack of an ice-rich core and seepage in the terminus zone, as well as the south-facing aspect and low elevation, provides more support for the earth flow classification. At this early stage in our investigations it is difficult to decide which classification is more dominant, but our field observations slightly favour a rock glacier interpretation.

CONCLUSIONS

The Dawson City landslide occurred predominantly in altered ultramafic rock that is heavily fractured with five dominant and two subordinate discontinuity sets. While the intact strength of the rock, as evaluated from point load tests, varies considerably its average value still corresponds to a strong rock. The fractured nature of the outcrop has reduced rock-mass strength, and led to probable pseudo-rotational failure.

Geomorphic evidence indicates that the middle to lower section of the landslide debris is currently moving. Preliminary dendrochonology results suggest that the minimum average movement rate is on the order of 4.5 cm/year. The moving debris exhibits traits common to both earth flows and rock glaciers. An array of survey pins was installed in July, 2006 to monitor and quantify movement of both the middle to lower portion of the debris and a potentially unstable mass of rock above the headscarp.

ACKNOWLEDGEMENTS

The authors would like to thank K. Fecova and E. Trochim for their assistance in the field, and G. Patton and A. Wolter for their assistance with the preparation and testing of the rock and soil samples. Discussions with J. Orwin regarding rock glaciers and J. Koch on dendrochronology are gratefully acknowledged. B. Ward is thanked for his constructive comments on the manuscript. This research was supported by the Northern Scientific Training Program, Natural Science and Engineering Research Council of Canada, Yukon Geological Survey and Yukon Geomatics.

REFERENCES

ASTM, 2006. Standard Test Methods for Liquid Limit, Plastic Limit, and Plasticity Index of Soils, Annual Book of ASTM Standards: Volume 4 - Construction Section 8 Soil and Rock (I). American Society for Testing and Materials, p. D 4318-05.

Barsch, D., 1996. Rock glaciers. Indicators for the present and former geoecology in high mountain environments. Springer, Berlin, Germany, 331 p.

Bond, J.D. and Sanborn, P.T., 2006. Morphology and geochemistry of soils formed on colluviated weathered bedrock: Case studies from unglaciated upland slopes in west-central Yukon. Yukon Geological Survey, Open File, 2006-19, 70 p.

Bovis, M.J., 1985. Earthflows in the Interior Plateau, southwest British Columbia. Canadian Geotechnical Journal, vol. 22, p. 313-334.

Brand, M., 2002. Archaeological investigations of transient residences on the hillsides surrounding Dawson City, Yukon. Occasional Papers in Archaeology, 12. Yukon Tourism, Heritage Branch, Whitehorse, Yukon, 202 p.

Brideau, M.-A., Stead, D., Roots, C. and Orwin, J., in press. Geomorphology and engineering geology of a landslide in ultramafic rocks, Dawson City, Yukon. Engineering Geology.

British Standard Institute, 1981. Description of soils and rocks, BS 5930. *In:* Code of Practice for Site Investigations, BSI Group, England.

Colpron, M. (compiler), 2006. Tectonic assemblage map of Yukon-Tanana and related terranes in Yukon and northern British Columbia (1:1 000 000 scale). Yukon Geological Survey, Open File 2006-1.

Coumantakis, J., 1982. Comportement des péridotites et des serpentinites de la Grèce en travaux publics et leurs propriétés physiques et mécaniques. Bulletin of the International Association of Engineering Geology, vol. 25, p. 53-60.

Craig, R.F., 2004. Craig's soil mechanics 7th Edition. Spon Press, New York, N.Y., 447 p.

Duk-Rodkin, A., 1996. Surficial geology, Dawson, Yukon Territory. Geological Survey of Canada Open File 3288, 1:250 000 scale.

Escartin, J., Hirth, G. and Evans, B., 2001. Strength of slightly serpentinized peridotites: Implications for the tectonics of the oceanic lithosphere. Geology, vol. 29, no. 11, p. 1023-1026.

Froese, D.G., Duk-Rodkin, A. and Bond, J.D. (eds.), 2001. Field guide to the Quaternary research in the central and western Yukon Territory, CANQUA 2001. Occasional Papers in Earth Sciences No. 2, Heritage Branch, Government of Yukon, 102 p.

Froese, D.G., Barendregt, R.W., Enkin, R.J. and Baker, J., 2000. Paleomagnetic evidence for multiple Late Pliocene - Early Pleistocene glaciations in the Klondike area, Yukon Territory. Canadian Journal of Earth Sciences, vol. 37, p. 863-877.

Giardino, J.R., Shroder, J.F. and Vitek, J.D., 1987. Rock glaciers. Allen and Unwin, England, 416 p.

Glawe, U. and Linard, J., 2003. High concrete dam on serpentinite. Quarterly Journal of Engineering Geology and Hydrogeology, vol. 36, p. 273-285.

Grasselli, G., 2006. Shear strength of rock joints based on quantified surface description. Rock Mechanics and Rock Engineering, vol. 39, no. 4, p. 295-314.

Green, L.H., 1972. Geology of Nash Creek, Larsen Creek, and Dawson Map-areas, Yukon Territory. Geological Survey of Canada, Memoir 364, 157 p.

Haeberli, W., Hallet, B., Arenson, L., Elconin, R., Humlum, O., Kaab, A., Kaufmann, V., Ladanyi, B., Matsuoka, N., Springman, S. and Muhll, D.V., 2006. Permafrost creep and rock glacier dynamics. Permafrost and Periglacial Processes, vol. 17, p. 189-214.

Hoek, E. and Brown, E.T., 1997. Practical estimates of rock mass strength. International Journal of Rock Mechanics and Mining Sciences, vol. 34, no. 8, p. 1165-1186.

Hungr, O., Evans, S.G., Bovis, M.J. and Hutchinson, J.N., 2001. A review of the classification of landslides and flow type. Environmental and Engineering Geoscience, vol. VII, no. 3, p. 221-238.

ISRM, 1985. Suggested method for determining point load strength. International Journal of Rock Mechanics, Mining Sciences and Geomechanic Abstract, vol. 22, p. 51-60.

Kilic, R., 1995. Geomechanical properties of the ophiolites (Cankiri/Turkey) and alteration degree of diabase. Bulletin of the International Association of Engineering Geology, vol. 51, p. 63-69.

Kilic, R., Kocbay, A. and Sel, T., 1998. The geomechanical properties and alteration degree of serpentinite in the Ankara Ophiolitic Melange, Turkey. *In:* 8th International IAEG Congress, O. Hungr and E. Moore (eds.), Balkema Rotterdam, p. 243-251.

Marinos, P. and Hoek, E., 2000. GSI: A geologically friendly tool for rock mass strength estimation. GEOENG 2000, Melbourne, Australia. CD-ROM.

Marinos, P., Hoek, E. and Marinos, V., 2006. Variability of the engineering properties of rock masses quantified by the geological strength index: The case of ophiolites with special emphasis on tunnelling. Bulletin of Engineering Geology and the Environment, vol. 65, no. 2, p. 129-142.

Marinos, V., Marinos, P. and Hoek, E., 2005. The Geological Strength Index: Applications and limitations. Bulletin of Engineering Geology and the Environment, vol. 64, p. 55-65.

Martin, E.H. and Whalley, W.D., 1987. Rock glaciers, Part 1: rock glacier morphology: classification and distribution. Progress in Physical Geography, vol. 11, p. 261-282.

Mortensen, J.K., 1988a. Geology, southwest Dawson map area, Yukon. Geological Survey of Canada, Open File 1927, 1:250 000 scale.

Mortensen, J.K., 1988b. Geology of southwestern Dawson Map Area, Yukon Territory. Geological Survey of Canada, Current Research, 88-1E, p. 73-78.

Mortensen, J.K., 1990. Geology and U-Pb geochronology of the Klondike District, west-central Yukon Territory. Canadian Journal of Earth Sciences, vol. 27, p. 903-914.

Paradis, S. and Simandl, G.J., 1996. Cryptocrystalline ultramafic-hosted magnesite veins in selected British Columbia mineral deposit profiles, Volume 2 - Metallic Deposits, D.V. Lefebure and T. Hõy (eds.), British Columbia Ministry of Employment and Investment, Open File 1996-13, p. 97-100.

Paventi, M., Scoble, M. and Stead, D., 1996. Characteristics of a complex serpentinized ultramafic rock mass at the Birchtree Mine, Manitoba. *In:* Rock Mechanics, Proceedings of the 2nd North American Rock Mechanics Symposium, M. Aubertin, F. Hassani and H. Mitri (eds.), p. 339-346.

Thomas Heritage Consulting, 2005. Heritage resource impact assessment for proposed Dawson Bridge. Final Report to Transportation and Engineering Branch, Department of Highways and Public Works, Government of Yukon, 22 p.

Tyrrell, J.B., 1910. "Rock glaciers" or chrystocrenes. Journal of Geology, vol. 18, p. 549-553.

VanDine, D.F., 1980. Engineering geology and geotechnical study of Drynoch Landslide, British Columbia. Geological Survey of Canada Paper 79-31, 34 p.

Wahl, H.E., Fraser, D.B., Harvey, R.C. and Maxwell, J.B., 1987. Climate of Yukon. Climatological Studies Number 40. Atmospheric Environment Service, Environment Canada, 323 p.

Wildman, W.E., Jackson, M.L. and Whittig, L.D., 1968. Iron-rich montmorillonite formation in soils derived from serpentinite. Soil Science Society American Journal, vol. 32, p. 787–794.

Wilford, D.J., Cherubini, P. and Sakals, M.E., 2005. Dendroecology: a guide for using trees to date geomorphic and hydrologic events. British Columbia Ministry of Forests, Research Branch, Victoria, B.C., Land Management Handbook no. 58, 20 p.

Yagi, N., Yatabe, R., Yokota, K. and Mukaitani, M., 1996. A case study of failure of cut slope consisting of weathered serpentine. *In:* Landslides, J. Chacon, C. Irigaray and T. Fernandez (eds.), Balkema, Rotterdam, p. 307-319.

Yukon Ecoregions Working Group, 2004. Klondike Plateau Ecoregion. *In:* Ecoregions of the Yukon Territory: Biophysical properties of Yukon landscapes, C.A.S. Smith, J.C. Meikle and C.F. Roots (eds.), Agriculture and Agri-Food Canada, PARC Technical Bulletin No. 04-01, Summerland, British Columbia, p. 159-168.

Appendix 1. *Moosehide Slide Monitoring Network (July 26, 2006).*

Site No.	Occupation time (min)	Comments/Location	Easting	Northing	Elevation
			UTM Zone 7, NAD83		(m)
Moosehide Slide Differential GPS survey					
Dyke Bench Mark	32	NRCAN bench mark on dyke at south end of town	576126.770	7103962.889	334.426
Base Station	9 hrs 15 min	existing benchmark on dyke, at ferry landing	576735.886	7105541.625	333.434
MAB-06-18-1	30	rebar post in contoured debris	576937.413	7105781.203	361.822
MAB-06-18-2	21	rebar post in contoured debris	576976.878	7105809.586	373.597
MAB-06-18-3	24	rebar post at top of freshly exposed debris train toe	577096.079	7105900.851	399.512
MAB-06-18-4	18	rebar post on south flank near debris train toe	577119.580	7105874.333	405.826
MAB-06-18-5	26	rebar post halfway up debris train on south side	577158.807	7105888.599	428.911
MAB-06-18-6	32	rebar post in upper debris train, north flank	577172.752	7105914.620	441.403
MAB-06-18-7	28	wooden post in loose heaved material (significant fines)	577204.986	7105935.453	462.515
MAB-06-18-8	22	rebar post in stable levee on south flank	577235.723	7105913.771	467.829
MAB-06-18-9	25	rebar post on south flank, near fresh trench and split tree	577186.408	7105891.336	444.296
Handheld GPS coordinates					
MAB-06-18-10		1st crack monitoring site - big split spruce tree	577495	7106006	
MAB-06-18-11		2nd crack monitoring site - scarp about 1.5 m high	577493	7106012	
MAB-06-18-12		3rd crack monitoring site - scarp about 80 cm high	577486	7106033	

Developing a new method to identify previously unrecognized geochemical and morphological complexity in placer gold deposits in western Yukon

***Evan C. Crawford*[1]**
Earth and Ocean Sciences, University of British Columbia[2]

Robert K. Chapman
School of Earth and Environment, University of Leeds[3]

***William P. LeBarge*[4]**
Yukon Geological Survey

***James K. Mortensen*[5]**
Earth and Ocean Sciences, University of British Columbia[2]

Crawford, E.C., Chapman, R.K., LeBarge, W.P. and Mortensen, J.K., 2007. Developing a new method to identify previously unrecognized geochemical and morphological complexity in placer gold deposits in western Yukon. *In:* Yukon Exploration and Geology 2006, D.S. Emond, L.L. Lewis and L.H. Weston (eds.), Yukon Geological Survey, p. 139-148.

ABSTRACT

Placer gold has been, and is, a notable resource in the western Yukon; however, identification of the lode sources feeding these placer deposits has been difficult. Previous studies have used electron microprobe (EMP) and manual morphological analyses of gold grains with some success to define source-mineralization-style areas, but have not been able to accurately predict lode locations. This study utilizes EMP in conjunction with a new method for morphological analysis based on semi-automated digital image analysis to re-examine this problem. Examination of a sample suite collected over the entire Klondike goldfields area demonstrates that there is significant complexity in Yukon placer gold deposits that has not previously been recognized. Confronting this complexity using a statistical approach based on this new shape analysis method, EMP and a planned future laser ablation mass spectroscopy study will hopefully produce a method for locating lode gold sources.

RÉSUMÉ

L'or placérien a été et reste encore une ressource appréciable au Yukon occidental; cependant l'identification des sources filoniennes alimentant ces dépôts placériens s'est avérée difficile. Dans des études antérieures on a utilisé avec un certain succès des analyses à la microsonde électronique (MÉ) et des analyses morphologiques manuelles pour définir des styles de régions minéralisées d'origine, mais ces études n'ont pas permis de prévoir avec exactitude les emplacements des gîtes filoniens. Dans le cadre de la présente étude, la MÉ est utilisée avec une nouvelle méthode d'analyse morphologique basée sur une analyse semi-automatisée d'images numériques comme nouvelle approche pour la solution de ce problème. L'examen d'un ensemble d'échantillons recueillis sur toute la région des champs aurifères du Klondike démontre une grande complexité jusqu'à maintenant insoupçonnée des gisements d'or placérien au Yukon. On espère que le fait d'aborder cette complexité par une approche statistique fondée sur cette nouvelle méthode d'analyse morphologique utilisée avec la MÉ dans le cadre d'une étude projetée des échantillons traités par ablation au laser et spectrométrie de masse fournira une méthode de localisation des sources d'or filonien.

[1]*ecrawfor@eos.ubc.ca*
[2]*6339 Stores Road, Vancouver, British Columbia, Canada, V6T 1Z4*
[3]*Leeds, United Kingdom, LS2 9JT*
[4]*bill.lebarge@gov.yk.ca*
[5]*jmortens@eos.ubc.ca*

INTRODUCTION

The composition of placer gold grains has been analysed in many studies to establish geochemical 'fingerprints' of gold from specific lode sources worldwide (e.g., Mortensen *et al.*, 2004; Grigorova *et al.*, 1998; Watling *et al.*, 1994). Placer gold grains have also been noted to change systematically with the distance travelled from the lode source, and several studies (e.g., Townley *et al.*, 2003; Knight *et al.*, 1999a; Youngson and Craw, 1999; Loen, 1995; Knight *et al.*, 1994) have attempted to develop variation curves between grain shape and the distance specific grains have travelled. Such a relationship could provide important constraints for identifying the most likely source location for gold from specific placer deposits.

Previous morphological studies of placer gold have followed the general procedure of identifying and measuring a morphological parameter of selected gold grains, estimating the distance those grains had travelled, and then trying to develop a model for the evolution of grain shape (proxied by the parameter) over distance. These methods are oversimplified in that they do not take into account the possibility of polymodality in the parameter. If a sample is polymodal, the use of an average parameter value for a sample to generate a model can have serious ramifications. For example, in a sample with two populations of equal proportions, the average value of the parameter for that sample may be a value which none of the grains individually record. Another limiting factor of previous morphological studies is that they have not attempted to correlate morphological parameters with other available data such as composition. While it has not yet been determined if composition plays a role in shape development (e.g., grains of differing alloy composition will vary in hardness and therefore deform differently during transport), assuming it does not may lead to erroneous conclusions.

Another problem faced when interpreting these data sets is visualizing the data. There is no standard parameter used to characterize gold grain shape evolution, nor any standard method of presenting the data. Although useful for comparing a few samples, many of the methods used in the literature become incomprehensible when applied to the increasingly large data sets that can now be easily generated using new computerized image analysis methods such as are discussed in this contribution.

Kernel density analysis provides a solution to many of the problems previously mentioned. It reduces all of the measurements on a sample to a single curve which accurately retains and easily presents the information available from those measurements. The shape of these curves allows for plots of multiple data sets to remain legible. Extending the analysis into two dimensions produces a 3D surface plot that allows for easy identification of the relationships between paired data, the contributing populations present, as well as the shape, location and relative contributions of those populations.

This contribution reports the preliminary results obtained from the application of a new semi-automated method for the objective measurement of morphological information on placer gold samples from a number of drainages within the Klondike District of western Yukon. It also presents the novel results that can be extracted from the data using one and two dimensional kernel density analysis with a case example. This method is currently being expanded to a much larger sample suite, and will hopefully yield new insights on the behaviour of gold in the alluvial environment.

PREVIOUS WORK

There have been many previous studies that investigated the evolution of gold grain shape with alluvial transport (Márquez-Zavalía *et al.*, 2004; Wierchowiec, 2002, and previously mentioned works). A number of these studies have utilized semi-quantitative or qualitative parameters, which, although easy to measure, are overly susceptible to operator bias, and their use will not be discussed further. Fully quantitative studies have generally been limited in scope, due to the amount of labour previously required to measure each grain manually. They are also limited in that only a few basic measurements (minor, intermediate and major axis lengths) can be reliably made in this fashion. Parameters that have been used which incorporate measurements of all three axes include the Cailleux flatness index (Cailleux, 1945) and the Corey (Corey, 1949) and Zingg (Zingg, 1935) parameters. Other previously used morphological parameters include roundness, flatness, rim thickness, and percentage of rimmed grains. Analysis of these measurements has generally been limited to plotting parameter values against distance, or using x,y plots to try to correlate between parameters (e.g., Knight *et al.*, 1999a; Youngson and Craw, 1999).

Extensive gold compositional studies have also been carried out (Mackenzie and Craw, 2005; Chapman *et al.*, 2000; Knight *et al.*, 1999b; Leake *et al.*, 1998; Loen, 1994);

however, no attempt has been made previously to link the compositions of individual grains to the shape parameters measured for those grains. The almost universally utilized method is electron microprobe analysis (EMP), which is generally restricted to the quantification of major and some minor elements (Au, Ag, Cu and Hg) that are present in sufficient concentrations to be measured reliably. Analysis of the compositional data obtained has typically been constrained to determining average concentrations for a sample, or plotting one concentration value against another.

COMPUTERIZED IMAGE ANALYSIS

Until now, quantitative shape measurements of placer gold grains has required manual measurement using a light or electron microscope. This method is slow, labour intensive and subject to operator bias. It is also restrictive in that it is difficult to record any measurements excluding the three major axis lengths.

The use of digital image analysis in this study has dramatically improved the speed and objectivity of grain analysis. ImageJ (a java implementation of NIHImage) is a freeware image analysis program that can be customized by the addition of user-generated macros. A new macro was developed specifically for morphological characterization of placer gold using this program. The new macro combines built-in features of ImageJ with several other open source macros, and has some novel capabilities. This macro allows for the simple and quick quantitative morphological characterization of large sample suites.

Although it would be ideal to record and digitize the entire 3D physical shape of every grain, then extract the desired parameters from the digital model, developing a method of that type was beyond the scope of this project. Instead, two perpendicularly oriented 2D images of every grain down the long or intermediate and short axes were collected, allowing for three-dimensional information on the grains to be determined. The macro developed for this purpose measured the feret and breadth, area, perimeter, convex area, convex perimeter, largest inscribed circle radius and smallest circumscribing circle radius on each bisecting image. Then it performed a fourier analysis on the outline shape. At present, only the feret and breadth measurements are used to obtain short, intermediate and long axis lengths for each grain.

The method is mentioned briefly here because it has allowed the generation of large morphological data sets. These data sets, along with other data recorded on placer gold grains, provide interesting insight on the study of placer gold. More than 7500 grains from 53 locations have been analysed using this program thus far, as compared to the most extensive previous quantitative morphological study in the literature which measured only the three axis lengths on 1502 grains from 60 locations (Townley *et al.*, 2003). This study uses the Hofmann (Hofmann, 1994) shape parameter (or Hofmann shape entropy) as the primary descriptor of shape. Unpublished ongoing studies by the authors indicate that this parameter will be the most useful for quantifying the evolution of shape with transport. The form of the parameter is given by equation 1.

KERNEL DENSITY ANALYSIS

Kernel density analysis (KDA, also known as kernel density estimation or the Parzen window method; Parzen, 1962) is a way to calculate a probability density function for a variable in a population from a number of measurements made on the variable. The equation for a kernel density analysis using a normal distribution kernel is given by equation 2.

For this study, Silverman's rule of thumb (Silverman, 1986) for bandwidths provides an objective method for selecting bandwidths. The calculation for the bandwidth is the minimum of the standard deviation and the interquartile range divided by 1.34, multiplied by 0.9, and

$$H = \frac{-1}{1.0986}\left(\frac{l \times \ln\left(\frac{l}{l+i+s}\right)}{l+i+s} + \frac{i \times \ln\left(\frac{i}{l+i+s}\right)}{l+i+s} + \frac{s \times \ln\left(\frac{s}{l+i+s}\right)}{l+i+s}\right)$$

Equation 1. *The Hofmann shape parameter. l, i and s are the lengths of the long, intermediate and short axes, respectively.*

$$p_x = \sum_{0}^{n} N(o_n, w, x)$$

Equation 2. *The 1D kernel density estimation:* p_x *is the probability of a randomly sampled member of the population having the value x, N is a normal distribution function with a mean* o_n *(the observed values for the parameter) and standard deviation or bandwidth w evaluated at value x, summed over all observations n.*

divided by the number of observations to the one fifth power. Since the choice of bandwidth can have a significant impact on the results of the analysis, it is necessary to have specific criteria for selecting bandwidth values instead of just subjectively choosing values.

The KDA method can be also extended to multiple dimensions to examine relationships between variables, and generate probability distribution functions for those relationships.

CASE STUDY

A sample of placer gold grains (n=54; sample number EC-06) was recovered by hand panning from a location near Fox Gulch in the Klondike placer district in western Yukon (63°57'N, 139°21'W). After drying and hand picking, the grains were mounted on packing tape and imaged for analysis using the previously mentioned computerized image analysis method. The grains were then transferred to a conductive tape mount and examined by scanning electron microscopy (SEM) – backscattered (BS) and secondary electron (SE). Subsequently, the grains were mounted in epoxy, ground down and polished to expose a section roughly bisecting the grain along the major axis. After carbon coating the mounts, images of the cross-sections were recorded using SEM (BS only), and the major element composition (Au, Ag, Hg and Cu) of the core of the grains was determined by EMPA. Individual grains were tracked with unique identification numbers through all steps to allow for correlation of results.

ONE DIMENSIONAL KDA

The kernel density estimation method was applied to the data for sample EC-06; the results of those analyses are shown in Figures 1 and 2. In stark comparison to the methods used in previously published studies, these plots clearly show that the data is at least bimodal in both cases, and likely even more complex. The smooth curve and the ease of locating relative maxima makes plots of multiple samples much more readable when compared to plots of multiple samples using the cumulative percentage method.

After the KDA has been performed, the next step is to identify all of the component populations in a sample. To accomplish this, a number of normal distributions are generated and summed. The parameters (mean, standard deviation and relative weighting) of the individual

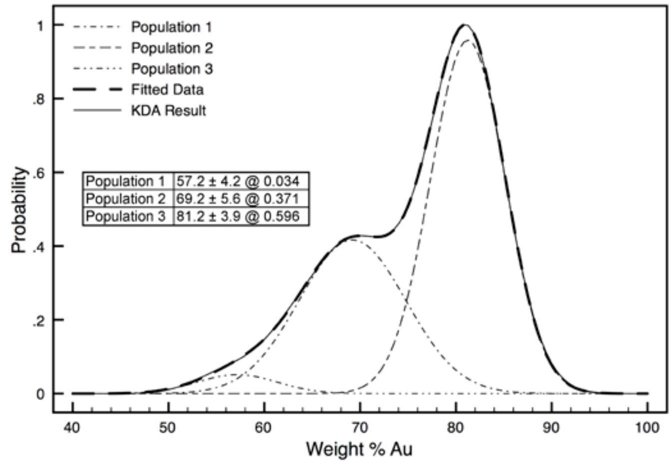

Figure 1. *One-dimensional KDA output, and fitted component populations for wt% Au data on sample EC-06. Included table contains the following parameters: mean, standard deviation and relative weighting for each identified peak.*

distributions are then modified to minimize the difference between the summed curve and the curve calculated from the data. Assuming a good fit to the data is achieved, the parameters of those fitted distributions then provide information on the parameter values for the component populations in the sample. This method is far superior to previous methods of data analysis because it allows quantitative objective information on the parameters of interest to be recovered. It is also a vast improvement over using simple arithmetic means. The arithmetic means for sample EC-06 are 76.0 ± 7.6 for wt% Au and 0.897 ± 0.051 for the Hofmann shape parameter; the KDA shows that in neither case does the arithmetic mean correctly identify a component population (Figs. 1 and 2).

A visual examination of the KDA results (Figs. 1 and 2) clearly indicates that for both cases (wt% Au and the Hofmann shape parameter), the sample contains at least two component populations. Fitting the data to identify those populations reveals that in both cases there are three populations; it also returns the parameter values for those populations.

This analysis has been applied to a number of samples from the Klondike District, and has revealed significant complexity not previously recognized in samples. Furthermore, qualitative examination confirms consistent trends in the Hofmann shape parameter during alluvial transport (Fig. 3), suggesting that the development of a predictive model for the evolution of gold grain shape will be possible.

A preliminary shape evolution curve has been created using the fitted peak locations from the 1D analysis, using data from samples known distances apart or for which the distance to the lode source is known with a high level of confidence (Fig. 4).

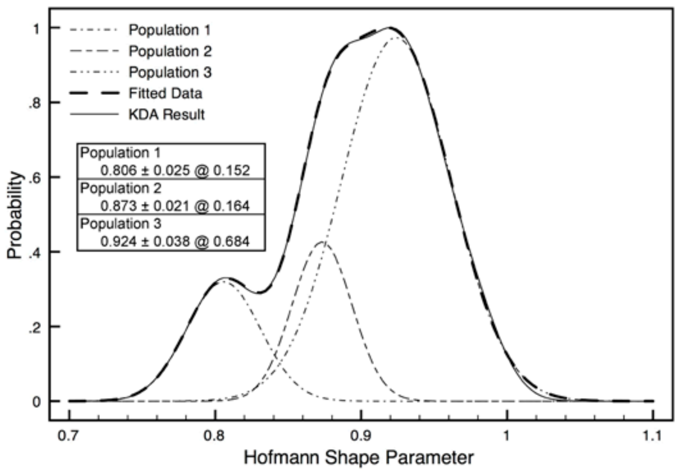

Figure 2. *One-dimensional KDA output, and fitted component populations for Hofmann shape parameter data on EC-06. Included table contains the following parameters: mean, standard deviation and relative weighting for each identified peak.*

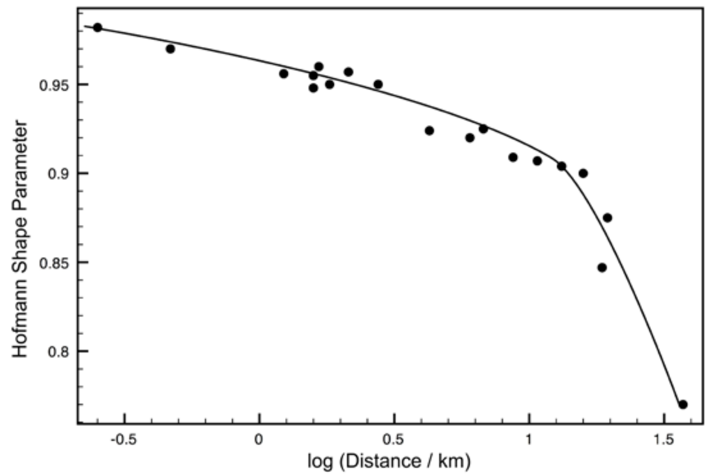

Figure 4. *A preliminary shape evolution curve for placer gold from the Klondike placer district.*

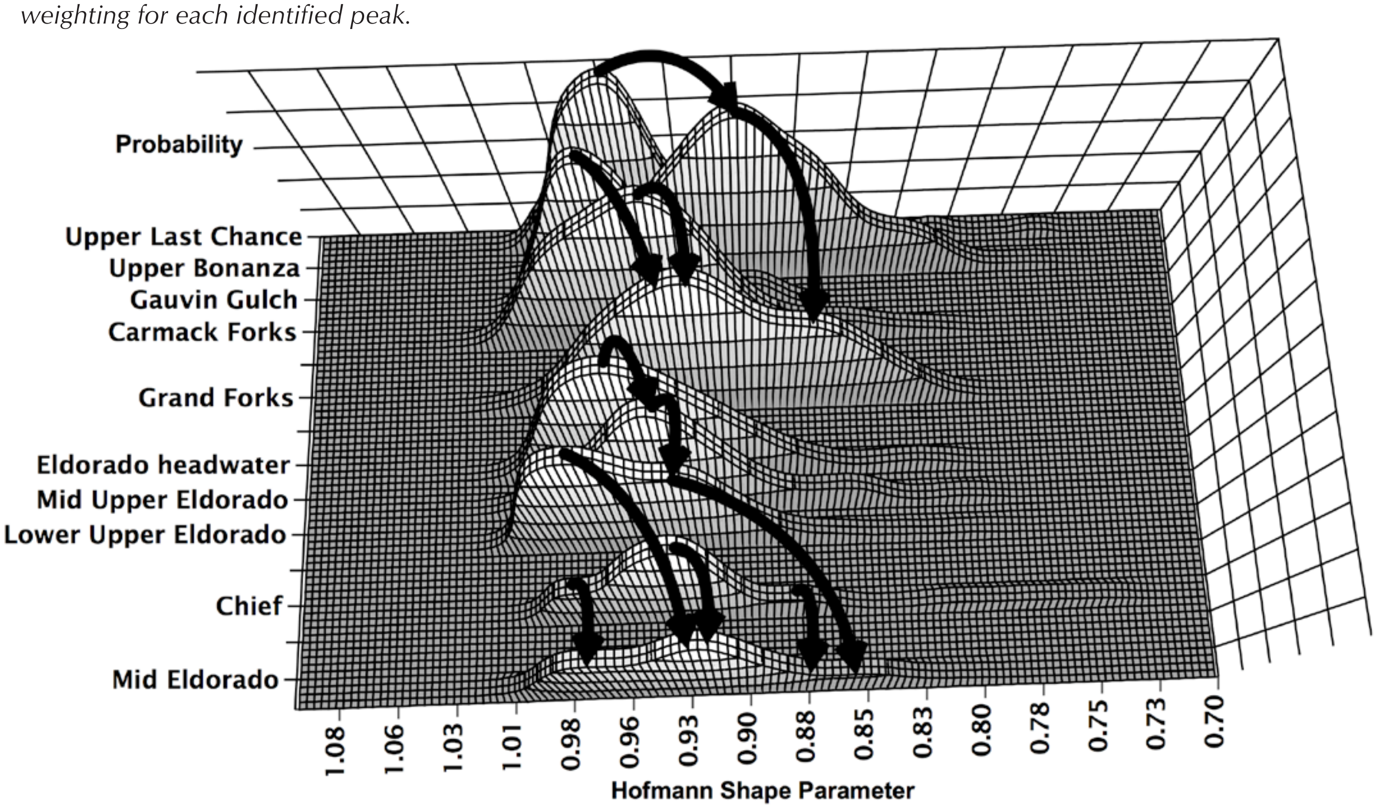

Figure 3. *Probability density plots of the Hofmann shape parameter for samples progressing down two drainage systems in the Klondike District. Five samples each from the two drainages are shown, with arrows indicating quantitatively identified evolution paths for grain populations with downstream transport.*

This shape evolution curve allows for prediction of distance to source; however, there is still significant scatter in the data, and the accuracy of the curve is uncertain. Several source types for Klondike placer gold are known, and it is likely that each source will have a different initial shape. Further complicating the issue is that each source has a different major element alloy composition, potentially resulting in different malleability, and hence a different rate of shape evolution during alluvial transport.

If the average composition of each grain-shape population were known, it would be possible to model many of these complications and eliminate much of the scatter. If identical numbers of populations were found from both the Hofmann and composition 1D analyses, and the relative weights of those populations were identical, then those populations would likely be identical. In this example, however, it is clear that this is not the case, so there is still confusion and an inability to determine both the Hofmann shape parameter and wt% Au values for individual populations. Fortunately, it is possible to extend the KDA into two dimensions and recover this information.

TWO DIMENSIONAL KDA

The traditional method for identifying correlation between variables is to plot results on an x,y plot and look for continuous relationships or groupings of data. This method works well when there are few or very distinct populations, but tends to be of decreased utility with more broadly distributed observations or when objective quantitative information is desired. There is no standardized method for visualizing paired data from placer gold (i.e., isochron diagrams in geochronology, or the many plots used to define geochemical composition fields, e.g., TAS plots). Since placer gold data tends to be broadly distributed, and quantitative information is desired from this analysis, two-dimensional KDA provides an excellent method for examining the available data in this case.

The method for performing a two-dimensional kernel density analysis is directly analogous to the one dimensional case. The formula for a 2D KDA is given by equation 3.

As with the 1D results, it is possible to fit a series of normal distributions to the KDA result obtained, and thus identify the populations present in a sample.

$$p_{x,y} = \sum_{0}^{n} N(o_{n_x}, w_x, x) \times N(o_{n_y}, w_y, y)$$

Equation 3. *The 2D kernel density estimation: $p_{x,y}$ is the probability of a randomly sampled member of the populations having the values x,y. n is the number of paired x,y data, N is the normal distribution function, evaluated using means of o_{n_x} and o_{n_y} which are the x and y observations for each pair and using standard deviations w_x and w_y which are the bandwidths for those variables.*

This method does suffer in that the output generated is a probability surface, and must therefore be viewed in 3D, making it difficult to display data from several samples in a single plot. However, the benefit of identifying the locations and distribution parameters of the component populations in a sample greatly outweighs this downside.

With the 2D KDA method, it would be possible to obtain an exact fit to the KDA results if one fitted the same number of populations as data points used to perform the KDA. It is vital that the number of populations chosen should have some kind of geological reasoning. For example, a sample collected near the top of a drainage should be expected to contain only a few contributing sources, whereas a major tributary draining a large area is much more likely to have more contributors.

Figure 5 shows a traditional x,y plot of the EC-06 data for comparison, and Figure 6 shows the two-dimensional KDA result. Six peaks were fitted to the KDA results; the summed results are presented in Figure 7, and the individual fitted component peaks are shown in Figure 8. All plots also show the projection of the 3D surface onto

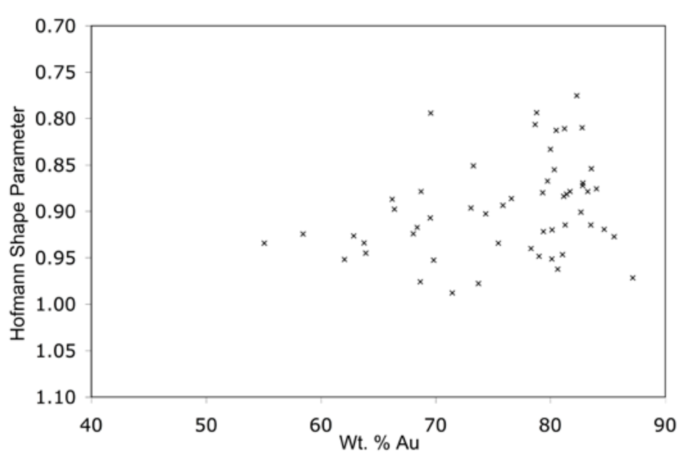

Figure 5. *An x,y plot of the data for EC-06.*

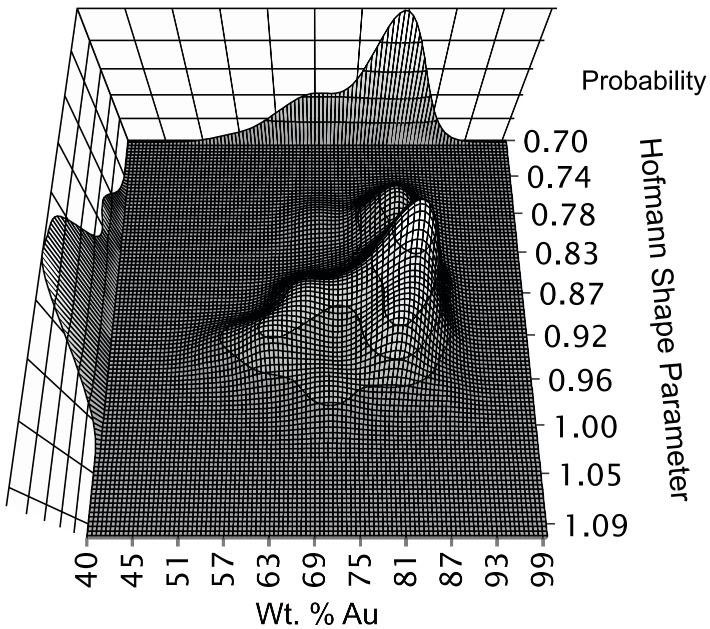

Figure 6. *Two-dimensional KDA results for sample EC-06.*

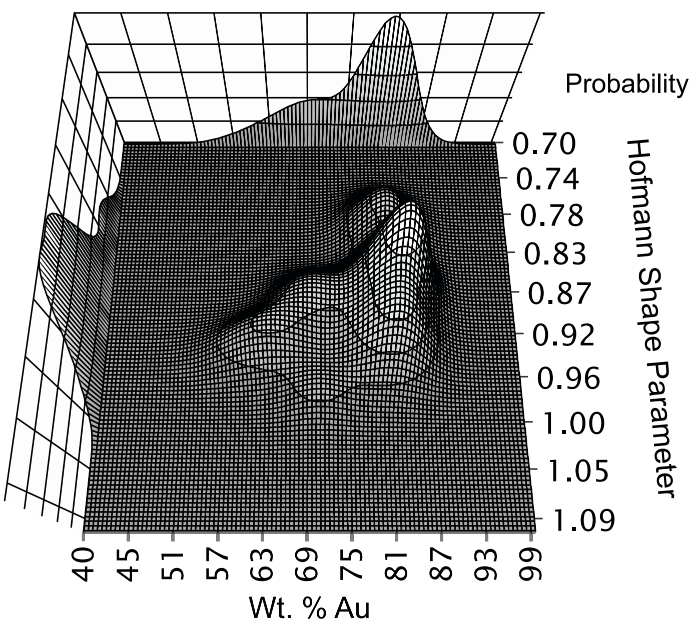

Figure 7. *The summed results of seven normally distributed peaks fitted to the KDA output for EC-06.*

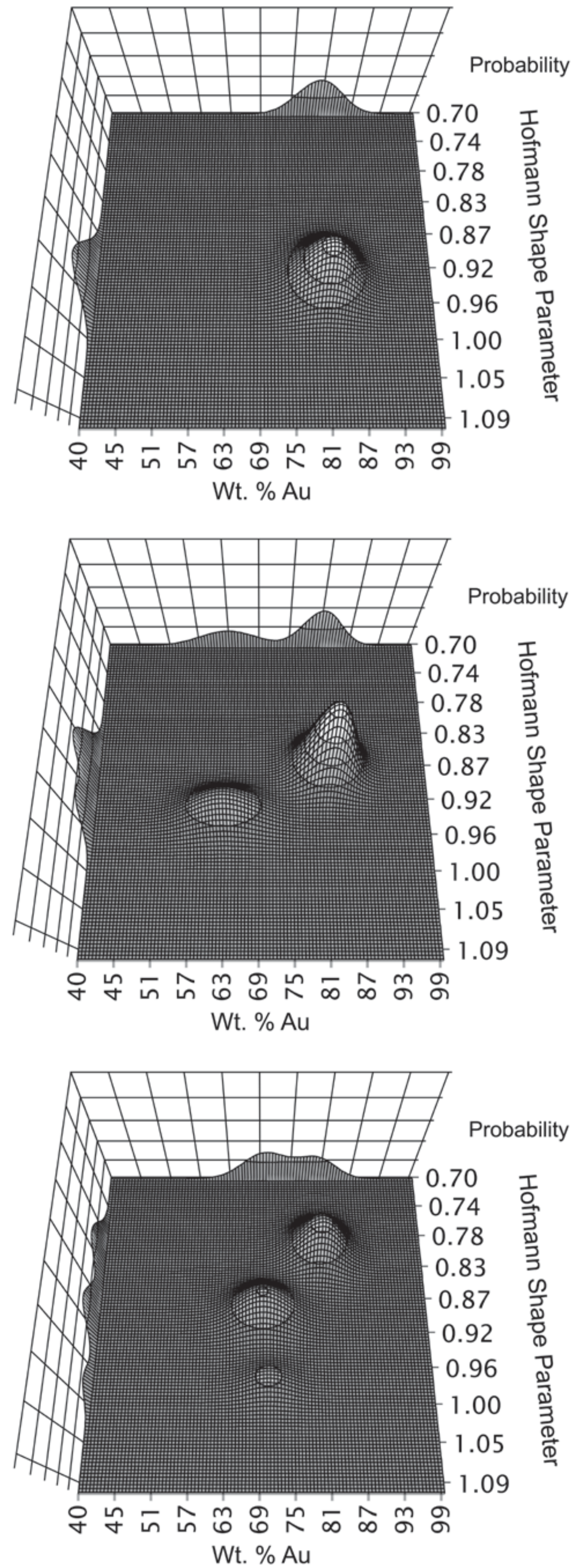

Figure 8. *(right column) The six component populations identified from the 2D KDA of sample EC-06.*

each individual axis for visual comparison to the 1D KDA results.

The EC-06 example illustrates the scrutiny required in choosing the number of peaks to be used in the fit. Although there is a definite peak at ~ 70, 0.8 (Fig. 6), when fitted, this peak represented a single observation. In a sample of n=54, this is likely to represent the sampling of a tail of one population rather than a unique population.

Two-dimensional KDA is far superior to previously used methods (e.g., the x,y plot) in demonstrating the presence and location of multiple contributing populations in the sample. It is also preferred over performing two 1D analyses because it returns correlated information for the two variables. It is interesting to compare the results of the 2D and 1D analyses. Table 1 shows that the 2D peak locations can be roughly grouped to correspond to the populations identified by the 1D analysis. The weights are given because although the mathematical analysis of the data provides interesting results, it is important to ensure that the results are not an artifact of the analysis, and do pertain to some true feature of the samples.

Although the following comparisons are qualitative, they provide another level of support for the method of analysis. In this case, grains were selected randomly from those grains that unambiguously belonged to each of the six identified populations. The whole grain BS and SE SEM images, as well as the BS SEM cross-section images (Fig. 9) were then visually compared. The compositional

Table 1. *Comparison of 1D and 2D KDA (shaded) results. S.D. = standard deviation.*

		1D Shape Results - Hofmann Parameter Values			
		Mean S.D. Weight Group	**Mean S.D. Weight Group**	**Mean S.D. Weight Group**	
	Mean S.D. Weight Group	0.806 ± 0.025 0.152 **C**	0.873 ± 0.021 0.164 **B**	0.924 ± 0.038 0.684 **A**	
1D Composition Results	57.2 ± 4.2 0.034 **1**			63.6 ± 5.6 0.935 ± 0.022 0.153 8	Mean S.D. Weight # of grains
	69.2 ± 5.6 0.371 **2**		69.9 ± 4.6 0.894 ± 0.024 0.148 8	70.9 ± 3.8 0.980 ± 0.019 0.055 3	Mean S.D. Weight # of grains
	81.2 ± 3.9 0.596 **3**	80.5 ± 3.9 0.808 ± 0.026 0.147 8	81.6 ± 3.7 0.875 ± 0.022 0.228 12	80.7 ± 4.4 0.932 ± 0.029 0.268 15	Mean S.D. Weight # of grains

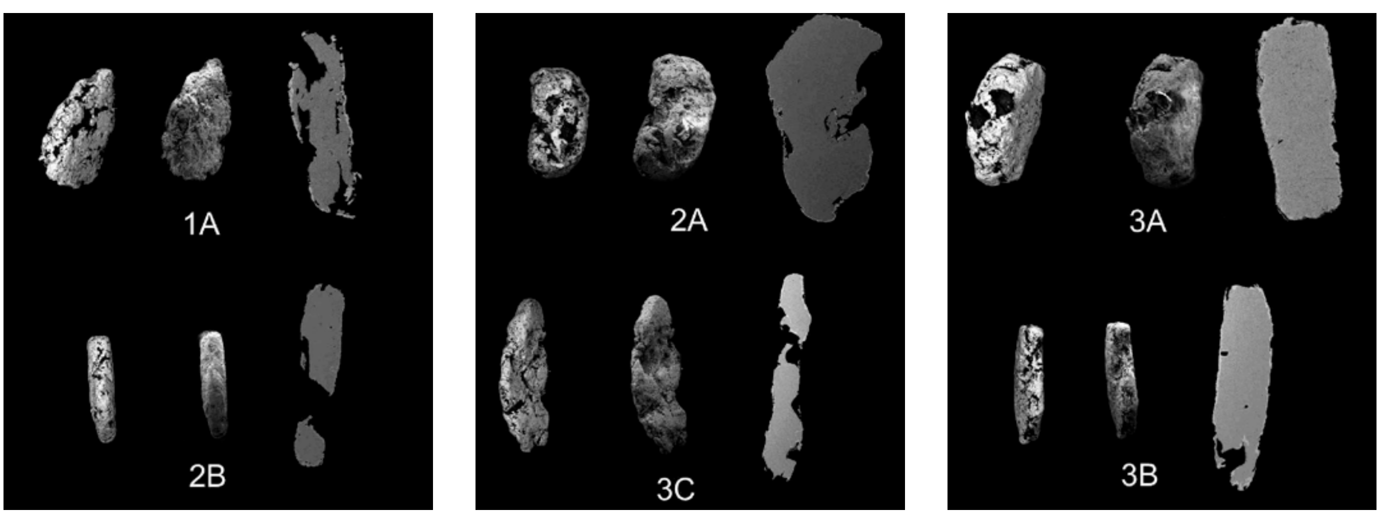

Figure 9. *Qualitative comparison of the six identified component populations in sample EC-06. Labels indicate compositional (letter) and morphological (number) groupings as per Table 1.*

populations are difficult to visually compare: the shade of the BS images generally relates to average atomic number, so the group 3 grains should be lighter than group 2, which should be lighter than group 1; however, this relationship can be complicated by the settings used to record the images. This comparison, if made, must be made on the sectioned grains since it is the core composition that is being examined due to the presence of gold-rich rims on many grains.

It is also interesting to note the differences in rimming between the populations: populations 3A, 3B and 1A show well developed rims, while those in the remaining groups are sparse and much thinner where present. A qualitative shape comparison is slightly easier. Group A contains the most boxy and irregular grains, whereas group B grains are mostly tabular, and the group C grain is flakier still. Overall, the correspondence between determined parameters and physical observations appears to be good, and provides some evidence that the method is revealing true information and not statistical artifacts.

CONCLUSIONS AND FUTURE WORK

Automating the measurement of morphological parameters on gold grains makes the collection of large, quantitative and unbiased sets of data relatively quick and easy. Although this provides a large amount of potentially useful information, a new problem arises in finding a way to visualize the data in a clear and concise manner that allows useful information to be extracted.

The use of kernel density analysis provides an easy way to process data into clearly interpretable diagrams. It also provides an excellent way to identify and extract quantitative information on individual populations within a sample. The 1D analysis has been shown to be an improvement over previous methods; however, it is still not sufficient to fully explain placer deposit complexity. The 2D method is a significant improvement; however, only once the predictive model is generated and tested will it be possible to determine if it adequately describes alluvial placer gold-shape evolution. Work currently underway to obtain correlated compositional data will allow the development of this model.

It is anticipated that laser ablation inductively coupled plasma mass spectroscopy (LA-ICP-MS) will be applied to further characterize the composition of Klondike placer gold. If compositional populations identified by electron microprobe and LA-ICP-MS are shown to be identical, then prior identification of those component populations using the KDA methods presented here will reduce the number of samples that need be examined by LA-ICP-MS.

REFERENCES

Cailleux, A., 1945. Distinction des galets marin et fluviatiles. Bulletin de la Société Géologique de France. Ser. 5, nu. 15, p. 374-404.

Chapman, R.J., Leake, R.C. and Moles, N.R., 2000. The use of microchemical analysis of alluvial gold grains in mineral exploration: experiences in Britain and Ireland. Journal of Geochemical Exploration, vol. 71, p. 241-268.

Corey, A.T., 1949. Influence of shape on the fall velocity of sand grains. Unpublished M.Sc. thesis, Colorado A&M University, Fort Collins, Colorado, 102 p.

Grigorova, B., Anderson, S., de Bruyn, J., Smith, W., Stülpner, K. and Barzev, A., 1998. The AARL gold fingerprinting technology. Gold Bulletin, vol. 31, no. 1, p. 26-29.

Hofmann, H.J., 1994. Grain shape indices and isometric graphs. Journal of Sedimentary Research, vol. 40, p. 1054-1056.

Knight, J.B., Morison, S.R. and Mortensen, J.K., 1999a. The relationship between placer gold particle shape, rimming and distance of fluvial transport as exemplified by gold from the Klondike district, Yukon Territory, Canada. Economic Geology, vol. 94, p. 635-648.

Knight, J.B., Mortensen, J.K. and Morison, S.R., 1999b. Lode and placer gold composition in the Klondike district, Yukon Territory, Canada: Implications for the nature and Genesis of Klondike placer and lode gold deposits. Economic Geology, vol. 94, p. 649-664.

Knight, J.B., Mortensen, J.K. and Morison, S.R., 1994. Shape and composition of lode and placer gold from the Klondike district, Yukon, Canada. Exploration and Geological Services Division, Indian and Northern Affairs Canada, Yukon Region, Bulletin 3, 142 p.

Leake, R.C., Chapman, R.J., Bland, D.J., Stone, P., Cameron, D.G. and Styles, M.T., 1998. The origin of alluvial gold in the Leadhills area of Scotland: Evidence from interpretation of internal chemical characteristics. Journal of Geochemical Exploration, vol. 63, p. 7-36.

Loen, J.S., 1995. Use of placer gold characteristics to locate bedrock gold mineralization. Exploration and Mining Geology, vol. 4, no. 4, p. 335-339.

Loen, J.S., 1994. Origin of placer gold nuggets and history of formation of glacial gold placers, Gold Creek, Granite county, Montana. Economic Geology, vol. 89, p. 91-104.

Mackenzie, D.J. and Craw, D., 2005. The mercury and silver contents of gold in quartz vein deposits, Otago Schist, New Zealand. New Zealand Journal of Geology and Geophysics, vol. 48, p. 265-278.

Márquez-Zavalía, M.F., Southam, G., Craig, J.R. and Galliski, M.A., 2004. Morphological and chemical study of placer gold from the San Luis range, Argentina. The Canadian Mineralogist, vol. 42, p. 169-192.

Mortensen, J.K., Chapman, R., LeBarge, W. and Jackson, L., 2004. Application of placer and lode gold geochemistry to gold exploration in western Yukon. *In:* Yukon Exploration and Geology 2004, D.S. Emond, L.L. Lewis and G.D. Bradshaw (eds.), Yukon Geological Survey, p. 205-212.

Parzen, E., 1962. On estimation of a probability density function and mode. Annals of Mathematical Statistics, vol. 33, p. 1065-1076.

Silverman, B.W., 1986. Density estimation for statistics and data analysis. Chapman and Hall, New York, 175 p.

Townley, B.K., Hérail, G., Maksaev, V., Palacios, C., de Parseval, P., Sepulveda, F., Orellana, R., Rivas, P. and Ulloa, C., 2003. Gold grain morphology and composition as an exploration tool: application to gold exploration in covered areas. Geochemistry: Exploration, Environment, Analysis, vol. 3, p. 29-38.

Watling, R.J., Herbert, H.K., Delev, D. and Abell, I.D., 1994. Gold fingerprinting by laser ablation inductively coupled plasma mass spectrometry. Spectrochimica Acta, vol. 49B, no. 2, p. 205-219.

Wierchowiec, J., 2002. Morphology and chemistry of placer gold grains – indicators of the origin of the placers: and example from the East Sudetic Foreland, Poland. Acta Geologica Polonica, vol. 52, p. 563-576.

Youngson, J.H. and Craw, D., 1999. Variation in placer style, gold morphology, and gold particle behaviour down gravel bed-load rivers: an example from the Shotover/Arrow-Kawarau-Clutha river system, Otago, New Zealand. Economic Geology, vol. 94, p. 615-634.

Zingg, T., 1935. Beitrag zur Schotteranalyse. Schweizerische Mineralogische und Petrographische Mitteilungen, vol. 15, p. 39-140.

Micropetrology and mineral geochemistry of the Tombstone and Deadman plutons, Tombstone Plutonic Suite, central Yukon

Ashley M. Flanders, Michael J. Harris*[1] *and Lance Kearns
Department of Geology and Environmental Science, James Madison University[2]

Craig J.R. Hart
Centre for Exploration Targeting (M006), School of Earth and Geographical Science, The University of Western Australia[3]

Flanders, A.M., Harris, M.J., Kearns, L. and Hart, C.J.R., 2007. Micropetrology and mineral geochemistry of the Tombstone and Deadman plutons, Tombstone Plutonic Suite, central Yukon. *In:* Yukon Exploration and Geology 2006, D.S. Emond, L.L. Lewis and L.H. Weston (eds.), Yukon Geological Survey, p. 149-156.

ABSTRACT

Micropetrographic observations and mineral geochemistry data, along with previously reported whole-rock geochemistry, defined an A-type granite-affinity for the Tombstone and Deadman plutons of the 120-km-long, mid-Cretaceous Tombstone-Tungsten plutonic belt. This plutonic belt was intruded into the western Selwyn Basin, the western-most edge of the ancestral North American craton, and is situated well inboard of any potential subduction-zone plutonism, which is found in the accreted terranes that were juxtaposed with the North American craton during the Jura-Cretaceous.

Over a dozen mineral specimens were petrographically observed and five were chemically analysed. Similarities found among the two plutons are their alkalic nature, minimal quartz content, presence of igneous andradite garnets and the presence of rare-earth-bearing minerals. Differences between the two plutons include the fact that the Tombstone pluton contains Th, Ce and La with magnetite and titanite, while the Deadman pluton contains Nd with Ce and La, as well as Ba-rich alkali feldspars. These observations are not commonly found in tectonic-related I- or S-type granitoids, and distinguish the Tombstone plutonic suite as being most similar to A-type granites.

RÉSUMÉ

Des observations micropétrographiques et des données sur la géochimie des minéraux, de même que des données déjà publiées sur la géochimie de la roche entière, ont permis de définir une affinité avec le granite de type A pour les plutons de Deadman et de Tombstone de la ceinture de roches plutoniques de Tombstone Tungsten du Crétacé moyen (d’une longueur de 120 km). Cette ceinture de roches plutoniques a pénétré le bassin de Selwyn, le rebord le plus occidental de l’ancestral craton de l’Amérique du Nord; cette ceinture est située bien à l’intérieur de tout éventuel plutonisme de subduction observé dans les terranes accrétés qui se sont juxtaposés au craton nord-américain du Jurassique-Crétacé.

Plus d’une douzaine d’échantillons de minéraux ont fait l’objet d’une analyse chimique. Les similarités observées entre les deux plutons comprennent leur nature alcaline, leur teneur minimale en quartz, la présence de grenats andradites ignés et de minéraux contenant des éléments des terres rares. Les deux plutons diffèrent sur le plan de la composition : le pluton de Tombstone contient du Th, du Ce et du La, de même que de la magnétite et de la titanite, tandis que le pluton de Deadman contient du Nd avec du Ce et du La, ainsi que du Ba dans les feldspaths alcalins. Ces compositions ne sont pas courantes pour les granitoïdes d’origine tectonique des types S ou I.

[1]*harrismj@jmu.edu, phone: 540-568-6480, fax: 540-568-8058*
[2]*Department of Geology and Environmental Science, James Madison University, MSC 6903, Harrisonburg, VA, 22807, USA*
[3]*Crawley, Western Australia, 6009, Australia*

INTRODUCTION

During the mid-Cretaceous, an extensive magmatic episode occurred throughout western North America from the Alaskan and Canadian Cordillera to as far south as Mexico. A number of plutonic belts have been identified based on their geographical distributions; in some cases, plutonic suites, which are defined by similar petrological, mineralogical, geochemical and age characteristics have also been identified (Armstrong, 1998). Some of the least-studied plutonic belts exist in the northern Canadian Cordillera and Alaska, where they have only recently been divided into smaller plutonic suites (Hart *et al.,* 2004a).

The most eastern, or inboard, of these plutonic belts in Yukon is the 800-km-long Tombstone-Tungsten Belt (TTB) which comprises the Tombstone, Mayo and Tungsten suites (Fig. 1). The distribution of the numerous plutons that make up this belt is largely within the northern margin of the Neoproterozoic and Paleozoic Selwyn Basin, a site of episodic clastic deposition within the otherwise carbonate-dominant platforms of the ancient North American miogeoclinal margin. This plutonic belt comprises more than 100 plutons and associated east-trending dyke swarms, and is directly associated with the formation of hundreds of mineral occurrences, the most significant being intrusion-related gold deposits (e.g., Dublin Gulch) and tungsten skarns (e.g., Mactung; Hart *et al.,* 2002, 2004a).

The nature of the associated plutonic rocks has been considered to represent a distinct post-collisional tectonic setting (Mair *et al.,* 2006), and this greatly influenced the nature of the associated mineralization. Although all three plutonic suites have associated gold mineralization, the metallogeny, lithology and geochemistry of the Tombstone suite is particularly anomalous as it is characterized by large lithologically variable, highly alkalic, silica-saturated and undersaturated, variably zoned mafic and felsic granitoids with unusual U-Th-F and Cu-Au-Bi metallogenic associations (Anderson 1987; Hart *et al.* 2004a). These diverse features are characteristic of A-type granitoids (Loiselle and Wones, 1979; Eby, 1990; Martin, 2006). This paper focuses on the micropetrology and mineral chemistry of two critical plutons that define this suite, the Tombstone and Deadman plutons.

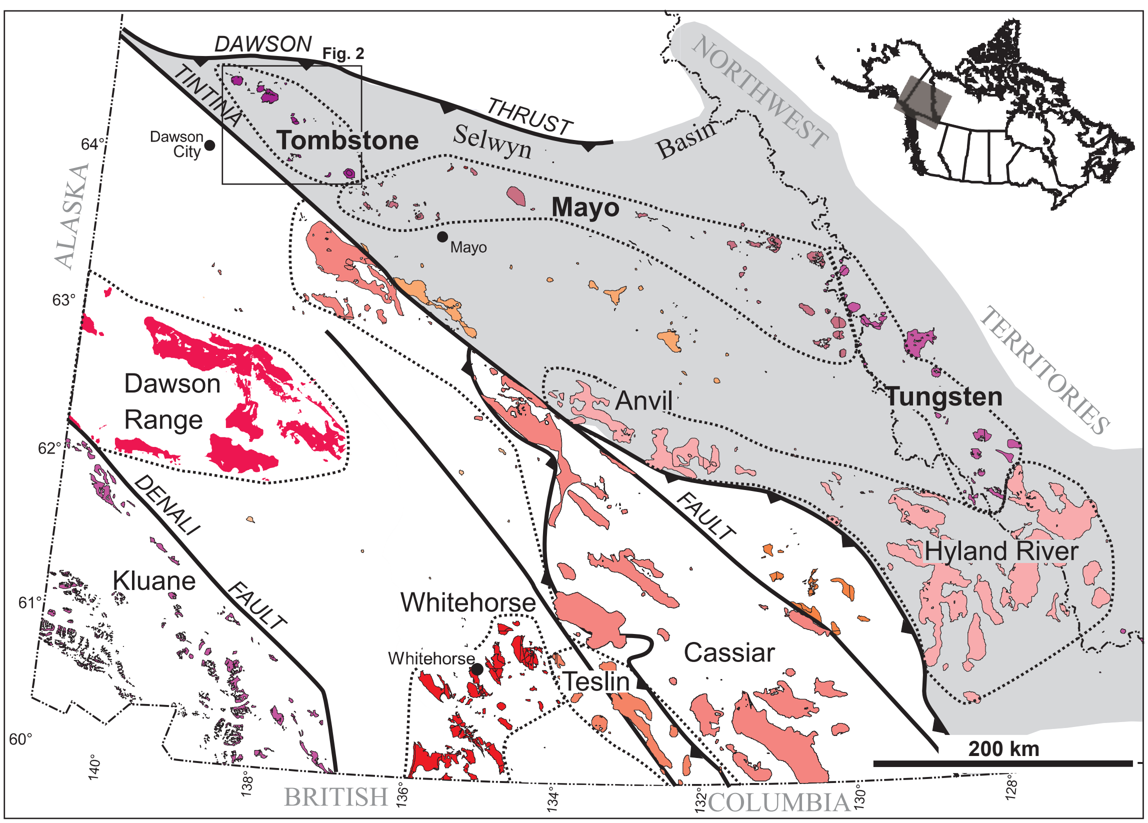

Figure 1. *Regional tectonic elements of the Yukon, and the distribution of mid-Cretaceous plutonic suites (dotted lines). The Tombstone-Tungsten Belt includes the Tombstone and Deadman plutons (Fig. 2) of this study (modified from Hart et al., 2004b).*

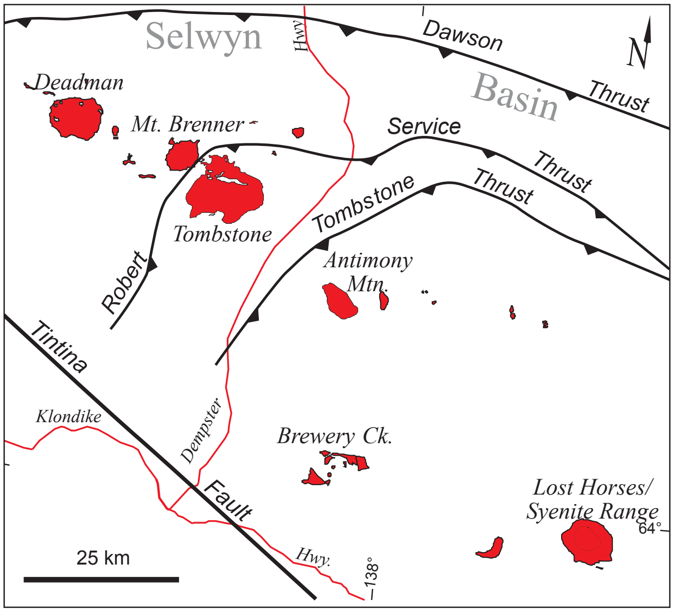

Figure 2. *Distribution of the plutons which form the Tombstone Plutonic Suite (modified from Hart et al., 2004b).*

REGIONAL

The Tombstone and Deadman plutons are located about 55 km north-northeast of Dawson City, Yukon (Fig. 2). The stocks are among the most northerly members of a 120-km-long northwest-trending string of five large mid-Cretaceous plutons and numerous assorted stocks, dykes and sills that parallel the Tintina Fault (Anderson, 1987; Hart *et al.,* 2004b). They are likely equivalent with the Livengood suite in east-central Alaska. The plutons intrude deformed and weakly metamorphosed strata of the Selwyn Basin, and appear to be entirely post-deformational. However, paleomagnetic studies of the Deadman pluton by Symons *et al.* (2006) indicate notable tilting and likely displacement of the pluton. Selwyn Basin assemblages at this location include Neoproterozoic coarse clastic Hyland Group; lower Paleozoic Road River Group black shales and chert; Mississippian Keno Hill Quartzite; Permian shale and chert; Triassic quartzite, calcareous siltstone, limestone and gabbro; and Jurassic black shale.

The Deadman and Tombstone plutons are both circular, and about 7 and 9 km in diameter, respectively. Both plutons have mostly steep sides, but both plutons host roof pendants and have some irregular contacts indicating shallow-dipping shoulders. Both plutons are variably concentrically zoned, multiphase alkalic plutons composed mostly of medium- to coarse-grained alkali-feldspar syenite and biotite-hornblende monzonite, with lesser amounts of quartz monzonite and pseudoleucite-phyric tinguaite (Anderson, 1987).

Vein, skarn and disseminated mineral occurrences are located within, and adjacent to, the Tombstone suite plutons and have the following metal associations: uranium-thorium-fluorine, antimony-arsenic-gold, tin-silver and gold-copper-bismuth (Hart *et al.,* 2004a). In both the Deadman and Tombstone plutons, uranium-thorium mineralization is associated with the tinguaite, a silica-undersaturated, highly potassic leucite porphyry.

The plutons have several age determinations, but the most accurate is likely the 91 ± 1 Ma determination by the U-Pb SHRIMP[1] (C. Hart, unpublished) on zircons, that are large and mostly unzoned, from the Deadman pluton (Hart *et al.,* 2004a). This date is similar to K-Ar dates from the Tombstone pluton and likely indicates that the plutons cooled rapidly within a few million years (Anderson, 1987; Hart *et al.,* 2004a). Based on petrographic observations and slightly elevated aeromagnetic responses and magnetic susceptibility values, Hart *et al.* (2004a) deemed the Tombstone suite to be magnetite-series granitoids (Ishihara, 1981).

A-TYPE GRANITE CHARACTERISTICS

A-type granites refer to those felsic units that are alkali-rich or have intruded into anorogenic environments, free of any tectonic or deformational events. In both cases, the likely source of magma formation is partial melting of the lower crust due to extreme crustal thickness. A-type granites comprise quartz syenites to peralkaline granites that are characterized by high modal concentrations of orthoclase and sodic plagioclase, and high total modal feldspar concentrations (>60%). Further, the mafic contents include the presence of iron-rich micas, amphiboles and pyroxenes. Geochemically, there are commonly high total concentration of alkali contents and low CaO contents (at SiO_2 = 70%, $Na_2O + K_2O$ = 11%, CaO < 1.8%, high FeO_T/MgO = 8-80), plus elevated halogens such as F contents (F = 1.7%). The Y/Nb ratio has also been used to determine source environments with Y/Nb < 1.2 suggesting sources chemically similar to oceanic island basalts, while those with Y/Nb > 1.2 suggest sources chemically similar to island-continental margin basalts (Eby, 1990; Hess, 1989).

[1]*Sensitive, high-resolution, ion microprobe*

EXPERIMENTAL METHODS

A total of five polished thin sections from both plutons were petrographically analysed. The Scanning Electon Microscope (SEM) and Energy Dispersive Spectrometer (EDS) provided further analyses for mineral content and chemical composition. A 200-point count was used for modal mineral percentages to determine appropriate IUGS igneous rock nomenclature. Element mapping and backscatter imagery on the SEM provided informal mineral identifications and EDS analyses gave oxide chemistry of garnet and other accessory minerals.

ANALYTICAL RESULTS

Recently determined whole-rock analyses are shown in Table 1 for the Deadman pluton (Hart *et al.,* 2004b). They all show peraluminous values, high alkalis versus CaO values (>10% Na_2O + K_2O vs <4% CaO), FeO_T/MgO ratios of 7 to 26, and F between 0.01 and 1.5%. LOI and H_2O+ values are all less than 0.7%. The Y/Nb ratios range from 0.65 to 0.89.

New petrologic observations of the Tombstone and Deadman plutons showed some mineral compositional similarities along with some very distinct differences. Table 2 shows the results of 200-point count analyses, and the resulting IUGS rock calculations and names. Petrologically, both plutons consistently contained > 60% total modal feldspar content. Many of the feldspars showed obvious zoning patterns, albite zoning in the plagioclase and Carlsbad twinning in the orthoclase (Figs. 3 and 4). Further, several isotropic minerals were observed, some with subhedral to euhedral garnet shapes.

Table 1. *Selected whole-rock geochemistry for the Deadman pluton (from Hart et al., 2004b).*

	DM 1	DM 2	DM 3	DM 4
SiO_2	57.8	64.7	58.6	68.3
TiO_2	0.304	0.198	0.303	0.175
Al_2O_3	19.3	17.6	21.1	16.1
FeO_T	2.85	1.92	2.53	1.8
Fe_2O_3	1.65	0.92	0.53	1.0
FeO	1.2	1.0	2.0	0.8
MnO	0.13	0.05	0.06	0.04
MgO	0.11	0.24	0.23	0.26
CaO	3.76	2.34	0.85	1.53
Na_2O	3.59	5.84	2.98	5.38
K_2O	8.6	5.43	12.1	4.9
P_2O_5	0.03	0.02	0.02	0.01
Cr_2O_3	0.005	0.005	0.005	0.005
LOI	0.65	0.6	0.4	0.65
H_2O^+	0.5	0.3	0.7	0.2
Total	**98.8**	**99.4**	**99.4**	**99.4**
Cl	347	30	157	69
F	1050	479	1520	10
B	47	45	29	37
V	38	23	15	21
Co	1	1	2	1
Ga	22	24	32	27
Ge	1.2	1.2	1.5	1.3
Rb	197	178	705	211
Sr	3380	1110	599	637
Y	11.4	17.2	30.4	15.5
Zr	175	414	518	287
Nb	12.8	22.9	40.3	24.0

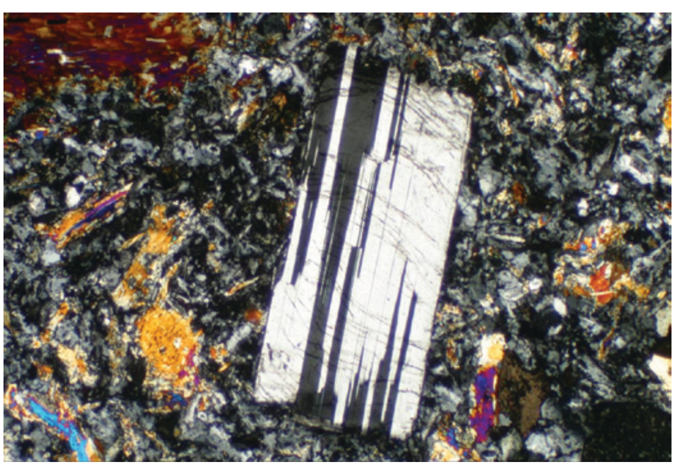

Figure 3. *Polysynthetic twinning of plagioclase shown in thin section (bipolarized light).*

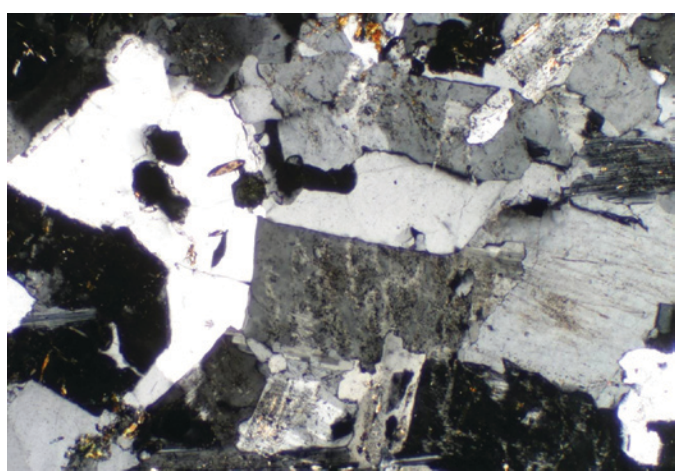

Figure 4. *Orthoclase feldspar and small titanite crystals in thin section (bipolarized light).*

Table 2. *Results from 200-point count analyses of the five polished sections. Q = Q/Q+A+P, (F = F/F+A+P), A = A/Q+A+P, M = biotite + amphibole + opaques + titanite.*

	DM 1	DM 3	Tomb 6A	Tomb 20	Tomb 22
Quartz	0	2.25	6.74	0	0
K-feldspar	76.9	83.95	48.69	77.42	29.3
Biotite	2.56	13.5	0.75	1.38	1.84
Amphibole	5.13	0.98	39.7	0.46	16.6
Opaques	15.38	0.98	0	20.74	52.3
Titanite	0	0.98	4.12	0	0
Q	0	2.6	12.16	0	0
A	100	97.4	77.84	100	100
P	0	0	0	0	0
M	23.07	16.44	44.57	22.56	70.74
IUGS name	leucocratic alkali-feldspar syenite	leucocratic alkali-feldspar syenite	alkali-feldspar quartz syenite	leucocratic, nepheline-bearing alkali-feldspar syenite	melanocratic alkali-feldspar syenite

EDS analyses confirmed the zoning in the feldspars and the presence of andradite garnets ($Ca_3Fe_2(SiO_4)_3$). As well, both plutons contain minerals with several uncommon rare-earth and radioactive elements that are also uncommon in most granitoids (Tables 3-7).

One of the most enigmatic differences between the two plutons is the presence of up to 2 wt.% Ba in the alkali feldspars of the Deadman pluton, and the absence of the Ba in the Tombstone pluton. Both plutons contain minerals with the REEs, Ce and La. However, Tombstone also contains Th (Fig. 5), which is recordable on a Geiger counter. The Deadman pluton contains Nd rather than Th.

One EDS analysis of a mineral from the Tombstone pluton suggests a possible occurrence of the rare-earth mineral fluoro-carbonate synchesite or parasite. Proper verification would require XRD analysis, which was not possible due to the small sample grain in thin section.

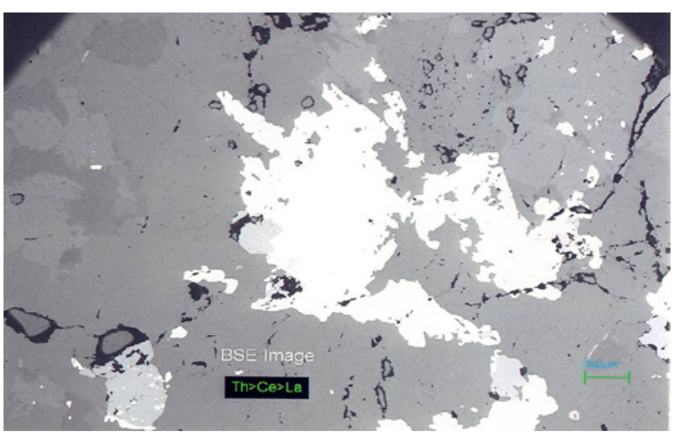

Figure 5. *Backscatter-electron image of a radioactive rare-earth mineral containing greater Th concentration than Ce, La or Nd.*

Table 3. *Mineral chemistry data from Tombstone sample 6A, from EDS analyses (all measured in weight percent, estimated from bar graph). Sample: (1) alkali feldspar; (2) albitic feldspar; (3) andradite garnet; (4) possibly Ca-Mg-Fe clinopyroxene.*

	1	2	3	4
O	66	68	48	22
Si	21	17	22	22
Al	6	6		1
Ca			11	12
Fe			12	12
K	4	1		
Mg			4	5
Mn			1	
Na	3	8	2	1

Table 4. *Mineral chemistry data from Tombstone sample 22, from EDS analyses (all measured in weight percent). Sample: (1-5) zoned garnet from rim to core; (6) a rare-earth element (REE)-bearing mineral.*

	1	2	3	4	5	6
O	45.02	46.76	43.13	45.85	45.16	35.15
Si	15.78	20.98	15.04	14.79	14.93	3.34
Al	1.31	2.12	2.19	1.77	1.87	
C						12.91
Ca	20.94	13.09	21.02	20.35	20.35	3.33
Ce						19.16
F						8.5
Fe	14.73	11.11	14.84	13.26	13.67	
La						14.36
Mg		3.42			0.37	
Mn	0.42	0.39	0.34	0.27	0.38	
Na		1.52				
Ti	1.8	0.6	3.44	3.7	3.26	

Table 5. *Mineral chemistry data from Tombstone sample 20, from EDS analyses (all measured in weight percent). Sample: (1,2) orthoclase; (3-7) different garnet crystals; (8) a REE-bearing mineral; (9,10) nepheline.*

	1	2	3*	4	5	6	7	8	9	10
O	59.37	49.89	45	30.37	48.58	50.16	48.53	41.8	50.04	55.42
Si	24.39	28.07	16	22.34	15.85	15.87	15.62	7.72	17.71	15.07
Al	8.26	8.95	2	2.38	1.51	1.33	2.21		16.4	14.1
C								9.9		
Ca			21	25.7	18.58	18.19	18.75	9.65		
Ce								6.55		
F								2.98		
Fe			14	16.88	13.19	12.38	13.25			
K	6.4	12.66							3.77	2.18
La								2.98		
Mn			1	0.6	0.66	0.69	0.73			
Na	1.61	0.43							12.1	13.2
P								1.77		
Th								16.6		
Ti			1	1.73	1.65	1.38	0.91			

*data estimated from bar graph

Table 6. *Mineral chemistry data from Deadman sample 1, from EDS analyses (all measured in weight percent). Sample: (1-4) mainly perthitic orthoclase; (5) albitic feldspar; (6, 7) same zoned crystal, with (6) the orthoclasic core, and (7) part of the rim of unknown affinity.*

	1	2	3	4	5	6	7
O	66.1	64.16	62.73	51.79	61.42	53.5	54.31
Si	20.24	21.2	21.96	27	20.75	26.4	16.25
Al	8.17	8.02	8.16	9.17	8.54	9.14	7.15
Ba	0.28	0.41	0.3	1.21		0.92	
Ca					0.44	0.25	5.28
Cl							0.2
Fe						0.42	11.07
K	4.27	4.23	4.88	9.38	0.96	6.99	1.59
Mg							0.95
Mn							0.52
Na	0.94	1.99	1.98	1.46	7.89	2.38	1.95
Ti							0.74

Table 7. *Mineral chemistry data from Deadman sample 3, from EDS analyses (all measured in weight percent). Sample: (1) orthoclase; (2,3) albite; (4) possible Fe-spinel; (5) REE-bearing apatite; (6) biotite; (7,8) REE-bearing minerals.*

	1	2	3	4	5	6	7	8
O	61.77	60	50.59	47.78	63.09	55.15	64.32	50.84
Si	23.03	18.03	17.92		1.21	14.81	13.94	14.43
Al	8.16	11.8	15.8	29.6		11.3	9.82	10
Ca		2.45	1.16		18.39		3.52	5.47
Ce					1.09		4.71	8.8
Fe				16.4		9.8	2.19	5.2
K	5.62		2.7			5.96		
La							1.5	3.66
Mg						1.44		
Mn				0.86		0.33		
Na	1.42	7.71	11.8		1.16			
Nd					0.65			1.59
P					14.4			
Ti						1.22		
Zn				5.34				

Accessory minerals, found petrographically and through the SEM, show that the Tombstone pluton contains titanite (Fig. 6), magnetite, and in one sample, nepheline. Within the Deadman pluton apatite and spinel, and possibly hercynite ($FeAl_2O_4$) are common.

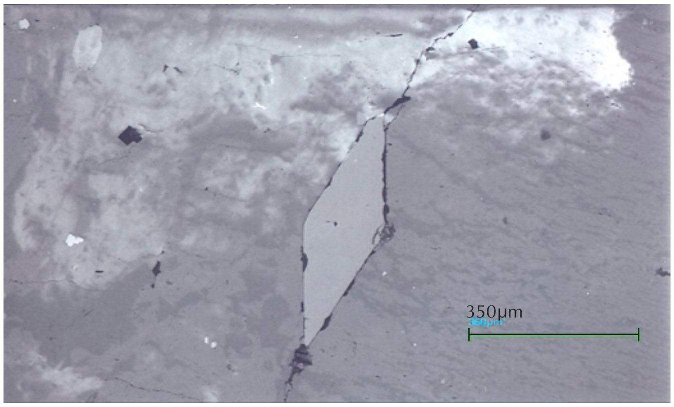

Figure 6. *Backscatter-electron image of a titanite crystal from the Tombstone pluton.*

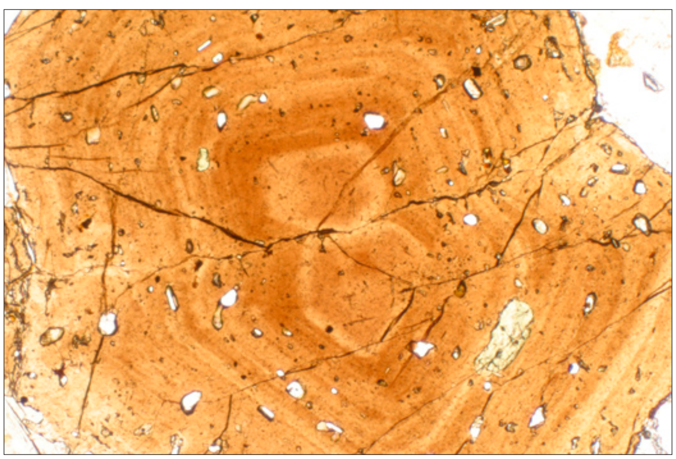

Figure 7. *Backscatter-electron image of the zoned garnet from the Tombstone 22 sample.*

CONCLUSIONS

The *ca.* 91 Ma Deadman and Tombstone plutons were emplaced into the ancient North American continental margin during the mid-Cretaceous, following a period of terrane collision, crustal thickening and lower greenschist-facies metamorphism. The plutons are related to extensional events following the compressional events. There are multiple variations in mineral composition of the intrusions, even though they are from one contemporaneous belt. This is likely due to the heterogeneity of source material, as is common of A-type granites. As has been suggested by Behnia *et al.* (2004), A-type granites are associated with either continental or oceanic plate interiors, in a tensional anorogenic regime, or even immediately post-orogenic environment (Pitcher, 1993), with definite alkaline and anhydrous imprints. Although more chemical data from other plutons would provide more confidence on the A-type nature of the granitoids, the location of the Tombstone-Tungsten Belt and the two plutons, well inboard, and formed very late within the suites, suggests quite a different environment than most other types of granitoids.

REFERENCES

Anderson, R.G., 1987. Plutonic rocks in the Dawson map area, Yukon Territory. *In:* Current Research, Part A, Geological Survey of Canada, Paper 87-1A, p. 689-697.

Armstrong, R.L., 1988. Mesozoic and early Cenozoic magmatic evolution of the Canadian Cordillera. *In:* Processes in Continental Lithospheric Deformation, S.P. Clark Jr., B.C. Burchfiel and J. Suppe (eds.), Geological Society of America Special Paper, vol. 218, p. 55-92.

Behnia, P., Darvishzadey, A. and Collins, L.G., 2004. Geochemical peculiarities in K- and Si-metasomatic processes of Qooshchi Complex, Northwest Iran. Iranian International Journal of Science, vol. 5, no. 1, p. 77-90.

Eby, G.N., 1990. The A-type granitoids: A review of their occurrence and chemical characteristics, speculation on the petrogenesis. Lithos, vol. 26, 115-134.

Hart, C.J.R., McCoy, D.T., Goldfarb, R.J., Smith, M., Roberts, R., Hulstein, R., Bakke, A.A. and Bundtzen, T.K., 2002. Geology, exploration and discovery in the Tintina Gold Province. *In:* Geology, Exploration and Discovery in the Tintina Gold Province, Alaska and Yukon, R.J. Goldfarb and R. Neilson (eds.), Geological Society of America Special Paper, vol. 9, p. 241-274.

Hart, C.J.R., Goldfarb, R.J., Lewis, L.L. and Mair, J.L., 2004a. The northern Cordilleran mid-Cretaceous plutonic province: Ilmenite/magnetite series granitoids and intrusion-related mineralization. Resource Geology, vol. 54, p. 253-280.

Hart, C.J.R., Mair, J.L., Goldfarb, R.J. and Groves, D.I., 2004b. Source and redox controls on metallogenic variations in intrusion-related ore systems, Tombstone-Tungsten Belt, Yukon Territory, Canada. Transactions of the Royal Society of Edinburgh: Earth Sciences, vol. 95, p. 339-356.

Hess, P.C., 1989. Origins of Igneous Rocks. Harvard University Press, Massachusetts, 336 p.

Ishihara, S., 1981. The granitoid series and mineralization. Economic Geology, 75th Anniversary Volume, p. 458-484.

Loiselle, M.C. and Wones, D.R., 1979. Characteristics and origin of anorogenic granites. Geological Society of America, Abstracts, 11, p. 468.

Mair, J.L., Hart, C.J.R. and Stephens, J., 2006. Deformation history of the western Selwyn Basin, Yukon, Canada: Implications for orogen evolution and mid-Cretaceous magmatism. Geological Association of America, Bulletin, vol. 118, p. 304-323.

Martin, R.F., 2006. A-type granites of crustal origin ultimately result from open-system fenitization-type reactions in an extensional environment. Lithos, vol. 91, p. 125-136.

Pitcher, W.S., 1993. The Nature and Origin of Granites. Blackie Academic & Professional, London, 321 p.

Symons, D.T.A., Harris, M.J., Hart, C.J.R. and McCausland, P.J.A., 2006. Paleomagnetism of the ~91 Ma Deadman pluton: Post-mid-Cretaceous tectonic motion in central Yukon. *In:* Yukon Exploration and Geology 2005, D.S. Emond, G.D. Bradshaw, L.L. Lewis and L.H. Weston (eds.), Yukon Geological Survey, p. 299-313.

Field investigations of the Upper Devonian to Lower Carboniferous Tuttle Formation, eastern Richardson Mountains, Yukon

***Tiffani A. Fraser*[1] *and Tammy L. Allen*[2]**
Yukon Geological Survey

Fraser, T.A. and Allen, T.L., 2007. Field investigations of the Upper Devonian to Lower Carboniferous Tuttle Formation, eastern Richardson Mountains, Yukon. *In:* Yukon Exploration and Geology 2006, D.S. Emond, L.L. Lewis and L.H. Weston (eds.), Yukon Geological Survey, p. 157-173.

ABSTRACT

The Upper Devonian to Lower Carboniferous Tuttle Formation was an exploration target for oil and gas in the Peel Plateau and Eagle Plain in the 1960s and 1970s. To date, seven minor gas shows have been identified in the Tuttle Formation in the Peel region. This study is part of a long-term project to investigate the sedimentology, stratigraphy and hydrocarbon potential of this unit in the Peel region.

The Tuttle Formation forms the upper part of a siliciclastic wedge that was deposited in the foreland basin of the Yukon and Ellesmerian fold belts. In the eastern Richardson Mountains, on Trail and Road rivers, it occurs as alternating packages of resistant and recessive intervals. Resistant intervals, 23 to 54 m thick, comprise five lithofacies including fining-upward sandstone, massive sandstone, siltstone, conglomerate and diamictite. Recessive intervals, 55 and 144 m thick, consist of siltstone and shale and are mostly covered.

RÉSUMÉ

La Formation de Tuttle datant du Dévonien supérieur au Carbonifère inférieur a constitué dans les années 60 et 70 une cible d'exploration à la recherche de pétrole et de gaz sur le plateau Peel et dans la plaine Eagle. Jusqu'à maintenant, on a identifié sept vindices mineurs de gaz dans la Formation de Tuttle dans la région de Peel. Cette étude s'insère dans un projet de recherche à long terme sur la sédimentologie, la stratigraphie et le potentiel en hydrocarbures des couches du Paléozoïque supérieur dans la région de Peel.

La Formation de Tuttle forme la partie supérieure d'un biseau silicoclastique déposé dans le bassin d'avant pays des zones de plissement Ellesmerienne et du Yukon. Dans la partie orientale des monts Richardson le long des rivières Trail et Road, elle prend la forme d'ensembles alternants d'intervalles récessifs et résistants. Les intervalles résistants d'une épaisseur de 23 à 54 m comprennent cinq unités lithologiques dont un grès à granodécroissance vers le haut, un grès massif, un siltstone, un conglomérat et une diamictite. Les intervalles récessifs d'une épaisseur de 55 à 144 m se composent de siltstone et de shale, et sont principalement couverts.

[1]*tiffani.fraser@gov.yk.ca*

[2]*tammy.allen@gov.yk.ca*

INTRODUCTION

In 2006, the Yukon Geological Survey began fieldwork in the eastern Richardson Mountains as part of the "Regional Geoscience Studies & Petroleum Potential, Peel Plateau and Plain" study, known informally as 'The Peel Project'. The project is a working partnership that involves the efforts of the Geological Survey of Canada, Northwest Territories Geoscience Office, Yukon Geological Survey, and university and industry affiliates (Pyle *et al.*, 2006). It is a four-year project ending in 2009.

Upper Paleozoic strata comprising the Canol, Imperial and Tuttle formations and the overlying 'Cf' map unit (Norris, 1981b; 1982b) were studied as part of this investigation, with the Upper Devonian to Lower Carboniferous Tuttle Formation as the main focus. This paper summarizes preliminary findings of work on the Tuttle Formation to date.

LOCATION, ACCESS AND EXPOSURE

The study area is in the northeast corner of the Yukon in the eastern Richardson Mountains, on Trail River map sheet (NTS 106L; Fig. 1). During summer 2006, field studies were based out of an exploration camp on a tributary of the upper Caribou River. Access to camp was via a 30-minute helicopter ride from Eagle Plains Hotel located on the Dempster Highway. Fieldwork was helicopter-supported, as there is no infrastructure in the region.

The Paleozoic succession in the region crops out along the eastern flank of the Richardson Mountains as well as along the northern Mackenzie Mountains, allowing for surface investigation of rocks equivalent to those that are in the subsurface of the Peel Plateau and Plain.

Exposures of the Tuttle Formation and neighbouring units were mainly limited to river cuts. Sandstone bodies of the

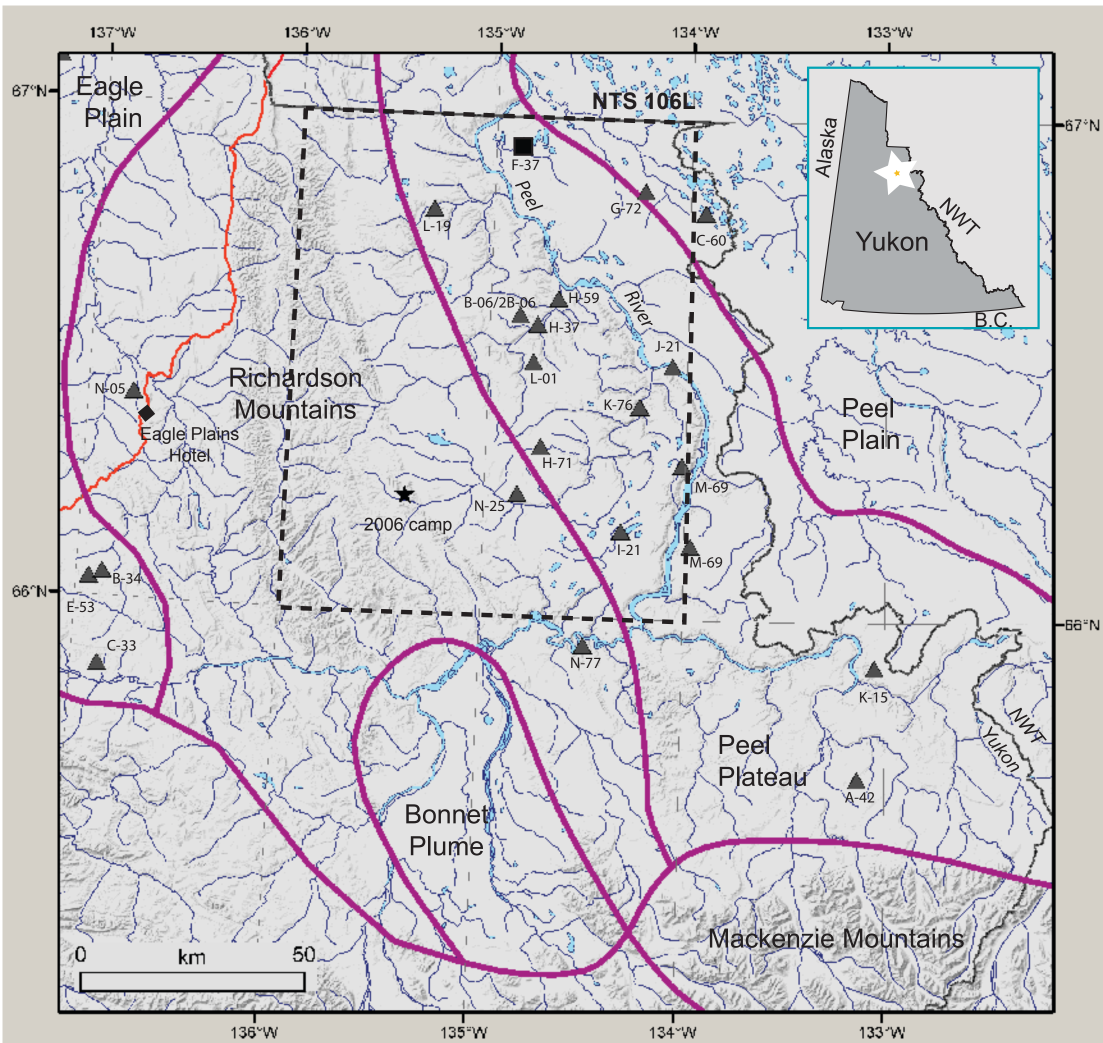

Figure 1. *Map of study area displaying well locations (triangles), summer 2006 camp (star) and Eagle Plains Hotel (diamond). NTS mapsheet 106L is highlighted with a dashed box. Tuttle Formation type section in the F-37 well is represented by a square.*

Tuttle Formation form resistant units that crop out on Trail and Road rivers, as well as along a north-trending ridge extending south of Trail River to north of Road River. A number of site visits were made in areas mapped as the Tuttle Formation by Norris (1981b), as well as recessive units that lie stratigraphically above and below, including the Canol and Imperial formations and Norris' (1981b) map units 'Dus' and 'Cf' (see Fig. 2 for locations).

PREVIOUS STUDIES

During the 1960s and 1970s, the Richardson Mountains and the neighbouring Peel Plateau and Plain were mapped at a 1:250 000 scale by the Geological Survey of Canada as part of Operation Porcupine. Bedrock maps for the Yukon portion of the Peel region include NTS map sheets 106E (Wind River) and 106F (Snake River) by Norris (1982a,b), and 106L (Trail River) and 106K (Martin House) by Norris (1981b,c). No bedrock mapping has been completed since. This mapping has contributed to an understanding of the geology on a regional scale, however our field observations indicate that some detailed remapping is required.

In addition to bedrock mapping, a number of reports pertain to the study area.

Norris (1968) provided a summary of early exploration and geological work on Devonian formations of the Operation Porcupine area, including the Peel Region, up to about 1964. Norris (1985) provided a revised account of the Devonian geology of this same area from additional field work and biostratigraphic studies.

A comprehensive litho/environmental facies analysis of the Mississippian Clastic Wedge (Tuttle Formation) was made by Lutchman (1977) as a part of the Lower Mackenzie Energy Corridor Study conducted by

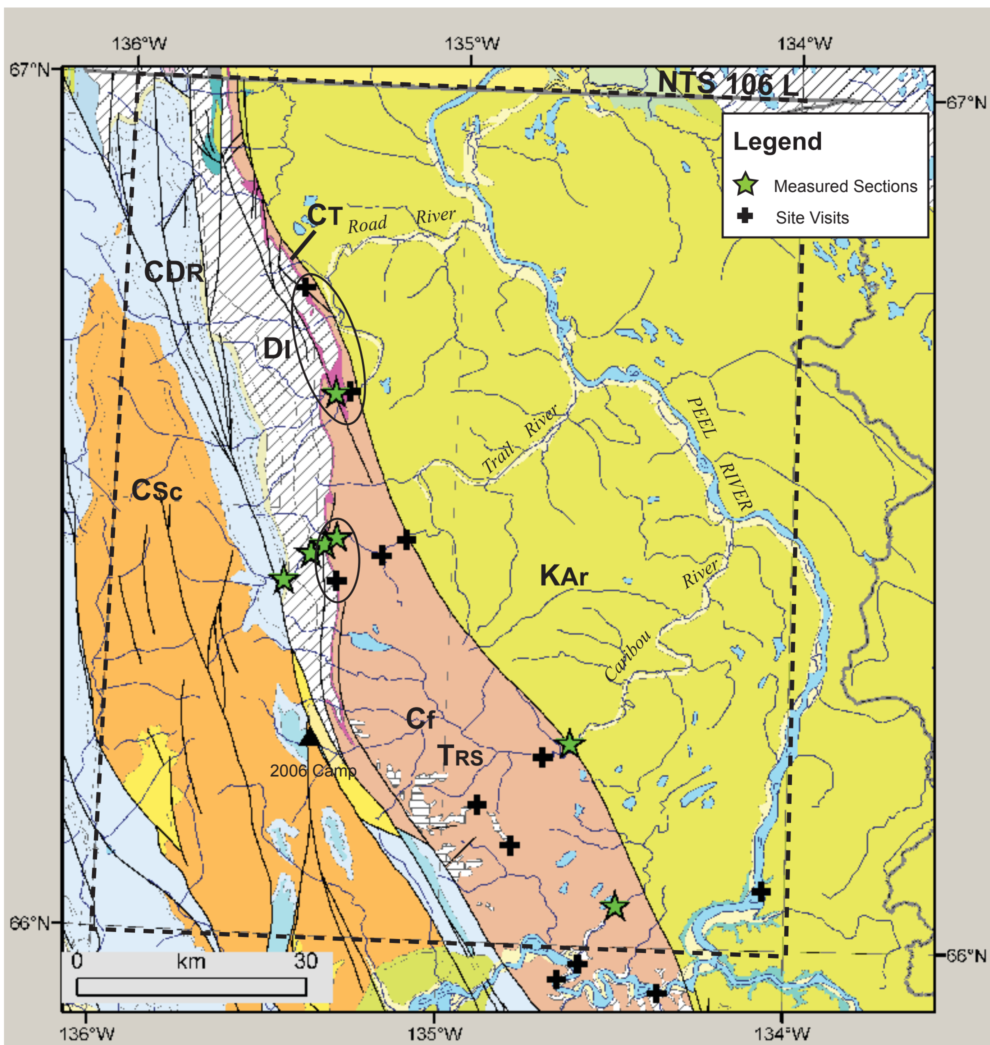

Figure 2. *Close-up map of 106L (dashed line) showing measured sections, site visits and summer 2006 camp location. Circled areas highlight Tuttle locations.*
KAr = Arctic Red Formation
Cf = Carboniferous shale
CT = Tuttle Formation
DI = Imperial Formation
CDR = Road River Formation
CSc = Slats Creek Formation.
TRS = Shublik limestone (skeletal, marine)
Geology from Norris (1981b; 1982a) and Gordey and Makepeace (2001).

Geochem Laboratories and AGAT Consultants. The study involved examination of core, cuttings and mechanical logs from available boreholes.

Pugh (1983) published a subsurface study of the Peel River map area (64° to 68° North latitude and 128° to 144° West longitude), based on regional correlation of well logs and examination of drill cuttings.

Braman and Hills (1992) reported ages of the Imperial and Tuttle formations based on miospores collected from outcrop in the eastern Richardson Mountains and Peel region.

A compilation volume of the efforts of Operation Porcupine was published in 1997 (Norris, D.K., 1997, ed.). Portions of Chapter 7 by Norris (1997) on Devonian strata and Chapter 8 by Richards *et al.* (1997) on Upper Devonian to Permian strata are pertinent to this study.

In 2000, the Government of Yukon published a petroleum resource assessment of the Peel Plateau (National Energy Board of Canada, 2000). This study was conducted by the National Energy Board on behalf of the Yukon government.

Petrel Robertson Consulting Limited (2002) completed a regional geological and geophysical assessment of the central Mackenzie Valley, Northwest Territories, and Eagle Plain, Yukon, which includes the Peel Plateau and Richardson Mountains. The data used in the assessment were derived from logs, core tests and geochemical data obtained from wells and seismic data.

Osadetz *et al.* (2005) published a petroleum resource assessment of the Peel Plateau and Plain of the Yukon Territory, which identified and used statistics to analyse eight plays in three assessment regions.

Lutchman (1977) interpreted a fluvial-deltaic model for the Tuttle Formation based on subsurface analysis. In contrast, based on outcrop observations, Hills *et al.* (1984), and Braman and Hills (1992) interpreted the Tuttle Formation to be deposited as a turbidite sequence.

EXPLORATION HISTORY

During the 1940s to 1970s, a number of oil and gas companies were actively exploring in the Peel region. Studies by these companies included photogeology, geological mapping, section measuring, drilling and seismic acquisition. A number of reports summarizing the results of these studies are available at the National Energy Board (NEB) in Calgary, Alberta.

Nineteen exploratory oil and gas wells were drilled on the Yukon side of the Peel region between 1965 and 1977 (Fig. 3). Eighteen of these wells intersected the Tuttle Formation. Various wireline geophysical logs exist for 18 of the 19 wells and are available to the public.

At least 2039 km of 2D seismic data was acquired from the Yukon Peel region between 1963 and 1976 (Oil and Gas Management Branch, 2001; Fig. 4). All 409-km of data acquired in 1976 is available in paper format from the NEB. The remainder is not publicly available.

In 1977, exploration activity in the Peel region ceased due to the Berger Commission recommendations that a ten-year moratorium be placed on pipeline construction in the Mackenzie Valley (Morrell, 1995). Renewed interest in the Peel region is expected should the proposed Mackenzie Gas Pipeline be constructed.

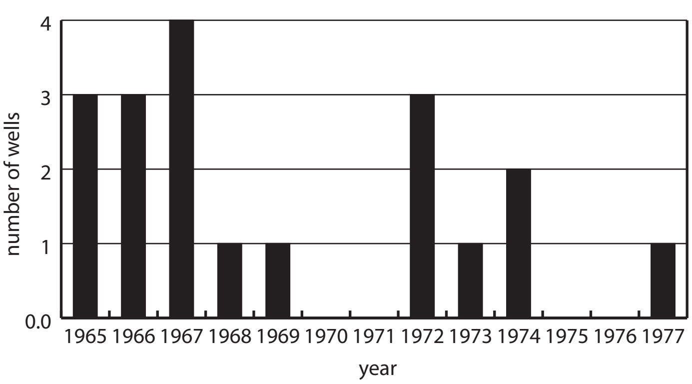

Figure 3. *History of exploratory wells drilled in the Peel Region, Yukon (Government of Canada, 1980).*

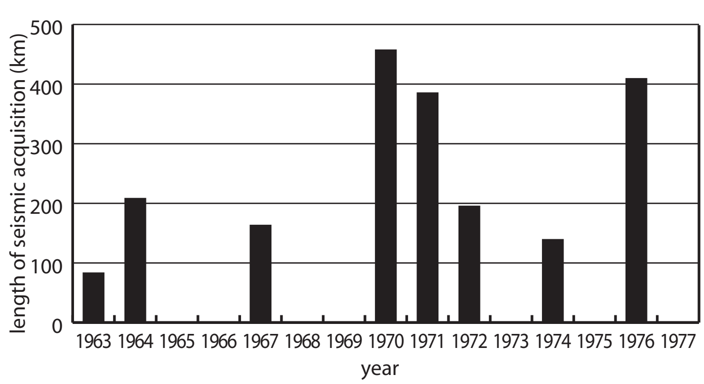

Figure 4. *History of 2D seismic acquisition in the Peel Region, Yukon (Oil and Gas Management Branch, 2001).*

GEOLOGICAL SETTING AND STRATIGRAPHIC FRAMEWORK

The Peel Plateau and Plain in the Yukon is underlain by a westerly thickening wedge of Phanerozoic sedimentary rock (up to 4.5 km thick), that unconformably overlies a poorly understood Proterozoic succession (Osadetz *et al.*, 2005). Phanerozoic strata in the region can be divided into three main depositional systems (Fig. 5): 1) Cambrian to Upper Devonian carbonates and shales of the Mackenzie Peel Shelf and Richardson Trough (Morrow, 1999); 2) an Upper Devonian to Carboniferous clastic

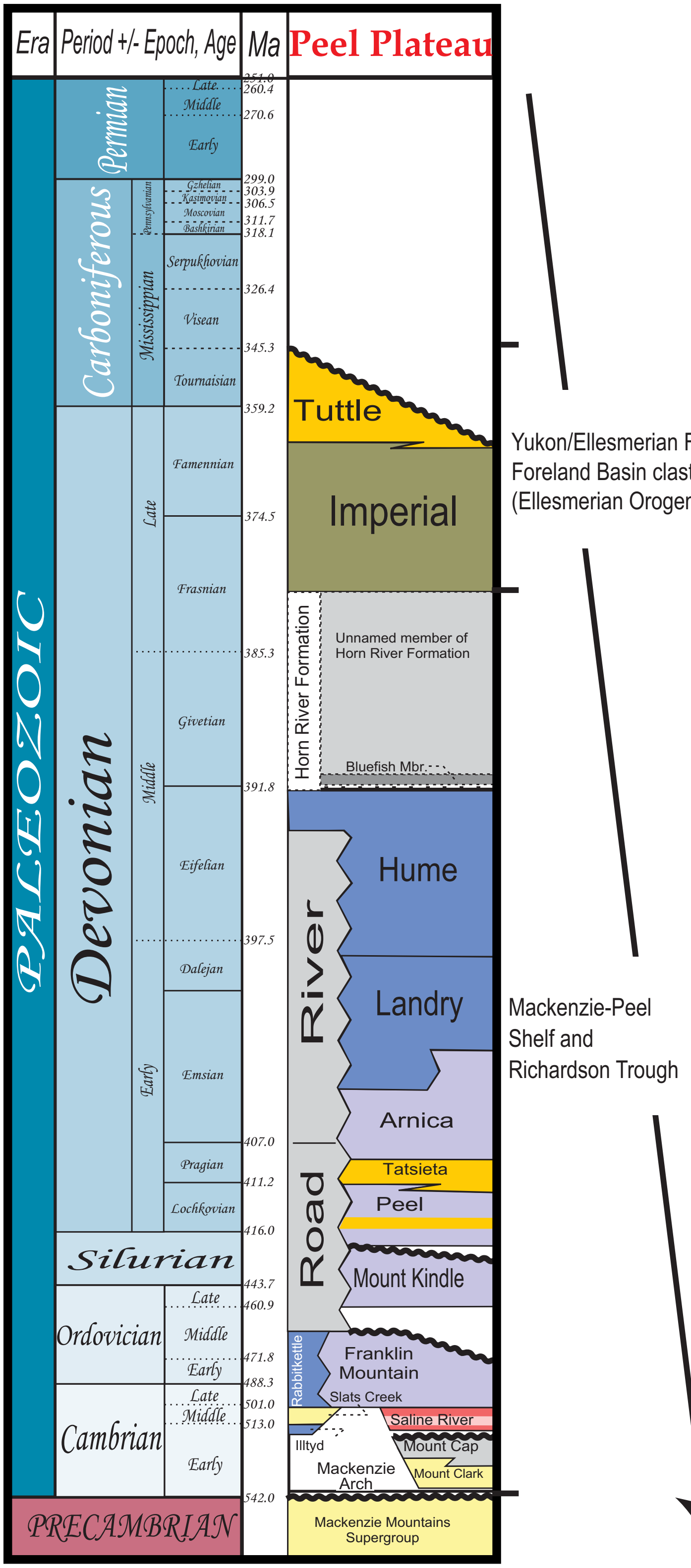

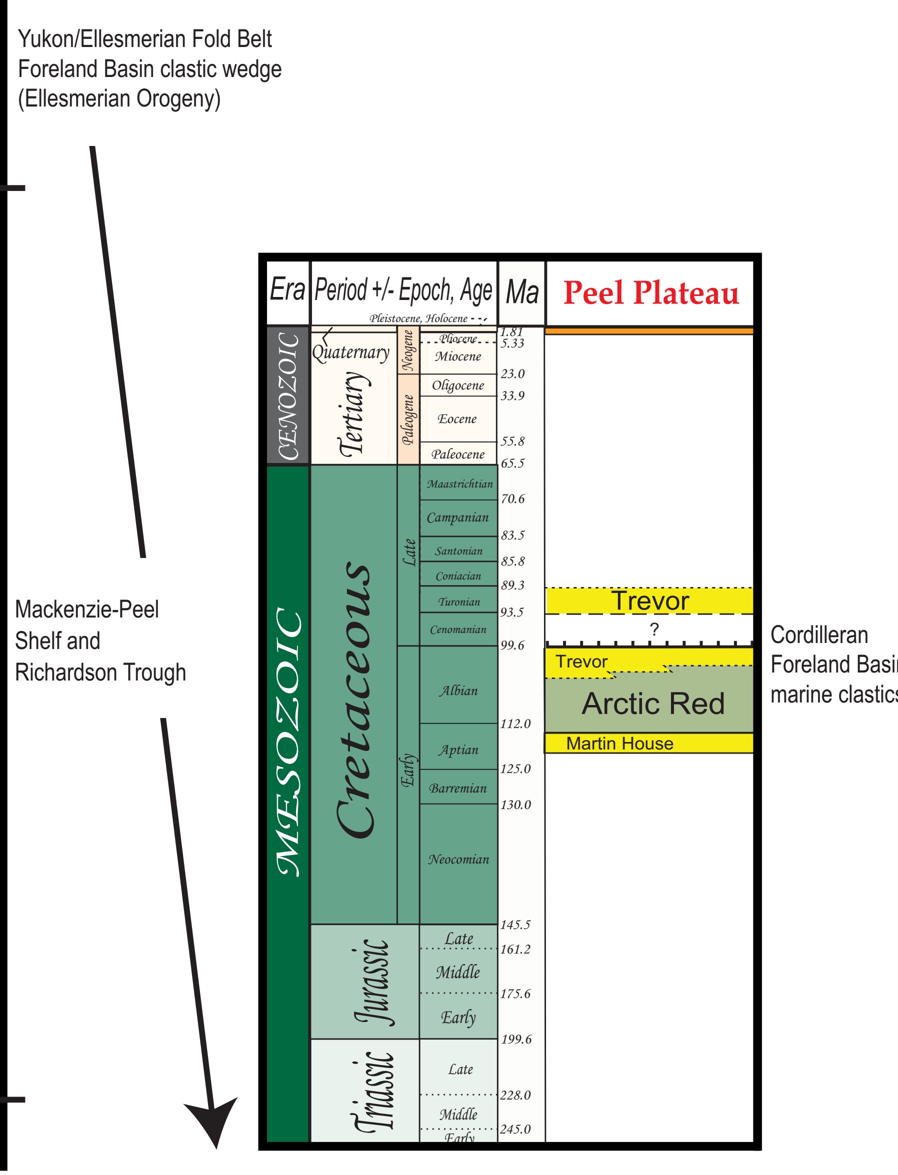

Figure 5. *Stratigraphic column for the Peel Plateau (from Morrow et al., 2006) highlighting the three main depositional systems of the Phanerozoic. Note that the column for the Richardson Mountains is similar except that this Cretaceous section has been removed by erosion.*

wedge that was deposited in a foreland basin of the Yukon and Ellesmerian fold belts associated with the Frasnian to Tournaisian Ellesmerian Orogeny (Richards *et al.* 1997); and 3) Cretaceous marine shelf deposits that were deposited in the foreland basin of the Cordilleran Orogen (Dixon, 1992).

The southern Richardson Mountains border the Peel Plateau to the west. The mountain ranges trend north and are an expression of the Richardson Anticlinorium, which is a broad, north-plunging structure bounded to the east by the Trevor Fault and to the west by Deception Fault (Norris, 1985). The Anticlinorium is a structural inversion of the Richardson Trough that occurred during the Laramide Orogeny (Osadetz *et al.*, 2005). The stratigraphy for the Richardson Mountains is correlative to the Peel Plateau and Plain, with the exception that most of the Cretaceous section has been removed by erosion.

The Upper Devonian to Carboniferous clastic wedge represents synorogenic deposition in the foreland of the Yukon and Ellesmerian fold belts (Richards *et al.*, 1997). The Ellesmerian Orogeny created a complex depositional setting across northern Yukon and the Northwest Territories with sedimentation derived from the west and north (Gordey, 1988). The clastic wedge consists of a thick (up to 1909 m, according to Richards *et al.* 1997) package of shale and siltstone, with lesser sandstone and limestone, comprising the Frasnian to Famennian Imperial Formation, and the overlying Famennian to Tournaisian Tuttle Formation (up to 1420 m, according to Pugh, 1983; see description below). Upper Devonian to Upper Mississippian Ford Lake Shale (Brabb, 1969) is the basinal equivalent to the Tuttle Formation and occurs further south and west of the Peel region (Pugh, 1983).

TUTTLE FORMATION

The Tuttle Formation has been described by many authors in the past, including Norris (1968, 1985, 1997), Lutchman (1977), Pugh (1983), Braman and Hills (1992) and Richards *et al.* (1997). Our definition of the Tuttle Formation follows Pugh (1983): he proposed the name Tuttle Formation for an alternating succession of coarse- to fine-grained clastic rocks overlying the Imperial Formation and unconformably overlain by Mesozoic strata in an area flanking the eastern, northern and western Richardson Mountains.

TYPE SECTION

The type section for the Tuttle Formation is the Pacific Peel Y.T. F-37 borehole which was drilled in 1972 in the Peel region of the Yukon (Fig. 6). In this well, the Tuttle Formation occurs between depths of 106.7 and 980.2 m from the surface and is 873.5 m in total thickness. At this

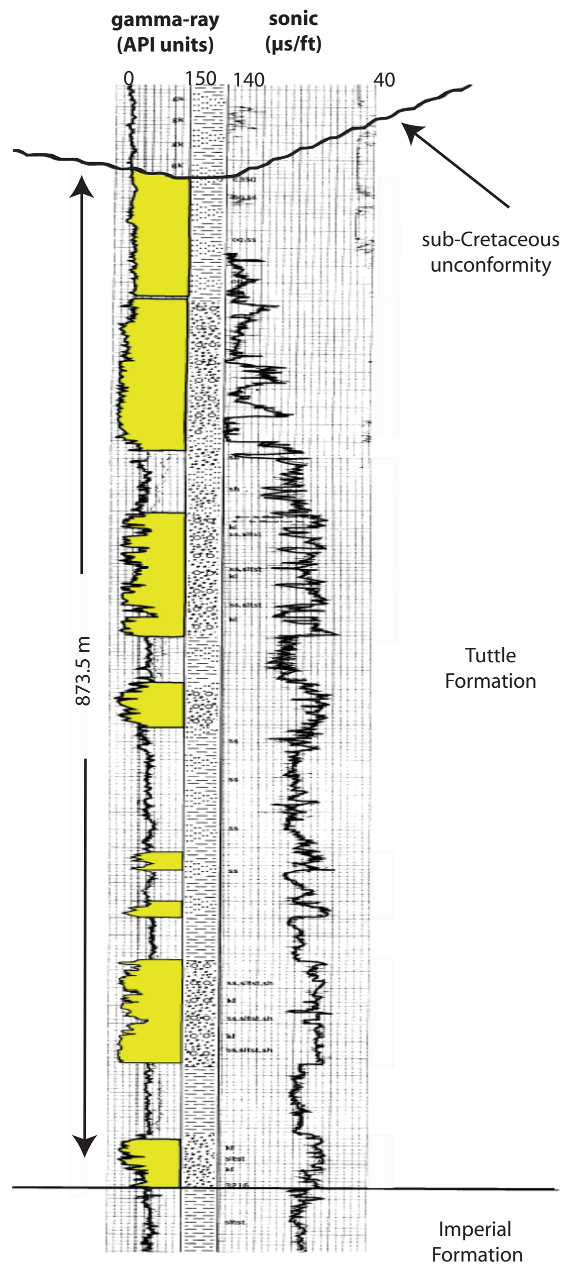

Figure 6. *Gamma-ray and sonic curves for the Tuttle Formation type section interval (106.7 to 980.2 m) in the Pacific Peel Y.T. F-37 borehole (see location on Fig. 1). Shaded areas represent coarser grained intervals (after Pugh, 1983).*

location, the Tuttle Formation overlies shale of the Upper Devonian Imperial Formation, and is eroded above by the sub-Cretaceous unconformity. Cretaceous marine siliciclastic rocks lie above the unconformity.

Pugh (1983) described the Tuttle Formation type-section as chert conglomerate, very poorly sorted quartz and chert sandstone, siltstone and shale. The conglomerate is predominantly multicoloured chert, including white, buff, grey, yellow, orange and pale green clasts. Most of the sandstone and shale beds are micaceous, with sandstone also containing kaolinite pore-filling cement. The top 100 m of the formation contains orthoquartzite beds. Pugh's (1983) definition of the Tuttle Formation includes the interval between the Imperial Formation and the overlying Mesozoic strata, including the map units 'Dus' and 'Cf' of Norris (1981b).

DISTRIBUTION

The Tuttle Formation is found at surface on the western and eastern flanks of the Richardson Mountains (northwestern circle area in Fig. 7). Norris (1982a,b) mapped a Carboniferous sandstone and shale, designated map unit 'MO', along the northern front of the Mackenzie Mountains on NTS map sheets 106E (Wind River) and 106F (Snake River) (southern circled area in Fig. 7). In the Yukon digital geology compilation map by Gordey and Makepeace (2001), the Tuttle Formation and map unit 'MO' were combined into the lower Carboniferous Tuttle Formation (i.e., map unit 'lCT'). Further field investigations are required to confirm this correlation. Surface exposures of the Tuttle Formation and map unit 'MO' are limited almost exclusively to the Yukon Territory.

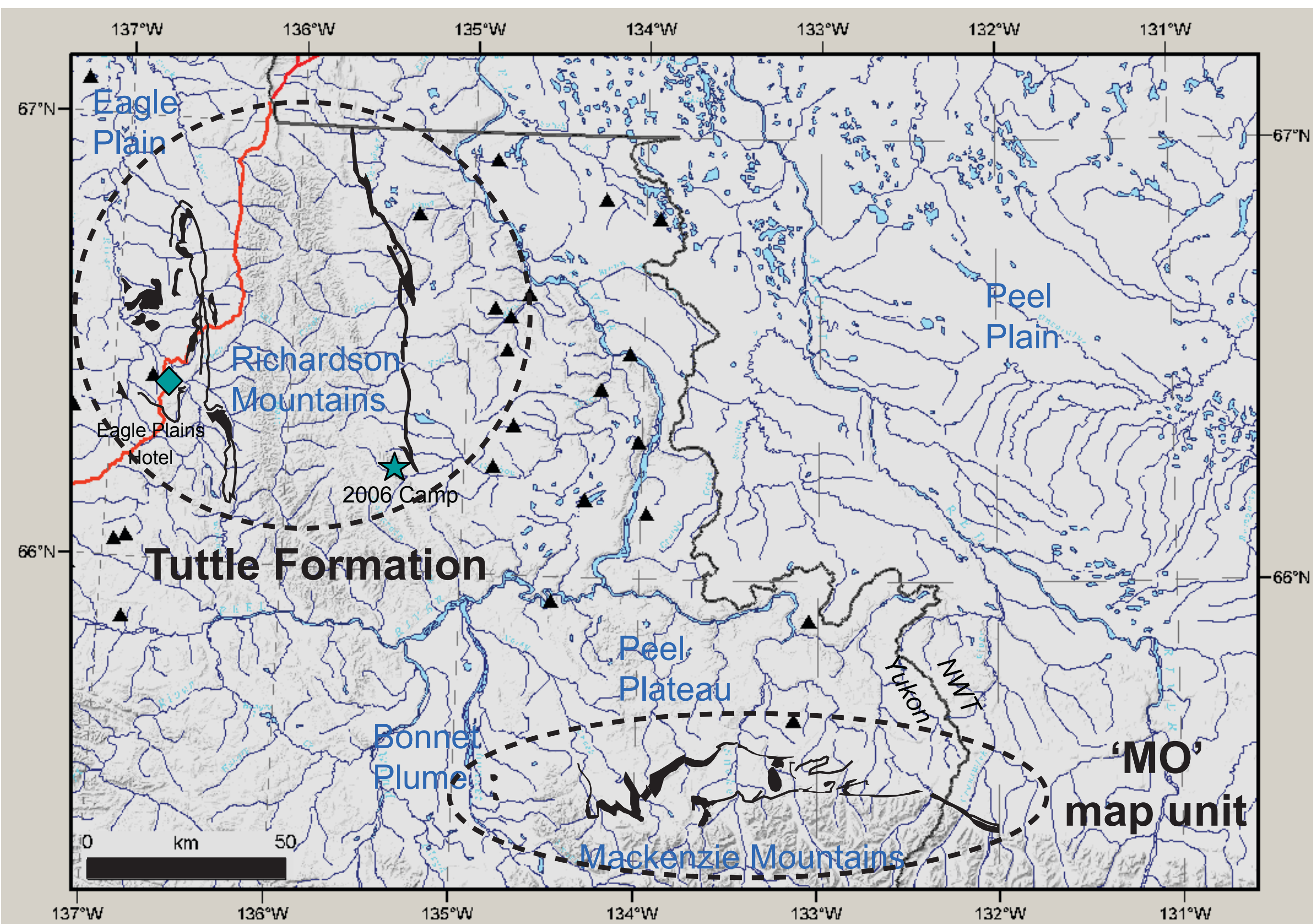

Figure 7. *Surface expression (black polygons) of the Tuttle Formation and map unit 'MO' of Norris (1981a,b; 1982 a,b). Triangles represent Yukon well locations.*

In the Peel region, the Tuttle Formation is intersected in eighteen Yukon and nine Northwest Territories boreholes. Figure 8 displays an isopach map of the Tuttle Formation in the Peel region, based on Pugh (1983), showing the range in thickness from 0 m at the western and eastern erosional edges to 1198.7 m in borehole H-37.

Pugh (1983) interpreted a maximum thickness of over 1250 and 1420 m for the Tuttle Formation on the east and west sides of the Richardson Mountain Anticlinorium, respectively. Norris (1985) suggests the depocentre of the Tuttle Formation was within what is now the Richardson Anticlinorium, before it was uplifted and Tuttle strata subsequently removed by erosion.

AGE

The Tuttle Formation on Trail and Road rivers has been assigned an early-middle Famennian to early Tournaisian age based on miospores (Hills *et al.*, 1984; Braman and Hills, 1992). Within the Tuttle Formation on Trail River, there is a change from possible middle Famennian miospores to latest Famennian or early Tournaisian miospores, suggesting that there may be a hiatus in the Formation (Braman and Hills, 1992). Parts of the section are missing, however, and in other parts the spores are highly carbonized making age determinations uncertain through this interval (Braman and Hills, 1992).

FIELD WORK AND PRELIMINARY FINDINGS

The 2006 field season involved an initial reconnaissance study of the distribution and accessibility of potential stratigraphic sections of the Tuttle Formation. Once exposures were identified, sections were measured and

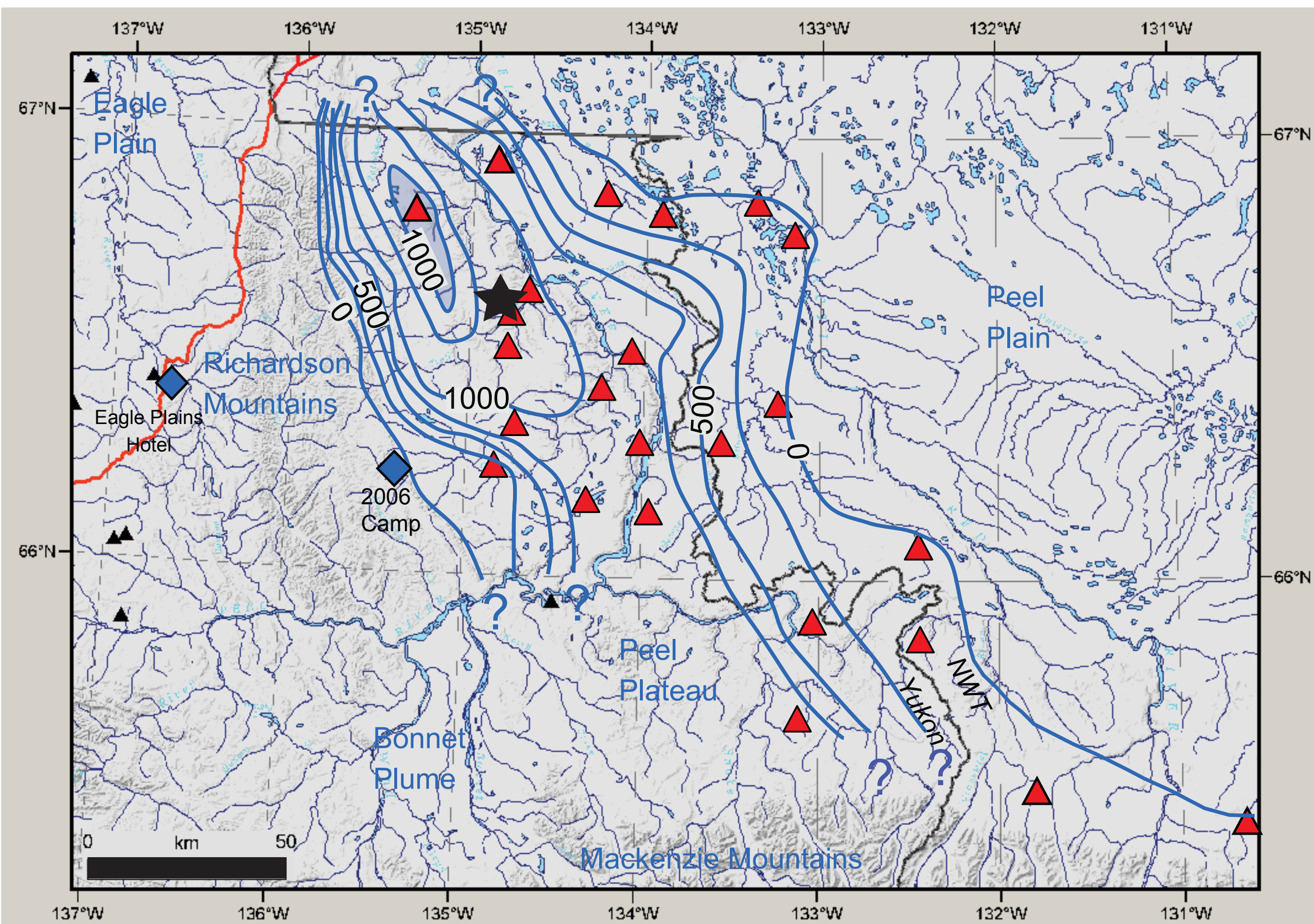

Figure 8. *Subsurface distribution of the Tuttle Formation in the Peel region. Contours represent thickness of Tuttle Formation in metres based on well data (after Pugh, 1983). Borehole H-37 (star) has the thickest Tuttle section in the Peel region at 1198.7 m. Dark grey triangles represent Peel region wells that intersect the Tuttle Formation.*

sampled to obtain data for use in future resource assessments. Samples were collected for porosity and permeability analysis for reservoir potential; Rock-Eval pyrolysis, total organic carbon, and hydrocarbon extraction analyses for source rock potential and thermal maturation determination; microfossils (i.e., spores and foraminifera) for dating; and thin sections for lithology and rock fabric. Most of the samples are still undergoing lab analysis.

Detailed sections of the Tuttle Formation were measured on the Trail and Road rivers. In addition, two visits to exposures of Tuttle Formation were made. Section and visit locations can be found on Figure 2.

MEASURED SECTIONS

The first impression of the Tuttle Formation in the field is its alternating resistant and recessive nature in outcrop. Resistant 'ribs' of dominantly sandstone, with lesser amounts of conglomerate and siltstone, alternate with recessive, covered units that are interpreted as siltstone and shale. In this paper, siltstone is applied to fine-grained clastic rocks composed primarily of silt-size grains and tends to be flaggy; shale is applied to rocks that exhibit fissility and are made up of clay-size material; while mudstone is applied to fine-grained rocks that are made up of silt- and clay-size material and lack fissility.

A total of 300 m of the Tuttle Formation was measured, but no complete section was observed in the field. Detailed sections were measured on both Trail and Road rivers, and for most of the sections, sedimentary structures were difficult to distinguish due to inaccessibility, lichen, cementation and mud cover.

The best exposed section of Upper Paleozoic strata was the Trail River section (Fig. 9). This section provided individual bed thicknesses, grain-size distribution, and sedimentary structures associated with the sandstone and shale of the Tuttle Formation and adjacent units. A total of 225 m of strata were measured (Fig. 10), which consisted of 81 m of resistant sandstone, with an intervening covered interval measuring 144 m. It was unclear in the field whether this section represented the base of the Tuttle Formation: the unit below the first sandstone rib consisted predominantly of shale, with lesser sandstone and siltstone. This is possibly the map unit 'Dus' of Norris (1981b). Norris (1981b) assigned strata above the Tuttle Formation to map unit 'Cf' (i.e., Carboniferous shale) on Trail River. However, we suggest that the Tuttle Formation may extend eastward to the Trevor Fault. This interpretation would be consistent with the findings of Braman and Hills (1992).

The section measured on Road River is 108 m thick, and consists of 53 m of resistant sandstone and a covered interval of 55 m. The strata are structurally complex and

Figure 9. *Sandstone interval of the Tuttle Formation exposed on Trail River (location within circled area on Trail River, Fig. 2). Stratigraphic thickness measured is 55 m. Top of section is to the right. Rock hammer (30 cm long) circled for scale.*

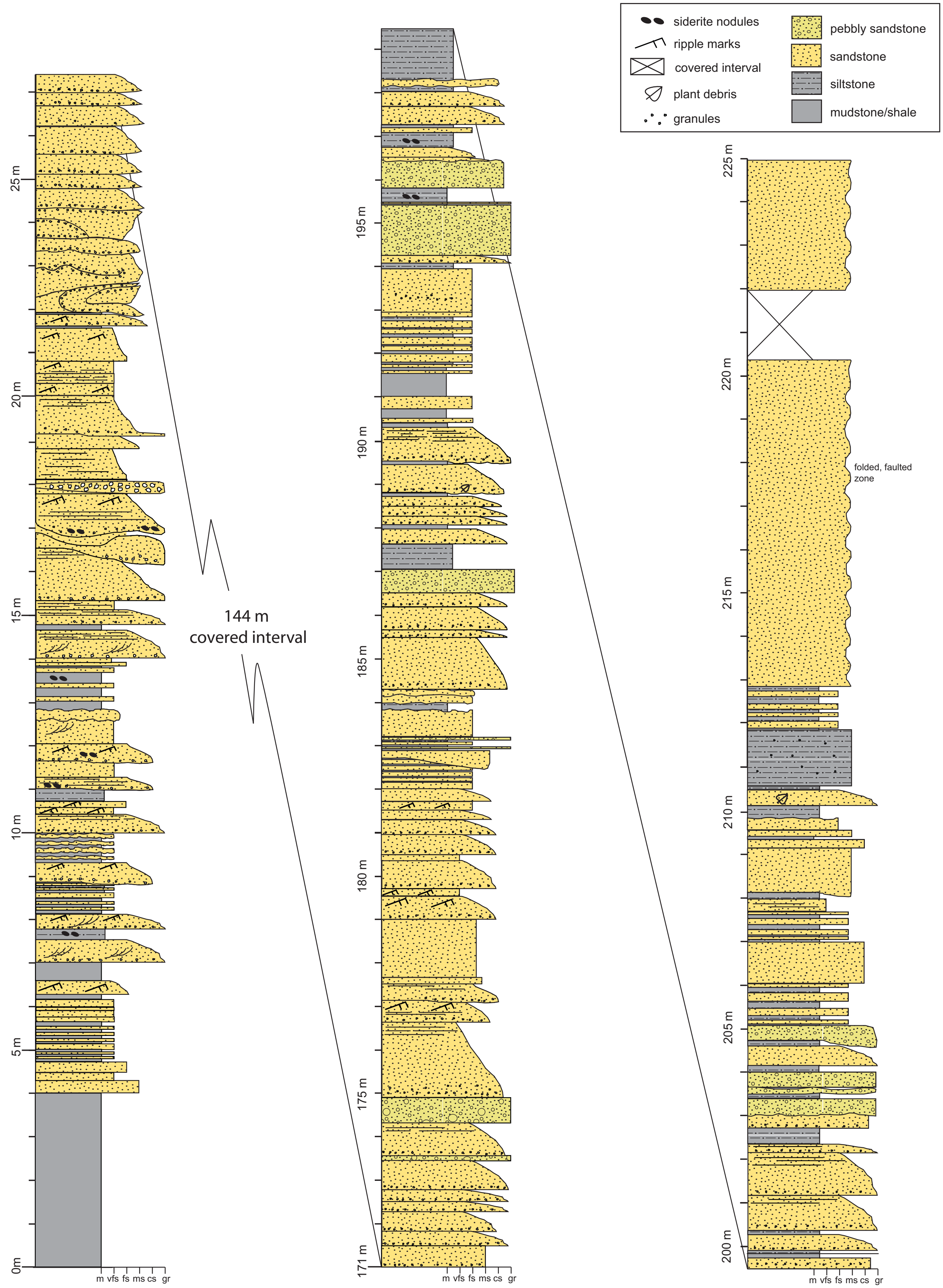

Figure 10. Measured stratigraphic section on Trail River.

an upper contact could not be determined. An additional 57 m of shale, with lesser amounts of sandstone and siltstone, was also measured below the Tuttle Formation, and tentatively assigned to the Imperial Formation.

SITE VISITS

Two visits to other Tuttle Formation exposures were made in the study area. The first was on a north-trending ridge south of Trail River (Fig. 2). At this location, the Tuttle Formation was exposed on surface and no fresh rock faces were observed due to lichen cover. Sandstone and conglomerate samples were taken for thin-section analysis and porosity and permeability determinations.

The second visit was to a large, steep exposure of the Tuttle Formation on a north-trending ridge north of Road River (Fig. 2). At this location approximately 8-10 m of conglomerate and lesser sandstone were exposed. A sample of conglomerate from the topmost 3 m of the exposure was obtained for thin section, and porosity and permeability determinations.

Figure 11. *Fining-upward sandstone on Trail River. Note the gradual fining up from granule-rich sandstone at the base to medium sandstone at the top. Granules are predominantly chert. Parallel laminae to large-scale planar crossbeds are evident in the sandstone. Hammer is 30 cm long.*

SEDIMENTOLOGY

The Tuttle Formation, as observed in outcrop along the eastern flank of the Richardson Mountains, consists of alternating packages of coarse-grained clastic rocks including medium- to very coarse-grained sandstone and conglomerate, with finer grained intervals of siltstone and shale that are largely covered. The sections measured on Trail and Road rivers indicate the coarse-grained packages range from 23 to 54 m thick, while the largely covered finer grained intervals range from 55 to 144 m thick.

Field investigations of the coarse-grained Tuttle Formation on Trail and Road rivers revealed five lithofacies that could readily be identified, including fining-upward sandstone, massive sandstone, siltstone, conglomerate and diamictite. These units are described in order of abundance observed in the field.

Fining-upward sandstone

Fining-upward sandstone is the most common lithofacies observed within measured sections of the Tuttle Formation (Fig. 11). The sandstone is light olive-grey to medium-grey on the fresh surface and weathers medium grey, dark yellowish orange or light brown. Individual fining-upward beds average 60 cm thick, with 100 cm being the thickest observed bed. The base of each bed is commonly marked by scours (up to 25 cm deep) and exhibits sole marks and/or load casts. Fining-upward beds tend to be stacked on top of one another and are locally separated by siltstone intervals less than 10 cm thick.

Fining-upward beds consist of coarse- to very coarse-grained sandstone with, or without, granules and pebbles at the base, grading to medium- to very fine-grained sandstone at the top. At the base, the sandstone is poorly sorted, containing up to 20% subangular to subrounded very coarse sandstone, granules or pebbles (less than 1.7 cm in diameter). The larger grains consist of varicoloured chert (i.e., grey, black, yellow, green), tripolitic chert (white) and quartz (smoky grey). The matrix consists of finer grained chert and quartz sandstone, which is generally more rounded than the larger grains. This basal zone is massive or cross-bedded. The top portion of the fining-upward beds are lithologically similar to the base, and are either massive, or parallel laminated. In the fine- to very fine-grained sandstone at the top, ripples were observed in laminations and beds 2 mm to 3 cm thick.

Commonly observed in this lithologic unit was a fine-grained, white chalky mineral precipitated in pore spaces. This mineral has been identified in previous work as kaolinite (Lutchman, 1977; Pugh, 1983). Fossilized plant debris occur as millimetre-size plant fragments on bedding planes, or as randomly oriented tree fragments. No *in situ* plant remains were identified.

Massive sandstone

The second most common lithofacies noted within measured sections of the Tuttle Formation is massive sandstone. The sandstone is light to medium grey and weathers dusky yellow, moderate brown, light olive-grey and greyish-orange. Beds range from 30 to 450 cm thick and have abrupt lower contacts. The sandstone is typically resistant, well indurated and blocky, but locally is friable and fractured.

The sandstone is poorly sorted and ranges from fine sand to granules (Fig. 12). Coarse sand to granule-sized grains comprise 5 to 25% of the overall rock texture. Larger grains are predominantly tripolitic chert (white) with lesser quartz (smoky grey). The chert grains are subangular to rounded, and contain a variety of internal structures including laminae and circular fragments (possibly radiolarian fossils), or are structureless. The matrix of the finer grained sandstone is chert- and quartz-rich. The sandstone on Road River has a greater proportion of quartz in the matrix than that on Trail River, resulting in a more indurated rock. Quartz overgrowths and fused-grain boundaries were observed in thin section. Other material includes 3% carbonaceous material, mud clasts up to 10 cm across, and white chalky pore filling interpreted as kaolinite.

Carbonized tree fragments, millimetre-size plant debris, and grey mudchips are common in this lithofacies, notably at the base of beds. Millimetre-sized carbonaceous material was concentrated along parallel laminae in the top portion of some beds. Siderite nodules and continuous bands were also observed locally.

Siltstone

Poorly exposed, recessive intervals of siltstone were noted between some of the sandstone beds described above. These intervals are typically less than 10 cm thick, but can be up to 50 cm thick. This lithofacies is dominated by siltstone with lesser mudstone and is dark grey to black, with rusty weathering. Thin laminae and beds of sandstone up to 3 cm thick were also observed in this unit. The sandstone is very fine-grained and quartz-rich with beds 1 to 10 cm thick, giving the unit a striped appearance (Fig. 13).

Conglomerate

The coarsest lithofacies observed was a matrix-supported, small-pebble conglomerate (Fig. 14). In the literature, conglomerate is described as one of the more abundant facies within the Tuttle Formation, however on Trail and Road rivers, it is a subordinate unit.

In measured sections, conglomerate beds normally did not exceed 60 cm in thickness. An exception is the north-trending ridge north of Road River, where conglomerate 8 to 10 m thick was exposed.

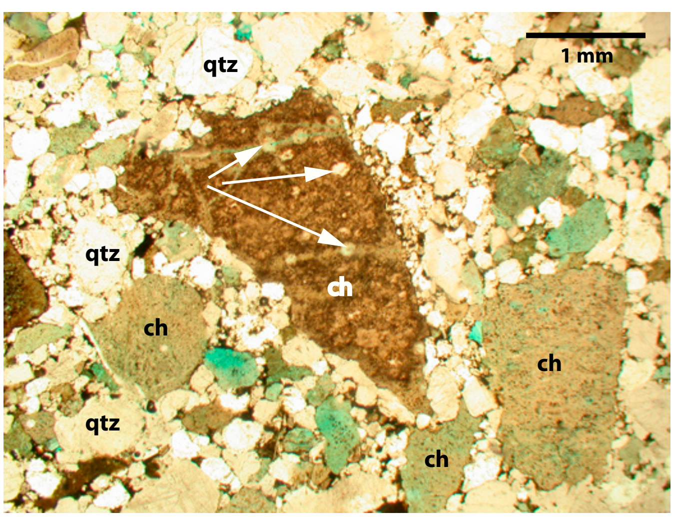

Figure 12. *Thin section of massive sandstone. Note the poor sorting and the larger chert (ch) and quartz (qtz) grains in a predominantly quartz matrix. There are possible radiolarian fossils in the chert clast in the middle of the figure (arrows).*

Figure 13. *Siltstone. Note the striped appearance enhanced by the alternating beds of light grey very fine-grained sandstone and dark grey siltstone.*

Figure 14. *Chert-pebble conglomerate from Trail River. Note the abundance of chert clasts. Chert in this sample is varicoloured including white, grey, black, yellow, and light green.*

Figure 15. *Diamictite on Road River consisting of rounded clasts within a blocky finer grained matrix. This lithology is very distinctive in the sections due to its dark colour and structureless appearance.*

On Trail and Road rivers, the conglomerate is typically matrix-supported with clasts averaging 1 cm across, although cobbles were observed locally. Conglomerate beds are lensoidal and are either massive or normally graded. Pebbles are subangular to rounded and are predominantly varicoloured chert (i.e., white, medium to light grey, light yellowish-grey, black, greyish-pink, bluish-grey, light and dark green and grey banded varieties) and quartz (white and smoky grey). Clasts are spherical. The matrix is composed of poorly sorted chert and quartz grains of variable sand sizes. Weathered surfaces are rusty.

Diamictite

Diamictite is the least abundant lithofacies observed and was only found on Road River. It is medium dark grey on the fresh surface and weathers blackish-red to greyish-red. This lithofacies appears dirty in contrast to neighbouring units and is extremely friable.

Diamictite consists of a disorganized mixture of mudstone, siltstone or very fine-grained sandstone supporting clasts of coarse sandstone, granules, pebbles and cobbles (up to 10 cm across). Clasts comprise up to 20% of the composition and are subrounded to round (Fig. 15). No internal sedimentary structures were observed, and the bases were scoop- or lobate-shaped. Beds vary in thicknesses from 85 to 220 cm. Disseminated carbonaceous plant debris is present locally.

POROSITY AND PERMEABILITY

Thirty Tuttle samples were submitted to AGAT Laboratories, Core Services Division in Calgary for analysis of porosity and permeability using standard procedures of AGAT Laboratories.[1] Out of the samples submitted, 28 were analysed using 38.1- to 25.4-mm (1.5- to 1.0-inch) plugs, with 2 samples insufficient for this type of analysis (i.e., plugs could not be made). A fracture in another sample produced permeability errors and is not reported here. All samples submitted were hand samples collected from the field and were chosen to represent a wide range of grain sizes from various Tuttle Formation outcrops.

Note that outcrop-based predictions of subsurface reservoir quality has certain limitations, including differences in diagenetic history and pore system evolution between surface and subsurface samples and the fact that recent outcrop diagenesis (leaching, cementation, sediment infill, etc.) may enhance or destroy porosity and permeability that occurs in the subsurface (Tobin, 1997). Hence, the results from this analysis will be used as an approximation of subsurface reservoir quality in a frontier region with otherwise sparse subsurface data.

[1]*AGAT Laboratories, 2006. Final Core Analysis Report, Outcrop Samples Miscellaneous Locations. Prepared for Yukon Geological Survey, 16 p.*

Figure 16 is a cross-plot of porosity (percent) versus permeability (millidarcies). Samples were divided into five classes based on grain size, including fine, medium and coarse sandstone, granule to pebble conglomerate, and a poorly sorted fine sandstone to granule conglomerate. The figure also displays reservoir porosity and permeability classes defined by Levorsen (2001).

Porosity ranged from 1.6% in coarse-grained sandstone to 18.6% in medium-grained sandstone. Permeability ranged from 0 to 13.7 mD in coarse-grained sandstone. Based on these surface samples, the best prospects for reservoir rock are medium-grained sandstone, followed by coarse-grained sandstone and then the poorly sorted fine sandstone to granule conglomerate.

The granule- to pebble-conglomerate has the poorest reservoir characteristics of samples analysed. Exceptions to these results are observations at a large conglomerate outcrop in the northern part of the study area. Vugs measuring up to approximately 15 cm in diameter were observed (Fig. 17). Two samples from this outcrop were submitted for porosity/permeability analyses. The first had poor to fair reservoir characteristics, and the second was unsuitable for testing because it was too friable to make a plug. We expect this second sample would have fair to good reservoir characteristics as it appeared porous in hand specimen.

Figure 17. *Vuggy conglomerate indicating high porosity at a Tuttle exposure north of Road River. Notebook is 18 cm long.*

HYDROCARBON OCCURRENCES

The Tuttle Formation has historically been an exploration target in both the Peel region and Eagle Plain. In the Peel, minor gas has been detected in six Yukon wells and in one Northwest Territories well (Table 1 and Fig. 18).

In Eagle Plain, gas has been detected in the Tuttle Formation in six wells. Four have had minor gas shows, and two wells, the Western Minerals Chance #1 L-08 (UWI 300L086610137300) and the Mobil Oil Birch Y.T. B-34 (UWI 300B346610136405), have estimated reserves of 57 x 10^6 and 81 x 10^6 m^3(2 and 3 billion cubic feet (BCF)), respectively (National Energy Board of Canada, 2000).

No record of oil shows exist in the literature, however a sample of bitumen-stained sandstone found in what is believed to be Tuttle Formation on Trail River is currently undergoing analysis as part of this study.

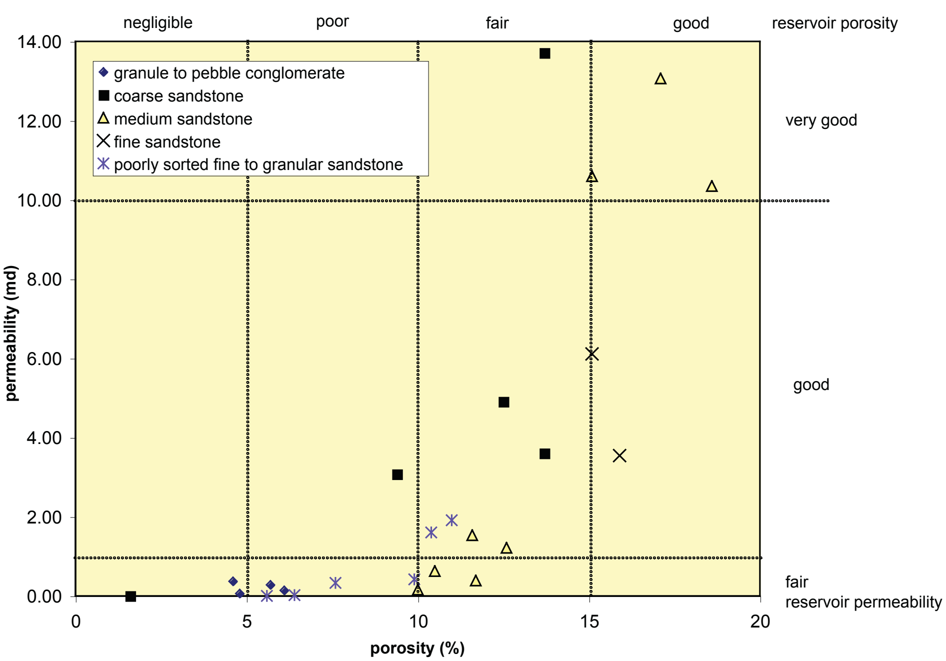

Figure 16. *Porosity/permeability cross-plot for 25 Tuttle surface samples. Samples were classified into five groups (granule to pebble conglomerate, coarse sandstone, medium sandstone, fine sandstone, and poorly sorted fine to granular sandstone) based on predominant grain size.*

***Table 1.** Historical gas shows in the Tuttle Formation in the Peel region (Government of Canada, 1980; Indian and Northern Affairs, 1966a and 1966b).*

Well name and unique well identifier (UWI)	Drill stem test (DST) depth	Recoveries
Shell Peel River Y.T. **B-06** (UWI300B066640134450)	DST #2 312.4-430.4 m (1025-1412 ft)	18.3 m (60 ft) mud; 18.3 m (60 ft) mud-cut water; gas to surface in 30 seconds; too small too measure
Shell Peel River Y.T. **B-06A** (UWI302B066640134450)	DST #1 798.3-866.9 m (2619-2844 ft)	789.4 m (2590 ft) partly gasified water; gas to surface in 45 minutes
McD GCO Northup Taylor Lake Y.T. **K-15** (UWI300K156600133000)	DST #1 729.4-737.0 m (2393-2418 ft)	30.5 m (100 ft) water-cut mud; 121.9 m (400 ft) mud-cut gassy fresh water
Shell Peel River Y.T. **M-69** (UWI300M696610133450)	DST #4 1742.8-1799.8 m (5718-5905 ft)	94 m (310 ft) mud; gas to surface too small to measure
Shell Peel River Y.T. **I-21** (UWI300I216620134150)	DST #2 767.5-888.8 m (2518-2916 ft)	418.5 m (1373 ft) fresh water, slightly gasified
Shell Canada Peel River Y.T. **L-01** (UWI300L016640134450)	DST #2 1338.7-1394.2 m (4392-4574 ft)	91.4 m (300 ft) water-cut mud; 182.9 m (600 ft) mud-cut water; 640 m (2100 ft) slightly gasified water
Arco Shell Sainville River **D-08** (UWI300D08662013330)	DST #5 898.6-907.7 m (2948-2978 ft)	gas to surface in 25 minutes; too small to measure

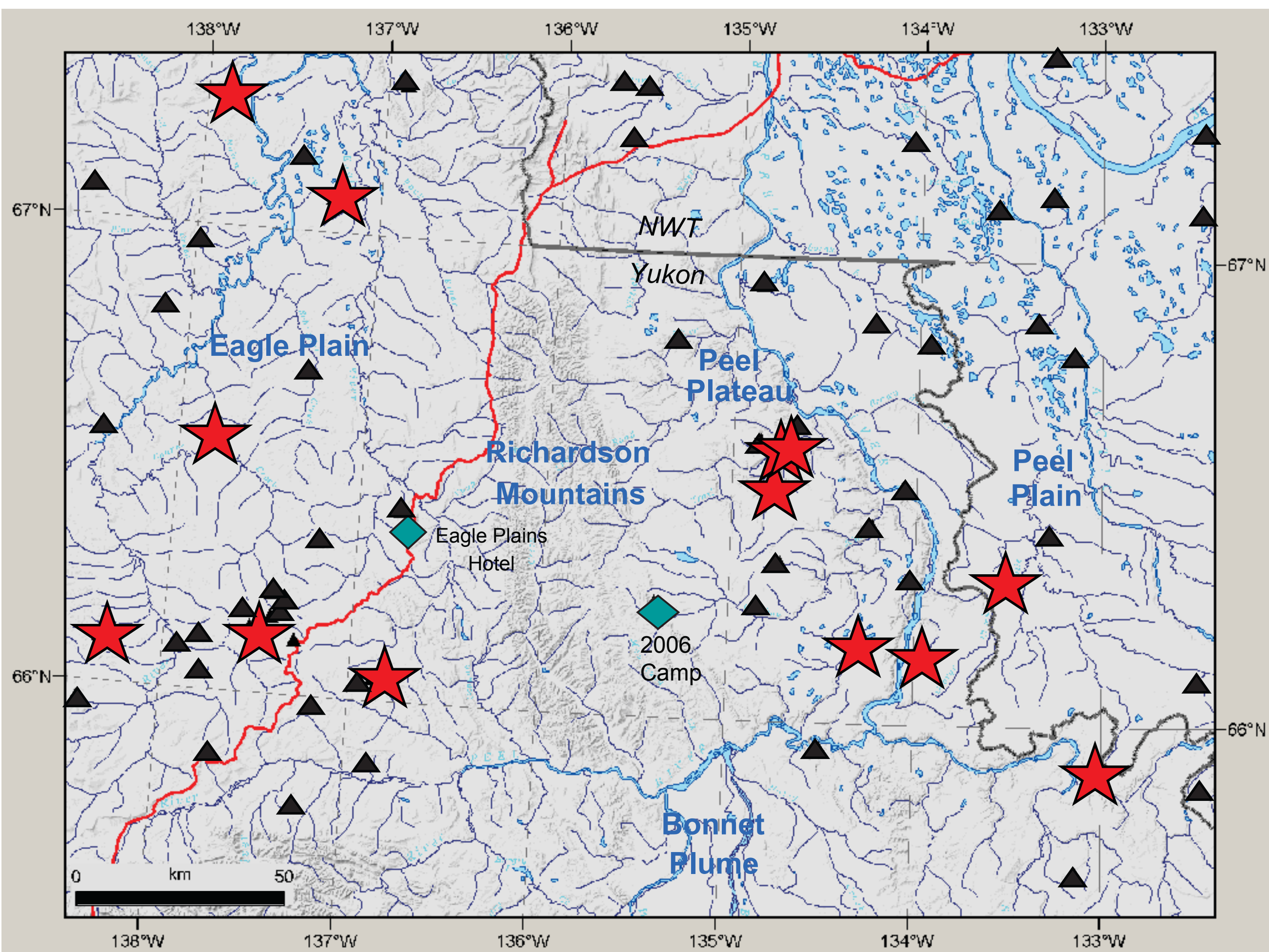

***Figure 18.** Map highlighting wells which have had gas shows (stars) in the Tuttle Formation in the Peel region (Government of Canada, 1980; Indian and Northern Affairs, 1966a,b) and Eagle Plain (National Energy Board of Canada, 2000; Osadetz et al., 2005a). Triangles indicate other wells in vicinity.*

CONCLUSIONS

The Tuttle Formation on the eastern flank of the Richardson Mountains was investigated as part of the four-year, multi-partner "Regional Geoscience Studies & Petroleum Potential, Peel Plateau and Plain" project. Field studies in 2006 in NTS map sheet 106L (Trail River) identified the Upper Devonian to Lower Carboniferous Tuttle Formation as alternating resistant and recessive intervals. Resistant intervals comprise chert- and quartz-rich sandstone, with lesser conglomerate and siltstone. Intervening poorly exposed, recessive intervals consist predominantly of siltstone and shale.

Exposed resistant sections of the Tuttle Formation on Trail and Road rivers are divided into five lithofacies, including fining-upward sandstone, massive sandstone with lesser siltstone, conglomerate and diamictite. In our map area we found only limited exposure of conglomerate. However, the distribution of conglomerate is reported as variable in the map area (Pugh, 1983; Norris, 1985).

Based on surface-sample analyses of porosity and permeability, the best prospects for reservoir rock are medium-grained sandstone, followed by coarse-grained sandstone, and then poorly sorted fine sandstone to granule conglomerate. Noticeable vuggy porosity was observed in Tuttle conglomerates on a ridge north of Road River. Minor gas shows have been found in the Tuttle Formation in the Peel region in six Yukon wells and in one NWT well. These gas shows, along with gas shows and combined reserve estimates of 138 x 10^6 (5 BCF) in the Tuttle Formation in Eagle Plain, show a promising future for the Tuttle Formation as a reservoir unit, and warrant further investigation.

ACKNOWLEDGMENTS

We would sincerely like to thank International KRL Resources Corporation for their helicopter and camp support this summer. Our research this year is greatly enhanced by their support. We would also like to thank Prism Helicopters and especially Simon the Australian pilot for providing safe and friendly flights. We would also like to thank the scientists at GSC Calgary for their support and enthusiasm towards our project. Thanks to Grant Lowey for critical review of this manuscript.

REFERENCES

Brabb, E.E., 1969. Six new Paleozoic and Mesozoic formations in east-central Alaska. U.S. Geological Survey, Bulletin, 27 p.

Braman, D.R. and Hills, L.V., 1992. Upper Devonian and Lower Carboniferous miospores, western District of Mackenzie and Yukon Territory, Canada. Palaeontolographica Canadiana, no. 8, 97 p.

Dixon, J., 1992. A review of Cretaceous and Tertiary stratigraphy in the Northern Yukon and adjacent Northwest Territories. Geological Survey of Canada, Paper 92-9, 79 p.

Gordey, S.P., 1988. Devono-Mississippian clastic sedimentation and tectonism in the Canadian Cordilleran Miogeocline. *In:* Devonian of the World, N.J. McMillan, A.F. Embry and D.J. Glass (eds.), Canadian Society of Petroleum Geologists, Memoir 14, vol. II Sedimentation, p. 1-14.

Gordey, S.P. and Makepeace, A.J. (compilers), 2001. Bedrock Geology, Yukon Territory. Geological Survey of Canada, Open File 3754; Exploration and Geological Services Division, Yukon Region, Indian and Northern Affairs Canada, Open File 2001-1, 1:1 000 000 scale.

Government of Canada, 1980. Schedule of Wells 1920-1979. Northwest Territories and Yukon Territory, Northern Non-Renewable Resources Branch, Oil and Gas Resources Evaluation Division, Exploratory Operations Section. Indian Affairs and Northern Development.

Hills, L.V., Hyslop, K., Braman, D.R. and Lloyd, S., 1984. Megaspores from the Tuttle Formation (Famennian-Tournasian) of the Yukon, Canada. Palynology, vol. 8, p. 211-224.

Indian and Northern Affairs, 1966a. Microfiche Well-History Report for Shell Peel River Y.T. I-21. Page 2 of Well Completion Data report.

Indian and Northern Affairs, 1966b. Microfiche Well-History Report for Shell Peel River Y.T. L-1. Page 1 of Water Analysis report by Chemical and Geological Laboratories.

Levorsen, A.I., 2001. Geology of Petroleum (2nd edition). AAPG Foundation, Oklahoma, p. 97-143.

Lutchman, M., 1977. Lower Mackenzie Energy Corridor Study. Geochem Laboratories Canada Ltd. and AGAT Consultants Ltd., 42 p.

Morrell, G.R. (ed.), 1995. Petroleum Exploration in Northern Canada: A Guide to Oil and Gas Exploration and Potential. Indian and Northern Affairs Canada, p. 12.

Morrow, D.W., 1999. Lower Paleozoic stratigraphy of northern Yukon Territory and northwestern District of Mackenzie. Geological Survey of Canada, Bulletin 538, 202 p.

Morrow, D.W., Jones, A.L. and Dixon, J., 2006. Infrastructure and Resources of the Northern Canadian Mainland Sedimentary Basin. Geological Survey of Canada, Open File 5152, 59 p.

National Energy Board of Canada, 2000. Petroleum resource assessment of the Eagle Plain, Yukon Territory, Canada. National Energy Board report for Yukon Department of Economic Development, Energy Resources Branch, 74 p.

Norris, A.W., 1968. Reconnaissance Devonian stratigraphy of Northern Yukon Territory and Northwestern District of Mackenzie. Geological Survey of Canada, Paper 67-53, 74 p.

Norris, A.W., 1985. Stratigraphy of Devonian outcrop belts in northern Yukon Territory and northwestern District of Mackenzie (Operation Porcupine area). Geological Survey of Canada, Memoir 410, 81 p.

Norris, A.W., 1997. Devonian. *In:* The Geology, Mineral and Hydrocarbon Potential of Northern Yukon Territory and Northwestern District of Mackenzie, D.K. Norris (ed.), Geological Survey of Canada, Bulletin 422, p. 163-200.

Norris, D.K., 1981a. Geology: Eagle River, Yukon-Northwest Territories. Geological Survey of Canada, Map 1523A, scale 1:250 000.

Norris, D.K., 1981b. Geology: Trail River, Yukon-Northwest Territories. Geological Survey of Canada, Map 1524A, scale 1:250 000.

Norris, D.K., 1981c. Geology: Martin House, Yukon-Northwest Territories. Geological Survey of Canada, Map 1525A, scale 1:250 000.

Norris, D.K., 1982a. Geology: Snake River, Yukon-Northwest Territories. Geological Survey of Canada, Map 1529A, scale 1:250 000.

Norris, D.K., 1982b. Geology: Wind River, Yukon-Northwest Territories. Geological Survey of Canada, Map 1528A, scale 1:250 000.

Norris, D.K. (ed.), 1997. Geology and mineral and hydrocarbon potential of Northern Yukon Territory and Northwestern District of Mackenzie. Geological Survey of Canada, Bulletin 422, 401 p.

Oil and Gas Management Branch, 2001. Whitehorse, Department of Energy, Mines and Resources, Yukon Government.

Osadetz, K.G., MacLean, B.C., Morrow, D.W., Dixon, J. and Hannigan, P.K., 2005. Petroleum Resource Assessment, Peel Plateau and Plain, Yukon Territory, Canada. Yukon Geological Survey, Open File 2005-3; Geological Survey of Canada, Open File 4841, 76 p.

Petrel Robertson Consulting Ltd., 2002. Regional Geological and Geophysical Assessment, Central Mackenzie Valley, NWT and Eagle Plain, YT, 553 p.

Pugh, D.C., 1983. Pre-Mesozoic geology in the subsurface of Peel River map area, Yukon Territory and District of Mackenzie. Geological Survey of Canada, Memoir 401, 61 p.

Pyle, L.J., Jones, A.L. and Gal, L.P., 2006. Geoscience Knowledge Synthesis: Peel Plateau and Plain, a prospective hydrocarbon province in the Northern Mackenzie Corridor. GSC Open File 5234; NWT Open File 2006-01, 85 p.

Richards, B.C., Bamber, E.W. and Utting. J., 1997. Upper Devonian to Permian. *In:* The Geology, Mineral and Hydrocarbon Potential of Northern Yukon Territory and Northwestern District of Mackenzie, D.K. Norris (ed.), Geological Survey of Canada, Bulletin 422, p. 201-251.

Tobin, R.C., 1997. Porosity prediction in frontier basins: a systematic approach to estimating subsurface reservoir quality from outcrop samples. *In:* Reservoir Quality Predication in Sandstones and Carbonates, J.A. Kupecz, J. Gluyas and S. Bloch (eds.), AAPG Memoir, vol. 69, p. 1-18.

Are mafic dykes in the Nor and Hart River areas of the Yukon correlative to the Bonnet Plume River Intrusions? Constraints from geochemistry

Julie Hunt[1]
Yukon Geological Survey

Derek Thorkelson[2]
Simon Fraser University

Hunt, J.A. and Thorkelson, D.J., 2006. Are mafic dykes in the Nor and Hart River areas of the Yukon correlative to the Bonnet Plume River Intrusions? Constraints from geochemistry. *In:* Yukon Exploration and Geology 2006, D.S. Emond, L. L. Lewis and L.W. Weston (eds.), Yukon Geological Survey, p. 175-180.

ABSTRACT

Samples of mafic to intermediate dykes were collected from the Nor and Hart River areas of the Yukon in regions underlain by metasedimentary rocks and breccia that have been correlated to Wernecke Supergroup and/or Wernecke Breccia. The samples were analysed for whole-rock and trace-element geochemistry and the results compared to those for intrusive suites in the northern Yukon.

RÉSUMÉ

Des échantillons de dykes mafiques à intermédiaires ont été prélevés dans les roches et les brèches métasédimentaires de la région des rivières Nor et Hart, pour lesquelles une corrélation a été établie avec le Supergroupe de Wernecke et les brèches de Wernecke. Ces échantillons ont été soumis à des analyses géochimiques de la roche entière et des éléments traces. Les résultats ont été comparés à ceux obtenus pour les suites intrusives dans le nord du Yukon.

[1]*currently at CODES, University of Tasmania, Julie.hunt@utas.edu.au*

[2]*dthorkel@sfu.ca*

INTRODUCTION

The Wernecke and Ogilvie mountains of the northern Yukon are largely underlain by metasedimentary rocks of the Wernecke Supergroup (WSG; Fig. 1; *e.g.*, Delaney, 1981; Abbott, 1997; Thorkelson, 2000). The Supergroup is host to a regional-scale mineralized breccia system known as Wernecke Breccia that is being actively explored for iron oxide-copper (± U ± Au) deposits (*e.g.*, Yukon MINFILE, Deklerk and Traynor, 2005; Hunt *et al.*, 2005). The absolute age of the Supergroup is not known but is constrained by the *ca.* 1710 Ma age of cross-cutting mafic to intermediate dykes and sills of the Bonnet Plume River intrusive suite (Thorkelson *et al.*, 2001).

Metasedimentary rocks and breccia also locally underlie the Nor and Hart River areas (Fig. 1). Little is known about these rocks, but they have been interpreted to be correlative with those of the WSG and Wernecke Breccia (*e.g.,* Norris, 1997; Abbott, 1997). Like those in the Wernecke and Ogilvie mountains, metasedimentary rocks in these areas are cut by mafic to intermediate dykes. Samples of the dykes were collected for geochemical and geochronological analyses to determine if they are correlative with the Bonnet Plume River intrusive suite. This paper presents the results of the geochemical analyses. Dating of the samples is currently taking place at the University of British Columbia.

BONNET PLUME RIVER INTRUSIONS – PREVIOUS WORK

The Bonnet Plume River Intrusions (BPRI) were emplaced as short dykes and small stocks, and most are composed of fine- to medium-grained diorite and gabbro; other (rare) compositions include syenite and anorthosite (Thorkelson, 2000; Thorkelson *et al.*, 2001). Primary mineralogy of the dioritic intrusions is dominated by plagioclase and clinopyroxene. However, regional low-grade metamorphism associated with the Paleoproterozoic Racklan orogeny and metasomatic alteration related to emplacement of the Wernecke Breccias have typically altered the mineral assemblage (*ibid.*). For example, pyroxene has altered to chlorite or actinolite, and plagioclase is pseudomorphed by sericite or scapolite. Other metasomatic effects include the introduction of hematite, magnetite, silica, carbonate, pyrite and chalcopyrite, in addition to sodium and potassium.

Generally, BPRI have a significant degree of large-ion lithophile element (LILE) enrichment and steep down-to-the-right trace-element profiles with modest depletions of Nb and Zr (Fig. 2a; Thorkelson *et al.*, 2001). Based on the geochemical data, Thorkelson *et al.* (2001) suggest that the BPRI were generated from mantle similar to that involved in the genesis of normal Mesozoic and Cenozoic sea floor. They suggest that the geochemical data are best explained by relatively small degrees of mantle anatexis,

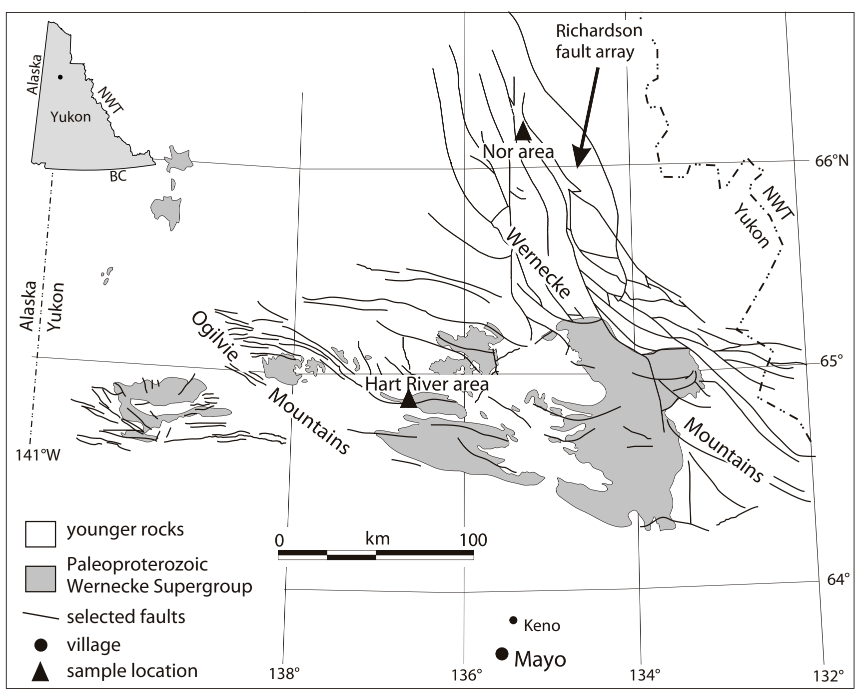

Figure 1. *Location map showing Nor and Hart River areas.*

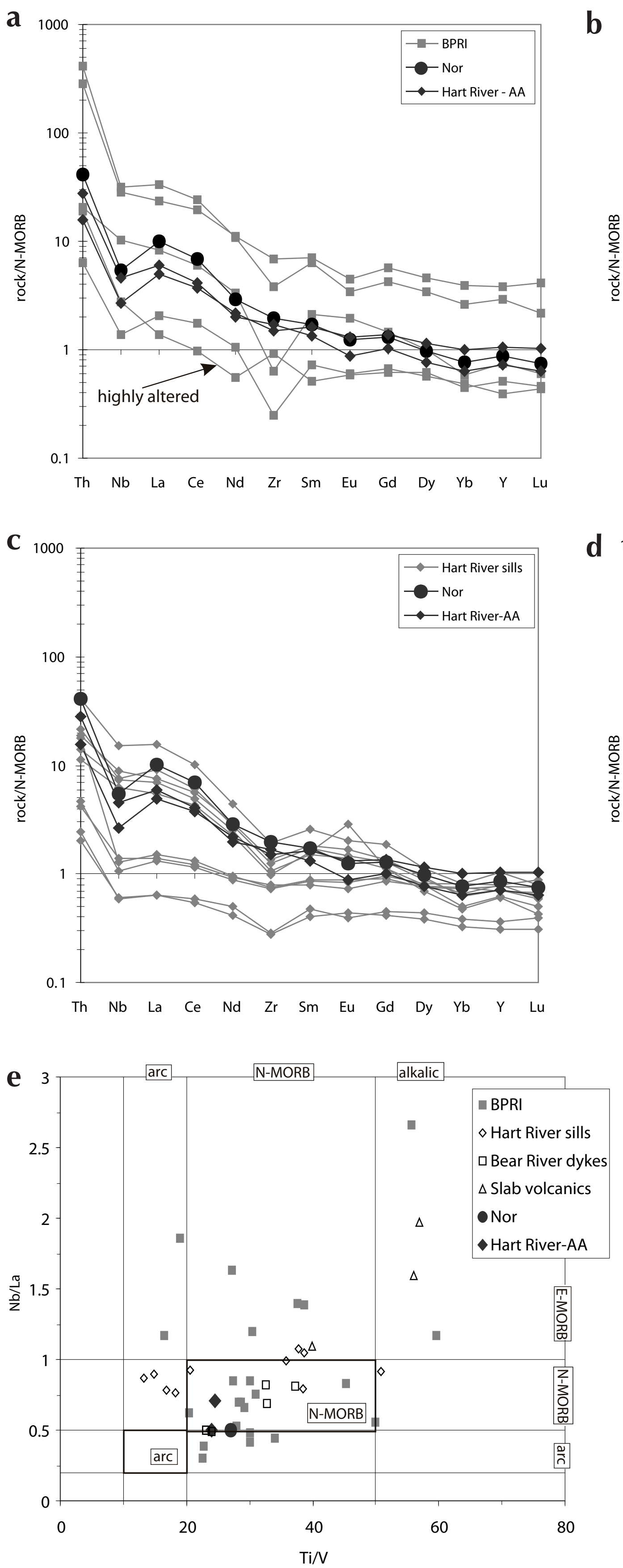

Figure 2. *Geochemical diagrams for the Nor and Hart River samples compared to those of intrusive suites in the northern Yukon.* ***(a) to (d)*** *N-MORB-normalized trace-element profiles:* ***(a)*** *compared to ca. 1710 Ma Bonnet Plume River Intrusions;* ***(b)*** *compared to > 1600 Ma Slab volcanics;* ***(c)*** *compared to ca. 1380 Ma Hart River sills;* ***(d)*** *compared to ca. 1270 Ma Bear River dykes;* ***(e)*** *bivariate plot using elemental ratios for distinguishing tectonic affinity (after Gill, 1981 and Shervais, 1982).*

possibly coupled with crustal assimilation; genesis in an extensional continental environment is their favoured interpretation.

PRESENT STUDY

LOCATION AND FIELD RELATIONS

Nor Area

The Nor area is located in the southern Richardson Mountains of north central Yukon, approximately 275 km north of the town of Mayo, and includes the Ewen (Nor) MINFILE occurrence located at 66°15'N, 135°23'W on NTS map sheets 106L/3 and 6 (Fig. 1; Yukon MINFILE 106L 061, Deklerk and Traynor, 2005). The Nor area is underlain by metasedimentary rocks that are likely correlative with the Fairchild Lake Group of the Wernecke Supergroup. These rocks are cut by hematitic breccia similar in appearance to bodies of Wernecke Breccia.

Subcrop, approximately 10 m x 3 m, of medium-grained, dark green chloritic 'syenite' occurs in an area of breccia (location: NAD83, UTM E0482884, N7349174, Zone 8). Specular hematite occurs locally on fractures within the syenite. Additional subcrop (~10 m x 2 m) of 'syenite' occurs approximately 1 km to the south (location: NAD83, UTM E0482697, N7348130, Zone 8); here, grey carbonate veins up to 1 cm across cut the syenite. A sample of the syenite was collected for petrographic and geochemical analyses and geochronology (sample JH05-22; Table 1).

Hart River Area

The Hart River area is approximately 150 km northwest of the town of Mayo and includes the AA mineral property located at 64°50'58" N, 136°40'48"W on NTS map sheet 116A/15 (Fig. 1). The AA area is underlain by metasedimentary rocks that are likely correlative with the Fairchild Lake and Quartet groups of the Wernecke Supergroup (Norris, 1997). Like the Nor area, the metasedimentary rocks are cut by hematitic breccia similar in appearance to bodies of Wernecke Breccia.

Subcrop (~10 m x 2 m) of medium-grained, dark green-grey, chloritic, weakly foliated diorite (location: NAD83, UTM E0419922, N7192733, Zone 8) occurs within limey, fine-grained metasedimentary rocks that are locally brecciated. Blebs of sulphide minerals up to 5 cm across and red iron-staining occur locally within the diorite. Additional diorite outcrops approximately 1 km to the east within an area of breccia (location: NAD83, UTM E0421245, N7192037, Zone 8). This diorite is medium- to fine-grained, dark to medium green, and chloritic. Minor disseminated epidote, specular hematite and specular hematite-bearing quartz veins occur locally within the diorite. Samples of the diorite were collected for petrographic and geochemical analyses and geochronology (samples JH05-H56 and JH05-H57; Table 1).

GEOCHEMISTRY

Samples from the Nor and Hart River areas were analysed by x-ray fluorescence for major oxides and by research-grade inductively coupled plasma mass spectrometry for trace elements; results are in Table 1.

The samples are somewhat altered; however, aspects of original composition can be revealed by using elements of relatively low mobility (*cf.* Thorkelson *et al.*, 2001). Figure 2 shows profiles of selected high-field-strength elements (HFSE), including rare-earth elements (REE) that have been normalized to normal mid-ocean ridge basalt (N-MORB). For comparative purposes, the Nor and Hart River area samples are plotted along with results for Bonnet Plume River Intrustions (BPRI; Thorkelson *et al.*, 2001) and other intrusive suites known to occur in the northern Yukon. BPRI data are from Thorkelson *et al.*, 2001. Remaining comparative data are from the Yukon Geochemical Database (Héon, 2003).

Results for the Nor and Hart River areas samples are similar (Fig. 2 a to d). They plot in the middle of the range for *ca.* 1710 Ma BPRI, have values lower than those of the >1600 Ma Slab volcanics, plot towards the upper part of the range for *ca.* 1380 Ma Hart River sills and are similar to *ca.* 1270 Ma Bear River dykes. Figure 2e is a bivariate plot that indicates tectonic affinity. The Nor and Hart River area samples plot in the N-MORB field and are similar to the BPRI and Bear River dykes in this respect.

SUMMARY

Geochemical results for samples of mafic to intermediate rocks from the Nor and Hart River areas are similar to those for a number of intrusive suites in the northern Yukon (Fig. 2). Thus, they cannot be definitively correlated with a particular regional intrusive suite based solely on chemistry. Results of geochronology, currently underway at the University of British Columbia, should help resolve this.

Table 1. *Geochemical analyses of samples from Hart River and Nor areas.*

sample # material: NTS map area: UTM Easting: UTM Northing:	JH05 22 syenite 106L/6 482884 7349174	JH05 H56 diorite 116A/15 419922 7192733	JH05 H57 diorite 116A/15 421245 7192037
SiO_2	50.03	52.23	48.53
Al_2O_3	13.57	12.78	14.02
Fe_2O_3	10.04	10.08	16.97
MnO	0.13	0.18	0.12
MgO	7.41	6.52	6.07
CaO	7.36	7.06	4.77
Na_2O	5.03	3.97	3.71
K_2O	0.71	0.61	0.78
TiO_2	1.03	0.88	1.73
P_2O_5	0.11	0.09	0.16
Cr_2O_3	0.05	0.03	0.01
LOI	4.57	4.71	2.56
original totals	100	99.14	99.41
V	229	215	434
Cr	340	200	60
Co	36	34	51
Ni	130	90	50
Cu	80	10	40
Zn	40	100	<30
Ga	18	15	19
Ge	2.2	1.8	2.4
As	<5	<5	<5
Rb	19	9	25
Sr	96	69	115
Y	24.2	20.1	29.3
Zr	146	125	110
Nb	12.7	10.6	6.2
Mo	<2	<2	<2

sample # material: NTS map area: UTM Easting: UTM Northing:	JH05 22 syenite 106L/6 482884 7349174	JH05 H56 diorite 116A/15 419922 7192733	JH05 H57 diorite 116A/15 421245 7192037
Ag	<0.5	<0.5	<0.5
In	<0.1	0.2	0.1
Sn	<1	<1	<1
Sb	3	2.9	3.1
Cs	0.6	0.5	0.5
Ba	157	89	141
La	25.2	14.9	12.3
Ce	51.8	30.6	28.1
Pr	5.91	3.73	3.82
Nd	21.2	14.5	15.9
Sm	4.54	3.49	4.3
Eu	1.27	0.892	1.33
Gd	4.77	3.75	5.03
Tb	0.8	0.63	0.91
Dy	4.46	3.51	5.27
Ho	0.88	0.71	1.08
Er	2.48	2.09	3.16
Tm	0.374	0.309	0.479
Yb	2.36	1.94	3.07
Lu	0.339	0.29	0.473
Hf	3.4	3	2.7
Ta	0.93	0.73	0.49
W	0.6	0.6	<0.5
Tl	<0.05	0.09	0.09
Pb	<5	10	<5
Bi	0.4	2.3	1.2
Th	4.96	3.36	1.89
U	3.72	0.81	0.37

Note: Sample locations are in Fig. 1. Major oxides are in wt.% and trace elements in ppm. LOI, loss on ignition (as reported in original total. NTS, National Topographic system; UTM, Universal transverse Mercator coordinates (Zone 8); Original total, all oxides plus LOI as reported by the laboratory.

ACKNOWLEDGEMENTS

We would like to thank International KRL Resources Corp. and Shawn Ryan for their hospitality and help with sample collection.

REFERENCES

Abbott, G., 1997. Geology of the upper Hart River area, eastern Ogilvie Mountains, Yukon Territory. Exploration and Geological Services Division, Yukon Region, Indian and Northern Affairs Canada, Bulletin 9, 92 p.

Deklerk, R. and Traynor, S., 2005. Yukon MINFILE – A database of mineral occurrences. Yukon Geological Survey, CD-ROM.

Delaney, G.D., 1981. The Mid-Proterozoic Wernecke Supergroup, Wernecke Mountains, Yukon Territory. *In:* Proterozoic Basins of Canada, Geological Survey of Canada, Paper 81-10, p. 1-23.

Gill, J.B., 1981. Orogenic andesites and plate techtonics. Springer Berlin, Heidelberg, New York, 358 p.

Héon, D., 2003. Yukon Regional Geochemical Database. Yukon Geological Survey, CD-ROM.

Hunt, J.A., Baker, T. and Thorkelson, D.J., 2005. Regional-scale Proterozoic IOCG-mineralised breccia systems: examples from the Wernecke Mountains, Yukon, Canada. Mineralium Deposita, vol. 40, no. 5, p. 492-514.

Norris, D.K., 1997. Geology and mineral and hydrocarbon potential of northern Yukon Territory and northwestern district of Mackenzie. Geological Survey of Canada, Bulletin 422, 401 p.

Shervais, J.W., 1982. Ti-V plots and the origin of modern and ophiolitic lavas. Earth and Planetary Science Letters, vol. 59, p. 101-118.

Thorkelson, D.J., 2000. Geology and mineral occurrences of the Slats Creek, Fairchild Lake and “Dolores Creek” areas, Wernecke Mountains, Yukon Territory. Exploration and Geological Services Division, Yukon Region, Indian and Northern Affairs Canada, Bulletin 10, 73 p.

Thorkelson, D.J., Mortensen, J.K., Creaser, R.A., Davidson, G.J. and Abbott, J.G., 2001. Early Proterozoic magmatism in Yukon, Canada: constraints on the evolution of northwestern Laurentia. Canadian Journal of Earth Sciences, vol. 38, p. 1479-1494.

A reconnaissance inventory of permafrost-related landslides in the Pelly River watershed, central Yukon

***Panya Lipovsky*[1]**
Yukon Geological Survey

Crystal Huscroft
Thompson Rivers University

Lipovsky, P. and Huscroft, C., 2007. A reconnaissance inventory of permafrost-related landslides in the Pelly River watershed, central Yukon. *In:* Yukon Exploration and Geology 2006, D.S. Emond, L.L. Lewis and L.H. Weston (eds.), Yukon Geological Survey, p. 181-195.

ABSTRACT

A reconnaissance inventory of permafrost-related landslides in the Pelly River watershed was conducted in 2006, largely in response to local community concerns regarding the potential impacts of climate change on slope stability and possible effects on water quality. Using aerial photograph analysis, satellite imagery, and visual inspection from a fixed-wing aircraft, over 100 permafrost-related slides were located near the Pelly and MacMillan rivers and various tributaries. Basic geomorphic characteristics were determined for many of the failures based on analysis of remote sensing data, and reviews of existing literature and surficial geology maps. Most of the landslides identified were small active-layer detachments and retrogressive thaw failures. Several large failures also illustrate important characteristics associated with permafrost-related landslides, including their source-area setting, triggers, high mobility, the longevity of their activity and their ability to impact very large areas. The nature and distribution of the identified failures highlights a number of implications for land-use in central Yukon and emphasizes the need for enhanced methods of permafrost detection and regional mapping in the Territory.

RÉSUMÉ

Un inventaire de reconnaissance des glissements de terrain associés au pergélisol dans le bassin versant de la rivière Pelly a été entrepris pendant l'été de 2006. Ces travaux ont été effectués en réponse à des inquiétudes de la communauté quant aux incidences possibles du changement climatique sur la stabilité des talus et les effets possibles sur la qualité de l'eau de la rivière Pelly. D'après l'analyse de photographies aériennes et d'images satellites ainsi qu'une inspection visuelle par avion, plus de 100 glissements associés au pergélisol ont été repérés près des rivières Pelly et MacMillan ainsi que de divers tributaires. Les caractéristiques géomorphologiques de base d'un grand nombre de ces glissements ont été déterminées d'après des analyses de données de télédétection et des examens de la documentation et des cartes existantes sur la géologie des dépôts meubles. La plupart des glissements de terrain identifiés étaient de petits décollements de la couche active et effondrements régressifs dus au dégel. Plusieurs grands effondrements illustrent en outre d'importantes caractéristiques associées aux glissements de terrain reliés au pergélisol dont le cadre de l'aire d'origine, les mécanismes de déclenchement, la durée d'activité et l'aptitude à perturber de très grandes étendues. La nature et la distribution des effondrements identifiés mettent en lumière un certain nombre d'incidences pour l'utilisation des terres dans la région du centre du Yukon et soulignent la nécessité de méthodes améliorées de détection et de cartographie à l'échelle régionale du pergélisol dans le territoire.

[1]*panya.lipovsky@gov.yk.ca*

INTRODUCTION

Several recent studies have documented the occurrence of permafrost-related landslides in south and central Yukon (Ward *et al.*, 1992; Huscroft *et al.*, 2004; Lipovsky *et al.*, 2006; Lyle, 2006) and northern British Columbia (Geertsema *et al.*, 2006; Geertsema and Pojar, 2006). These highlight the fact that such failures are common in discontinuous permafrost regions. Findings from these studies demonstrate that permafrost-related landslides commonly occur in, or proximal to, valley bottoms, suggesting that they are a source of significant sediment into watercourses. Recent increased turbidity in the Pelly River has raised community concerns about possible new sediment sources in the Pelly River watershed. In addition, there are growing concerns about the potential impacts of projected climate change on slope stability in permafrost terrain and the implications this may have for land use in the region.

In light of these facts, a reconnaissance inventory of permafrost-related landslides in the Pelly River watershed was completed during the summer of 2006 to determine the general nature and distribution of these types of failures. This paper describes the results of this work and reviews a number of examples that illustrate some key characteristics of permafrost-related landslides that are important to consider for land-use planning and development in central Yukon.

BACKGROUND

Permafrost contributes to slope stability through its influence on soil drainage, soil moisture and soil strength (McRoberts and Morgenstern, 1974; Dyke, 2004). Ice-rich permafrost, in particular, leads to highly unstable conditions if it thaws. In flat terrain, thermokarst develops when large amounts of ice thaws, allowing the remaining soil particles to consolidate and the ground surface to settle. On slopes, thawing of ice-rich permafrost releases excess water, creating very high pore pressures and highly unstable conditions.

There are two main types of permafrost-related landslides that occur in permafrost terrain. Retrogressive thaw slumps (also known as bimodal flows) are triggered by the initial exposure of massive ground ice, leading to melting and the growth of a steep frozen headscarp. Initial exposure can result from many types of disturbances including river erosion, forest fires, small slope failures, groundwater piping, or even tree blow-downs and animal burrows (McRoberts and Morgenstern, 1974; Lyle, 2006). Ice exposed in the headscarp rapidly and steadily thaws, and the headscarp can retreat up to tens of metres per year (Lyle, 2006). The headscarp eventually stabilizes when either all the ice has thawed, or the headscarp becomes insulated by debris that has fallen from above (Mackay, 1966). The thawing soil is continually transported away in highly mobile debris flows that can travel several kilometres down very gentle slopes to valley bottoms or directly into watercourses. Retrogressive thaw slumps can remain active for decades and can expand in size quite rapidly, as will be shown in the discussion.

Active-layer detachments occur entirely within the active layer, the shallow surface layer of soil (generally < 2 m thick) that thaws and refreezes annually. The permafrost table (the upper surface of permafrost located at the base of the active layer) is impermeable and restricts drainage due to its high ice content. Active-layer detachments are commonly triggered in large numbers by events that lead to rapid increases in active-layer depth, rapid thawing of ice-rich permafrost, and/or sustained soil saturation, such as intense rainstorms or forest fires (Lekowicz and Harris, 2005). They occur on shallow slopes as low as 6° (McRoberts and Morgenstern, 1974) and commonly have a long narrow shape (Lewkowicz and Harris, 2006). While generally relatively small in size (5-20 m wide by up to 200 m long), they commonly occur in large numbers on individual slopes (Lipovsky *et al.*, 2006). Where they reach valley bottoms, they can also contribute a large amount of sediment into watercourses.

STUDY AREA SETTING

The areas investigated for this study included slopes immediately adjacent to the Pelly, MacMillan and South MacMillan rivers and selected major tributaries. The study area was generally limited to within 5 km of the aforementioned rivers, within the region bounded by the communities of Pelly Crossing to the west and Ross River to the south, the North Canol Road to the east, and the South MacMillan River to the north (Fig. 1).

PHYSIOGRAPHY

The study area largely lies within the Yukon Plateaus physiographic region (comprised of the Klondike, Stewart and Lewes Plateaus, MacMillan Highland and Willow and Ross Lowlands). The Tintina Trench dissects the plateau areas in a northwesterly trending direction. Upland areas in the eastern part of the study area include the Selwyn Mountains (Hess and Simpson Ranges) north of the

Tintina Trench, and the Kaska Mountains (Pelly Mountains) to the south (Fig. 1).

The Pelly River flows for over 500 km, draining nearly 50 000 km^2 (Water Survey of Canada[1]). Its headwaters lie in the southern Selwyn Mountains. For nearly half of its length, it flows northwesterly along the Tintina Trench, draining the Pelly Mountains to the south and the Anvil Range to the north. It then cuts westward across the Lewes Plateau, just above its confluence with the MacMillan River about 40 km east of Pelly Crossing, and empties into the Yukon River approximately 40 km west of the same community.

The MacMillan River drains approximately 14 000 km^2 (Water Survey of Canada) with the headwaters of the North and South MacMillan rivers located in the central Selwyn Mountains. The South MacMillan and MacMillan rivers flow westward for approximately 200 km through the Yukon Plateaus, draining the Wilkinson Range to the south, and the Russell Range and Clark Hills to the north.

Bedrock geology on the northeast side of the Tintina Trench is generally dominated by Selwyn Basin sedimentary formations of shales, cherts and sandstones that formed off the margin of ancient North America prior to 320 million years ago. Southwest of the trench, a wide variety of younger lithologies from the Yukon-Tanana and Cassiar terranes are found (Gordey and Makepeace, 2003).

Earthquakes have been recorded in the study area, mostly south of the Tintina Trench; the largest (since 1953) occurred 20 km west of Ross River in November, 2002 with a magnitude of 4.6. Only one other earthquake greater than magnitude 4 has been recorded throughout the study area since 1953 (Geological Survey of Canada records).

GLACIAL HISTORY AND SURFICIAL GEOLOGY

Surficial geology throughout most of the study area is primarily a product of the Late Pleistocene McConnell glaciation. This glaciation occurred between 26 000 and 10 000 years ago, covering south and eastern Yukon and reaching its western limit near the confluence of the Pelly and MacMillan rivers (Ward and Jackson, 1993a). During

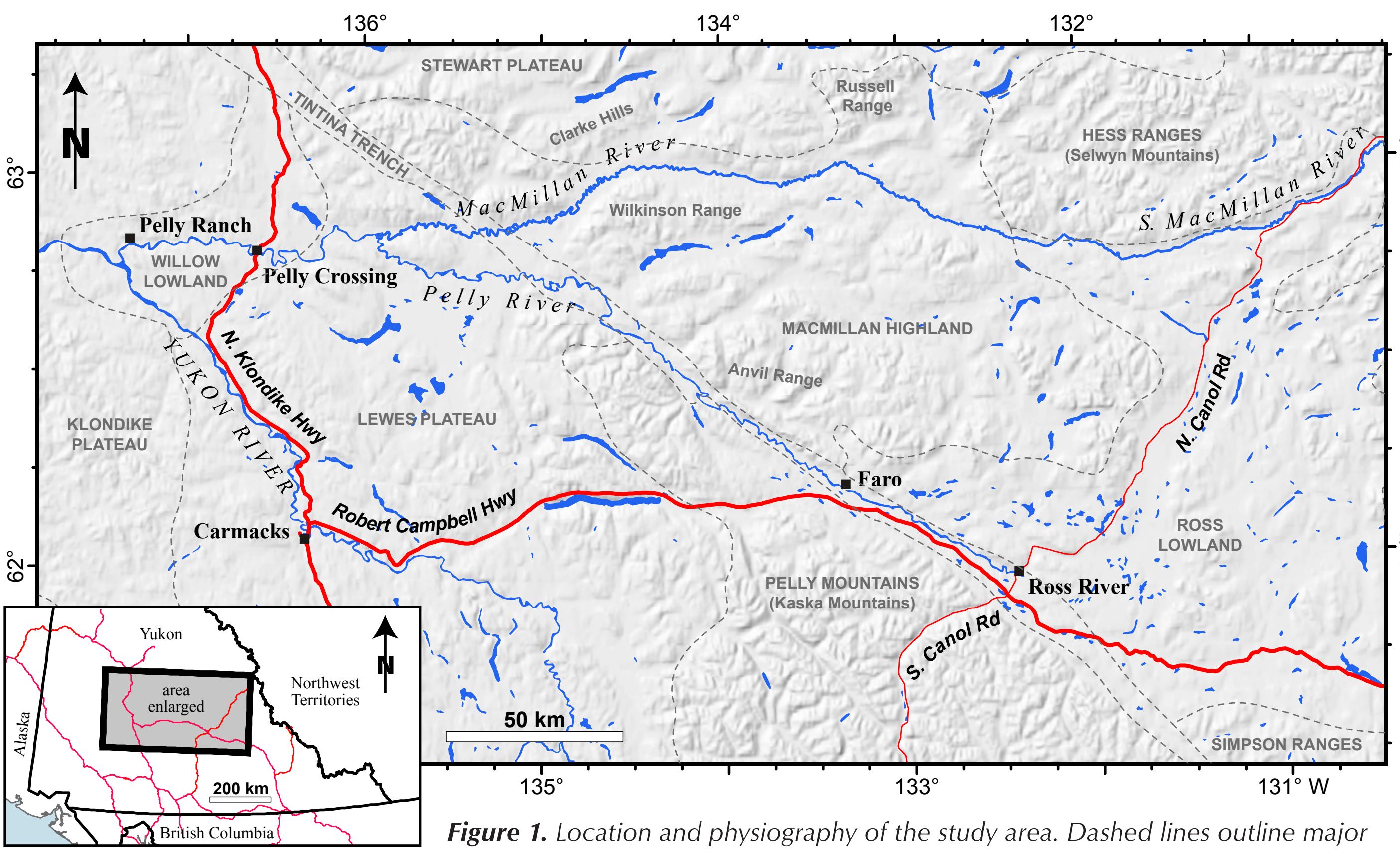

Figure 1. *Location and physiography of the study area. Dashed lines outline major physiographic regions. Inset map shows major roads in southern Yukon and regional location of study area.*

[1]*http//www.wsc.ec.gc.ca/hydat/H2O/index_e.cfm*

the maximum extent of the McConnell glaciation, the Selwyn lobe of the Cordilleran Ice Sheet flowed out of the Selwyn Mountains in a westerly and northwesterly direction following the main valley of the Tintina Trench (Jackson *et al.*, 1991; Ward and Jackson, 2000). Middle Pleistocene Reid glacial deposits are found west of the McConnell glacial limit near the mouth of the MacMillan River, down to the confluence of the Pelly and Yukon rivers (Jackson, 1997).

As a result of these glaciations, extensive blankets of silt-rich till, derived from the sedimentary Selwyn Basin lithologies, were deposited in low-lying valleys and on most slopes in the study area. Streamlined landforms are common in plateau areas, indicating westerly and northwesterly ice-flow directions, following the general trend of major valleys. As glacial retreat occurred, coarse-grained glaciofluvial meltwater materials were deposited in large meltwater channels and outwash plains that occupied the main valleys. During glacial retreat, large glacial lakes were dammed by ice in many of the main valleys and thick deposits of fine-grained glaciolacustrine material are now found along the lower reaches of the MacMillan River (Ward and Jackson, 1993a,b), and along the Pelly River between Ross River and about 50 km downstream of Faro (Jackson, 1993c).

PERMAFROST

Most of the study region is located in the extensive discontinuous permafrost zone, although the area south of the Pelly River where it flows through the Tintina Trench is located at the northern margin of the sporadic discontinuous permafrost zone (Heginbottom *et al.*, 1995). Local permafrost distribution and ground ice-content is controlled by a number of site-specific factors including aspect, surficial material texture, slope position, elevation, drainage conditions, vegetation cover, microclimate, duration and depth of snow cover, and past and present hydrogeological conditions (Rampton *et al.*, 1983). In general, ice-rich permafrost is most commonly found within silt-rich and organic-rich surficial materials on north-facing slopes and in valley bottoms.

A variety of permafrost features occur throughout the study area, as shown on regional-scale surficial geology maps (Jackson, 1993a,b,c,d,e and 1997; Jackson *et al.*, 1993a,b; Ward and Jackson, 1993a,b,c). Thermokarst commonly occurs in fine-grained glaciolacustrine terraces and in organic-rich alluvial and morainal materials along the MacMillan and Pelly rivers. Pingos also occur in a few locations within till, glaciofluvial and alluvial materials.

CLIMATE

The study area experiences a subarctic continental climate with long cold winters and short warm summers. Environment Canada online climate normals for the period 1971-2000 were used to summarize the following climate characteristics for climate stations at Pelly Ranch (62°49'N, 137°22'W, elevation 454 m, located 35 km west of Pelly Crossing) and Faro (62°12'N, 133°22'W, elevation 717 m) (Fig. 1). Mean annual temperatures are -3.9°C and -2.2°C, respectively. Mean annual precipitation is 310 mm and 316 mm, respectively, and two-thirds of this falls in the summer months.

Monthly temperature and precipitation normals indicate very similar conditions and seasonal variations for the two climate stations (Fig. 2). Mean daily temperatures at Pelly Ranch range between -27.5°C (daily minimum -32.8°C) in January to +15.5°C in July (daily maximum 22.6°C). July is the wettest month, receiving a mean monthly precipitation of up to 59 mm in Faro and 55 mm at Pelly Ranch. Snow depths reported for the two climate stations are up to 33 cm (at the end of each month), and snow cover generally persists between October and April.

HYDROLOGY

Table 1 shows average daily discharges for the Pelly and MacMillan rivers at various times throughout the year (data from Water Survey of Canada online archives). Peak flows are dominated by snowmelt and generally occur in early June, with discharge rates gradually diminishing into the winter. Local spikes in the discharge occur in response to intense rainfall events.

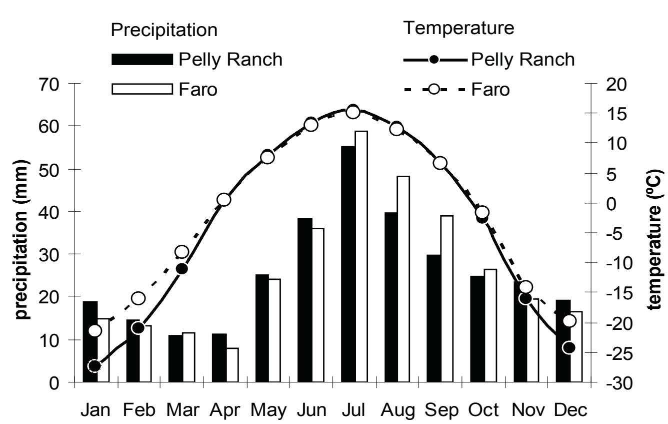

Figure 2. *Monthly temperature and precipitation normals (1971-2000) for Pelly Ranch and Faro (from Environment Canada online climate data).*

Table 1. *Range of average daily flows for the Pelly and MacMillan rivers throughout the year. (Data from Water Survey of Canada online archives).*

	Mean peak discharge (m^3/s) (early June)	Peak discharge range (m^3/s) (early June)	Discharge range (m^3/s) (Nov. 1)	Period of record
Pelly River				
~100 km east of Ross River (below Fortin Creek)	350	275–600	20–75	1986–1994
near Faro (below Vangorda Creek)	850	500–1800	50–150	1972–2005
at Pelly Crossing	1600	700–4300	80–500	1951–2005
South MacMillan River at North Canol Road	85	55–190	5–15	1974–1996
MacMillan River near confluence with Pelly River	600	250–1100	40–95	1984–1996

LANDSLIDE INVENTORY

SURVEY METHODOLOGY

A variety of sources were used to locate over 150 landslides within the corridor surrounding the Pelly, Ross, MacMillan and South MacMillan rivers. Eleven 1:100 000-scale surficial geology maps by Jackson (1993a,b,c,d,e and 1997), Jackson *et al*. (1993a,b) and Ward and Jackson (1993a,b,c) provide nearly complete coverage of the entire study area. Thirty-four large landslides were located on these maps, which were interpreted primarily in the early 1980s. A detailed review of the most recent (1988-2004) 1:40 000-scale aerial photographs available along the corridor was used to classify these landslides, and locate 67 smaller and more recent failures. Finally, a fixed-wing reconnaissance survey was flown on July 11, 2006 up the Pelly River to Ross River, north to the South MacMillan, and back down the MacMillan River to Pelly Crossing. Forty-three additional landslides were identified during this fixed-wing aerial survey. Both previously described and newly identified landslides were documented with digital photographs and GPS locations.

The landslides were described and classified as completely as possible to determine type, relative size, area and setting by analysis of digital photographs, aerial photographs, satellite imagery (GoogleEarth[2]), 1:50 000-scale digital topographic maps and 1:100 000-scale surficial geology maps. The ages of selected large landslides were also constrained from historical aerial photographs.

RESULTS

Permafrost-related landslides were classified as active-layer detachments or retrogressive thaw slumps, and where the type could not be confirmed, they were classified as 'probable' based on setting and/or morphology (Table 2). Relative sizes were assigned to each landslide: those wider than 500 m or having travel distances or runouts longer than 500 m were considered large; those less than about 100 m wide or 100 m long were considered small; and all remaining intermediate sizes were considered medium. The distribution of the identified landslides is shown in Figure 3.

Table 2. *Numbers and relative sizes of landslides identified in 2006 survey.*

Landslide type	Total	Large	Medium	Small
Permafrost-related landslides	114	32	48	34
active-layer detachments	47	10	18	19
probable active-layer detachments	5	1	1	3
retrogressive thaw slump	52	12	27	13
probable retrogressive thaw slump	11	8	2	1
Non-permafrost-related landslides	36	7	18	11
slumps along cutbanks	19	2	9	8
probable slumps along cutbanks	3		2	1
debris flows/slides in alpine areas	9		7	2
rock slumps	5	5		

Active-layer detachments

At least 47 active-layer detachments were identified throughout the study area. These occurred primarily on north-facing slopes covered by till veneers and blankets, but also within colluvial

[2]earth.google.com/

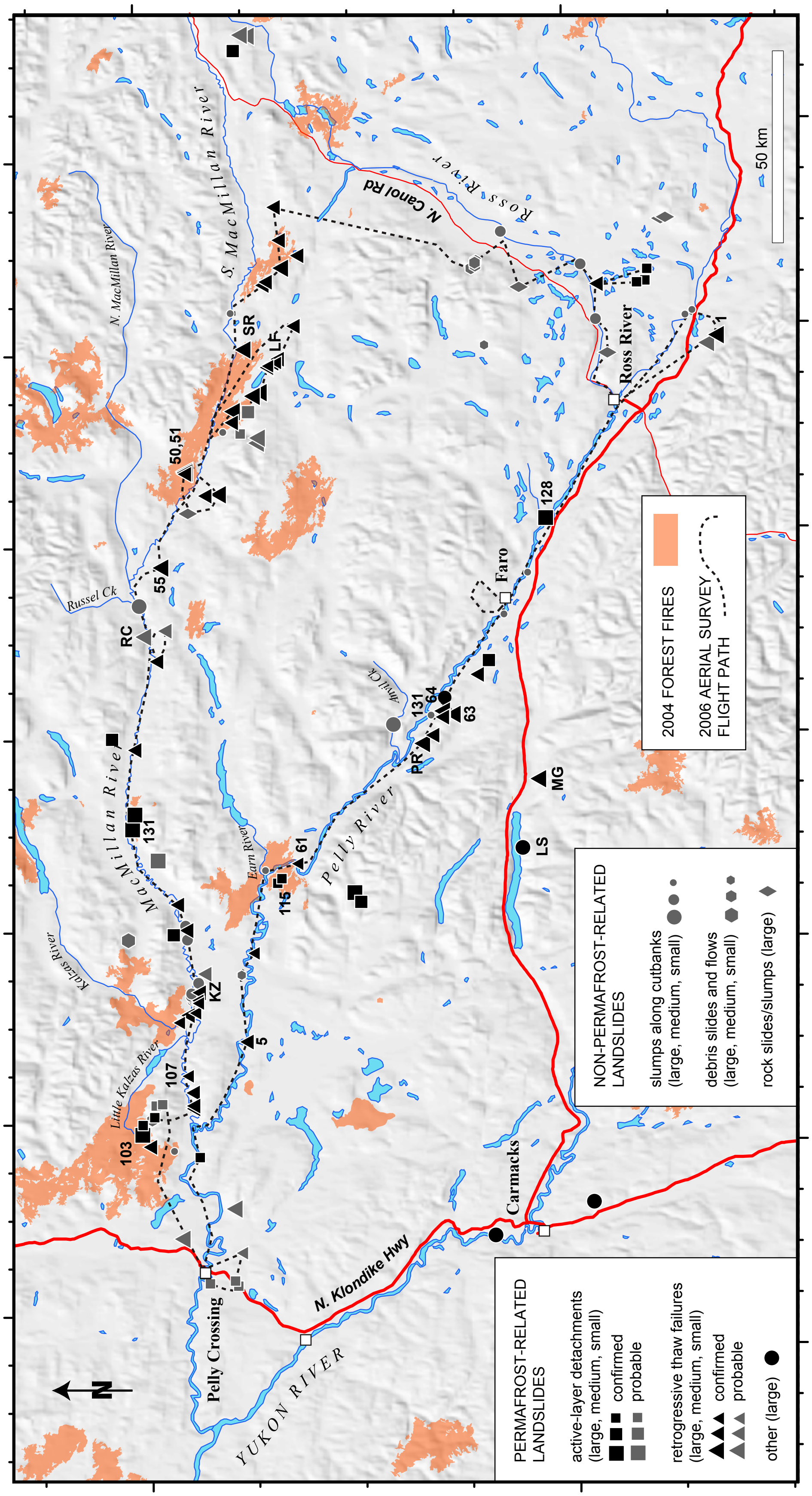

Figure 3. Location and classification of landslides described in the inventory. Numbers and letters refer to specific landslides mentioned in the text.

Figure 4. *A large active-layer detachment was initiated on a gentle north-facing slope near the mouth of Excell Creek following forest fires in 2004. The failure is estimated to be approximately 300 m long. Photo taken in July, 2006.*

Figure 5. *Multiple small active-layer detachments (highlighted by arrows) were initiated by forest fires in 2004. The slides occur in colluviated till on northeast-facing slopes having angles between 13-16°. Photo taken in July, 2006.*

materials. Only 10 large active-layer detachments were identified. Two of these appeared to have occurred very recently based on the sharply defined headscarps and lack of vegetation regeneration; these were likely initiated by forest fires that burned in 2004 near Faro (Fig. 4 and #128 in Fig. 3), and in the headwaters of the Little Kalzas River near the mouth of the MacMillan River (#103 in Fig. 3). At least 10 small active-layer detachments also appear to have been triggered by the 2004 forest fires on northeast-facing slopes adjacent to the Pelly River, approximately 2 km upstream from the mouth of Earn River (Fig. 5 and #115 in Fig. 3).

Most of the remaining active-layer detachments identified appeared as old overgrown scars. Seven large active-layer detachments occurred prior to 1949 on a north-facing slope south of the MacMillan River, just upstream from the mouth of Moose River (#131 in Fig. 3). The scars from these failures cover nearly 50% of an approximately 2-km-wide stretch of this slope, suggesting that this mode of failure is probably a significant slope-forming process in the area.

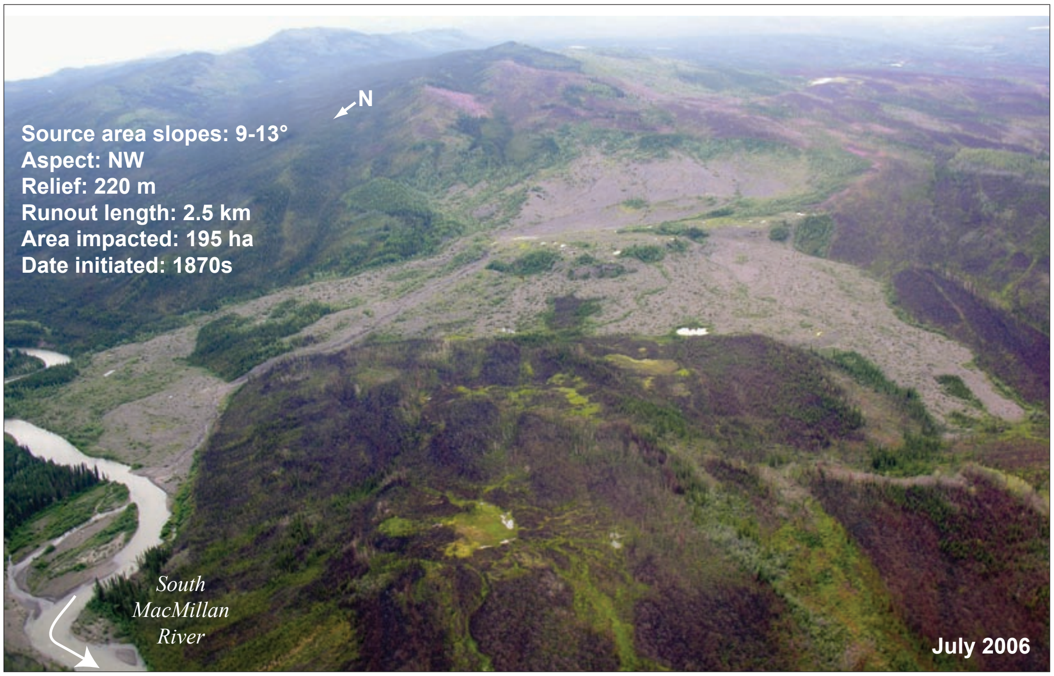

Figure 6. *The Surprise Rapids landslide covers nearly 2 km^2. Debris has traveled up to 2.5 km from the source area, which is approximately 700 m wide. View is to the southeast.*

Retrogressive thaw slumps

Twelve large retrogressive thaw failures were identified throughout the study area on slopes mantled by till blankets or veneers. Nine of these were located along the South MacMillan River on northwest- to northeast-facing slopes. One large failure suspected to be permafrost-related was located on a south-facing slope further down the MacMillan River, just downstream from the mouth of Russel Creek (RC in Fig. 3). Three large inactive failures occurred along the Pelly River upstream from the mouth of Anvil Creek (#63, 64 and PR in Fig. 3), and one occurred upstream of Ross River and south of Bruce Lake (#1 in Fig. 3). Nearly all of the large failures were initiated decades ago, prior to 1980 and as far back as 1870, with the exception of the two south-facing failures (Clarke Peak and Russel Creek), which occurred after 1988. At least five of the large slumps have been active within the last five years (#50, 51, 55, RC and SR in Fig. 3) and two of these (#50 and 51) appear to have been reactivated by forest fires in 2004.

The Surprise Rapids landslide (Fig. 6 and SR in Fig. 3), located 90 km north of Ross River on the South MacMillan River, is one of the largest retrogressive thaw slumps documented in central Yukon, impacting an area of almost 2 km^2. It was likely triggered by a forest fire in the 1870s, and initiated from gentle source slopes (9-13°) mantled by a blanket of clay-rich till with a high ice content (Ward *et al.*, 1992). The failure has remained active since it was initiated, and the highest levels of activity have coincided with a period in the 1940s when record early summer temperatures occurred in central Yukon (Ward *et al.*, 1992). The aerial survey in the summer of 2006 revealed that the thaw failure had not perceptively retrogressed since 1992 despite a forest fire adjacent to the eastern flank of its headscarp in 2004.

The Russel Creek landslide (Fig. 7) is a large probable retrogressive thaw failure located 150 km east of Pelly Crossing. It is unique due to its southerly aspect, which is uncommon for permafrost-related failures in central Yukon. The classification of the landslide as a probable retrogressive thaw failure is based on the bowl-shaped headscarp geometry and the mobility of the flows. The failure initiated on a gentle (13°) slope and was likely triggered by a 1989 forest fire. Surficial materials on the slope have been mapped as a till veneer.

Twenty-seven medium-sized retrogressive thaw failures were identified. Almost all of these occurred along near the South MacMillan (e.g., Fig. 8) and MacMillan rivers, while only four occurred along the Pelly River (e.g., Fig. 9). Most of the slides occurred in till-blanket or veneer materials, although at least seven occurred in glaciolacustrine deposits and four occurred in glaciofluvial complex deposits. Twenty-one of these medium-sized failures initiated in or prior to the 1980s. Six retrogressive thaw failures initiated since 1990; these are located

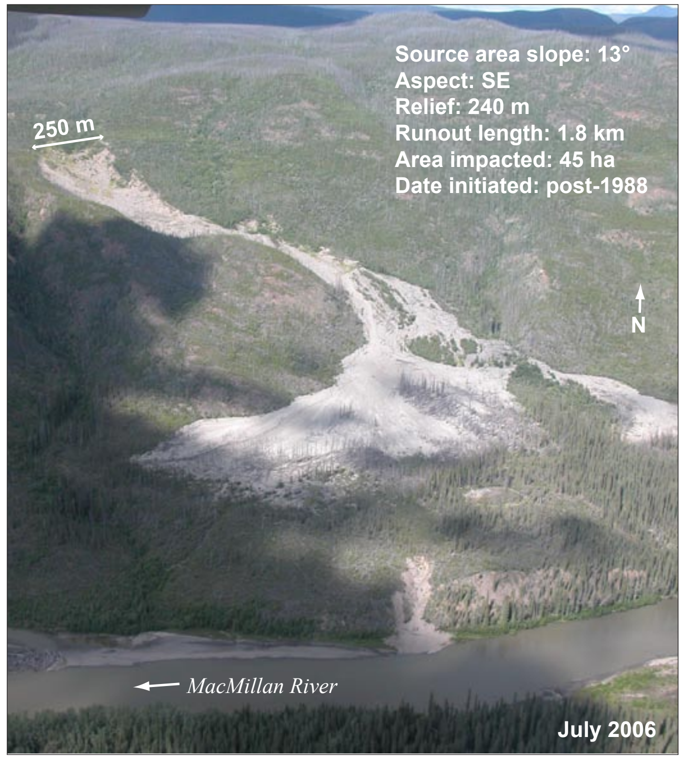

Figure 7. *The Russel Creek landslide covers an area of approximately 0.45 km². It has a runout length of approximately 1.8 km and the deposits are over 1 km wide at the toe.*

entirely along the South MacMillan River and have remained active to the present day. One of these appears to have been triggered by forest fires in 2004 (#51 in Fig. 3).

One very active medium-sized failure is located on the MacMillan River, 15 km upstream from the mouth of the Kalzas River (KZ in Fig. 3). Debris flows issuing from this retrogressive thaw slump have formed a tongue that has blocked three quarters of the river's width for at least the past three years. As shown in Figure 10, the headscarp has retreated about 150 m since 1989, averaging nearly 10 m/yr for the last 17 years. Rapid retreat rates are common for this type of failure, and rates as high as 40 m/yr have been documented for a retrogressive thaw failure near Little Salmon Lake (MG in Fig. 3) (Lyle, 2006).

Thirteen small retrogressive thaw slumps were identified within the study area. Seven of these occurred in the lower reaches of the watershed, immediately along the banks of the Pelly and MacMillan rivers and primarily within glaciolacustrine surficial materials. The remaining six occurred in the upper watershed on till-blanketed slopes above the South MacMillan River. Five of the small slumps were active in 2006 and appear to have been

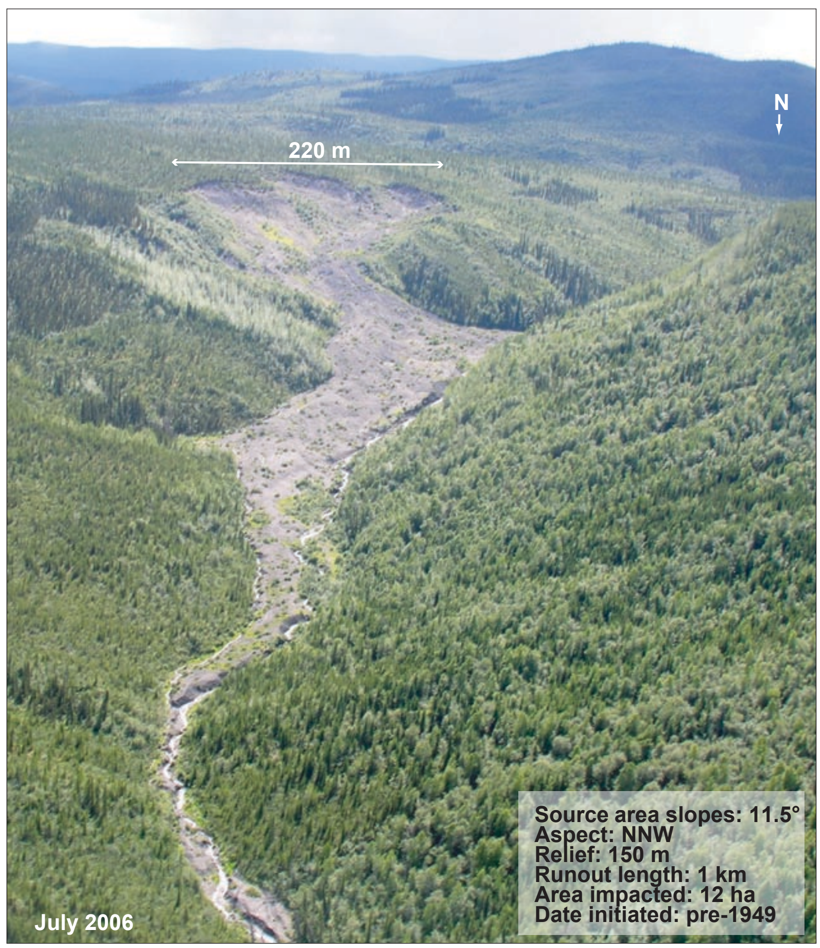

Figure 8. *This large retrogressive thaw slump (#55 in Fig. 3) is located 4 km up a tributary to the South MacMillan River. It was initiated prior to 1949 on a gentle north-facing slope that is mantled by till. Gradual headscarp retreat has caused ongoing deposition of debris along a 700-m-long segment of the creek. View is to the south.*

Figure 9. *Oblique aerial photograph of a retrogressive thaw slump (#5 in Fig. 3) that was contributing sediment to the Pelly River in 2006. This landslide has been active and increasing in size since at least 1989. View is to the south. Estimated width of main failure is approximately 200 m.*

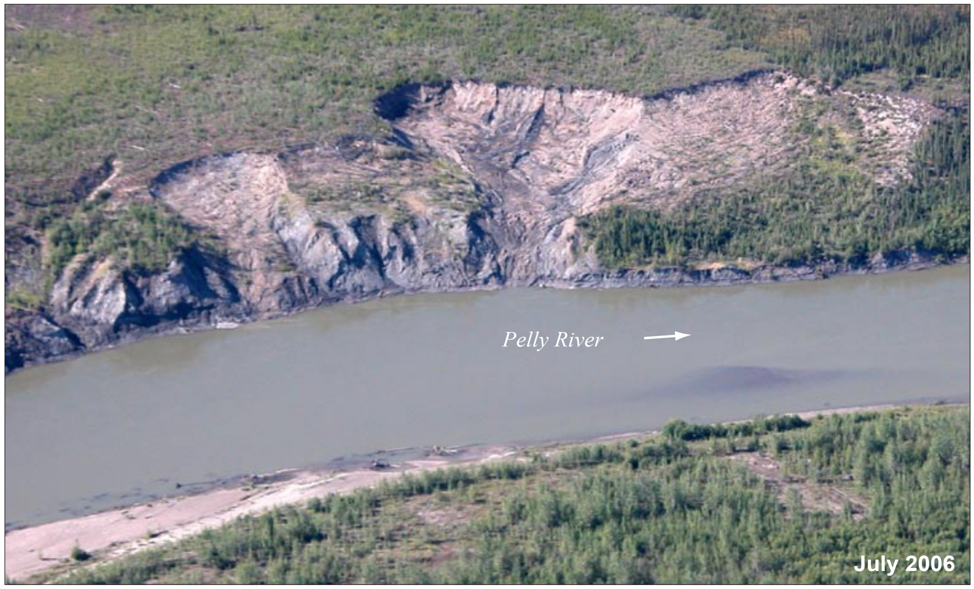

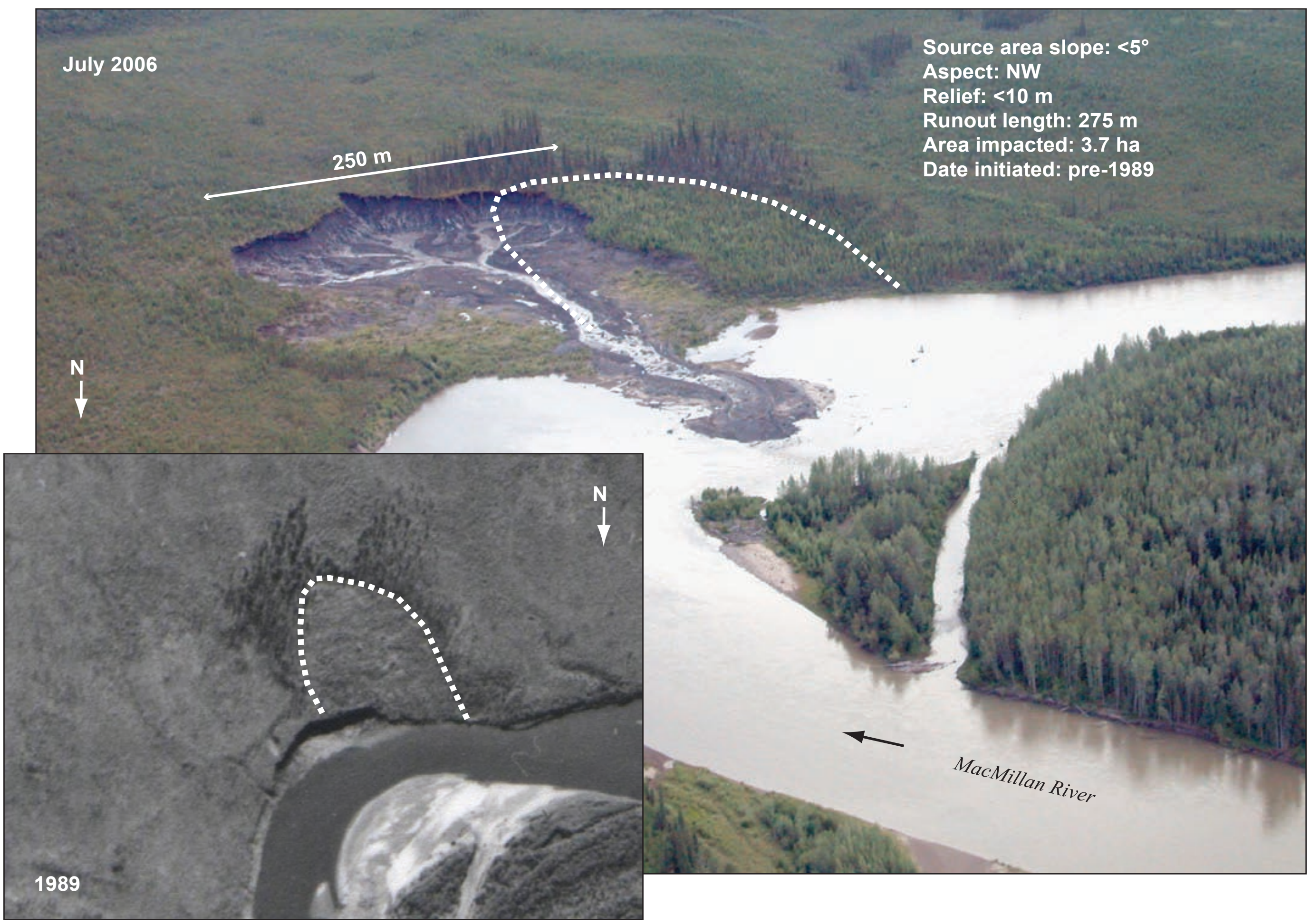

Figure 10. *The Kalzas landslide covered an area of nearly 4 ha and was approximately 250 m wide in 2006. The inset shows the location of the headscarp on a 1989 aerial photograph (National Air Photo Library, A27516-188). The dashed line traces the edge of an older overgrown retrogressive thaw slump.*

initiated in the last ten years. The rest occurred in or before the 1980s.

Surficial materials

The surficial material in which each landslide initiated in was determined from analysis of 1:100 000-scale surficial geology maps (Jackson, 1993a,b,c,d,e and 1997; Jackson *et al.*, 1993a,b; Ward and Jackson, 1993a,b,c). The majority (73%) of the permafrost-related landslides initiated in till blankets and veneers. This is a reflection of the fact that till deposits dominate the surficial geology on most slopes within central Yukon. However, the till in this region is also commonly rich in silt and clay (Lyle, 2006; Ward *et al.*, 1992; Ward and Jackson, 2000), which promotes the growth of ground ice in these materials.

Landslides initiated in glaciolacustrine plain and blanket materials, mapped at the surface, or where glaciolacustrine materials were mapped or interpreted beneath other surface materials, constitute 11% of the permafrost-related failures. These materials were commonly subject to thermokarst processes in the vicinity of the failures.

A total of 9% of the permafrost-related landslides (mostly active-layer detachments and alpine debris flows) occurred in colluvial apron materials; 5% of the landslides initiated in glaciofluvial complexes, plain and delta materials; and less than 2% occurred in organic-rich alluvial materials.

Impacts on water quality

The potential impact of the landslides on water quality in the Pelly and MacMillan River system was subjectively rated based on proximity to a river or stream. Where the debris from the landslide directly reached a river or tributary, it was considered a direct impact. If a landslide occurred on a slope and did not appear to contribute sediment directly to a watercourse, its impact was considered indirect.

Fifty-one landslides were classified as potentially having direct impacts on water quality in the Pelly and MacMillan rivers at some time in the recent past or present. Eight of these are permafrost-related failures that were directly contributing sediment to rivers or their major tributary streams in 2006. All of these failures were retrogressive thaw slumps, of which three are large (#55, Surprise Rapids and Russell Creek), two are medium-sized (#5 and KZ in Fig. 3) and two are small (#61 and 107 in Fig. 3). These medium and large-sized failures are further described in Table 3.

Another large retrogressive thaw slump that is indirectly related to sediment inputs into the Pelly River is shown in Figure 11 (PR in Fig. 3). This failure is known as the Pelly River landslide (Lyle, 2006) and is one of the largest permafrost-related landslides documented in central Yukon. It initiated prior to 1949 on a gentle slope in fine-grained till (Ward and Jackson, 2000), covering an area of approximately 2 km^2. While the landslide itself is not actively contributing sediment to the river, it may have altered local hydrology enough to cause the incision of a new tributary that now empties into the Pelly River.

Table 3. *Characteristics of various large and medium-sized permafrost-related landslides.*

Landslide name	Surficial materials	Date initiated	Source slope (°)	Aspect	Source elevation (m)	Area impacted (ha)	Runout (m)	Deposit width (m)	Relief (m)
Landslides potentially impacting water quality directly in 2006									
#55 (06PR055)	till blanket	pre-1949	11.5	NNW	1050	12	1000	700	150
SR (Surprise Rapids)	till blanket	1870s	9-13	NW	920	170	2100	1700	240
RC (Russel Ck)	till veneer	post-1988	13	SE	880	45.4	1800	1000	240
#5 (06PR005)	glaciofluvial/ glaciolacustrine	pre-1989	10	NE	520	<3	~150	-	10
KZ (Kalzas)	glaciolacustrine	pre-1989	<5	NW	550	3.7	275	-	<10
PR (Pelly River)	till veneer	pre-1949	17	NE	1100	200	4100	1500	450
Other major landslides not directly impacting water quality in 2006									
LF (Laforce)	till blanket	post-1992	10-14	NE	1060	4.7	370	250	70
#50 (06PR050)	till veneer	1949-1976	18-22	NNW	960	7.4	490	250	90

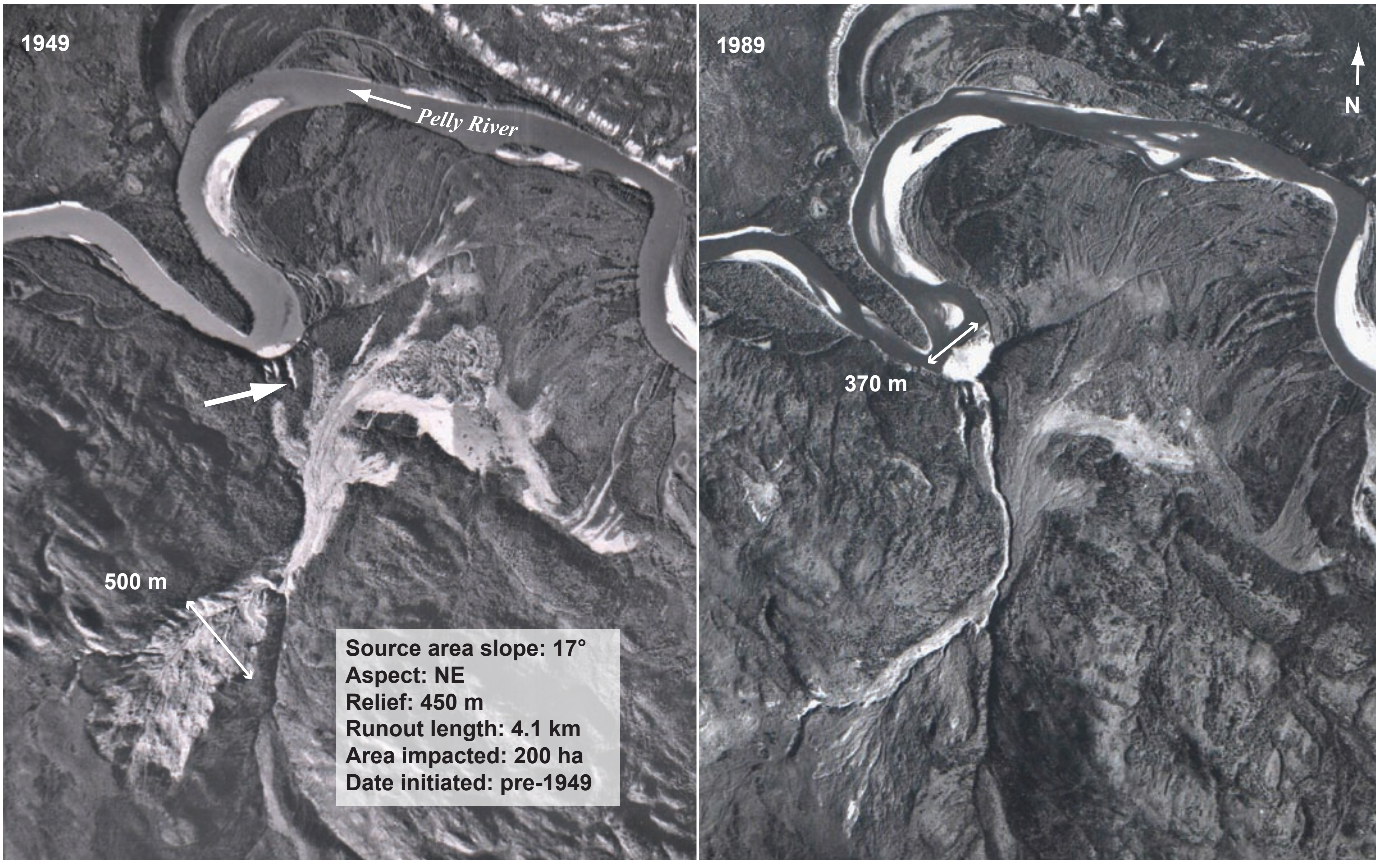

Figure 11. *Comparison of the Pelly River landslide scar in aerial photographs from 1949 (National Air Photo Library, A12182-128) and 1989 (National Air Photo Library, A27516-243). The landslide covered an area of approximately 2 km^2 and its debris traveled over 4 km. The 1989 photo shows a large fan that has grown into the Pelly River due to incision of a new tributary along the western edge of the landslide debris. The large arrow in the left photo shows the extent of the same gully in 1949.*

Ongoing incision of this gully has built a large fan that has constricted the Pelly River on a tight meander bend just upstream from the mouth of Anvil Creek.

DISCUSSION

LANDSLIDE TRIGGERS

Permafrost-related landslides are triggered by disturbances that cause the active layer to become saturated or ground-ice to thaw. Direct exposure of ice to the atmosphere or water will lead to rapid thawing. Alteration of runoff and groundwater flow can also cause thermal erosion or the build up of high pore pressure. The most common disturbances to permafrost and active-layer hydrology in the study area seem to be forest fires and river erosion, combined with the related influences of local synoptic weather conditions and long-term climate trends.

Seismicity is also a potential landslide trigger, although historical records show that all but two earthquakes recorded in the area since 1953 have had magnitudes less than 4. In addition, most epicentres are concentrated south of the Tintina Trench, so it is unlikely that seismicity is a major triggering factor in the study area.

Forest fires dramatically alter surface thermal and hydrological conditions during and immediately following the fire, leading to rapid increases in active-layer depth and changes in soil moisture regimes (Burn, 1998; Yoshikawa *et al*., 2002; Lipovsky *et al*., 2006). At least sixteen of the failures identified in the study area were likely triggered or re-activated by forest fires that occurred in 2004. Most of these were small active-layer detachment slides, although the initiation of several older large retrogressive thaw slumps was also coincident with the timing of earlier forest fires. McCoy and Burn (2005) have estimated that the maximum annual burned area may increase by greater than 300% by 2069 in central Yukon. The frequency of failures triggered by forest fires in the region can therefore also be expected to increase during this time.

Ten small to medium-sized retrogressive thaw failures occurred on river banks, primarily on outside meander bends in glaciolacustrine materials. These materials commonly underlie glaciofluvial materials in valley bottoms, and such stratigraphy is not always explicitly shown on surficial geology maps due to poor exposure. This highlights the potential limitations of performing landslide-hazard analyses based on surface-material characteristics alone, and emphasizes the need for a detailed understanding of the glacial history of an area when undertaking such evaluations.

CLIMATE CHANGE

While relatively few landslides identified in this study were triggered in the last 15 years, long-term climate warming in the past few centuries has likely played a role in initiating and promoting the ongoing growth of many of the largest permafrost-related landslides in the region. Lyle (2006) reported long-term climate change as a potential contributing factor in the initiation of two large permafrost-related landslides near Little Salmon Lake (MG and LS in Fig. 3). Ward *et al.* (1992) related warmer summers in the 1940s to a long period of increased activity at the Surprise Rapids landslide due to earlier melting of winter snowpack and faster seasonal thawing of frozen ground.

The potential effects of temperature and precipitation increases on slope stability as projected for southern Yukon in the next 50 years were discussed by Huscroft *et al.* (2004). Climate is intricately linked to a variety of factors that influence the frequency of common landslide triggers, including forest-fire frequency and severity, river-flow levels, bank-erosion rates and extreme synoptic events such as intense rainfall and snowmelt events. It is also strongly linked to many factors that control the distribution of permafrost, including the duration and depth of seasonal snow cover, summer and winter air temperatures, soil moisture, vegetation and microclimate effects.

Where undisturbed, permafrost is very slow to respond to air temperatures due to the fact that it is buffered by the active-layer soil, organic materials and snow cover. However, gradual warming of permafrost has been documented in central Alaska and northern Canada (Osterkamp and Romanovsky, 1999; Smith *et al.*, 2005). Burn (1998) estimated that it would take on the order of a century for permafrost 4-5 m thick in the Takhini River valley to thaw completely under the current climate regime. He also stated that the active layer may increase in thickness more rapidly. Anticipated warming in the next several decades will therefore likely have a more pronounced impact on the frequency and/or magnitude of landslide-triggering events than it will have on the regional distribution and degradation of permafrost (Lewkowicz and Harris, 2005).

WATER QUALITY

It is evident from this survey that permafrost-related landslides have occurred widely throughout the study area for several decades. While a small number of landslides have been initiated in the last 15 years, some of the older ones have remained active for long periods. Following initial failure, most of this ongoing activity is gradual, and very few landslides were directly contributing sediment into the Pelly and MacMillan rivers in 2006. Considering the large size of the study area, and the ongoing amount of sediment inputs from continual bank erosion, it seems unlikely that permafrost-related landslides have contributed enough sediment to cause noticeable impacts to water quality as far downstream as Pelly Crossing.

DEVELOPMENT IMPLICATIONS

As illustrated by the examples presented in this paper, permafrost-related landslides have the potential to impact extremely large areas for decades and they can travel distances up to 5 km down slope. The majority of the permafrost-related landslides identified in this study occurred on gentle north-facing slopes in ice-rich till or along north-facing river banks. However, one large failure, suspected to be permafrost-related, occurred on a southeast-facing slope in the past two decades. Development in the region, and elsewhere throughout south and central Yukon, should therefore avoid or mitigate any disruptions to local thermal and hydrological conditions in these settings. Geotechnical studies that characterize the permafrost distribution, ice-content, and surficial geology stratigraphy and history should also be performed to characterize not only the proposed development site, but also slopes several kilometres upslope and downslope of the site.

FUTURE WORK

Establishing the surficial geology stratigraphy and confirming the presence of permafrost in the initiation zones of the larger landslides documented in this study would be useful for defining the specific settings that permafrost-related failures occur in, and for providing more specific development implications. Monitoring ground temperatures at certain sites would also allow improved modeling of potential permafrost degradation in the future. As better methods of permafrost detection are developed and more detailed permafrost mapping and modeling is performed for central Yukon, refinement of landslide-susceptibility mapping techniques for discontinuous permafrost terrain will become greatly improved.

ACKNOWLEDGEMENTS

Ken Nordin brought the Pelly River water quality concern to our attention and provided much of the motivation to perform this study. Support from Selkirk First Nation was provided from Bonnie Hueberschwerlen. Dave Young of Big Salmon Air safely piloted the fixed-wing reconnaissance flight. Basic characterizations of many large landslides throughout the study area were greatly facilitated through the use of GoogleEarth. Extra special thanks to Jeff Bond for providing helpful comments and suggestions.

REFERENCES

Burn, C.R., 1998. The response (1958-1997) of permafrost and near-surface ground temperatures to forest fire, Takhini River valley, southern Yukon Territory. Canadian Journal of Earth Sciences, vol. 35, no. 2, p. 184-199.

Dyke, L., 2004. Stability of frozen and thawing slopes in the Mackenzie Valley, Northwest Territories. Géo Quebec 2004, 57th Canadian Geotechnical Society Conference, p. 31-38.

Geertsema, G., Clague, J.J., Schwab, J.W. and Evans, S.G., 2006. An overview of recent large catastrophic landslides in northern British Columbia, Canada. Engineering Geology, vol. 83, p. 120-143.

Geertsema, M. and Pojar, J.J., 2006. Influence of landslides on biophysical diversity – a perspective from British Columbia. Geomorphology, 2006. 15 p.

Gordey, S. P. and Makepeace, A.J., 2003. Yukon digital geology, Version 2.0. Geological Survey of Canada Open File 1749 and Yukon Geological Survey Open File 2003-9(D), 2 CD-ROMS.

Heginbottom, J.A., Dubreuil, M.A. and Harker, P.T., 1995. National Atlas of Canada (5th edition), Canada Permafrost, Plate 2.1, (MCR 4177), 1:7 500 000 scale.

Huscroft, C.A., Lipovsky, P.S. and Bond, J.D., 2004. A regional characterization of landslides in the Alaska Highway corridor, Yukon. Yukon Geological Survey, Open File 2004-18, 65 p. report and CD-ROM.

Jackson, L.E., Jr., Ward, B.C., Duk-Rodkin, A. and Hughes, O.L., 1991. The last Cordilleran ice sheet in southern Yukon Territory. Géographie physique et Quaternaire, vol. 45, p. 341-354.

Jackson, L.E., Jr., 1993a. Surficial geology, Earn River, Yukon Territory. Geological Survey of Canada, Map 1819A, 1:100 000 scale.

Jackson, L.E., Jr., 1993b. Surficial geology, South MacMillan River, Yukon Territory. Geological Survey of Canada, Map 1820A, 1:100 000 scale.

Jackson, L.E., Jr., 1993c. Surficial geology, Magundy River, Yukon Territory. Geological Survey of Canada, Map 1821A, 1:100 000 scale.

Jackson, L.E., Jr., 1993d. Surficial geology, Olgie Lake, Yukon Territory. Geological Survey of Canada, Map 1822A, 1:100 000 scale.

Jackson, L.E., Jr., 1993e. Surficial geology, Big Timber Creek, Yukon Territory. Geological Survey of Canada, Map 1834A, 1:100 000 scale.

Jackson, L.E., Jr., Morison, S.R. and McKenna, K., 1993a. Surficial geology, Dragon Lake, Yukon Territory. Geological Survey of Canada, Map 1832A, 1:100 000 scale.

Jackson, L.E., Jr., Morison, S.R. and McKenna, K., 1993b. Surficial geology, Prevost River, Yukon Territory. Geological Survey of Canada, Map 1833A, 1:100 000 scale.

Jackson, L.E., Jr., 1997. Surficial geology, Granite Canyon, Yukon Territory. Geological Survey of Canada, Map 1878A, 1:100 000 scale.

Lewkowicz, A.G. and Harris, C., 2005. Frequency and magnitude of active-layer detachment failures in discontinuous and continuous permafrost, northern Canada. Permafrost and Periglacial Processes, vol. 16, p. 115-130.

Lewkowicz, A.G. and Harris, C., 2006. Morphology and geotechnique of active-layer detachment failures in discontinuous and continuous permafrost, northern Canada. Geomorphology, vol. 69, p. 275-297.

Lipovsky, P.S., Coates, J., Lewkowicz, A.G. and Trochim, E., 2006. Active-layer detachments following the summer 2004 forest fires near Dawson City, Yukon. *In:* Yukon Exploration and Geology 2005, D.S. Emond, G.D. Bradshaw, L.L. Lewis and L.H. Weston (eds.), Yukon Geological Survey, p. 175-194.

Lyle, R.R., 2006. Landslide susceptibility mapping in discontinuous permafrost: Little Salmon Lake, central Yukon. Unpublished MSc thesis, Queen's University, Kingston, Ontario, 351 p.

Mackay, J.R., 1966. Segregated epigenetic ice and slumps in permafrost, Mackenzie Delta area, NWT. Geographical Bulletin, vol. 8, p. 59-80.

McCoy, V.M. and Burn, C.R., 2005. Potential alteration by climate change of the forest-fire regime in the boreal forest of central Yukon Territory. Arctic, vol. 58, p. 276-285.

McRoberts, E.C. and Morgenstern, N.R., 1974. Stability of slopes in frozen soil, Mackenzie Valley, N.W.T. Canadian Geotechnical Journal, vol. 11, p. 554-573.

Osterkamp, T.E. and Romanovsky, V.E., 1999. Evidence for warming and thawing of discontinuous permafrost in Alaska. Permafrost and Periglacial Processes, vol. 10, p. 17-37.

Rampton, V.N., Ellwood, J.R. and Thomas, R.D., 1983. Distribution and geology of ground ice along the Yukon portion of the Alaska Highway gas pipeline. *In:* Proceedings of the 4th International Conference on Permafrost, Fairbanks, Alaska, July 17-22, 1983, p. 1030-1035.

Smith, S.L., Burgess, M.M., Riseborough, D. and Nixon, F.M., 2005. Recent trends from Canadian permafrost thermal monitoring network sites. Permafrost and Periglacial Processes, vol. 16, p. 19-30.

Ward, B.C. and Jackson, L.E., Jr., 1992. Late Wisconsinan glaciation of the Glenlyon Range, Pelly Mountains, Yukon Territory, Canada. Canadian Journal of Earth Science, vol. 29, p. 2007-2012.

Ward, B.C., Jackson, L.E., Jr. and Savigny, K.W., 1992. Evolution of Surprise Rapids landslide, Yukon Territory. Geological Survey of Canada Paper 90-18, 24 p.

Ward, B.C. and Jackson, L.E., Jr., 1993a. Surficial geology, Needlerock Creek, Yukon Territory. Geological Survey of Canada, Map 1786A, 1:100 000 scale.

Ward, B.C. and Jackson, L.E., Jr., 1993b. Surficial geology, Wilkinson Range, Yukon Territory. Geological Survey of Canada, Map 1787A, 1:100 000 scale.

Ward, B.C. and Jackson, L.E., Jr., 1993c. Surficial geology, Telegraph Mountain, Yukon Territory. Geological Survey of Canada, Map 1789A, 1:100 000 scale.

Ward, B.C., and Jackson, L.E., Jr., 2000. Surficial geology of the Glenlyon map area, Yukon Territory. Geological Survey of Canada, Bulletin 559, 60-page report and four 100 000-scale maps.

Yoshikawa, K., Bolton, W.R., Romanovsky, V.E., Fukuda, M. and Hinzman, L.D., 2002. Impacts of wildfire on the permafrost in the boreal forests of Interior Alaska. Journal of Geophysical Research, vol. 108, no. D1–8148, p. 14.

Structure of schist in the vicinity of the Klondike goldfield, Yukon

Doug MacKenzie and Dave Craw
Geology Department, University of Otago[1]

Jim K. Mortensen
Earth and Ocean Sciences, University of British Columbia[2]

Tim Liverton
Klondike Star Mineral Corporation[3]

MacKenzie, D.J., Craw, D., Mortensen, J.K. and Liverton, T., 2007. Structure of schist in the vicinity of the Klondike goldfield, Yukon. *In:* Yukon Exploration and Geology 2006, D.S. Emond, L.L. Lewis and L.H. Weston (eds.), Yukon Geological Survey, p. 197-212.

ABSTRACT

This study describes the structural evolution of the Klondike Schist and the structural setting of mineralized mesothermal veins from which over 500 tonnes of placer gold has been derived. The Klondike Schist was emplaced as a series of thrust slices on top of a structural stack that includes at least three additional thrust slices. A distinctive set of mesoscopic structures, particularly a set of recumbent folds, formed during thrust emplacement. These folds have a general southeast trend, and deform thrust-emplaced ultramafic rocks. Underlying thrust panels contain folds that resemble these thrust-related structures, but have a consistent northeast trend. The Klondike Schist may have been rotated about a vertical axis during the latter stages of thrusting along phacoidal cleavage zones. Extensional sites in post-thrust kink folds and faults host mesothermal gold veins. Hence, gold mineralization postdated thrust stacking. Normal faults offset mesothermal veins, and host late-stage hydrothermal alteration zones.

RÉSUMÉ

Dans cette étude on décrit l'évolution structurale du schiste de Klondike et le cadre structural des veines mésothermales minéralisées dont on a tiré plus de 500 tonnes d'or placérien. Le schiste de Klondike a été mis en place sous forme d'une succession d'écailles de chevauchement au sommet d'un empilement structural comprenant au moins trois autres écailles de chevauchement. Un ensemble distinctif de structures mésoscopiques, en particulier un ensemble de plis couchés, se sont formées pendant le chevauchement. Ces plis ont une orientation générale sud-est et déforment des roches ultramafiques mises en place par chevauchement. Les lames de chevauchement sous-jacentes présentent des plis ressemblant à ces structures associées au chevauchement, mais qui ont une orientation nord-est uniforme. Le schiste de Klondike peut avoir subi une rotation autour d'un axe vertical pendant les derniers stades du chevauchement le long de zones clivées lenticulaires. Des sites d'extension dans les plis et failles en chevrons post-chevauchement renferment les veines d'or mésothermales. La minéralisation en or est ainsi postérieure à l'empilement par chevauchement. Des failles normales décalent les veines mésothermales et renferment des zones d'altération hydrothermale de phase tardive.

[1]*P.O. Box 56, Dunedin, New Zealand, doug.mackenzie@stonebow.otago.ac.nz*
[2]*Vancouver, British Columbia, Canada, jmortensen@eos.ubc.ca*
[3]*Whitehorse, Yukon, Canada*

INTRODUCTION

The Klondike goldfield (Fig. 1) has produced over 500 tonnes of alluvial gold from a remarkably small area (<2500 km^2; Knight *et al.*, 1999; Lowey, 2005). The sources for this gold are presumed to have been in the underlying bedrock, as the compositions of placer gold and compositions of gold in nearby gold-bearing quartz veins are closely related (Knight *et al.*, 1999; Mortensen *et al.*, 2005). These veins have mesothermal characteristics, fill fractures in the underlying schist (Rushton *et al.*, 1993), and have been the target of numerous exploration programs over the past 20 years, including a major effort over the past 3 years by Klondike Star Mineral Corporation.

Despite the potential economic significance of the Klondike gold-bearing veins, neither the structure of the host schist nor the structural setting of the veins are known in detail. Although the overall regional geology has been elucidated at the 1: 50 000 scale, and the tectonic setting is reasonably well understood (e.g., Mortensen, 1990, 1996; Gordey and Ryan, 2005), little is known about the structural evolution of the schists that host the auriferous veins. Likewise, the relative timing of gold-bearing vein emplacement, in relation to other structural events affecting the host schists, has not been examined in detail.

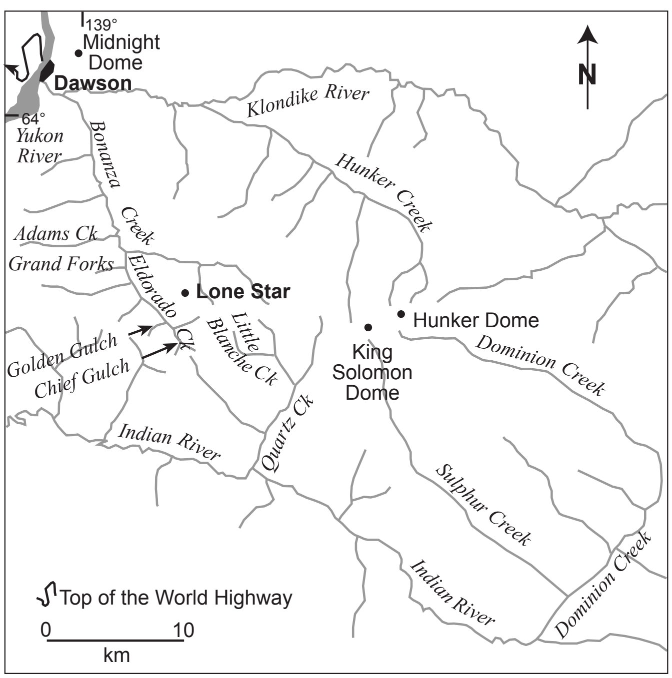

Figure 1. Location map showing the main study area in the Klondike District and specific localities discussed in the text.

This report outlines results of detailed structural observations in the Klondike area during the 2006 field season. Due to limited outcrop exposure, observations were obtained mainly from the best-exposed parts of the central and northern Klondike, in areas of recent or current mineral exploration or placer mining activity, as well as in road and stream cuts. We have determined a readily recognizable sequence of structural events that occurred during the evolution of the Klondike Schist, and we have placed the gold mineralization stage within this structural framework. This report provides extensive illustration of the key structural features, with the intention of facilitating further structural mapping and event correlation throughout the Klondike District.

This work has been carried out as part of a regional study of the entire Klondike District and adjacent Indian River area (J. Mortensen, D. MacKenzie and D. Craw, work in progress) that is being funded by the Klondike Star Mineral Corporation.

REGIONAL STRUCTURE

The Klondike Schist in the vicinity of the Klondike goldfield is part of the Yukon-Tanana Terrane, and consists of medium-grade metamorphic rocks of Late Permian age (Fig. 2; Mortensen, 1996). The schist includes a wide range of metasedimentary and meta-igneous rock types, now represented as quartzofeldspathic, micaceous and chloritic schists. These rocks are interlayered on the 1-100 m scale and are pervasively foliated and recrystallized, with few primary features recognizable.

The Klondike Schist forms the upper part of a stacked pile of thrust slabs that includes lithologically distinct Nasina Assemblage (Mortensen, 1990, 1996; Table 1) and a composite slice of little-metamorphosed greenstone and ultramafic rocks of probable Slide Mountain Terrane origin (Mortensen, 1996). The thrust slices of metamorphic rocks are locally separated by additional ultramafic slices (Mortensen, 1996; Mortensen, unpublished mapping), but exposure of the bounding faults is poor. The structure of the Klondike Schist in the Klondike goldfield is, in part, directly linked to the structure of this thrust pile (Table 1, 2). Detailed mapping of rocks within the lower thrust slabs is beyond the scope of this study, but we provide general descriptions of these underlying rocks to facilitate comparison and contrast with the Klondike Schist.

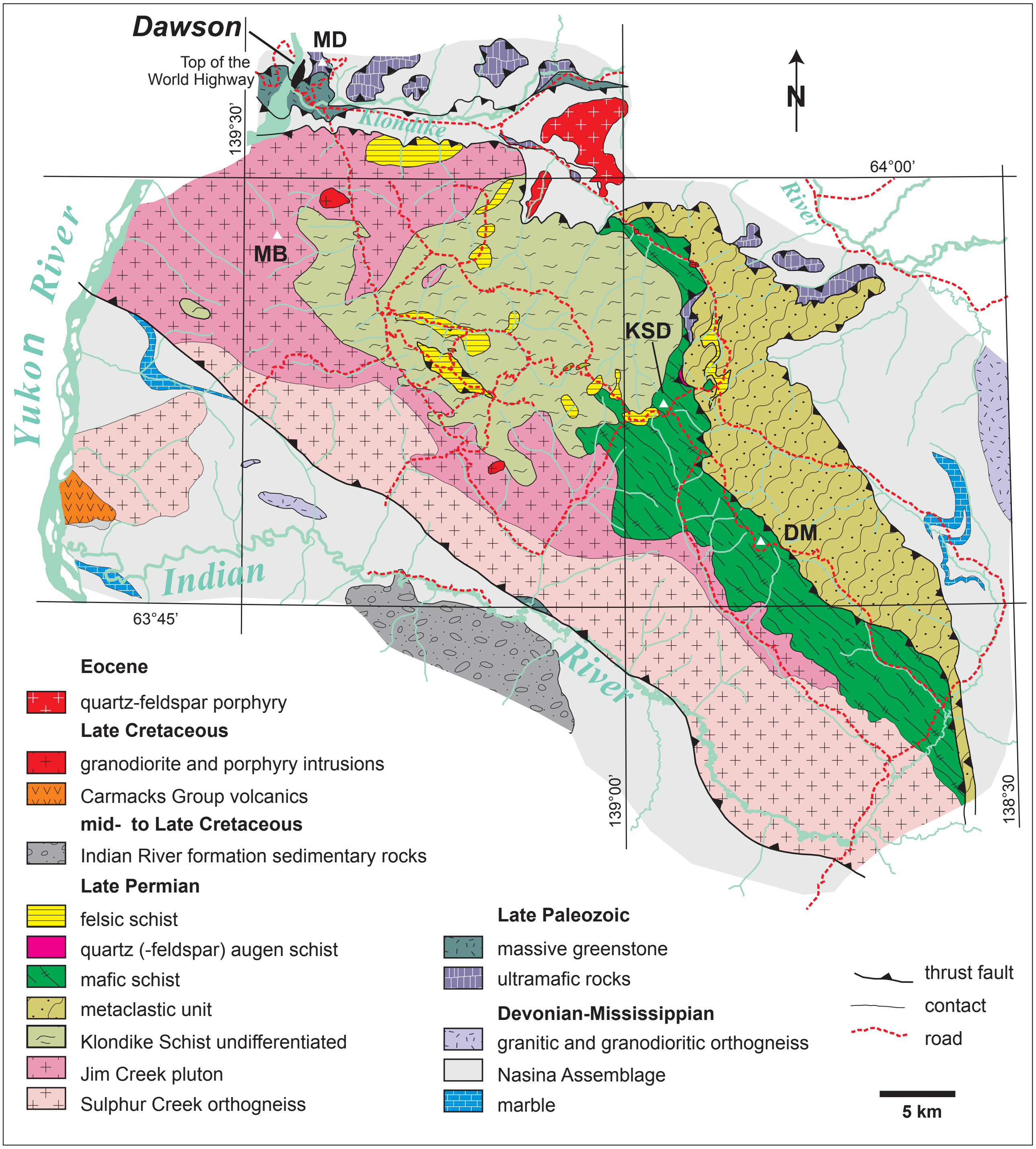

Figure 2. *Geological map of the Klondike District. KSD = King Solomon Dome; MD = Midnight Dome; DM = Dominion Mountain; MB = Mount Bronson.*

The thrust slices in the central and northern parts of the Klondike District, which have been the main focus of our work thus far, have generally increasing metamorphic grade and degree of textural reconstitution up the pile, although the two slices of Nasina Assemblage near the base of the structural stack are separated by greenstone, with little foliation development (Table 1). The Klondike Schist shows the highest metamorphic grade, most pervasive metamorphic reconstitution, and coarsest metamorphic grain size. The syn-metamorphic structures

***Table 1.** Summary comparison of thrust slices (in relative structural order) in the Klondike district (after Mortensen, 1996).*

Thrust slice	Rocks	Metamorphic grade	Textural reconstitution	Metamorphic structures
Klondike Schist (may include 2-3 slices)	micaceous schist, quartzofeldspathic schist, chloritic schist	upper greenschist facies (biotite zone)	pervasive recrystallization, coarse (0.1-1 mm) metamorphic grain size	pervasive coarse mica foliation, strong metamorphic segregation
Nasina Assemblage	dark grey micaceous schist	middle greenschist facies	pervasive recrystallization, fine (0.01-0.1 mm) metamorphic grain size	pervasive slaty foliation, weak metamorphic segregation
greenstone and ultramafic rocks	massive metabasalt and metadiabase, chlorite schist zones; serpentinite	lower greenschist facies	variable recrystallization, fine (0.01-0.1 mm) metamorphic grain size	minor local foliation development
Nasina Assemblage	dark grey micaceous schist	lower greenschist facies	pervasive recrystallization, fine (0.01-0.1 mm) metamorphic grain size	pervasive slaty foliation, weak metamorphic segregation

***Table 2.** Summary of principal structural events relevant to the structure of hydrothermal gold deposit rocks (shown from oldest at bottom, to youngest at top) that affect the Klondike Schist, as compiled in this study.*

Deformation stage	Klondike Schist event	Main feature	Orientation	Mineralization	Deformation	Age*
normal faults	normal faults	gouge zones	NW to N	pyrite in silicified schist and porphyry dykes	regional extension	Late Cretaceous?
mesothermal veins	Au veins	massive discordant quartz veins	variable, commonly NW	Au, pyrite, other sulphide minerals	local extensional sites	Early or Middle Jurassic?
kink folds and faults	D_4	angular folds, faults, shears, gouge zones	two orthogonal, N to NE; E to SE	?	compression	Early or Middle Jurassic?
thrust stacking	D_3	phacoidal cleavage	shallow dip	nil	compression	Early Jurassic?
		recumbent folds, spaced cleavage (S_3)	variable, mainly shallow dip, NW trend	nil		
		serpentine emplacement	shallow dip	nil		
pervasive foliation	S_2	foliation, isoclinal folds	variable	nil	compression	Late Permian?
first foliation	S_1	foliation, segregations	variable	nil	compression	Late Permian?
deposition	S_0	bedding etc.	not seen	sulphide minerals in some rocks		mid-Permian

*Age of events is deduced from regional considerations, after Mortensen (1996)

in the Klondike Schist were imposed on the rocks before thrust stacking, and there are some distinct differences in structural elements between thrust slices (Table 1).

STRUCTURES IN THE NASINA ASSEMBLAGE

Both slices of Nasina Assemblage (Table 1; Fig. 2) have similar structural features, although earlier structures are more readily seen in the lower slice. The Nasina units are typically finely laminated (commonly cm-scale), predominantly micaceous and at least weakly carbonaceous. The schist structure is dominated by a pervasive slaty foliation (S_1) that is defined by oriented fine-grained (<100 micron) metamorphic muscovite and chlorite. Only minor metamorphic segregation has occurred, locally accentuating primary lamination. The foliation is folded by tight to isoclinal folds (F_2) that have some mica recrystallization along fold-axial surfaces (S_2), generally subparallel to S_1 (Fig. 3). The composite S_1 and

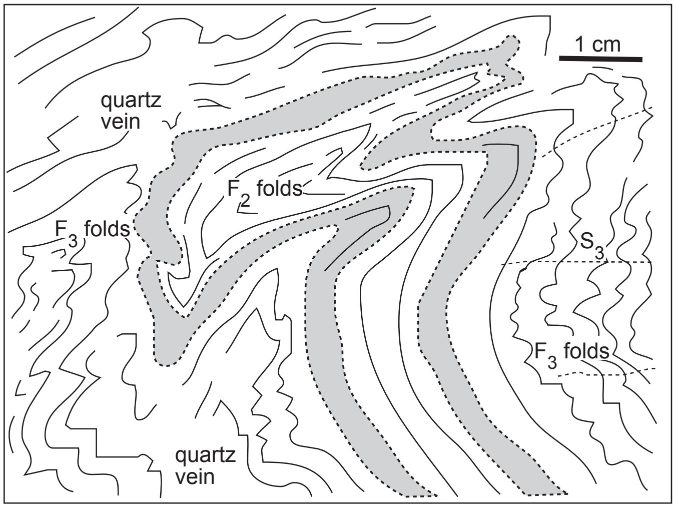

Figure 3. *Field sketch (from photograph) of a complex fold zone in the Nasina Assemblage structurally below the greenstone thrust slice, near Dawson City. The prominent foliation (S_1; grey layer) has been folded by F_2 folds with variable development of S_2 fold-axial surface foliation. These folds have been folded in turn by F_3 crenulations with a spaced cleavage (S_3; dashed). A distinctive chloritic lamina (grey) is traceable through the fold zone.*

S_2 fabric is generally shallow-dipping, except where modified by later structures.

Both earlier fabrics are folded by crenulations (F_3; cm-scale) that are only weakly developed in the lower Nasina thrust slice (Fig. 3). The crenulations have a shallow-dipping spaced cleavage (S_3) with little or no recrystallization of micas (Fig. 3). The crenulations are related to mesoscopic and macroscopic folding of metamorphic fabrics that are visible in some outcrops, both above and below the greenstone slice. A well exposed macroscopic example in the upper Nasina thrust slice on lower Bonanza Creek has recumbent folds with >10-m wavelength (Fig. 4a). The angular relationships between metamorphic foliation and S_3 spaced cleavage vary around both macroscopic and mesoscopic folds (Fig. 4b, c, d). A prominent crenulation lineation (L_3) on the metamorphic foliation has a consistent northeast trend in both the upper and lower Nasina thrust slices (Fig. 5a, b).

The above-described structures are cut or modified by a prominent phacoidal cleavage that has locally reactivated the shallow-dipping foliation. This cleavage is best exposed near the top of the lower Nasina thrust slice, where cleavage surfaces are spaced from 0.1 to 10 m apart and become progressively more closely spaced towards the overlying serpentinite. The cleavage anastomoses around relatively competent lensoidal blocks of schist. Cleavage surfaces are polished, marked by slickensides, and locally coated in recrystallized chlorite. Minor cataclasis has occurred on many surfaces, yielding sub-millimetre zones of grey-black cataclasite.

The pervasive foliation is deformed by small-scale (1-10 cm) angular kink folds in many areas. These kink folds typically have a northwest trend and steeply dipping fold-axial surfaces. Two sets of intersecting kinks are commonly observed, with the second (subordinate) set oriented perpendicular to the dominant set.

STRUCTURES IN THE COMPOSITE GREENSTONE-ULTRAMAFIC THRUST SLICE

The greenstone-ultramafic thrust slice comprises an upper sheet of massive greenstone (mainly massive metabasalt and metadiabase), which is structurally underlain by a laterally less-extensive lens-shaped body of partially to wholly serpentinized harzburgite. The greenstone unit is well exposed in road cuts on the Midnight Dome road, in natural outcrops on both sides of the Klondike River near Dawson and on the bluffs immediately across the Yukon River from Dawson, and in road cuts along the Top of the World Highway (Figs. 1 and 2).

The underlying ultramafic rocks comprise the top of the Midnight Dome and, together with the greenstone unit, form a south-dipping composite slab that is both underlain and overlain by Nasina Assemblage metasedimentary rocks. The greenstone has been extensively chloritized, but foliation is only developed in localized zones, 1-5 m across. Within these zones, the foliation (S_1) is defined by oriented chlorite, and anastomoses around pods of massive greenstone. The foliation has been deformed by synmetamorphic similar folds that are generally intrafolial and have a variably developed fold-axial-surface cleavage (S_2) that is subparallel to the earlier foliation. This relationship is displayed more clearly in a localized zone of deformation around a massive metadiabase clast in a greenstone agglomerate (Fig. 6a). Both these fabrics are folded in places by shallow-plunging crenulations (cm-scale; Fig. 6b) that have a weak fold-axial-surface fabric defined by the sub-parallel orientation of recrystallized chlorite.

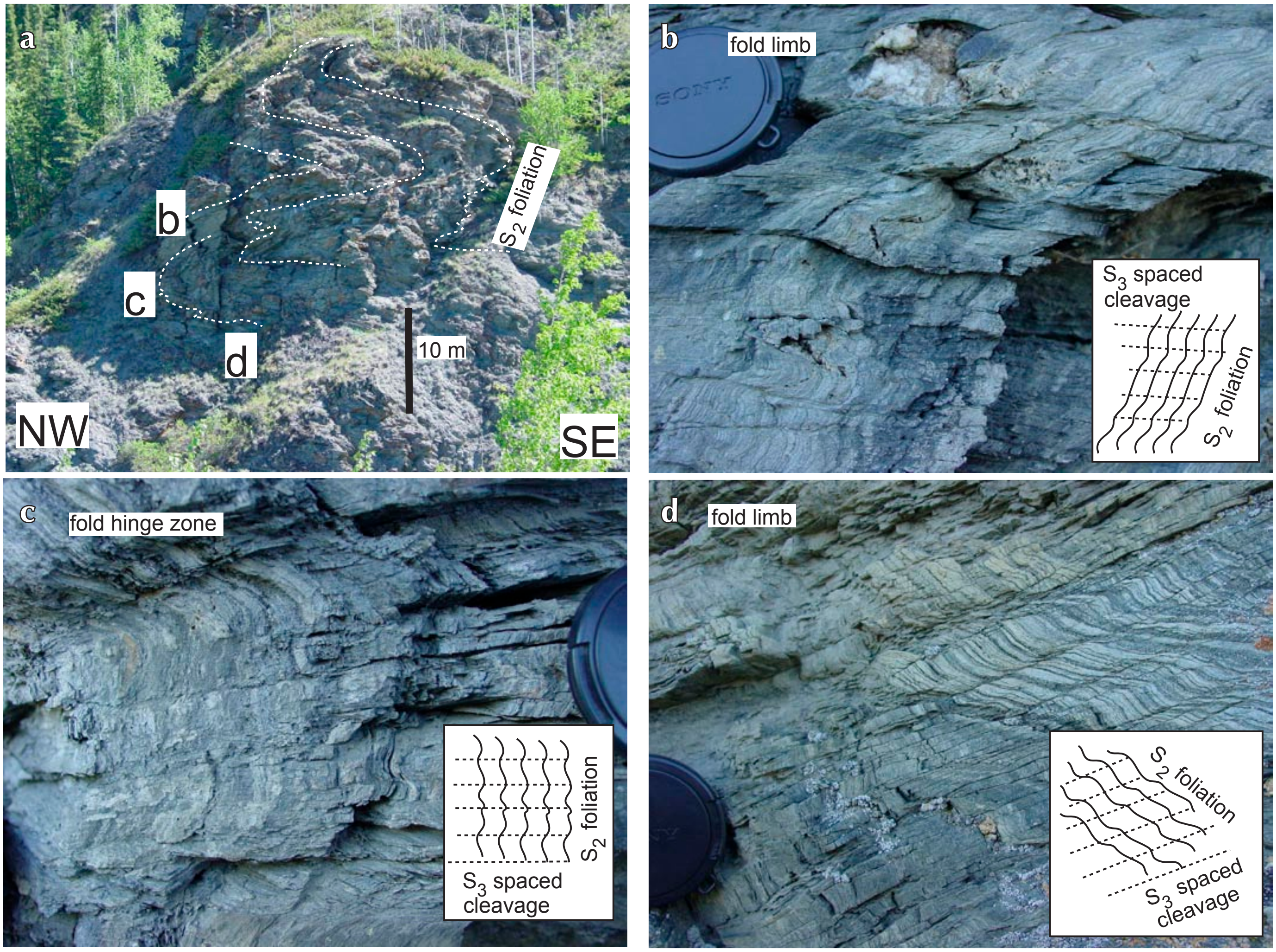

Figure 4. *A set of recumbent F_3 folds in the Nasina Assemblage on a right-limit bluff, 2 km above the mouth of Bonanza Creek. The outcrop in* ***(a)*** *shows the scale of the folds; the whole outcrop is similar to the portions at the top that have the S_2 foliation outlined. Photographs* ***(b)*** *to* ***(d)*** *show the relative dips of S_2 foliation and the S_3 spaced cleavage in different parts of the fold. Simplified sketches on each photo show the interpreted relationships. Note the almost brittle nature of the spaced cleavage, with negligible recrystallization of new micas characterizing the low metamorphic grade of the Nasina Assemblage (Table 1).*

The hinges of F_3 crenulations in S_2 foliation planes define a prominent lineation (L_3; Fig. 6b), and a spaced fold-axial-surface cleavage that cuts across the early fabrics at moderate to high angles. The lineation has a consistent northeast trend (Fig. 5c). All fabrics in the greenstones are cut by spaced (1-10 m) brittle fractures with surfaces marked by slickensides (Fig. 6b). Fabrics and structures within the ultramafic rocks are similar to those described above in the greenstone, except that an early (S_1) foliation is generally not developed.

STRUCTURES IN THE KLONDIKE SCHIST

The Klondike Schist is structurally more complex than rocks in the underlying thrust slices (Table 1). Structural features of the Klondike Schist are summarized in Table 2 (oldest at the bottom, youngest at the top), and these are described in the following sections. No single outcrop contains evidence of all of these structural features.

Within the Klondike District, the Klondike Schist comprises at least three separate thrust slices, with

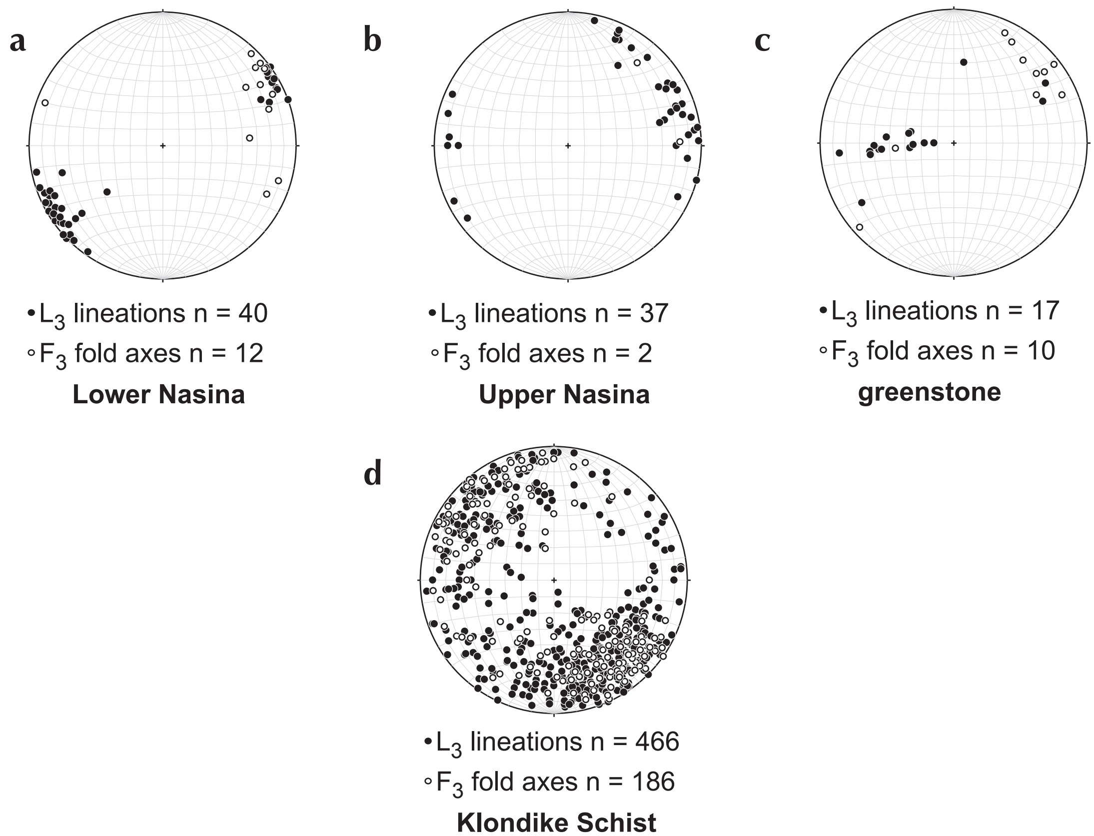

Figure 5. *Lower hemisphere equal-area stereonets for F_3 fold axes and L_3 intersection lineations on the S_2 foliation surfaces.* ***(a)*** *Lower Nasina Assemblage,* ***(b)*** *Upper Nasina Assemblage,* ***(c)*** *Greenstone-ultramafic thrust slice,* ***(d)*** *Klondike Schist.*

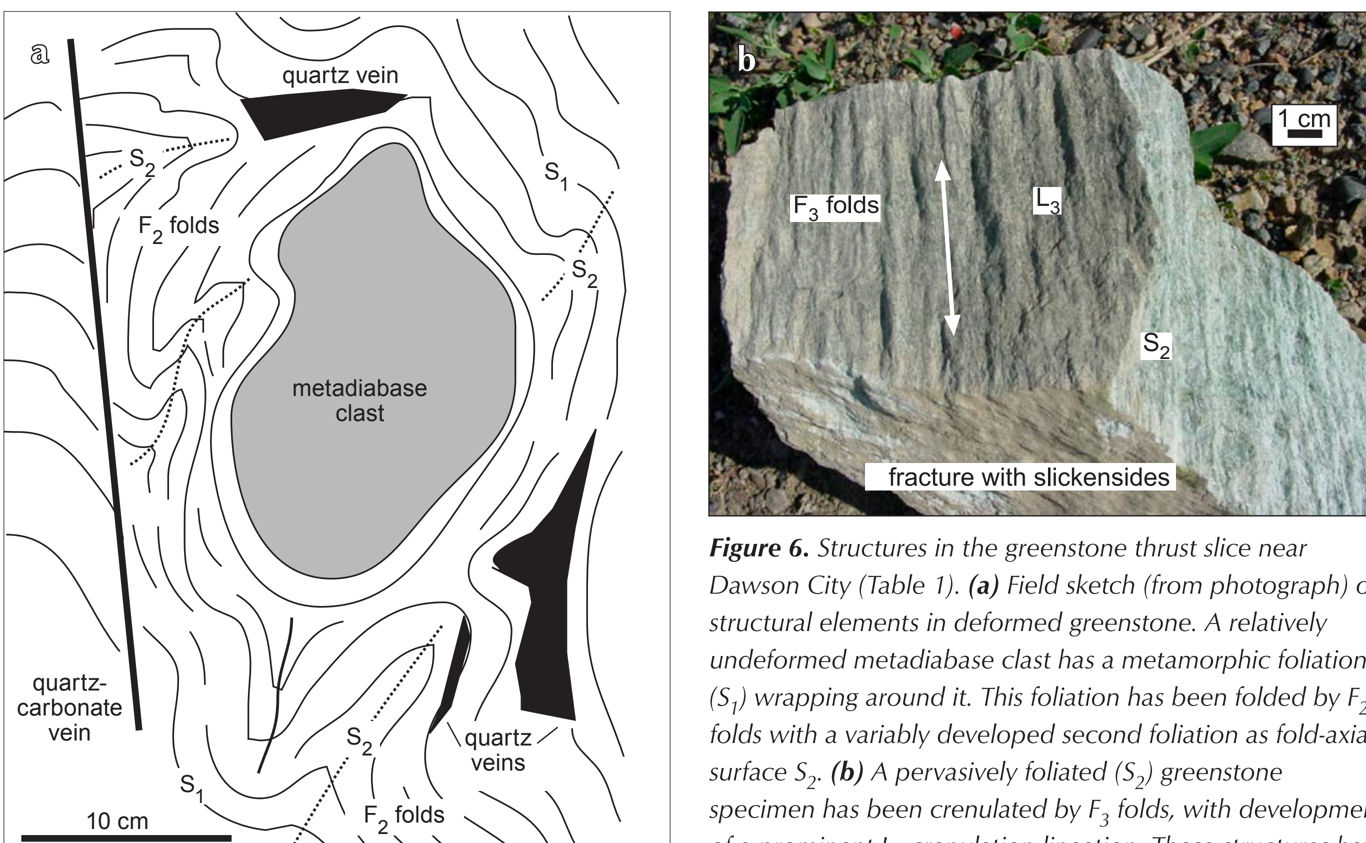

Figure 6. *Structures in the greenstone thrust slice near Dawson City (Table 1).* ***(a)*** *Field sketch (from photograph) of structural elements in deformed greenstone. A relatively undeformed metadiabase clast has a metamorphic foliation (S_1) wrapping around it. This foliation has been folded by F_2 folds with a variably developed second foliation as fold-axial-surface S_2.* ***(b)*** *A pervasively foliated (S_2) greenstone specimen has been crenulated by F_3 folds, with development of a prominent L_3 crenulation lineation. These structures have been cut by a fracture marked by slickensides (bottom).*

distinctly different types of schist occurring above and below thrust boundaries (Fig. 2; Mortensen, 1996). The bounding faults are irregular surfaces deformed by folding and a later phacoidal cleavage (described below). Discontinuous ultramafic horizons of serpentinite and/or talc-carbonate schist mark these thrust faults (Mortensen, 1996; Fig. 7).

A pervasive foliation is the most prominent structural feature in the Klondike Schist. This is a composite feature, being made up of an early metamorphic foliation (S_1) that was folded and reactivated by a second phase of ductile deformation (F_2) during peak metamorphism. F_2 folds, where observed, are generally intrafolial and isoclinal, with a well developed fold-axial-surface foliation (S_2) defined by the parallel orientation of metamorphic micas. The composite foliation development was accompanied by metamorphic segregation (mm- to cm-scale), so that rocks are generally finely laminated (Fig. 8a, b). In addition, numerous foliation-parallel quartz veins occur throughout all host-rock types. These concordant veins locally contain pyrite, especially along their margins, but are apparently barren of gold. The composite foliation is generally shallowly to moderately dipping over most of the Klondike Schist, but later deformation has locally caused steepening near specific structures.

The most prominent folds (F_3) seen in many parts of the Klondike Schist deform the foliation, and overprint and largely obscure the F_1 and F_2 structures. The F_3 folds seen at outcrop scale are minor structures on larger scale recumbent folds similar to those in the Nasina Assemblage (Fig. 4a) that are difficult to recognize in the Klondike area. A prominent spaced cleavage (S_3) has developed parallel to F_3 fold-axial surfaces, and this has been accentuated by recrystallization of micas (Fig. 9). The spaced cleavage in the Klondike Schist (Figs. 8a and 9) has had more extensive mineral recrystallization than in

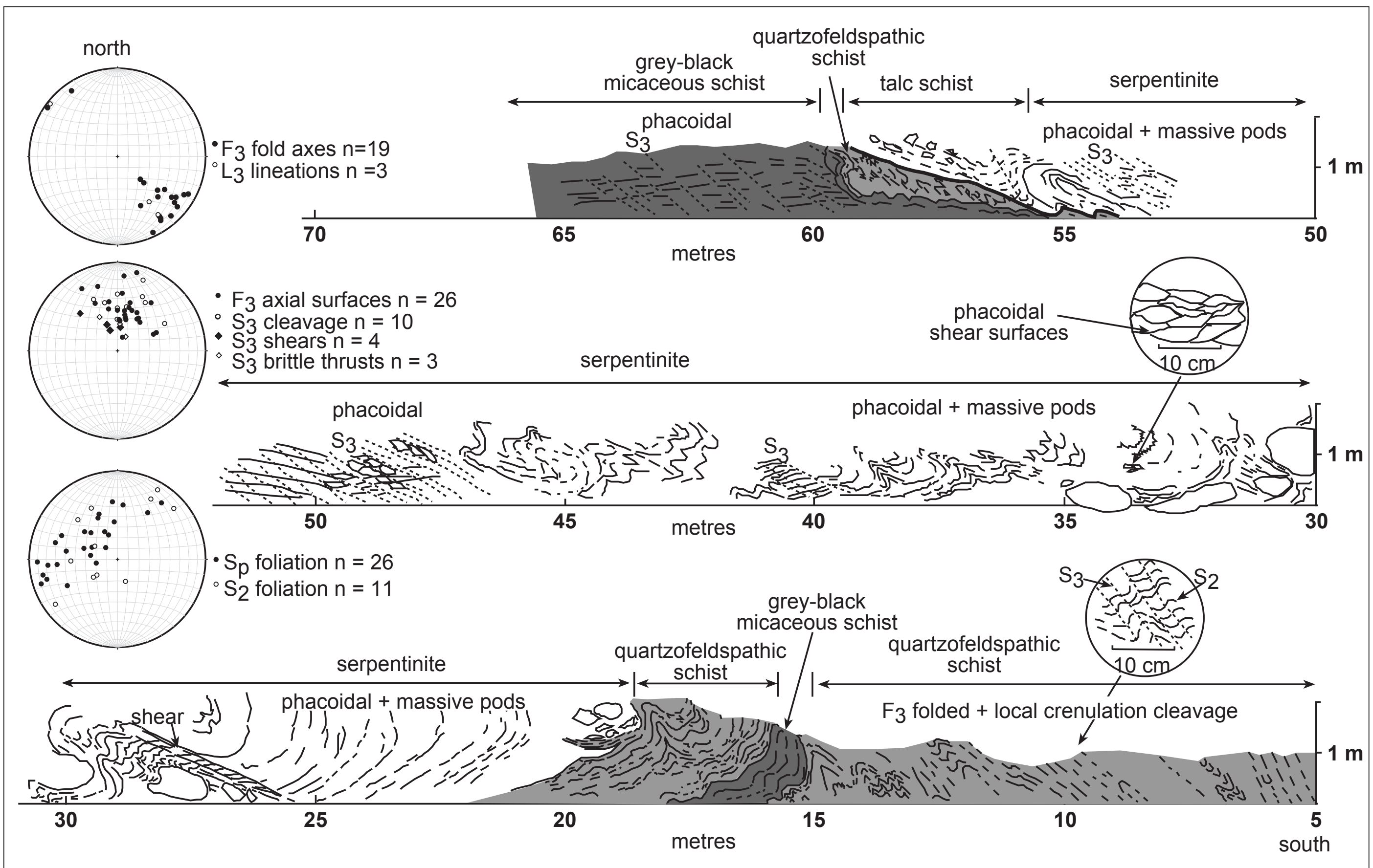

Figure 7. Sketch of a trench wall through a thrust boundary between two slices of Klondike Schist immediately east of the historic Lone Star mine (see Fig. 1). Sketch covers ca. 60 m from north (upper left) to south (lower right) in three composite sections. Serpentinite (no colour) deformed by F_3 and later phacoidal cleavage separates schist of the lower slice (top left) from schist of the upper slice (lower right). Lower hemisphere equal-area stereonets show orientations of structural elements in the three composite sections. S_p is the prominent undifferentiated foliation.

the Nasina Assemblage, and many Klondike Schist outcrops are dominated by the S_3 fabric. Small-scale F_3 folds form a prominent crenulation lineation on composite foliation surfaces, and this is accentuated by a lineation defined by intersection of S_3 with the foliation. This prominent lineation (L_3) has widely varying orientations, but it generally plunges southeast (east to south; Figs. 5d and 7).

At least locally, F_3 folds deform and overprint the thrust faults bounding individual thrust slices in the Klondike Schist. At one locality near the historic Lone Star mine (Fig. 1) that was examined in detail in this study, F_3 folds deform one of the thrust faults and the serpentinite marking it (Fig. 7). The locally intense F_3 folds and associated S_3 fabric are traceable both up-section and down-section into the Klondike Schist (Fig. 7).

F_3 folded zones near serpentinite-bearing thrusts in the Klondike Schist are locally overprinted by a phacoidal cleavage (Figs. 7 and 10). Cleavage surfaces are spaced between 0.1 and 10 m apart, and spacing becomes closer towards the thrusts, especially in micaceous schist (Fig. 7). Cleavage surfaces are polished, marked by slickensides, and locally cataclastic, with minor recrystallization of chlorite in chloritic schists (Fig. 10). Cleavage surfaces are partially defined by reactivated foliation, and partially defined by reactivated S_3, although truncation of S_3 is common also (Fig. 10).

The Klondike Schist and thrusts imbricating it are cut by D_4 reverse faults and related kink folds (F_4; Table 2). These structures are variably developed throughout the Klondike District, with locally intense zones separated by large areas that display little or no evidence of this deformation. The structures have developed in two mutually perpendicular directions (Table 2), and some outcrops have structures of both orientations. The folds and faults deform F_3 structures (Figs. 8b and 11), and form broad (km-scale) warps of the pervasive foliation (Fig. 12a). The most prominent features are zones of fault gouge (metre-scale) bordered by zones of steeply dipping sheared foliation (Figs. 13a,b). These zones are commonly accompanied by zones of F_4 folds in adjacent schist (Fig. 12b). The intensity of this F_4 folding decreases over 100 m from the main deformation zone. However, scattered F_4 kinks and associated fractures occur over most of the Klondike Schist.

The youngest deformation event recognizable in the Klondike Schist is a set of normal faults that cut across all earlier structural features (Table 2). These are defined by wide (metre-scale) gouge zones, with locally developed silicification and pyritization of adjacent schist. Some of these normal faults appear to have been controlled by pre-existing D_4 deformation zones (Fig. 12c). The normal-fault zones commonly host dykes of mafic to intermediate composition, and these dykes are variably altered (Fig. 14).

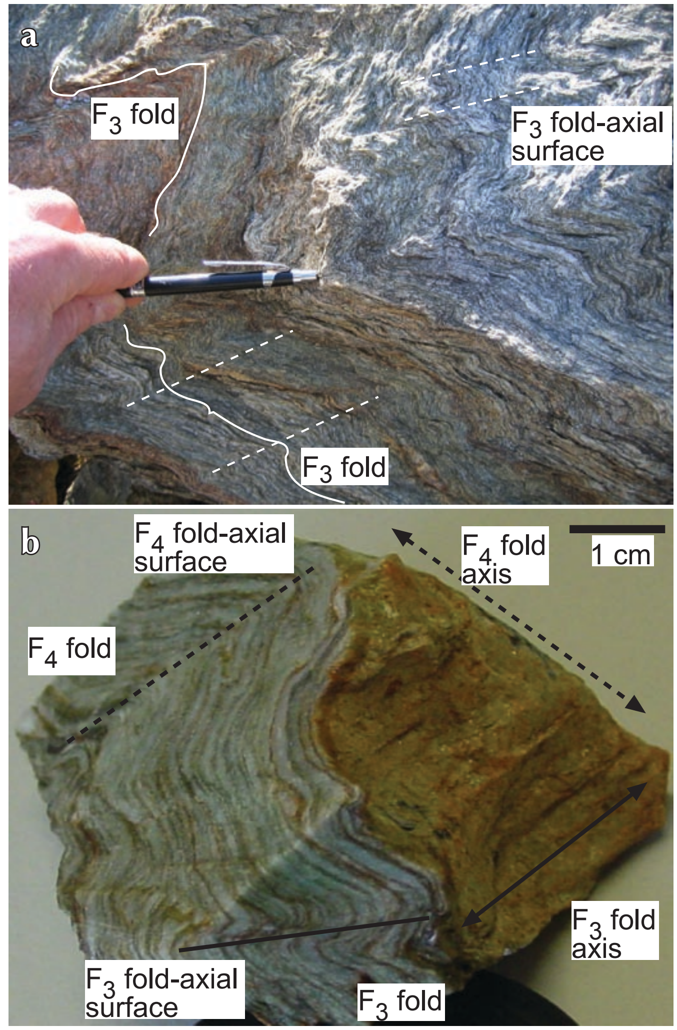

Figure 8. *Photographs of F_3 folds in Klondike Schist, east of Eldorado Creek. Note the finely laminated and segregated host schist, alignment of micas in the spaced cleavage, and local development of a recrystallized mica fabric.*
(a) *Moderately developed F_3 folds of segregated foliation (solid line), with a spaced cleavage parallel to the fold axial surface (dashed lines);* ***(b)*** *specimen showing interference between F_3 folds and F_4 folds (as labelled).*

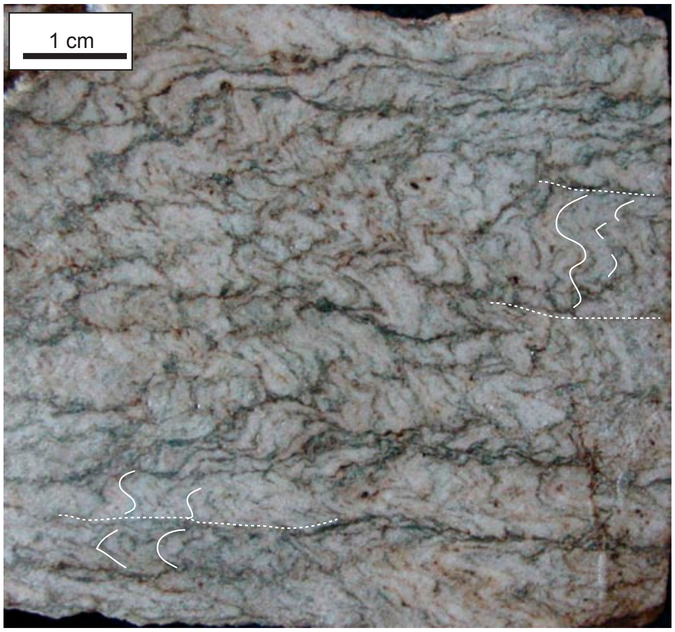

Figure 9. *A slab of quartzofeldspathic Klondike Schist, showing remnants of metamorphic foliation (S_1+S_2; solid white lines) that have been folded by F_3 crenulations. Well developed S_3 spaced cleavage (parallel to dashed white lines) locally dominates the rock fabric.*

STRUCTURAL CONTROLS ON VEIN FORMATION

Discordant quartz veins (distinct from metamorphic segregations) form in a wide variety of structural settings in the Klondike Schist. Many, but not all, of these veins contain gold, and these are typically mesothermal in style as described by Rushton *et al.* (1993). Detailed examination of gold-bearing vein structures is beyond the scope of this regional structural study, but will be addressed in future work. The following is a summary of observations on these discordant veins in relation to the structures described previously.

Individual veins can follow several different structural features along their strikes and/or dips. The main criterion for structural hosting of veins appears to be whether any pre-existing structural weaknesses in the rock are suitably oriented to open in superimposed extension. Additional mineralized rock has been created by hydrothermal alteration of wall rocks adjacent to extensional zones, whether those extensional zones host quartz veins or not.

D_4 structures are the most common hosts of quartz veins, particularly in fractures parallel to F_4 fold-axial surfaces (Figs. 11, 13b and 15). The geometric relationship between veins, F_4 'axial surface' fractures and F_4 folds is consistent, regardless of orientation of the foliation. Where F_4 folds have upright fold-axial-surface fractures, and foliation is flat-lying, veins have a steep dip (Figs. 11 and 16). Where foliation is steeply dipping and F_4

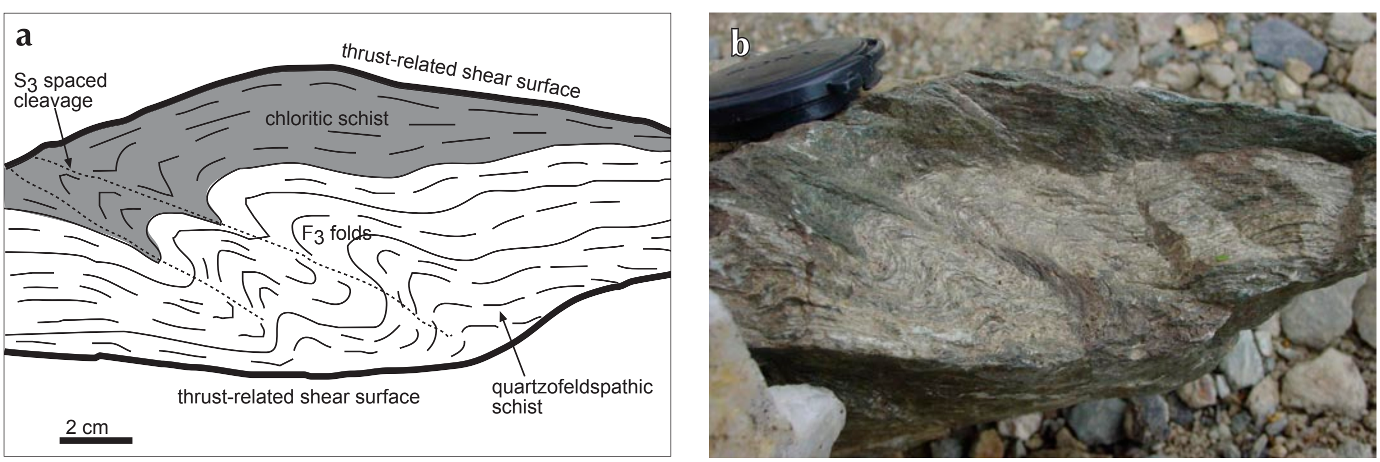

Figure 10. *Sketch **(a)** and photograph **(b)** of a block from a thrust zone between slabs of Klondike Schist near Hunker Dome (see Fig. 1). F_3 folds and S_3 spaced cleavage are visible in the core of the block, especially in the quartzofeldspathic layer. These features are truncated on the margin of the block by thrust-related shears (thick lines in **a**) that form a phacoidal cleavage around more resistant lenses of rock.*

Figure 11. *Large F_4 fold exposed in the northeast bank of Bonanza Creek at Grand Forks (see Fig. 1). The rocks are strongly affected by F_3 structures, and the prominent layering (white lines) is a combination of S_2 and S_3. The F_3 fold axes plunge steeply down this composite surface. These structural features are folded by the F_4 structure. A prominent set of fractures has developed subparallel to the F_4 fold-axial surface. One of these has been filled by a discordant quartz vein (left).*

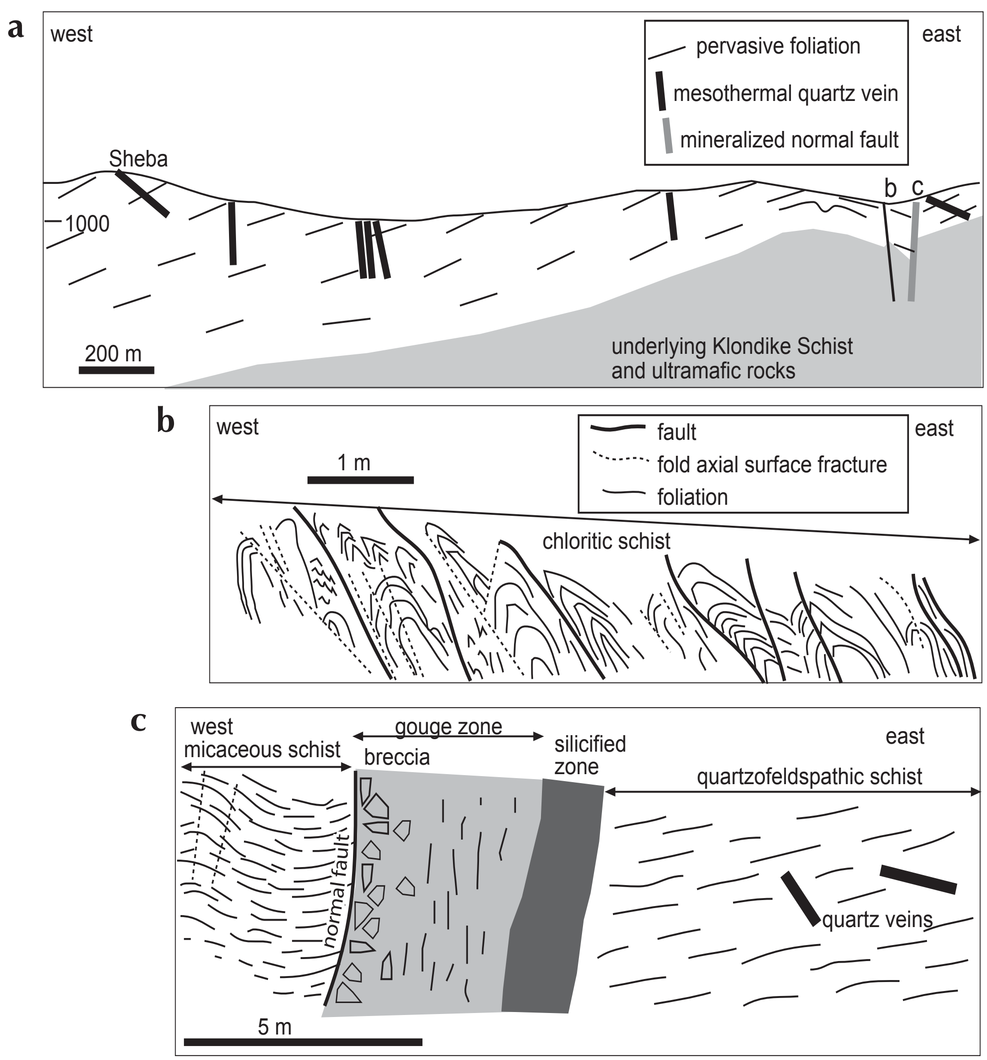

Figure 12. *Sketch sections through some portions of the King Solomon Dome-Hunker Dome area (see Fig. 1), showing structural elements relevant to vein formation in the Klondike Schist.*
(a) *Regional cross-section, east from the Sheba vein system, based on trench mapping, with locations of sections b and c. A broad F_4 antiformal fold of metamorphic foliation is on the east (right) side.*
(b) *F_4 deformation zone adjacent to a steeply dipping F_4 fault on the limb of the large antiform (see **a**).*
(c) *Eastern margin of the F_4 deformation zone, with a combination of normal-fault structures superimposed on F_4 structures. Mesothermal quartz veins fill F_4-related structures and the later normal fault has been hydrothermally altered.*

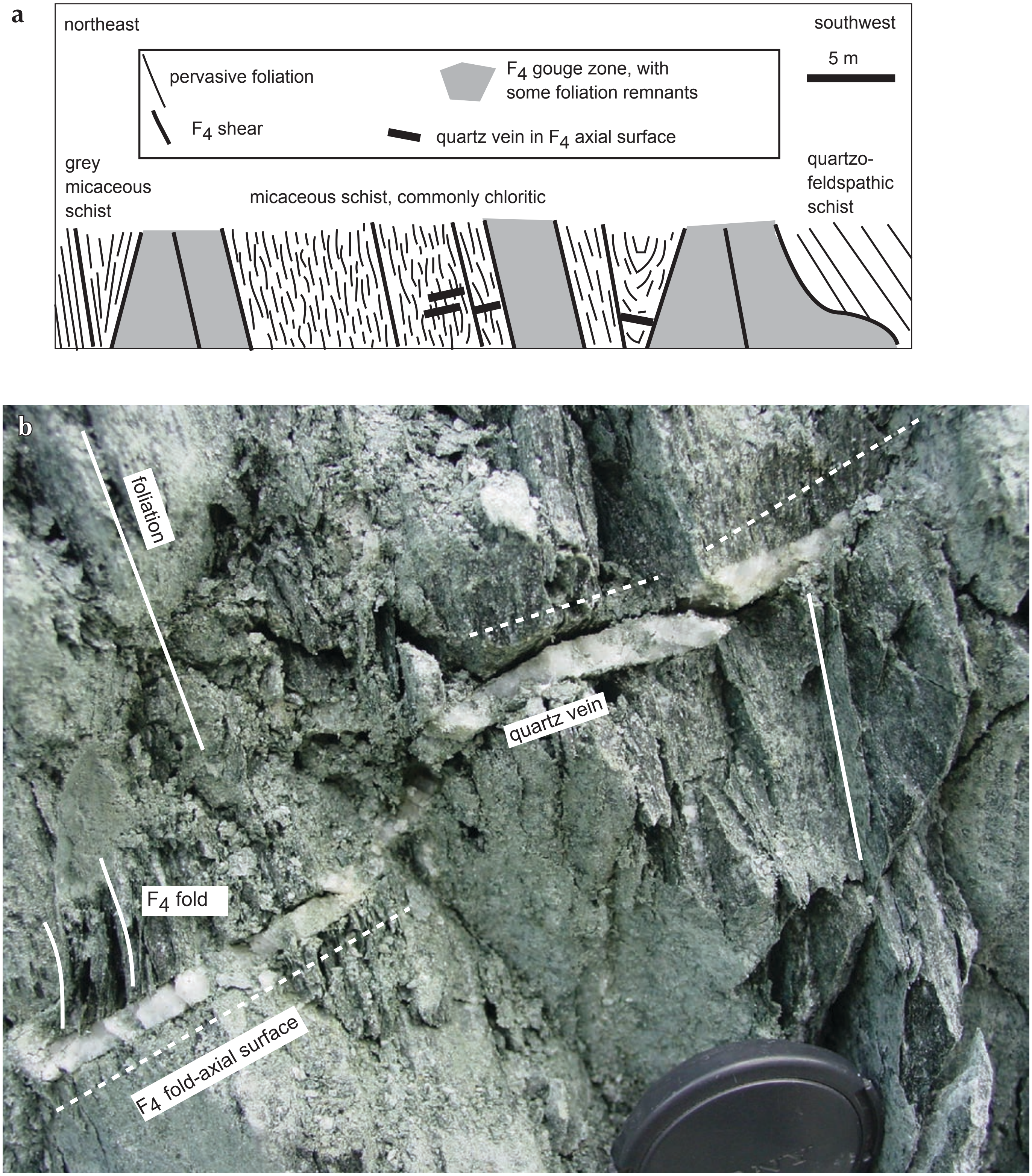

Figure 13. (a) *Section through a trench in the bed of Eldorado Creek near the mouth of Golden Gulch (see Fig. 1), showing an F_4 reverse fault and wide deformation zone cutting across Klondike Schist. Zones of gouge separate zones of more intact rock. F_4 folds have developed on a steep foliation, and their axial surface fractures are shallow-dipping to the northeast and southwest (northeast in* ***b****). Some of these fractures (dashed lines in* ***b****) are filled with quartz veins, as shown in* ***b****.*

folds have shallowly dipping axial surfaces, fractures and veins are also shallowly dipping (Fig. 13b). Weak F_4 deformation in the King Solomon Dome-Hunker Dome area (Fig. 12a) has resulted in spaced fractures parallel to fold-axial surfaces of two perpendicular F_4 fold sets. Both sets host quartz veins.

In addition, opening of the S_2 pervasive foliation during F_4 deformation, assisted by strong differences in rock types, has produced some near-concordant mineralized veins. Likewise, opening of the S_3 spaced cleavage associated with tight F_3 folding hosts some mineralized veins, especially near F_3 fold hinges.

Further hydrothermal alteration and vein formation occurred along the late-stage normal faults. This hydrothermal activity mainly resulted in alteration, silicification and pyritization of adjacent host rocks

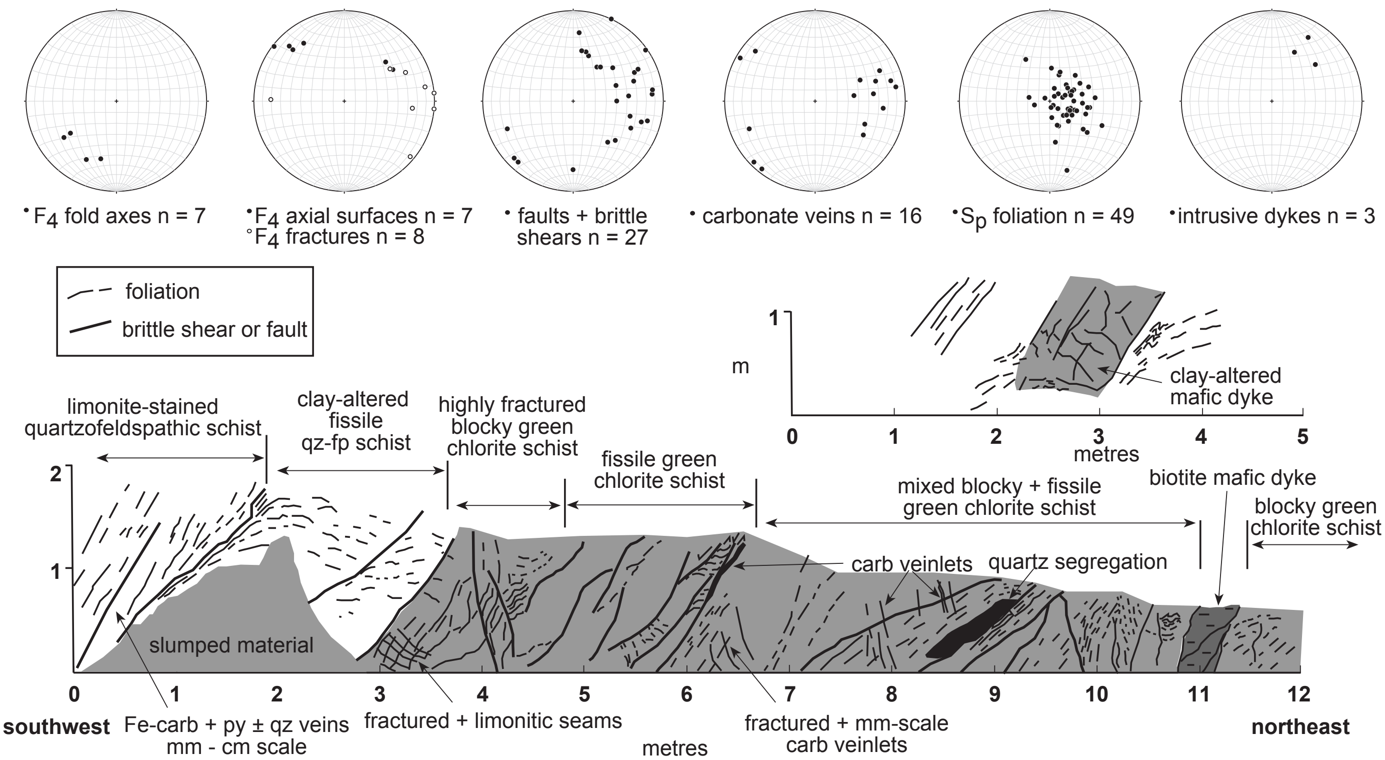

Figure 14. *Section through two parallel trenches cut across a variably mineralized northwest-striking normal fault zone on the ridge crest between the heads of Chief Gulch and Little Blanche Creek (see Fig. 1). In the lower section, chlorite schist (light-grey shading) has been juxtaposed against quartzofeldspathic schist (white, left). The upper section shows an altered, biotite-phyric mafic dyke intruded into quartzofeldspathic schist. Lower hemisphere equal-area stereonets are shown for structures, veins and dykes.* S_p *is the prominent undifferentiated foliation.*

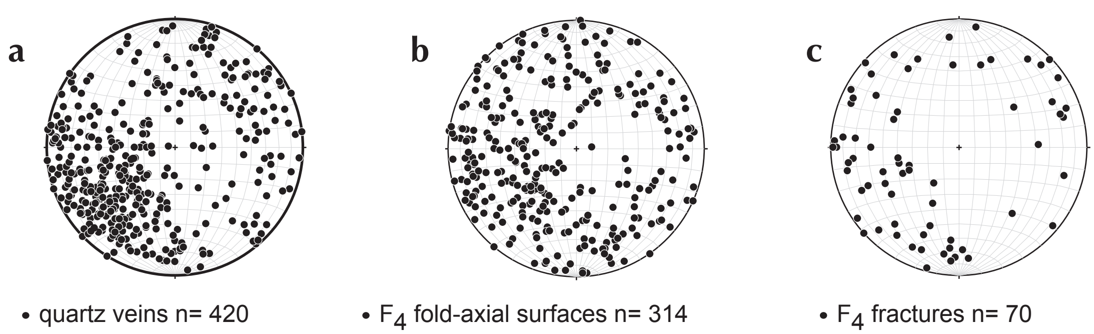

Figure 15. *Lower hemisphere equal-area stereonets from the Klondike Schist.* ***(a)*** *Poles to quartz veins. Main populations are northeast- and east-dipping.* ***(b)*** *Poles to* F_4 *axial surfaces.* ***(c)*** *Poles to* F_4 *axial surface-parallel fractures.*

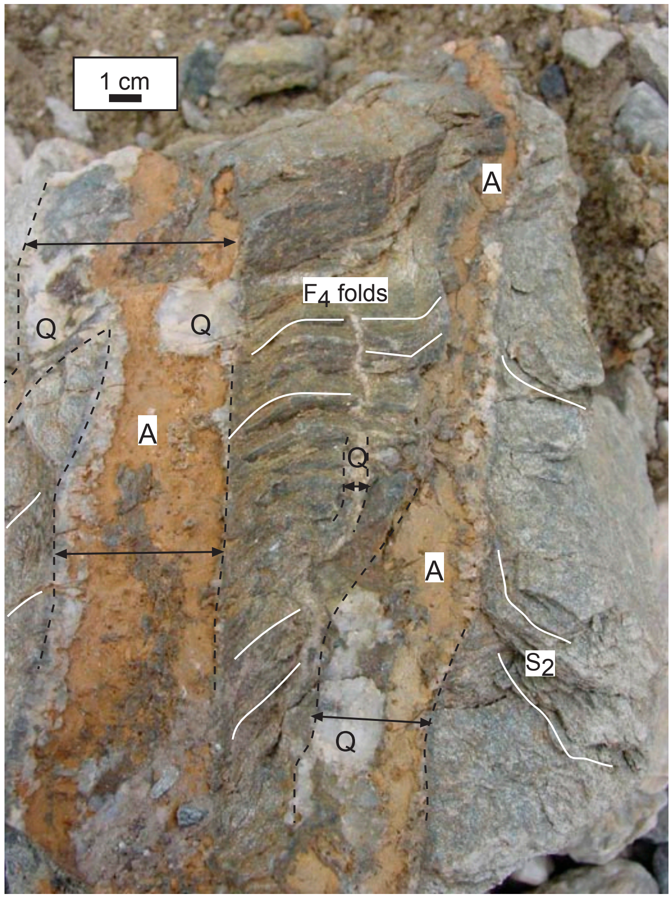

Figure 16. *Quartz (Q) and ankeritic carbonate (A) veins fill steeply dipping extensional fractures (dashed black lines) that have developed parallel to the fold-axial surfaces of F_4 kink folds of metamorphic foliation in Klondike Schist (white lines).*

(Fig. 12c). This style of alteration is structurally later than the mesothermal veins described previously, and normal fault offsets (metre-scale) of mesothermal veins have occurred. The co-existence of the two styles of mineralization in close proximity (e.g., Fig. 12c) results from reactivation of F_4 zones by normal faults that subsequently control later fluid flow.

CORRELATION OF STRUCTURAL EVENTS THROUGH THE THRUST SLICES

All the thrust slices (Table 1) have similar sets of structures: composite foliation (S_1 and S_2), later folds with a spaced cleavage (F_3), and post-F_3 cataclastic phacoidal cleavage or shears. However, correlation of structural features is hindered by lack of appropriate age data and outcrop. Similarly, comparison of bounding faults is hindered by poor exposure. Hence, the correlations outlined below are tentative and subject to revision, but provide useful starting points for further work.

The most plausible structural link between thrust slices is the widespread set of folds and spaced cleavage that is designated F_3 in each slice. The F_3 folds have similar style and northeast trend through the two Nasina Assemblage slices and the intervening greenstone-ultramafic slice (Fig. 5a, b, c). Since the Nasina Assemblage and greenstone have disparate tectonic origins (Mortensen, 1996), having these F_3 structures in common suggests that ductile fold structures formed during, or just after, juxtaposition of the slices. The phacoidal cleavage that is strongly developed near the thrusts postdates the folding and may have involved reactivation of thrust surfaces.

Despite the apparent correlation of F_3 and phacoidal cleavage in the lower three thrust slices, correlation of these structures into the overlying Klondike Schist is more problematic. Regional and local observations support the close relationship between thrust stacking and serpentinite emplacement (Mortensen, 1996). Serpentinite between two Klondike Schist slices has been folded by F_3 (Fig. 7), further supporting the contention that F_3 deformation accompanied or postdated thrust stacking. However, L_3 in the Klondike Schist, while highly variable, has orientations at a high angle to L_3 in the lower thrust stacks (Fig. 5d). One plausible explanation for this discrepancy is that the Klondike Schist slices were rotated about a vertical axis during final emplacement on the well developed phacoidal cleavage zones (Fig. 10) that occur at the thrust zones. If this is correct, thrust-stacking structures in the Klondike Schist include three stages: serpentine emplacement, F_3 deformation, and phacoidal cleavage development. We include all three of these Klondike Schist structural stages in the D_3 thrust-stacking generation in Table 2.

The D_4 faults that are widespread in the Klondike Schist of the Eldorado and Bonanza creek catchments clearly post-date thrust emplacement according to the above structural correlations. These D_4 faults have not yet been traced beyond the Klondike Schist into the underlying thrust slices, but kink folds with similar orientations to D_4 in the Klondike Schist occur throughout the Nasina Assemblage. D_4 structures are steeply dipping, so their extension into the underlying slices should be detectable.

Since mesothermal gold-bearing vein emplacement was partially controlled by F_4 structures, regional mapping of F_4 structures is of potential economic interest.

CONSTRAINTS ON ABSOLUTE AGES OF DEFORMATION EVENTS

The absolute ages of specific deformation and/or mineralization events in the Klondike District are still not well known, although some progress has been made on this front. The early deformation events (D_1 and D_2) that affected both the structurally lower Nasina Assemblage units and the Klondike Schist itself are constrained to be pre-latest Permian on the basis of crosscutting undeformed intrusive rocks. Field relationships described in this paper demonstrate that the regional-scale thrust faulting and F_3 deformation event are broadly synchronous, and, from regional considerations, the thrust faulting appears to be mainly Early Jurassic in age (Dusel-Bacon *et al.*, 2002). We have no direct age constraints on the timing of the D_4 event. The age of formation of gold-bearing quartz veins is still problematical. K-Ar ages of ~140-145 Ma for muscovite within the Sheba vein were reported by Rushton *et al.* (1993), and subsequent re-analysis of material from this same location using Ar-Ar methods yielded data that could be interpreted to indicate either a Late or Early Jurassic age for the veins (M. Villeneuve, pers. comm., 2003). Ar-Ar and K-Ar ages for the host schists in the general area of the Sheba vein (Mortensen, unpublished data), however, suggest that these are all cooling ages and thus provide only a minimum age for the veining. Muscovite from a gold-bearing vein and surrounding schists in the Adams Creek area west of Bonanza Creek (Fig. 1) yield Ar-Ar ages in the range of 178-184 Ma (Mortensen, unpublished data), suggesting a minimum age of 178 Ma for the veining, at least in that area. Since veining was late- or post-D_4, it therefore appears that the D_4 event was Early or early-Middle Jurassic in age and may have immediately followed the D_3 folding and thrust faulting.

The D_5 folding and high-angle reverse fault zones locally contain biotite- and/or feldspar-phyric porphyry dykes that, although not yet directly dated, are most reasonably correlated with the Late Cretaceous Carmacks Group magmatism. These dykes were strongly fractured and faulted within the D_5 deformation zones and locally display strong hydrothermal alteration and pyritization, all suggesting that they were emplaced prior to, or during, the D_5 deformation. High-angle normal faults and hydrothermal alteration (locally including epithermal vein and other forms of epigenetic mineralization) are known to be widely associated with Carmacks Group magmatism elsewhere in western Yukon. Additional work is underway to attempt to better constrain the ages of the various deformation and mineralizing events in the Klondike District.

CONCLUSIONS

This preliminary study presents an internally consistent structural evolutionary framework for the Klondike Schist (Table 2). The structural events and associated features described in Table 2 are readily distinguishable in outcrop, hand specimen and drill core, and provide an additional useful set of observations that help to understand the nature of the rocks of the area.

The Klondike Schist occurs as at least two thrust slices on top of at least three other thrust slices. A distinctive set of crenulation folds (F_3), that are locally parasitic on larger scale (>10 m) recumbent folds of foliation, accompanied thrust stacking and the emplacement of serpentinite in the thrust stack. These folds have a distinctive spaced axial-planar cleavage in all thrust slices. This cleavage has developed locally into a new rock fabric with recrystallized micas in the Klondike Schist. The crenulations associated with this set of folds trend northeast through the otherwise-disparate thrust slices beneath the Klondike Schist, but trend southeast in the Klondike Schist. Syn-emplacement rotation of the Klondike Schist thrust slices along phacoidal cleavage zones is suspected.

The Klondike Schist has been further deformed by a set of orthogonal faults and related kink folds (F_4) and fractures. These structures post-date thrust stacking, and have not yet been traced into underlying thrust slices. Mesothermal vein formation and gold mineralization occurred during or after fault and kink-fold formation, and were partly controlled by local extensional sites developed in the faults and kink folds. Fractures parallel to kink-fold axial surfaces are particularly common hosts for mesothermal veins. Late-stage normal faults have been partially localized by pre-existing F_4 structures, and these late faults offset some mesothermal veins. Hydrothermal alteration and silicification of host rocks accompanied normal fault movement, with a different style of mineralization from the mesothermal veins.

ACKNOWLEDGEMENTS

This research was supported financially and logistically by the Klondike Star Mineral Corporation. Field work was facilitated by Bill Mann, and keen field assistance was provided by Kathryn Denommee, Kelsey Dodge and Martin To.

REFERENCES

Dusel-Bacon, C., Lanphere, M.A., Sharp, W.D., Layer, P.W. and Hansen, V.L., 2002. Mesozoic thermal history and timing of structural events for the Yukon-Tanana Upland, east-central Alaska: $^{40}Ar/^{39}Ar$ data from metamorphic and plutonic rocks. Canadian Journal of Earth Sciences, vol. 39, p. 1013-1051.

Gordey, S.P. and Ryan, J.J., 2005. Geology, Stewart River area (115N, 115O and part of 115J), Yukon Territory. Geological Survey of Canada, Open File 4970, 1:250 000 scale.

Knight, J.B., Mortensen, J.K. and Morison, S.R., 1999. Lode and placer gold compositions from the Klondike District, Yukon Territory, Canada: Its implications for the nature and genesis of Klondike placer and lode gold deposits. Economic Geology, vol. 94, p. 649-664.

Lowey, G.W., 2005. The origin and evolution of the Klondike goldfields, Yukon, Canada. Ore Geology Reviews, vol. 28, p. 431-450.

Mortensen, J.K., 1990. Geology and U-Pb chronology of the Klondike District, west-central Yukon. Canadian Journal of Earth Sciences, vol. 27, p. 903-914.

Mortensen, J.K., 1996. Geological compilation maps of the northern Stewart River map area, Klondike and Sixtymile Districts (115N/15, 16; 115O/13, 14; and parts of 115O/15, 16). Exploration and Geological Services Division, Yukon Region, Indian and Northern Affairs Canada, Open File 1996-1(G), 43 p.

Mortensen, J.K., Chapman, R., LeBarge, W. and Jackson, L., 2005. Application of placer and lode gold geochemistry to gold exploration in western Yukon. *In:* Yukon Exploration and Geology 2004, D.S. Emond, L.L. Lewis and G.D. Bradshaw (eds.), Yukon Geological Survey, p. 205-212.

Rushton, R.W., Nesbitt, B.E., Muehlenbachs, K. and Mortensen, J.K., 1993. A fluid inclusion and stable isotope study of Au quartz veins in the Klondike district, Yukon Territory, Canada: a section through a mesothermal vein system. Economic Geology, vol. 38, p. 647-678.

Laser ablation ICP-MS U-Pb zircon ages for Cretaceous plutonic rocks in the Logtung and Thirtymile Range areas of southern Yukon

Jim Mortensen*[1] *and Allison Brand
Pacific Centre for Isotopic and Geochemical Research,
Earth & Ocean Sciences, University of British Columbia[2]

Tim Liverton
Klondike Star Mineral Corporation[3]

Mortensen, J.K., Brand, A. and Liverton, T., 2007. Laser ablation ICP-MS U-Pb zircon ages for Cretaceous plutonic rocks in the Logtung and Thirtymile Range areas of southern Yukon. *In:* Yukon Exploration and Geology 2006, D.S. Emond, L.L. Lewis and L.H. Weston (eds.), Yukon Geological Survey, p. 213-221.

ABSTRACT

Plutonic rocks of Early and mid-Cretaceous age are associated with tungsten-molybdenum porphyry- and skarn-style mineralization in the Logtung area (Yukon MINFILE 105B 039, Deklerk and Traynor, 2005) in southwestern Wolf Lake map area (105B), and with tin-tungsten (-copper, lead, zinc) skarn mineralization at the Mindy and Ork occurrences (Yukon MINFILE 105C 038 and 054, respectively, Deklerk and Traynor, 2005) in the Thirtymile Range in eastern Teslin map area (105C). We have determined laser ablation U-Pb zircon ages of 109.4 ± 0.9 Ma and 110.5 ± 0.8 Ma for two samples of a biotite monzogranite stock that is inferred to be comagmatic with the felsic dyke system that partially hosts the Logtung mineralization. The latter sample is from the same locality from which a U-Pb zircon age of ~58 Ma was previously reported for zircons inferred to be hydrothermal in origin. Two separate phases of the Thirtymile Stock gave U-Pb ages of 102.7 ± 1.1 Ma and 100.9 ± 1.4 Ma.

RÉSUMÉ

Des roches plutoniques datant du Crétacé moyen au Crétacé supérieur sont associées à du porphyre renfermant du tungstène et du molybdène ainsi qu'à la minéralisation typique des skarns dans la région de Logtung (MINFILE 105B 039) au sud-ouest de la région de la carte Wolf Lake (105B), ainsi qu'au skarn minéralisé en étain et tungstène (-cuivre, plomb, zinc) des indices Mindy et Ork (MINFILE 105C 038 et 054, respectivement) dans la chaîne Thirtymile située dans la partie orientale de la région de la carte Teslin (105C). Nous avons déterminé par datation des zircons à l'U/Pb des âges de 109,4 ± 0,9 Ma et de 110,5 ± 0,8 Ma pour deux échantillons d'un stock de monzogranite à biotite que l'on déduit contemporain du magmatisme ayant engendré le réseau de filons intrusifs renfermant en partie la minéralisation de Logtung. Le dernier de ces deux échantillons provient du même emplacement où une datation antérieure à l'U/Pb de zircons qui seraient d'origine hydrothermale a fourni une âge d'environ 58 Ma. Deux phases distinctes du stock Thirtymile ont fourni des âges U/Pb de 102,7 ± 1,1 Ma et 100,9 ± 1,4 Ma.

[1]*jmortens@eos.ubc.ca*

[2]*6339 Stores Rd., Vancouver, British Columbia, Canada V6B 1Z4*

[3]*Box 393, Watson Lake, Yukon, Canada Y0A 1C0*

INTRODUCTION

Plutonic rocks are widespread in the Cassiar Terrane in southeastern and south-central Yukon (Fig. 1). Most of these are of Early to mid-Cretaceous age and have been included within the Cassiar Plutonic Suite of Mortensen *et al*. (2000) or the Anvil-Hyland-Cassiar belt of Hart (2004) and Hart *et al*. (2004). The broad range of lithological and geochemical compositions of these plutons and their diverse metallogenic signatures (including tungsten skarns, tin skarns and greisens, lead-zinc-silver-rich veins and tungsten-molybdenum porphyries; e.g., Liverton and Alderton, 1994; Driver *et al.*, 2000; Liverton and Botelho, 2001; Liverton *et al*., 2001, 2005), together with the wide range of isotopic ages previously reported for various intrusions in the Cassiar Terrane, however, indicates that more than one plutonic suite is present.

Most published isotopic ages for this region were calculated using K-Ar or Rb-Sr methods, and some of these ages have likely been disturbed by subsequent reheating events. Several recent studies employing the more robust U-Pb dating method on zircons and/or monazite (e.g., Stevens *et al*., 1993; Liverton *et al*., 2005; Mortensen *et al*., 2006) have demonstrated that most intrusive rocks in this area were emplaced 115-97 Ma, but that two older intrusive suites, one giving Early Jurassic crystallization ages and one giving Late Permian ages, are also present. Mihalynuk and Heaman (2002) also reported a U-Pb age of 58 ± 6 Ma for zircons recovered from a hydrothermally altered sample of monzonite from the Logtung W-Mo porphyry occurrence (Fig. 1) that they interpreted to have been hydrothermal in origin.

In view of the renewed interest in a variety of intrusion-related styles of mineralization in the Cassiar Terrane, a more complete understanding of temporal, geochemical and metallogenic evolution of magmatism in this region is desired. To this end, we have been carrying out a series of focused studies aimed at better constraining the ages, metallogenic associations and paleotectonic settings of

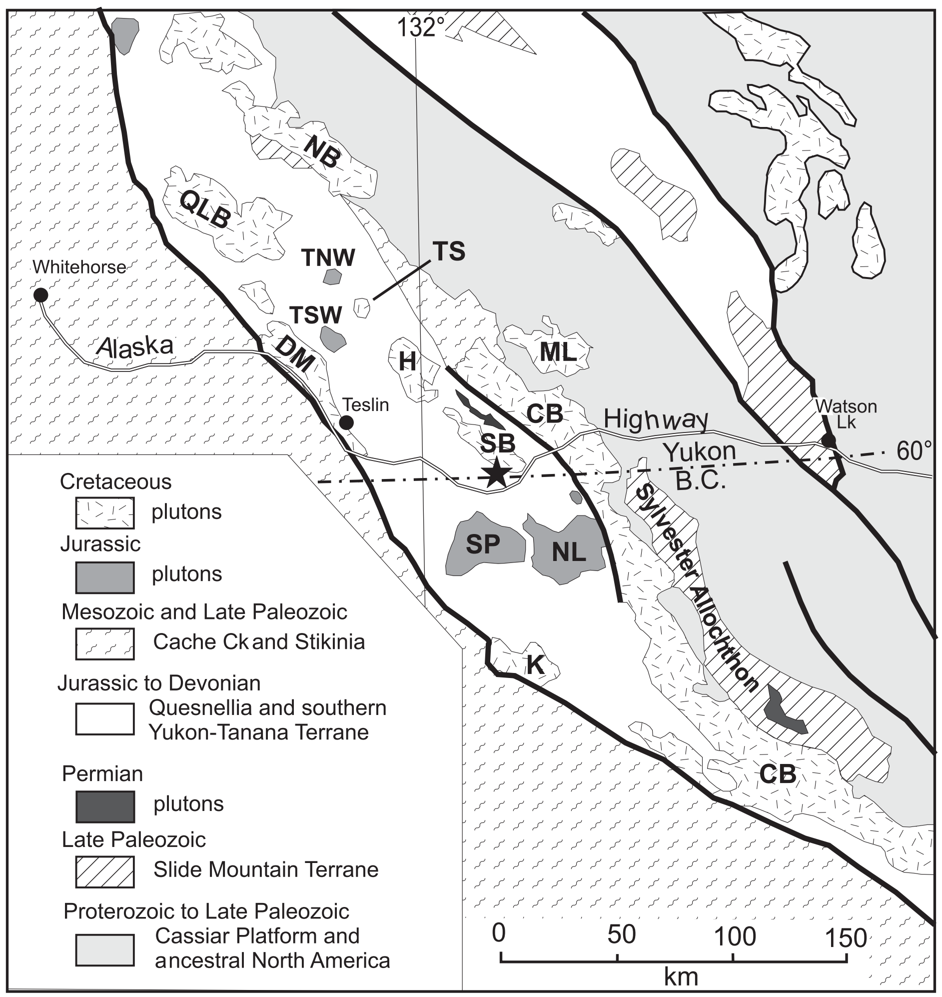

Figure 1. *Simplified geology of southern Yukon and northern British Columbia, with major plutons labelled.*
CB=Cassiar Batholith
SP=Simpson Peak pluton
NL=Nome Lake pluton
K= Klinkit pluton
SB=Seagull Batholith
ML=Marker Lake Batholith
H=Hake Batholith
DM=Deadman pluton
QLB=Quiet Lake Batholith
NB=Nisutlin Batholith
TNW=Thirtymile pluton northwest
TSW=Thirtymile pluton southwest
TS=Thirtymile Stock
Star shows the location of the Logtung area (see Fig. 2).

various intrusions in the Cassiar Terrane (e.g., Mortensen and Gabites, 2002; Liverton *et al.*, 2005; Mortensen *et al.*, 2006). In this contribution we report four new U-Pb zircon ages for two samples of intrusive rocks in the vicinity of the Logtung tungsten-molybdenum porphyry occurrence (Yukon MINFILE 105B 039, Deklerk and Traynor, 2005) in the southwest part of the Wolf Lake sheet, including a resampling of the unit previously dated by Mihalynuk and Heaman (2002), and two lithofacies of the Thirtymile Stock, in the Thirtymile Range, in the east part of the Teslin 1:50 000 mapsheet 105C/9 (Fig. 1).

INTRUSIVE ROCKS IN THE LOGTUNG AREA

The oldest intrusion in the Logtung area (preliminary Early Jurassic U-Pb zircon age; Mortensen, unpublished data) is a zoned diorite which locally grades to granodiorite, and predates mineralization. Two diorite intrusions, each approximately 0.5 x 1 km, intrude the metasedimentary country rocks to the northeast and southwest of the main monzogranite body and felsic dyke complex (Fig. 2). Primary mineralogy consists of hornblende and plagioclase, with minor quartz, biotite, clinopyroxene and K-feldspar. In places, textures become porphyritic with hornblende phenocrysts up to 8 mm, but the main diorite is dominantly heterogeneous and equigranular, with an average grain size of 1-2 mm. A sporadic aureole consisting of early reaction skarns is associated with this unit up to 30 m from the contacts (Noble *et al.*, 1984). The reaction skarns contain biotite and disseminated sulphide minerals including pyrrhotite and chalcopyrite. Disseminated sulphide minerals (possibly including molybdenite and chalcopyrite) have also been observed within the diorite near the contact.

The main intrusive body associated with the felsic dyke system and tungsten-molybdenum mineralization is a biotite monzogranite stock, approximately 2 km^2 in area. The slightly elongate monzogranite dips ~45° to the northwest below the felsic dyke system. It is characterized by a high silica content (74.6 – 77.5% SiO_2), 3% modal biotite, a molar $Al_2O_3/(Na_2O+K_2O+CaO)$ ratio of 1.00 and maximum W and Mo concentrations of 510 ppm and 235 ppm, respectively (Stewart, 1983). Accessory minerals include fluorite, scheelite, ilmenite, pyrite, zircon, allanite, apatite and beryl. Porphyritic textures dominate throughout the body; however, there is a fine-grained (1-5 mm) contact phase up to 90 m across, and satellite dykes associated with the intrusion are (rarely) pegmatitic. Hydrothermal alteration is variable in intensity throughout

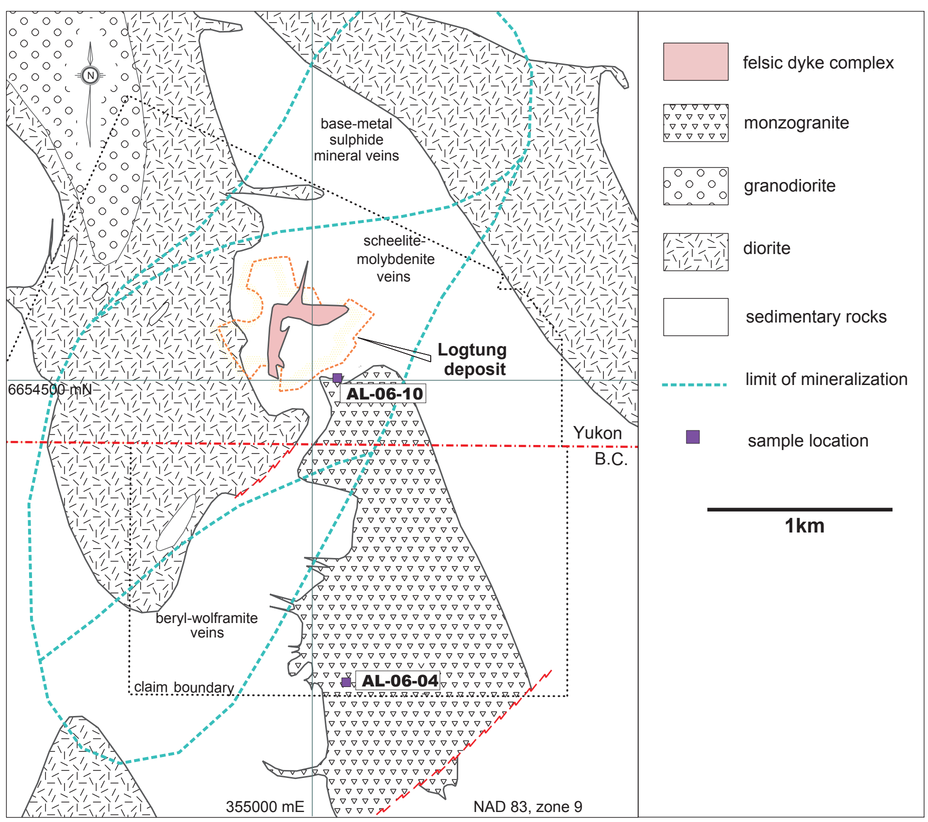

Figure 2. *Geology of southwestern Wolf Lake map area showing location of Logtung deposit and geochronological samples.*

the monzogranite stock, and consists of feldspar replacement by sericite, calcite and fluorite; and scheelite and biotite replacement by chlorite.

Tungsten-molybdenum mineralization is most intensely centred on the felsic dyke system, which is inferred to be associated with the monzogranite stock. The system consists of an irregularly shaped bilobate intrusion, approximately 500 m across, which outcrops on both sides of the northeast-trending Logtung ridge, a topographical high between the two diorite intrusions. The felsite is porphyritic, with a high SiO_2 content (75.1-76.7 wt%), and tungsten/molybdenum values similar to the monzogranite. Quartz, plagioclase, K-feldspar and spessartine garnet phenocrysts (all up to 1.5 mm) are set in a fine-grained felsite groundmass (~0.06-0.09 mm) (Stewart, 1983). Ribbon-banded material consisting of alternating layers (1-4 mm thick) of quartz, apatite needles and felsite locally developed in the main felsite body. Areas of coarsely crystalline, monominerallic massive quartz also occur. Alteration is similar to the monzogranite; however, the felsic dyke system is crosscut by a system of thin (~1-3 mm) quartz-molybdenite veins. In places, the felsite is fractured, with pyrite and molybdenite infilling. A contact aureole ~70 m wide affects the reaction skarns intruded by the felsite.

THIRTYMILE STOCK

The Thirtymile Stock, together with the Hake Batholith and Seagull Batholith (Fig. 1), have been described as a 'sub-suite' of the Cassiar intrusions. Rb-Sr dating yielded an isochron age of 101 ± 5.6 Ma for the megacrystic lithofacies of the Thirtymile Stock and an errorchron (interpreted as a cooling age) of 98.3 ± 2.9 Ma for the marginal facies of the Hake Batholith (Liverton *et al.*, 2001). All of the intrusions are highly fractionated metaluminous to weakly peraluminous one-mica granites *sensu stricto*, with only the least-evolved facies of the Thirtymile Stock (porphyry) displaying any hornblende or titanite. The Thirtymile Stock conveniently contains four lithofacies (Fig. 3) that span the complete compositional range of these intrusions (Liverton and Alderton, 1994). These include the Li-mica leucogranite and the following three biotite-bearing lithofacies: porphyry, megacrystic granite and even-grained granite. The Li-mica leucogranite is a zinnwaldite-topaz-fluorite alkali granite that forms the smallest areal extent in the Thirtymile Stock and occurs as various small sills and dykes peripheral to the stock. A lithology virtually identical to the Li-mica leucogranite exists in the apophyses of the Ork Stock, 4 km to the south. The chemistry of these granites is distinctive in their progression from relatively 'evolved' compositions (Thornton-Tuttle indices, 'D' of 86.8 (porphyry, specimen POR) to 96.2 in the biotite-bearing facies; Thornton and

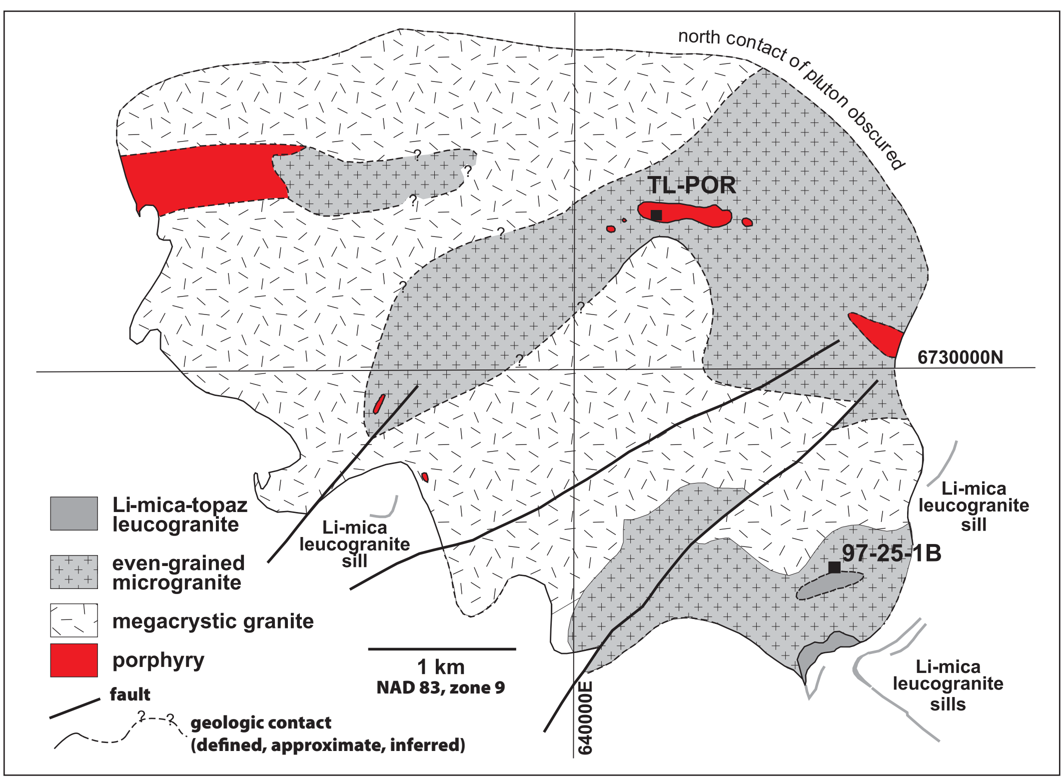

Figure 3. *Simplified geology of the Thirtymile Stock.*

Tuttle, 1960) to an extremely fractionated final lithofacies (D= 99.4 in the Ork stock). This final lithofacies has Rb/Sr ratios to >7000, and trace element compositions that fall in the 'A-type' or 'within-plate' fields of tectonic discriminant diagrams. Biotite compositions indicate that these granites are reduced-type, plotting between the nickel-nickel oxide (NNO) and quartz-fayalite-magnetite (QFM) buffers, with some below the QFM oxygen fugacity buffers (Liverton and Botelho, 2001). The Sr_i ratio of 0.7074 for the Thirtymile megacrystic facies indicates that these are I-type granites. The reduced nature and elevated halogen contents of the magma from which these granites were derived are reflected in peripheral mineralization: tin-fluorine-boron greisen-skarn at the Mindy prospect (Yukon MINFILE 105C 038, Deklerk and Traynor, 2005), tin-fluorine skarn at the Ork stock and nearby un-named scheelite-bearing skarns. The chemical signature of these granites being transitional between I-types and anorogenic granites is consistent with their generation in a late-tectonic extensional setting, which fits the H_{LO} ('Hybrid Late Orogenic') classification of Barbarin (1990).

U-PB GEOCHRONOLOGY

In this study we determined U-Pb crystallization ages for 1) two intrusive units in the vicinity of the Logtung tungsten-molybdenum porphyry occurrence (Yukon MINFILE 105B 039, Deklerk and Traynor, 2005) in the southwest part of the Wolf Lake mapsheet and 2) two lithofacies of the Thirtymile Stock in the Thirtymile Range of the Teslin mapsheet (Figs. 1 and 3) using laser ablation inductively coupled plasma mass spectrometry (LA-ICP-MS) methods. All of the analytical work was done at the Pacific Centre for Isotopic and Geochemical Research (PCIGR) at the University of British Columbia.

METHODOLOGY

The methodology used for LA-ICP-MS U-Pb dating at the PCIGR has been described by Mortensen *et al.* (2006). Minor modifications to the dating method in this study include using a 116 Ma in-house zircon as an external standard rather than the ~1100 Ma FC-1 standard, using higher laser power (60%) for the ablation, and collecting data in mixed analog and ion counting mode, with the strongest isotopic peaks (for ^{238}U and ^{232}Th) being counted in analog mode and the other weaker peaks in ion counting mode. These changes have resulted in substantially stronger ion beams and much-improved counting statistics, leading to better precision and accuracy on individual analyses. In this study, a total of 20 line scans were collected for each sample. The time-resolved signal from each analysis was carefully examined, and portions of the signal that likely reflect the effects of post-crystallization Pb-loss and/or the presence of older inherited zircon cores were excluded from calculation of the final isotopic ratios. Data from some analyses are thought to indicate that the entire scan covered portions of zircon that had experienced at least minor Pb-loss or were entirely on inherited core material. These analyses were not included in the final age calculation. Interpreted crystallization ages are based on a weighted average of the calculated ^{206}Pb/^{238}U ages for 10-20 individual analyses from each sample. Errors for the calculated ages are given at the 2 sigma level using the method of Ludwig (2003).

SAMPLE LOCATIONS AND DESCRIPTIONS

Two samples of the monzogranite stock were collected from the Logtung area. Sample AL-06-04 was obtained from the main monzogranite body (UTM 355284E, 6653271N; zone 9; all locations given use the NAD83 datum) south of the defined deposit boundary (Fig. 2). Approximately 15 kg of coarse-grained material was collected, with primary mineralogy consisting of quartz, plagioclase, K-feldspar and biotite. Minor garnet and accessory pale blue beryl, black tourmaline and fluorite are also present. Textures are porphyritic, with quartz phenocrysts up to 5 mm and euhedral K-feldspar crystals up to 1.0 cm in length. The groundmass is equigranular, with grains ~0.5-1.5 mm. Although relatively unaltered, there is evidence of minor replacement of feldspar by fluorite.

Sample AL-06-10 (~20 kg) was obtained from approximately the same location (UTM 354631E, 6655505N, zone 9; Fig. 2) as that of Mihalynuk and Heaman (2002), near the contact with the metasedimentary country rock. The primary mineralogy consists of quartz-plagioclase, K-feldspar and biotite, with accessory garnet. Although the monzogranite at this locality is also porphyritic, the average size of phenocrysts is smaller (~5-8 mm) than that of the previous sample, with an average groundmass grain size of ~0.3-1.0 mm. This sample is more intensely altered than AL-06-04, with sericite replacing feldspar.

Two samples were analysed from two separate phases of the Thirtymile Stock (Fig. 3). The geochemically least-evolved portion of the stock comprises a fine-grained seriate-textured granodiorite locally with 1-cm-sized potassium feldspar phenocrysts that grades into a similar groundmass containing cumulates of potassium feldspar megacrysts in metre-scale masses. Sample TL-POR (640568E, 6731078N, zone 9) is from the latter phase. Sample 97-25-1B (611778E, 6728670N, zone 9) is the most evolved lithofacies of the stock, which consists of even-grained biotite granite. Sample sizes ranged from 3-15 kg each.

ANALYTICAL RESULTS

The two samples of monzonite from the Logtung area each yielded a moderate amount of zircon, which consisted of clear, colourless to pale yellow, stubby prisms with multifaceted terminations. Many of the grains were fractured and contained abundant clear bubble- and rod-shaped inclusions. A total of 21 individual analyses were done on zircons from sample AL-06-04 (Fig. 4a). One grain yielded an older (~125 Ma) age that appears to reflect the presence of inherited zircon throughout the entire analysis; three grains gave slightly younger ages and are interpreted to have suffered Pb-loss throughout (Table 1). A weighted average of the $^{206}Pb/^{238}U$ ages of the remaining 17 analyses gives an age of 109.4 ± 0.9 Ma, which is interpreted to be a reasonable estimate of the crystallization age of the sample. Twenty analyses were obtained from the second sample (AL-06-10; Fig. 4b, Table 1); a weighted average $^{206}Pb/^{238}U$ age of 110.5 ±

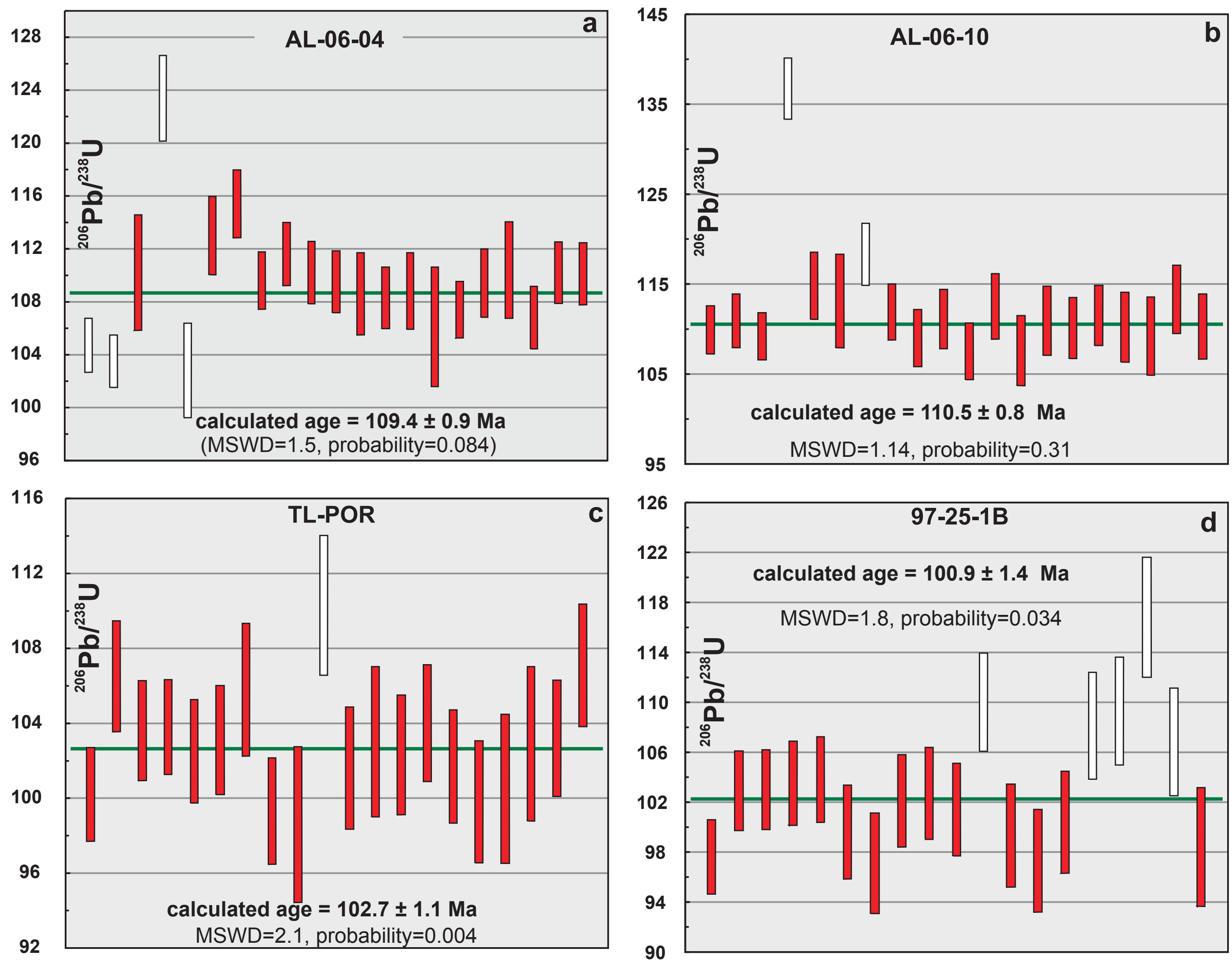

Figure 4. *Plot of $^{206}Pb/^{238}U$ ages for individual LA-ICP-MS analyses from two samples from the Logtung area* ***(a, b)*** *and two samples of the Thirtymile Stock* ***(c, d)****. Open bars are analyses that were excluded from the calculated weighted average age. MSWD = mean square of weighted deviates.*

0.8 Ma is based on a total of 18 individual analyses. Two analyses give slightly older ages, apparently due to the presence of minor inherited zircon.

The two Thirtymile Stock samples yielded abundant zircon that mainly formed square, stubby to elongate prismatic grains with simple terminations. Most of the zircon grains were fractured and contained abundant fine clear inclusions. No inherited cores were observed. The most colourless, least fractured and inclusion-free grains were selected from each sample for analysis. Nineteen out of a total of 20 analyses from sample TL-POR (Table 1) yield a weighted average $^{206}Pb/^{238}U$ age of 102.7 ± 1.1 Ma (Fig. 4c), which gives the crystallization age of the sample. One analysis yields a slightly older age,

Table 1. *LA-ICP-MS U-Pb analytical data for samples from the Logtung area and the Thirtymile Stock.*

Sample number	$^{206}Pb/^{238}U$ age	Error (1σ)	Sample number	$^{206}Pb/^{238}U$ age	Error (1σ)
AL-06-04-1	104.7	1.02	AL-06-10-20	110.3	1.81
AL-06-04-2	103.5	0.99	TL-POR-1	100.2	1.25
AL-06-04-3	110.2	2.18	TL-POR-2	106.5	1.48
AL-06-04-4	123.4	1.62	TL-POR-3	103.6	1.34
AL-06-04-5	102.8	1.78	TL-POR-4	103.8	1.27
AL-06-04-6	113	1.47	TL-POR-5	102.5	1.38
AL-06-04-7	115.4	1.28	TL-POR-6	103.1	1.46
AL-06-04-8	109.6	1.09	TL-POR-7	105.8	1.77
AL-06-04-9	111.6	1.19	TL-POR-8	99.3	1.42
AL-06-04-10	110.2	1.18	TL-POR-9	98.6	2.08
AL-06-04-11	109.5	1.18	TL-POR-10	110.3	1.86
AL-06-04-12	108.6	1.56	TL-POR-11	101.6	1.63
AL-06-04-13	108.3	1.16	TL-POR-12	103	2.01
AL-06-04-14	108.8	1.45	TL-POR-13	102.3	1.6
AL-06-04-15	106.1	2.26	TL-POR-14	104	1.56
AL-06-04-16	107.4	1.07	TL-POR-15	101.7	1.51
AL-06-04-17	109.4	1.29	TL-POR-16	99.8	1.63
AL-06-04-18	110.4	1.82	TL-POR-17	100.5	1.99
AL-06-04-19	106.8	1.18	TL-POR-18	102.9	2.06
AL-06-04-20	110.2	1.17	TL-POR-19	103.2	1.55
AL-06-04-21	110.1	1.17	TL-POR-20	107.1	1.63
AL-06-10-1	109.9	1.35	97-25-1B-1	97.6	1.49
AL-06-10-2	110.9	1.51	97-25-1B-2	102.9	1.59
AL-06-10-3	109.2	1.31	97-25-1B-3	103	1.6
AL-06-10-4	136.7	1.71	97-25-1B-4	103.5	1.7
AL-06-10-5	114.8	1.88	97-25-1B-5	103.8	1.72
AL-06-10-6	113.1	2.6	97-25-1B-6	99.6	1.88
AL-06-10-7	118.3	1.73	97-25-1B-7	97.1	2.02
AL-06-10-8	111.9	1.56	97-25-1B-8	102.1	1.85
AL-06-10-9	109	1.59	97-25-1B-9	102.7	1.84
AL-06-10-10	111.1	1.64	97-25-1B-10	101.4	1.86
AL-06-10-11	107.5	1.57	97-25-1B-11	110	1.97
AL-06-10-12	112.5	1.83	97-25-1B-12	99.3	2.06
AL-06-10-13	107.6	1.94	97-25-1B-13	97.3	2.06
AL-06-10-14	110.9	1.92	97-25-1B-14	100.4	2.04
AL-06-10-15	110.1	1.69	97-25-1B-15	108.1	2.14
AL-06-10-16	111.5	1.68	97-25-1B-16	109.3	2.16
AL-06-10-17	110.2	1.95	97-25-1B-17	116.8	2.4
AL-06-10-18	109.2	2.17	97-25-1B-18	106.8	2.16
AL-06-10-19	113.3	1.9	97-25-1B-19	98.4	2.38

presumably reflecting minor inheritance. Sixteen of twenty analyses from sample 97-25-1B (Table 1) give a weighted average $^{206}Pb/^{238}U$ age of 100.9 ± 1.4 Ma (Fig. 4d), which gives the crystallization age of the sample. The four outliers give slightly older ages, indicating older inherited zircon cores were present.

DISCUSSION

Results from the Logtung area confirm previous work by K-Ar and Rb-Sr dating that suggested an age of ~110 Ma (e.g., Hunt and Roddick, 1987) for these bodies. The results that were reported previously by Mihalynuk and Heaman (2002) are difficult to explain. Our sample AL-06-10, which was collected from the same outcrop as that of Mihalynuk and Heaman (2002), did not contain any of the brownish zircons that yielded an apparent age of 58 Ma and were interpreted by Mihalynuk and Heaman (2002) to be of hydrothermal origin. Two samples of molybdenite from the Logtung deposit have yielded Re-Os ages that are identical to the U-Pb zircon ages that we report here (D. Selby, pers. comm., 2006); thus, the nature and origin of the ~58 Ma zircons in the Mihalynuk and Heaman sample is uncertain.

The Thirtymile Stock and other bodies in the Thirtymile Range (e.g., the Ork Stock) represent some of the most evolved mid-Cretaceous plutons in the Cassiar Terrane. The mineralogy of these bodies is substantially different from most other Cassiar Suite plutons, however, in that they contain both magnetite and titanite. This mineral assemblage is generally more typical of more oxidized magmas, although geochemical investigations of the Thirtymile and Ork stocks (Liverton and Alderton, 1994; Liverton and Botelho, 2001) indicate that the magmas were in fact moderately reduced. In the northern Cordillera they are closest in composition to the reduced I-type of the Tungsten Suite (Hart *et al*., 2004), except for Sr_i and age. However, some relatively reduced granitoids have been noted in the northern part of the Cassiar Suite (Driver *et al*., 2000), and the Sr_i ratio for the Thirtymile pluton is only just less than the lower values reported for that suite. Ages reported for the Anvil-Hyland-Cassiar intrusions (110-96 Ma, Hart *et al*., 2004) overlap the 100.9-102.7 Ma age reported in this study.

ACKNOWLEDGMENTS

We thank the staff of the Pacific Centre for Isotopic and Geochemical Research, especially Bert Mueller, for assistance in generating the analytical data reported here. We also thank Richard Friedman for providing a critical review of the manuscript.

REFERENCES

Barbarin, B., 1990. Granitoids: main petrogenetic classifications in relation to origin and tectonic setting. Geological Journal, vol. 25, p. 227-238.

Deklerk, R. and Traynor, S. (compilers), 2005. Yukon MINFILE 2005 – a database of mineral occurrences. Yukon Geological Survey, CD-ROM.

Driver, L.A., Creaser, R.A., Chacko, T. and Erdmer, P., 2000. Petrogenesis of the Cretaceous Cassiar Batholith, Yukon-British Columbia, Canada: Implications for magmatism in the North American Cordilleran interior. Geological Society of America Bulletin, vol. 112, p. 1119-1133.

Hart, C.J.R., 2004. Mid-Cretaceous magmatic evolution and intrusion-related metallogeny of the Tintina Gold Province, Yukon and Alaska. Unpublished Ph.D. thesis, University of Western Australia, 198 p.

Hart, C.J.R., Goldfarb, R.J., Lewis, L.L. and Mair, J.L., 2004. The northern Cordilleran mid-Cretaceous plutonic province: Ilmenite/magnetite series granitoids and intrusion-related mineralization. Resource Geology, vol. 54, p. 253-280.

Hunt, P.A. and Roddick, J.C., 1987. A compilation of K-Ar ages: Report 17. *In:* Radiogenic Age and Isotopic Studies: Report 1, Geological Survey of Canada, Paper 87-2, p. 143-210.

Liverton, T. and Alderton, D.H.M., 1994. Plutonic rocks of the Thirtymile Range, Dorsey Terrane: Ultrafractionated tin granites in the Yukon. Canadian Journal of Earth Sciences, vol. 31, p. 1557-1568.

Liverton, T. and Botelho, N.F., 2001. Fractionated alkaline rare-metal granites: Two examples. Journal of Asian Earth Sciences, vol. 19, p. 399-412.

Liverton, T., Thirlwall, M.F. and McClay, K.R., 2001. Tectonic significance of plutonism in the Thirtymile Range, southern Yukon. *In:* Yukon Exploration and Geology 2000, D.S. Emond and L.H. Weston (eds.), Exploration and Geological Services Division, Yukon Region, Indian and Northern Affairs Canada, p. 171-180.

Liverton, R., Mortensen, J.K. and Roots, C.F., 2005. Character and metallogeny of Permian, Jurassic and Cretaceous plutons in the southern Yukon-Tanana Terrane. *In:* Yukon Exploration and Geology 2004, D.S. Emond, L.L. Lewis and G.D. Bradshaw (eds.), Yukon Geological Survey, p. 147-165.

Ludwig, K.R., 2003. Isoplot 3.0, a geochronological toolkit for Microsoft Excel. Berkeley Geochronological Center Special Publication, no. 4, 71 p.

Mihalynuk, M.G. and Heaman, L.M., 2002. Age of mineralized porphyry at the Logtung deposit W-Mo-Bi-Be (Beryl, Aquamarine), northwest BC. *In:* Geological Fieldwork 2001, BC Ministry of Energy and Mines, Paper 2002-1, p. 35-39.

Mortensen, J.K. and Gabites, J.E., 2002. Lead isotopic constraints on the metallogeny of southern Wolf Lake, southeastern Teslin and northern Jennings River map areas, Yukon and British Columbia: Preliminary results. *In:* Yukon Exploration and Geology 2001, D.S. Emond, L.H. Weston and L.L. Lewis (eds.), Exploration and Geological Services Division, Yukon Region, Indian and Northern Affairs Canada, p. 179-188.

Mortensen, J.K., Hart, C.J.R., Murphy, D.C. and Heffernan, S., 2000. Temporal evolution of Early and mid-Cretaceous magmatism in the Tintina Gold Belt. *In:* The Tintina Gold Belt: Concepts, Exploration and Discoveries, J. Jambor (ed.), British Columbia and Yukon Chamber of Mines, Special Volume 2, p. 49-57.

Mortensen, J.K., Sluggett, C., Liverton, T. and Roots, C.F., 2006. U-Pb zircon and monazite ages for the Seagull and Cassiar batholiths, Wolf Lake map area, southern Yukon. *In:* Yukon Exploration and Geology 2005, D.S. Emond, G.D. Bradshaw, L.L. Lewis and L.H. Weston (eds.), Yukon Geological Survey, p. 257-266.

Noble, S.R., Spooner, E.T.C. and Harris, F.R., 1984. The Logtung large tonnage, low-grade W (scheelite)-Mo porphyry deposit, south-central Yukon Territory. Economic Geology, vol. 79, p. 848-868.

Stevens, R.A., Mortensen, J.K. and Hunt, P.A., 1993. U-Pb and ^{40}Ar-^{39}Ar geochronology of plutonic rocks from the Teslin suture zone, Yukon Territory. *In:* Radiogenic and Isotopic Studies: Report 7, Geological Survey of Canada, Paper 93-2, p. 83-90.

Stewart, J.P., 1983. Petrology and geochemistry of the intrusives spatially associated with the Logtung W-Mo prospect, south-central Yukon Territory. Unpublished M.Sc. thesis, University of Toronto, Toronto, Ontario, 243 p.

Thornton, C.P. and Tuttle, O.F., 1960. Chemistry of igneous rocks - I. Differentiation index. American Journal of Science, vol. 258, p. 664-684.

The three 'Windy McKinley' terranes of Stevenson Ridge (115JK), western Yukon

Donald C. Murphy[1]
Yukon Geological Survey

Murphy, D.C., 2007. The three 'Windy McKinley' terranes of Stevenson Ridge (115JK), western Yukon. *In:* Yukon Exploration and Geology 2006, D.S. Emond, L.L. Lewis and L.H. Weston (eds.), Yukon Geological Survey, p. 223-236.

ABSTRACT

Rocks assigned to the Windy McKinley Terrane occur in Stevenson Ridge and Kluane map areas of western Yukon. Based on new mapping in Stevenson Ridge area, rocks mapped as Windy McKinley Terrane have been divided into three fault-bound assemblages: 1) a structurally lowest assemblage of muscovite-quartz schist, calcsilicate schist, and minor marble, carbonaceous quartzite and schist, pebble meta-conglomerate and granitic meta-plutonic rocks; 2) an imbricated ophiolitic assemblage of meta-chert, probably intrusive greenstone, leucogabbro, variably serpentinized dunite and harzburgite, and mafic greywacke; and 3) an assemblage of fine-grained clastic and calcareous rocks intruded and variably hornfelsed by voluminous Early Triassic (Mortensen and Israel, 2006) gabbro. Assemblage 1 probably correlates with Yukon-Tanana Terrane. Assemblage 2 more strongly resembles the Chulitna Terrane of Alaska rather than either the Windy or McKinley terranes as originally defined. Assemblage 3 resembles part of McKinley Terrane, as well as the Aurora Peak and Pingston terranes. These terrane re-assignments have implications for the area's mineral potential.

RÉSUMÉ

Les roches attribuées au terrane de Windy McKinley se trouvent dans la région des cartes Stevenson Ridge et Kluane au Yukon occidental. D'après de nouveaux travaux de cartographie dans la région de Stevenson, le terrane a été subdivisé en trois assemblages limités par des failles : 1) un assemblage structural inférieur de schiste à muscovite et quartz, de schiste à silicates calciques et de quantités mineures de marbre, de quartzite et de schiste carbonés, de conglomérat caillouteux métamorphisé et de roches granitiques plutoniques métamorphisées; 2) un assemblage ophiolitique imbriqué de chert métamorphisé, de roche verte probablement intrusive, de leucogabbro, de dunite et de harzburgite serpentinisées à des degrés variables et de grauwacke mafique; et 3) un assemblage de roches clastiques et calcaires à grain fin pénétrées et cornéennisées à des degrés variables par un volumineux gabbro du Trias précoce (Mortensen et Israel, 2006). L'assemblage 1 est probablement corrélé avec le terrane de Yukon-Tanana. L'assemblage 2 ressemble davantage au terrane de Chulitna en Alaska qu'aux terranes de Windy ou de McKinley auxquels il avait à l'origine été attribué. L'assemblage 3 ressemble au terrane de McKinley. Ces attributions à de nouveaux terranes ont des conséquences pour le potentiel minéral de la région.

[1]*don.murphy@gov.yk.ca*

INTRODUCTION

One of the least understood components of Yukon geology is the Windy McKinley Terrane of western Yukon (Wheeler and McFeeley, 1991; Fig. 1). Occurring in two outcrop areas in southwestern Stevenson Ridge and north-central Kluane map areas, the rocks assigned to the terrane are generally poorly exposed and with local exception, have not been mapped in detail finer than 1:250 000 scale. Furthermore, no fossils have been extracted from rocks of the Windy McKinley Terrane in the Yukon and until recently, no isotopic ages have been determined. Modern lithogeochemical data are completely lacking. Consequently, neither the lithological character of the terrane is known in detail, nor are its age or geodynamic setting(s). The interpretation of the terrane's role in the evolution of the North American Cordillera and the assessment of its mineral potential have largely been derived from proposed correlations with rocks in Alaska, where the Windy and McKinley terranes were originally defined.

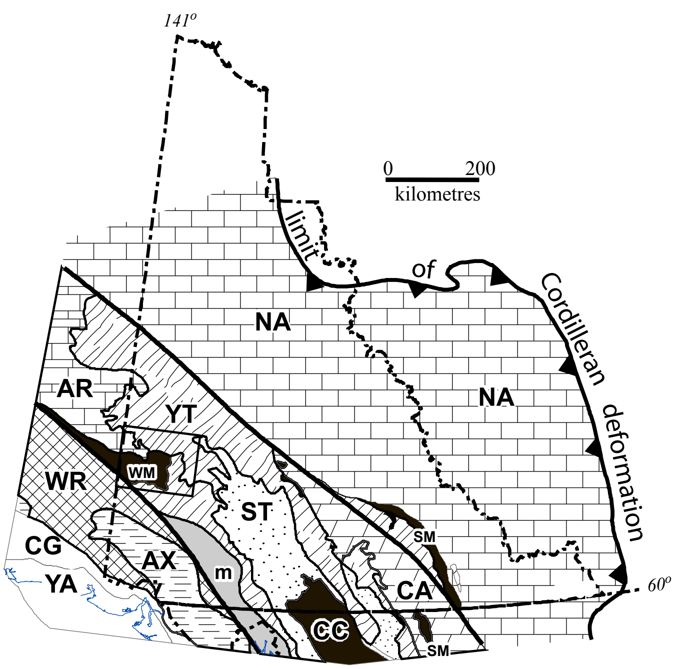

Figure 1. *Terrane map of distribution of Windy McKinley Terrane in western Yukon and eastern Alaska (modified after Colpron and Nelson, 2006). Stevenson Ridge map area is indicated by box.* ***Laurentian elements:*** *NA = Ancestral North American margin; CA = Cassiar Terrane, North American continental margin displaced on Tintina Fault; AR = Alaska Range, parautochthonous North American continental margin;* ***Intermontane Superterrane:*** *SM = Slide Mountain Terrane; YT = Yukon-Tanana Terrane; ST = Stikinia; CC = Cache Creek Terrane; WM = Windy McKinley Terrane; m = undifferentiated metamorphic rocks;* ***Insular Superterrane:*** *WR = Wrangellia; AX = Alexander Terrane; CG = Chugach Terrane; YA = Yakutat block.*

The purpose of this report is to present the results of reconnaissance mapping of Windy McKinley Terrane in the southwestern corner of Stevenson Ridge area (NTS 115JK; Figs. 1 and 2). Outcrops were examined and mapped in a reconnaissance fashion along the Alaska Highway, and three upland areas along the western and southwestern borders of the Wellesley Basin, an extensive gravel- and swamp-dominated lowland area between the White and Donjek rivers (Fig. 2). When considered in the light of previous work on the 'type' Windy and McKinley terranes of Alaska, the new observations reported herein result in the following conclusions:

1. The rocks mapped as Windy McKinley Terrane in Stevenson Ridge map area can be divided into three fault-bound subdivisions, none of which resembles either Windy or McKinley terranes as defined in Alaska.
2. Rocks of the southern-most subdivision resemble the pre-Late Devonian Snowcap assemblage of Yukon-Tanana Terrane.
3. The most extensive subdivision, underlying much of the unexposed Wellesley Basin and surrounding areas, is an imbricated, but stratally intact, ophiolite, unlike the stratally disrupted mafic and ultramafic rocks of the Windy or McKinley terranes. Its character is more reminiscent of the Chulitna Terrane of the southern Alaska Range.
4. The remainder of the terrane, exposed mainly in sporadic outcrops on either side of the Alaska Highway from Snag Junction to the Alaska border, closely resembles descriptions of the Pingston or Aurora Peak terranes, Late Paleozoic and Early Mesozoic calcareous and pelitic phyllite-dominated terranes voluminously intruded by Triassic gabbro.

These new terrane assignments require a change in the way in which these rocks may be viewed in terms of mineral potential and their role in the tectonic evolution of the North American Cordillera.

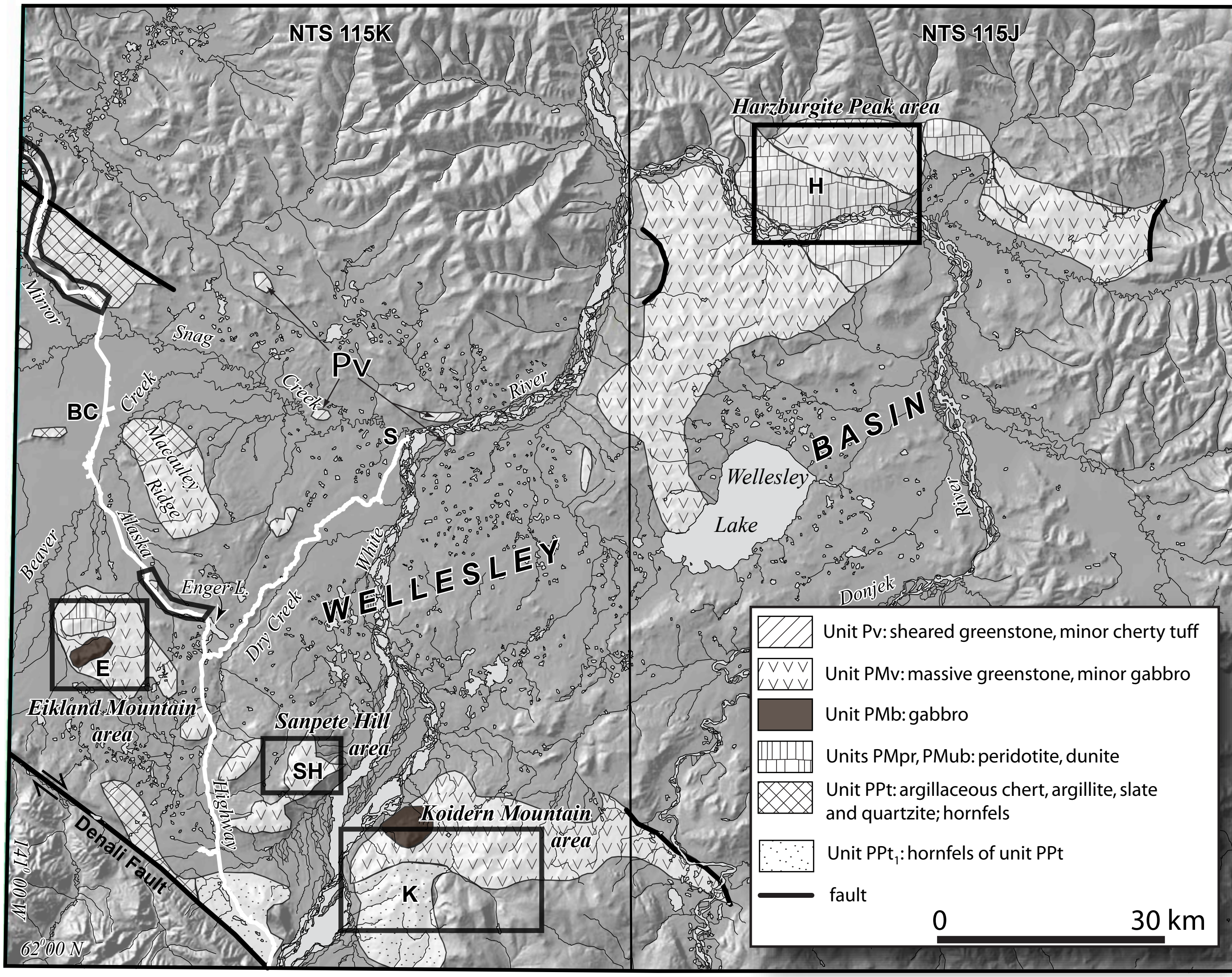

Figure 2. *Southwestern Stevenson Ridge map area. Boxes indicate areas of reconnaissance mapping as well as areas examined in recent work by Mortensen and Israel (2006, areas along Alaska Highway), and Canil and Johnston (2003; Harzburgite Peak). Rock units outlined are from Tempelman-Kluit (1974). BC = Beaver Creek; S = Snag cabin site; E, SH, K, H = Summits of Eikland Mountain, Sanpete Hill, Koidern Mountain and Harzburgite Peak, respectively.*

PREVIOUS WORK

Stevenson Ridge map area was first systematically mapped at 1:250 000 scale by Tempelman-Kluit (1974). The rocks that were later included in Windy McKinley Terrane comprise sheared greenstone, tuff and chert (unit Pv, *op. cit.*); peridotite (harzburgite and dunite, units PMpr and PMub, *op. cit.*); massive greenstone, also locally associated with chert (unit PMv, *op. cit.*); hornblende gabbro, spatially associated with massive greenstone and peridotite (unit PMb, *op. cit.*); and argillaceous chert and hornfels (unit PPt and PPt_1, *op. cit.*). Tempelman-Kluit (1974) noted a similarity of these rocks with Cache Creek Group and on that basis, inferred a Late Paleozoic age. Petrographic descriptions of many of these rock units form the basis of a bachelor's thesis by Delich (1972).

The rocks of southwestern Stevenson Ridge map area that are northeast of the Denali Fault have been assigned various terrane names, starting with the original definitions of tectonostratigraphic terranes in the late 1970s based on work done primarily in Alaska. Coney *et al.* (1980) originally assigned them to the composite Pingston McKinley Terrane, an assignment that was later superceded by Jones *et al.*'s (1984) application of the name 'Windy McKinley Terrane'. In spite of attempts to apply the name 'Windy Terrane' to these rocks (e.g., Nokleberg *et al.*, 1985, 1992, 1994), the Windy McKinley Terrane assignment has persisted into the most recent compilations and literature (Wheeler and McFeeley, 1991; Gordey and Makepeace, 2001; Canil and Johnston, 2003; Mortensen and Israel, 2006).

Nearly 30 years passed between Tempelman-Kluit's (1974) fieldwork and the start of the subsequent generation of bedrock geological research on Windy McKinley Terrane of Stevenson Ridge map area. Canil and Johnston (2003) described the rocks and relationships near Harzburgite Peak (Fig. 2); they interpreted the harzburgite body as a mantle tectonite massif, inferred that it was thrust to the north over sheeted dykes and gabbro, and concluded that all rock units were part of a large imbricated ophiolite complex. They further went on to correlate the rocks of Windy McKinley Terrane to the Seventy Mile – Slide Mountain Terrane. Mortensen and Israel (2006) investigated the western part of Windy McKinley Terrane exposed along the Alaska Highway and reported the preliminary results of U-Pb detrital-zircon and igneous isotopic dating studies. They describe the western part of the terrane as comprising mainly "...argillites interlayered with massive mafic flows and breccias (greenstones), all of which are intruded by large bodies of gabbro." (*op. cit.*); quartz-rich sandstone and limestone also occur in the argillite package. U-Pb isotopic analyses of baddeleyite and zircon from gabbro indicated a *ca.* 229 Ma (late Middle Triassic) crystallization age. U-Pb zircon analysis of detrital zircons yielded a spectrum of ages with peaks at 400-600 Ma, 900-1300 Ma, 1500-2000 Ma and 2500-2800 Ma. From these data, Mortensen and Israel (2006) inferred that Windy McKinley Terrane is a thrust flap of Wrangellia or Alexander Terrane on top of Yukon-Tanana Terrane.

THIS STUDY

Approximately three weeks were spent in Stevenson Ridge map area during the 2006 field season. During this time, outcrops of Windy McKinley Terrane rocks along the Alaska Highway were examined, as well as rocks in the following upland areas, Koidern Mountain, Sanpete Hill and Eikland Mountain (Fig. 2).

UNIT PPt, ALASKA HIGHWAY

Unit PPt is exposed in two areas along the Alaska Highway. A few outcrops occur in a 4-km-long stretch northwest of Enger Lakes, but the most extensive outcrops occur in the 10-km-long stretch north of where the highway crosses Mirror Creek (Fig. 2). In both areas, unit PPt is composed primarily of folded and foliated, medium to dark grey phyllitic argillite with variable amounts of interbedded tan-brown, variably calcareous quartz siltstone (Fig. 3a), sandstone and pebbly sandstone (Fig. 3b). North of Mirror Creek, tightly folded and strongly foliated dark-grey calcareous phyllite and argillaceous limestone predominate (Fig. 3c). Extensive bodies of dark, brown-green gabbro (Fig. 3d) are ubiquitous in these outcrops, intruding and imparting a hornfels texture on the host argillaceous rocks. Cherty, cream-coloured, green and pink calcsilicate rock and spotted porphyroblastic meta-pelite occur near intrusive contacts (Fig. 3e). Gabbro is fractured, veined and locally foliated; it is not possible to tell whether it is post-kinematic with respect to the host rocks.

KOIDERN MOUNTAIN AREA

The summit ridges of Koidern Mountain and an adjacent upland to the east afford the best opportunity to examine units PPt_1, PMv and PMb of Tempelman-Kluit (1974) and evaluate the relationships between them (Fig. 4). It also provides the best opportunity to evaluate Tempelman-Kluit's (1974) inference that unit PPt_1 is the hornfelsed equivalent of unit PPt. The units occur in a north-dipping structural succession which has been intruded by the Nisling Range Batholith, a body of mid-Cretaceous granodiorite. All units are offset by a previously unrecognized northwest-striking, post-mid-Cretaceous, dextral strike-slip fault with a horizontal offset of >4 km.

Unit PPt_1 underlies the southern part of the area, dipping to the north beneath the other rock units included in Windy McKinley Terrane. It comprises primarily slabby, psammitic biotite-muscovite-quartz schist (mineral modifiers in order of increasing amounts), intercalated with lesser biotite schist and biotite-muscovite metapelitic schist (Fig. 5a). Amphibolitic calc-silicate schist, marble (Fig. 5b), dark grey, somewhat carbonaceous schist and quartzite are minor constituents. The summit of Koidern Mountain is underlain by quartzofeldspathic schist inferred to be a granitic metaplutonic rock (Fig. 5c).

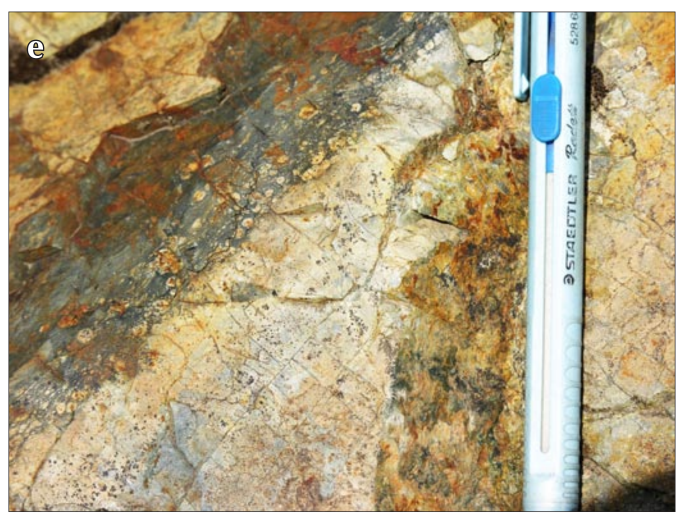

Figure 3. *Rock types included in Tempelman-Kluit's (1974) unit PPt (argillaceous chert):* ***(a)*** *phyllitic argillite and sandstone (Station 06DM010);* ***(b)*** *pebbly calcareous quartz sandstone (Station 06DM006);* ***(c)*** *calcareous phyllite (Station 06DM031);* ***(d)*** *gabbro (Station 06DM001);* ***(e)*** *spotted hornfels within a few metres of contact with massive gabbro. Protolith was probably argillite; calc-silicate hornfels locally developed.*

In contrast to the strongly recrystallized, primarily quartz-rich metasedimentary rocks of unit PPt_1, unit PMv comprises massive, greenschist-grade greenstone, chert and dark argillite. Greenstone is dark green, massive and fine grained (Fig. 6a); it is generally well fractured and cut by pale green epidote-quartz veins. Bodies of greenstone are generally concordant with respect to bedding in the strongly foliated chert, although one example of a cross-cutting body was noted. The discordant body had a slightly coarser grained diabasic texture and is clearly intrusive. With rare exception (Fig. 6b), volcanic features and textures are lacking in the other bodies, suggesting that these may be sills rather than flows. Chert is thin- to medium-bedded (ribbon-bedded to 40 cm) and is observed in many colours of matte grey, tan, green and pink (Figs. 6c, d). In the northern part of the upland area east of Koidern Mountain, unit PMv also includes tightly folded, dark green, mafic greywacke (Fig. 6e), intercalated with dark green argillite and pale green, cherty, fine-grained tuff (Fig. 6f); these rock types were not included in Tempelman-Kluit's (1974) original description.

Unit PMb in this area consists of two portions of a gabbro stock that are several square kilometres in size and that are offset along a post-mid-Cretaceous strike-slip fault. The stock is composed of generally massive and fractured, but locally foliated, medium- to coarse-grained gabbro and leucogabbro (Fig. 6g). Mafic minerals are blocky and appear to have been converted to chlorite and/or

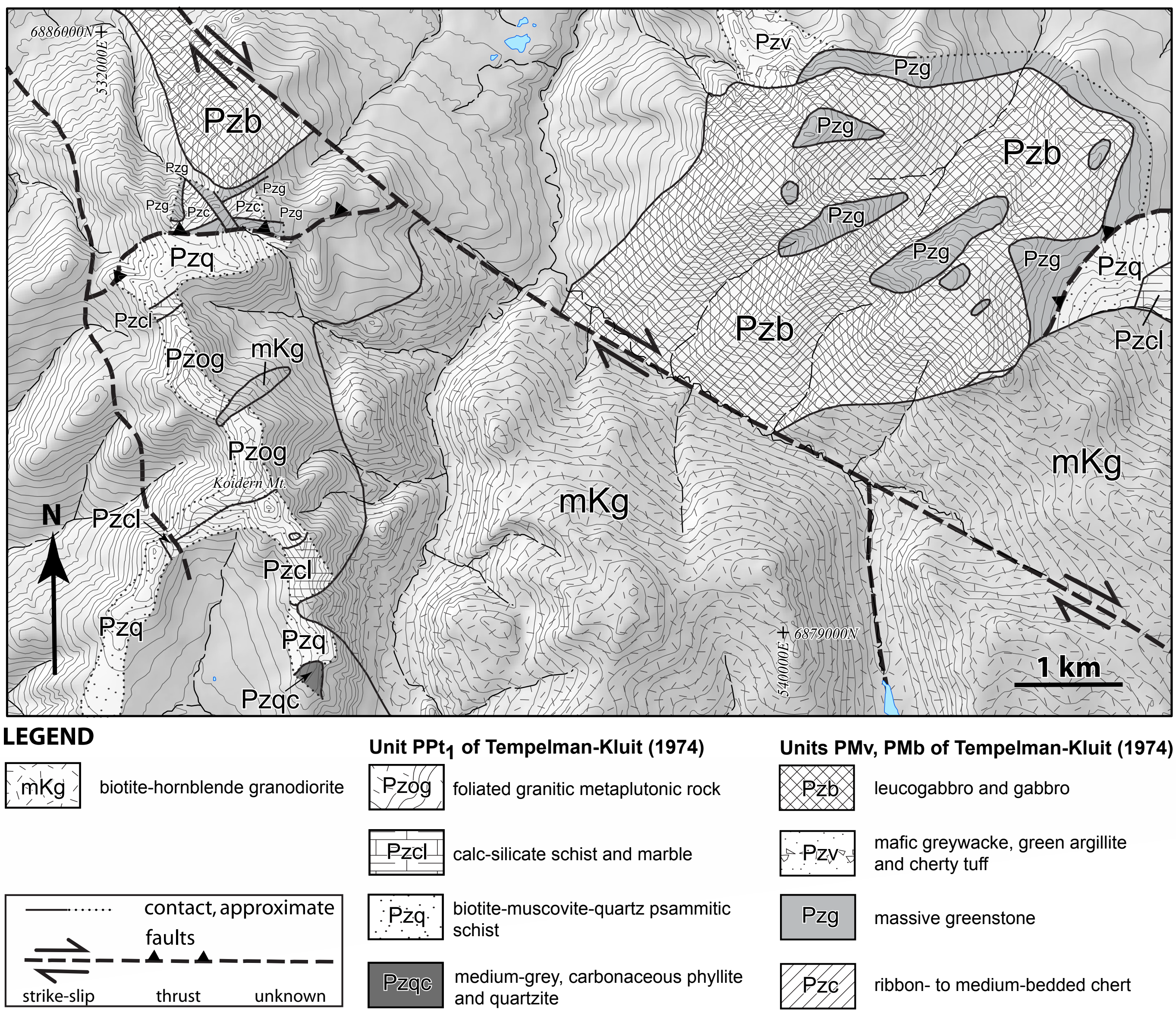

Figure 4. *Reconnaissance geology of Koidern Mountain area (UTM zone 7).*

actinolite. Preliminary thin-section work suggests that the original mafic mineralogy may have been pyroxene rather than hornblende as reported by Tempelman-Kluit (1974). The occurrence of gabbro dykes cutting massive greenstone and numerous blocks and rafts of greenstone in the gabbro stock indicate that gabbro intrudes and post-dates unit PMv. However, greenstone dykes locally intrude gabbro (Fig. 6a), suggesting that they are broadly coeval.

The contrasts in composition, degree of metamorphic recrystallization and metamorphic grade between unit PPt_1 and units PMv and PMb imply different and likely unrelated geological histories. A faulted contact is inferred to separate these units. The contact is not exposed, but can be constrained to within 20 m. A zone of foliated and lineated feldspathic greenstone (metadiabase or metagabbro; Fig. 7) is immediately above the contact. The north-dipping foliation is defined by the parallel orientation of chlorite and the long axes of elongate feldspars, and also by a weak, discontinuous compositional layering or lenticularity. A second foliation occurs within the foliation-parallel compositional lenses; this internal foliation is locally sigmoidal, deflecting to the boundaries of the lenses, and locally, asymmetrically folded. The north-trending and north-plunging lineation is defined by chlorite smears and the long axes of sub-parallel feldspar porphyroclasts. When combined with the orientation of the lineation, the sense of inclination of the two foliations in the shear zone and the vergence of asymmetrical folding of the internal foliation suggests that the fault separating unit PPt_1 and units PMv and PMb is a south-directed thrust fault.

SANPETE HILL

Sanpete Hill is underlain exclusively by monotonous massive greenstone of unit PMv, except in the lower slopes overlooking the White River which are underlain by granodiorite. Three textural variants of greenstone were observed: massive, fine-grained greenstone (most

Figure 5. *Schists of Tempelman-Kluit's (1974) unit PPt_1 in the southern part of Koidern Mountain area:* ***(a)*** *psammitic biotite-muscovite-quartz schist (Station 06DM062);* ***(b)*** *isolated outcrop of marble (view to southeast from Station 06DM141);* ***(c)*** *band of medium-grained, quartzofeldspathic rock intercalated with quartz-rich metasedimentary schist near margin of granitic metaplutonic rock (Station 06DM062). Quartzofeldspathic band is inferred to be a transposed dyke.*

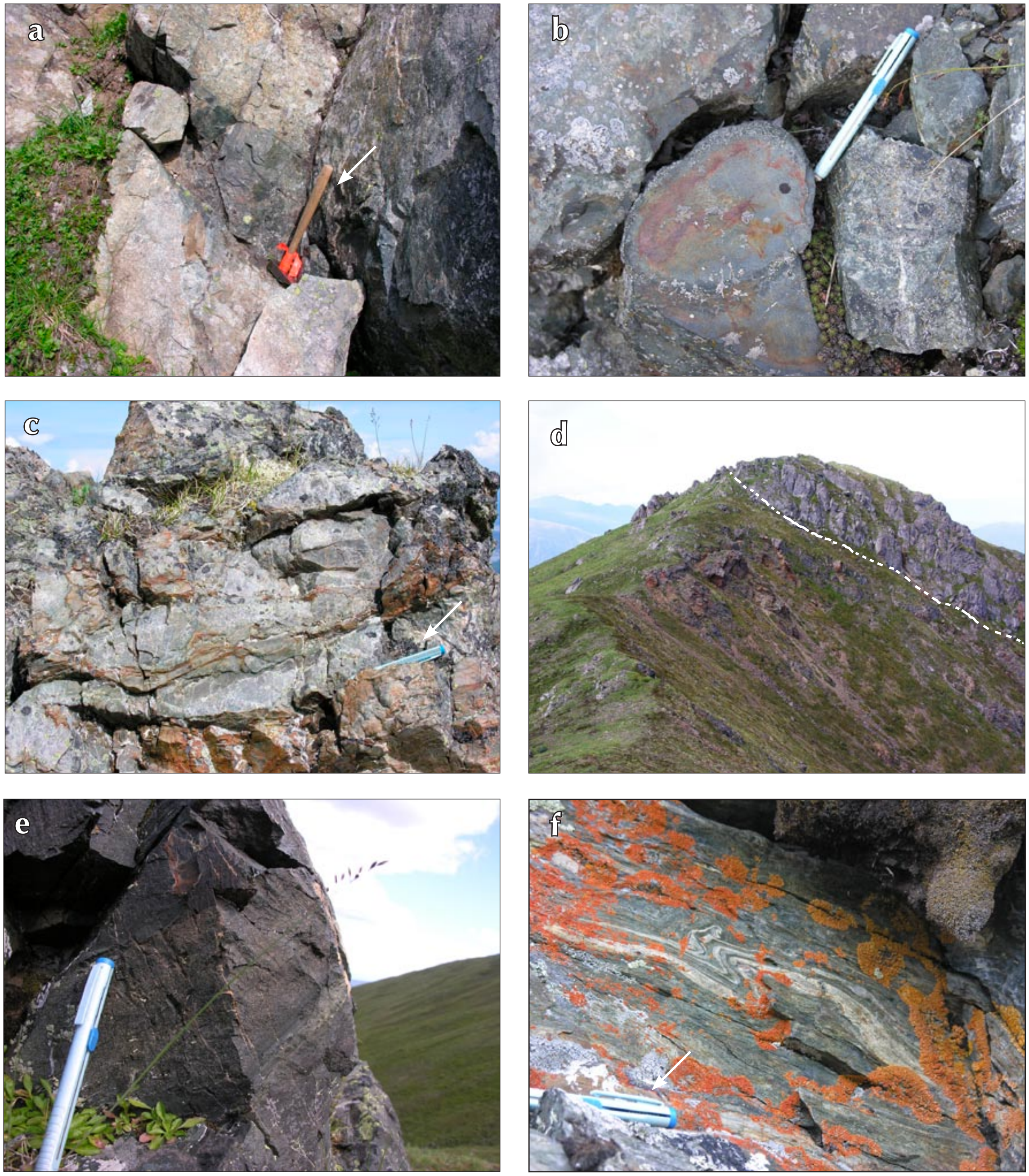

Figure 6. *Rock types in Tempelman-Kluit's (1974) units PMv (massive greenstone), PMb (gabbro), Koidern Mountain area.* ***(a)*** *Massive, fine-grained greenstone dyke intruding gabbro;* ***(b)*** *Bomb-like feature in generally massive greenstone (Station 06DM114). This is the only feature reminiscent of a volcanic origin for massive greenstone of unit PMv.* ***(c)*** *Medium-bedded, grey chert (Station 06DM073);* ***(d)*** *Section through unit PMv: massive greenstone and chert at top, chert and argillite below (Station 06DM074);* ***(e)*** *Mafic greywacke and argillite (Station 06DM122);* ***(f)*** *Folded cherty tuff (Station 06DM124);* ***(g)*** *Leucogabbro (Station 06DM077). Width of photo is about 1 m.*

Figure 7. *Foliated and lineated greenstone above contact with underlying schists of unit PPt_1 (Station 06DM081). Foliation dips to the north and is locally folded (one hinge visible in shadowed area to left of hammer head).*

common, Fig. 8a); massive, feldspar-porphyritic, fine-grained greenstone (less common, Fig. 8b); and massive, feldspar-porphyritic diabase (rare, Fig. 8c). All textural variants are unfoliated, despite the presence of fractures and veins. These rocks are interpreted as a sheeted dyke complex since volcanic textures were not observed.

EIKLAND MOUNTAIN

According to Tempelman-Kluit (1974), the Eikland Mountain massif is underlain primarily by massive greenstone of unit PMv spatially associated with bodies of gabbro and partly serpentinized dunite and harzburgite. Traverses along the ridge crest of the massif indicate that these rocks occur in a southeastwardly dipping panel with massive greenstone and small bodies of gabbro in the south. Further to the north, these rocks are successively underlain by massive gabbro, foliated and lineated gabbro, and finally by layered, foliated and lineated, variably serpentinized harzburgite and dunite (Figs. 9, 10). The

Figure 8. *Textural variation in greenstones of Tempelman-Kluit's (1974) unit PMv, Sanpete Hill:*
(a) *massive greenstone (PMv) intruded by granite (Kg) (Station 06DM097);* ***(b)*** *feldspar-porphyritic greenstone with fine-grained groundmass (Station 06DM098);*
(c) *feldspar-porphyritic greenstone with medium-grained diabasic groundmass (Station 06DM100).*

contact between gabbro and greenstone is cut by an unfoliated body of leucogabbro or diorite (unit PMb of Tempelman-Kluit, 1974). This leucogabbro or diorite has a fresh appearance and different composition and texture, suggesting that it is younger than, and unrelated to, the host rocks.

Tempelman-Kluit (1974) mapped unit PMv in the area southeast of Eikland Mountain and extending to the Alaska Highway. In a small hilltop west of the highway and north of Dry Creek, unit PMv comprises unfoliated, polymictic, pebble to cobble conglomerate (Fig. 11). Conglomerate clasts include various intermediate volcanic rock types, quartzite and amphibolite. The relationship of this rock unit to more typical greenstone of unit PMv is not known.

DISCUSSION

With these new observations, and those of Mortensen and Israel (2006) and Canil and Johnston (2003), some first-order questions about Windy McKinley Terrane in Yukon can start to be addressed. First of all, should all of

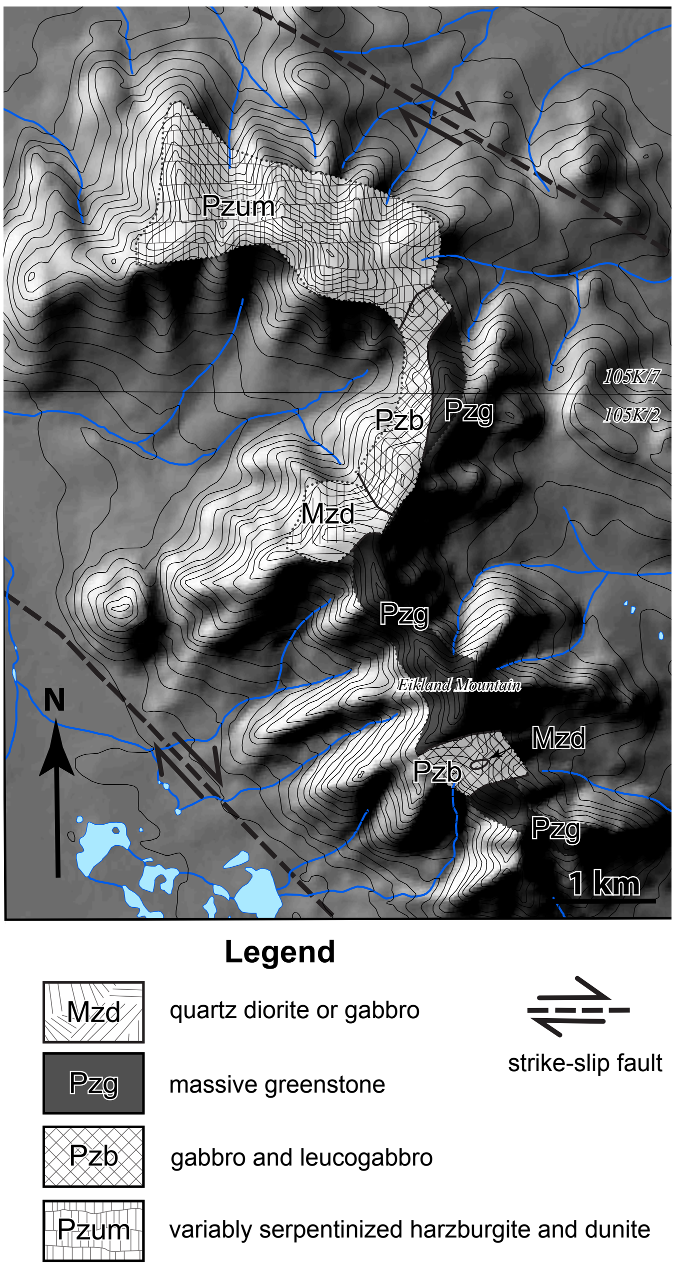

Figure 9. *Reconnaissance geology of Eikland Mountain.*

Figure 10. *Harzburgite of Tempelman-Kluit's (1974) unit PMpr (Station 06DM159).*

Figure 11. *Polymictic conglomerate observed north of Dry Creek in the area of Tempelman-Kluit's (1974) unit PMv.*

the rocks currently mapped as Windy McKinley Terrane be included in the terrane? Secondly, what are the relationships between the rock assemblages that are included in the terrane? Thirdly, what is the relationship between the rocks included in Windy McKinley Terrane and surrounding rocks of Yukon-Tanana Terrane? Fourthly, how do rocks in Yukon assigned to Windy McKinley Terrane compare with the Alaskan type localities of these terranes, that is, is the cross-border correlation with these terranes valid? Finally, what are the implications of any new insights into the nature and evolution of Windy McKinley Terrane for the mineral potential of Stevenson Ridge area?

From this study, it is not clear that all rocks of Stevenson Ridge map area mapped as Windy McKinley Terrane should be included in the terrane. Rocks currently included in Windy McKinley Terrane can be divided into three assemblages: 1) an assemblage of fine-grained and variably calcareous metaclastic rocks intruded by Middle Triassic gabbro (Mortensen and Israel, 2006; unit PPt of Tempelman-Kluit, 1974); 2) quartz-rich and locally calcareous metasedimentary and granitic metaplutonic schists such as those that underlie the southern part of the Koidern Mountain area and that have been inferred to be the hornfelsed equivalent of the rocks along the Alaska Highway (unit PPt_1 of Tempelman-Kluit, 1974); and 3) an ophiolitic assemblage (following Canil and Johnston, 2003) of massive greenstone, chert, gabbro and variably serpentinized dunite and harzburgite as observed at Eikland Mountain, Sanpete Hill, and the northern part of Koidern Mountain area (units PMv, PMb, PMpr and PMub of Tempelman-Kluit, 1974). Subdivision 1 and 2 are sufficiently dissimilar as to cast doubt on Tempelman-Kluit's (1974) inference that one is the hornfelsed equivalent of the other. Several observations illustrate the differences between these units. For example, carbonaceous argillite is nearly ubiquitous in exposures of unit PPt and only a minor constituent of unit PPt_1; slabby psammitic schist (metasandstone) is the most common rock type in unit PPt_1, yet sandstone is only a minor constituent of outcrops of unit PPt; granitic metaplutonic rock is an important constituent of unit PPt_1, yet absent in outcrops of unit PPt; and finally, gabbro, which locally makes up more than 50% of the outcrops of unit PPt, was not observed in unit PPt_1 outcrops. Unit PPt_1 most strongly resembles rocks of Yukon-Tanana Terrane, in particular, the Snowcap assemblage, the oldest and generally structurally deepest assemblage of the terrane (*cf.* Colpron and Nelson, 2006). Consequently, unit PPt_1 is herein removed from Windy McKinley Terrane.

The nature of the relationship between the remaining two assemblages in Windy McKinley Terrane is not yet known. Gabbro is the only rock type in common between them, but it differs in grain size and texture. Contacts between the two assemblages have not been observed, but appear to coincide with pronounced northwest-trending topographic lineaments along which aeromagnetic trends are offset or truncated (Fig. 12). One of these lineaments coincides with the extension of the post-mid-Cretaceous strike-slip fault documented in the Koidern Mountain area, suggesting that these lineaments mark dextral strike-slip faults. Owing to the large number of northwest-trending topographic lineaments in the area, dextral strike-slip faults may be more important than previously recognized. Aeromagnetic trends are also truncated by northeast-trending, topographic lineaments, indicating the presence of a second previously unrecognized set of faults in the area.

The nature of the contacts between the assemblages of Windy McKinley Terrane and the rocks of the surrounding Yukon-Tanana Terrane is known only locally. In the Koidern Mountain area, units of the ophiolitic assemblage (units PMv and PMb) structurally overlie rocks herein correlated with Yukon-Tanana Terrane along a south-directed, pre-mid-Cretaceous thrust fault. Near where the Alaska Highway crosses the Alaska-Yukon border, unit PPt is juxtaposed against rocks of Yukon-Tanana Terrane to the north along a topographic and geophysical lineament, implying that the contact at this location could be a strike-slip fault. This inference is supported by the steep orientation of foliations in rocks on both sides of this contact.

The new information about these assemblages, in this and recent studies, provides the basis for a test of the assignment of these rocks to the composite Windy McKinley Terrane, which was made more than 20 years ago, on the basis of the reconnaissance mapping available at that time. Windy Terrane was originally defined on the basis of outcrop exposures in the southern part of Denali National Park, Alaska. It was originally described as a stratally disrupted assemblage with a characteristic feature being "...large blocks of limestone, mainly of Devonian age, floating in a matrix of sandstone, conglomerate and limy argillite that contains late Mesozoic fossils" (Jones *et al.*, 1982 and references therein). Other large blocks include "...altered basalt, serpentinite, green and maroon argillite (tuff), and recrystallized chert (possibly an ophiolitic assemblage)..." which are "...structurally associated with black siltstone and argillite that contain

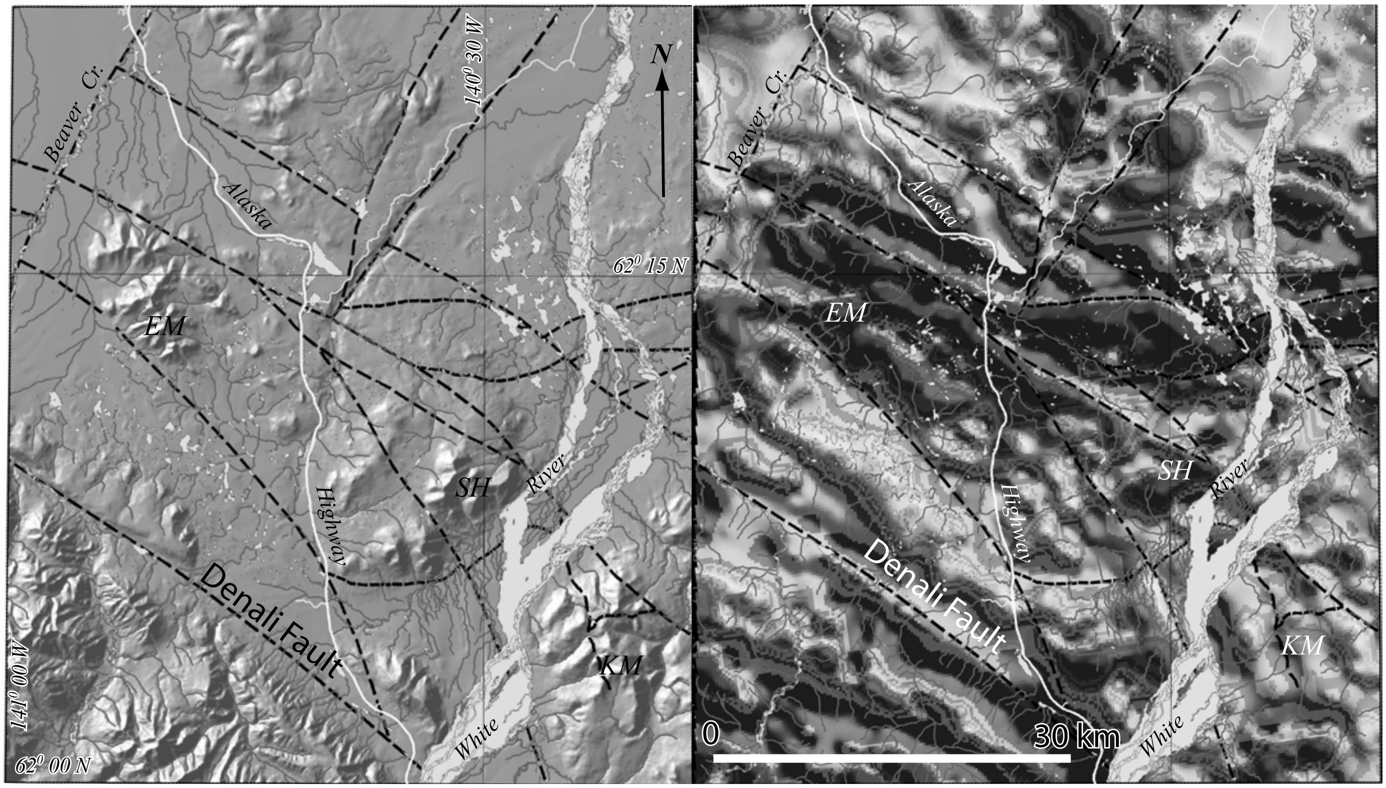

Figure 12. *Digital elevation model with hill-shading and first vertical derivative aeromagnetic map of southwestern Stevenson Ridge map area with traces of dextral strike-slip and normal faults inferred from these data. EM = Eikland Mountain; SH = Sanpete Hill; KM = Koidern Mountain.*

fossils, including a trilobite, of probable Silurian age" (*op. cit.*). Well rounded conglomerate clasts are dominantly greywacke and chert, the latter of which has yielded Mississippian, Triassic, Jurassic and Early Cretaceous radiolarian (*op. cit.*). McKinley Terrane was originally defined on the basis of outcrops in the eastern part of Denali National Park (Jones *et al.*, 1982 and references therein). It comprises three stratigraphic units. The lowest unit is composed of "...highly folded, fine-grained flyschlike rocks with abundant trace fossils and sporadic thin layers of displaced fossiliferous detritus, mainly bryozoans and rare brachipods *(sic)* of late Paleozoic (Permian?) age" (*op. cit.*); the top of this unit also includes radiolarian chert and argillite containing Triassic fossils and enclosing slump blocks of Devonian limestone. The middle unit is several thousand metres thick and consists of pillow basalt with associated dykes and sills of gabbro and sporadic sedimentary interbeds containing Late Triassic monotid bivalves; the dykes and sills also cut the underlying sedimentary rocks. The uppermost unit consists of "...poorly fossiliferous, flyschlike assemblage of greywacke, argillite, minor conglomerate and radiolarian chert that is of late Mesozoic (mainly Cretaceous) age" (*op. cit.*). With these descriptions in mind, it seems clear that the rocks in Stevenson Ridge map area that have been assigned to Windy McKinley Terrane bear little resemblance to the type Windy Terrane and only some similarity to the type McKinley Terrane. The extensive areas of relatively intact, although imbricated (Canil and Johnston, 2003), ophiolitic rocks in Stevenson Ridge map area are unlike the kilometre-scale blocks of disrupted ophiolitic rocks in the type Windy Terrane. Mélange-like stratal disruption, blocks of limestone, and thick pillow basalt sequences are not characteristics of either of the Stevenson Ridge assemblages. The variably calcareous and argillaceous siliciclastic rock assemblage of Stevenson Ridge area is lithologically similar only to the older part of the McKinley Terrane and is likewise intruded by voluminous amounts of Triassic, albeit Middle Triassic, gabbro (Mortensen and Israel, 2006). If this assemblage is indeed McKinley Terrane, the remaining parts of the terrane are notably absent in Stevenson Ridge map area.

Although unlike Windy Terrane and only partly resembling McKinley Terrane, the two assemblages in Stevenson Ridge map area are lithologically similar to other terranes in the Alaska Range. The Pingston Terrane, with which the Stevenson Ridge rocks were originally affiliated (Coney *et al*., 1980), comprises an older, Pennsylvanian to Permian unit of tan-weathering phyllite, minor radiolarian chert, and very rare lenses of crinoidal marble, all of which are intruded by abundant gabbro and diorite. The younger unit is Late Triassic in age and consists of laminated, silty limestone, black sooty argillite and minor quartzite, also intruded by gabbro (Jones *et al*., 1982). The Aurora Peak Terrane (Nokleberg *et al*., 1985), which may correlate with the Pingston Terrane (*op. cit.*; Wilson *et al*., 1998), consists of a relatively older unit of calc-schist, marble, quartzite and pelitic schist, and a relatively younger unit of metaplutonic rocks including metagabbro. Relatively intact ophiolitic rocks (basal serpentinite, gabbro, pillow basalt and chert) associated with intermediate to mafic volcaniclastic rocks make up the lower part of the Chulitna Terrane, a relatively narrow and lithologically and paleontologically distinctive terrane in the southern Alaska Range (Jones *et al*., 1982). These terranes may appear to be a better match for the Stevenson Ridge rocks, but more information is needed before any terrane re-assignments would be credible. If these new correlations are indeed valid, they have implications for the magnitude of displacement of the Denali Fault (including the Hines Creek strand), implications that are beyond the scope of this paper.

The new appreciation of the nature of the rocks in southwestern Stevenson Ridge map area, derived from this and recent work by Canil and Johnston (2003) and Mortensen and Israel (2006), has implications for mineral exploration in the area. If, as inferred by Mortensen and Israel (2006), the McKinley- or Pingston-like assemblage of variably calcareous and argillaceous clastic rocks and gabbro is reminiscent of Wrangellia or Alexander Terrane, then gabbro in this assemblage could be a potential target for Cu-Ni-PGE magmatic sulphide deposits. If present, any volcanic rocks coeval with the voluminous gabbro bodies could potentially host volcanic-associated massive sulphide deposits. Ophiolitic terranes, such as the Chulitna-Terrane-like assemblage in Stevenson Ridge area, are known to host podiform chromite in their upper mantle-lower crustal sections, and Cyprus-style volcanic-associated massive sulphide deposits in their upper crustal sections. Finally, the re-assignment of Tempelman-Kluit's (1974) unit PPt_1 to Yukon-Tanana Terrane increases the local extent of this terrane. As Yukon-Tanana Terrane locally hosts a diversity of massive sulphide deposits (*e.g.* the Finlayson Lake district, southeastern Yukon (Murphy *et al*., 2006 and references therein)), this new area of Yukon-Tanana Terrane may also hold promise for these types of deposits.

SUMMARY

Rocks in southwestern Stevenson Ridge map area that have been correlated with Windy McKinley Terrane in Alaska were re-examined in 2006. These rocks have been subdivided into three assemblages, one of which probably belongs to Yukon-Tanana Terrane; one that may correlate with part of McKinley Terrane, but also resembles other terranes in Alaska such as the Pingston or Aurora Peak terranes; and an ophiolitic assemblage that may correlate with the Chulitna Terrane of the southern Alaska Range. Assessments of the region's mineral potential need to be revised in light of these new correlations.

ACKNOWLEDGEMENTS

I would like to thank Stephen Horton for excellent assistance, both in the field and in the office; Doug Makkonen and Stephen Soubliere of Trans North Helicopters for safe and efficient flying; Carl Schulze of All-Terrane Geological Consulting and Richard Niemenen, formerly of Falconbridge, for invaluable logistical assistance; and Jim Mortensen for ongoing interest and discussion. Steve Israel provided an internal critical review and I would like to thank him for that, as well as his interest in, and discussion about, the Insular terranes in Yukon and Alaska.

REFERENCES

Canil, D. and Johnston, S.T., 2003. Harzburgite Peak: A large mantle tectonite massif in ophiolite from southwest Yukon. *In:* Yukon Exploration and Geology 2002, D.S. Emond and L.L. Lewis (eds.), Exploration and Geological Services Division, Yukon Region, Indian and Northern Affairs Canada, p. 77-84.

Colpron, M. and Nelson, J.L., 2006. Paleozoic Evolution and Metallogeny of Pericratonic Terranes at the Ancient Pacific Margin of North America, Canadian and Alaskan Cordillera. Geological Association of Canada, Special Paper 45, 523 p.

Coney, P.J., Jones, D.L. and Monger, J.W.H., 1980. Cordilleran suspect terranes. Nature, vol. 288, p. 329-333.

Delich, M.W., 1972. Petrology of some new ultramafic occurrences between Shakwak and Tintina Trenches, western Yukon. Unpublished BSc thesis, The University of British Columbia, Vancouver, British Columbia, Canada, 40 p.

Gordey, S.P. and Makepeace, A. (compilers), 2001. Bedrock Geology, Yukon Territory. Geological Survey of Canada, Open File 3754 and Exploration and Geological Services Division, Yukon Region, Indian and Northern Affairs Canada, Open File 2001-1, scale 1:1 000 000.

Jones, D.L., Silberling, N.J., Gilbert, W. and Coney, P., 1982. Character, distribution, and tectonic significance of accretionary terranes in the central Alaska Range. Journal of Geophysical Research, vol. 87, no. B5, p. 3709-3717.

Jones, D.L., Silberling, N.J., Coney, P.J. and Plafker, G., 1984. Part A – Lithotectonic terrane map of Alaska (west of the 141st Meridian). *In:* Lithotectonic Terrane Maps of the North American Cordillera, D.L. Jones and N.J. Silberling (eds.), United States Geological Survey, Open File Report 84-523, p. A1-A12.

Mortensen, J.K. and Israel, S., 2006. Is the Windy-McKinley terrane a displaced fragment of Wrangellia? Evidence from new geological, geochemical and geochronological studies in western Yukon. Geological Society of America, Abstracts with Programs, vol. 38, No. 5, Abstract 43-10.

Murphy, D.C., Mortensen, J.K., Piercey, S.J., Orchard, M.J. and Gehrels, G.E., 2006. Mid-Paleozoic to early Mesozoic tectonostratigraphic evolution of Yukon-Tanana and Slide Mountain terranes and affiliated overlap assemblages, Finlayson Lake massive sulphide district, southeastern Yukon. *In:* Paleozoic and Mesozoic Evolution and Metallogeny of Pericratonic Terranes at the Ancient Pacific Margin of North America, Canadian and Alaskan Cordillera, M. Colpron and J.L. Nelson (eds.). Geological Association of Canada, Special Paper 45, p. 75-105.

Nokleberg, W.J., Jones, D.L. and Silberling, N.J., 1985. Origin and tectonic evolution of the Maclaren and Wrangellia terranes, eastern Alaska Range, Alaska. Geological Society of America Bulletin, vol. 96, p. 1251-1270.

Nokleberg, W.J., Aleinikoff, J.N., Lange, I.M., Silva, S.R., Miyaoka, R.T., Schwab, C.E. and Zehner, R.E., 1992. Preliminary geologic map of the Mount Hayes quadrangle, eastern Alaska Range, Alaska. U.S. Geological Survey, Open File Report 92-594, scale 1:250 000.

Nokleberg, W.J., Plafker, G. and Wilson, F.H., 1994. Geology of south-central Alaska. *In:* The Geology of Alaska, Geological Society of America, The Geology of North America, G. Plafker and H.C. Berg (eds.), vol. G-1, p. 311-366.

Tempelman-Kluit, D.J., 1974. Reconnaissance geology of Aishihik Lake, Snag and part of Stewart River map areas, west-central Yukon. Geological Survey of Canada, Paper 73-41.

Wheeler, J.O. and McFeeley, P. (compilers), 1991. Tectonic assemblage map of the Canadian Cordillera and adjacent parts of the United States of America, Geological Survey of Canada, Map 1712A, scale 1:2 000 000.

Wilson, F.H., Dover, J.H., Bradley, D.C., Weber, F.R., Bundtzen, T.K. and Haeussler, P.J., 1998. Geologic map of central (interior) Alaska. U.S. Geological Survey, Open File Report 98-133, 63 p.

Morphological and compositional analysis of placer gold in the South Nahanni River drainage, Northwest Territories

K.L. Rasmussen[1] and J.K. Mortensen[2]
Department of Earth and Ocean Sciences, University of British Columbia

H. Falck
Geological Survey of Canada/Northwest Territories Geoscience Office[3]

Rasmussen, K.L., Mortensen, J.K. and Falck, H., 2007. Morphological and compositional analysis of placer gold in the South Nahanni River drainage, Northwest Territories. *In:* Yukon Exploration and Geology 2006, D.S. Emond, L.L. Lewis and L.H. Weston (eds.), Yukon Geological Survey, p. 237-250.

ABSTRACT

Placer gold has been reported in small amounts throughout the South Nahanni river drainage; however, the original source of the gold is uncertain. This study focuses on two types of placer gold in the area: (1) locally abundant grains derived from near Selena Creek, and (2) scattered grains recovered from streams throughout the South Nahanni drainage area. A shape analysis of all gold grains was completed and representative grains from each sample population were selected for imaging on the scanning electron microscope, along with analysis for Au-Ag-Cu-Hg values on the electron microprobe. The gold grains are typically >700 fineness and mercury is below detection levels (<0.20%). Approximately half the grains analysed from the Selena Creek area registered near to, or slightly greater than, detection levels of copper (<0.04%), whereas the majority of grains from the isolated showings had copper contents below detection levels. The results are compared with published morphological and compositional data for placer and lode gold in other regions.

RÉSUMÉ

La présence d'or placérien a été signalée en petite quantité dans l'ensemble du bassin versant de la rivière Nahanni Sud dans les Territoires du Nord-Ouest, mais une grande conjecture persiste quant à son origine. Cette étude est focalisée sur les deux types d'or placérien trouvés dans la région : 1) les grains abondants par endroits près du ruisseau Selena et 2) les grains épars récupérés dans des cours d'eau dans l'ensemble du bassin. Une analyse de la forme de tous les grains d'or a été effectuée et des grains représentatifs de chaque population échantillonnée ont été sélectionnés à des fins d'imagerie au microscope électronique à balayage suivie d'analyses pour Au-Ag-Cu-Hg à la microsonde électronique. De manière caractéristique le titre des grains est supérieur à 700 et leur teneur en mercure est inférieure aux seuils de détection (< 0,20 %). Approximativement la moitié des grains provenant de la région du ruisseau Selena ne présentaient que des concentrations de cuivre légèrement supérieures aux seuils de détection (< 0,04 %), alors que la majorité des grains provenant d'indices isolées renfermaient des concentrations de cuivre inférieures aux seuils de détection. Les résultats obtenus sont comparés aux données de morphologie et de composition publiées pour l'or placérien et l'or filonien provenant d'autres régions.

[1]*6339 Stores Road, Vancouver, British Columbia, Canada, V6T 1Z4, krasmuss@eos.ubc.ca*

[2]*jmortens@eoc.ubc.ca*

[3]*P.O. Box 1500, 4601-B 52nd Avenue, Yellowknife, NT, Canada, X1A 2R3*

INTRODUCTION

Since the 1920s, the South Nahanni River has been known as a 'dangerous river' by the people entering the region for various reasons (e.g., trapping, route to the Klondike, adventure, etc.), including the prospectors who were searching for gold in the area. An account of their efforts has been partially preserved by the names of the lakes, creeks and felsic intrusions, many of which are named after many of the early prospectors; Deadman and Headless valleys give some indication of the fates of those who did not survive their time in the region. The stories are also documented in books such as R.M. Patterson's "Dangerous River" (1953) and P. Berton's "The Mysterious North" (1956). Certainly the fate of the McLeod Brothers, who are alleged to have been discovered without their heads in the early 1900s after reportedly having found a mother-lode, or a 'good prospect', made for much speculation as to the cause of their deaths (e.g., cannibal Indian tribes, eight-foot-tall sasquatches, scavenging grizzly bears), and even more so with respect to the location of their lost gold mine (Turner, 1975).

While literature on the legends abounds (with varying degrees of exaggeration), the geological understanding of the source of the placer gold has lagged far behind. A study of placer gold-grain morphology and composition for the South Nahanni River watershed of the Selwyn and Mackenzie mountains, Northwest Territories, was undertaken in order to investigate the nature of, and to make inferences as to the origin of, the placer gold (Fig. 1). The study was initiated as part of the Mineral and Energy Resource Assessment (MERA II) conducted by the Geological Survey of Canada for Parks Canada over the 2004-2005 field seasons (Falck and Wright, 2007, in press). The purpose of the MERA II was to evaluate the precious- and base-metal potential of the South Nahanni River area; however, the question as to the source of scattered deposits of placer gold in the area was not fully addressed. This study aims to develop a preliminary characterization of the known placer gold in the area, in order to determine whether or not the gold is locally derived. This study will also make suggestions for possible mineral deposit settings from which the gold may have been derived (e.g., intrusion-related skarns or sheeted veins, Carlin-type sediment-hosted disseminated, orogenic vein, etc.).

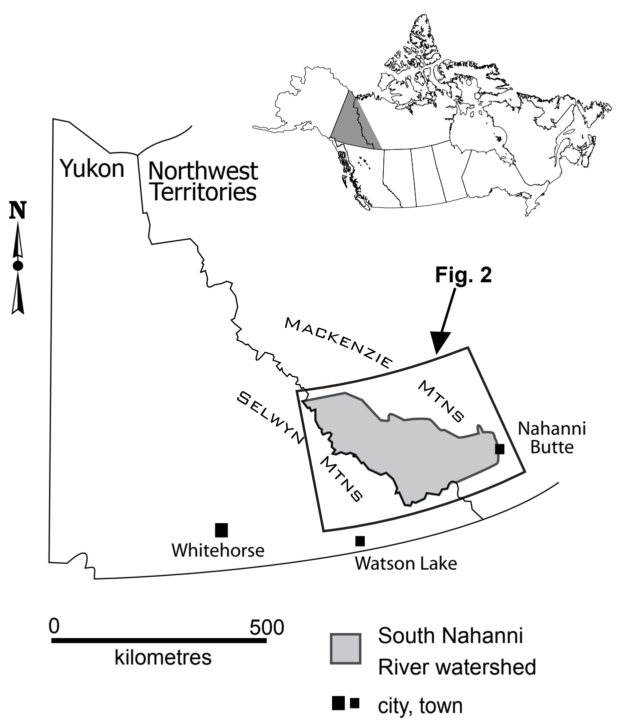

Figure 1. *Location of the South Nahanni River watershed in the Selwyn and Mackenzie mountains, southwestern Northwest Territories (adapted from Mortensen et al., 2000).*

To characterize and determine the source of the placer gold in the area, samples from two 'types' of placer occurrences were investigated:

(1) Locally abundant placer gold grains were recovered from Chuck Creek, in the Selena Creek area (referred to as the 'Chuck sample'). This sample was collected adjacent to the intermediate to mafic volcanic rocks hosting the Chuck copper (-gold) mineral showings documented in the Northern Minerals Database[4] (NORMIN) (Fig. 2). This area also has several known placer gold occurrences, as documented in NORMIN. Locations of these placer occurrences are shown in Figure 2. Gold grains were panned from a sample of light-coloured, clay-rich material with small limestone fragments. In the field, this material underlies an immature, cobble-boulder lag in the streambed. It is uncertain whether the clay-rich material is an oxidized till forming a basal layer of the creek, or part of an underlying linear feature, such as a fault (T. Christie and H. Smith, writ. comm., 2006). The gold grains were separated by hand from a concentrate composed predominantly of ilmenite-magnetite-barite, but includes specular hematite and an iron- and/or calcium-rich garnet (no sulphide minerals were present).

[4]*NWT Geoscience Office, Government of the Northwest Territories, 2006. Northern Minerals Database (NORMIN), www.nwtgeoscience.ca/normin*

(2) A collection of placer gold grains referred to as 'isolated samples' (36 grains from 8 sample locations and 18 unidentified/unlocated grains) were recovered from approximately 450 stream silt and heavy mineral concentrate (HMC) samples (Fig. 2). These samples were collected during the 1985-1987 field seasons for an earlier Mineral and Energy Resource Assessment (MERA I) conducted over the Ragged Ranges and Nahanni Karst and Tlogotsho Plateau regions (Spirito *et al*., 1988; Jefferson and Pare, 1991) of the watershed (Fig. 2).

The distribution of the isolated samples is biased due to the limited HMC sample coverage within the entire South Nahanni River watershed. Areas that are not represented by the 'isolated placer gold samples', and which are thought to have a high potential for locally derived placer gold, are the southwestern corner where several placer gold occurrences are documented in NORMIN and where the Chuck sample is located, as well as the northern portion of the field area that has at least one primary intrusion-associated gold showing documented in NORMIN (Fig. 2). We are also restricted by the relatively small number of gold grains included in the isolated

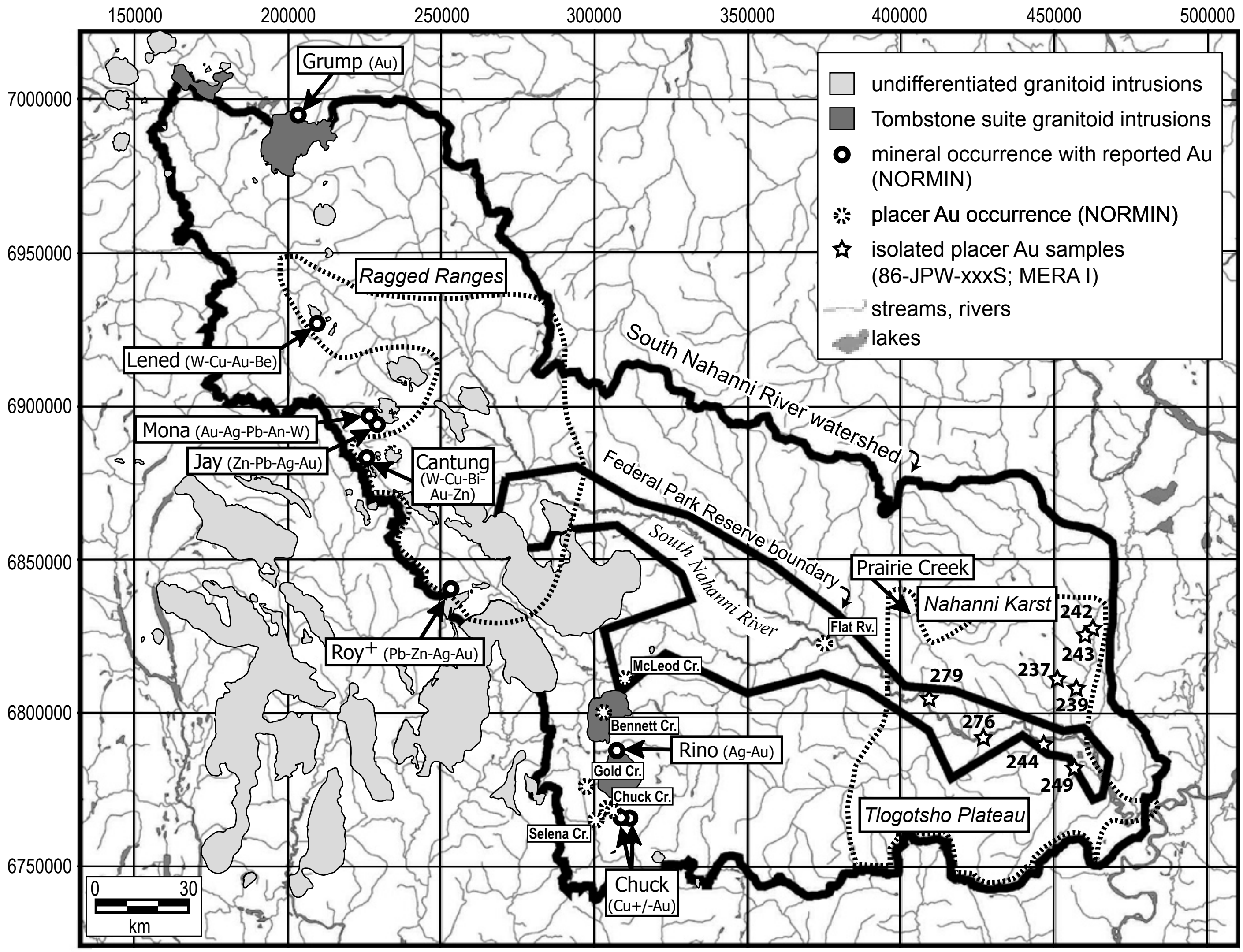

Figure 2. *Map of the South Nahanni River watershed area (Heffernan, 2004; Rasmussen et al., 2006). Approximate Ragged Ranges and Nahanni Karst-Tlogotsho Plateau HMC sampling regions from the MERA I are outlined by dashed black lines (Spirito et al., 1988). Locations of lode and placer gold occurrences (NORMIN) are also shown. Isolated samples of placer gold grains collected by C.W. Jefferson within Nahanni MERA I areas and made available for this study are represented by star symbols (Spirito et al., 1988; Jefferson and Spirito, 2003). The map grid is NAD 83, Zone 10 UTM coordinates.*

samples. A larger sample size is preferred in order to statistically characterize gold grain morphologies and compositions. This, in turn, limits the inferences we can make regarding the source of these samples. The Chuck sample, however, consisted of enough grains (>250) to completely characterize the placer gold morphology and composition for the Chuck placer gold showing.

PREVIOUS WORK IN THE SOUTH NAHANNI RIVER WATERSHED

Prospecting in the South Nahanni River region began near the turn of the 20th century, most likely as a result of historical reports by local First Nations (Dene) groups. The Dene discovered and mined large gold nuggets from local streambeds (as described by R.M. Patterson in "Dangerous River", 1953). This prospecting along the river and its tributaries has continued sporadically up until present day and has resulted in the filing of assessment work on six placer gold occurrences in the Nahanni region (Fig. 2; NORMIN). The majority of follow-up work was conducted on the five showings in the southwestern corner of the South Nahanni River watershed, which consist of the McLeod Creek, Bennett Creek, Gold Creek, Chuck Creek and Selena Creek placer occurrences (Fig. 2). The placer deposits were discovered either by prospectors panning, or during large regional stream sediment surveys (Gallup, 1973; Lenters, 1984). Following discovery, only a limited amount of work was conducted on these showings and consisted mainly of test pits on the placer deposits and minor prospecting to identify the source of the gold. Investigations of a select few of the claims included soil sampling and geophysical surveys, as well as geological mapping and prospecting (White and Cruz, 1973; Vulimiri and Crooker, 1989). The most comprehensive documented work has been in the Selena Creek area (Fig. 2), where there has been prospecting of two copper showings in the creek headwaters (McDougall, 1976; Stammers, 1983; Vulimiri, 1986) combined with several investigations of the placer gold deposits (Rowan and von Kursell, 1989; Cairns *et al.*, 1995).

Although anecdotal evidence suggests that small-scale placer gold testing and mining by individuals has taken place historically throughout the southwestern corner of the South Nahanni River watershed, records in NORMIN detailing exploration in the Selena Creek area only date from the early 1980s. The following geological summary of the Chuck occurrences is sourced from the NORMIN assessment files 095DNE0007 to 095DNE0010. From this area, anomalous placer gold and bedrock-hosted gold and copper (malachite, bornite and chalcopyrite) values were reported. The lode occurrences are hosted in intensely sericitized and locally highly silicified, intermediate to mafic volcanic rocks of the Lower Cambrian Sekwi Formation. The volcanic rocks are overlain by the calcareous Rabbitkettle Formation and crop out in the core of the southwest-plunging Caribou anticline. More recent work that has resulted in the completion of a second MERA in the South Nahanni River watershed (Falck and Wright, 2007, in press), as well as ideas proposed by Emsbo *et al.* (2006), have highlighted the possibility that the gold in the southwestern portion of the watershed may be derived from a Carlin-type gold deposit in the sedimentary and/or volcanic strata.

The results of the MERA I, conducted from 1986-1987 (Spirito *et al.*, 1988), also addressed the source of placer gold grains recovered by HMC sampling throughout the Ragged Ranges (none of which were available for this study), Nahanni Karst and Tlogotsho Plateau areas. The lack of evidence for continental glaciation in the western half of the South Nahanni River watershed led Spirito *et al.* (1988) to suggest that placer gold recovered from the Ragged Ranges area was locally sourced from intrusion-related vein or skarn mineralization. The most prospective suite of intrusions for hosting gold mineralization is the Tombstone suite (Fig. 2), which has a known affinity for gold mineralization both in the study area (Fig. 2) and elsewhere in Yukon (Mortensen *et al.*, 2000; Hart *et al.*, 2005). Some anomalous gold values are also associated with the tungsten skarns related to Tungsten suite intrusions (as documented in NORMIN) in the western part of the study area; however, no gold grains have been reported in proximity to the larger tungsten skarn occurrences, such as Lened or Cantung (Fig. 2), despite HMC sampling in that area. Unfortunately, none of the placer gold grains recovered from the western portion of the field area during the MERA I were available for this study.

Spirito *et al.* (1988) suggested two other possible sources for the fine placer gold recovered from isolated sample locations in the Nahanni Karst and Tlogotsho Plateau areas, south and east of the Prairie Creek minesite (Fig. 2). One hypothesis is that gold may have been locally derived from tetrahedrite-bearing sulphide veins with heterogeneous gold concentrations, such as those that crosscut base metal occurrences at Prairie Creek (Fig. 2). The spatial location of gold-bearing samples, that is, following a northerly trend not paralleled by till deposits, and at the intersection of north- and northwest-trending faults where gold-bearing quartz veins may occur, was thought to support such a local provenance for the gold grains (Jefferson and Pare, 1991; Jefferson and Spirito, 2003). Alternatively, gold may have been derived from the greenstone-hosted gold mineralization in the Precambrian basement of the Canadian Shield. This gold is believed to have been transported by continental glaciers from the east and concentrated by glaciofluvial reworking. The latter possibility has recently taken precedence based on the presence of granite clasts and garnet grains in glacial till, the lack of other precious- or base-metals with the gold, and the random locations of gold anomalies (Jefferson and Spirito, 2003).

ANALYTICAL TECHNIQUES

The shapes of gold grains were studied using image analysis employing ImageJ software, with which minor, intermediate and major axes lengths of grains were measured. This allowed the calculation of various flatness indices such as the Cailleux flatness index[5] (Cailleux and Tricard, 1959) as well as a statistical comparison of grain size and the degree of flattening each gold particle has undergone. Representative grains selected from the Chuck sample and all grains from the isolated placer samples were subsequently imaged with the minor axis of each grain parallel to the surface of the slide, using the secondary electron (SE) detector on the scanning electron microscope (SEM) in order to document surficial textures and particle morphologies (e.g., folding, crystallinity, etc.). Following SE imaging, a representative population of the Chuck sample (~180 grains) and all grains from the isolated samples were mounted in epoxy with the long axis of each grain perpendicular to the surface of the slide. The grain mounts were then brought to a high polish using 1 μ diamond paste, and analysed for gold, silver, copper and mercury on a fully automated CAMECA SX-50 electron microprobe (EMP) operating in wavelength-dispersion mode. The operating conditions were as follows: excitation voltage, 20 kV; beam current, 20 nA, peak count time, 40 s; background count time, 20 s; and spot diameter, 5 μ. The standards, X-ray lines, and crystals used for gold, silver, copper and mercury were as follows: Au element, AuMa, PET; Ag element, AgLa, PET; Cu element, CuKa, LIF; and HgTe, HgMb, PET. Data reduction was done using the 'PAP' (phi-rho-Z) method of Pouchou and Pichoir (1985). Detection limits for gold, silver, copper and mercury, respectively, were 0.30, 0.15, 0.07, 0.30 (wt% minimum), and 0.20, 0.10, 0.04, 0.20 (wt% limit). No sulphide inclusions were observed in any grains using the backscattered electron detector (BSE) on the EMP.

[5]Cailleux flatness index is a simple measure of the mass redistribution a malleable particle undergoes due to hammering and/or folding during transport in fluvial systems (Youngson and Craw, 1999); if (a), (b) and (c) are the lengths of the long, intermediate and short axes of a particle, respectively, the Cailleux flatness index = (a + b) / 2c

RESULTS

Chuck gold grains display relatively consistent morphologies, with somewhat flattened, smoothed grain outlines and limited local folding (Fig. 3a-f). Some grains, however, display complicated shapes with delicate protrusions; sub-spherical grains are rare. Gold grains from the isolated samples tend to have a more variable range of morphology, including commonly folded protrusions and/or grain margins (Fig. 3g-l). Some of these grains display smoothed but relict crystalline shapes, whereas others are almost spherical. Chuck gold grains also display less complex surficial textures than the isolated samples, which have abundant smear and groove marks, scratches, and dents (Fig. 3). It should be noted, however, that the isolated samples have been handled much more frequently with tweezers, which may explain some of the scratch marks or dents. Gold grains from the isolated samples also tend to be smaller in size compared to those grains from the Chuck sample (Fig. 3). Furthermore, the minor and major axes typically measure <0.05 mm and <0.20 mm respectively for gold grains of the isolated samples, while the gold grains from the Chuck sample have minor and major axes measuring <0.15 mm and <0.50 mm, respectively (Fig. 4).

Gold grains from the Chuck sample have a range of low Cailleux flatness index values, typically between one and six, which do not appear to be a function of gold fineness[6] (Fig. 5a). The gold fineness values are relatively high, typically from 800 to 975. In the Chuck sample, copper and mercury were typically below standard detection levels (wt% minimum), but approximately one-third contain copper concentrations between 0.04 (wt% limit) to 0.11 wt% (Fig. 5b). At copper concentrations above 0.04%, there is a clear covariant relationship between copper and gold fineness for gold grains of the Chuck sample. Despite the range of grain morphology

*[6]fineness = Au/(Au + Ag) * 1000, if Au and Ag are in wt%*

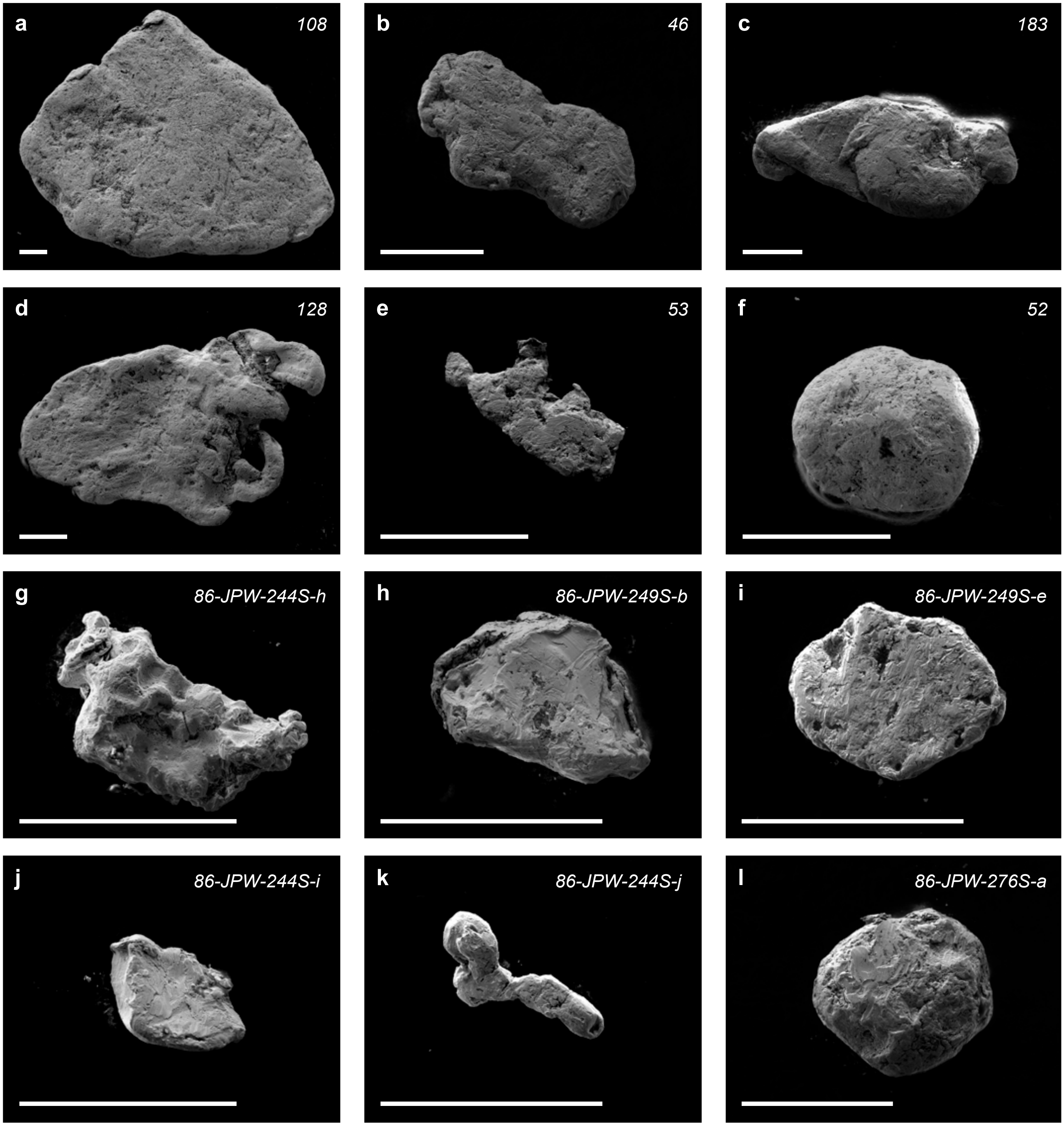

Figure 3. *Placer gold grain morphologies for grains from the Chuck sample (a-f) and grains from the isolated sample locations (g-l). Grain numbers for the Chuck sample, as well as sample number and grain letter for the isolated samples are noted; the minor axis of each grain is perpendicular to the surface and the white bar represents 200 microns.*

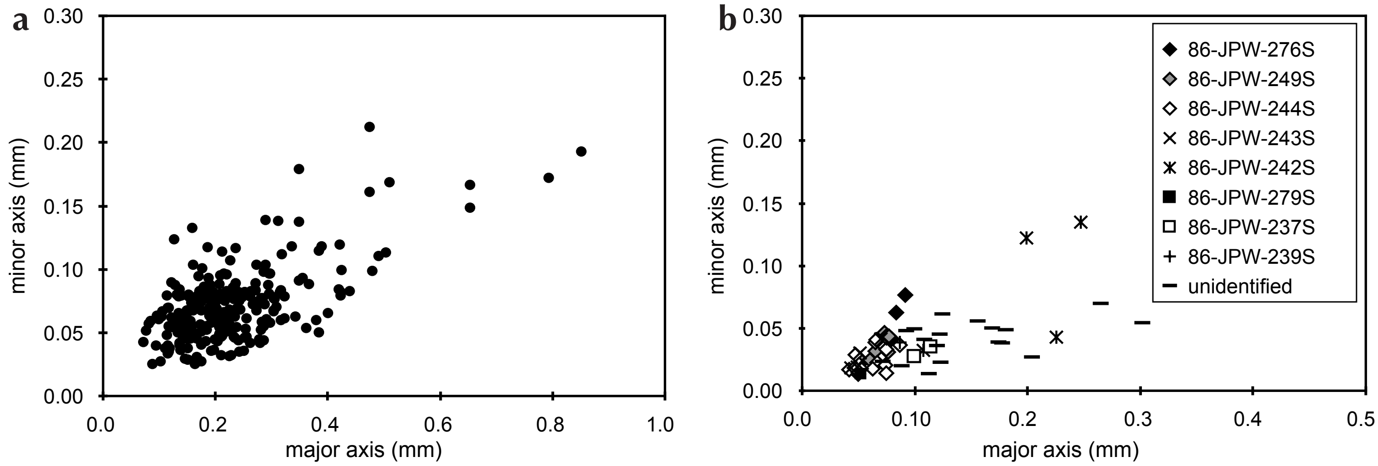

***Figure 4. (a)** Plot of minor axis vs. major axis for gold grains from the Chuck sample; **(b)** plot of minor axis vs. major axis for gold grains from isolated samples; note the different scales on the x-axis.*

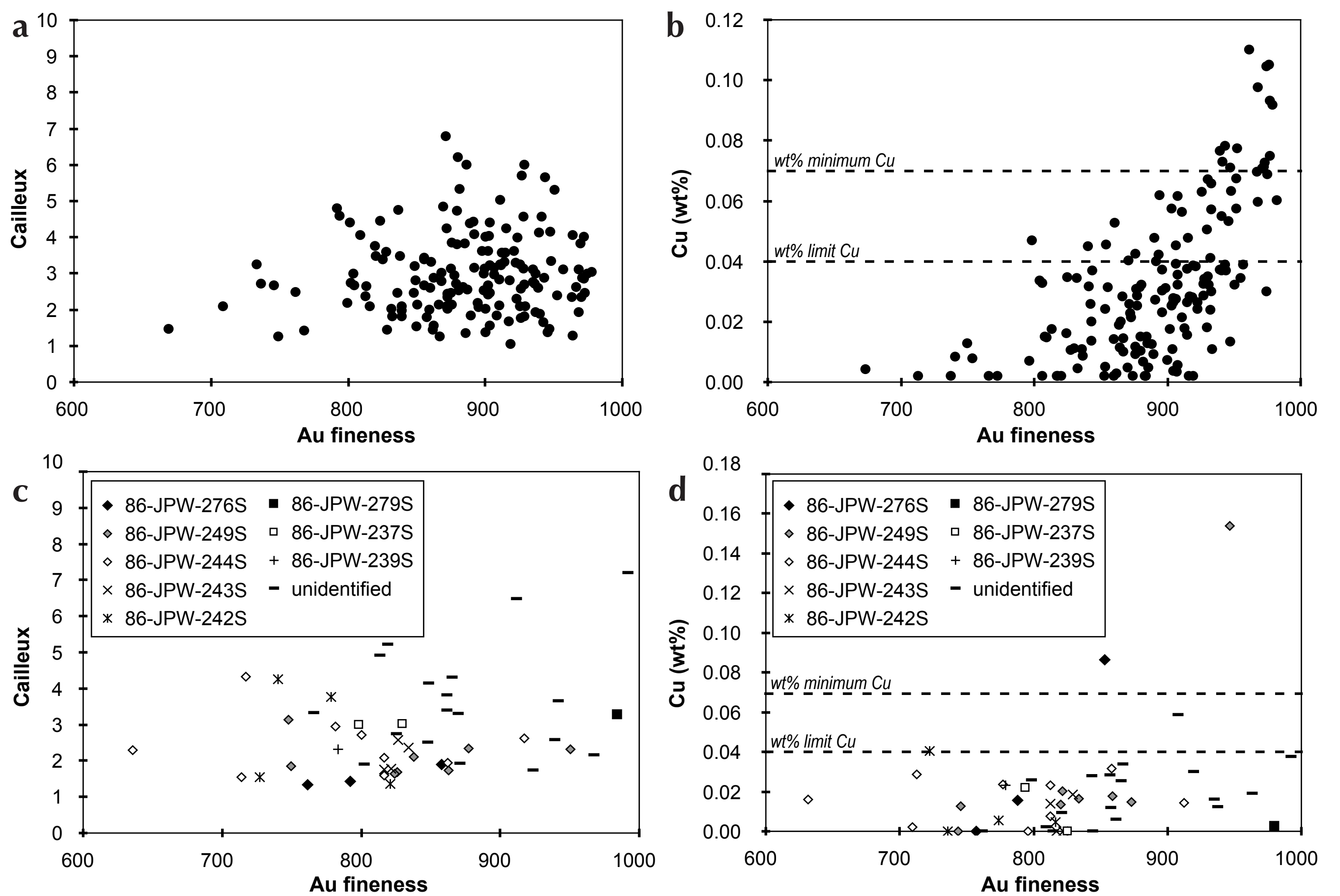

***Figure 5. (a**) Plot of Cailleux flatness index vs. gold fineness for the Chuck sample; **(b)** plot of copper content vs. gold fineness for the Chuck sample; **(c)** plot of Cailleux flatness index vs. gold fineness for isolated samples; **(d)** plot of copper content vs. gold fineness for isolated sample locations.*

observed, placer gold from the isolated samples are relatively consistent with respect to the Cailleux flatness index, typically between one and five for samples with known locations (Fig. 5c). Gold fineness values are also high, from 700 to 950, but have a greater range than the Chuck sample. Mercury (not shown) and copper were not detected by EMP analysis in the majority of these grains (Fig. 5d).

DISCUSSION

TRANSPORT DISTANCE

Measurements of the degree of flattening is one of the most useful parameters in determining approximate distances of transport for placer gold grains in fluvial systems (e.g., Knight *et al*., 1999a; Youngson and Craw, 1999). Detailed work on placer gold grain morphologies from known lode sources in the Klondike District, western Yukon, and the Otago Schist Belt of South Island, New Zealand, has resulted in semi-quantitative curves relating observed transport distances to the degree of flattening of a population of gold grains (Knight *et al*., 1999a; Youngson and Craw, 1999). The Shotover/Arrow-Kawarau-Clutha fluvial system in Otago, New Zealand, transects a back-arc region currently undergoing active exhumation, but with relatively low topographic gradients and low levels of precipitation (Youngson and Craw, 1999). This setting is similar to the tectonic regime experienced in the Selwyn and MacKenzie mountains from the mid-Jurassic through to at least the Cretaceous (e.g., Gordey and Anderson, 1993). Placer gold in Otago is sourced from sparse quartz veins hosted in schistose metasedimentary rocks of the Otago Schist. Youngson and Craw (1999) have shown that the Cailleux flatness index of placer gold grains increases with transport distance in the Otago Schist Belt. Flatness index ranges from approximately 1 (spherical or cubic) to just over 130 (highly flattened and folded discoids, or elongate/irregularly folded discoids, or sub-spherical/ellipsoidal) for the most far-traveled grains in Otago. Based on the data compiled by Youngson and Craw (1999), gold grains with maximum Cailleux flatness values of less than seven are found in proximal primitive-placer zones and are largely undeformed; they have traveled 1 to 10 km from the lode gold source. Furthermore, grains with maximum Cailleux flatness values of 1 to 3 are found in primary or colluvial sources and have crystalline and delicate morphologies; they in turn have traveled less than 1 km from the lode gold source. Although the distances determined in the Otago study apply specifically to Otago placer gold (Youngson and Craw, 1999), the validity of their data is extended to our study area based on a similar tectonic and geographic regime.

The majority of gold grains in the Chuck sample have variable, but anomalously low, Cailleux flatness indices of <7, indicating that they have been transported very little distance (e.g., 1-10 km) in a fluvial environment. Similarly, gold from the isolated samples also have anomalously low Cailleux flatness values, which for many of the samples is <3. The limited flattening of the grains could also indicate a local provenance rather than the glacially transported hypothesis first suggested by Spirito *et al*. (1988) for the isolated samples. Other possibilities are: (1) grains reworked from a local primitive paleoplacer; or (2) grains sourced from a nearby primary lode gold source (Youngson and Craw, 1999). Due to the statistically small number of grains recovered, each of the isolated samples cannot be fully or statistically characterized with respect to the degree of flattening, although the lack of highly flattened grains or higher Cailleux flatness index values significantly lowers the likelihood that the grains have traveled more than 10 km in a fluvial system, regardless of whether or not glacial transport was involved at some point in time.

POSSIBLE LODE GOLD SOURCES

As discussed previously, several possible lode sources have been suggested for the placer gold grains in the South Nahanni river watershed, including:

(1) intrusion-related mineralization, either in intrusion-hosted vein systems (similar to the Dublin Gulch deposit west of Mayo, Yukon; e.g., Mortensen *et al*., 2000), or possibly disseminated in skarn, or siliceous contact aureoles (Spirito *et al*., 1988);

(2) a Carlin-type lode source for at least the Chuck samples (e.g., Emsbo *et al*., 2006; Falck and Wright, 2007, in press);

(3) tetrahedrite-bearing sulphide veins cross-cutting fault-controlled base-metal mineralization such as at Prairie Creek (Spirito *et al*., 1988; Jefferson and Pare, 1991); and/or

(4) glacially transported gold derived from orogenic quartz veins in the Slave craton to the east (Spirito *et al*., 1988; Jefferson and Spirito, 2003).

Other possibilities include epithermal-related mineralization and gold formed within the fluvial system by chemically or microbially induced precipitation (authigenic). A derivation of placer gold from an epithermal lode is rejected because of the relative homogeneity and high levels of gold fineness for all the samples in the study area; a gold fineness range of 0-1000 is typically present in most epithermal systems. This is even the case within individual deposits, due to variable temperatures, mixing of mineralizing fluids and changing sulphidation states (McCready *et al.*, 2003; Shikazono and Shimizu, 1986, 1987; Morrison *et al.*, 1991; Knight *et al.*, 1999b; Chapman and Mortensen, 2006). The absence of pristine, sharply crystalline gold grains with very high fineness cores (>980; e.g., McCready *et al.*, 2003) eliminates the possibility of authigenic gold (e.g., Loen, 1994; McCready *et al.*, 2003).

Western portion of drainage

As described above, an intrusion-related lode source for placer gold in the western portion of the study area has been proposed for isolated placer gold grains (not available for analysis) by Spirito *et al.* (1988), and there is a spatial association between placer gold showings and Tombstone suite intrusions in the southwestern portion of the study area (Fig. 2). Specific to the Chuck sample, the increased or measurable copper concentrations in the gold grains are not unexpected as the gold was sampled from a creek near the Chuck lode copper (-gold) occurrences. The relationship of increasing copper concentration with gold fineness (as is demonstrated by the plot in Figure 5b) has been described by other researchers (e.g., Knight and McTaggart, 1990) and is explained as a copper-saturation curve in copper-poor and gold-rich mineralizing systems (Knight *et al.*, 1999b). This increase in copper with gold fineness indicates some form of environmental variation during formation of the lode gold source, perhaps a change in temperature, or pH over time. The occurrence of relatively high fineness gold, measurable copper and low mercury (not shown) is relatively consistent with various intrusion-related sources for gold (Fig. 6a) from several placer camps in the Stewart River map area, western Yukon (Dumula and Mortensen, 2002). Furthermore, the presence of Fe- and/or Ca-rich garnet in the heavy minerals collected with the gold grains and limestone fragments indicates some form of silicate-fluid reaction with iron-rich and/or calcareous rocks during the initial gold mineralizing event(s); this in turn could also point towards a skarn-type lode source adjacent to an intrusion. Anomalous gold values are also reported in the NORMIN database for the Rino skarn occurrence, which is adjacent to a Tombstone suite intrusion near the Chuck sample location (Fig. 2). However, the lack of typical intrusion-derived or contact aureole minerals such as titanite, zircon, pyrite, pyrrhotite, andalusite, etc., observed in the heavy minerals panned from the Chuck sample, or as inclusions within the Chuck gold grains, does not lend support to a proximal, intrusive derivation for the gold (Loen, 1994).

Another possible gold source for the Chuck gold grains is nearby, or adjacent, Carlin-type mineralization. Emsbo *et al.* (2006) suggested that the association of gold with specific Tombstone suite intrusions throughout Yukon and Alaska (a continuation of the belt of Tombstone suite intrusions that crops out in the study area) is analogous to the Carlin-type mineralization trend in southwestern USA. This inference is based largely on a similar tectonic regime to that of northern Nevada (Emsbo *et al.*, 2006) where the majority of large Carlin-type gold deposits are hosted in a distal back-arc environment with far-ranging, deep-seated (transpressional?) structures, spatially and temporally associated with magmatism (Hart *et al.*, 2005; Rasmussen *et al.*, 2006; Gabrielse *et al.*, 2006, in press). Carlin-type gold deposits (summarized from Li and Peters, 1998) are commonly found near, but outside, the contact aureole of felsic intrusions and are typically hosted in impure carbonate-argillite strata; however, they may be hosted in intermediate to mafic volcanic rocks or felsic plutonic rocks. These deposits are generally associated with structurally controlled zones of silicification, sericitization, stockwork, and/or brecciation. Gold mineralization is very fine grained (micron scale, or ~0.01 mm), has a range of gold fineness (typically >500), and is disseminated in the host rock with limited associated sulphide minerals, although arsenic-mercury-antimony-bearing minerals are commonly observed. Base metals such as copper are usually not reported with Carlin-type gold; however, copper mineralization has been observed in association with gold at some Carlin-type deposits in China and Nevada (Li and Peters, 1998). The copper measured in the Chuck sample gold grains may be derived from the intermediate to mafic volcanic rocks and remobilized along the same structures that carry Carlin-type fluids. The intensely sericitized, and locally silicified, intermediate to mafic volcanic rocks hosting anomalous copper (-gold) mineralization and the overlying Rabbitkettle Formation limestones are both possible hosts for a Carlin-type deposit. Despite the lack of any associated sulphide minerals with the Chuck sample, and the relatively large gold-grain size compared to those grains of most Carlin-type gold deposits (particularly in the southwestern USA), this option remains a viable possibility for the source of

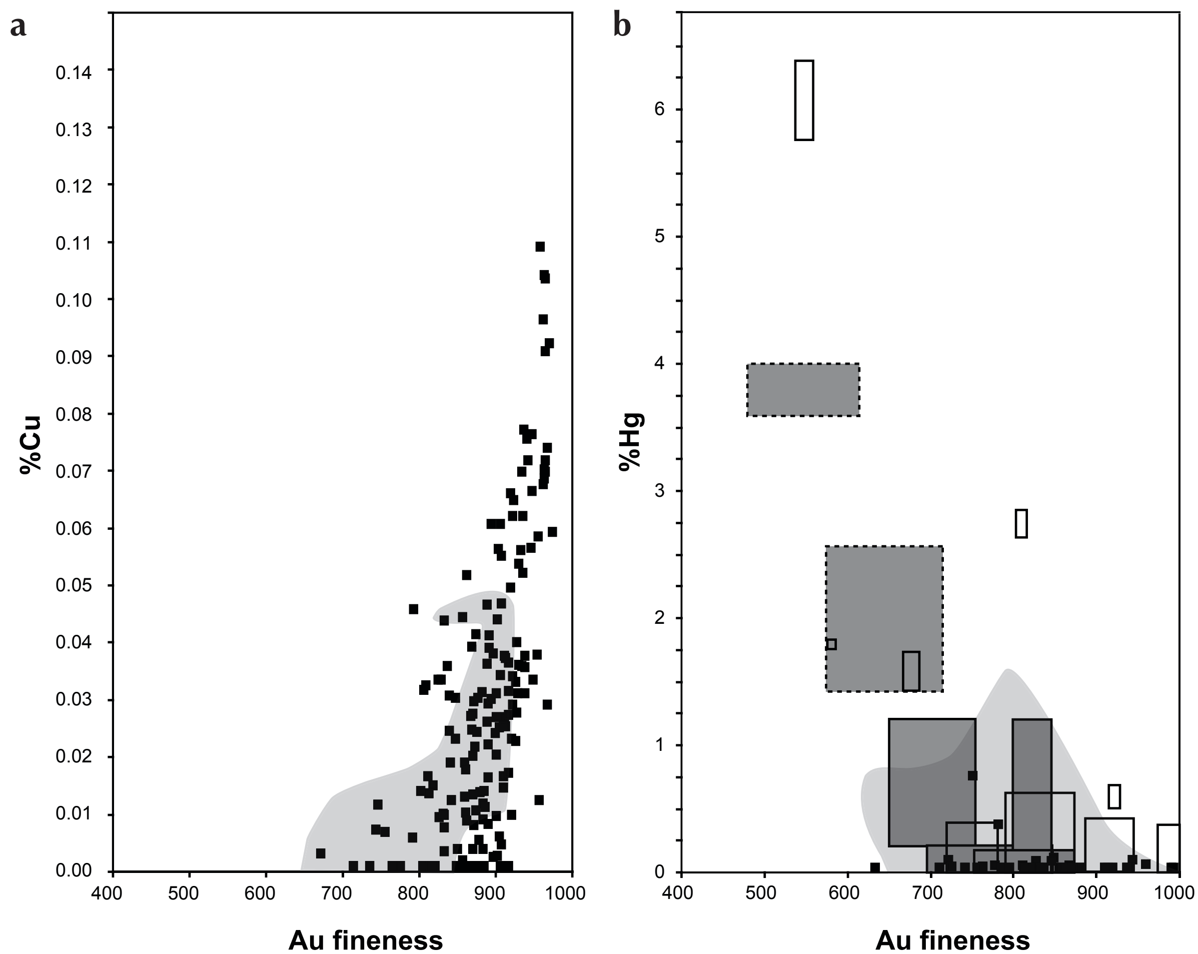

Figure 6. ***(a)*** *Plot of copper content vs. gold fineness for intrusion-related gold and the Chuck placer gold sample. The compositional field of intrusion-related gold from the Stewart River map area (Dumula and Mortensen, 2002) is indicated by the pale grey underlay, and compositions exhibited by the Chuck sample are indicated by small black squares;* ***(b)*** *plot of mercury content vs. gold fineness for orogenic and intrusion-related gold, and the isolated placer gold samples. Compositional fields of Archean greenstone-hosted orogenic gold in the Yellowknife Greenstone Belt, Slave craton are indicated by unfilled black outlines (data from Armstrong and Gochnauer, 2000; Gochnauer, unpublished data, 2001), compositional fields for Mesozoic orogenic gold from Yukon are indicated by dark grey boxes (dashed fields are inferred from a few data points; data from Knight* et al.*, 1999b), compositions of intrusion-related gold from the Stewart River map area are indicated by the pale grey underlay (Dumula and Mortensen, 2002), and the compositions exhibited by isolated samples of placer gold are indicated by small black squares.*

the placer gold due to the many other similarities listed above. At this time, the lack of access to compositional data for gold from Carlin-type mineralization does not allow for a compositional comparison with the Chuck sample.

Eastern portion of drainage

Studies of placer gold deposits have documented the presence of quartz and commonly pyrite, as well as other sulphide or silicate inclusions in gold grains sourced from orogenic veins (e.g., Loen, 1994; Knight *et al.*, 1999b). Sulphide inclusions (e.g., pyrite, chalcopyrite and galena; Loen, 1994) are common in gold grains sourced from intrusion-related deposits. Therefore, it is plausible that gold associated with tetrahedrite-bearing sulphide veins could contain inclusions of tetrahedrite, and possible galena, sphalerite and Cu-sulphides from the base-metal veins that they postdate. However, it should also be noted that the size and abundance of inclusions tends to decrease with increasing transport distance due to the effects of 'hammering' of the gold grains (Mortensen *et al.*, 2005). The lack of mineral inclusions (sulphide, silicate, or carbonate) in the isolated samples of gold grains, as viewed under the EMP, does not discount the possibility of a distal, intrusion-related source, especially for isolated samples collected from the South Nahanni River (Fig. 2). A more proximal, vein-derived source as described above can not be discounted by the absence of inclusions, particularly if the small size of the grains and the relatively flat or spherical nature of some of the grains are as a result of increased transport distances rather than primary features of the lode gold source (Mortensen *et al.*, 2005). Figure 6b demonstrates that gold compositions of the isolated samples in the study area overlap with placer gold compositions in the Stewart River map area that have an intrusion-related lode source (Dumula and Mortensen, 2002), although the absence of copper in most of the grains from the isolated samples (Fig. 5d) is inconsistent with the range of low copper concentrations observed in the Stewart River placer gold (Fig. 6a). Several mineral occurrences with anomalous gold concentrations are present in the study area. These are typically adjacent to granitoid intrusions (Fig. 2; as documented in NORMIN). The isolated samples, however, are not spatially associated with granitoid intrusions, nor are they from tributaries that currently drain valleys containing granitoid intrusions, with the exception of samples 86-JPW- 276S and -279S located on the South Nahanni River. These two samples do not have Cailleux flatness indices indicative of the great distances of travel in a fluvial system (i.e., >12 for more than 100 km travel; Youngson and Craw, 1999) necessary for these samples to have been sourced from intrusion-related mineralization (Fig. 5c). Unfortunately, the lack of compositional data for gold from the tetrahedrite-bearing veins in the study area does not allow for a similar compositional comparison.

Another possibility for the origin of the isolated gold grains is a glacially transported, distal source from Archean greenstone gold deposits in the Precambrian shield (Spirito *et al.*, 1988; Jefferson and Spirito, 2003). Gold grains transported by southwest-flowing continental ice sheets would be deposited within glacial till as poorly concentrated and poorly sorted, relatively large and/or irregular grains displaying crystalline outlines and low degrees of flattening due to their initial glacial transport in host rock clasts. Striations, grooves, crush marks and folded grain edges would also be common (Herail *et al.*, 1989). It is also possible, however, for gold grains with a nearby lode source to have some, or all, of these features (Loen, 1994; Youngson and Craw, 1999). Most gold grains from the isolated samples have relatively low Cailleux flatness values and range in morphology from delicate with relict crystallinity, to partially or entirely flattened and rounded grains, to almost spherical grains. These grains also display much more complex surficial textures, such as scratch and smear marks, dents, and more frequently folded grain margins than the Chuck sample. All of these observations are consistent with glacially transported material.

Gold compositions of the isolated samples in the study area are compared with available data for multiple Archean greenstone-hosted orogenic gold deposits in the Yellowknife greenstone belt (YGB), Slave craton, NWT (Armstrong and Gochnauer, 2000; Gochnauer, unpublished data, 2001; Fig 6b). Results of EMP analyses of gold, silver and mercury for *in situ* gold from the Archean deposits indicate that gold fineness and mercury concentration form several distinct compositional fields (Fig. 6b); gold fineness typically ranges from 720 to 1000 and mercury is typically <0.5%, although a couple of individual deposits of lower gold fineness (500 to 750) have anomalously high mercury concentrations (Gochnauer, unpublished data, 2001). Copper was not measured for the YGB lode gold. The lack of mercury in several of the YGB deposits, with the exception of two grains from the isolated samples, combined with an overlapping range of gold fineness (Fig. 6b), allows for a viable Archean-derived and glacially transported model for the placer gold. Although Yukon orogenic gold has not been proposed as a possible lode source, compositional fields of several lode gold deposits in the Klondike region, Yukon (Knight *et al.*, 1999b) also overlap with many of the placer gold grain compositions (Fig. 6b). This compositional overlap with orogenic gold from the Klondike indicates that the same, or a similar, Mesozoic mineralizing event could also be regarded as a possible lode gold source for the isolated placer gold samples. Ultimately, whether there are one or more sources of gold for the isolated placer gold occurrences, the lack of a statistically valid population for each sample does not allow us to make any inferences as to the original gold source(s), aside from describing compositional similarities or dissimilarities between the placer gold and gold from specific lodes.

FUTURE WORK

Further imaging of gold grains using the back-scattered electron detector (BSE) will be carried out on the polished grain mounts in order to document the nature and thicknesses of high gold-fineness rims and any mineral inclusions that were not obvious under the EMP. The identification of particular sulphide, sulphate, or silicate mineral phases or combinations thereof will be important in addressing the possible lode gold sources, particularly with respect to Carlin-type gold for the Chuck sample and glacially transported Archean greenstone-derived gold for the isolated samples. Additional analyses on the grains will include laser ablation inductively coupled plasma mass spectrometry methods to determine trace-element signatures by measuring lower concentrations of copper and mercury, and trace amounts of other elements such as arsenic, bismuth, tellurium, antimony, chromium, arsenic, tungsten, rubidium, strontium, tin, barium, etc. (e.g., Outridge *et al*., 1998). This compositional data, combined with a statistical Kernal Density estimation (KDE) of shape and trace element composition, will accurately define specific populations within a sample group. This, in turn, will allow stronger inferences as to the distance of travel the grains have undergone and the most prospective lode gold deposit-type(s) (e.g., intrusion-related, Carlin-type, Archean greenstone, etc.) for the placer gold in the South Nahanni River watershed. The more detailed work will be particularly useful for the Chuck sample. This work is expected to take place early in 2007.

ACKNOWLEDGEMENTS

Funding for this project was provided by an NSERC Discovery Grant to Dr. J.K. Mortensen (University of British Columbia). We are very grateful to C. Jefferson (GSC Ottawa) for contributing the placer gold grains obtained during the MERA I, and Archer Cathro & Associates Ltd. for contributing the Chuck placer sample. Access to unpublished gold compositional data for the Yellowknife Greenstone Belt was kindly provided by J. Armstrong (currently with Stornoway Diamond Corporation) and K. Gochnauer (Department of Indian and Northern Affairs Canada). We also thank E. Crawford (University of British Columbia) for his help with the image analysis process he is currently developing, and to L. Ootes (Northwest Territories Geoscience Office), who provided many useful comments and a review of this manuscript.

REFERENCES

Armstrong, J.P. and Gochnauer, K., 2000. A preliminary discussion of intra and inter sample variation in gold fineness from a variety of Au-showings, EXTECH-III field area. *In:* Abstract volume - 28th Annual Yellowknife Geoscience Forum; Yellowknife, Northwest Territories, Nov 22-24; p. 5-6.

Berton. P., 1956 (reprinted 1989). The Mysterious North. McClelland and Stewart Ltd., Toronto, Ontario, 391 p.

Cailleux, A. and Tricart, J., 1959. Initiation à l'étude des sables et des galets, vol. 1, Paris, Centre de Documentation Universitaire, 369 p.

Cairns, S., Roman, R. and Adams L., 1995. Report on prospecting and sampling on claims Peter 1, X and Gilbert, District of MacKenzie, NWT. Department of Indian Affairs and Northern Development, Assessment Report 83599, 113 p.

Chapman, R.J. and Mortensen, J.K., 2006. Application of microchemical characterization of placer gold grains to exploration for epithermal gold mineralization in regions of poor exposure. Journal of Geochemical Exploration, vol. 91, p. 1-26.

Dumula, M.R. and Mortensen, J.K., 2002. Composition of placer and lode gold as an exploration tool in the Stewart River map area, western Yukon. *In:* Yukon Exploration and Geology 2001, D.S. Emond, L.H. Weston and L.L. Lewis (eds.), Exploration and Geological Services Division, Yukon Region, Indian and Northern Affairs Canada, p. 87-102.

Emsbo, P., Groves, D.I., Hofstra, A.H. and Bierlein, F.P., 2006. The giant Carlin gold province: a protracted interplay of orogenic, basinal, and hydrothermal processes above a lithospheric boundary. Mineralium Deposita, vol. 41, no. 6, p. 517-525.

Falck, H. and Wright, D.F. (eds.), 2007 (in press). Mineral and Energy Resource Potential of the Proposed Expansion to the Nahanni National Park Reserve, Northern Cordillera, Northwest Territories. Geological Survey of Canada Open File 5344. 1 CD-ROM.

Gabrielse, H., Murphy, D.C. and Mortensen, J.K., 2006 (in press). Cretaceous and Cenozoic dextral orogen-parallel displacements, magmatism, and paleogeography, north-central Canadian Cordillera. *In:* Paleogeography of the North American Cordillera: Evidence For and Against Large-Scale Displacements, J.W. Haggart, R.J. Enkin and J.W.H. Monger (eds.), Geological Association of Canada, Special Paper 46, p. 255-276.

Gallup, W.B., 1973. Geology of the Nahanni placer claims, Flat River, NWT; Windfall, Binker and Epler Groups. Department of Indian Affairs and Northern Development Assessment Report 80393, 19 p.

Gordey, S.P. and Anderson, R.L., 1993. Evolution of the northern cordilleran miogeocline, Nahanni map area (105I), Yukon and Northwest Territories. Geological Survey of Canada, Memoir 428, 214 p.

Hart, C.J.R., Mair, J.L., Goldfarb, R.J. and Groves, D.I., 2005. Source and redox controls on metallogenic variations in intrusion-related ore systems, Tombstone-Tungsten belt, Yukon Territory, Canada. Geological Society of America, Special Paper, vol. 389, p. 339-356.

Heffernan, R.S., 2004. Temporal, geochemical, isotopic and metallogenic studies of mid-Cretaceous magmatism in the Tintina Gold Province, southeastern Yukon and southwestern Northwest Territories, Canada. Unpublished MSc thesis, University of British Columbia, British Columbia, Canada, 83 p.

Herail, G., Fornar, G., Viscarra, G. and Miranda, V., 1990. Morphological and chemical evolution of gold grains during the formation of a polygenetic fluviatile placer: the Mio-Pleistocene Tipuani placer example (Andes, Bolivia). Chronique de la Recherche Minière, vol. 500, p. 41-49.

Jefferson, C.W. and Pare, D., 1991. New placer gold anomalies in the northern Liard Range – southern Ram Plateau area, South Nahanni River region, District of Mackenzie, Northwest Territories. Current Research, Part E, Geological Survey of Canada Paper 91-1E, 4 p.

Jefferson, C.W. and Spirito, W.A. (eds.), 2003. Mineral and Energy Resource Assessment of the Tlogotsho Plateau, Nahanni Karst, Ragged Ranges and adjacent areas under consideration for expansion of Nahanni Nation Park Reserve, Northwest Territories. Geological Survey of Canada Open File 1686, 1 CD-ROM.

Knight, J.B. and McTaggart, K.C., 1990. Lode and placer gold of the Coquihalla and Wells areas, British Columbia. British Columbia Ministry of Energy, Mines and Petroleum Resources, Exploration in British Columbia 1989, Paper 1990-1, p. 387-394.

Knight, J.B., Morison, S.R. and Mortensen, J.K., 1999a. The relationship between placer gold particle shape, rimming, and distance of fluvial transport as exemplified by gold from the Klondike district, Yukon Territory, Canada. Economic Geology, vol. 94, p. 635-648.

Knight, J.B., Morison, S.R. and Mortensen, J.K., 1999b. Lode and placer gold composition in the Klondike district, Yukon Territory, Canada: implications for the nature and genesis of Klondike placer and lode gold deposits. Economic Geology, vol. 94, p. 649-664.

Lenters, M.H., 1984. Report on prospecting and geochemical sampling permits 969, 970, 971, 972, Flat River Prospect. Department of Indian Affairs and Northern Development Assessment Report 81741, 26 p.

Li, Z. and Peters, S.G., 1998. Comparative geology and geochemistry of sedimentary-rock-hosted (Carlin-Type) gold deposits in the People's Republic of China and in Nevada, USA. United States Geological Survey Open-File Report 98–466, 104 p.

Loen, J.S., 1994. Origin of placer gold nuggets and history of formation of glacial gold placers, Gold Creek, Granite County, Montana. Economic Geology, vol. 89, p. 91-104.

McCready, A.J., Parnell, J. and Castro, L., 2003. Crystalline placer gold from the Rio Neuquen, Argentina: Implications for the gold budget in placer gold formation. Economic Geology, vol. 98, p. 623-633.

McDougall, G., 1976. Report on the Deb property. Department of Indian Affairs and Northern Development Assessment Report 80508, 81 p.

Morrison, G.W., Rose, W.J. and Jaireth, S., 1991. Geological and geochemical controls on the silver content (fineness) of gold in gold-silver deposits. Ore Geology Reviews, vol. 6, no. 4, p. 333-364.

Mortensen, J.K., Hart, C.J.R., Murphy, D.C. and Heffernan, S., 2000. Temporal evolution of Early and mid-Cretaceous magmatism in the Tintina Gold Belt. *In:* The Tintina Gold Belt: Concepts, Exploration and Discoveries, J. Jambor (ed.), British Columbia and Yukon Chamber of Mines, Special Volume 2, p. 49-57.

Mortensen, J.K., Chapman, R., LeBarge, W. and Jackson, L., 2005. Application of placer and lode gold geochemistry to gold exploration in western Yukon. *In:* Yukon Exploration and Geology 2004, D.S. Emond, L.L. Lewis and G.D. Bradshaw (eds.), Yukon Geological Survey, p. 205-212.

Outridge, P.M., Doherty, W. and Gregoire, D.C., 1998. Determination of trace elemental signatures in placer gold by laser ablation – inductively coupled plasma – mass spectrometry as a potential aid for gold exploration. Journal of Geochemical Exploration, vol. 60, p. 229-240.

Patterson, R.M., 1953 (reprint 1999). Dangerous River: Adventure on the Nahanni. Boston Mill Press, Erin, Ontario, 276 p.

Pouchou, J.-L. and Pichoir, F., 1985. “PAP” (phi-rho-Z) procedure for improved quantitative microanalysis. *In:* Microbeam Analysis, J.T. Armstrong (ed.), San Francisco Press, San Francisco, California, p. 104-106.

Rasmussen, K.L., Mortensen, J.K. and Falck, H., 2006. Mid-Cretaceous granitoids in the southwestern Northwest Territories and southeastern Yukon: implications for magma source regions, tectonic setting, and metallogeny. *In:* Abstract volume - 34th Annual Yellowknife Geoscience Forum, Yellowknife, Northwest Territories, Nov. 21-23, p. 46.

Rowan, L.G. and von Kursell, A.H., 1989. Geological report on the evaluation survey of the Selena Creek property, Nahanni Mining District, NWT. Department of Indian Affairs and Northern Development Assessment Report 82830, 77 p.

Samusikov, V.P. and Petrova, N.I., 1983. Correlations between the content of silver, antimony and copper in native gold (deposits of the Yana-Kolyma belt as examples). Chemical Abstracts, vol. 101, p. 114-234.

Shikazono, N. and Shimizu, M., 1986. Compositional variations in gold-silver series minerals from some gold deposits in the Korean Peninsula. Kozan Chishitsu, vol. 36, no. 200, p. 545-553.

Shikazono, N. and Shimizu, M., 1987. The silver/gold ratio of native gold and electrum and the geochemical environment of gold vein deposits in Japan. Mineralium Deposita, vol. 22, no. 4, p. 309-314.

Spirito, W.A., Jefferson, C.W. and Pare, D., 1988. Comparison of gold, tungsten and zinc in stream silts and heavy mineral concentrates, South Nahanni resource assessment area, District of Mackenzie. Current Research, Part E, Geological Survey of Canada Paper 88-1E, p. 117-126.

Stammers, M.A., 1983. Geological and geochemical report on the Chuck 1 and 2 claims, Nahanni Mining District, NWT. Department of Indian Affairs and Northern Development Assessment Report 81665, 27 p.

Turner, D., 1975. Nahanni. Hancock House Publishing, Blaine, Washington, 286 p.

Vulimiri, M.R., 1986. Geological report on the Chuck 1 mineral claim, Caribou River area, Nahanni Mining District, NWT. Department of Indian Affairs and Northern Development Assessment Report 82082, 17 p.

Vulimiri, M.R. and Crooker, G.E., 1989. Geological, geophysical and geochemical report on the Chuck 1 mineral claim, Caribou River Area, Nahanni Mining District, NWT. Department of Indian Affairs and Northern Development Assessment Report 82859, 36 p.

White, G.E. and Cruz, E.D., 1973. Geochemical, geophysical report, Andrew and Becker, Rino Claims, East Skinboat Lake, NWT. Department of Indian Affairs and Northern Development Assessment Report 82032, 16 p.

Youngson, J.H. and Craw, D., 1999. Variation in placer style, gold morphology, and gold particle behavior down gravel bed-load rivers: an example from the Shotover-Arrow-Kawarau-Clutha river system, Otago, New Zealand. Economic Geology, vol. 94, p. 615-634.

PROPERTY DESCRIPTION

New data on the geology and mineralization of the Skukum Creek gold-silver deposit,
southern Yukon (NTS 105D/3)
S.G. Soloviev 253

New data on the geology and mineralization of the Skukum Creek gold-silver deposit, southern Yukon (NTS 105D/3)

Serguei G. Soloviev
CME Consultants Inc.[1]

Soloviev, S.G, 2007. New data on the geology and mineralization of the Skukum Creek gold-silver deposit, southern Yukon (NTS 105D/3). *In:* Yukon Exploration and Geology 2006, D.S. Emond, L.L. Lewis and L.W. Weston(eds.), Yukon Geological Survey, p. 253-268.

ABSTRACT

Detailed exploration conducted during 2006 in the western part of the Skukum Creek deposit has revealed new structural, mineralogical and geochemical features.

The deposit incorporates a number of (at least six or seven) sub-parallel narrow mineralized zones, coincident with andesite-dacite-rhyolite dyke swarms extending for at least 1 km along strike and for hundreds of metres down-dip. Various mineralized zones differ in size, structural setting, intensity and composition of mineralization, and, in total, form a large mineralized package more than 200 m wide, corresponding to a property- to district-scale fault zone extending for over 10 km and traced by a dyke belt. Significant potential exists for the exploration of these structures along strike and down-dip.

The diamond drilling intersected numerous high-grade intercepts of gold and silver mineralization corresponding to the low-sulphidation sub-type of epithermal gold-silver deposits. However, strong enrichment in base metals (up to 25% of combined Zn+Pb+Cu) and arsenic suggests essential differences from typical epithermal mineralized systems.

RÉSUMÉ

Les travaux d’exploration en détail de la campagne 2006 sur la portion occidentale du gîte de Skukum Creek ont permis de révéler de nouveaux aspects structuraux, minéralogiques et géochimiques.

Le gîte comprend plusieurs zones minéralisées sous-parallèles étroites (au moins six ou sept) qui coïncident avec une série de dykes de composition andésitique-dacitique-rhyolitique. Ces dykes s’étendent sur une longueur d’au moins 1 km et sur plusieurs centaines de mètres de profondeur. Les zones minéralisées sont différentes entre-elles par leurs dimensions, conditions structurales, intensités, et type de minéralisation. Au total, ces zones forment un ensemble minéralisé de plus de 200 m de large, correspondant à une zone de faille d'échelle régionale s’étendant sur plus de 10 km et marquée par une série de dykes. Ces structures possèdent un important potentiel pour l’exploration autant en longueur et qu’en profondeur.

Plusieurs intersections à haute teneur en or et en argent ont été obtenues pendant la campagne. Cette minéralisation correspond à un sous-type de gisement épithermal or-argent pauvre en soufre. Toutefois, un enrichissement important en métaux de base (jusqu’à 25% d’un ensemble en Zn+Pb+Cu) et arsenic suggère des différences primordiales avec les systèmes épithermaux typiques.

[1]*CME Consultants Inc., 2130-21331 Gordon Way, Richmond, British Columbia, Canada V6W 1J9*

INTRODUCTION

The Skukum Creek gold-silver deposit is located in the Wheaton River area, within the Skukum property, 60 km southwest of Whitehorse. The property is 100% owned by Tagish Lake Gold Corp.

The deposit is the focus of the current exploration and mining development program, with the goal of increasing the resource base of the deposit. Conducted as a part of this program, the 2006 detailed exploration of the deposit included extension of 1300-m level adit for some 400 m further west, followed by almost 6500 m of core drilling (72 drill holes in total) from underground locations.

This paper deals with preliminary field results obtained during the May-November, 2006 drilling program and accompanying mapping (with compilation of older results) of the underground 1300-m level of the Skukum Creek deposit. Special attention was given to possible exploration and genetic consequences foreseeable on the basis of the fieldwork results.

SOME ASPECTS OF REGIONAL AND DISTRICT GEOLOGY AND METALLOGENY

The 171-km^2 Skukum property encompasses several significant mineral occurrences, including the past-producing Mount Skukum gold mine, Skukum Creek gold-silver deposit, Goddell Gully gold-antimony prospect, Becker-Cochran antimony prospect, as well as numerous gold, gold-silver, lead-zinc, copper and other related showings within the Wheaton River mining district (Yukon MINFILE, Deklerk and Traynor, 2005; Fig. 1). Small copper-porphyry mineral occurrences are known near the Skukum Creek deposit. In total, these deposits and

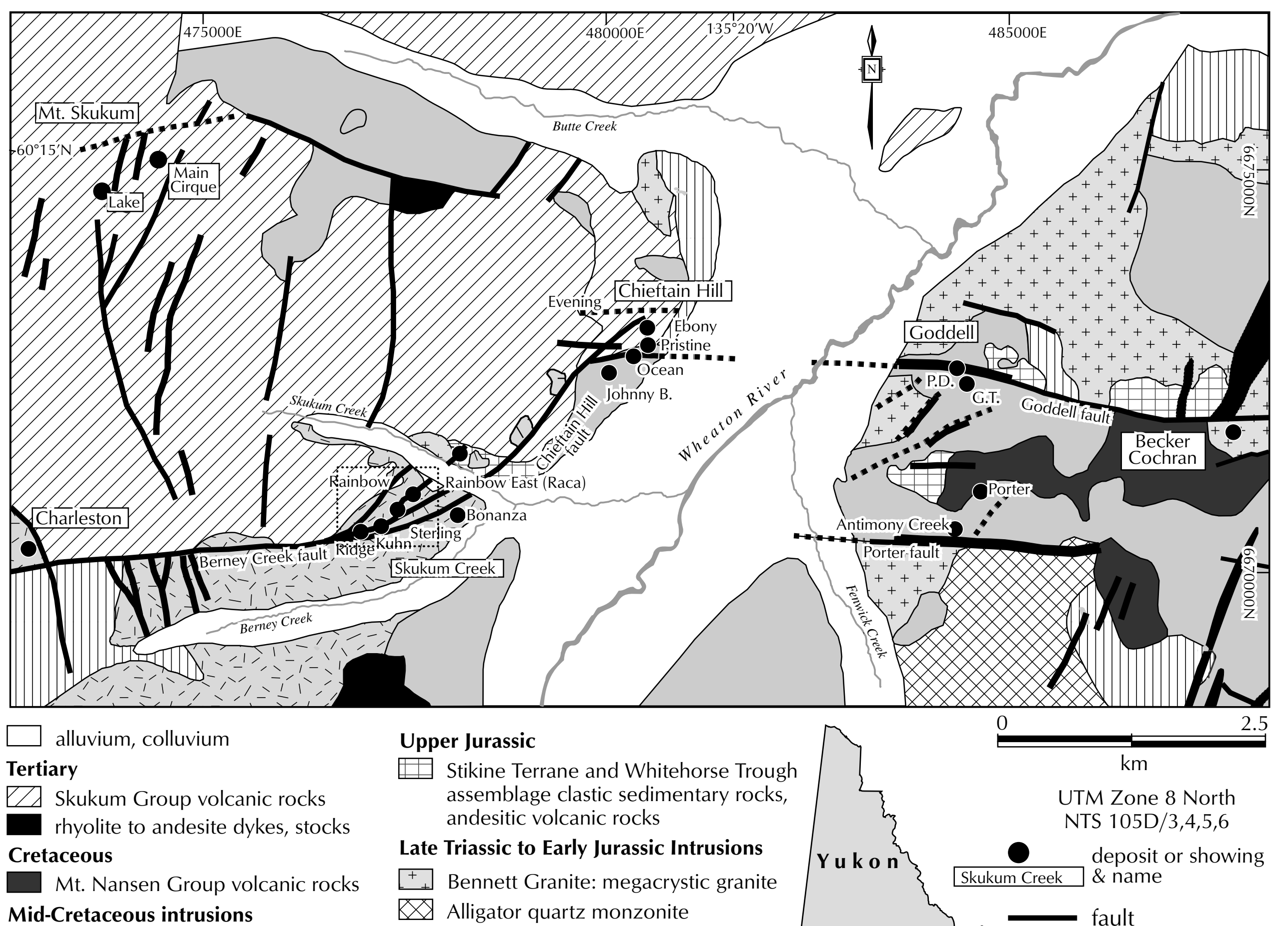

Figure 1. *Geology of the Skukum project area (after Lang et al., 2003). Data compiled from Hart and Radloff (1990) and unpublished company maps. Dotted rectangle shows area of Figure 2.*

occurrences form an important mineralized district exhibiting a long-lasting, multi-episode history of mineral formation.

The regional geology was described in a number of papers (Wheeler, 1961; Doherty and Hart, 1988; Hart and Radloff, 1990) and summarized by Lang *et al.* (2003). The Wheaton River area covers the boundary between the Stikine and Nisling terranes of the Intermontane Superterrane (or Intermontane Belt) of the Canadian Cordillera. The rocks consist of Paleozoic(?) gneiss assigned to the Nisling Terrane, Jurassic andesite and siliciclastic rocks of the Stikine Terrane, and Whitehorse Trough overlap assemblage.

The older rocks were intruded by late Triassic or early Jurassic K-feldspar megacrystic Bennett Granite (175 Ma), and then by metaluminous Cretaceous intrusions of the Coast Plutonic Complex, including the most abundant Whitehorse Plutonic Suite (116-119 Ma), locally represented by the Mt. McNeil granodiorite pluton and associated rocks, and the Mt. McIntyre plutonic suite (96-119 Ma); the latter includes the Mt. Ward granite and Carbon Hill quartz monzonite. Intermediate Cretaceous volcanic rocks of the Mt. Nansen Group, thought to be approximately coeval with the Coast Plutonic Complex, are present regionally, and in the property area occur east of the Wheaton River (Lang *et al.,* 2003).

As noted by Lang *et al.* (2003), the early Eocene Mount Skukum volcanic complex, part of the widespread late Paleocene to early Eocene felsic to intermediate volcanism of the Skukum Group (Smith, 1982 and 1983; Pride, 1986), is a caldera sequence that underlies the western portion of the district. The Mount Skukum complex consists of up to 800 m of mainly porphyritic andesitic flows and tuff, exposed over an area of approximately 200 km^2. These volcanic rocks are locally separated from pre-Tertiary rocks by curved, east- to northeast-trending structures such as Berney Creek fault and Wheaton lineament (coincident with the Wheaton River valley on Fig. 1) that have been inferred to be syn-volcanic, caldera-bounding faults (Hart and Radloff, 1990). These and parallel structures host gold-silver mineralization in the district.

On a regional scale, most of these tectonic and magmatic events have or may have been accompanied by respective metallogenic assemblages (e.g., Mihalynuk *et al.,* 1997). In particular, Upper Triassic arc rocks of the Whitehorse Trough are lithologically and temporally equivalent to those hosting important copper-molybdenum-gold porphyry deposits in southern British Columbia. Early Jurassic intrusive rocks are also known to host copper-gold mineralization in the central-western Yukon (Minto and Williams Creek deposits; Tafti and Mortensen, 2004). Cretaceous plutons produce copper skarns where they cut Upper Triassic carbonate rocks in the Whitehorse copper belt (Mihalynuk *et al.,* 1997), as well as copper-gold porphyry mineralization; and the southern end of the belt may extend into the Skukum area. Epithermal gold-silver mineralization related to volcanic rocks forms a distinct belt extending from north to south across southern Yukon; this incorporates the Mount Nansen cluster of epithermal gold deposits and occurrences related to 100-Ma Mount Nansen volcanics, the Laforma epithermal gold deposit related to the Carmacks Group volcanics (75 Ma), and finally the Mt. Skukum gold prospect, further south, related to Tertiary volcanic rocks (55 Ma). Some of these volcanic rocks are responsible for both epithermal and possibly related copper-porphyry deposits (i.e., the Laforma gold veins and the Casino copper-molybdenum-gold deposit), suggesting the respective epithermal-porphyry transitions.

The Mount Skukum mine, situated north of the Skukum Creek deposit, occurs within the Mt. Skukum Volcanic Complex and is represented by typical epithermal gold-silver mineralization occurring in quartz, quartz-carbonate and quartz-fluorite veins bearing high gold values (approximately 14 g/t Au in average; McDonald, 1990). Some of the veins are controlled by generally meridianal (north-trending) faults, which locally also host andesite and rhyolite dykes. Most of this epithermal mineralization represents its low-sulphidation sub-type that is evidenced by characteristic mineral assemblages (quartz-adularia-sericite) and textures (open-space filling, hydrothermal brecciation, cryptocrystalline quartz, bladed calcite replaced by silica, etc.; *cf.* Heald *et al.,* 1987; White and Hedenquist, 1990). On deeper levels, crackle breccia-style quartz and quartz-carbonate stockwork, locally with quite abundant pyrite, occur in andesite dykes. Epithermal high-sulphidation mineralization is also present, evidenced by the presence of alunite sinters (caps) in immediate vicinity to the Mount Skukum prospect area (McDonald, 1990).

LOCAL GEOLOGICAL SETTING

The Skukum Creek deposit is related to a large (possibly district-scale) fault zone that exceeds 200 m in width and extends in an east-northeast direction for several kilometres (possibly up to 10-20 km) along strike. This fault zone hosts the major mineralized zones of the Skukum Creek deposit, including the Rainbow, Rainbow 2, Kuhn and other zones bearing gold and silver. Further east, this fault controls the Rainbow East mineralized zone, the Goddell Gully gold-antimony prospect, the Becker-Cochran antimony prospect, as well as numerous gold, gold-silver, lead-zinc, copper, and other showings previously mentioned (Fig. 1).

This fault zone is considered to be a part of a fault system bordering and terminating the Mt. Skukum Volcanic Complex, in particular, rimming a large caldera (volcanic depression) composed of volcanic rocks. A large composite pluton of the mid-Cretaceous Coast Plutonic Suite occurs in the immediate vicinity of the Skukum Creek deposit. This pluton is composed of larger masses of gabbro, monzonite/diorite, McNeil granodiorite, as well as smaller quartz monzonite, monzonite-porphyry and granite dykes (Fig. 2).

Some features of the local geology suggest that this fault zone was established before the Tertiary volcanic event. This zone, in particular, is in part traceable by a 'chain' of roof pendants composed of monzonite/diorite and, to lesser extent, by highly metamorphic possibly Precambrian metasedimentary rocks enclosed in the McNeil granodiorite. Also, there are numerous small dykes and apophyses of younger (than McNeil granodiorite) intrusive rocks, particularly quartz monzonite, monzonite-porphyry, granite, elongated in accordance to the general strike of the fault zone.

The fault zone is expressed by a very large number of subparallel and commonly subvertical andesite, dacite,

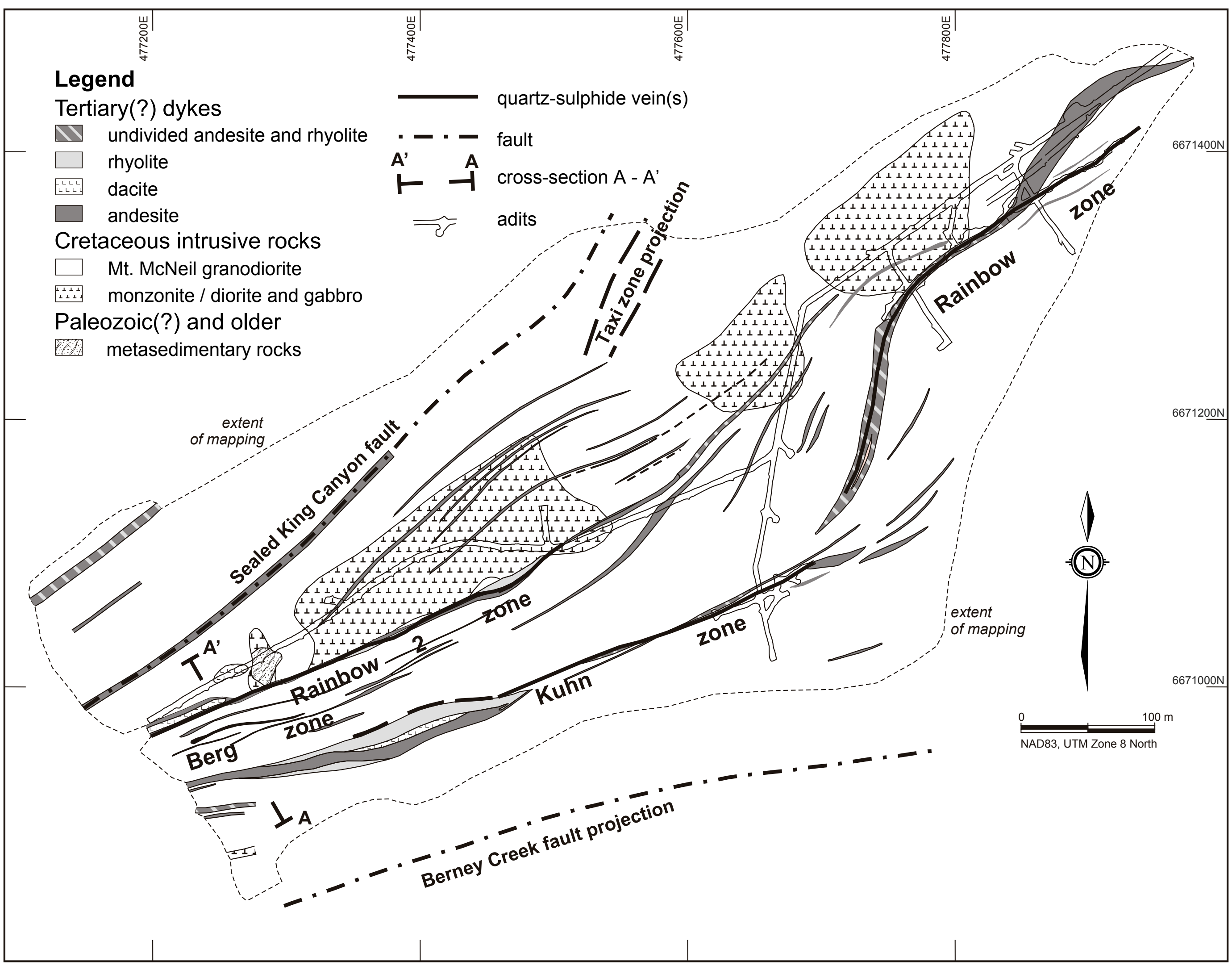

Figure 2. *Geological map of the Skukum Creek deposit, 1300-m level.*

rhyolite dykes and their swarms tracing more localized shear-like structures distinguishable within the wide fault zone. Individual dykes can attain some 15 to 20 m in thickness but commonly are 0.5 to 2 m thick; the largest dykes extend for hundreds of metres along strike and down dip. Smaller dykes commonly form 'en echelon' structures. The dykes are reliable markers of mineralized shear zones. These dykes are typically considered to represent the Tertiary volcanic event (as subvolcanic analogues of the aerial volcanic rocks); however, some of them may be in fact late mafic dykes accompanying the Cretaceous intrusive rocks (Fig. 2). Multiple episodes of dyke emplacement possibly correspond to the re-activation events of the hosting shear zone(s), with the dykes intruding into these shear zones or their re-activated intervals. Thus, individual dykes, being syn- or post-tectonic in relation to the corresponding tectonic event, occur as pre-tectonic in relation to later tectonic re-activation accompanied, in turn, by another set of related dykes.

Among the dykes found in the deposit area, the zoned dykes composed of andesite-dacite, and more complex composite andesite-dacite-rhyolite and andesite-rhyolite dykes are of special interest, as the largest of them are coincident with the most important mineralized zones. In the zoned dykes, dacite occupies the core position and exhibits gradational contacts to the 'rimming' andesites. These relationships can be considered as revealing intra-chamber magmatic differentiation rather than successive emplacement of various rock types. The differential zoning occurs where the dykes display a greater thickness, and generally grade into andesite along strike and down dip.

Composite andesite-rhyolite and andesite-dacite-rhyolite dykes are something different from the zoned andesite-dacite dykes mentioned above. These rock types are found in cross-cutting relationships rather than in gradual transitions, suggesting these complex dykes were likely formed by subsequent intrusion of portions of magma with different composition, accompanying respective re-activation of the hosting shear zone. In all cases, rhyolite appears to be younger than other rock types (dykes). It is important that the largest dykes identified on the prospect (namely, the Rainbow 2, Kuhn, and possibly Rainbow dykes) represent this type of composite dyke, and include perhaps earlier zoned andesite-dacite and/or unzoned andesite dykes intruded by rhyolite dykes.

Another important feature of the deposit structure is represented by the abundance of various hydrothermal and eruptive magmatic breccias. These include intrusive (eruptive) magmatic breccia with granodiorite fragments in monzonite-porphyry cement, as well as monolithic and polylithic phreatomagmatic breccias with andesite and rhyolite cement. Most of these breccias occur in the local shear zones.

Individual local shear zones are traceable for hundreds of metres along strike and down dip and are typically some 10 to 30 m thick. The larger shear zones hosting mineralization were studied in detail by Lang *et al.* (2003) and include the Rainbow and Kuhn mineralized zones, linked by the north-trending Sterling zone, a dilatational stepover that connects the eastern end of the Kuhn zone with the western end of the Rainbow zone. The Rainbow East zone represents a possible eastern extension of the Rainbow zone. North-northeast trending, steeply dipping quartz-sulphide extension veins in the Taxi zone, and similar veins developed throughout the underground workings, have orientations consistent with formation during sinistral displacement along the Rainbow and Kuhn faults. The Rainbow 2 zone represents a western extension of the Rainbow zone. In addition, a new mineralized zone (Berg) was discovered in 2006 between the Rainbow 2 and Kuhn mineralized zones in the western part of the deposit, an almost equal distance (some 20 to 30 m) from each of these zones.

Also, a number of either hydrothermally altered or geochemically anomalous intercepts related to andesite dyke swarms may be indicative of the presence of other (hidden on the upper levels) mineralized zones. In total, the deposit structure may be presented as a thick mineralized package incorporating at least six to seven mineralized zones related to subparallel subvertical shear zones. Total width of the mineralized package possibly exceeds 200 m. It is noteworthy that this mineralized package appears to be just a small part of a much more extensive district-scale fault zone controlling mineral occurrences on the adjacent territory.

The Rainbow mineralized zone is so far the largest mineralized zone found within the Skukum Creek deposit and hosts the majority of mineral resources. It is subvertical, coincident with a large composite andesite+rhyolite dyke, trends 50-55/78-83°S, and has been traced by drilling over a strike length of 265 m and 360 m down dip, and remains open at depth. A thick northwest-trending felsic dyke, referred to as the Portal dyke, bounds the zone to the northeast. According to Lang *et al.* (2003), the controlling fault itself pinches and swells, attaining widths of 1 to 10 m, but may reach widths to 20 m. Mineralization is represented by pinching and swelling lensoid and more uniform lenticular quartz-sulphide veins developed along the dyke contacts. The veins are younger than the dykes, and commonly contain their fragments or crosscut them, although they occur mostly close to, or along, the dyke contacts. The formation of the mineralized veins is definitely coincident with an additional (postdating the dykes) episode of tectonic shearing. Multiple generations of veins are present, including early veins incorporated as fragments into cataclasites and younger veins that overprint cataclastic breccias. The quartz-sulphide veins comprise several generations of quartz, pyrite, sphalerite, galena, arsenopyrite, stibnite, chalcopyrite, etc., with common breccia textures. The breccias exhibit textural relationships suggestive for both cataclastic and hydrothermal processes (Lang *et al.,* 2003). Coarse-grained pyrite, arsenopyrite and sphalerite are locally abundant but, generally, fine-grained sulphide minerals predominate. Total sulphide mineral contents vary from a few percent to 20-30% and higher in local massive sulphide-rich intervals.

MINERALIZED ZONES IN THE WESTERN PART OF THE DEPOSIT

The 2006 exploration program focused on the Rainbow 2, Berg and Kuhn mineralized zones from the 1300-m level, situated in the western part of the Skukum Creek deposit. Figure 2 shows the 1300-level geological plan with the position of the three mineralized zones. A typical cross-section (A-A′) through the zone is illustrated in Figures 3 and 4.

RAINBOW 2 ZONE

The Rainbow 2 zone, discovered in 2003 while completing an underground drift, is similar to the Rainbow zone. It is situated 250 m southwest of the Rainbow zone and is possibly hosted by the same shear zone striking 050°/80°SE. In 2006, the Rainbow 2 mineralized zone was traced for almost 300 m along strike; this brings the total identified and partially explored strike length of the zone to some 350 m.

The zone incorporates a composite andesite-rhyolite or zoned andesite-dacite dyke of variable thickness, with general thickening toward the west-southwest (from a few metres up to 10 m). The hosting fault zone is represented by numerous, although quite short, intervals of fracturing, tectonic brecciation, gouging, cataclasis, etc., reflecting the dilatational shear nature of the Rainbow 2 fault zone. Over significant strike extent, this shear is roughly coincident with the contact of granodiorite and monzonite/diorite, although it is not a rule, as the shear can occur far from this contact (mostly in granodiorite).

The granodiorite and monzonite/diorite commonly show increased sericite and chlorite alteration near the Rainbow 2 zone or in the hanging wall in most instances, which passes to moderate to weak alteration with distance away from the structural break. The rocks show moderate to strong chloritic alteration in the mafic minerals and moderate sericite alteration of plagioclase; a tight stockwork of epidote-carbonate with a narrow bleached envelope is also present. Within the zone, the rocks are strongly to completely silicified, bear intense quartz-sericite and quartz-carbonate-sericite alteration, and locally are strongly argillically altered. An intense stockwork of thin quartz to quartz-carbonate and quartz-pyrite stringers, and background fine-grained pyrite dissemination are also common.

Mineralized intervals occupy a relatively minor part of the fault zone (Figs. 3 and 4, see pages 260 and 261). In general, the mineralized intervals, composed of quartz-sulphide veins and intervals of intense quartz-sulphide veining, form a series of lenticular bodies up to 5-6 m thick, extending for 200-250 m along strike and 50-100 m in a vertical direction, pinching out and swelling into the next lens.

The Rainbow 2 fault zone and coincident mineralized zone are generally vertical, but dip steeply (90° to 75°) to the southwest in a few places.

The gold and silver mineralization in the Rainbow 2 zone exhibits close association with pyrite, sphalerite, arsenopyrite, chalcopyrite and galena. In most cases, a positive correlation between the amount of sulphide minerals and gold/silver grades can be established. Both coarse- and fine-grained sulphide minerals are present; the quartz-sulphide veins are characterized by brecciated, banded, locally crustiform textures (Fig. 5 and 6). Pyrite and sphalerite predominate but arsenopyrite, chalcopyrite and, less commonly, galena are locally abundant. Some veins contain magnetite and associated chalcopyrite. The quartz-sulphide veins commonly show internal zonation from sulphide-rich rims (commonly with banded and massive sulphide minerals) to sulphide-poor quartz core (with fine to coarse, disseminated, but generally minor, sulphide minerals).

Drilling during 2006 returned significant high-grade mineralization over substantial widths. Significant

Table 1. *Selected significant intersections, Rainbow 2 zone.*

Hole	Grade (g/t)		Drill length (m)
	Au	Ag	
SC06-41	18.98	137.1	0.67
including	48.5	215.0	0.25
SC06-48	13.49	218.8	3.76
including	34.24	411.9	1.40
SC06-50	77.50	487.0	1.15
SC06-60	14.90	248.0	0.55
SC06-61	17.21	103.3	2.57
including	41.80	234.0	1.05
SC06-73	18.58	244.9	2.50
including	36.80	424.0	1.00
SC06-75	51.30	437.0	0.80
SC06-78	10.95	59.1	3.61
including	33.30	145.0	1.11
SC06-85	32.53	306.9	1.59
including	68.50	600.0	0.59

intersections of gold-silver mineralization within the Rainbow 2 zone are listed in Table 1.

The Ag:Au ratio for the Rainbow 2 zone is quite low (13:1) and significantly less than that for the mineralization in the Rainbow zone (37:1).

The Rainbow 2 mineralized zone still remains open to the west-southwest as well as down dip along its entire strike length.

BERG ZONE

The discovery of a new significant mineralized zone, the Berg zone, parallel to, and located between the Rainbow 2 and Kuhn zones, is of special interest and potential importance. As with the other zones, the Berg zone is also associated with large andesite dykes and the mineralization is lenticular with limited vertical extent probably not exceeding 60-80 m.

The presence of several narrow but heavily mineralized veins within this mineralized lens is also quite common for the Berg zone.

However, in contrast to the Rainbow 2 mineralized zone, the Berg zone is characterized by a distinct plunge down from the west (west-southwest) to east (east-northeast) at a 40-50° angle. Mineralization progressively occurs at deeper levels toward the east, and on shallower levels toward the west.

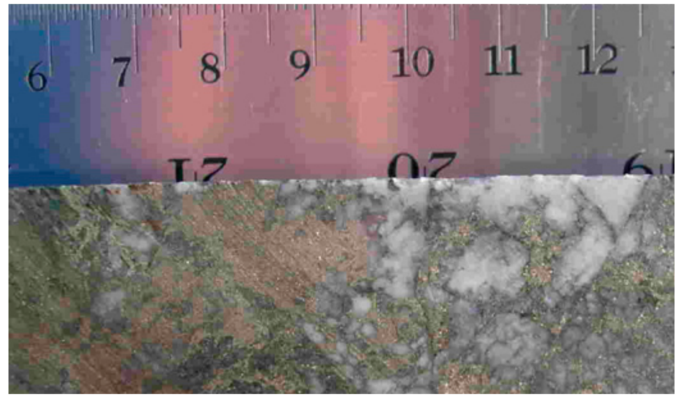

Figure 5. *Quartz-sulphide mineralization of the Rainbow 2 zone showing the brecciated nature of the zone. Sulphide minerals consist mainly of pyrite and sphalerite. SC06-61, 41.80 g/t Au, 234.0 g/t Ag.*

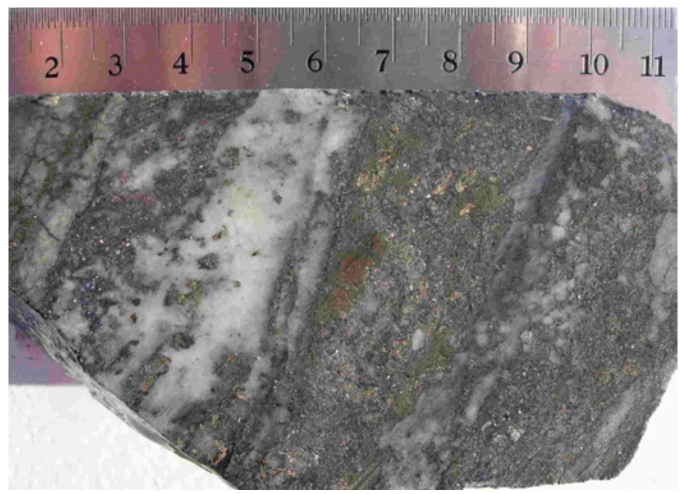

Figure 6. *Disseminated and banded textures of the quartz-sulphide mineralization of the Rainbow 2 zone. Sulphide minerals consist mainly of pyrite, arsenopyrite and sphalerite. SC06-41, 48.50 g/t Au, 215.0 g/t Ag.*

In regard to this structural feature, it has to be noted that some aspects of the distribution of higher gold and silver values within the Rainbow 2 zone (most visible on its longitudinal projection) may form a similar trend 'plunging' from the west to east.

Outside of its most mineralized portion of 60-80 m long (and 1-3 m wide), the Berg zone splits into a series of small subparallel veins, veinlets and narrow stockwork zones, locally loses its continuity, but then starts again as another set of mineralized veins tracing the general controlling structure.

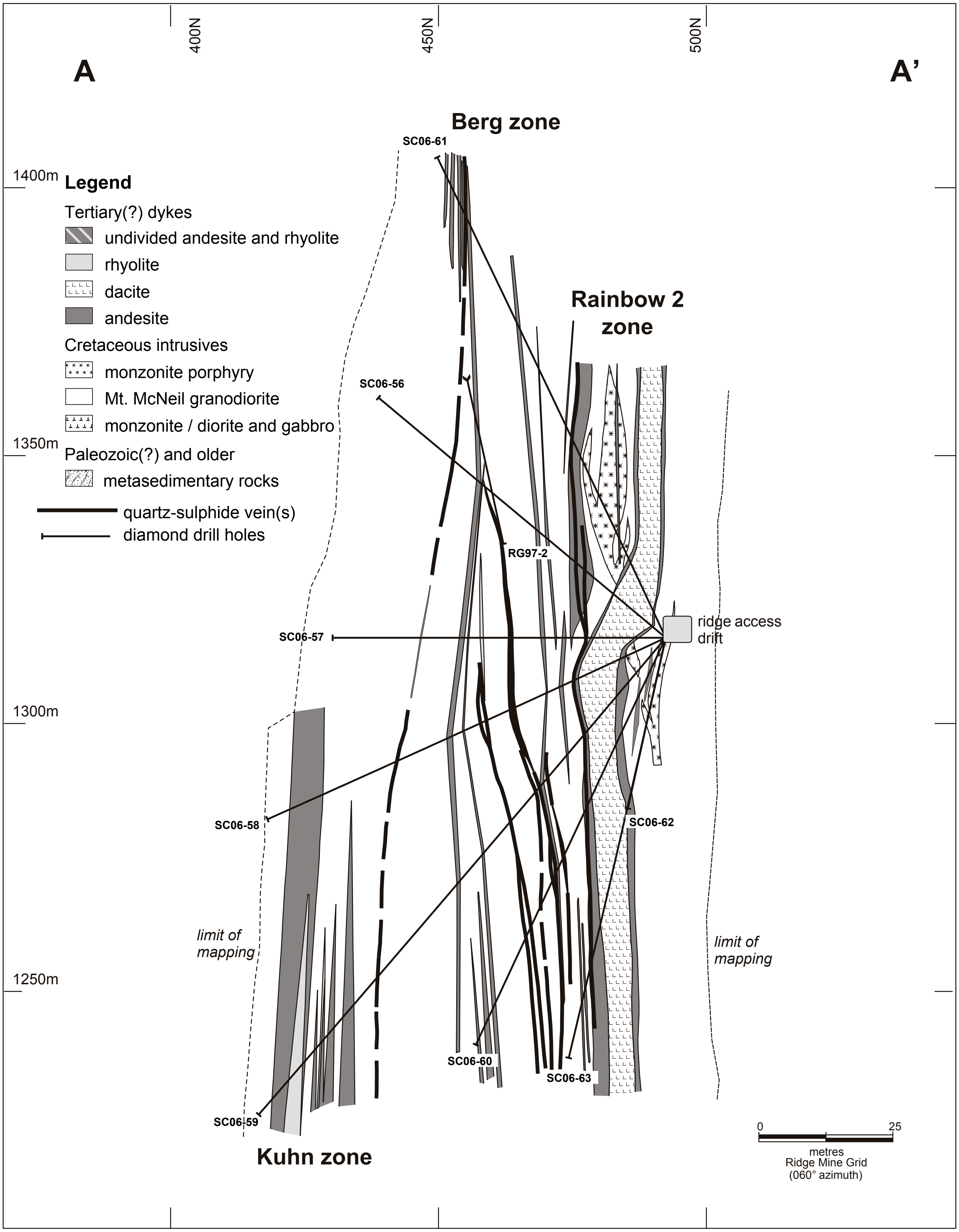

Figure 3. *DDH Cross Section A-A', geological interpretation. Location shown on Figure 2.*

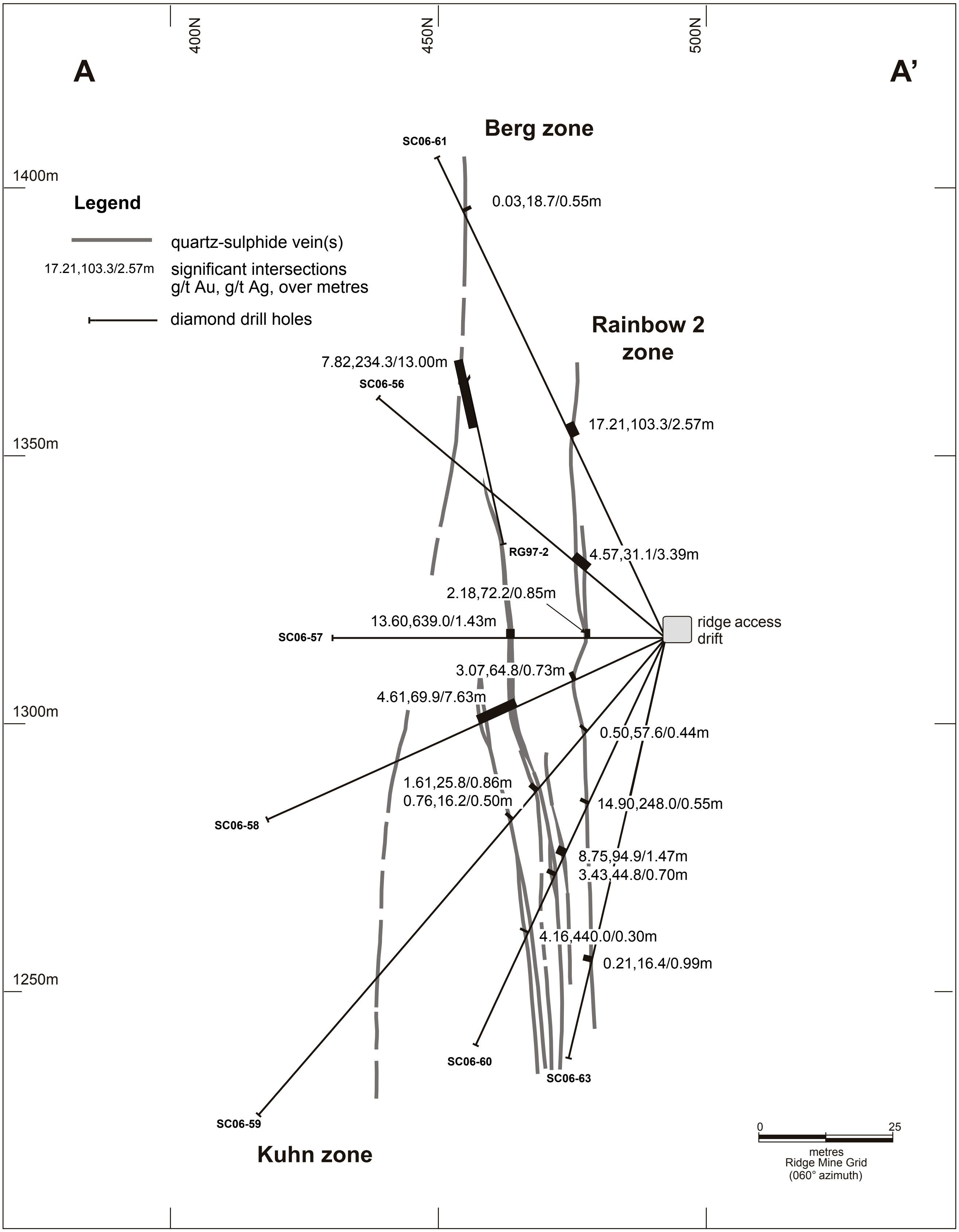

Figure 4. *DDH Cross Section A-A', mineralization and results. Location shown on Figure 2.*

Table 2. *Selected significant intersections, Berg zone.*

Hole	Grade (g/t)		Drill length (m)
	Au	Ag	
SC06-57	13.60	639.0	1.43
SC06-58	11.57	183.3	1.86
including	23.80	329.0	0.75
SC06-70	24.57	90.0	0.95
SC06-73	18.58	244.9	2.50
SC06-78	8.15	568.0	0.30
SC06-86	23.25	397.0	1.59
including	44.23	751.7	0.83

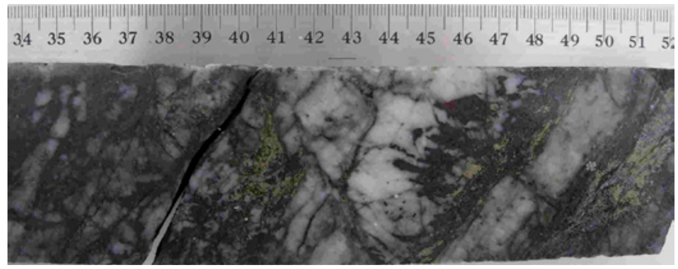

Figure 8. *Brecciated and banded textures of the quartz-sulphide mineralization of the Berg zone. Sulphide minerals consist mainly of pyrite, arsenopyrite and sphalerite. SC06-86, 23.30 g/t Au, 665.0 g/t Ag.*

The gold and silver mineralization found in the Berg zone is quite similar to that located in the Rainbow 2 zone. This is well manifested by the presence of the same set of sulphide minerals (including abundant arsenopyrite, sphalerite, galena and pyrite), high sulphide content in mineralized quartz-sulphide veins, their similar textural appearance (banded, brecciated, locally crustiform textures), etc. (Figs. 7 and 8). Perhaps, the difference is a relatively higher content of arsenopyrite in the Berg zone (with lower chalcopyrite and pyrite?), as compared to that in the Rainbow 2 zone. Another difference is observed in higher average Ag:Au ratio of the mineralization in the Berg zone (22:1), indicating greater abundance of silver, as compared to that in the Rainbow 2 zone (13:1). Finally, the mineralization found in the Berg zone more commonly bears significant antimony contents than that in the Rainbow 2 zone.

As a result of similar mineral composition, the drill intercepts of the Berg zone are also quite comparable to those of the Rainbow 2 zone in terms of the presence of high-grade gold and silver values (Table 2).

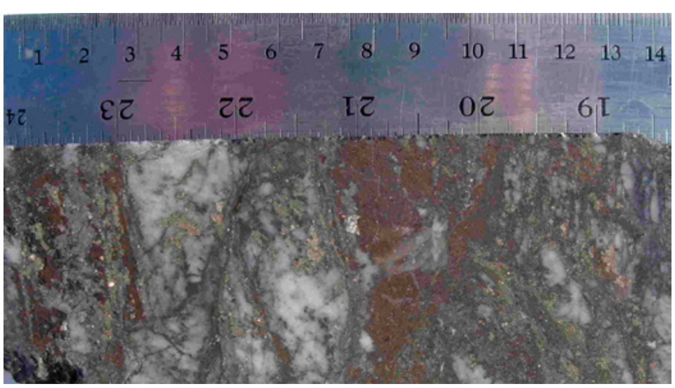

Figure 7. *Quartz-sulphide mineralization of the Berg zone showing the sheared nature of the zone. Sulphide minerals consist mainly of pyrite, arsenopyrite and sphalerite. SC06-58, 10.50 g/t Au, 519.0 g/t Ag.*

In general, the Berg mineralized zone (especially, its general controlling structure) represents an attractive exploration target for the follow-up drilling, as other large 'mineralized lenses' can be expected within this structure.

KUHN ZONE

The Kuhn mineralized zone trends 070°/ 80-85°S, and, prior to 2006, was traced by drilling over a strike length of 200 m and 350 m down dip, remaining open along strike and at depth.

The Kuhn zone geology is similar to that of the other mineralized zones. It includes a shear zone marked by intense fracturing, tectonic brecciation, faulting, commonly with tension clay, andesite, rhyolite, and composite and zoned andesite-dacite-rhyolite dykes, lenticular quartz-sulphide veins, and intense sulphide-bearing quartz, quartz-carbonate and quartz-carbonate-sericite stockwork.

The Kuhn zone carries 11.11 g/t Au and 93.5 g/t Ag over an average width of 2.89 m along a 41.0-m strike extent from the 1308-m level drift; and 29.31 g/t Au and 197.8 g/t Ag across an average width of 2.0 m and a 30.0-m strike length from the 1350-m level drift from channel samples collected in 1988. In 2003, an oblique diamond drillhole testing the northeastern depth extent of the Kuhn zone returned an incomplete intercept (due to caving) of 8.3 g/t Au, 69 g/t Ag over 2.9 m in hole SC02-16 (C.O. Naas, pers. comm., 2003).

In 2005, the Kuhn zone was intersected across 17.8 m in drillhole SC05-37, with three significant quartz-sulphide breccia/veins. The drilling returned a number of significant intercepts, including 2.83 g/t Au over 3.75 m;

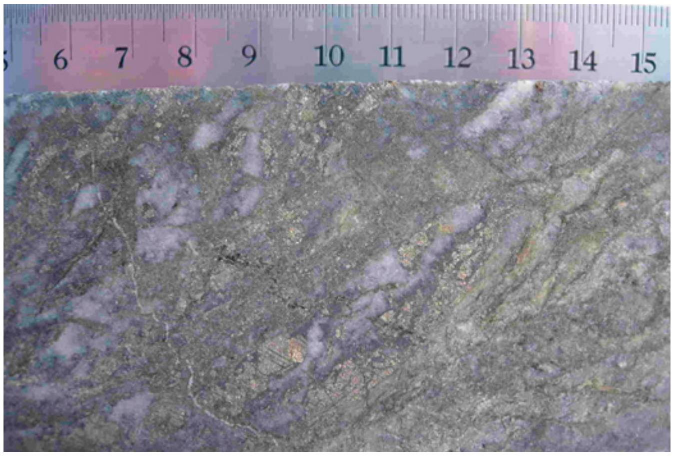

Figure 9. *Quartz-sulphide mineralization of the Kuhn Zone. Sulphide minerals consist mainly of pyrite. SC06-78, 4.58 g/t Au, 82.9 g/t Ag.*

5.04 g/t Au and 172 g/t Ag over 0.95 m in DDH SC05-37; 1.23 g/t Au and 16.0 g/t Ag over 1.2 m in DDH SC05-38; and other similar generally quite low-grade intercepts (C.O. Naas, pers. comm., 2005).

In 2006, the Kuhn zone was extended for some 310 m along strike; this brings its total identified and partially explored strike length of the zone to some 550 m. It was demonstrated that the large portion of the zone outlined in 2006 is essentially coincident with a large composite andesite-dacite-rhyolite dyke evolving into a much narrower unzoned andesite dyke toward its west-southwestern end. Similarly, the distance between the Kuhn dyke and the Berg and Rainbow 2 zones gradually becomes narrower with their possible merger expected some 200-300 m west of the end of the drift. The portion of the Kuhn zone explored in 2006 differs from previously explored sections by the presence of this large zoned andesite-dacite-rhyolite dyke.

This dyke is situated within a broad zone of intense fracturing, brecciation, quartz-sericite alteration and background disseminated pyrite, with local small zones of quartz and quartz-carbonate stringers bearing disseminated pyrite, galena, chalcopyrite, arsenopyrite, etc. (Fig. 9). Total width of the Kuhn mineralized zone may attain some 20-25 m, but decreases toward the west-southwest; it has a subvertical or very steep (80-85°) southwestern dip.

Table 3. *Selected significant intersections, 2006, Kuhn zone.*

Hole	Grade (g/t)		Drill length (m)
	Au	Ag	
SC06-73	2.48	72.9	2.82
including	3.54	120.0	1.45
SC06-78	4.58	82.9	0.27
and	5.04	53.1	0.26

Significant intercepts of the Kuhn zone obtained in 2006 are presented in Table 3.

Remarkably, average Ag:Au ratio of the mineralization in the Kuhn zone (30:1) is lower than that in the Rainbow zone (37:1) but higher than that in the Berg zone (22:1), and much higher than that in the Rainbow 2 zone (13:1).

Most of the higher gold intercepts in drilling were obtained from the highest levels of the Kuhn zone intersected by up-holes drilled at high angles at the western (west-southwestern) flank of the zone, with less gold from drill holes intersecting the Kuhn zone on the drift level in the western part of the deposit. This may suggest that the better mineralized part of the Kuhn zone plunges from the west toward the east, in similar manner to that of the Berg zone. If so, this structural pattern occurring on the Skukum Creek deposit may be one of the leading structural features controlling the mineralization.

STYLES (TYPES) OF MINERALIZATION

As noted previously, the mineralization of the Skukum Creek deposit is represented by numerous narrow lensoid and lenticular quartz (-carbonate-sericite) veins, mineralized stockwork, zones of pervasive silicification, quartz-carbonate-sericite alteration, etc. Among them, the quartz-sulphide veins are most significant and constitute the ‘pivotal’ element of the larger mineralized zones (Rainbow, Rainbow 2, Berg, Kuhn). Individual quartz-sulphide veins vary from several centimetres to a few metres in thickness, extending from several metres to several tens of metres along strike and down dip. Commonly, the veins merge or split into several smaller ones, locally distinguished as veining zones, pinch and swell, and experience flexure-like and sigmoid curving both along strike and down dip. The veins have essentially quartz-sulphide composition, with typically light-grey milky quartz brecciated and then cemented by dark-grey quartz, fine-grained sulphidic material, and coarser grained sulphide minerals, including pyrite, arsenopyrite, sphalerite, galena, chalcopyrite, etc.

The quartz-sulphide veins are surrounded by wide halos of mineralized stockwork, pervasive silicification and quartz-

Table 4. *Selected wider significant intersections, Skukum Creek deposit.*

Hole	Grade (g/t)		Drill length (m)
	Au	Ag	
SC06-41	2.16	22.7	6.40
SC06-58	4.61	69.9	7.63
SC06-60	2.67	43.4	6.35
SC06-65	1.92	10.1	11.66
SC06-66	0.38	60.1	12.43
SC06-68	2.43	24.4	8.02
SC06-84	4.54	48.6	8.91

carbonate-sericite alteration, containing background disseminated pyrite. Some (typically much smaller) zones contain abundant pyrrhotite, commonly associated with a propylitic-style gangue assemblage of amphibole, chlorite, epidote and quartz.

Currently, the larger quartz-sulphide veins represent the major value of the deposit; they commonly contain very high gold and/or silver values over limited widths, typically together with high sulphide contents (as well as high concentrations of Cu, Pb, Zn). Selected lower grade but much wider (than single quartz-sulphide veins) intercepts are presented in Table 4.

Most of these intervals are found in the westernmost part of the deposit, where the Rainbow 2, Berg and Kuhn mineralized zones exhibit a tendency to merge due to possible merging of the respective controlling structures. Alternatively, many of these intervals occur due to local splitting of major mineralized structures.

The productive mineralization found on the Skukum Creek deposit is characterized by significant variability in terms of mineral composition and geochemical features. The new, significantly expanded set of geochemical data makes it possible to distinguish various geochemical (and respectively mineral) types of mineralization, and to trace geochemical and mineralogical differences of mineralization occurring in different mineralized zones (Table 5).

The data presented in Table 5 illustrate several important geochemical features of gold and silver mineralization found at the Skukum Creek deposit.

In particular, at least seven different gold- and/or silver-bearing geochemical (and mineral) assemblages can be distinguished on the Skukum Creek deposit, including (1) gold-silver-bearing assemblage, with low sulphide content; (2) gold-silver-bearing assemblage, with low content of all sulphide minerals but arsenopyrite; the latter is constantly present in significant amounts providing strong enrichment in arsenic (typically more than 1% As), as a most stable geochemical signature; (3) silver-gold-bearing assemblage, also with low content of all sulphide minerals but arsenopyrite; (4) silver-gold-antimony polysulphidic assemblage, with consistant presence and great abundance of chalcopyrite, sphalerite, galena and arsenopyrite; (5) similar silver-gold polysulphidic assemblage, also with consistant presence and great abundance of chalcopyrite, sphalerite, galena and arsenopyrite, but with no essential antimony values; (6) essentially silver-bearing polysulphidic assemblage, with consistant presence and great abundance of chalcopyrite, sphalerite and galena; and (7) essentially silver-bearing assemblage, with or without bismuth mineralization and with generally low sulphide content.

The presence and abundance of various gold- and/or silver-bearing assemblages varies for different mineralized zones. In particular, the silver-gold-antimony polysulphidic assemblage (4), with consistant presence and great abundance of chalcopyrite, sphalerite, galena and arsenopyrite, appears to occur only in the Berg zone indicating the abundance of antimony as one of the most remarkable features of the Berg zone, whereas similar silver-gold polysulphidic assemblage (5), also with consistant presence and great abundance of chalcopyrite, sphalerite, galena and arsenopyrite, but with no essential antimony values predominates in the Rainbow 2 zone. The silver-gold-arsenic assemblage (4) and essentially silver polysulphidic assemblage (6) also occur in the Rainbow 2 zone only and are apparently absent in the Berg zone. In contrast, the gold-silver assemblage (1), with low sulphide content, and the gold-silver-arsenic assemblage (2) appear to be present in both the Rainbow 2 and Berg mineralized zones. Finally, the essentially silver and silver-bismuth assemblages occur both within and outside the large mineralized zones, forming typically small stockwork and veining zones.

Among these mineral assemblages, those with high sulphide content (4-6) sharply predominate the deposit and form the majority of significant intercepts obtained for the Rainbow 2, Berg and Kuhn mineralized zones during the 2006 exploration program. In addition, there appears to be some correlation between the amount of sulphide minerals and gold+silver grades, with the highest values more or less corresponding to the higher sulphide contents. Overall sulphide contents of some 10-20% are most common for gold-silver-bearing mineralized intervals,

Table 5. *Representative assay results for various mineral assemblages on the Skukum Creek deposit.*

Drill hole	Interval, m	Au, g/t	Ag, g/t	Ag:Au	Cu, %	Pb, %	Zn, %	As, %	Sb, g/t	Bi, g/t	Zone
1. Gold-silver assemblage, with low sulphide mineral content											
SC06-58	37.20-38.14	10.80	5.1	0.5:1	0.013	0.050	0.193	0.0055	15	<5	Berg
SC06-65	23.53-24.79	16.90	43.2	2.6:1	0.034	0.596	1.230	0.0080	10	<5	Berg
SC06-74	22.19-22.63	31.60	52.4	1.7:1	0.088	0.134	1.280	0.0065	<5	<5	Rainbow 2
2. Gold-silver-arsenic assemblage											
SC06-44	62.07-62.47	14.40	72.4	5.0:1	0.108	1.040	0.641	>1	10	<5	Rainbow 2
SC06-70	36.25-37.20	24.57	90.0	3.7:1	0.128	0.590	2.388	>1	145	<5	Berg
SC06-82	39.84-40.30	30.40	94.7	3.1:1	0.104	0.664	0.637	>1	75	<5	Rainbow 2
3. Silver-gold-arsenic assemblage											
SC06-51	30.49-30.94	19.70	296.0	15.0:1	1.620	0.412	1.350	>1	<5	<5	Rainbow 2
SC06-78	44.64-45.75	33.30	145.0	4.4:1	0.215	0.410	1.740	>1	15	<5	Rainbow 2
SC06-81	37.10-37.28	70.70	710.0	10.0:1	2.140	0.298	0.517	>1	30	<5	Rainbow 2
SC06-87	21.06-22.31	16.80	133.0	7.9:1	0.227	0.800	1.450	>1	55	35	Rainbow 2
4. Silver-gold-antimony polysulphidic assemblage											
SC06-57	28.24-29.67	13.60	639.0	47.0:1	1.34	1.68	3.43	>1	1450	<5	Berg
SC06-58	30.51-31.26	23.80	329.0	13.8:1	0.49	3.17	2.96	>1	6185	<5	Berg
SC06-58	36.61-36.85	10.50	518.0	49.3:1	0.875	2.240	11.600	>1	5380	<5	Berg
SC06-86	44.76-45.59	44.23	751.7	17.0:1	1.277	8.754	14.360	>1	488	103	Berg
5. Silver-gold polysulphidic assemblage											
SC06-40	42.00-42.22	59.60	476.0	8.0:1	0.917	2.930	7.540	>1	40	135	Rainbow 2
SC06-71	19.00-19.43	16.60	805.0	48.5:1	1.800	0.579	8.940	0.9615	50	<5	Rainbow 2
SC06-75	24.30-25.10	51.30	437.0	8.5:1	0.686	2.570	5.840	0.1395	<5	<5	Rainbow 2
SC06-84	39.76-40.14	58.50	640.0	10.9:1	1.900	0.355	4.940	>1	20	<5	Rainbow 2
SC06-89	25.65-26.14	17.40	710.0	40.8:1	0.765	1.760	3.560	0.5400	<5	90	Rainbow 2
6. Essentially silver polysulphidic assemblage											
SC06-44	64.61-64.91	1.35	329.0	243.7:1	1.190	0.440	3.760	0.0050	<5	<5	Rainbow 2
SC06-76	33.75-34.75	1.44	424.0	294.4:1	1.590	2.450	6.070	0.0025	<5	<5	Rainbow 2
SC06-77	28.75-29.26	1.71	910.0	532.2:1	2.380	1.230	7.470	0.0680	<5	<5	Rainbow 2
7. Essentially silver and silver-bismuth assemblages, with low sulphide mineral content											
SC06-40	0.99-1.15	0.02	690.0	34500:1	0.012	1.050	0.370	0.0005	<5	640	-
SC06-45	3.30-3.37	0.32	1550.0	4843.8:1	0.045	0.827	0.013	0.0020	<5	3715	-
SC06-74	39.31-39.69	0.24	489.0	2037.5:1	1.180	0.193	0.374	<0.0005	25	<5	-

with locally much higher contents (up to 80-100% sulphide minerals in local parts of the mineralized intervals).

Distinct geochemical signatures of various mineral assemblages make it possible to suggest some mineralogical features, especially as to the mineral form of gold and silver; there seems to be no doubt that gold and silver are represented by various minerals (such as native gold, electrum, etc.) occurring in various proportions. In particular, comparable amounts of gold and silver in the gold-silver assemblages (1 and 2) support electrum as the major gold-silver-bearing mineral, although native gold with a high-fineness may also be present in rare cases. In contrast, the silver-gold assemblages (3-5) require the presence of one or more additional silver-bearing phases to provide very high silver grades. Finally, only silver-bearing mineral(s) occur in essentially silver-bearing assemblages (6-7). These suggestions on gold-silver mineralogy of the Rainbow 2, Berg and Kuhn mineralized zones are consistent with the data of Lang *et al.* (2003). They concluded, on the example of the Rainbow and Kuhn mineralized zones, that gold occurs mostly as electrum and minor to trace native gold, whereas silver is hosted predominantly in freibergite, with trace to minor native silver and argentite; trace amounts occur also within galena, chalcopyrite, stibnite and sphalerite.

No distinct vertical or lateral deposit-scale geochemical zonation can be established at the present stage of exploration, although, as noted above, various mineralized zones differ in their geochemical signatures. Within the mineralized zones, a larger number of productive mineral assemblages occur in structurally more complex intervals (such as their swellings). On the other hand, the lack of geochemical trends and stable geochemical variability within some 100-m vertical extent of the mineralized zones explored during the 2006 program may be attributed to significant vertical extent of mineralization.

DISCUSSION

The 2006 exploration program has resulted in additional resource expansion and delineation on the Skukum Creek deposit, with the extension of the Rainbow 2 mineralized zone for an additional 270 m further west-southwest, and discovery of the Berg mineralized zone. The program provided additional geological, structural, geochemical and mineralogical information to highlight some important features of the Skukum Creek deposit.

In particular, the exploration program has highlighted the structural position of the deposit as situated within an extended fault zone marked by numerous subparallel dyke swarms, with the respective position of the mineralization in relation to these swarms and controlling local shear structures. In total, three subparallel shears controlling larger lensoid to lenticular mineralized zones (Rainbow-Rainbow 2, Berg, Kuhn) are known; the mineralized zones are generally subvertical, with some of them possibly merging at depth, perhaps in total forming a tree-like structure. Additional structures are also marked by dyke swarms, linear hydrothermal alteration halos, and intense geochemical anomalies, with the potential to host gold mineralization.

The four presently known mineralized zones vary in the abundance of mineralized material, strike and down-dip extent, width, gold and silver grades and geochemical and mineralogical features of mineralization. In particular, the Rainbow zone is the largest and hosts the majority of the deposit resources; it is characterized by the highest average Ag:Au ratio (37:1). In contrast, the Rainbow 2 zone extends the Rainbow zone further west-southwest, and has the lowest average Ag:Au ratio (13:1), but possibly higher sulphide-mineral content. The Berg zone, also with high sulphide-mineral content, is characterized by a moderate average Ag:Au ratio (22:1), higher arsenic and especially antimony contents. The Kuhn zone also has quite high average Ag:Au ratio (30:1). Thus, several mineralized zones with different geochemical (and mineralogical) features occur together, emphasizing the complexity of the area.

In general, the Skukum Creek deposit shows structural and compositional similarities to many low-sulphidation epithermal gold-silver deposits worldwide, including Ken Snyder and Comstock Lode (Nevada, USA), Kupol and Kubaka (northeast Russia), Hishikari (Japan), El Penon (Chile), Martha Hill (New Zealand), and others. These other deposits are characterized by subvertical mineralized zones with significant depth extent (800 m and 600 m at Comstock Lode and Martha Hill, respectively; some 200 m at Hishikari and Ken Snyder; 300-400 m at Kupol; etc.) and variable Ag:Au ratio (1:1 at Kubaka, Hishikari, and Martha Hill; 10:1 at Ken Snyder; 12:1 at Kupol; 19:1 at El Penon; 23:1 at Comstock Lode). Occurrence of several mineralized veins on the upper level and their merging into a much larger single mineralized body down dip is common for some of these deposits (e.g., Kubaka, etc.). All this may suggest significant potential of the Skukum Creek deposit at depth.

However, the majority of these large epithermal deposits have much lower sulphide-mineral content (typically 1-3% sulphide minerals), that significantly distinguishes them from the Skukum Creek deposit, which typically has some 10-20%, locally greater than 80%, sulphide minerals in the mineralized zones hosting gold-silver mineralization. No such features as open-space filling textures, crypto-crystalline quartz, bladed calcite replaced by silica, typical for epithermal gold-silver deposits are observed at the Skukum Creek deposit. Interestingly, the Skukum Creek deposit differs in this regard from the Mount Skukum deposit situated nearby and related to the same volcanic-plutonic complex.

To some extent, these differences can be explained by assuming essentially deeper conditions of formation of the Skukum Creek deposit. This explanation, in particular, is favoured by the occurrence of a greater amount of sulphide minerals on deeper levels of the Mount Skukum mine. Respectively, the Skukum Creek deposit would be considered as transitional from epithermal to porphyry (rather gold-porphyry) environment.

An alternative explanation could be provided, if one considers the variability of sulphide-mineral contents within the epithermal class of gold-silver deposits. Actually, some of the epithermal gold-silver deposits are formed at shallow depths but are still characterized by the abundance of sulphide minerals. Commonly, these deposits are distinguished as epithermal gold-silver-base metal deposits. In particular, the Victoria deposit (Luzon, Philippines) is characterized by close association of gold with quartz, sphalerite, galena and chalcopyrite. In relatively high-gold zones, sphalerite and galena are abundant (Claveria *et al.,* 1999). Another example is represented by numerous epithermal gold-base metal deposits in southeast Europe (Baia Mare and others; Grancea *et al.,* 2002). Some of these deposits are clearly related to volcanic complexes with shoshonitic affinity. It is interesting that, in turn, some of these deposits are considered as links (or precursors) to gold-rich volcanic-hosted massive sulphide deposits. In general, these considerations would suggest yet stronger geological complexity of the area, with possible occurrence of different volcanic suites.

ACKNOWLEDGEMENTS

The author wishes to thank Robert Rodger, President, and T. Gregory Hawkins, Chairman of the Board, Tagish Lake Gold Corp. Thanks are also expressed to Barry Way, general manager on site during the 2006 exploration program, and to Chris Naas, Ted VanderWart and Marthe Archambault for their assistance in preparing this paper. The manuscript benefited from critical review by Lee Pigage.

REFERENCES

Claveria, R.J.R., Cuison, A.G. and Andam, B.V., 1999. The Victoria gold deposit in the Mankayan mineral district, Luzin, Phillipines. *In:* International Congress on Earth Sciences, Exploration and Mining around the Pacific Rim (the PACRIM Congress), October 10-13, 1999, Bali, Indonesia.

Deklerk, R. and Traynor, S., 2005. Yukon MINFILE - A database of mineral occurrences. Map 105D – Whitehorse area. Yukon Geological Survey, 1:250 000 scale.

Doherty, R.L. and Hart, C.J.R., 1988. Preliminary geology of Fenwick Creek (105D/3) and Alligator Lake (105D/6) map areas. Exploration and Geological Services Division, Yukon Region, Indian and Northern Affairs Canada, Open File 1988-2 (2 maps), 1:50 000 scale.

Hart, C.J.R. and Radloff, J.K., 1990. Geology of Whitehorse, Alligator Lake, Fenwick Creek, Carcross and part of Robinson map areas (105D/11,6,3,2, and 7). Exploration and Geological Services Division, Yukon Region, Indian and Northern Affairs Canada, Open File 1990-4, 113 p.

Heald, P., Foley, N.K. and Hayba, D.O., 1987. Comparative anatomy of volcanic-hosted epithermal deposits: Acid-sulfate and adularia sericite types. Economic Geology, vol. 82, p. 1-26.

Grancea, L., Bailly, L., Leroy, J., Banks, D., *et al.,* 2002. Fluid evolution in the Baia Mare epithermal gold/polymetallic district, Inner Carpathians, Romania. Mineralium Deposita, vol. 37, p. 630-647.

Lang, J., Rhys, D. and Naas, C., 2003. Structure and alteration related to gold-silver veins at the Skukum Creek deposit, southern Yukon. *In:* Yukon Exploration and Geology 2002, D.S. Emond and L.L. Lewis (eds.), Exploration and Geological Services Division, Yukon Region, Indian and Northern Affairs Canada, p. 267-280.

McDonald, B.W.R., 1990. Geology and genesis of the Mount Skukum epithermal gold-silver deposits, southwestern Yukon Territory (105D/3,6). Exploration and Geological Services Division, Yukon Region, Indian and Northern Affairs Canada, Bulletin 2, 65 p.

Mihalynuk, M.G., Mountjoy, K.J., Smith, M.T., Currie, L.D., Gabites, J.E., Tipper, H.W., Orchard, M.J., Poulton, T.P. and Cordey, F., 1997. Geology and mineral resources of the Tagish Lake area (104M/8,9,10E,15 and 104N/12W), Northwestern British Columbia. British Columbia Ministry of Energy, Mines and Petroleum Resources, Bulletin 105.

Pride, M.J., 1986. Description of the Mount Skukum Volcanic Complex, southern Yukon. *In:* Yukon Geology, Volume 1, J.A. Morin and D.S. Emond (eds.), Exploration and Geological Services Division, Yukon Region, Indian and Northern Affairs Canada, p. 148-160.

Smith, M.J., 1982. Petrology and geology of high level rhyolite intrusives of the Skukum area, 105D/SW, Yukon Territory. *In:* Yukon Exploration and Geology 1981, Exploration and Geological Services Division, Yukon Region, Indian and Northern Affairs Canada, p. 62-73.

Smith, M.J., 1983. The Skukum Volcanic Complex, 105D/SW: geology and comparison to the Bennett Lake cauldron complex. *In:* Yukon Exploration and Geology 1982, Exploration and Geological Services Division, Yukon Region, Indian and Northern Affairs Canada, p. 68-72.

Tafti, R. and Mortensen, J.K., 2004. Early Jurassic porphyry (?) copper(-gold) deposits at Minto and Williams Creek, Carmacks Copper Belt, western Yukon. *In:* Yukon Exploration and Geology 2002, D.S. Emond and L.L. Lewis (eds.), Yukon Geological Survey, p. 289-303.

Wheeler, J.O., 1961. Whitehorse map-area, Yukon Territory. Geological Survey of Canada, Memoir 312, 156 p.

White, N.C. and Hedenquist, J.W., 1990. Epithermal environments and styles of mineralization; variations and their causes and guidelines for exploration. *In:* Epithermal Gold Mineralization of the Circum-Pacific; Geology, Geochemistry, Origin and Exploration, II, J.W. Hedenquist, N.C. White and G. Siddeley (eds.), Journal of Geochemical Exploration, vol. 36, p. 445-474.